

UNCLASSIFIED

AD 2 4 1 7 1

DEFENSE DOCUMENTATION CENTER

FOR

SCIENTIFIC & TECHNICAL INFORMATION

CAMERON STATION, ALEXANDRIA, VIRGINIA



UNCLASSIFIED

NOTICE: When government or other drawings, specifications or other data are used for any purpose other than in connection with a definitely related government procurement operation, the U. S. Government therefor incurs no responsibility, nor any obligation whatsoever; and the fact that the Government may have furnished, or in any way supplied the said drawings, specifications, or other data is not to be regarded by implication or otherwise as in any manner licensing the holder or any other person or corporation, or conveying any rights or permission to manufacture, use or sell any patented invention on that may in any way be related thereto.

**Best
Available
Copy**

NAVY DEPARTMENT

THE DAVID W. TAYLOR MODEL BASIN

WASHINGTON 7, D. C.

**A REANALYSIS OF THE ORIGINAL TEST DATA
FOR THE TAYLOR STANDARD SERIES**

BY MORTON GERTLER

MARCH 1954

REPORT 806

TABLE OF CONTENTS

	PAGE
Acknowledgments	i
Notation	iii
Formulas	v
List of Illustrations	vii
List of Tables	xi
History of the Taylor Standard Series	1
Geometry of the Taylor Standard Series	2
Characteristics of the Parent	4
Derivation of Series Forms from Parent	4
Configuration of Derived Forms	13
Characteristics of Actual Forms Tested	17
Reduction of the Original Test Data	17
Temperature Corrections	21
Transitional Flow Corrections	21
Restricted Channel Corrections	24
Cross-Fairing of Resistance Data	27
Final Presentation of Data	30
Calculation of Effective Horsepower Using Revised Contours	37
Validity of Taylor Series Comparisons	42
Use of the Revised Taylor Series Contours With Frictional-Resistance Formulations Other Than Schoenherr	44
References	45

APPENDICES

- Appendix 1 - Curves of Half-Breadth and Waterline Endings Versus Longitudinal Prismatic Coefficient for Derived Forms of the Taylor Standard Series
- Appendix 2 - Contours of Wetted-Surface Coefficients for Standard Series Vessels Plotted Against Prismatic Coefficient and Volumetric Coefficient
- Appendix 3 - Curves of Residual-Resistance Coefficient Versus Speed-Length Ratio and Froude Number for Standard Series Vessels Having a Beam-Draft Ratio of 2.25
- Appendix 4 - Curves of Residual-Resistance Coefficient Versus Speed-Length Ratio and Froude Number for Standard Series Vessels Having a Beam-Draft Ratio of 3.00
- Appendix 5 - Curves of Residual-Resistance Coefficient Versus Speed-Length Ratio and Froude Number for Standard Series Vessels Having a Beam-Draft Ratio of 3.75
- Appendix 6 - Tables of the Schoenherr Frictional-Resistance Coefficients Versus Reynolds Numbers
- Appendix 7 - Tables of Density and Kinematic Viscosity of Water

ACKNOWLEDGMENTS

The author is extremely grateful for the continued encouragement and support given to this work by Dr. F. H. Todd, Chief Naval Architect; Mr. R. B. Couch, Head of the Ship Division; Captain A. G. Mumma, USN, Commanding Officer and Director; Captain F. X. Forest, USN, former Officer in Charge of the Hydromechanics Laboratory; and Rear Admiral C. O. Kell, USN (retired), former Commanding Officer and Director of the David Taylor Model Basin. He is greatly indebted to Mr. W. Kopko, Mr. J. L. Beveridge, Mr. A. D. Williams and others of the staff of the Taylor Model Basin who assisted materially in the laborious calculations and preparation of figures and charts which are most essential in a work of this nature. The author further wishes to express his appreciation for the comments received from naval architects throughout the United States; many of their suggestions were incorporated in the final draft.

NOTATION

DIMENSIONS

COEFFICIENTS

Symbol	Description	Dimensions in Mass- Length-Time System
L	Waterline length	L
B	Beam measured at midlength	L
H	Draft measured at midlength	L
S	Wetted surface area	L^2
∇	Immersed volume	L^3
A_x	Area of a transverse section at midlength	L^2
v	Speed	LT^{-1}
V_k	Speed expressed in knots	LT^{-1}
v'	Speed in a restricted channel	LT^{-1}
v''	"Schlichting's intermediate speed"	LT^{-1}
R	Acceleration due to gravity	LT^{-2}
ρ	Mass density	ML^{-3}
ν	Kinematic viscosity	$L^2 T^{-1}$
R_t	Total resistance	MLT^{-2}
R_f	Frictional resistance	MLT^{-2}
R_r	Residual resistance	MLT^{-2}
ΔR	Resistance due to roughness	MLT^{-2}
r	Hydraulic radius	L
d	Characteristic depth of channel	L
EHP	Effective horsepower	

Symbol

B/H	Beam-draft ratio
L/B	Length-beam ratio
C_p	Longitudinal prismatic coefficient
C_w	Volumetric coefficient
C_S	Wetted-surface coefficient
C_x	Midship-section coefficient
C_t	Total-resistance coefficient
C_f	Frictional-resistance coefficient
C_r	Residual-resistance coefficient
ΔC_f	Roughness-allowance coefficient
R_e	Reynolds number
$Froude$	Froude number
$\text{Total-resistance coefficient}$	Total-resistance coefficient
$\text{Wetted-surface coefficient}$	Wetted-surface coefficient
Speed coefficient	Speed coefficient
$\text{Displacement-flow coefficient}$	Displacement-flow coefficient

$\left. \begin{array}{l} \text{Total-resistance coefficient} \\ \text{Wetted-surface coefficient} \end{array} \right\} \text{ "circle coefficient"}$
 $\left. \begin{array}{l} \text{Speed coefficient} \\ \text{Displacement-flow coefficient} \end{array} \right\} \text{ system}$

FORMULAS

Volumetric Coefficient:

$$C_v = \frac{v}{L^3}$$

Longitudinal Prismatic Coefficient:

$$C_P = \frac{v}{A_x L}$$

Beam-Draft Ratio:

$$\frac{B}{H}$$

Wetted-Surface Coefficient:

$$C_S = \frac{S}{\sqrt[3]{vL}}$$

Total-Resistance Coefficient:

$$C_t = \frac{R_t}{\frac{\rho}{2} S v^2}$$

Frictional-Resistance Coefficient:

$$C_f = \frac{R_f}{\frac{\rho}{2} S v^2}$$

Residual-Resistance Coefficient:

$$C_r = \frac{R_r}{\frac{\rho}{2} S v^2}$$

Effective Horsepower:

$$EHP = \frac{C_t \times \frac{\rho}{2} S v^3}{550 \text{ ft-lb/sec}} = A v^3 K C_t$$

where

$$A = 0.004380 \rho S$$

Roughness-Allowance Coefficient:

$$\Delta C_f = \frac{\Delta R}{\frac{\rho}{2} S v^2}$$

Reynolds Number:

$$R_e = \frac{vL}{\nu}$$

Froude Number:

$$F = \frac{v}{\sqrt{gL}}$$

Speed-Length Ratio:

$$\frac{V_k}{V/L}$$

“CIRCLE COEFFICIENT” SYSTEM:

Total-Resistance Coefficient:

$$\textcircled{C} = \frac{1000}{8\pi} \textcircled{S} C_t$$

Wetted-Surface Coefficient:

$$\textcircled{S} = \frac{S}{v^{2/3}}$$

Speed Coefficient:

$$\textcircled{K} = \frac{v}{v^{1/6}} \sqrt{\frac{4\pi}{g}}$$

LIST OF ILLUSTRATIONS

Figure 1	Lines and Offsets for the Parent Form of the Taylor Standard Series.	PAGE 3
Figure 2	Sketch Showing Relocation of Sections of a Parent Form to Produce a Derived Form Having a Different Longitudinal Prismatic Coefficient	4
Figure 3	Sectional-Area Curves for the Derived Forms of the Taylor Standard Series.	6
Figure 4	Curves of Geometrical Parameters Used to Define Mathematically the Sectional-Area Curves for the Taylor Standard Series.	8
Figure 5	Comparison of the Taylor Displacement-Length Ratio and Wetted-Surface Coefficients with the Redefined Coefficients.	9
Figure 6	Contours of Volumetric Coefficient Versus Longitudinal Prismatic Coefficient and Length-Beam Ratio for a Beam-Draft Ratio of 2.25	10
Figure 7	Contours of Volumetric Coefficient Versus Longitudinal Prismatic Coefficient and Length-Beam Ratio for a Beam-Draft Ratio of 3.00	11
Figure 8	Contours of Volumetric Coefficient Versus Longitudinal Prismatic Coefficient and Length-Beam Ratio for a Beam-Draft Ratio of 3.75	12
Figure 9	Effects of Longitudinal Prismatic Coefficient Variation on the Shapes of Derived Forms	14

	PAGE
Figure 10 Effects of Volumetric Coefficient Variation on the Shapes of Derived Forms	15
Figure 11 Effects of Beam-Draft Ratio Variation on the Shapes of Derived Forms	16
Figure 12 Water Temperature in the U.S. Experimental Model Basin Versus Calendar Date for the Years of 1913 to 1918	22
Figure 13 Curves of Residual-Resistance Coefficient Versus Speed-Length Ratio, Showing Typical Data Spots	23
Figure 14 Auxiliary Charts for Restricted Channel Corrections to the Taylor Series Models Tested in the U.S. Experimental Model Basin	26
Figure 15 Sample Curve of Residual-Resistance Coefficient Versus Speed-Length Ratio, Showing Restricted Channel Corrections	28
Figure 16 Curves of Residual-Resistance Coefficient Versus Longitudinal Prismatic Coefficient for Equal Values of Volumetric Coefficient	29
Figure 17 Curves of Residual-Resistance Coefficient Versus Volumetric Coefficient for Equal Values of Longitudinal Prismatic Coefficient	30
Figure 18 Comparison of the Residual-Resistance Coefficient Obtained from Tests of New Taylor Series Models with Values Read from Contours of Appendices 3 and 4	31
Figure 19 Factors for Converting the Total-Resistance Coefficient C_t to the C Resistance Coefficient	34
Figure 20 Factors for Converting the Froude Number F to the K Speed Coefficient	35

	PAGE
Figure 21 Schoenherr Frictional-Resistance Coefficients for a 400-Foot Vessel Operating in Salt Water of 3.5 Percent Salinity and a Temperature of 59F.	36
Figure 22 The Variation in Effective Horsepower of Taylor Series Vessels with Change in Longitudinal Prismatic Coefficient for a Volumetric Coefficient of 1.5×10^{-3}	37
Figure 23 The Minimum Effective Horsepowers of Taylor Series Vessels of Various Lengths with a Volumetric Coefficient Equal to 1.5×10^{-3}	38
Figure 24 Comparison of the Effective Horsepower of a 650-Foot Passenger Vessel with an Equivalent Standard Series Vessel	40
Figure 25 Effect of Sectional-Area Shape on the Selection of Geometrical Parameters for Taylor Series Comparisons . .	43
Figure 26 Residual-Resistance Coefficient Corrections	44

LIST OF TABLES

	PAGE
Table 1 - Ordinates of the Sectional-Area Curves for the Taylor Standard Series Expressed as Ratios to the Maximum Area.	5
Table 2 - Functions for Calculation of Mathematically Defined Sectional-Area Curves and Waterlines.	7
Table 3 - Dimensions and Coefficients for Taylor Series Models with a Nominal Beam-Draft Ratio of 2.25 (Series 22)	18
Table 4 - Dimensions and Coefficients for Taylor Series Models with a Nominal Beam-Draft Ratio of 2.92 (Series 20)	19
Table 5 - Dimensions and Coefficients for Taylor Series Models with a Nominal Beam-Draft Ratio of 3.75 (Series 21)	20
Table 6 - Sample Form for the Calculation of Effective Horsepower from the Taylor Standard Series	39
Table 7 - Particulars for a 650-Foot Passenger Vessel	40

PREFACE

The reanalysis of the original test data for the Taylor Standard Series was accomplished at the David Taylor Model Basin during the period of 1948 to 1951. The work was originally prompted by the decision of the American Towing Tank Conference of 1947 to adopt the Schoenherr frictional-resistance formulation for use in predicting the effective horsepower of ships from model resistance test data. This decision, it was realized, would result in effective horsepower values that were not directly comparable with those calculated from the original Taylor Standard Series contours using the procedures which are given in Taylor's "Speed and Power of Ships."

The differences in the calculated effective horsepower result from two causes: the differences between the frictional resistances obtained from the Schoenherr formula and those from the old Experimental Model Basin 20-foot plank data in the model range and the differences between the corresponding frictional resistances obtained from the Schoenherr formula and from the Tideman constants in the ship range. The former is reflected as a difference in residual resistance and thus would require that a lengthy correction be made to the Taylor residual-resistance per ton contours to make them comparable to modern data. The latter merely requires a substitution of the Schoenherr formula with the appropriate roughness allowance for the Tideman constants in the ship calculation procedure.

When the original Taylor Series contours were prepared, no effort was made to compensate for changes in resistance caused by the normal change in towing basin water temperature over the year, to insure that flow about the models was fully turbulent, or to correct for possible restricted channel effects. In view of these considerations, it was believed that a revision of the results was warranted and could be accomplished only by reanalyzing the original test data and not by directly converting the existing faired residual resistance per ton contours.

In the reanalysis, the methods and procedures used were essentially the same as those currently used at the Taylor Model Basin. A total-resistance coefficient for the model was computed, from which a Schoenherr frictional-resistance coefficient was deducted to give a residual-resistance coefficient which in turn formed the basis for expansion from model to full scale.

The aforementioned corrections were made to the Taylor Series data as follows:

The Schoenherr frictional-resistance coefficient is a function of Reynolds number, so that compensation for differences in basin water temperature can be made by using the appropriate kinematic viscosity in the computation of Reynolds number. For the majority of the Taylor model tests, the basin water temperature was not recorded. A chart was therefore used of the day-by-day averages of the water temperature at the U. S. Experimental Model Basin during the years 1913 to 1918. In view of the variations shown by these records, the selected temperatures are, in most cases, believed to be accurate to within $\pm 1^\circ\text{F}$ of the temperatures actually prevailing at the times of model tests. A range of temperature from 53 to 80°F was experienced during a given year of testing, representing a change in frictional resistance of about 7 percent for a 20-foot model.

The method for correcting for the effects of transitional flow is based on the assumption that at low Froude numbers the residual-resistance coefficient, as defined, is a constant. The original data showed that in general the residual-resistance coefficient decreased with decreasing speed so long as wavemaking resistance was important. There was then a short range of speed for which the residual-resistance coefficient remained constant, after which, as the speed was still further reduced, the coefficient began to decrease again. This latter decrease has been attributed to transitional flow and has been ignored, the constant value of the coefficient being

used for all lower Froude numbers. Although this procedure is not rigorous, a number of recent tests of 20-foot models which were towed with and without a turbulence-stimulating device indicate that in general such conditions obtain for models which experience only minor transitional effects at the lowest speeds. Good agreement between the residual-resistance coefficient curves from the experiments without turbulence stimulation, faired in the way described above, and those resulting from the tests with the turbulence device was attained in most of these cases. This seems to be especially true with forms having the Taylor Series type of bow. Two new 20-foot Taylor Series models, having longitudinal prismatic coefficients of 0.613 and 0.746, were tested at the Taylor Model Basin in 1951. In both cases it was found that turbulent stimulation was required only at low speeds and that the aforementioned procedure gave reasonable agreement with the turbulent curve. The results of these tests are given in the 1951 Transactions for the Society of Naval Architects and Marine Engineers in a paper entitled, "A Proposed New Basis for the Design of Single Screw Merchant Ship Forms and Standard Series Lines," by Dr. F. H. Todd and Captain F. X. Forest.

Corrections for restricted channel effects were made by using the formulas given in TMB Report 460 entitled,

"Tests of a Model in Restricted Channels," by L. Landweber, May 1939, with the appropriate model dimensions and the dimensions of the cross section of the U. S. Experimental Model Basin. This correction was small in most cases, and even for the fullest model of the series, it amounted to a decrease in resistance of only 2 percent.

The results of the reanalysis of the Taylor Standard Series data are given in a form which employs a completely nondimensional representation. The faired resistance data are given as curves of residual-resistance coefficient versus Froude number. The major geometrical parameters used are beam-draft ratio, longitudinal prismatic coefficient, volumetric coefficient, and wetted-surface coefficient, the latter two being redefinitions of Taylor's displacement-length ratio and wetted-surface coefficient.

The scope of the series has been enlarged to include a third beam-draft ratio of 3.00 in addition to the beam-draft ratios of 2.25 and 3.75 published in Taylor's "Speed and Power of Ships." These values were obtained by interpolation, using the reworked data for the hitherto unpublished Series 20 which had a beam-draft ratio of 2.92.

HISTORY OF THE TAYLOR STANDARD SERIES

The Taylor Standard Series was the first of the methodical series of ship forms to receive wide attention and usage throughout the United States. The series, as it is known today, was the result of an evolution of several parent forms before the final parent, which was used to develop the series, was chosen.* The original parent was patterned after the British armored cruiser LEVIATHAN of the Drake class (1900), a model of which was tested in the U. S. Experimental Model Basin at Washington in 1902. The salient features of the LEVIATHAN consisted of a bulbous ram bow extended on a raised forefoot and a twin-screw cruiser type of stern. These features were retained in the first parent which was designed in 1906 using the sectional-area curve, load waterline, and bow and stern profiles of the LEVIATHAN together with mathematically derived body lines. The parent form so obtained was used to construct EMB Model 632, and, together with mathematically derived sectional-area curves, was used to develop the lines for the construction of 38 additional models. These models, designated Series 18, were tested to investigate the effect of changes in longitudinal prismatic coefficient and displacement-length ratio on the resistance of ship forms. The resulting data were prepared in reproducible form as contours of residual resistance per ton, for constant values of speed-length ratio, on grids of displacement-length ratio and longitudinal prismatic coefficient, but were not published.

The first parent was altered during 1906 by eliminating the bulbous ram bow. The resulting parent was used with the sectional-area curves of Series 18 to develop and construct 25 additional models. These models were tested to determine the effect on resistance of the variation of the same form parameters as those of Series 18. The results were similarly prepared for reproduction but were not published.

The final alteration to the parent consisted of dropping the forefoot to the baseline, adopting a 3 percent bulb, and moving the maximum section to midlength. The resulting parent became the basis of Series 20, 21, and 22. These series were developed using the sectional-area curves of Series 18 which were extended by the addition of mathematically derived sectional-area curves for longitudinal prismatic coefficients from 0.68 to 0.80 and by extrapolation to 0.86.

*References are listed on page 45.

Series 20 consisted of 38 models each having a constant beam-draft ratio of 2.92 but with systematically varied values of longitudinal prismatic coefficient and displacement-length ratio. Series 20 was tested during 1906 and 1907, and the results of these tests appeared only briefly in publication as Figure 70 in Taylor's "Speed and Power of Ships" to illustrate the variation of residual resistance with midship section area.

Series 21 and 22, having beam-draft ratios of 3.75 and 2.25, respectively, were then formulated. These two series consisted of a total of 80 models, which were tested in 1907 and 1908. The results of these model tests were published in the first edition of Taylor's "Speed and Power of Ships" in 1910. The scope of Series 21 and 22 was extended during 1913 and 1914 by tests of 40 additional models. The augmented results of both series were published first in the 1933 edition and then in the 1943 revised edition of Taylor's "Speed and Power of Ships." The data appeared as contours of residual resistance per ton plotted against longitudinal prismatic coefficient and displacement-length ratio, a presentation which is now familiar to the profession as the Taylor Standard Series contours.

The contours of residual resistance per ton which are found in the 1943 edition are based upon concepts which existed in 1910. No effort had been made, up to now, to alter the contours in accordance with the changes in analytical methods throughout the years. Thus, as in 1910, the data for the Experimental Model Basin 20-foot friction plane were used to reduce the model data to residual resistance, and the Tideman frictional-resistance constants were used in the prediction of the effective horsepower of the full-scale vessels.

In 1923, the U. S. Experimental Model Basin began to use the Gebers frictional-resistance formulation to compute the frictional resistance in both the model and full-scale ranges, and this practice was continued at the Taylor Model Basin through 1947. During this period the Taylor Series Contours continued to be widely used. The validity of the Taylor Series comparisons was not altered, however, because it was the practice to use an empirical factor, denoted G, with the Gebers formula to arrive at effective horsepower values equal to those predicted by the EMB-Tideman method. Since 1947, in accordance with a decision

made by the American Towing Tank Conference, the Schoenherr frictional-resistance formulation has been in general use by all American towing tanks to predict the effective horsepower of ships from model test data.²

The present use of the Schoenherr formula does not involve arbitrary factors solely for the purpose of seeking agreement with predictions obtained with past methods. However, since the basic Schoenherr coefficients apply to a hydraulically smooth surface, a roughness-allowance coefficient is normally added to allow for the deviation of the actual ship's hull surface from hydraulic smoothness. The roughness-allowance coefficient is generally based upon information obtained from correlation of ship trial data with model test data and may vary with ship type, with bottom paints, and with construction details. The value of 0.0004 adopted for this roughness-allowance coefficient by the American Towing Tank Conference in 1947² appears to be a suitable figure for average merchant ships, as borne out by recent merchant ship trials. The value of 0.0004 added to the Schoenherr coefficients coincidentally gives good agreement with the Froude coefficients for the range of ship lengths and speeds of average medium speed cargo vessels.

As the result of the introduction of the roughness allowance concept, the effective horsepower calculated with the Schoenherr formula should differ from the values calculated by the EMB-Tideman method to an extent which would depend upon the assigned value of roughness-allowance coefficient. If the Schoenherr formula plus the appropriate roughness-allowance coefficient were substituted for the Tideman values in the calculation procedure, the original Taylor Series contours could still be used for comparative purposes if there were no inherent errors in the contours themselves. This is on the assumption that the frictional-resistance coefficients versus Reynolds numbers obtained from the EMB plank results and from the Schoenherr formula are equal so that the residual resistances obtained with either would also be equal. The agreement is actually within 2 percent when they are compared upon the basis of a water temperature of 70F. The EMB plank was towed at a temperature of 70F and the values so obtained were used, without adjustment, for the calculation of the residual resistances of all of the series models regardless of the temperature of the water in which they were tested. This procedure introduced errors in the

Taylor contours which have not been corrected since their original presentation.

The present reanalysis of the original data for the Taylor Standard Series was started in 1948 for the purpose of correcting these errors. Prior to that time, consideration was given to the advisability of salvaging the original faired contours either by using them directly with the Schoenherr formula in the ship range or by the more complicated device of correcting the contours to account for the differences in residual resistances that would result if the Schoenherr formula were used instead of the EMB plank values. This approach was rejected because of the inherent errors in the contours which, as mentioned previously, were due to failure to correct for temperature, the probability that laminar flow existed in some cases since no effort was made to stimulate turbulence, and the restricted channel effects as will be subsequently discussed. Since the original data were being reworked, the data for the hitherto unpublished Series 20 were included in the reanalysis. This was done to provide an intermediate value of beam-draft ratio when it appeared that Taylor's assumption (that residual resistance varies linearly with beam-draft ratio) introduced further error in the interpolation between the values of beam-draft ratio of 2.25 and 3.75.

GEOMETRY OF THE TAYLOR STANDARD SERIES

The geometry of any methodical series should be completely and accurately defined. This prerequisite is necessary when the resistance data are expressed as functions of prescribed geometrical parameters since the resulting relationships apply, in the strictest sense, only to the particular parent form which has been varied according to the specified procedure. It is assumed, however, that within reasonable limits, similar trends can be expected for off-spring of other parent forms which have been derived by the same process. This assumption determines the validity of the accepted use of the Taylor Standard Series as a criterion for the performance of specific ship designs. Experience has shown that such a procedure is valid if the departures from the parent form being investigated are not too great.

The process of developing a series covering a wide range of geometrical parameters from a single parent form will

Stations	0.1	0.2	0.3	0.4	0.5	0.6	0.7	0.8	0.9	LWL	1.0	1.2	1.4	1.6	1.8
F.P. (Ext.)	0.036	0.048	0.062	0.077	0.092	0.107	0.122	0.137	0.152	0.167	0.182	0.197	0.212	0.227	0.242
1	0.044	0.057	0.071	0.085	0.100	0.114	0.129	0.143	0.158	0.172	0.187	0.201	0.216	0.230	0.245
2	0.054	0.074	0.097	0.120	0.143	0.166	0.189	0.212	0.235	0.258	0.281	0.304	0.327	0.350	0.373
3	0.069	0.101	0.122	0.145	0.168	0.191	0.214	0.237	0.260	0.283	0.306	0.329	0.352	0.375	0.398
4	0.089	0.132	0.161	0.184	0.207	0.230	0.253	0.276	0.299	0.322	0.345	0.368	0.391	0.414	0.437
5	0.114	0.168	0.207	0.246	0.285	0.324	0.363	0.402	0.441	0.480	0.519	0.558	0.597	0.636	0.675
6	0.142	0.209	0.259	0.318	0.377	0.436	0.495	0.554	0.613	0.672	0.731	0.790	0.849	0.908	0.967
8	0.205	0.302	0.379	0.456	0.533	0.610	0.687	0.764	0.841	0.918	0.995	1.072	1.149	1.226	1.303
10	0.289	0.422	0.522	0.622	0.722	0.822	0.922	1.022	1.122	1.222	1.322	1.422	1.522	1.622	1.722
12	0.399	0.561	0.693	0.825	0.957	1.089	1.221	1.353	1.485	1.617	1.749	1.881	2.013	2.145	2.277
14	0.549	0.795	0.994	1.193	1.392	1.591	1.790	1.989	2.188	2.387	2.586	2.785	2.984	3.183	3.382
16	0.691	1.021	1.282	1.543	1.804	2.065	2.326	2.587	2.848	3.109	3.370	3.631	3.892	4.153	4.414
18	0.777	1.183	1.483	1.783	2.083	2.383	2.683	2.983	3.283	3.583	3.883	4.183	4.483	4.783	5.083
20	0.779	1.183	1.483	1.783	2.083	2.383	2.683	2.983	3.283	3.583	3.883	4.183	4.483	4.783	5.083
22	0.705	1.039	1.299	1.559	1.819	2.079	2.339	2.599	2.859	3.119	3.379	3.639	3.899	4.159	4.419
24	0.568	0.841	1.063	1.285	1.507	1.729	1.951	2.173	2.395	2.617	2.839	3.061	3.283	3.505	3.727
26	0.421	0.602	0.742	0.882	1.022	1.162	1.302	1.442	1.582	1.722	1.862	2.002	2.142	2.282	2.422
28	0.274	0.446	0.568	0.690	0.812	0.934	1.056	1.178	1.300	1.422	1.544	1.666	1.788	1.910	2.032
30	0.133	0.265	0.338	0.411	0.484	0.557	0.630	0.703	0.776	0.849	0.922	0.995	1.068	1.141	1.214
32	0.079	0.153	0.237	0.321	0.405	0.489	0.573	0.657	0.741	0.825	0.909	0.993	1.077	1.161	1.245
34	0.037	0.077	0.116	0.155	0.194	0.233	0.272	0.311	0.350	0.389	0.428	0.467	0.506	0.545	0.584
36	0.038	0.068	0.104	0.139	0.175	0.211	0.247	0.283	0.319	0.355	0.391	0.427	0.463	0.499	0.535
38	0.036	0.063	0.093	0.123	0.153	0.183	0.213	0.243	0.273	0.303	0.333	0.363	0.393	0.423	0.453
40	0.034	0.053	0.073	0.093	0.113	0.133	0.153	0.173	0.193	0.213	0.233	0.253	0.273	0.293	0.313
F.P.	0.036	0.048	0.062	0.077	0.092	0.107	0.122	0.137	0.152	0.167	0.182	0.197	0.212	0.227	0.242

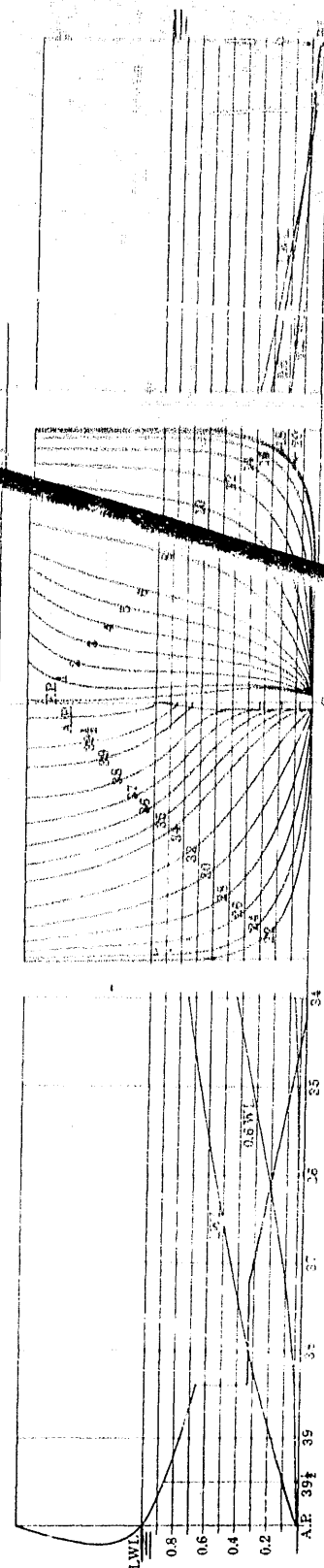


FIGURE 1.—Lines and offsets for the parent form of the Taylor Standard Series.

This is the final parent form which was used to derive the forms of U.S. Experimental Model Basin Series 20, 21, and 22. It incorporates the following changes to the original parent represented by EMB Model 20: (1) the bulb section was eliminated, the forefoot was dropped to the baseline, a 3 percent at bulb was adopted, and the forefoot section was moved to midlength.

often result in some forms which are not useful for practical ship designs. Nevertheless, it is desirable to know what these forms are so that final evaluations can be made. Unfortunately, the offsets of the offspring forms of the Taylor Series have not been published, and even the procedure for deriving these forms has not been given in much detail.^{1,3} Consequently an attempt is made here to explain the derivation procedures as well as to provide data whereby the individual resulting form of the series can be easily reproduced.

CHARACTERISTICS OF THE PARENT

The historical statement mentions that the final parent form for the Taylor Series was the result of several successive modifications of the basic form of the British cruiser LEVIATHAN. The form designated as the parent in Reference 1 incorporates all of these modifications except for the shift of the maximum section from Station 0.2 to midships. It is not possible, therefore, to develop the offspring forms of the Taylor series directly from the offsets and characteristics given therein. To fully establish the parent which was actually used to develop the series, the offsets were remeasured from the original lines drawings of the final parent. The lines and nondimensional offsets and characteristics derived from these measurements are shown by Figure 1.

The characteristics of the final parent form are similar in many respects to those of some of the more modern higher speed ship types. The midship section is roughly rectangular except for a small deadrise and a relatively large bilge radius. The forward sections, with the exception of the three percent bulb, are generally U-shaped whereas the extreme after sections are inclined to be somewhat V-shaped. The keel is flat for the major part of the length but rises at the extreme stern to form a centerline skeg which is designed to receive a single hinged type of rudder. It may be noted that the bow prismatic coefficient is 0.574 whereas the stern prismatic coefficient is 0.532. Thus the longitudinal center of buoyancy is forward of midships. This characteristic was modified in the development of the series proper by the selection of sectional-area curves for the offspring which had equal forebody and afterbody prismatic coefficients.

DERIVATION OF SERIES FORMS FROM PARENT

Most methodical series make use of the procedure of effecting variations in form parameters one at a time while other significant parameters are kept constant. This objective is usually achieved by resorting to some system for relating the geometrical parameters which are being investigated. Various methods, both graphical and mathematical, have been either used or considered for this purpose.^{1,4,5} It is important to know which system was used to derive a given series in addition to the geometrical parameters for a full understanding of the nature of the offspring which result from a given parent.

The method used to derive the Taylor Standard Series is essentially a graphical process. The parameters which are varied are the longitudinal prismatic coefficient C_p , the beam-draft ratio B/H , and the displacement-length ratio. The midship section coefficient C_x was held constant and the longitudinal center of buoyancy was fixed at midships. The change in C_p is the only one of the three parameters which involve changes in the nondimensionally defined body sections whose offsets are the half breadths expressed as ratios to the half maximum beam and heights expressed as ratios to the load waterline draft.

The procedure for accomplishing changes in C_p is illustrated by the sketch of Figure 2. Curve A is the sectional-area curve of the parent form and curve B is the sectional-area curve of the desired offspring. Point e is the point of intersection of any integrally numbered station ab with curve B. Point f is the horizontal projection of point e on curve A. Station cd, which is drawn through f, is the station of the parent form which has the same body section as that

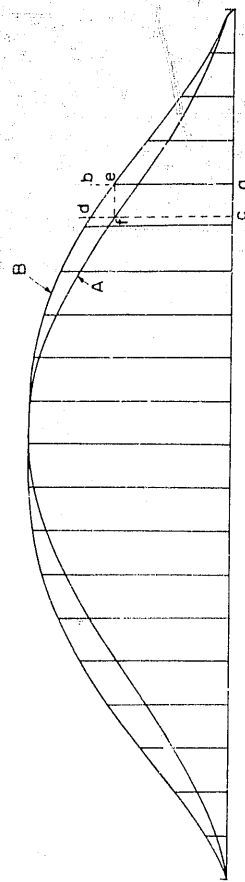


FIGURE 2.--Sketch showing relocation of sections of a parent form to produce a derived form having a different longitudinal prismatic coefficient

of the derived form at station ab. Thus, having the sectional-area and the various waterline curves of the parent form together with the sectional-area curve for the proposed offsprings, the offsets for the latter can be completely determined.

Although this graphical process is relatively simple, its execution for a large number of forms becomes quite laborious. Unfortunately, a search of the original files failed to produce the offsets for the individual forms comprising the Taylor Series. Consequently, it was considered advisable to redevelop the series in the prescribed manner to reproduce these offsets in a form enabling their direct use. The resulting information is given in Appendix 1 as contours of the nondimensional half breadths plotted against longitudinal prismatic coefficient for each of a number of selected stations between and including the forward and after perpendiculars. Separate sets of contours are given for each waterline height in suitable increments to define completely the forms covered by the series. The contours for each waterline height are given separately for the bow and stern so that they can be used in combination to produce changes in position of longitudinal center of buoyancy through the use of unequal bow and stern prismatic coefficients.

It is apparent that the success of a methodical series which is developed according to the aforementioned process depends largely upon the system used to vary the sectional-area curves. Obviously, if no attempt is made to systematize, large distortions in form would result and any resemblance that the offspring might bear to the parent would be destroyed. As stated previously, the sectional-area curves for the Taylor Series were mathematically defined. Consequently, they were varied systematically through a proper choice of the parameters for the governing equations. The values of these parameters were never published and a search of the original files produced values for only a limited number of curves. The original delineations and nondimensional ordinates and abscissas for all of the curves were available, and these are given in Figure 3 and Table 1, respectively. It is believed, however, that the mathematical approach is inherently more precise and, in addition, provides an excellent tool which can be used to produce the area curves for intermediate values of longitudinal prismatic coefficient. Therefore, Taylor's mathe-

Station Number	Longitudinal Prismatic Coefficients								
	0.48	0.52	0.56	0.60	0.64	0.68	0.74	0.80	0.86
F.P.	0.000	0.0000	0.000	0.000	0.000	0.000	0.000	0.000	0.000
0.2	.022	.025	.026	.029	.030	.035	.45	.055	.074
0.4	.032	.035	.038	.042	.045	.050	.064	.083	.112
0.5	.038	.042	.045	.048	.055	.064	.080	.108	.153
1	.046	.050	.058	.065	.074	.087	.110	.159	.229
2	.066	.078	.092	.107	.128	.152	.206	.298	.423
4	.126	.152	.184	.221	.264	.316	.423	.564	.751
6	.211	.257	.307	.364	.426	.499	.625	.766	.913
8	.323	.382	.446	.514	.587	.668	.784	.892	.977
10	.450	.517	.587	.658	.731	.803	.893	.959	.995
12	.586	.655	.722	.786	.846	.901	.957	.988	0.999
14	.724	.784	.838	.886	.928	.961	.987	0.998	1.000
16	.853	.893	.929	.955	.976	.990	0.998	1.000	1.000
18	0.955	0.971	0.983	0.992	0.997	0.999	1.000	1.000	1.000
20	1.000	1.000	1.000	1.000	1.000	1.000	1.000	1.000	1.000
22	0.964	0.974	0.984	0.991	0.996	0.999	1.000	1.000	1.000
24	.870	.903	.932	.957	.976	.988	0.998	1.000	1.000
26	.745	.797	.846	.891	.928	.958	.987	0.998	1.000
28	.604	.669	.731	.793	.848	.898	.957	.992	1.000
30	.460	.528	.596	.667	.737	.804	.895	.963	0.999
32	.322	.385	.450	.522	.595	.671	.789	.898	.987
34	.200	.251	.304	.368	.433	.506	.631	.773	.920
36	.103	.136	.173	.217	.265	.322	.428	.567	.745
37	.065	.090	.115	.149	.185	.231	.315	.436	.599
38	.034	.050	.066	.087	.112	.142	.201	.290	.414
39	.012	.018	.027	.037	.048	.060	.092	.140	.208
A.P.	0.000	0.000	0.000	0.000	0.000	0.000	0.000	0.000	0.000

TABLE 1.--Ordinates of the sectional-area curves for the Taylor Series expressed as ratios to the maximum Area
These values have been reread from the original sectional-area curves.

tical approach is redeveloped herein, and the resulting equations have been applied to obtain suitable fits to the sectional-area curves defined by Figure 3 and Table 1. The notation originally used by Taylor in his equations has been changed to avoid conflict with present day nomenclature and an additional term has been provided to take care of special cases.

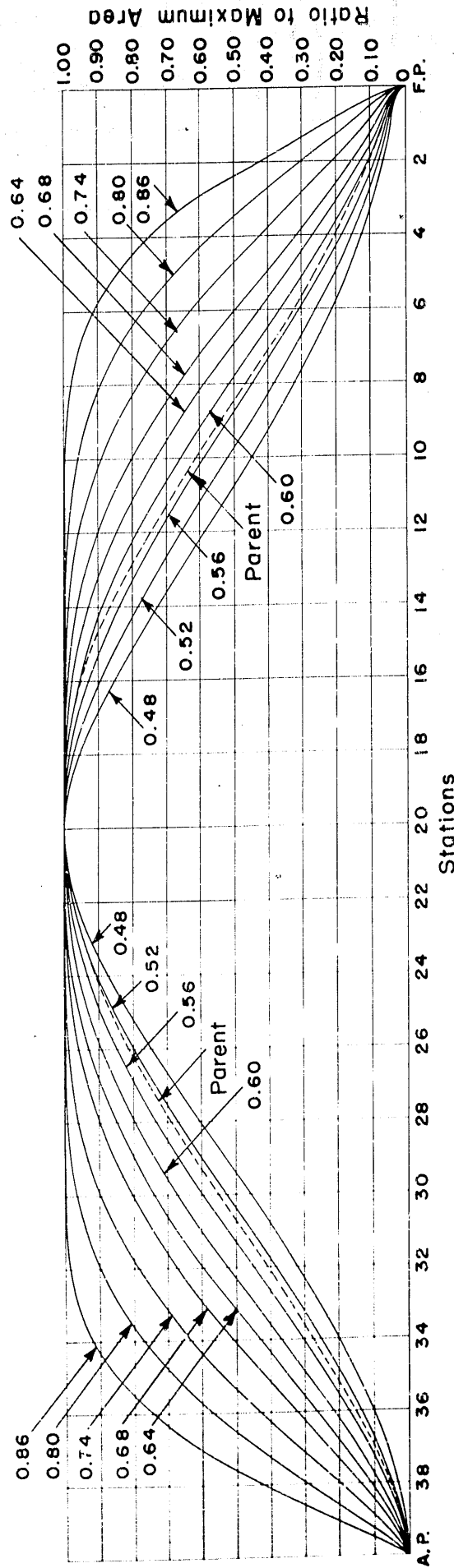


FIGURE 3.--Sectional-area curves for the derived forms of the Taylor Standard Series

Taylor's mathematical approach defines either the bow half or the stern half of the sectional-area curve by the equation of a fifth degree parabola

$$y = a_1x^5 + a_2x^4 + a_3x^3 + a_4x^2 + a_5x^5 \quad [1]$$

The values of the coefficients a_1 a_2 , ---- are determined in terms of prescribed geometrical parameters by imposing the end conditions and solving either by simultaneous equations or the determinant rule. The same results can be achieved more directly by the method of Reference 5. Thus Equation [1] can be restated in terms of four basic polynomials of the fifth degree in x which involve the selected geometrical parameters as follows:

$$y = C(x) + C_p P(x) + tI(x) + nN(x) \quad [2]$$

where

$$C(x) = -30x^2 + 100x^3 - 105x^4 + 36x^5 \quad [2a]$$

$$P(x) = 60x^2 - 180x^3 + 180x^4 - 60x^5 \quad [2b]$$

$$I(x) = x - 6x^2 + 12x^3 - 10x^4 + 3x^5 \quad [2c]$$

$$N(x) = -\frac{1}{2}x^2 + 2x^3 - \frac{5}{2}x^4 + x^5 \quad [2d]$$

and

y is the nondimensional ordinate $\frac{A}{A_x}$, and is unity for the section of maximum immersed area,

x is the nondimensional abscissa $\frac{x}{L}$ and is unity at the maximum section when x is measured from the extremity of either the bow or stern,

C_p is the longitudinal prismatic coefficient for either the bow or stern,

t is the tangent to the sectional-area curve at either the forward or after extremity, and

n is the second derivative of the sectional-area curve at $x = 1$ and $y = 1$.

In Equation [2], $C(x)$, $P(x)$, $I(x)$, and $N(x)$ are independent of the parameters C_p , t , and n . Thus, general working tables can be prepared for a number of values of x for the bow or stern halves of the sectional-area curves. Since y

x	$Q(x)$	$P(x)$	$T(x)$	$N(x)$	$F(x)$
0	0	0	0	0	+1.000000
0.02	-0.011217	+0.022589	+0.017694	-0.000816	0.994281
0.04	.041865	.0 8 935	.031143	.000678	.956930
0.06	.087733	.179406	.040865	.001400	.908327
0.08	.144983	.299016	.047344	.002275	.845967
0.10	.210140	.437400	.051030	.003240	.772740
0.12	.280077	.588815	.052337	.004238	.691285
0.14	.352001	.748002	.051648	.005326	.603999
0.16	.423438	.910393	.049313	.006142	.513045
0.18	.492222	1.071859	.045653	.006971	.420363
0.20	.556480	1.228800	.040960	.007680	.327680
0.22	.614616	1.378099	.035496	.008245	.236517
0.24	.665299	1.517101	.029499	.008650	.148198
0.26	.707452	1.643589	.023179	.008884	+0.063863
0.28	.740231	1.755759	.016722	.008941	-1.015527
0.30	.763020	1.852200	.010290	.008820	.089180
0.32	.775409	1.931870	+0.004025	.008523	.156461
0.34	.777185	1.994072	-0.001955	.008057	.216887
0.36	.768319	2.038432	.007550	.007432	.270113
0.38	.748946	2.064874	.012679	.006661	.315896
0.40	.719360	2.073600	.017280	.005760	.354240
0.42	.679992	2.065065	.021306	.004747	.385073
0.44	.631403	2.039955	.024727	.003643	.410363
0.46	.574262	1.999163	.027525	.002468	.424901
0.48	.509343	1.943750	.029696	-0.001246	.434422
0.50	.437500	1.875000	.031250	0	.437500

x	$Q(x)$	$P(x)$	$T(x)$	$N(x)$	$F(x)$
.52	.359662	1.794245	.032204	+0.001246	.434582
.54	.276815	1.702991	.032588	.002468	.426176
.56	.189986	1.602816	.032438	.003643	.412836
.58	.100236	1.495392	.031799	.004747	.393656
.60	-0.008640	1.382400	.030720	.005760	.373760
.62	+0.083725	1.265568	.029258	.006661	.349293
.64	.175799	1.146617	.027471	.007432	.322412
.66	.266524	1.027249	.025422	.008057	.293774
.68	.354916	0.909115	.023174	.008523	.264031
.70	.440020	.793800	.020790	.008820	.233820
.72	.517955	.682795	.018334	.008941	.203750
.74	.596919	.577477	.015868	.008884	.174396
.76	.667207	.479085	.013448	.008650	.146291
.78	.731219	.388694	.011129	.008245	.119914
.80	.788480	.307200	.008960	.007680	.095680
.82	.838650	.235286	.006982	.006971	.073936
.84	.881537	.173408	.005230	.006142	.054945
.86	.917116	.121768	.003729	.005219	.038884
.88	.945537	.080290	.002494	.004238	.025732
.90	.967140	.048600	.001530	.003240	.015740
.92	.982475	.026001	.000829	.002275	.008475
.94	.992304	.011452	.000369	.001400	.003755
.96	.997628	.003539	.000116	.000678	.001167
.98	+0.999692	+0.000461	-0.000015	+0.000192	-0.000153
1.00	+1.000000	0	0	0	0

TABLE 2.—Functions for calculation of mathematically defined sectional-area curves and waterlines
The nondimensional abscissas x are given as ratios to the half length.

is a linear function of C_p , t , and n , the offsets of a particular sectional-area curve can be directly determined for any value of x by adding algebraically the products shown in Equation [2].

It may be noted that Equation [2] is not satisfied when γ at $x=0$, as is the case where a projected bulb or transom stern is shown by the sectional-area curve. When these conditions exist, it is necessary to redefine C_p and γ to use Equation [2], as follows:

$$\gamma' = \frac{\lambda - f}{A_m - f} \quad [3]$$

where

$$F(x) = 1 - 30x^2 + 80x^3 - 75x^4 + 25x^5 \quad [2e]$$

$$C_p' = \frac{C_p - f}{1 - f} \quad [4]$$

and

where f is the ratio of the bulb or transom area to the maximum area.

This redefinition is objectionable because it introduces numerical values for the C_p and the area ordinates which are not those desired in the end result and which may lead to confusion. This obstacle can be suitably overcome by the introduction of the term $fF(x)$ to Equation [2],

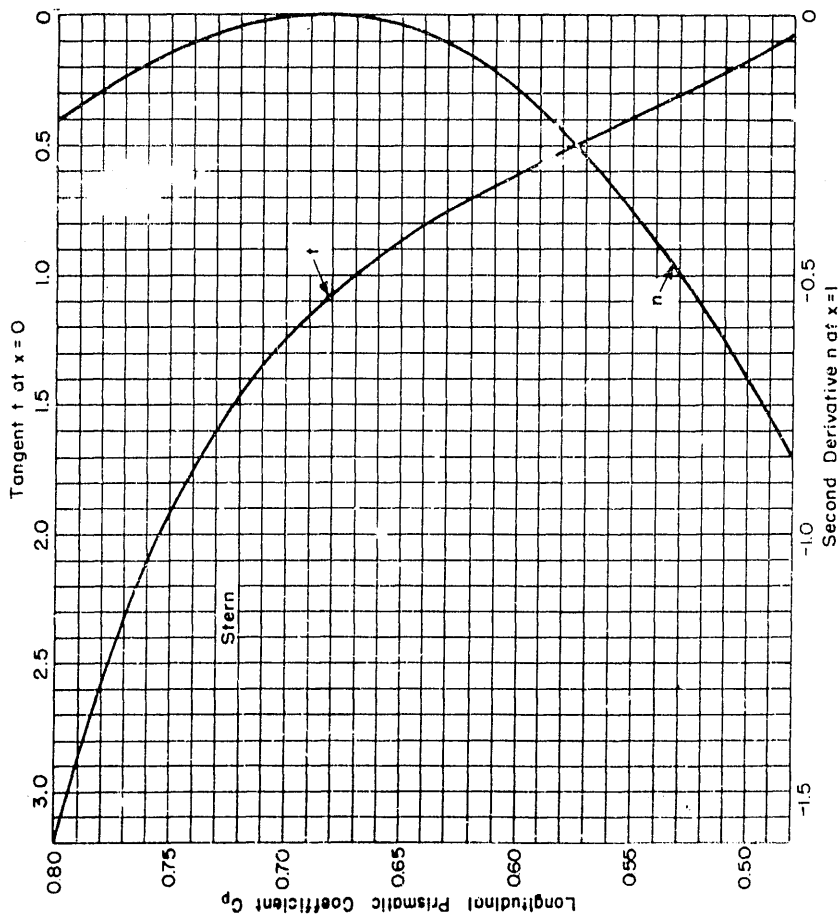


FIGURE 4.--Curves of geometrical parameters used to define mathematically the sectional-area curves for the Taylor Standard Series

The parameter f is constant and equal to 0.03 for the bow and 0.00 for the stern

Thus Equation [2] evolves to the more general expression

$$v = \zeta(x) + C_p P(x) + tI(x) + nN(x) + fF(x) \quad [5]$$

where the term $fF(x)$ drops out when the conditions for a bulb or transom do not exist.

Equation [5] can be directly used to define waterline curves by substituting the waterplane coefficient for C_p and the half siding for f . Values of $\zeta(x)$, $P(x)$, $I(x)$, $N(x)$, and $f(x)$ are listed in Table 2 for suitable incremental values of x to assist in the calculation of sectional-area or waterline curves for prescribed values of the appropriate geometrical parameters. The sectional-area curves for the Taylor Series have been fitted with Equation [5], and the resulting values of t and n are plotted against C_p in Figure 4. The value of f is constant and equal to 0.03 for the bow and 0.00 for the stern. Thus, with these values and Equation [5], any sectional-area curve belonging to the family for Taylor's Series can be easily reproduced.

The variation of C_p for the Taylor Series is thus accomplished by the preceding method involving the sectional-area curves. The variation of the other defining parameters, namely the displacement-length ratio and beam-draft ratio is obtained simply by selecting the appropriate over-all proportions of beam to draft to length. This can be accomplished nondimensionally as follows:

$$\left(\frac{L}{B}\right)^2 = \frac{C_x C_p}{B \frac{C_v}{H}} \quad [6]$$

The volumetric coefficient $C_v = \frac{V}{L^3}$ [7]

where V is the immersed volume and L is the load waterline length, is used as a defining parameter in place of Taylor's familiar displacement-length ratio. This change was considered desirable since the displacement-length ratio is not nondimensional. Furthermore, since it has the dimension of density, its definition depends upon specified units and standards, such as the requirement that the displacement be given in tons calculated for a given draft in salt water. However, the numerical values of displacement-length ratio have often been associated by members of the profession with certain types of vessels. To retain this use,

the relationship between C_v and displacement-length ratio is shown by Figure 5.

The relationships of Equation [6] are shown in Figures 6, 7, and 8 for the range of parameters covered by the series. Obviously, these curves apply to any form which has been derived from a parent having a midship section coefficient of 0.925, the value used for the Taylor Series parent.

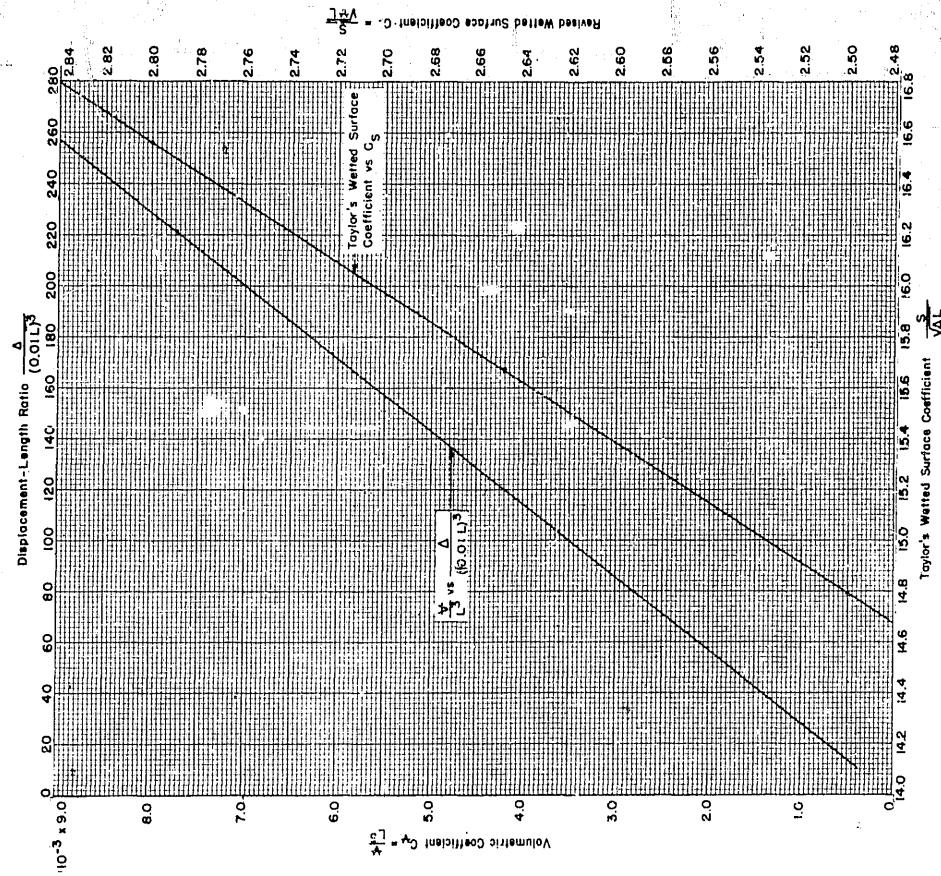


FIGURE 5.--Comparison of the Taylor displacement-length ratio and wetted-surface coefficients with the redefined coefficients

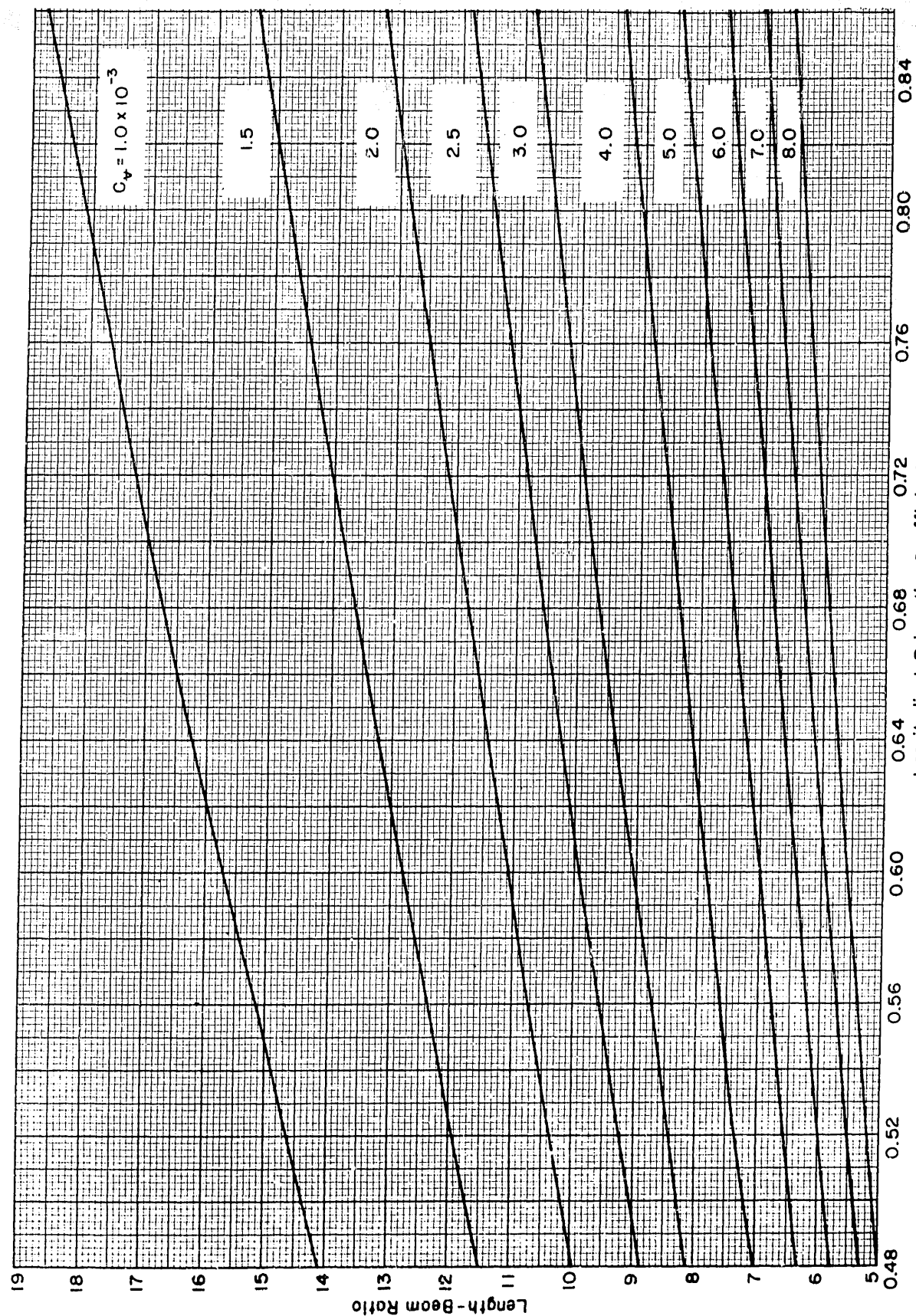


FIGURE 6.--Contours of volumetric coefficient versus longitudinal prismatic coefficient and length-beam ratio for a beam-draft ratio of 2.25

Values apply to all forms having a midship section coefficient of 0.925

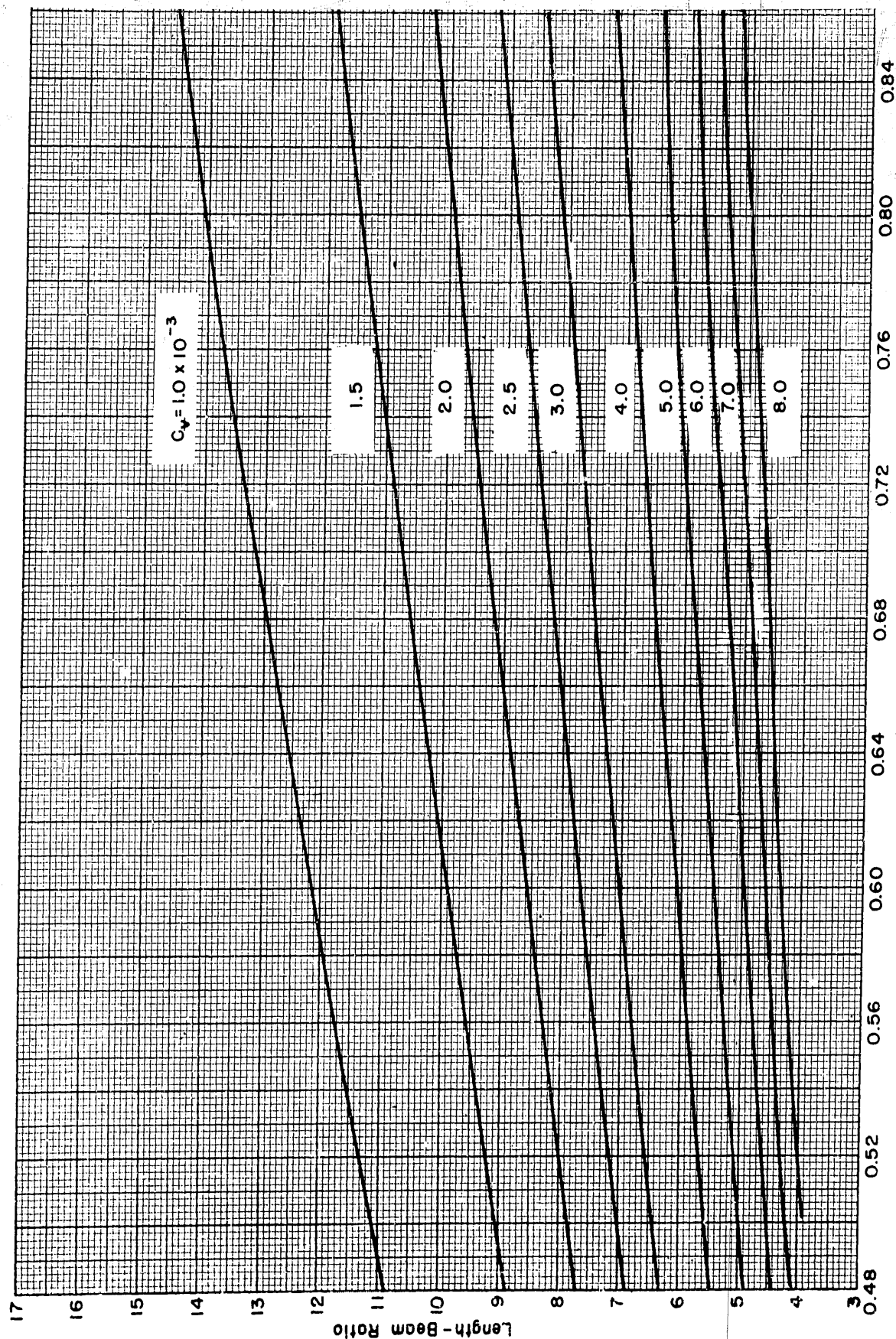


FIGURE 7.—Contours of volumetric coefficient versus longitudinal prismatic coefficient and length-beam ratio for a beam-draft ratio of 3.00

Values apply to all forms having a midship section coefficient of 0.925

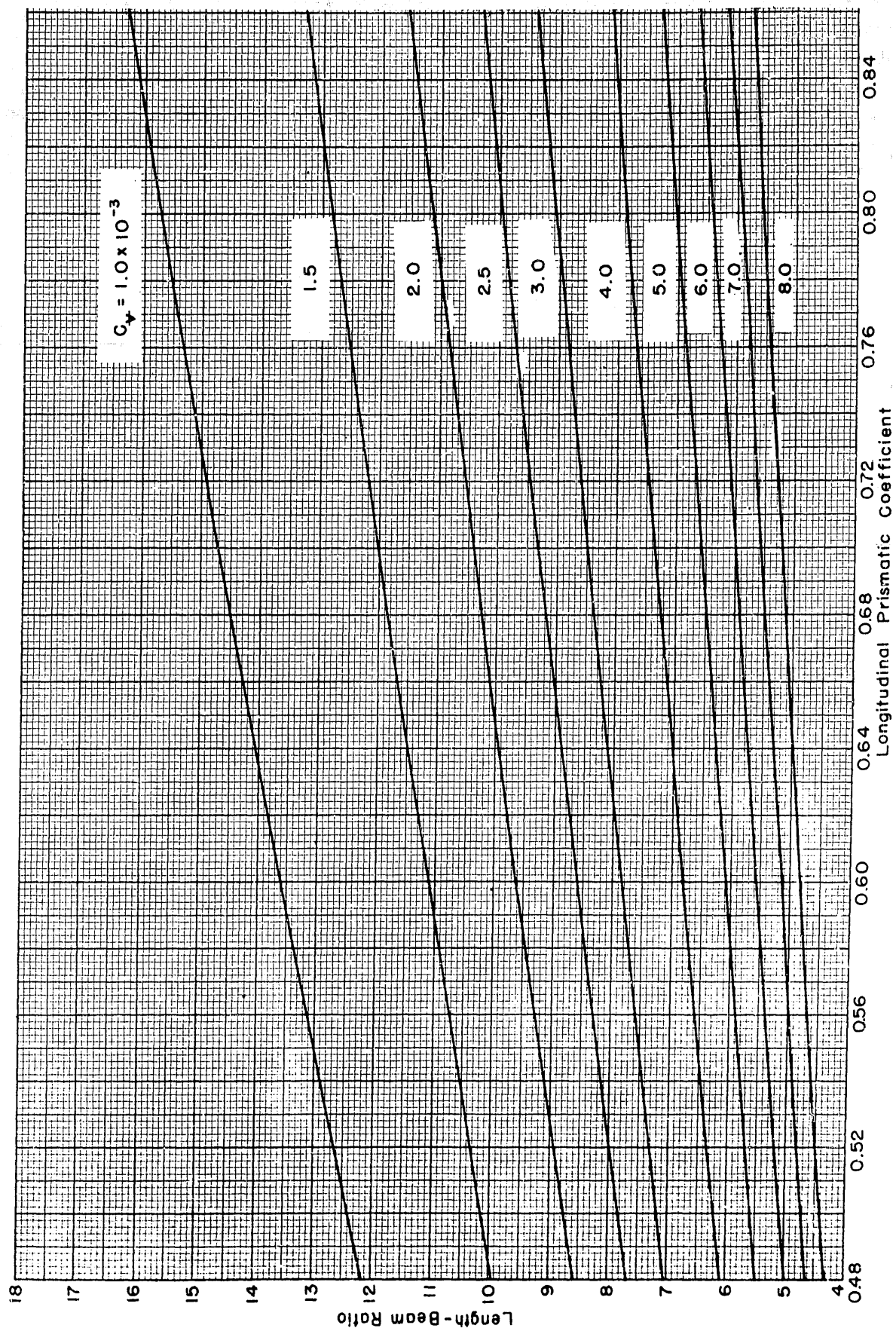


FIGURE 8.--Contours of volumetric coefficient versus longitudinal prismatic coefficient and length-beam ratio for a beam-draft ratio of 3.75

Values apply to all forms having a midship section coefficient of 0.925

As stated previously, the only variation which affects the nondimensional offsets of the individual forms is the longitudinal prismatic coefficient. The other variations must be shown either by selecting proportional scales on beam, draft, or length or by dimensionalizing to produce specific prototypes. The steps which are taken to determine any individual form of the series may be summarized as follows:

1. For the assigned value of C_p , read the nondimensional offsets from the waterline curves of Appendix 1.
2. For the assigned values of C_F and B/H , obtain the value of L/B from Formula [6] or Figures 6, 7, and 8.
3. Assign a characteristic linear dimension to the prototype such as length, beam, or draft. The other linear dimensions can be readily obtained from the values of B/H and L/B which have already been determined.
4. Multiply the nondimensional values for the half breadths, heights, and station spacings by the dimensional values of beam, draft, and length, respectively.

When the values of C_p , C_F , and B/H are assigned for any Taylor Series form, the corresponding wetted-surface coefficient can be determined. Unfortunately, as is the case with all complex forms such as ship shapes, it is not possible to express the wetted-surface coefficient as a function of these three parameters in a form which is capable of mathematical solution. This would be true even if the lines themselves were mathematically defined. Consequently, it is necessary to resort to the usual numerical procedures for calculating the wetted surfaces of individual series forms. If such calculations are made for a sufficient number of forms covering the desired range, the functional relationships can be shown graphically. The wetted surfaces of the models comprising the Taylor Series were originally calculated at the time of the model tests. Since these calculations were carefully made and spot checks indicated their accuracy, it was not necessary to repeat them. The wetted surfaces were originally calculated using the trapezoidal rule with measured girths and applying corrections for obliquity. The over-all obliquity factor was small, amounting to not less than 1.0015 and not more than 1.0070.¹ The original calculations were cross-faired to arrive at the contours of wetted-surface coefficient given

in Appendix 2. Contours are given for a B/H of 3.00 instead of the original 2.92 for ease of interpolation between the other two values of B/H . To achieve nondimensionality, the wetted-surface coefficient

$$C_s = \frac{S}{\sqrt{V}L} \quad [8]$$

where S is the wetted-surface area,
 \sqrt{V} is the immersed volume, and
 L is the load waterline length,

is used instead of the characteristic Taylor wetted-surface coefficient. The numerical values of C_s and Taylor's coefficient are related by Figure 5. It may be noted that the contours of Appendix 2 vary considerably in appearance in going from one value of B/H to the next. Unlike the contours for the other two values of B/H , the contours for a B/H of 2.25 have a distinct minimum at $C_p = 0.66$. It is difficult to prove mathematically why this should be so. However, it would appear that at values of B/H near 2.0, some of the resulting forms would approximate a half prolate spheroid. The latter has a $C_p = 0.667$ and represents the type of form for which the wetted-surface coefficient for a given L/B is the minimum value obtainable.

CONFIGURATION OF DERIVED FORMS

In planning a series of forms to be derived from a common parent, it may be difficult in some cases to visualize what the resulting forms will look like without going through the labor of the deriving process. From this standpoint, it appears desirable to survey generally the effects of the geometrical variations on the individual forms of the Taylor Series. To accomplish this, the profile, the load waterline curve, and the midship section for selected forms are shown drawn to proportionate scales in Figures 9, 10, and 11. The most interesting effects result from the C_p variation which is illustrated for fixed values of $B/H = 3.00$ and $C_F = 4.00 \times 10^{-3}$ in Figure 9. It may be noted that in addition to the usual changes in fullness of the waterlines which are attendant with C_p changes, there are distinct changes in stern profile. Most apparent of these are the change of the overhang of the stern counter and the change in the rise angle of the skeg. The variation in the overhang may lead to certain ramifications in comparing the resistances of offspring of dissimilar parents, as will be explained in a later section. The changes of form due to the

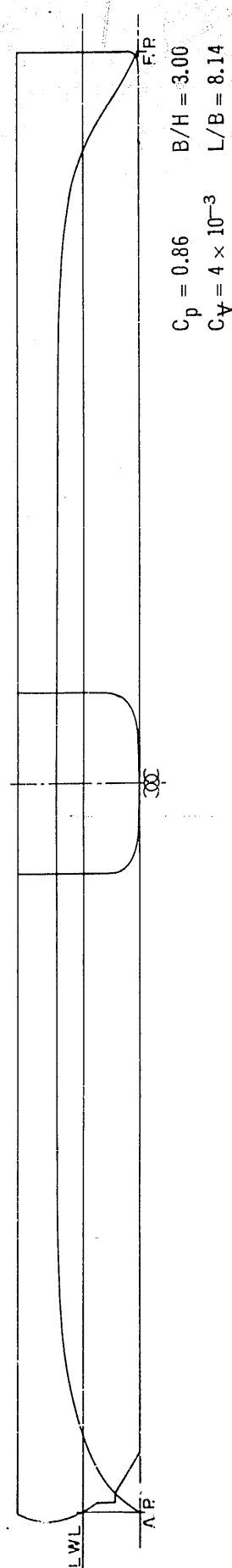
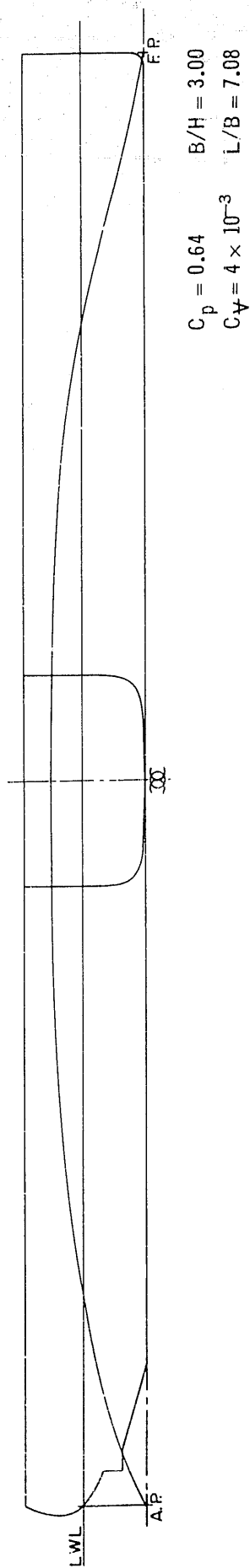
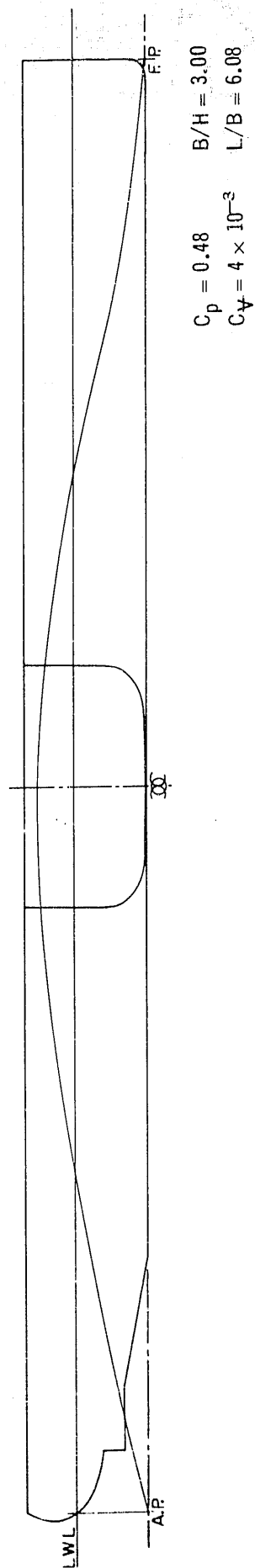
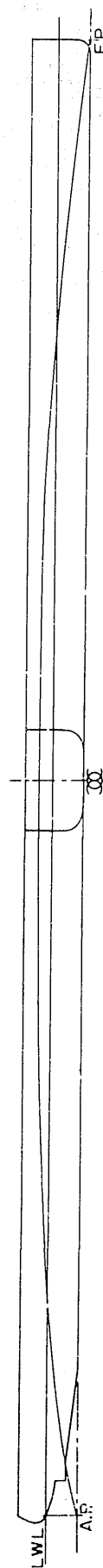
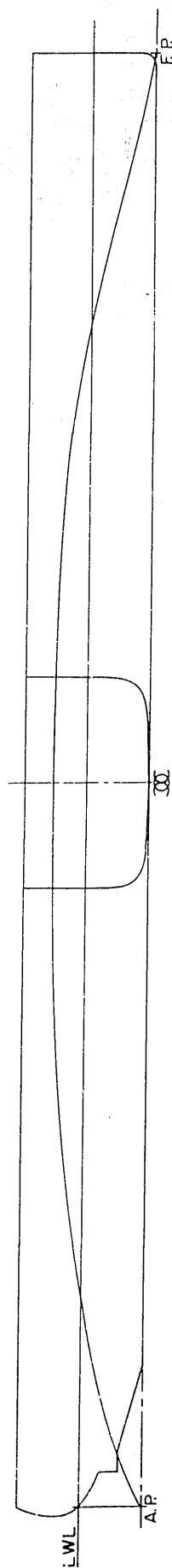


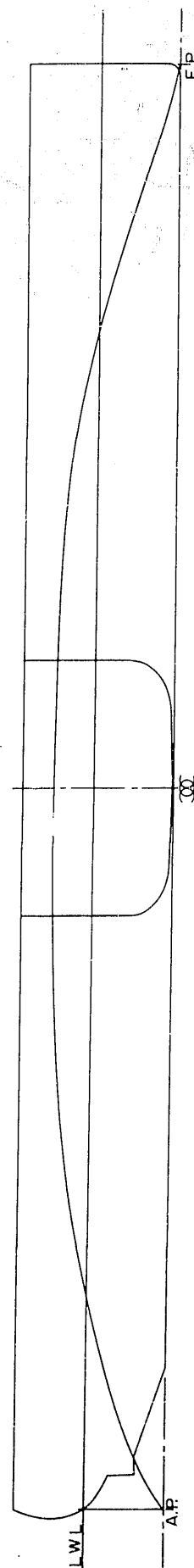
FIGURE 9.—Effects of longitudinal prismatic coefficient variation on the shapes of derived forms
 These forms have been derived for fixed values of beam-draft ratio = 3.00 and volumetric coefficient = 4.0×10^{-3}



$C_p = 0.64$ $B/H = 3.00$
 $C_V = 1 \times 10^{-3}$ $L/B = 14.05$



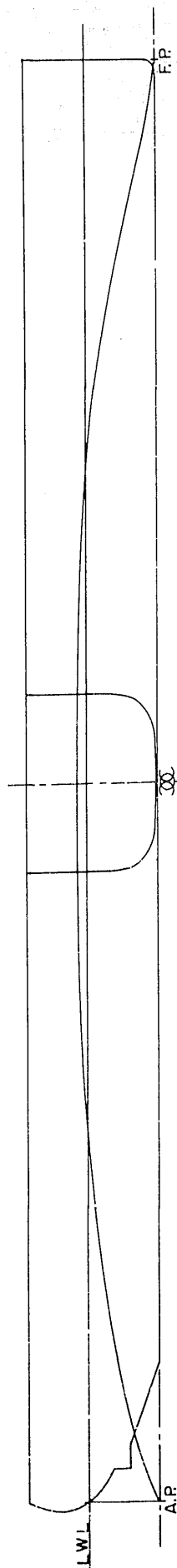
$C_p = 0.64$ $B/H = 3.00$
 $C_V = 4 \times 10^{-3}$ $L/B = 7.03$



$C_p = 0.64$ $B/H = 3.00$
 $C_V = 7 \times 10^{-3}$ $L/B = 5.32$

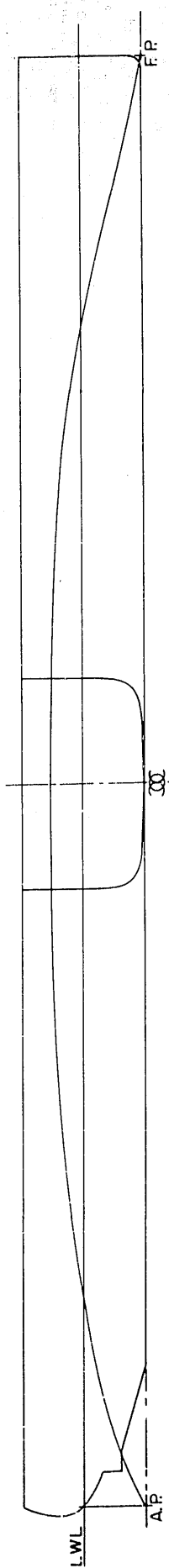
FIGURE 10.--Effects of volumetric coefficient variation on the shapes of derived forms

These forms have been derived for fixed values of beam-draft ratio = 3.00 and longitudinal prismatic coefficient = 0.64



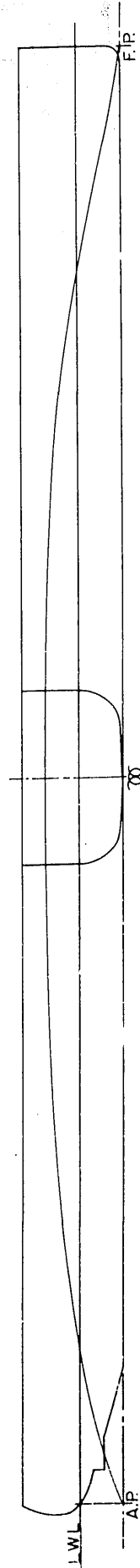
$$C_p = 0.64 \quad B/H = 2.25$$

$$C_V = 4 \times 10^{-3} \quad L/B = 8.11$$



$$C_p = 0.64 \quad B/H = 3.00$$

$$C_V = 4 \times 10^{-3} \quad L/B = 7.03$$



$$C_p = 0.64 \quad B/H = 3.75$$

$$C_V = 4 \times 10^{-3} \quad L/B = 6.30$$

FIGURE 11.—Effects of beam-draft ratio variation on the shapes of derived forms

These forms have been derived for fixed values of volumetric coefficient = 4.0×10^{-3} and longitudinal prismatic coefficient = 0.64

variation of C_f are shown for fixed values of $B/H = 3.00$ and $C_p = 0.64$ in Figure 10. Since effectively only L/B is being changed, the changes appear as proportionate changes of beam and draft, if length is held fixed. The changes in form due to the variation in B/H are shown for fixed values of $C_f = 4.00 \times 10^{-3}$ and $C_p = 0.64$ in Figure 11. Since L/B varies with B/H , the changes also appear as proportionate changes of beam and draft, if length is held fixed.

CHARACTERISTICS OF ACTUAL FORMS TESTED

The geometrical characteristics of the individual forms which were actually tested to provide resistance data are listed for record purposes in Tables 3, 4, and 5. The tabulated dimensions were originally obtained by actual measurements of the model template drawings, the drafts being corrected to the figure obtained by ballasting to the predetermined displacement. It may be noted that, due to human error, the individual model parameters differ to a small extent from the nominal values sought. These differences were taken into account in the fairing of the resistance data pursuant to the development of the final contours.

REDUCTION OF THE ORIGINAL TEST DATA

The original test data for the Taylor Series models were recorded on U. S. Experimental Model Basin "Hull Resistance" data forms. The model resistance in pounds and the change of level at bow and stern in inches were listed for each of the various towing carriage speeds. The displacement of the model in pounds and the agreement between actual and calculated drafts were also noted. In general, data values were listed for increments of approximately 0.1 to 0.2 knot to speeds up to 6.0 knots and at increments not greater than 0.3 knot at higher speeds.

The methods and procedures which were used to reduce the tabulated original data to nondimensional form are essentially the same as those currently used at the Taylor Model Basin.⁶ The procedure is as follows:

The total-resistance coefficient, which is defined as

$$C_t = \frac{R_t}{\frac{\rho}{2} S v^2} \quad [9]$$

where C_t is the total-resistance coefficient,
 R_t is the total resistance,
 ρ is the mass density, and
 v is the speed,

is calculated for each of the test values of resistance versus speed. The frictional-resistance coefficient is obtained from the Schoenherr formula

$$\frac{0.242}{\sqrt{C_f}} = \log_{10} (R_e \cdot C_f) \quad [10]$$

where C_f is the frictional-resistance coefficient,
 R_e is the Reynolds number, equal to $\frac{vL}{\nu}$

v is the speed,
 L is the waterline length, and
 ν is the kinematic viscosity

The frictional-resistance coefficients are subtracted from the total-resistance coefficients to obtain the residual-resistance coefficients, or

$$C_t - C_f = C_r = \frac{R_r}{\frac{\rho}{2} S v^2} \quad [11]$$

where C_r is the residual-resistance coefficient and R_r is the residual resistance.

It should be observed that the frictional-resistance coefficients used in Formula [10] to obtain the defined residual-resistance coefficient apply to the equivalent flat plate's as derived by the Schoenherr formula. Consequently, it is possible that the residual resistance may include not only wavemaking and form resistance but also the difference between the true frictional resistance of the vessel and that of the corresponding flat plate. If the frictional-resistance coefficient versus Reynolds number curve for the actual vessel is parallel to that calculated for the flat plate, the comparisons based on the final predicted effective horsepower will not be affected. However, when the residual-resistance coefficients of two dissimilar vessels are directly compared, the possibility of discrepancies due to such differences should

TABLE 3.--Dimensions and coefficients for Taylor Series models with a nominal beam-draft ratio of 2.25 (Series 22)

Model	Date Tested	Dimensions										Coefficients									
		L	B	H	V	A _T	A _L	S	C _p	C _f	C _p	C _p	C _p	C _p	C _p	C _p	C _p	C _p	C _p	C _p	C _p
815	27 Sep 07	20.52	1.418	0.624	500	8.02	0.812	32.91	0.4419	0.9178	0.5883	0.928	26.56	2.272	14.470	10.310	8.410	6.849	5.932	5.426	15.070
816	27 Sep 07	20.52	1.362	0.603	500	8.02	0.748	32.82	0.4781	0.9117	0.5221	0.928	26.56	2.259	15.070	10.310	8.410	6.849	5.932	5.426	15.070
817	28 Sep 07	20.53	1.312	0.581	500	8.02	0.695	32.77	0.5128	0.9117	0.5221	0.928	26.56	2.254	15.070	10.310	8.410	6.849	5.932	5.426	15.070
818	27 Sep 07	20.52	1.260	0.556	500	8.02	0.652	32.65	0.5581	0.9306	0.5998	0.928	26.56	2.245	15.070	10.310	8.410	6.849	5.932	5.426	15.070
819	22 Oct 07	20.53	1.222	0.544	500	8.02	0.611	32.61	0.5879	0.9192	0.6400	0.927	26.53	2.242	16.800	11.830	9.661	7.986	6.838	5.997	15.070
820	21 Oct 07	20.52	1.188	0.525	500	8.02	0.578	32.59	0.6270	0.9272	0.6761	0.928	26.56	2.240	17.270	12.250	9.537	7.883	6.753	5.997	15.070
821	25 Sep 07	20.53	1.074	0.477	1000	16.06	0.158	46.20	0.6249	0.9249	0.6756	0.928	26.56	2.243	12.250	10.830	8.845	7.687	6.753	5.997	15.070
822	25 Sep 07	20.53	1.074	0.477	1000	16.06	0.158	46.20	0.6249	0.9249	0.6756	0.928	26.56	2.243	12.250	10.830	8.845	7.687	6.753	5.997	15.070
823	9 Mar 08	20.53	1.546	0.685	1000	16.03	0.978	46.44	0.7373	0.9235	0.7983	0.928	26.56	2.259	13.280	10.830	8.845	7.687	6.753	5.997	15.070
824	10 Mar 08	20.51	1.894	0.839	1500	24.05	1.470	56.94	0.7379	0.9215	0.7976	0.928	26.56	2.254	10.830	8.845	7.687	6.753	5.997	15.070	15.070
825	4 Mar 08	20.52	2.300	1.031	2250	36.07	2.210	69.88	0.7349	0.9239	0.7953	0.928	26.56	2.259	10.830	8.845	7.687	6.753	5.997	15.070	15.070
826	2 Mar 08	20.51	2.668	1.187	3000	48.09	2.938	80.66	0.7403	0.9276	0.7981	0.928	26.56	2.259	10.830	8.845	7.687	6.753	5.997	15.070	15.070
827	11 Apr 14	20.51	2.330	1.292	3587	57.54	3.507	88.60	0.7410	0.9263	0.7999	0.928	26.56	2.259	10.830	8.845	7.687	6.753	5.997	15.070	15.070
828	17 Apr 14	20.51	3.148	1.393	4153	66.66	4.063	95.20	0.7411	0.9266	0.7999	0.928	26.56	2.259	10.830	8.845	7.687	6.753	5.997	15.070	15.070
829	21 Jul 13	20.51	1.488	0.658	1000	16.07	0.911	27.40	0.8002	0.9304	0.8603	0.928	26.56	2.252	13.780	11.290	9.209	7.968	6.775	5.997	15.070
830	23 Jul 13	20.51	1.818	0.991	1500	24.11	1.366	33.44	0.7980	0.9274	0.8604	0.928	26.56	2.252	13.780	11.290	9.209	7.968	6.775	5.997	15.070
831	22 Jul 13	20.51	2.574	1.141	3000	48.21	2.733	47.44	0.8002	0.9306	0.8601	0.928	26.56	2.252	13.780	11.290	9.209	7.968	6.775	5.997	15.070
832	22 Jul 13	20.50	2.226	0.991	2250	36.16	2.054	40.85	0.7996	0.9310	0.8587	0.928	26.56	2.252	13.780	11.290	9.209	7.968	6.775	5.997	15.070
833	21 Jul 13	20.51	1.816	0.811	1500	24.11	1.366	33.44	0.7980	0.9274	0.8604	0.928	26.56	2.252	13.780	11.290	9.209	7.968	6.775	5.997	15.070
834	21 Jul 13	20.51	1.488	0.658	1000	16.07	0.911	27.40	0.8002	0.9304	0.8603	0.928	26.56	2.252	13.780	11.290	9.209	7.968	6.775	5.997	15.070
835	23 Jul 13	20.51	2.818	1.250	3587	57.64	3.273	51.90	0.7976	0.9290	0.8587	0.928	26.56	2.252	13.780	11.290	9.209	7.968	6.775	5.997	15.070
836	23 Jul 13	20.51	2.574	1.141	3000	48.21	2.733	47.44	0.8002	0.9306	0.8601	0.928	26.56	2.252	13.780	11.290	9.209	7.968	6.775	5.997	15.070
837	23 Jul 13	20.51	1.818	0.991	1500	24.11	1.366	33.44	0.7980	0.9274	0.8604	0.928	26.56	2.252	13.780	11.290	9.209	7.968	6.775	5.997	15.070
838	23 Jul 13	20.51	2.818	1.250	3587	57.64	3.273	51.90	0.7976	0.9290	0.8587	0.928	26.56	2.252	13.780	11.290	9.209	7.968	6.775	5.997	15.070
839	23 Jul 13	20.51	2.818	1.250	3587	57.64	3.273	51.90	0.7976	0.9290	0.8587	0.928	26.56	2.252	13.780	11.290	9.209	7.968	6.775	5.997	15.070
840	23 Jul 13	20.51	2.818	1.250	3587	57.64	3.273	51.90	0.7976	0.9290	0.8587	0.928	26.56	2.252	13.780	11.290	9.209	7.968	6.775	5.997	15.070
841	23 Jul 13	20.51	2.818	1.250	3587	57.64	3.273	51.90	0.7976	0.9290	0.8587	0.928	26.56	2.252	13.780	11.290	9.209	7.968	6.775	5.997	15.070
842	23 Jul 13	20.51	2.818	1.250	3587	57.64	3.273	51.90	0.7976	0.9290	0.8587	0.928	26.56	2.252	13.780	11.290	9.209	7.968	6.775	5.997	15.070
843	23 Jul 13	20.51	2.818	1.250	3587	57.64	3.273	51.90	0.7976	0.9290	0.8587	0.928	26.56	2.252	13.780	11.290	9.209	7.968	6.775	5.997	15.070
844	23 Jul 13	20.51	2.818	1.250	3587	57.64	3.273	51.90	0.7976	0.9290	0.8587	0.928	26.56	2.252	13.780	11.290	9.209	7.968	6.775	5.997	15.070
845	23 Jul 13	20.51	2.818	1.250	3587	57.64	3.273	51.90	0.7976	0.9290	0.8587	0.928	26.56	2.252	13.780	11.290	9.209	7.968	6.775	5.997	15.070
846	23 Jul 13	20.51	2.818	1.250	3587	57.64	3.273	51.90	0.7976	0.9290	0.8587	0.928	26.56	2.252	13.780	11.290	9.209	7.968	6.775	5.997	15.070
847	23 Jul 13	20.51	2.818	1.250	3587	57.64	3.273	51.90	0.7976	0.9290	0.8587	0.928	26.56	2.252	13.780	11.290	9.209	7.968	6.775	5.997	15.070
848	23 Jul 13	20.51	2.818	1.250	3587	57.64	3.273	51.90	0.7976	0.9290	0.8587	0.928	26.56	2.252	13.780	11.290	9.209	7.968	6.775	5.997	15.070
849	23 Jul 13	20.51	2.818	1.250	3587	57.64	3.273	51.90	0.7976	0.9290	0.8587	0.928	26.56	2.252	13.780	11.290	9.209	7.968	6.775	5.997	15.070
850	23 Jul 13	20.51	2.818	1.250	3587	57.64	3.273	51.90	0.7976	0.9290	0.8587	0.928	26.56	2.252	13.780	11.290	9.209	7.968	6.775	5.997	15.070
851	23 Jul 13	20.51	2.818	1.250	3587	57.64	3.273	51.90	0.7976	0.9290	0.8587	0.928	26.56	2.252	13.780	11.290	9.209	7.968	6.775	5.997	15.070
852	23 Jul 13	20.51	2.818	1.250	3587	57.64	3.273	51.90	0.7976	0.9290	0.8587	0.928	26.56	2.252	13.780	11.290	9.209	7.968	6.775	5.997	15.070
853	23 Jul 13	20.51	2.818	1.250	3587	57.64	3.273	51.90	0.7976	0.9290	0.8587	0.928	26.56	2.252	13.780	11.290	9.209	7.968	6.775	5.997	15.070
854	23 Jul 13	20.51	2.818	1.250	3587	57.64	3.273	51.90	0.7976	0.9290	0.8587	0.928	26.56	2.252	13.780	11.290	9.209	7.968	6.775	5.997	15.070
855	23 Jul 13	20.51	2.818	1.250	3587	57.64	3.273	51.90	0.7976	0.9290	0.8587	0.928	26.56	2.252	13.780	11.290	9.209	7.968	6.775	5.997	15.070
856	23 Jul 13	20.51	2.818	1.250	3587	57.64	3.273	51.90	0.7976	0.9290	0.8587	0.928	26.56	2.252	13.780	11.290	9.209	7.968	6.775	5.997	15.070
857	23 Jul 13	20.51	2.818	1.250	3587	57.64	3.273	51.90	0.7976	0.9290	0.8587	0.928	26.56	2.252	13.780	11.290	9.209	7.968	6.775	5.997	15.070
858	23 Jul 13	20.51	2.818	1.250	3587	57.64	3.273	51.90	0.7976	0.9290	0.8587	0.928	26.56	2.252	13.780	11.290	9.209	7.968	6.775	5.997	15.070
859	23 Jul 13	20.51	2.818	1.250	3587	57.64	3.273	51.90	0.7976	0.9290	0.8587	0.928	26.56	2.252	13.780	11.290	9.209	7.968	6.775	5.997	15.070
860	23 Jul 13	20.51	2.818	1.250	3587	57.64	3.273	51.90	0.7976	0.9290	0.8587	0.928	26.56	2.252	13.780	11.290	9.209	7.968	6.775	5.997	15.070
861	23 Jul 13	20.51	2.818	1.250	3587	57.64	3.273	51.90	0.7976	0.9290	0.8587	0.928	26.56	2.252	13.780	11.290	9.209	7.968	6.775	5.997	15.070
862	23 Jul 13	20.51	2.818	1.250	3587	57.64	3.273	51.90	0.7976	0.9290	0.8587	0.928	26.56	2.252	13.780	11.290	9.209	7.968	6.775	5.997	15.070
863	23 Jul 13	20.51	2.818	1.250	3587	57.64	3.273	51.90	0.7976	0.9290	0.8587	0.928	26.56	2.252	13.780	11.290	9.209	7.968	6.775	5.997	15.070
864	23 Jul 13	20.51	2.818	1.250	3587	57.64	3.273	51.90	0.7976	0.9290	0.8587	0.928	26.56	2.252	13.780	11.290	9.209	7.968	6.775	5.997	15.070
865	23 Jul 13	20.51	2.818	1.250	3587	57.64	3.273	51.90	0.7976	0.9290	0.8587	0.928	26.56	2.252	13.780	11.290	9.209	7.968	6.775	5.997	15.070
866	23 Jul 13	20.51	2.818	1.250	3587	57.64	3.273	51.90	0.7976	0.9290	0.8587	0.928	26.56	2.252							

Model	Date Tested	Dimensions							Coefficients										
		L	B	H	A	V	A _x	A _w	S	C _b	C _x	C _p	C _{p_v}	C _w	10 ³ × C _v	Δ (0.01 L) ³	C _s	B/H	L/B
751	27 Apr 07	20.53	1.604	0.550	500	8.03	0.814	19.34	32.19	0.4431	0.9227	0.4803	0.7544	0.5872	0.927	26.52	2.507	2.916	12.800
745	22 Apr 07	20.51	2.278	0.777	1000	16.04	1.629	27.26	45.73	.4419	.9203	.4801	.7573	.5835	0.927	53.17	2.521	2.932	9.004
727	18 Apr 07	20.51	2.775	0.954	1500	24.06	2.444	33.37	55.95	.4432	.9233	.4800	.7559	.5863	0.928	79.76	2.519	2.909	7.391
721	20 Mar 07	20.51	3.580	1.227	2500	40.08	4.074	43.12	72.73	.4448	.9274	.4796	.7575	.5872	0.928	132.9	2.537	2.918	5.729
715	26 Feb 07	20.51	4.376	1.504	3750	60.11	6.100	53.10	88.68	.4453	.9268	.4805	.7527	.5916	0.927	199.4	2.526	2.910	4.687
752	29 Apr 07	20.52	1.552	0.526	500	8.03	0.752	19.87	32.25	.4791	.9211	.5201	.7678	.6239	0.929	26.55	2.512	2.951	13.220
746	23 Apr 07	20.51	2.180	0.742	1000	16.04	1.499	27.85	45.73	.4833	.9265	.5218	.7762	.6230	0.929	53.17	2.521	2.938	9.408
728	18 Apr 07	20.51	2.664	0.911	1500	24.06	2.254	34.21	55.99	.4833	.9287	.5204	.7719	.6261	0.928	79.76	2.521	2.924	7.699
722	20 Mar 07	20.51	3.396	1.184	2500	40.08	3.785	43.53	72.73	.4860	.9413	.5163	.7776	.6250	0.929	132.9	2.537	2.868	6.039
716	11 Mar 07	20.51	4.220	1.441	3750	60.11	5.656	53.96	88.72	.4820	.9301	.5182	.7730	.6234	0.929	199.4	2.527	2.929	4.860
753	29 Apr 07	20.52	1.488	0.508	500	8.03	0.698	20.30	32.30	.5174	.9234	.5604	.7782	.6649	0.929	26.55	2.516	2.929	13.790
747	23 Apr 07	20.51	2.108	0.719	1000	16.04	1.396	28.62	45.81	.5159	.9208	.5603	.7794	.6619	0.929	53.17	2.525	2.932	9.730
729	19 Apr 07	20.51	2.564	0.878	1500	24.06	2.085	35.24	56.07	.5211	.9263	.5627	.7776	.6701	0.928	79.76	2.525	2.920	7.999
723	22 Mar 07	20.51	3.300	1.138	2500	40.08	3.501	45.05	72.82	.5204	.9324	.5581	.7817	.6656	0.929	132.9	2.540	2.900	6.215
717	25 Feb 07	20.51	4.052	1.392	3750	60.11	5.220	54.79	88.97	.5195	.9255	.5613	.7881	.6593	0.927	199.4	2.534	2.911	5.062
754	30 Apr 07	20.52	1.454	0.491	500	8.03	0.658	20.64	32.36	.5478	.9217	.5944	.7919	.6917	0.927	26.55	2.520	2.961	14.110
748	24 Apr 07	20.51	2.036	0.700	1000	16.04	1.313	29.08	45.89	.5488	.9214	.5956	.7878	.6964	0.929	53.17	2.530	2.909	10.070
730	20 Apr 07	20.51	2.492	0.851	1500	24.06	1.959	35.48	56.16	.5531	.9236	.5988	.7970	.6942	0.928	79.76	2.529	2.928	8.230
724	21 Mar 07	20.51	3.224	1.105	2500	40.08	3.290	45.79	72.90	.5484	.9234	.5940	.7921	.6925	0.929	132.9	2.543	2.918	6.362
718	11 Mar 07	20.51	3.920	1.345	3750	60.11	4.892	55.98	89.26	.5561	.9279	.5993	.7984	.6963	0.928	199.4	2.542	2.914	5.232
755	30 Apr 07	20.53	1.404	0.474	500	8.03	0.610	20.92	32.45	.5875	.9159	.6410	.8093	.7259	0.927	26.52	2.527	2.962	14.620
749	24 Apr 07	20.51	1.972	0.670	1000	16.04	1.226	29.55	45.98	.5921	.9281	.6378	.8105	.7303	0.929	53.17	2.535	2.943	10.400
731	20 Apr 07	20.51	2.412	0.824	1500	24.06	1.836	36.18	56.33	.5904	.9240	.6389	.8071	.7314	0.928	79.76	2.536	2.927	8.503
725	22 Mar 07	20.51	3.108	1.064	2500	40.08	3.073	46.49	73.07	.5909	.9292	.6359	.8102	.7292	0.929	132.9	2.549	2.921	6.599
719	12 Mar 07	20.51	3.808	1.305	3750	60.11	4.586	57.03	89.60	.5899	.9229	.6390	.8077	.7302	0.927	199.4	2.552	2.918	5.386
756	1 May 07	20.51	1.354	0.459	500	8.03	0.578	21.06	32.56	.6294	.9300	.6772	.8277	.7582	0.930	26.58	2.538	2.950	15.150
750	25 Apr 07	20.50	1.924	0.649	1000	16.04	1.153	29.88	46.06	.6266	.9230	.6785	.8272	.7576	0.930	53.24	2.541	2.965	10.650
732	22 Apr 07	20.50	2.348	0.796	1500	24.06	1.728	36.50	56.48	.6280	.9245	.6793	.8260	.7580	0.930	79.85	2.543	2.950	8.731
726	23 Mar 07	20.54	3.034	1.024	2500	40.08	2.888	47.15	73.49	.6280	.9295	.6757	.8286	.7565	0.930	132.3	2.562	2.963	6.770
720	18 Mar 07	20.51	3.704	1.261	3750	60.11	4.320	57.73	90.00	.6275	.9249	.6784	.8245	.7599	0.930	199.4	2.563	2.937	5.537
849	24 Oct 07	20.53	1.830	0.629	1000	16.05	1.062	30.32	46.45	.6792	.9227	.7362	.8390	.8074	0.930	53.05	2.559	2.909	11.220
848	24 Oct 07	20.54	2.238	0.770	1500	24.08	1.589	37.10	57.08	.6804	.9222	.7377	.8403	.8073	0.930	79.39	2.567	2.906	9.178
847	30 Oct 07	20.53	2.890	0.993	2500	40.10	2.666	47.86	73.80	.6806	.9289	.7327	.8418	.8066	0.930	132.6	2.572	2.910	7.104
846	31 Oct 07	20.52	3.546	1.212	3750	60.15	3.977	58.79	90.83	.6821	.9253	.7370	.8422	.8081	0.930	199.2	2.586	2.926	5.787
853	2 Nov 07	20.54	1.756	0.606	1000	16.04	0.977	30.83	46.79	.7341	.9182	.7992	.8567	.8548	0.930	52.93	2.578	2.898	11.700
852	1 Nov 07	20.53	2.162	0.740	1500	24.06	1.468	37.86	57.45	.7324	.9175	.7983	.8566	.8529	0.930	79.57	2.584	2.922	9.496
851	28 Oct 07	20.53	2.782	0.953	2500	40.10	2.446	48.77	74.39	.7367	.9227	.7985	.8606	.8540	0.930	132.6	2.593	2.919	7.380
850	29 Oct 07	20.53	3.414	1.167	3750	60.15	3.666	59.78	91.67	.7354	.9202	.7992	.8600	.8531	0.930	199.0	2.609	2.925	6.013

TABLE 4.--Dimensions and coefficients for Taylor Series models with a nominal beam-draft ratio of 2.92 (Series 20)

TABLE 5.--Dimensions and coefficients for Taylor Series models with a nominal beam-draft ratio of

Model	Date Tested	L	B	H	V	A	A ₁	A ₂	S	C _b	C _x	C _p	C _{p_u}	C _n	10 ³ x C _v	C _s	H	L	
782	7 Aug 07	20.53	1.824	0.488	500	8.63	0.816	21.81	32.58	0.4396	0.9168	0.4797	0.7542	0.5825	0.928	26.52	2.537	3.738	11.260
776	15 Jul 07	20.53	2.568	0.684	1000	16.07	1.627	30.92	46.24	0.4456	0.9263	0.4818	0.7598	0.5865	2.796	2.546	3.754	7.983	
770	9 Jul 07	20.50	3.148	0.837	1500	24.09	2.448	38.77	56.24	0.4460	0.9290	0.4801	0.7424	0.5990	2.796	2.531	3.761	6.494	
764	27 Jun 07	20.50	3.856	1.024	2250	36.14	3.676	46.47	69.14	0.4464	0.9301	0.4800	0.7594	0.5879	4.195	2.540	3.766	5.316	
758	22 Jun 07	20.49	4.448	1.182	3000	48.18	4.869	53.27	80.39	0.4472	0.9260	0.4829	0.7651	0.5600	5.600	2.552	3.763	4.607	
1524	27 May 14	20.51	4.869	1.295	3587	57.64	5.836	58.49	88.38	0.4457	0.9256	0.4816	0.7610	0.5857	6.681	2.571	3.760	4.212	
1515	2 Sep 14	20.51	5.232	1.392	4153	66.74	6.757	62.93	94.70	0.4468	0.9278	0.4816	0.7619	0.5864	7.735	2.559	3.759	3.920	
783	6 Aug 07	20.51	1.750	0.468	500	8.03	0.753	22.35	32.60	0.4782	0.9194	0.5209	0.7682	0.6227	0.931	2.539	3.739	11.720	
777	15 Jul 07	20.53	2.452	0.69	1000	16.07	1.406	31.54	46.32	0.4943	0.9257	0.5233	0.7733	0.6265	1.857	2.545	3.721	8.373	
771	11 Jul 07	20.51	3.014	0.804	1500	24.09	2.255	38.58	57.09	0.4847	0.9307	0.5183	0.7731	0.6240	2.792	2.547	3.749	6.805	
765	27 Jun 07	20.50	3.698	0.984	2250	36.14	3.384	47.48	69.35	0.4844	0.9300	0.5206	0.7735	0.6263	4.195	2.560	3.758	5.544	
759	22 Jun 07	20.51	4.276	1.134	3000	48.18	4.612	54.23	80.65	0.4842	0.9305	0.5216	0.7834	0.6185	5.677	2.579	3.748	4.947	
1524	27 May 14	20.50	4.716	1.260	3587	57.62	5.380	58.95	88.68	0.4827	0.9246	0.5221	0.7843	0.6185	6.677	2.593	3.741	4.392	
1516	1 Sep 14	20.51	5.073	1.343	4153	66.74	6.267	64.39	94.95	0.4824	0.9290	0.5192	0.7717	0.6250	7.735	2.568	3.750	4.083	
784	7 Aug 07	20.52	1.654	0.451	500	8.03	0.695	22.36	32.76	0.5248	0.9316	0.5634	0.7971	0.6589	0.930	2.551	3.667	12.410	
778	16 Jul 07	20.52	2.384	0.63	1000	16.07	1.406	32.25	46.41	0.5191	0.9320	0.5570	0.7873	0.6592	1.860	2.556	3.766	8.607	
772	11 Jul 07	20.53	2.922	0.777	1500	24.09	2.095	39.50	56.94	0.5170	0.9229	0.5601	0.7849	0.6584	2.784	2.560	3.761	7.026	
760	24 Jun 07	20.52	3.568	0.932	2250	36.14	3.240	48.30	69.78	0.5184	0.9255	0.5602	0.7859	0.6537	4.183	2.563	3.748	5.751	
766	24 Jun 07	20.51	4.118	1.093	3000	48.18	4.420	55.21	80.98	0.5219	0.9375	0.5667	0.7984	0.6537	5.584	2.578	3.768	4.981	
1525	27 May 14	20.51	4.496	1.193	3587	57.61	4.993	61.55	89.02	0.5237	0.9308	0.5626	0.7856	0.6					
1517	2 Sep 14	20.51	4.850	1.294	4153	66.70	5.808	65.61	95.25	0.5183	0.9255	0.5600	0.7856	0.6366	7.731	2.576	3.748	4.229	
785	8 Aug 07	20.51	1.628	0.438	500	8.03	0.653	23.11	32.90	0.492	0.9158	0.6001	0.7940	0.6222	0.931	2.538	3.717	12.600	
779	15 Jul 07	20.54	2.300	0.617	1000	16.07	1.305	32.79	46.70	0.5512	0.9196	0.5995	0.7943	0.6941	1.854	2.570	3.728	8.930	
773	9 Jul 07	20.54	2.822	0.721	1500	24.09	1.947	40.33	57.29	0.5518	0.9162	0.6024	0.7932	0.6983	2.780	2.576	3.747	7.279	
767	28 Jun 07	20.47	3.428	0.952	2250	36.14	2.619	46.79	69.81	0.5592	0.9202	0.6022	0.7932	0.6933	4.213	2.576	3.742	5.971	
761	24 Jun 07	20.52	3.975	1.057	3000	48.18	3.923	58.79	81.48	0.5589	0.9339	0.5985	0.8030	0.6961	5.617	2.592	3.760	5.164	
1526	26 May 14	20.49	4.370	1.165	3587	57.61	4.866	62.63	89.25	0.5523	0.9204	0.6000	0.7908	0.6964	6.697	2.598	3.751	4.689	
1518	19 Sep 14	20.51	4.680	1.248	4153	66.70	5.427	66.77	95.67	0.5568	0.9291	0.5993	0.8004	0.6956	7.731	2.586	3.750	4.382	
786	8 Aug 07	20.53	1.576	0.424	500	8.03	0.611	23.46	33.17	0.5856	0.9151	0.6402	0.8070	0.7250	0.928	2.532	3.717	13.030	
780	18 Jul 07	20.53	2.238	0.595	1000	16.07	1.226	33.74	47.31	0.5875	0.9204	0.6384	0.8071	0.7282	1.857	2.584	3.761	9.173	
774	10 Jul 07	20.52	2.736	0.727	1500	24.09	1.837	40.84	57.58	0.5900	0.9266	0.6368	0.8113	0.7270	2.784	2.593	3.753	7.404	
768	1 Jul 07	20.52	3.242	0.861	2250	36.14	2.591	50.56	72.42	0.6313	0.9272	0.6797	0.8202	0.7605	5.584	2.623	3.759	5.484	
762	26 Jun 07	20.52	3.846	1.025	3000	48.18	3.680	57.66	81.95	0.5956	0.9335	0.6380	0.8152	0.7306	5.576	2.607	3.752	5.335	
1527	17 Apr 14	20.51	4.224	1.121	3587	57.54	4.383	63.04	89.90	0.5925	0.9287	0.6400	0.8142	0.7277	6.669	2.617	3.768	4.856	
1519	19 Sep 14	20.51	4.537	1.209	4153	66.70	5.072	67.77	96.21	0.5929	0.9247	0.6413	0.8141	0.7283	7.731	2.601	3.753	4.521	
787	9 Aug 07	20.53	1.536	0.413	500	8.03	0.577	24.15	33.34	0.6171	0.9095	0.6781	0.8056	0.7659	0.928	2.595	3.719	13.370	
781	22 Jul 07	20.53	2.164	0.576	1000	16.07	1.155	33.74	47.31	0.6282	0.9270	0.6778	0.8271	0.7594	1.857	2.605	3.757	9.487	
775	12 Jul 07	20.52	2.652	0.705	1500	24.09	1.729	41.38	57.90	0.6278	0.9246	0.6790	0.8258	0.7604	2.788	2.605	3.762	7.738	
769	26 Jun 07	20.52	3.240	0.861	2250	36.14	2.591	50.56	72.42	0.6313	0.9272	0.6797	0.8202	0.7605	5.584	2.623	3.759	5.484	
763	26 Jun 07	20.52	3.740	0.995	3000	48.18	3.450	58.37	82.45	0.6394	0.9272	0.6794	0.8295	0.7609	5.584	2.632	3.759	5.484	
1528	16 Apr 14	20.50	3.949	1.053	3587	57.54	3.793	65.62	91.25	0.6750	0.9122	0.7400	0.8340	0.8094	6.679	2.656	3.750	5.191	
1529	16 Apr 14	20.50	4.125	1.125	4153	66.74	4.403	68.00	98.02	0.6848	0.9122	0.7400	0.8340	0.8094	6.679	2.650	3.748	4.860	
865	25 Feb 08	20.52	1.927	0.529	1000	16.03	0.976	34.99	48.13	0.7411	0.9265	0.8000	0.8660	0.8559	1.855	2.653	3.766	10.300	
864	25 Feb 08	20.51	2.448	0.645	1500	24.05	1.465	42.95	58.98	0.7425	0.9278	0.8003	0.8682	0.8554	2.787	2.656	3.795	8.378	
863	24 Feb 08	20.51	2.992	0.793	2250	36.07	2.207	52.43	72.70	0.7411	0.9300	0.7968	0.8675	0.8544	4.180	2.673	3.773	6.855	
862	24 Feb 08	20.52	3.450	0.920	3000	48.09	2.938	66.12	92.39	0.7384	0.9256	0.7976	0.8642	0.8545	5.566	2.681	3.750	5.948	
1530	11 Apr 14	20.52	3.768	0.999	3587	57.54	3.497	66.12	92.39	0.7450	0.9291	0.8018	0.8642	0.8552	6.659	2.688	3.772	5.446	
1522	29 Aug 14	20.51	4.058	1.083	4153	66.70	4.065	71.17	99.29	0.7400	0.9249	0.8001	0.8653	0.8551	7.731	2.684	3.747	5.054	
1514	21 Jul 13	20.51	1.920	0.509	1000	16.07	0.914	35.38	48.63	0.8018	0.9354	0.8571	0.8923	0.8984	1.863	2.679	3.772	10.680	
1513	21 Apr 14	20.51	2.352	0.627	1500	24.06	1.914	43.29	59.61	0.7953	0.9295	0.8556	0.8865	0.8974	2.789	2.684	3.751	8.720	
1512	21 Apr 14	20.51	2.881	0.767	2250	36.09	2.052	53.04	73.54	0.7963	0.9286	0.8574	0.8872	0.8976	4.183	2.703	3.756	7.119	
1511	24 Jul 13	20.51	3.334	0.986	3000	48.21	2.730	61.38	85.11	0.7954	0.9242	0.8610	0.8855	0.8979	5.568	2.706	3.762	6.151	
1509	25 Jul 13	20.51	3.650	0.966	3587	57.64	3.268	67.22	93.31	0.7954	0.9250	0.8610	0.8855	0.8979	5.568	2.714	3.770	5.619	

be considered, although it is presently believed that such discrepancies would be small.

Since the aforementioned procedure for calculating C_r had to be performed on data from tests of 158 models, it was deemed practical to perform the calculations on a high-speed computing machine. The individual constants were calculated using desk machines and these constants were supplied to an IBM card-punch computing machine. A system of cross-checking was instituted to insure the accuracy of individual data points.

TEMPERATURE CORRECTIONS

One of the largest errors which is prevalent in the original Taylor Series contours resulted from the failure to account for the effects of changes in basin water temperature. Since the frictional-resistance coefficient is a function of Reynolds number, the temperature of the water must be accurately known to determine the appropriate kinematic viscosity to use in the computation of the Reynolds number. The basin water temperatures had not been recorded for the majority of Taylor's model tests. To estimate these temperatures, the chart of Figure 12 was prepared showing the water temperature in the Experimental Model Basin versus calendar date. The chart covers a five-year period (1913-1918) beginning with the time when the temperature was first recorded at the Experimental Model Basin and embraces the temperature values recorded for the later Taylor Series models. The chart indicates the maximum and minimum temperatures by width of line. Although there was considerable fluctuation in the air temperatures and a variation of from 53 to 80°F in water temperature over the course of a given year, it was quite surprising to find that the five-year averages of water temperatures at any given calendar date were generally repeated to within 2 to 3°F. In most cases, the assigned values of temperature used in the new calculations are believed to be accurate to within ± 1 °F.

The temperature differential of 53 to 80°F will, according to the Schoenherr formula, change the frictional resistance on a 20-foot model by approximately 7 percent. When it is considered that the calculated frictional resistance of slow-speed vessels amounts to approximately 80 percent of the total resistance, it can be readily seen that

if the temperature corrections were neglected, an attempt to cross-fair the relatively small remaining residual resistance would become complicated and large distortions might result.

The temperature of the basin water also tends to change the nature of the flow about the model, that is, whether or not appreciable laminar flow would exist. This is discussed in connection with the corrections for the effect of transitional flow upon resistance.

TRANSITIONAL FLOW CORRECTIONS

At the time when Taylor's model tests were conducted, modern turbulence stimulation techniques were unknown and their need was not anticipated. Therefore, when the data were originally reduced for the preparation of the original Taylor Series contours, no consideration was given to the problem of whether adequate turbulence had been established in the boundary layer of any given model. Even at a comparatively recent date, it was believed that with a 20-foot model and with typical basin water temperatures, the Reynolds numbers were high enough to insure adequate natural turbulence in the boundary layer. Recent studies have shown, however, that the resistance of certain types of forms is affected by transitional flow even for 30-foot models, especially at Reynolds numbers below about 6.3×10^6 . In reanalyzing the original data, therefore, an attempt was made to correct for the transitional flow effects.

The procedure used to accomplish this was as follows: Reference is made to the typical plot of C_r versus speed-length ratio shown in Figure 13. The assumption is then made that at low Froude numbers (or speed-length ratios) the residual-resistance coefficient, as defined, is a constant. If the C_r curve is traced from high to low speed-length ratios, it may be seen that the C_r decreases with decreasing speed-length ratio so long as wavemaking resistance is important. There is then a short range of speed for which the residual-resistance coefficient remains constant, after which, as the speed-length ratio is still further reduced, the coefficient begins to decrease again. In the reanalysis, this latter decrease, which has been attributed to transitional flow, has been ignored and the constant value of the coefficient used for all lower Froude numbers.

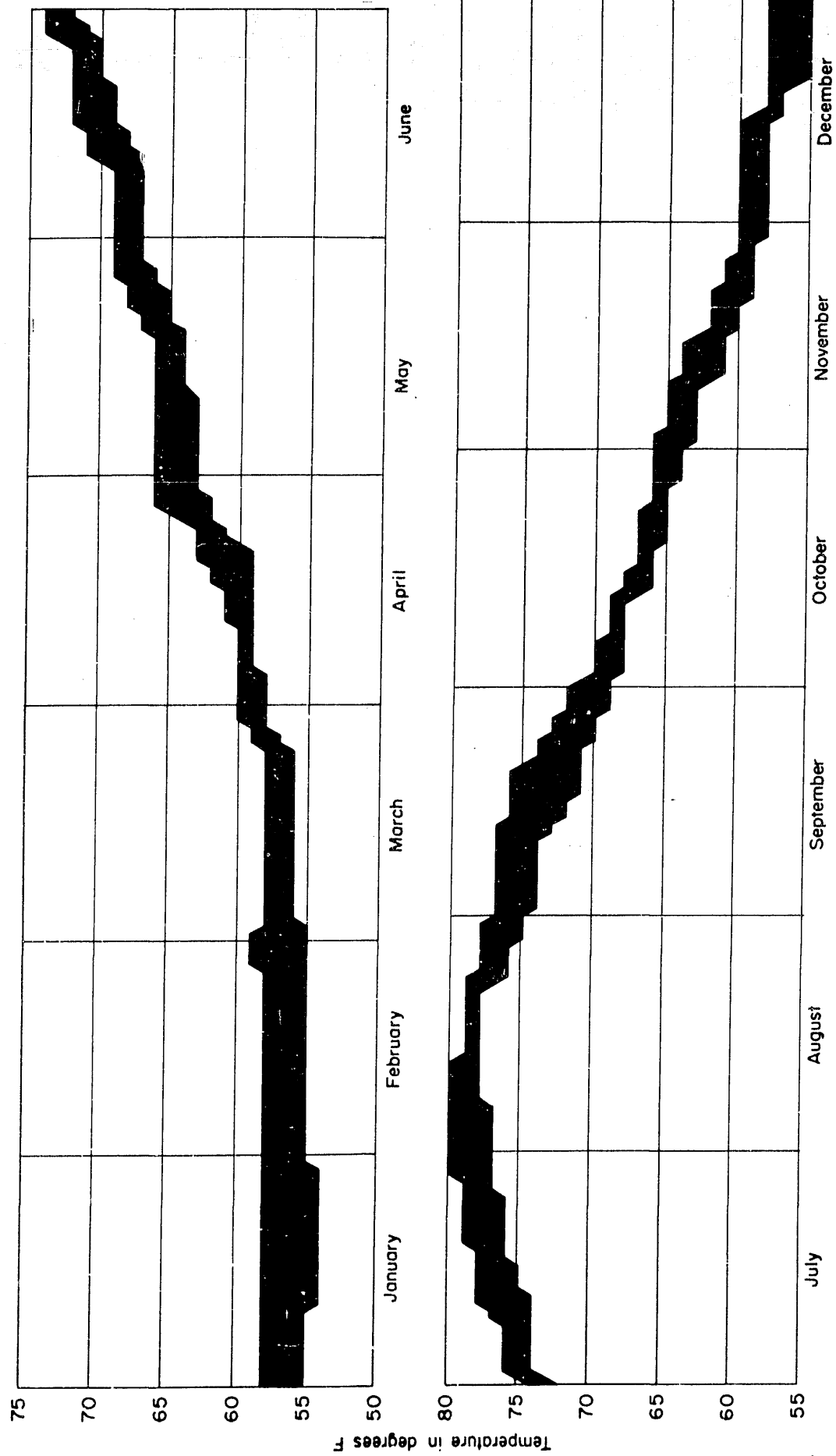


FIGURE 12.—Water temperature in the U.S. Experimental Model Basin versus calendar date for the years of 1913 to 1918

The width of the line indicates the variation in temperature from year to year

On the above basis, curve A of Figure 13, apparently needs no alteration since it continues to be constant at low speed-length ratios. This indicates that turbulent flow was probably attained in this case owing to one or more of the following variables: the higher water temperature, the shape of the model, the surface finish of the model, and the initial turbulence in the basin. Curve B, however, drops off considerably below a speed-length ratio of 0.55, which corresponded to a Reynolds number of 8.3×10^6 for the test. Consequently, applying the aforementioned procedure, the constant value of the coefficient is extrapolated as shown by the broken line.

Although this procedure for correcting for the effects of transitional flow is not rigorous, a number of recent tests of 20-foot models which were towed with and without a turbulence-stimulating device indicated that in general such conditions obtain for models which experience only

minor transitional effects at the lowest speeds. In such cases, the residual-resistance coefficient curves from the model experiments without turbulence stimulation, faired according to this procedure, have agreed reasonably well with those resulting from the tests with present types of turbulence devices. It is realized that such agreement does not completely establish the validity of the aforementioned procedure for correction of transitional flow effects since the problem of turbulence stimulation on ship models is not fully understood at the present time. However, it is believed that the corrections made in this work according to this procedure will prove to be reasonably good assumptions.

Experience has shown furthermore that 20-foot models with the Taylor Series type of bow, i.e., a bow with a vertical stem profile and with pronounced "U" sections, are less susceptible to laminar flow than bow shapes

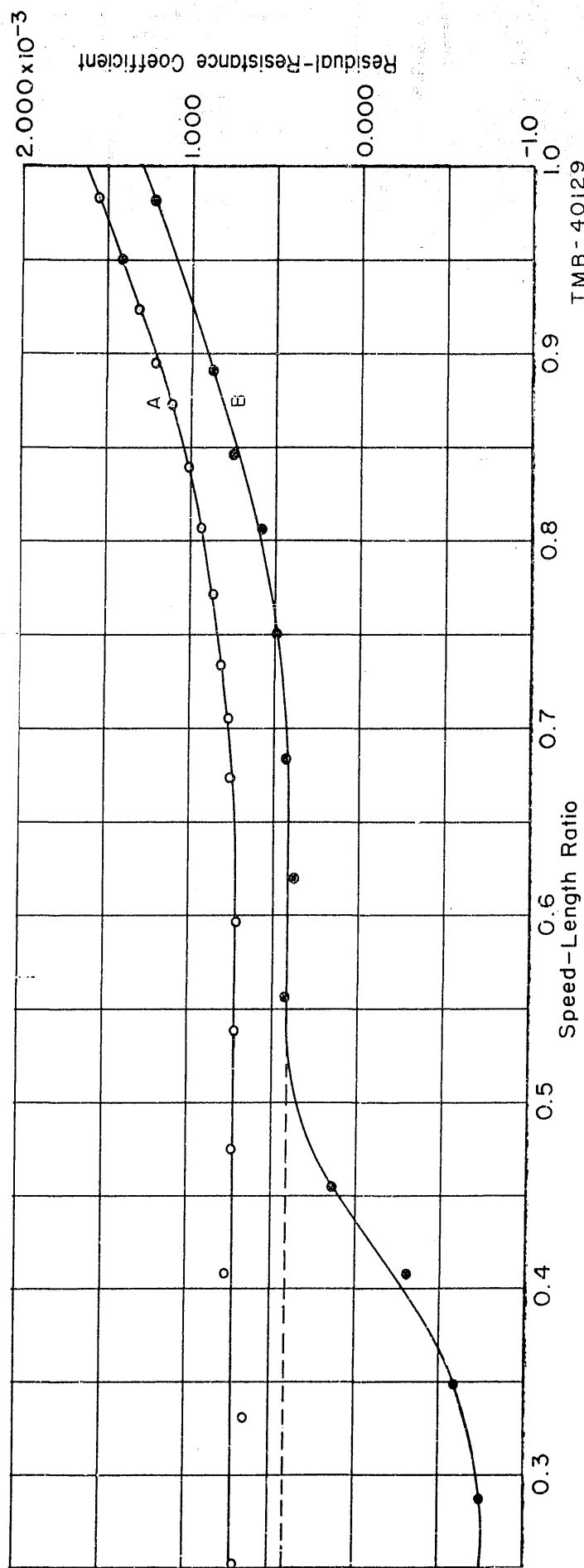


FIGURE 13.—Curves of residual-resistance coefficient versus speed-length ratio, showing typical data spots

Curve A is for a Taylor Series vessel with $C_p = 0.56$, $B/H = 2.25$, and $C_{\text{TP}} = 7.76 \times 10^{-3}$. Curve B is for a Taylor Series vessel with $C_p = 0.56$, $B/H = 2.25$, and $C_{\text{TP}} = 5.58 \times 10^{-3}$

which involve a raked stem and "V" sections. This effect is believed to be related to the pressure distribution characteristics associated with flow around the bows of the models. The degree to which models with U-type bows are affected by transitional flow was demonstrated by two 20-foot Taylor Series models, having longitudinal prismatic coefficients of 0.613 and 0.746, which were tested at the Taylor Model Basin in 1951.⁴ In both cases, it was found that turbulence stimulation was required only at low speeds and that the assumption of constancy of the residual-resistance coefficient at these low speeds gave reasonable agreement with the turbulent curve.

At longitudinal prismatic coefficients above 0.74, it became increasingly more difficult to establish the "plateau" in the residual-resistance coefficient curves of the Taylor Series models. This was essentially due to two reasons. First, the existence of more pronounced stabilizing pressure gradients for the fuller models caused the laminar flow at the bow to persist to higher Reynolds numbers. Second, the establishment of wavemaking humps at low Froude numbers made it more difficult to assess the speed at which laminar flow became unimportant. Fortunately, since the major part of the test data did not suffer from these defects, it was possible, by the process of cross-fairing on the related parameters for the series, to deduce reasonable values in these more difficult cases. However, in a few cases the highest values of longitudinal prismatic coefficient occur with the highest values of volumetric coefficient to become end points in the cross-fairing and therefore should be viewed with suspicion. These cases generally occur in a regime which is little used in actual ship design and consequently their accurate determination is somewhat academic.

RESTRICTED CHANNEL CORRECTIONS

It had been suspected for a long time that the cross-section of the U. S. Experimental Model Basin was not large enough to tow full-bodied 20-foot models without some restricted channel effect being present. Calculations based on existing restricted channel formulations tended to verify this suspicion.⁷ Furthermore, correlation tests of several 20- and 30-foot models, which were originally tested at the Experimental Model Basin, were made at the Taylor Model Basin in 1940 and 1941. These comparative tests exhibited trends for the larger and

fuller models at high speeds which could reasonably be due to the restricted channel effect. In view of the foregoing, it was considered desirable to incorporate restricted channel corrections in the reanalysis of the Taylor Standard Series.

The method selected to compensate for the restricted channel effects was the semi-empirical method of Reference 7. Since this procedure was developed for the general case, it is somewhat cumbersome for application to a large mass of data. The existence of certain fixed parameters in the present case has enabled the development of the following new procedure which greatly simplifies the restricted channel corrections in calculations of this kind. To avoid conflicts with existing notation, the superscripts prime (') and double prime (") are used in this section to denote quantities which apply to speed in a restricted channel and to "Schlichting's intermediate speed," respectively. The remaining quantities without the primes are the values sought for the unlimited case.

The procedure for deducing the corrections to be made for restricted channel effect is based upon two assumptions which may be summarized as follows:⁷

1. The theoretical assumption that the wavemaking resistance at "Schlichting's intermediate speed" v'' is equal to the wavemaking resistance at a corresponding speed in deep water v . The relation between v'' and v is given from wave theory by the formula

$$\left(\frac{v''}{v}\right) = \tanh\left(\frac{gd}{v^2}\right) \quad [12]$$

where d is the depth of the channel and g is the acceleration due to gravity.

2. The empirical assumption that the change in displacement flow around the ship or model hull due to limitations in depth or width of the channel necessitates a correction to the intermediate speed v'' to give the speed v' of the ship or model relative to the channel. This relationship is derived from systematic tests in restricted channels and is given as an empirical curve of the form⁷

$$\frac{v'}{v''} = \phi\left(\frac{2\sqrt{A_x}}{r}\right) \quad [13]$$

but has been changed herein to the more inclusive relationship

$$\frac{v'}{v''} = \varphi \left(\frac{\sqrt[3]{A_x L}}{r} \right) = \varphi (F_d) \quad [14]$$

where F_d is the displacement-flow parameter, A_x is the midship section area of the vessel, L is the waterline length of the vessel, and r is the hydraulic radius and is equal to

$$\frac{w d - A_x}{w + 2d + G} \quad [15]$$

where w is the width of the channel and G is the wetted girth of the vessel at the midship section.

The relationships between the various components of resistance which arise from the two foregoing assumptions are as follows:

$$R_t' = R_t - R_f + R_f'' \quad [16]$$

or

$$R_r = R_r' + R_f' - R_f'' \quad [17]$$

where R_t is the total resistance,

R_f is the frictional resistance, and

R_r is the residual resistance.

The superscripts or lack thereof denote the appropriate speeds for which the quantities are determined either by test measurement or by calculation using the stated formulas or empirical relationships.

The dimensional quantities given in Equation [17] can be converted to coefficient form as follows:

$$R_r = \frac{\rho}{2} S v^2 C_r = K v^2 C_r \quad [18a]$$

$$R_r' = \frac{\rho}{2} S (v')^2 C_r' = K (v')^2 C_r' \quad [18b]$$

$$R_f' = \frac{\rho}{2} S (v')^2 C_f' = K (v')^2 C_f' \quad [18c]$$

$$R_f'' = \frac{\rho}{2} S (v'')^2 C_f'' = K (v'')^2 C_f'' \quad [18d]$$

where C_r is the residual-resistance coefficient, C_f is the frictional-resistance coefficient, and the same convention is applied to the superscripts.

Equation [17] can now be restated as follows:

$$K v^2 C_r = K (v')^2 C_r' + K (v'')^2 C_f' - K (v'')^2 C_f'' \quad [19]$$

and rearranging

$$C_r = C_r' \left(\frac{v'}{v} \right)^2 + C_f' \left(\frac{v'}{v} \right)^2 - C_f'' \left(\frac{v''}{v} \right)^2 \quad [20]$$

or

$$C_r = C_r' \left(\frac{v'}{v} \right)^2 + C_f' \left(\frac{v'}{v} \right)^2 - C_f'' \left(\frac{v''}{v} \right)^2 \left(\frac{v'}{v} \right)^2 \quad [21]$$

thus

$$C_r = \left\{ C_r' + \left[C_f' - C_f'' \left(\frac{v''}{v'} \right)^2 \right] \right\} \left(\frac{v'}{v} \right)^2 \quad [22]$$

Let

$$\Delta C_r = C_r'' \left(\frac{v''}{v'} \right)^2 - C_f' \quad [23]$$

Then

$$C_r = (C_r' - \Delta C_r) \left(\frac{v'}{v} \right)^2 \quad [24]$$

To deduce the values of C_r versus speed-length ratio in an unrestricted channel from the corresponding values in a restricted channel, it has been found convenient to resort to the three sets of auxiliary curves given in Figure 14. Each set of curves consists of contours of equal values of the displacement-flow parameter F_d plotted on the common abscissa of speed-length ratio in a restricted channel. The ordinate in each case is a dependent variable whose numerical value can be used directly with Formula [24] to arrive at the unrestricted channel values of C_r and the appropriate speed-length ratios. The curves

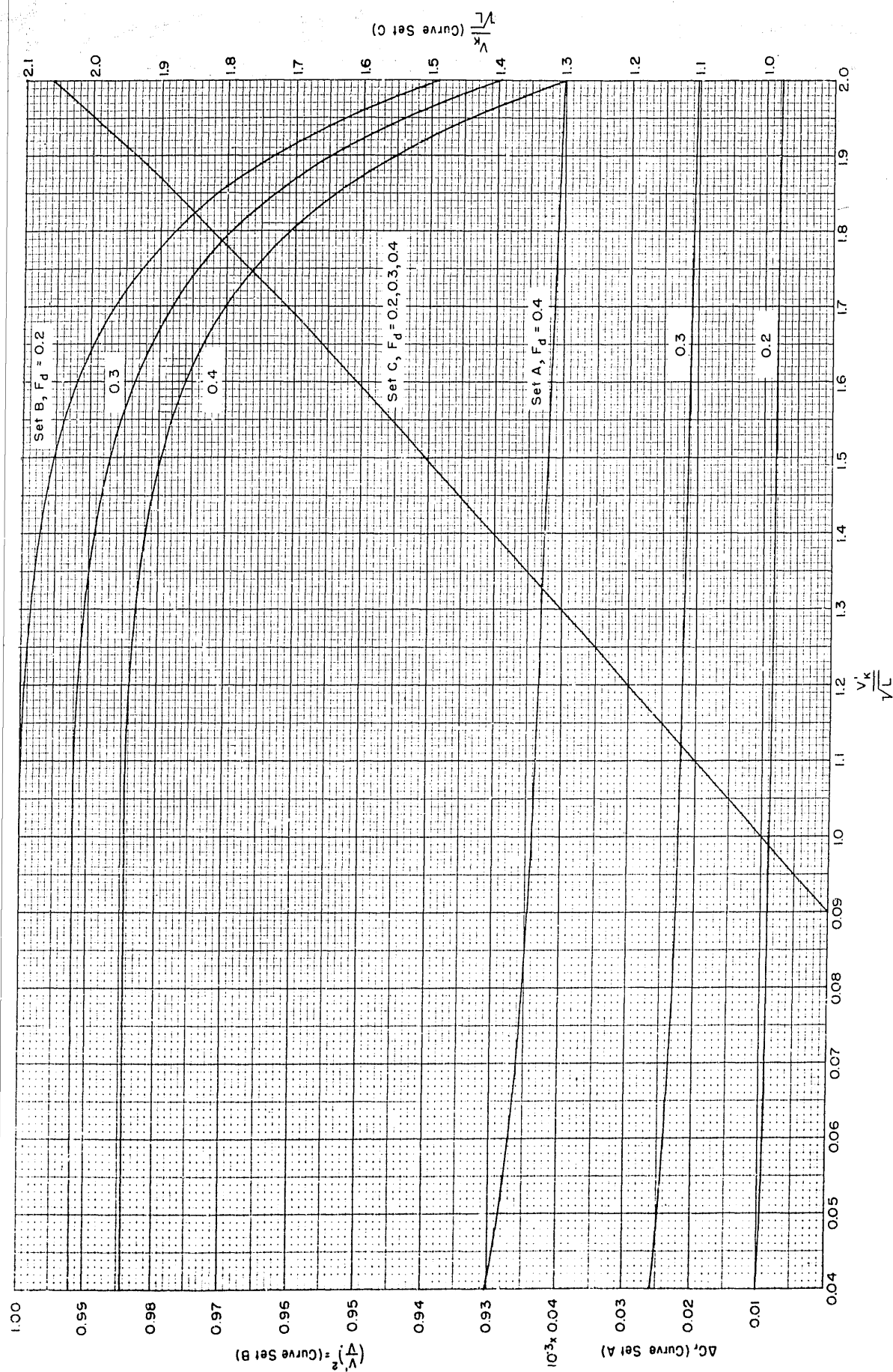


FIGURE 14.—Auxiliary charts for restricted channel corrections to the Taylor Series Models tested in the U. S. Experimental Model Basin

were derived using the speed relationships denoted by Equations [13] and [14], the corresponding Reynolds numbers, and the resulting Schoenherr frictional-resistance coefficients. Curve set A is used to determine ΔC_r which is subtracted from C_r to give a net value based on the speed in a restricted channel. Curve set B is used to obtain $\left(\frac{v'}{v}\right)^2$ which, when multiplied by the net value, gives the C_r for an unrestricted channel. Curve set C is used to convert the speed-length ratio from the restricted to unrestricted values. It may be noted that curve C is a single curve in the range of values required for the restricted channel corrections for the Taylor Series.

The procedure for applying the restricted channel correction to the faired C_r versus speed-length ratio data for a typical Taylor Series model is shown by the following numerical example:

Reference is made to the curve in Figure 15. For illustrative purposes, assume the speed-length ratio in a restricted channel to be 1.20. Then the uncorrected C_r taken from Figure 15 is 6.750×10^{-3} . The value of F_d for this model operating in the Experimental Model Basin is calculated from Formula [14] and is equal to 0.335. Entering Figure 15 with this value of F_d , $\Delta C_r = 0.0290 \times 10^{-3}$ from curve set A and $\left(\frac{v'}{v}\right)^2 = 0.9890$ from curve set B. Then from Formula [24], the value of C_r in an unrestricted channel is

$$(C_r' - \Delta C_r) \left(\frac{v'}{v}\right)^2 = (6.750 \times 10^{-3} - 0.0290 \times 10^{-3}) 0.9890 \\ = 6.647 \times 10^{-3}$$

Entering curve set C with the assumed value of 1.20 for the speed-length ratio in a restricted channel gives, in this case, the unchanged value of 1.20 for the restricted channel. These values are plotted with other values similarly obtained to give the corrected curve shown by the broken line in Figure 15.

Since the U. S. Experimental Model Basin does not have a rectangular cross section, the characteristic depth d which was used in the calculations was taken as the perpendicular distance from the centerline of the basin at the water surface to the nearest side of the basin. This gave a value of 13.6 feet as compared to the maximum depth on centerline of 14.0 feet.

It should be mentioned that the restricted channel corrections which were applied to the Taylor Series data were generally found to be quite small. The largest correction amounted to a decrease of approximately 2 percent of the predicted effective horsepower for a geometrically similar 400-foot vessel operating in salt water at a temperature of 59F. It is believed, however, that the corrections were significant and should not have been neglected since the cross-fairing of the residual-resistance coefficient curves was improved thereby and many inconsistencies eliminated.

CROSS-FAIRING OF RESISTANCE DATA

After the residual-resistance coefficient versus speed-length ratio curves were initially faired and the corrections for transitional flow and restricted channel effect applied, it remained to cross-fair the C_r against the geometrical parameters C_p , C_F and B/H . There were only three variations of B/H in the series as compared to a minimum of six variations of C_F and eight variations of C_p . Consequently, the latter two parameters were given the most consideration in the cross-fairing process.

The fairing procedure was as follows: From the faired curves of C_r versus speed-length ratio, for constant values of B/H and speed-length ratio, values of C_r were read and plotted against C_p for each of the given values of C_F . When faired, these data formed a set of contours of the type shown in Figure 16. In general, the curves of this type characteristically indicated a minimum value of C_r somewhere between C_p values of 0.52 to 0.66. Again at fixed values of B/H and speed-length ratio, cross curves of C_r versus C_F were prepared for even values of C_p using the faired values which were read from curves of the type illustrated in Figure 16. The resulting faired contours are exemplified by Figure 17. These contours showed a progressive increase of C_r with C_F and were in most cases very nearly linear. The sets of contours showing the variation of C_r with C_p were then cross-faired with the sets of contours showing the variation of C_r with C_F . This was accomplished by making minor adjustments in each of the sets until faired curves were obtained which satisfied the condition that each point on the C_r versus C_p contours was equal to the corresponding point on the C_r versus C_F contours. At this stage, the faired values from these two sets of contours were plotted against B/H for fixed values of C_p , C_F , and speed-length ratio in incremental steps

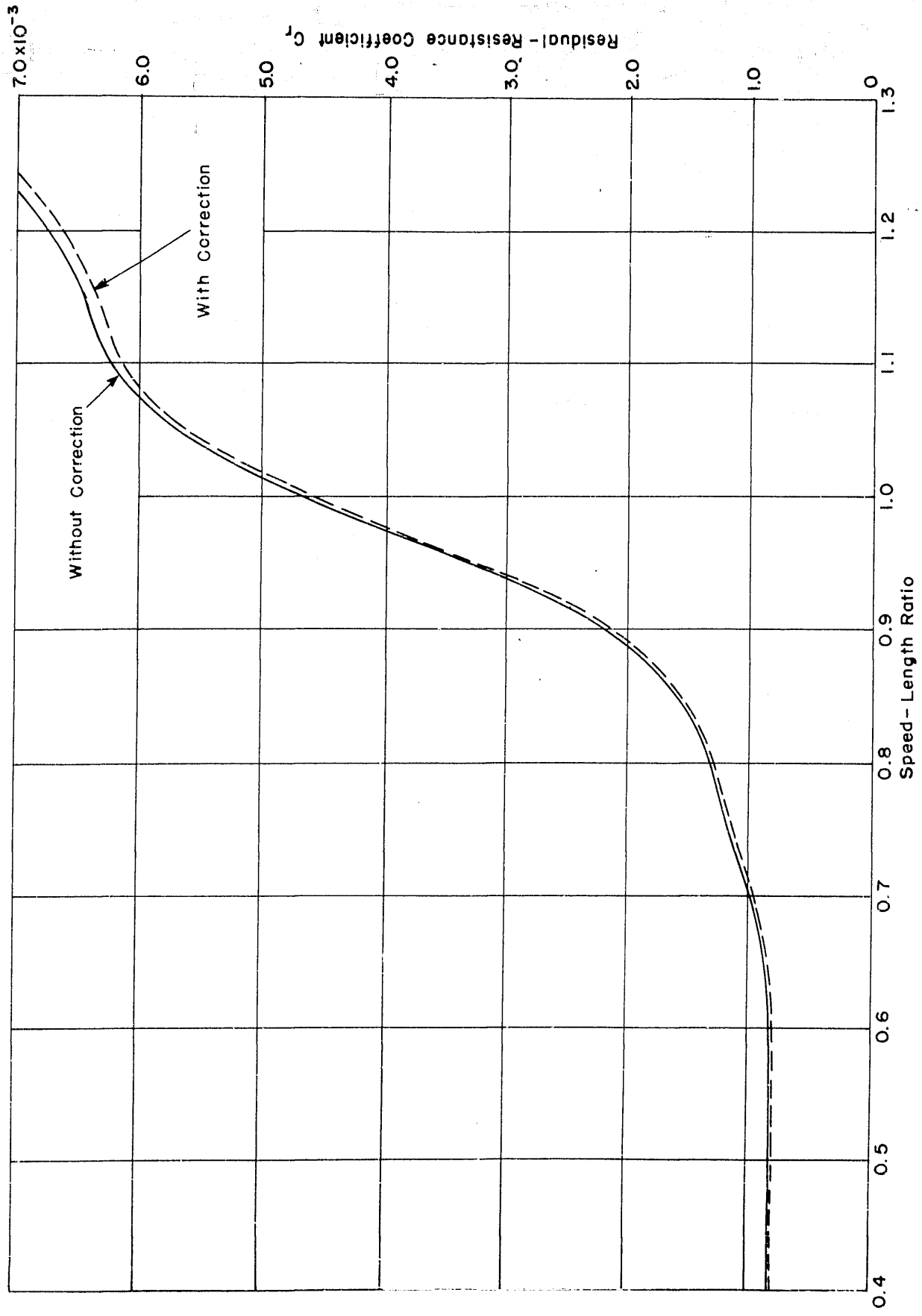


FIGURE 15.--Sample curve of residual-resistance coefficient versus speed-length ratio, showing restricted channel corrections

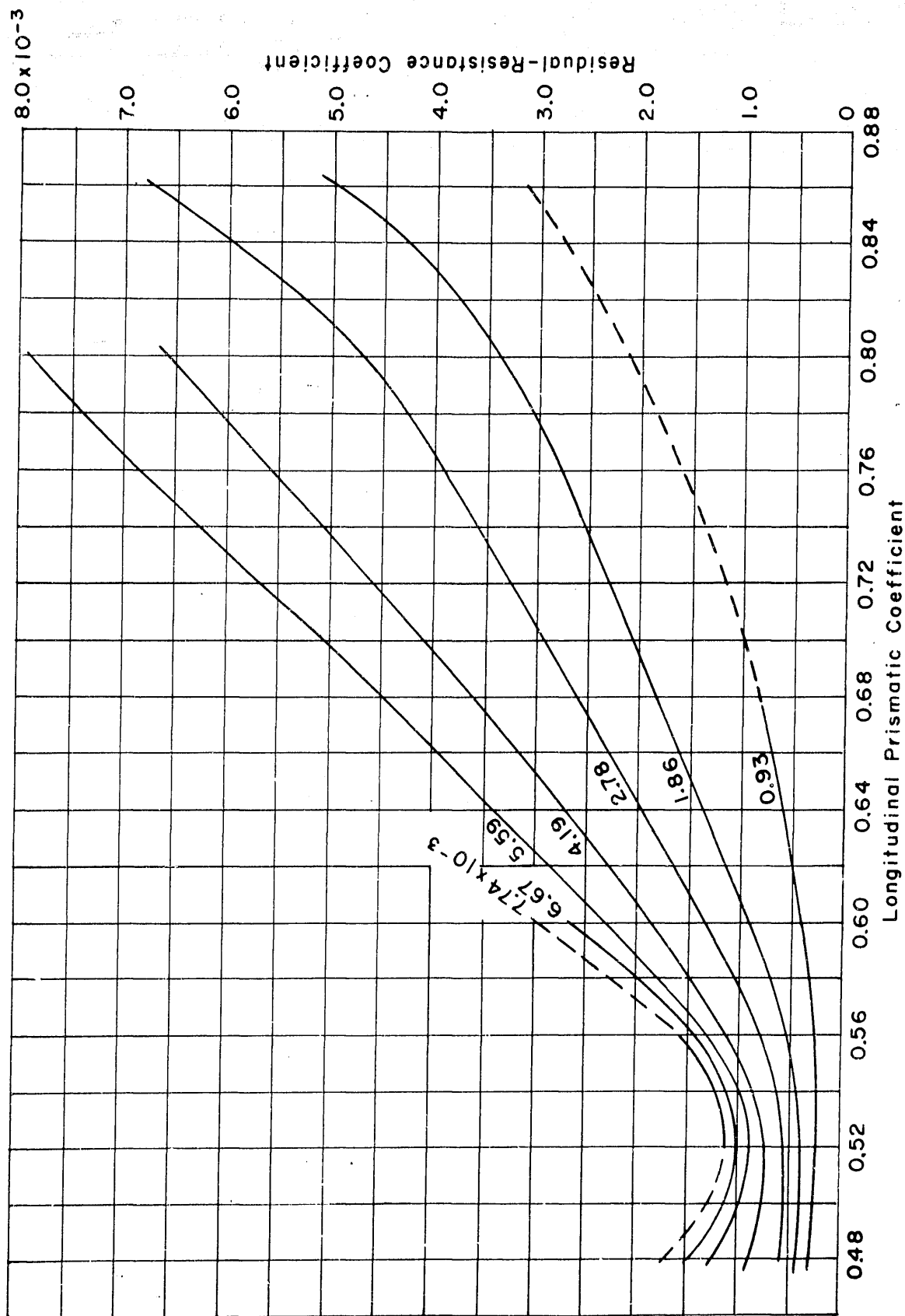


FIGURE 16.--Curves of residual-resistance coefficient versus longitudinal prismatic coefficient for equal values of volumetric coefficient

The curves are for fixed values of beam-draft ratio of 2.25 and speed-length ratio of 1.0

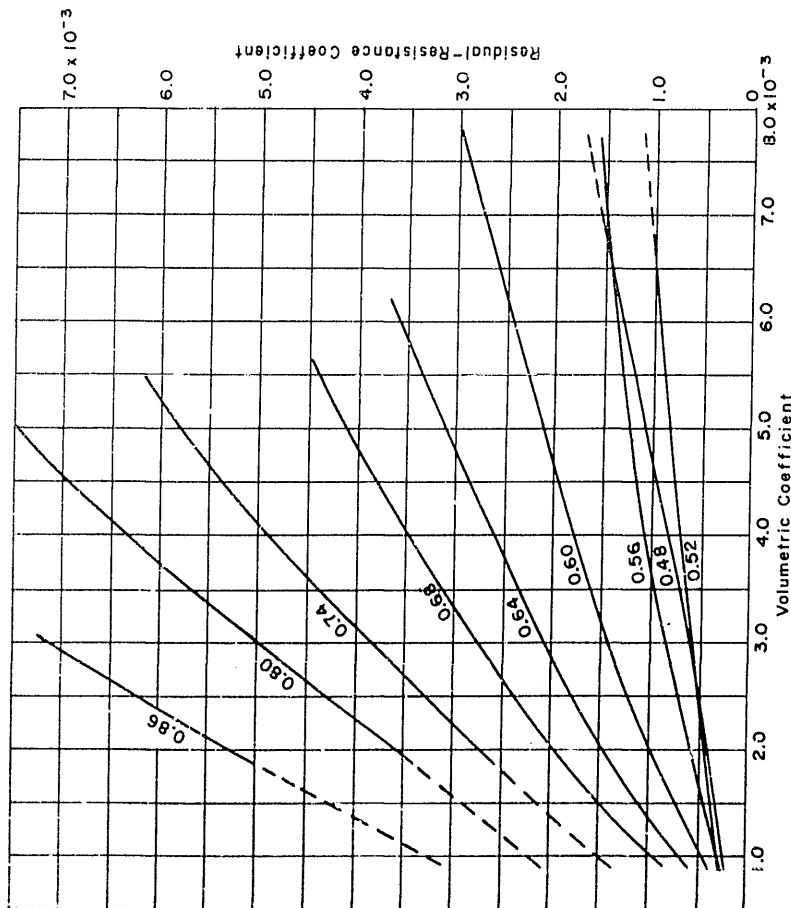


FIGURE 17.--Curves of residual-resistance coefficient versus volumetric coefficient for equal values of longitudinal prismatic coefficient

The curves are for fixed values of beam-draft ratio of 2.25 and speed-length ratio of 1.0

covering the range of the series. Any inconsistencies indicated in the B/D variation curves were similarly rectified by making adjustments in the other two sets of contours. Finally, the cross-faired values were replotted back on the original curves of C_r versus speed-length ratio. This was done not only to assure fairness in this view but to observe whether, in the cross-fairing process, significant departures were made from the original data spots.

It should be mentioned that, during the fairing process, special effort was made to adhere as strictly as possible to the original data which were corrected according to the aforementioned procedures. The humps and hollows normally found in resistance curves were retained. It was

gratifying to find that the data above speed-length ratios of 0.6 were excellent, even judging by present day standards. It was observed in this regime that, excluding a few obviously wild points, deviations of individual original data spots from the faired curves were less than 1 percent of the total resistance for C_p values up to 0.68 and less than 3 percent beyond this range. At the lower speed-length ratios, since the C_r is such a small percentage of the total-resistance coefficient in all cases, it is believed that through the combination of the corrections applied and the cross-fairing, very good standards of accuracy have been maintained.

During the cross-fairing process, curves of residual-resistance coefficient versus speed-length ratio were produced for a beam-draft ratio of 3.00 instead of the 2.92 used on the original models. This was done to provide an even value for interpolation purposes in the final presentation.

It would be of interest to compare the results obtained from the reanalysis of the original Taylor Series data with modern test results of Taylor Series models. Fortunately, the results for two Taylor Series models, which were recently constructed and tested at the Taylor Model Basin, are available.⁴ The residual-resistance coefficients for these models are compared in Figure 18 with the values interpolated from Appendices 3 and 4. It may be seen that for the fuller model, there is close agreement up to a speed-length ratio of 0.8 which, in general, represents the practical range for vessels of such characteristics. The maximum deviation in this range occurs at a speed-length ratio of 0.72 and amounts to less than 2 percent of the total model resistance. For the finer model, almost perfect agreement is obtained above a speed-length ratio of 0.9 which represents the range of most interest for vessels of such characteristics. The maximum deviation is obtained below this range at a speed-length ratio of 0.72 and amounts to approximately 3 percent of the total model resistance. It may also be noted that the wetted-surface coefficients which were calculated from measurements of the new models agree with in 0.1 percent of the values read from the contours of Appendix 2.

FINAL PRESENTATION OF DATA

The Taylor Standard Series was not only a comprehensive undertaking but also one which involved a program of

model construction and testing which could be reproduced at the present day only by large expenditures in time and money. Consequently, it seems only fitting that a special effort should be made to present the reanalyzed data in a form which will be most convenient and useful to the majority of the members of the profession. Obviously, the methods of presenting these data are numerous, and, while it seems worthwhile to present the same data in several different forms for the convenience of specialized groups, it is not always practical to do so. Therefore, the approach

used herein is to make one type of presentation of the data which can be universally applied, to suggest other methods of presentation, and to provide auxiliary curves to assist in rapid conversion of the generalized curves to some of the other desirable specialized curves.

The methods of presenting resistance data can be classified into two general types: one which facilitates the calculations for specific geometrically similar prototypes and a second which presents "merit" relationships, that is,

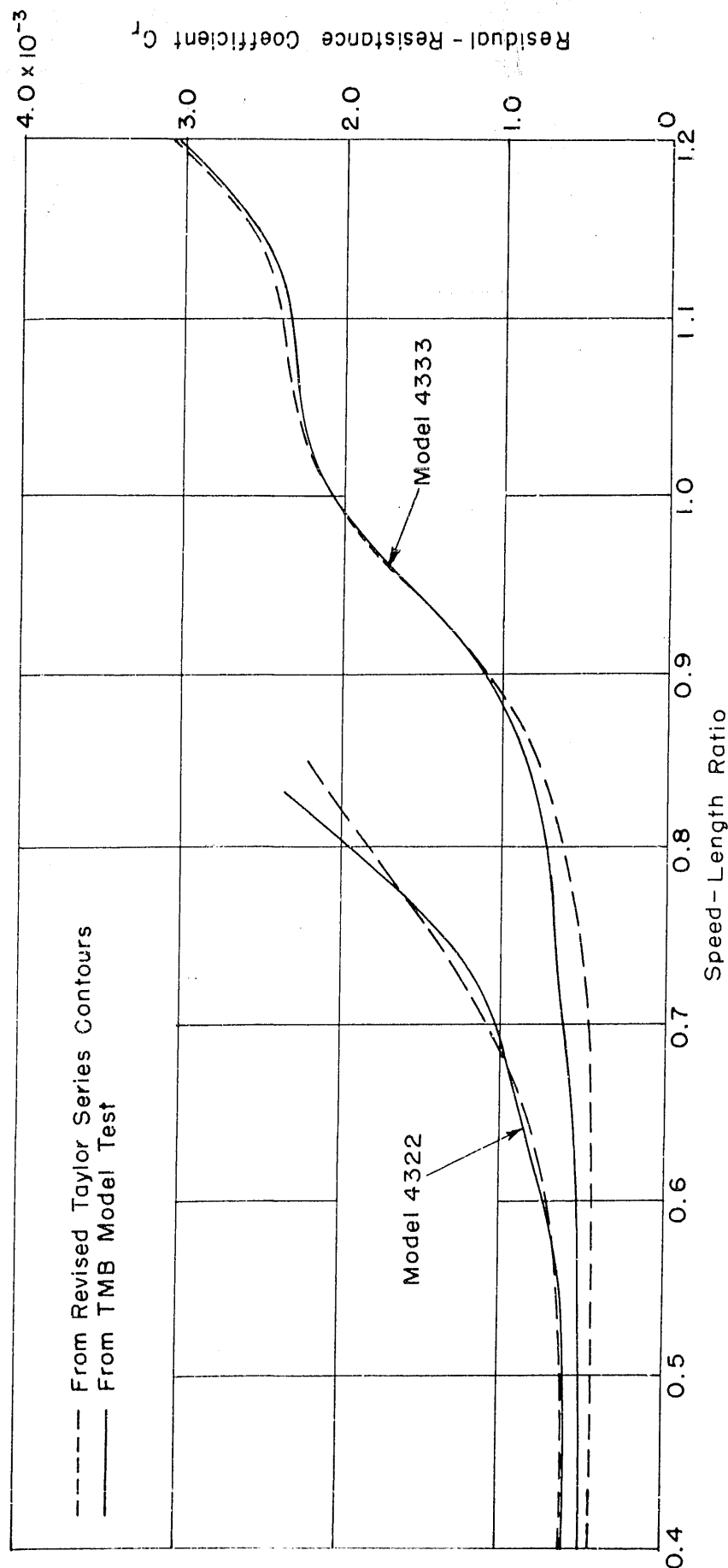


FIGURE 18.--Comparison of the residual-resistance coefficients obtained from tests of new Taylor Series Models with values read from contours of appendices 3 and 4

Model 4322 has the following characteristics:
 $C_p = 0.746$, $C_M = 5.26 \times 10^{-3}$, and $B/H = 2.50$. Model 4333 has the following characteristics: $C_p = 0.613$, $C_M = 4.05 \times 10^{-3}$, and $B/H = 2.50$

either qualitative or quantitative changes in resistance which would be expected to result from the variation of form parameters. A single method of presentation cannot efficiently combine these functions because the conflict in the dependency of components of resistance on the Froude and Reynolds laws requires the assignment of specific dimensions and conditions to establish true merit comparisons. Consequently, for more universal application, the primary method of presentation used here belongs to the first category.

The nondimensional coefficient which has been adopted to represent the resistance data is the residual-resistance coefficient. This coefficient is used in place of Taylor's well-known residual-resistance per ton of displacement. The speed-length ratio used by Taylor has been retained as the speed parameter, although it is not nondimensional both from the standpoint of the lack of \sqrt{g} in the denominator and the use of specified English units in its definition. An alternate scale of Froude number is provided, however, to facilitate international use.

The format used in the presentation also differs from that given in Taylor's "Speed and Power of Ships." It consists of curves of residual-resistance coefficient versus speed-length ratio (Froude number scale added) for various even values of volumetric coefficient. Separate families of curves are given for each longitudinal prismatic coefficient between 0.48 and 0.86 in increments of 0.01 for each of the three beam-draft ratios of 2.25, 3.00, and 3.75. For each family of curves, ranges of speed-length ratios of 0.5 to 1.0 and 1.0 to 2.0 are given on adjacent pages. The scale divisions, for both ordinate and abscissa, at the lower speed-length ratios are twice those of the higher range to permit accuracy of reading. To achieve the most efficient use of the grid, supplementary tables are provided for longitudinal prismatic coefficients above 0.80 where some of the residual-resistance coefficient curves are not constant below a speed-length ratio of 0.50. On each of the sets of curves, a decimal scale is used both for the low and high speed-length ratios to minimize errors of reading. The greatest magnification has been obtained by avoiding the use of overlapping scales. This has resulted in a small gap between the low and high speed-length ratio curves for a few of the higher values of longitudinal prismatic coefficient. This slight inconvenience is considered tolerable, however, in light of the improved scales for the remaining curves.

The use of the residual-resistance coefficient with the aforementioned format possesses several distinct advantages over the Taylor method:

1. Reference to only two pairs of pages is needed for a given case when an interpolation on $B//$ is required and only one pair of pages when such interpolation is not required.
2. The increments of longitudinal prismatic coefficient are small enough to give an accuracy in reading to the nearest five in the third significant figure without interpolation.
3. Interpolation on a given set of contours is along the ordinate and not normal to the contours, as in the original Taylor Series contours.
4. The values of the residual-resistance coefficient contours are read on the fine grid of the ordinate, permitting closer readings.
5. The shape of the residual-resistance coefficient versus speed-length ratio curves can be seen directly, showing significant features such as humps and hollows.
6. Values of residual-resistance coefficient can be read directly at uneven speed-length ratios or Froude numbers which correspond to even speed on the full-scale vessel. This permits computation of a single point, such as at the design speed, which is often all that is needed.
7. The residual-resistance coefficient curves of other vessels can be compared directly with those of the equivalent Standard Series vessels, an attribute which is desirable for preliminary analytical purposes.

An objection that has often been raised to the use of the residual-resistance coefficient as a parameter for residual resistance is that it contains the quantity wetted surface instead of the two-thirds power of the volume in the denominator. This objection is based on the premise that the residual resistance is a function of the immersed volume or displacement and not the wetted surface. This appears to be somewhat academic, however, when it is realized that neither the wetted surface nor the volume term implies any physical significance to the coefficient alone, but only serves to render the coefficient dimensionless. It can be further shown, by reference to the wetted-surface coefficients in Appendix 2, that the contours of residual-resistance coefficient for the various values of volumetric coefficient do not converge when C_r is redefined on the basis of volume to the two-thirds power. On the other hand, the present definition of the C_r is desirable

since it eliminates a step in the calculation of the effective horsepower. In this calculation, the C_r can be added directly to values of C_f , which can be represented by a single function of Reynolds number. A C_r based on volume to the two-thirds power would require either a conversion back to the definition based on wetted surface or separate calculations for values of a newly defined C_f for vessels of different immersed volumes but having equal Reynolds numbers.

Variations in the format for presenting the residual-resistance coefficients are shown in Figures 16 and 17. In addition, contours of C_r on C_p and C_T for even speed-length ratios, a format similar to the original Taylor Series contours, could be prepared. These are not considered desirable since small changes have a tendency to entirely change the appearance of such contours from one speed-length ratio to the next.

Merit relationships can be presented through the use of the so-called "circle coefficient" system which is widely used. The most popular presentation of this type consists of plots of \bar{C} versus \bar{K} . Fortunately, \bar{C} is simply related to the total-resistance coefficient C_t and can be readily obtained as follows:

$$\bar{C} = \frac{1000}{8\pi} \bar{S} C_t \quad [25]$$

where \bar{C} is the total-resistance coefficient, circle system, C_t is the total-resistance coefficient, \bar{S} is the wetted-surface coefficient, circle system, equal to $\frac{S}{L^{2/3}}$,

S is the wetted surface, and L is the immersed volume.

Since

$$C_s = \frac{S}{V^{1/3} L} = \bar{S} (C_T)^{1/6} \quad [26]$$

where C_s is the wetted-surface coefficient used in the reanalysis of Taylor's Series, L is the waterline length, and C_T is the volumetric coefficient,

then

$$\bar{C} = \frac{1000 C_s}{8\pi (C_T)^{1/6}} C_t = B C_t \quad [27]$$

where B is considered to be a function of C_s and C_T . The calculation of B from the contours of C_s versus C_T of Appendix 2 requires the use of tables of fractional powers or a log-log slide rule, facilities which are not always readily available. Consequently, it was considered desirable to prepare the specialized chart of Figure 19 which gives values of B for the range of values of C_s and C_T which are covered in the Taylor Series.

The \bar{K} coefficient is simply related to the Froude number by the equation:

$$\bar{K} = \frac{v}{L^{1/6}} \sqrt{\frac{4\pi}{g}} = \frac{\beta}{(C_T)^{1/6}} (\sqrt{4\pi}) = D \beta \quad [28]$$

where \bar{K} is the speed coefficient,

v is the speed,

β is the Froude number,

g is the acceleration due to gravity, and

D is a function of C_T .

Again to avoid calculations involving fractional powers, a specialized chart is provided by Figure 20 for values of D in the range covered by the Taylor Series data. If it is desired to convert directly from values of speed-length ratio to D , the values in Figure 20 must be multiplied by 0.2978, a factor based on a value of g for the North Atlantic Ocean.

When the plots of \bar{C} versus \bar{K} are used for merit comparisons, it is customary to base the calculations on standard conditions which apply to a 400-foot prototype vessel operating in salt water of 3.5 percent salinity and a temperature of 59°F. This permits the preparation of a chart of Schoenherr frictional resistance coefficient versus \bar{K} , Froude number, or speed-length ratio, as shown in Figure 21. These values can be added directly to the values of residual-resistance coefficient obtained from Appendices 3, 4, and 5 for the appropriate case to give the total-resistance coefficients. Then, by use of Formulas [27] and [28] and Figures 19 and 20, the values of \bar{C} versus \bar{K} are readily obtained.

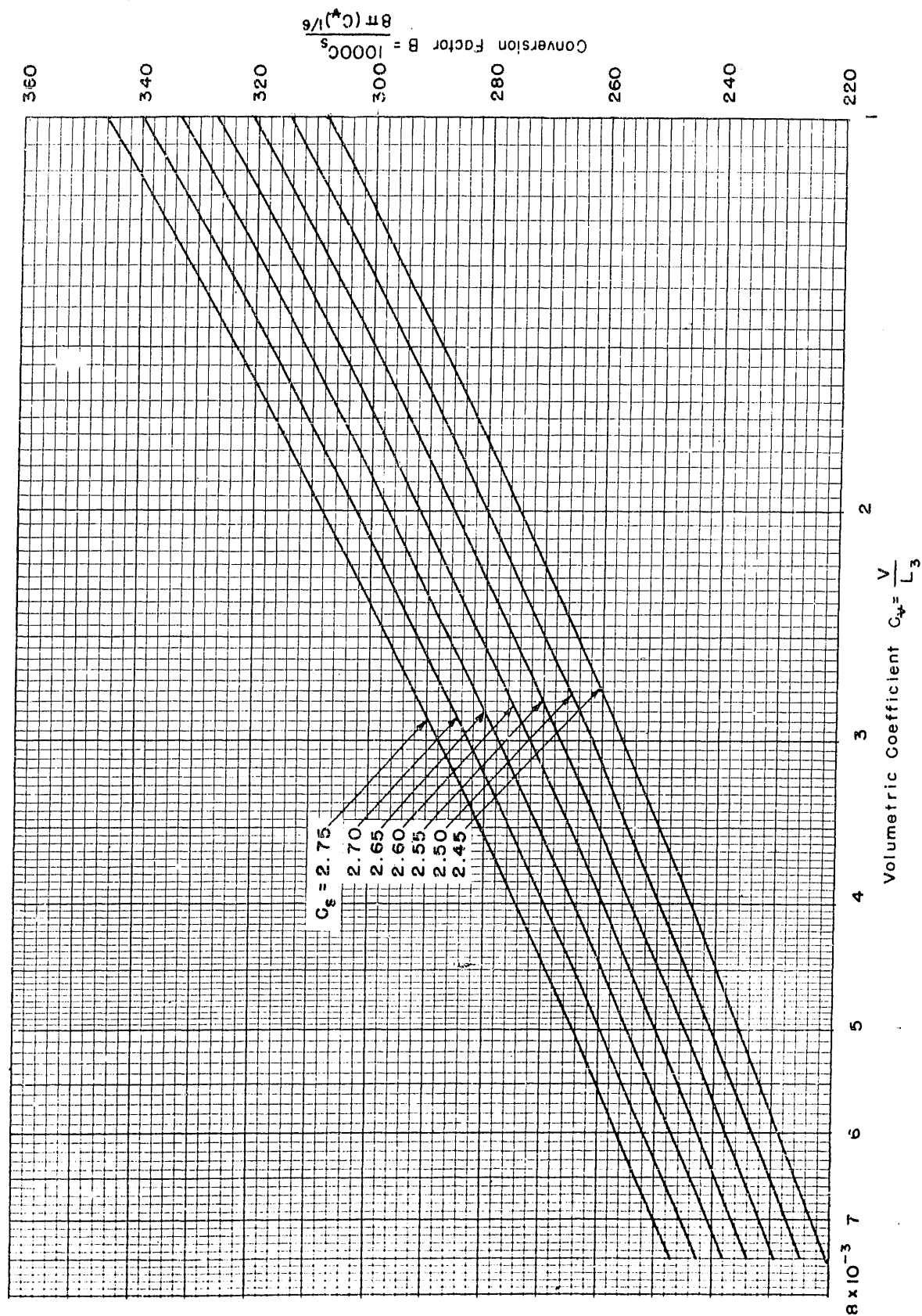


FIGURE 19.--Factors for converting the total-resistance coefficient C_t to the C resistance coefficient

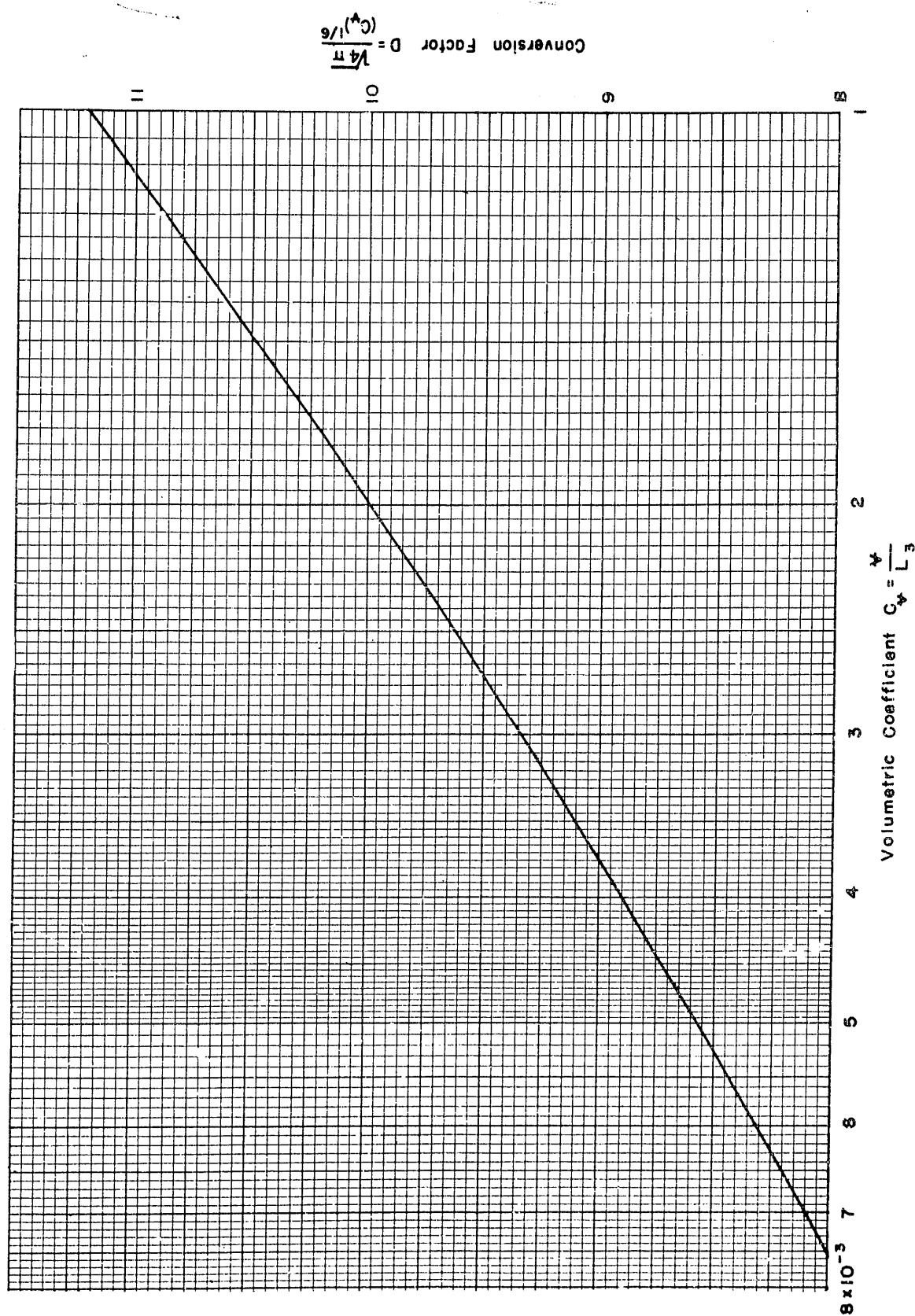


FIGURE 20.--Factors for converting the Froude number \bar{F} to the (K) speed coefficient

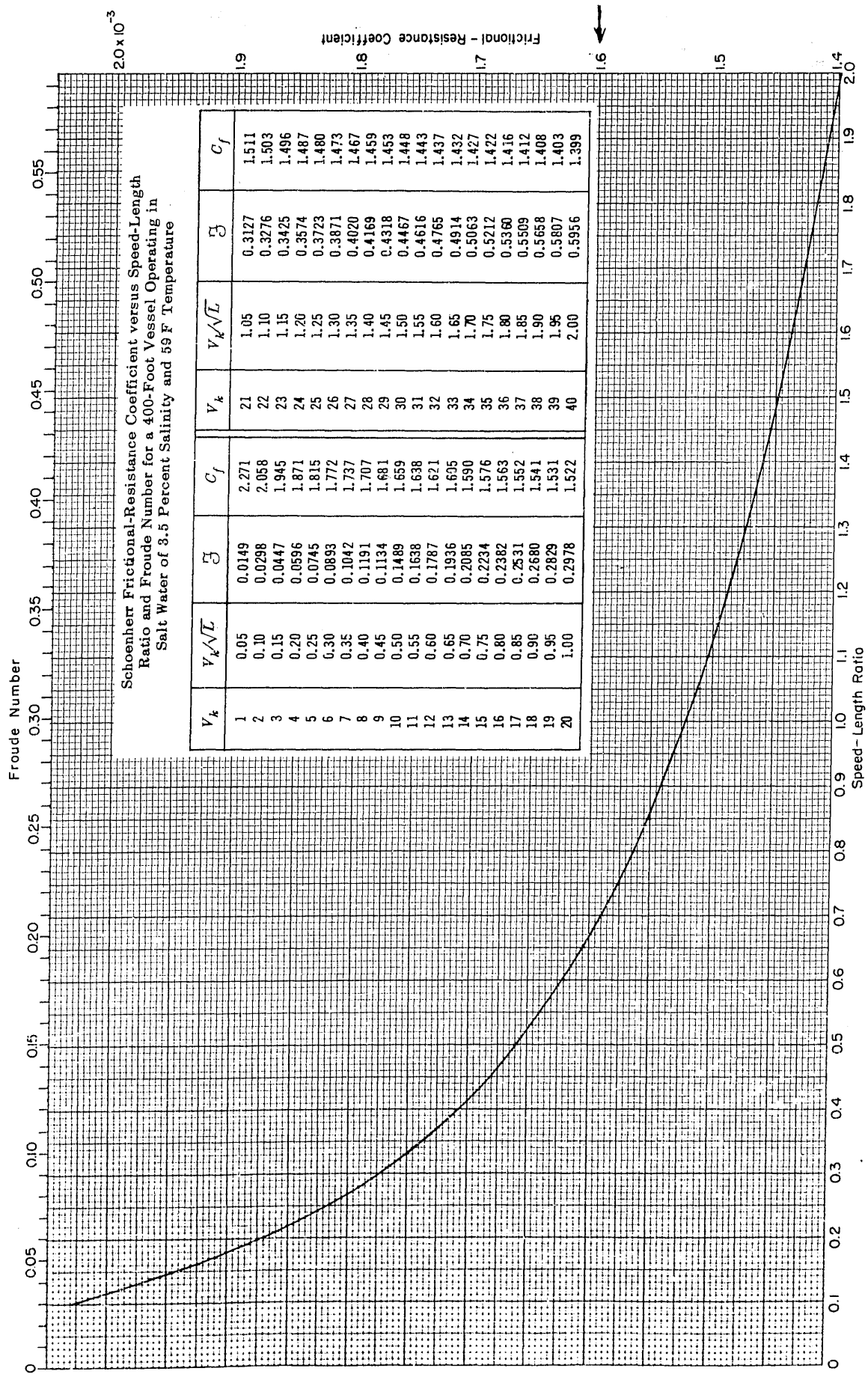


FIGURE 21.--Schoenherr frictional-resistance coefficients for a 400-foot vessel operating in salt water of 3.5 percent salinity and a temperature of 59F

Another device for showing merit relationships is exemplified in Figure 22. Here the effect of the variation in C_p for constant C_F is shown for each of the three values of R/H at each of several even speed-length ratios. The changes are shown as ratios of the effective horsepower to the minimum effective horsepower for each set of curves. The effective horsepower used to determine these ratios were calculated for the standard conditions of the 400-foot vessel operating in salt water of a temperature of 59F. The numerical values of these ratios apply reasonably to the second decimal place, however, to vessels ranging from 100 to 1000 feet in length.

The merit curves of the type shown in Figure 22 are also useful in the preliminary design stage for quickly reproducing the effective horsepower of a vessel of prescribed geometrical parameters if they are used in conjunction with curves of the type given in Figure 23. These are curves of effective horsepower for each of the minima shown in Figure 22 plotted against length for each of a number of even speed-length ratios. The effective horsepower for the desired vessel can be obtained by multiplying the effective horsepower from Figure 23 by the suitable ratios of Figure 22.

CALCULATION OF EFFECTIVE HORSEPOWER USING REVISED CONTOURS

Several methods of presenting the resistance data for the revised Taylor Series were suggested in the preceding section, and the method which uses the residual-resistance coefficient versus speed-length ratio curves was adopted for general application. The following discussion will demonstrate the use of these curves for specific types of calculations. The two most frequent uses of the original Taylor Series contours have been to estimate the effective horsepower of preliminary designs where only the overall dimensions and coefficients are known and to establish criteria for the performance of proposed and existing designs where either model or full-scale data are available. The method for accomplishing these types of calculations using the revised contours is shown in Table 6 by the sample form which briefly indicates the step-by-step procedure. The method is further illustrated by the following numerical example which involves a typical passenger vessel having the dimensions and coefficients given in Table 7.

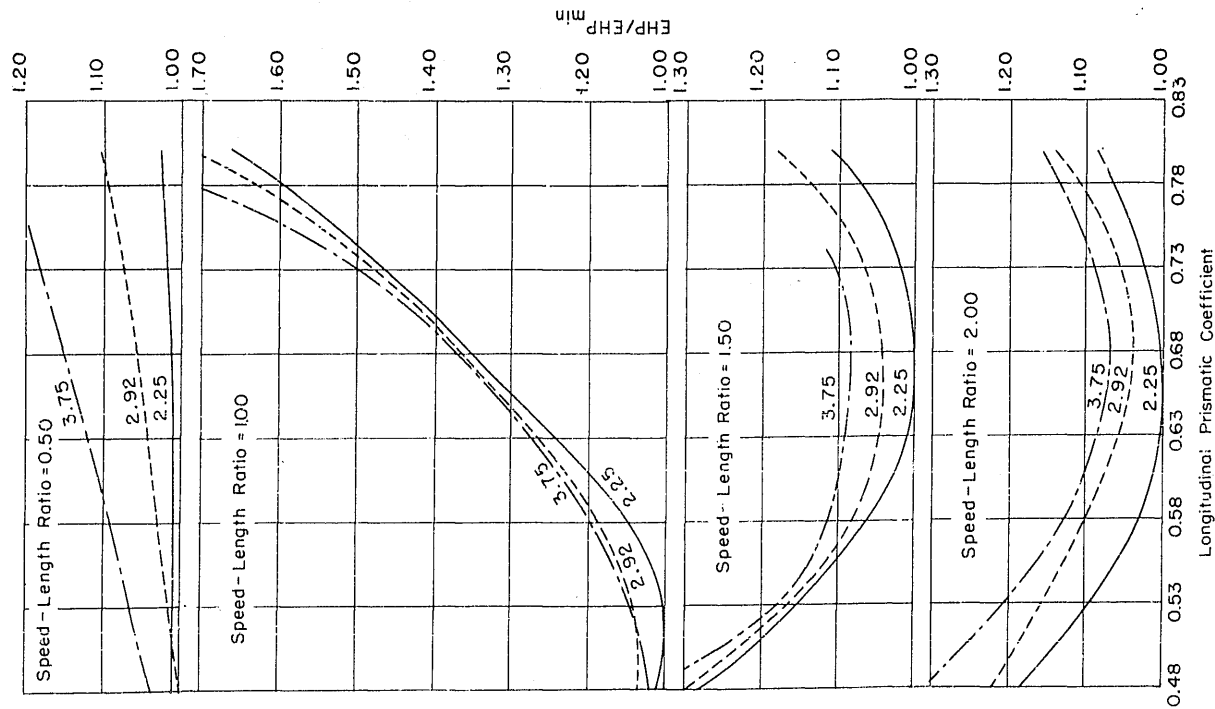
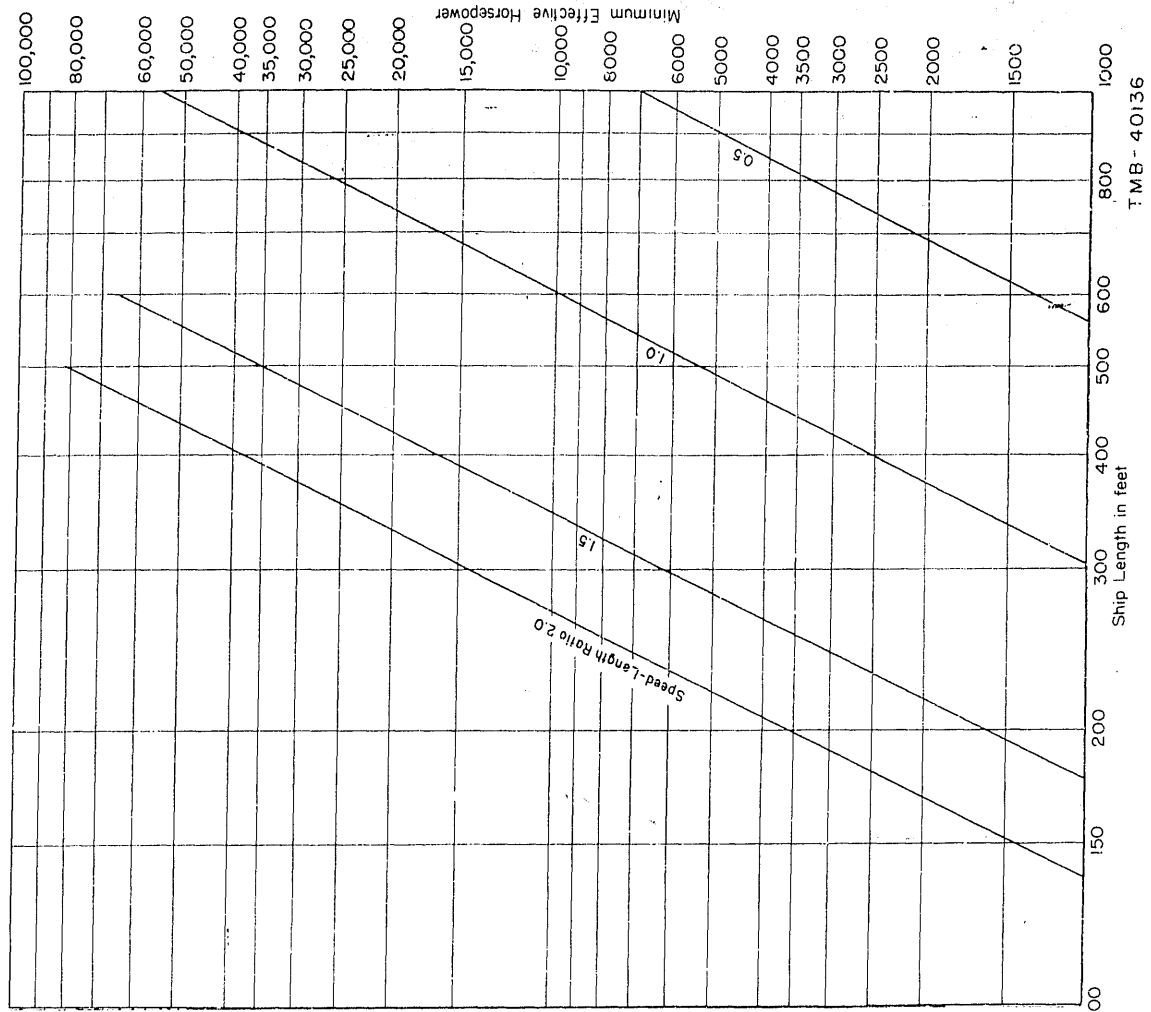
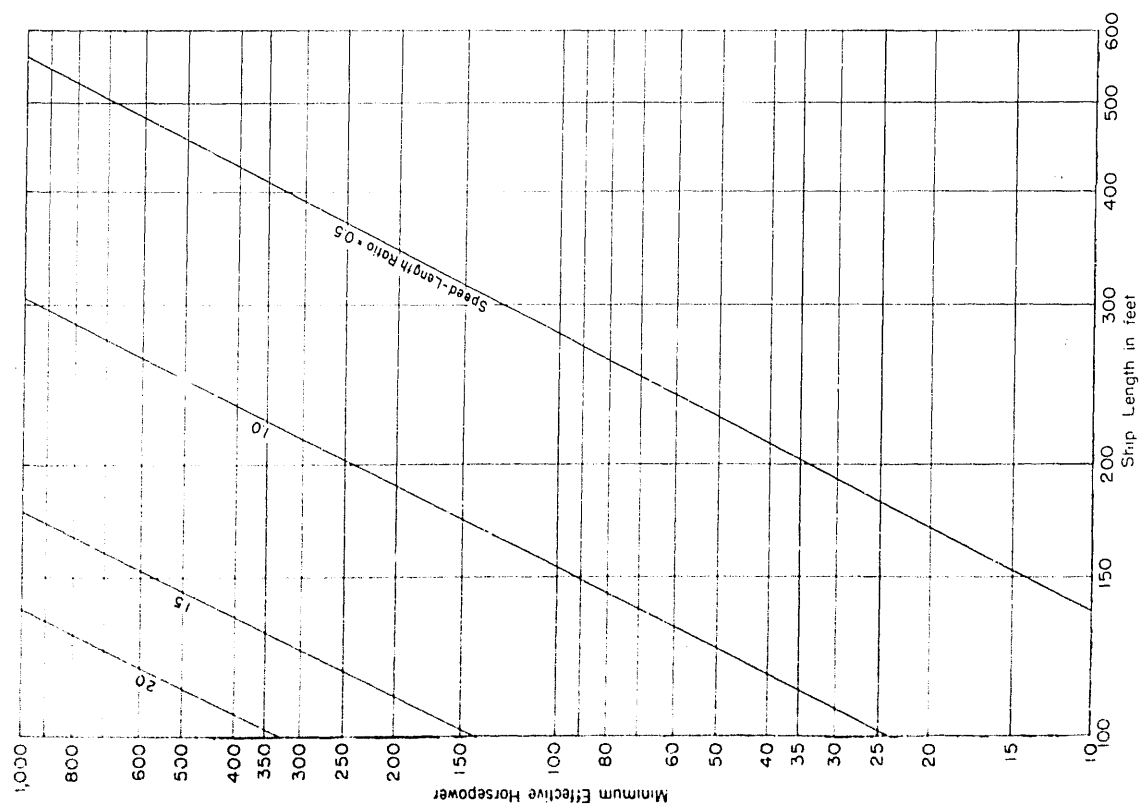


FIGURE 22.--The variation in effective horsepower of Taylor Series vessels with change in longitudinal prismatic coefficient for a volumetric coefficient of 1.5×10^{-3}

The effective horsepower pertain to a 400-foot ship operating in salt water of 3.5 percent salinity at a temperature of 59F and are expressed as ratios to the minimum EHP for each set of curves



TMB-40136

FIGURE 23.--The minimum effective horsepowers of Taylor Series Vessels of various lengths with a volumetric coefficient equal to 1.5×10^{-3}

SHIP-----MODEL-----

$$K = \frac{3.00 - \frac{B}{H}}{0.75} \quad A = 0.004380 \quad \rho, s' \quad \text{---}$$

COLUMN	PROCEDURE	COLUMN	PROCEDURE
1	From Formula 10 using speeds in Col. 17 with factor 1.689 to convert from knots to ft/sec	9	From Formula 9 using speeds in Col. 17 with factor 1.689 to convert from knots to ft/sec
2	From Formula 11 using speeds in Col. 17. (Need not be computed if Col. 1 is used.)	10	From Tables of Appendix 5 using values of R_e in Col. 9
3	From contours in Appendices 1, 2, and 3, using given values of C_p and C_{η} . (Only Col. 4 with either Col. 3 or Col. 5 is needed when linear interpolation is used.)	11	Col. 10 + ΔC_f
4		12	Col. 8 $\times \frac{C_5}{C_5'}$
5			
6	Col. 4 - Col. 3 when $\frac{B}{H} > 3.00$ or Col. 5 - Col. 4 when $\frac{B}{H} < 3.00$	13	Col. 11 + Col. 12
7	$\kappa \times$ Col. 6	14	Cube of speeds in Col. 17
8	Col. 4 + Col. 7	15	A from Formula 12 \times Col. 17
		16	Col. 13 \times Col. 15 (Formula 12)
		17	Assumed even ship speeds (knots)

(¹) Prime indicates that the quantity for the given ship is numerically different than that for the Standard Series vessel.

(2) When Standard Series EHP is compared with that computed for a given ship from model data, Columns, 9, 10, 11, 14, 15, and 17 have already been computed

TABLE 6.--Sample form for the calculation of effective horsepower from the Taylor Standard Series

If it is assumed for illustrative purposes that the desired value of effective horsepower is for a speed of 25.00 knots, then the speed-length ratio for the given vessel is

$$\frac{V/k}{\sqrt{L}} = \frac{25.00}{\sqrt{650.0}} = 0.980$$

From Table 7, the rounded-off values of longitudinal prismatic coefficient C_p and volumetric coefficient C_v are 0.62 and 3.78×10^{-3} , respectively. Since the beam-draft ratio B/H is 2.97, the residual-resistance coefficients must be interpolated between the contours for $B/H = 2.25$ and 3.00 in Appendices 3 and 4. Thus reading from these contours at $V/k = 0.980$, $C_p = 0.62$, and $C_v = 3.78 \times 10^{-3}$ for each B/H

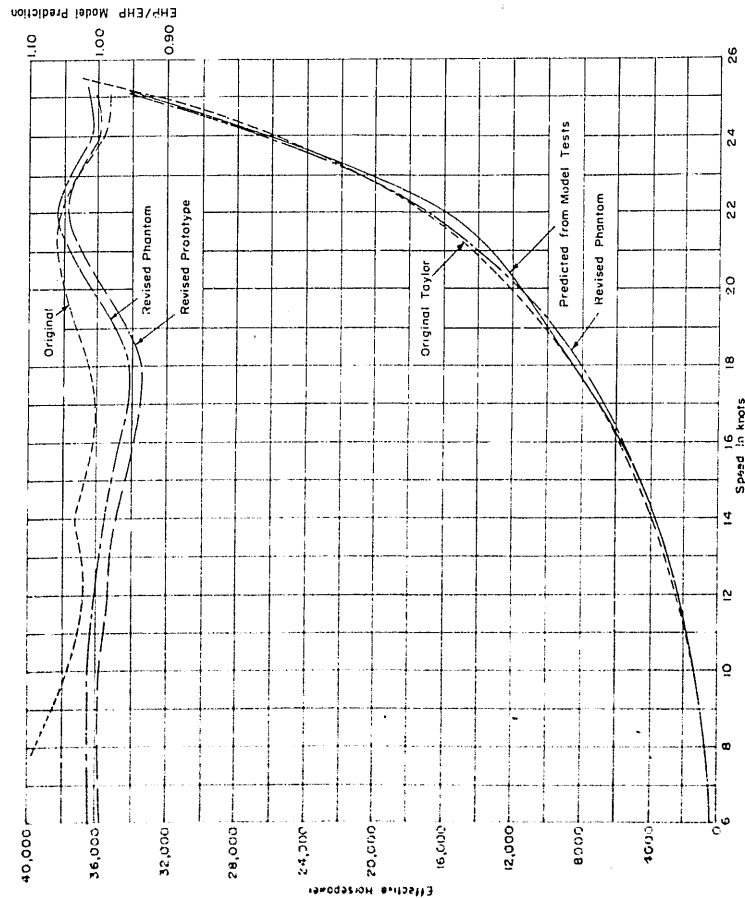


FIGURE 24.--Comparison of the effective horsepower of a 650-foot passenger vessel with an equivalent standard series vessel
The effective horsepower are calculated separately from model test data, the revised Taylor Series contours; and the original Taylor Series contours.

$$C_{r1} = 1.950 \times 10^{-3} \quad \text{for } B/H = 2.25$$

$$C_{r2} = 1.910 \times 10^{-3} \quad \text{for } B/H = 3.00$$

$$\text{and} \quad C_{r1} - C_{r2} = 0.040 \times 10^{-3}$$

The interpolation factor on B/H is

$$\frac{3.00 - 2.97}{3.00 - 2.25} = \frac{0.03}{0.75} = 0.04$$

Then the C_r for the Taylor Series vessel with a $B/H = 2.97$ is

$$1.910 \times 10^{-3} + 0.04(0.04 \times 10^{-3}) = 1.910 \times 10^{-3}$$

where the amount involved in interpolation in this case is negligible.

The Reynolds number for a 650-foot vessel operating in salt water of 59F at a speed of 25.00 knots is

$$\frac{vL}{\nu} = \frac{1.689 \, V/k \, L}{\nu} = \frac{1.689 \times 25.00 \times 650.0}{1.2817 \times 10^{-5}} = 2.142 \times 10^9$$

where 1.689 is the conversion factor from knots to feet per

Dimension	Model	Prototype
Length, feet	20.00	650.0
Beam, feet	2.738	88.98
Draft, feet	0.923	30.00
Displacement, pounds, tons	1892	29690
Wetted Surface, feet ²	63.64	6720
Coefficient		
Longitudinal Prismatic Coefficient C_p		0.616
Volumetric Coefficient C_v		3.784×10^{-3}
Wetted-Surface Coefficient C_s		2.595
Midship Section Coefficient C_x		0.972
Beam-Draft Ratio B/H		2.966

TABLE 7.--Particulars for a 650-foot passenger vessel

second and 1.2817×10^{-5} is the kinematic viscosity which is read from Appendix 7 for salt water at a temperature of 59F.

The Schoenherr frictional-resistance coefficient for a Reynolds number of 2.142×10^9 is, from the tables of Appendix 6,

$$C_f = 1.397 \times 10^{-3}$$

If the roughness-allowance coefficient ΔC_f is assumed to be 0.400×10^{-3} , then

$$\begin{aligned} C_t &= C_r + C_f + \Delta C_f \\ &= (1.910 + 1.397 + 0.400) \times 10^{-3} \\ &= 3.707 \times 10^{-3} \end{aligned}$$

Since

Power = resistance \times speed,

$$\begin{aligned} \text{EHP} &= \frac{C_t \times \frac{\rho}{2} S v^3}{550 \text{ ft-lb/sec}} \\ &= \frac{3.707 \times 10^{-3} \times \frac{1.991}{2} \times 65720 \times (25.00)^3 \times (1.689)^3}{550} \\ &= 33190 \end{aligned}$$

where 1.991 is the density in slugs per cubic foot which is read from Appendix 7 for salt water at 59F. The wetted surface of the Taylor Series vessel is computed from the wetted-surface coefficient which is interpolated from the contours of Appendix 2 using the assigned values of C_p , C_r , and B/l .

The preceding numerical example illustrates the direct computation of the effective horsepower for a Taylor Series prototype. In the past, the effective horsepower of the so-called "phantom vessel" was used in Taylor Series comparisons. The phantom vessel may be defined as one which has a residual resistance equal to that of the com-

parative Taylor Series vessel but with a frictional resistance equal to that of the subject vessel. This concept was probably originated to compensate for the fact that the wetted-surface coefficients of modern vessels are, in general, slightly higher than those of the comparable Taylor Series vessels. The phantom vessel procedure implies that the division of the total resistance into the components of residual and frictional resistance is an exact one, a fact which few would be willing to concede. Furthermore, if the wetted-coefficient used for the model differs from that for the full scale, a small error is introduced due to the difference in frictional-resistance coefficient between model and full scale, commonly designated as the D_f . This error, although small, leads to inconsistencies in comparisons because its magnitude depends on scale and choice of roughness-allowance coefficient.

For the aforementioned reasons, it is believed that the "phantom vessel" concept should be discontinued. However, the present calculation technique may be simply adapted to suit this concept if such is considered desirable. This may be accomplished either by separately calculating the residual and frictional horsepower or by conversion of the residual-resistance coefficient as follows:

The value of C_r based on the wetted surface of the Taylor Series form which is given in the numerical example is converted to C_r' based on the wetted surface of the subject vessel, or

$$C_r' = C_r \times \frac{C_s}{C_s'} = 1.910 \times 10^{-3} \times \frac{2.537}{2.595} = 1.867 \times 10^{-3}$$

where the prime indicates that the wetted surface of the subject vessel was used to calculate the coefficient. Then

$$\begin{aligned} C_t &= C_r' + C_f + \Delta C_f = (1.867 + 1.397 + 0.400) \times 10^{-3} \\ &= 3.664 \times 10^{-3} \end{aligned}$$

$$\begin{aligned} \text{and EHP} &= \frac{3.664 \times 10^{-3} \times \frac{1.991}{2} \times 29690 (25.00)^3 (1.689)^3}{550} \\ &= 33550 \end{aligned}$$

where 29690 is the wetted surface of the subject vessel in square feet.

The sample form of Table 6 is set up for the phantom vessel approach. The first approach can be used if the form is modified as follows:

1. Eliminate Column 12.
2. Add Column 8 to Column 11 to give Column 13.
3. Calculate Column 15 using a value of A based on the wetted surface of the Taylor Series vessel S .
4. Then Column 13 times Column 15 gives the desired EHP in Column 16.

When model test data are available for the subject vessel, it is likely that some of the calculations required are already available. The sample form indicates the steps that can be eliminated in these circumstances.

The effective horsepower curve for the subject vessel is shown in Figure 24 together with the effective horsepower curves derived from the original and revised Taylor Series contours. Ratios of the effective horsepower to those of the subject vessel are also given. It may be noted that at speeds up to 20 knots, there is considerable divergence between the predictions obtained with the original and with revised contours. At speeds below 14.0 knots, at least half of the discrepancy results from predicting with the EMB-Tideman method instead of the Schoenherr formula plus a roughness-allowance coefficient of 0.0004.⁶ At 18.0 knots, however, both EMB-Tideman and Schoenherr plus 0.0004 should give the same answer and yet there is a difference of approximately 6 percent. This difference is twofold in origin: first, the more refined interpolation between a B/H of 2.25 and 3.00 (in this case no interpolation) instead of the original linear interpolation between a B/H of 2.25 and 3.75 and second, the refairing process combining the corrections for water temperature, laminar flow, and restricted channel effects.

It may be further noted that for the case illustrated, the prediction based on a Taylor Series prototype gives an effective horsepower which is approximately 1.5 percent lower than that for the phantom vessel. The revised results for both the Taylor Series prototype and the phantom vessel characteristically show a lower effective horsepower than the subject vessel at some speeds at the expense of a higher effective horsepower at other speeds.

VALIDITY OF TAYLOR SERIES COMPARISONS

As previously stated, the results of methodical series are applicable, in the strictest sense, only to forms derived from the common parent. The common usage of series data to evaluate the performance of specific ship designs assumes, therefore, that the incremental changes in resistance with the given geometrical parameters will apply reasonably to offspring of other parents. Thus, if several competitive designs of a given ship type are to be compared, the Taylor Series data may be used to determine the resistance changes due to differences in C_p , C_f , and B/H among them, such that the remaining differences in resistance can be attributed to other variances in form. One method of accomplishing such comparisons is through the use of ratio curves similar to those shown in Figure 24. With this device, the effective horsepower of each design being studied are expressed as ratios to its equivalent Taylor Series vessel, and the ratios are compared instead of the absolute values of effective horsepower.

Direct comparisons with the Taylor Series prototype are permissible where the hull type of the subject vessel is similar to the equivalent series form. In such cases, the Taylor Series form may be considered as one of the possible alternative designs, and the effective horsepower can be directly compared without resorting to the intermediary ratios. If, however, it is desired to make direct comparisons or estimates of effective horsepower from Taylor's Series when the subject vessel is of entirely different type, a certain amount of interpretation may be involved. Significant departures in form which may affect the validity of series comparisons are often manifested by the comparable sectional-area curves. Features pertaining to the extremities of certain types of vessels such as transoms, pronounced counters, bulbous bows, and acutely raked stems, may significantly affect the load waterline length with very little change in immersed volume. As a consequence of this, the magnitude of the over-all longitudinal prismatic coefficient is affected by local changes, as may be seen from the sketches in Figure 25. The value of C_p for the Taylor Series variation, however, can only be altered by an over-all change in sectional-area curve. One possible solution to this problem would be to introduce an "effective" length to be used in the calculation of C_p , C_f , and C_s for the comparative Taylor Series vessel.

This concept can be illustrated by a numerical example involving Figure 25a. The sectional-area curve showing the transom is taken to represent a modern 664-foot cruiser. If the actual length of the subject vessel L_1 is used to define the geometrical parameters, $C_p = 0.613$, $C_F = 1.95 \times 10^{-3}$, $B/H = 3.00$, and $C_s = 2.641$. If, however, the sectional-area curve for the cruiser is extended to form an ending similar to that of the Taylor Series sectional-area curve as shown by the broken line, then the effective length L_2 is determined. The geometrical parameters based on L_2 are $C_p = 0.595$, $C_F = 1.78 \times 10^{-3}$, $B/H = 3.00$, and $C_s = 2.641$. The predicted effective horsepower for a speed of 30 knots and standard conditions are:

from model tests of subject vessel	36940
from Taylor's Series using L_1	40070
from Taylor's Series using L_2	36420

It can be seen that the series prediction based on L_1 is approximately 8 percent higher and that based on L_2 is 1 percent lower than the model test prediction of the subject vessel. The use of the effective length concept for prediction of the effective horsepower of dissimilar ship types does not appear unreasonable upon further consideration. If the stern of the longer Taylor Series vessel, length L_2 , is cut off to form a transom and the resulting length is L_1 , experiments have shown that, within reasonable limits, the change in total resistance would be small. Thus the closer prediction using the effective length appears to be valid.

Obviously the use of an effective length does not always reduce the Taylor Series predictions. If the subject vessel has an acutely raked stem, no bulb, or a relatively large counter, the effective length would be reduced with correspondingly higher values of C_p and C_F . Furthermore, Figure 22 shows that if C_p is reduced beyond a certain minimum, a further reduction in C_p would actually result in an increase in the predicted effective horsepower.

Direct comparisons with Taylor Series will also be affected if the midship coefficients or shapes of the subject vessel differ radically from that of the series. However, Taylor has previously shown that relatively small changes of resistance result from large changes in midship coefficients when the other parameters are held fixed.¹

To summarize, the Taylor Series data provide excellent criteria for selecting the over-all coefficients of various ship forms. They also provide a good intermediary for evaluating the performance of competitive forms of a given ship type. The data may be used for absolute comparisons or predictions of hull types similar to those of Taylor Series, but for widely dissimilar types, it may be necessary to redefine the geometrical parameters on the basis of an effective length.

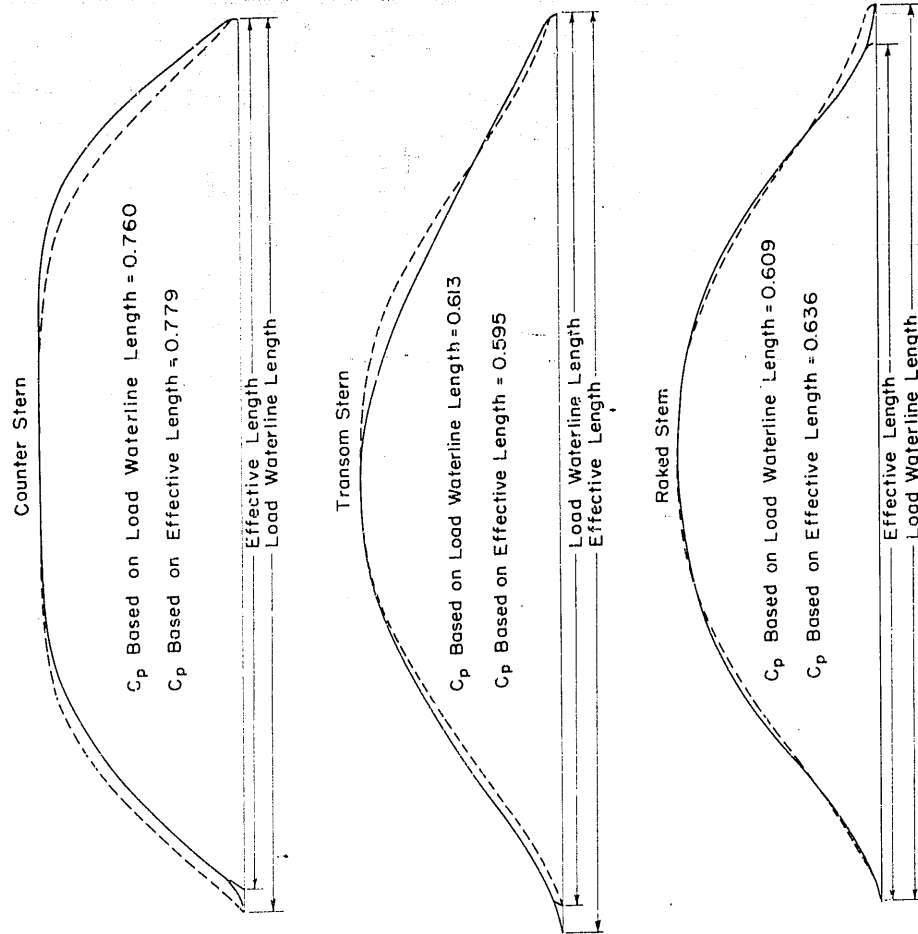


FIGURE 25.—Effect of sectional-area shape on the selection of geometrical parameters for Taylor Series comparisons
The broken line indicates the sectional-area curve for a Taylor Series vessel of an equivalent C_p based on load waterline length

USE OF THE REVISED TAYLOR SERIES CONTOURS WITH FRICTIONAL-RESISTANCE FORMULATIONS OTHER THAN SCHOENHERR

When dealing with residual resistances, the consequences of a change in frictional-resistance formulation are always a source of concern. The question is whether the laborious task of reducing the original data would have to be repeated. This question can be answered in the negative especially if the proposed formulation is a single function of Reynolds number. Such a change could be accomplished simply because of the existence of certain fixed parameters. Since all of the tests were conducted with models of the same length, namely 20.51 feet, the difference between the frictional-resistance coefficients can be expressed as functions of speed-length ratio and basin water temperature. This may be illustrated by considering the possibility of the use of Gebers formula which gives values for the frictional-resistance coefficient in the model range considerably different than those obtained with the Schoenherr formula. Since the differences in frictional-resistance coefficient are reflected as a change in residual-resistance coefficient, this quantity will be denoted ΔC_r . A set of curves of ΔC_r versus speed-length ratio and basin water temperature is shown in Figure 26. Thus, if it were desired to determine the effective horsepower predicted from the Gebers formula, the procedure for calculation would be essentially the same as that given in the preceding section, except that ΔC_r would be added to C_r and C_r would be deduced from Gebers formula.

Similar charts could be prepared for establishments using other frictional resistance formulations or, if it is desired, the conversions can be made on the total effective horsepower by the methods given in References 6 and 8.

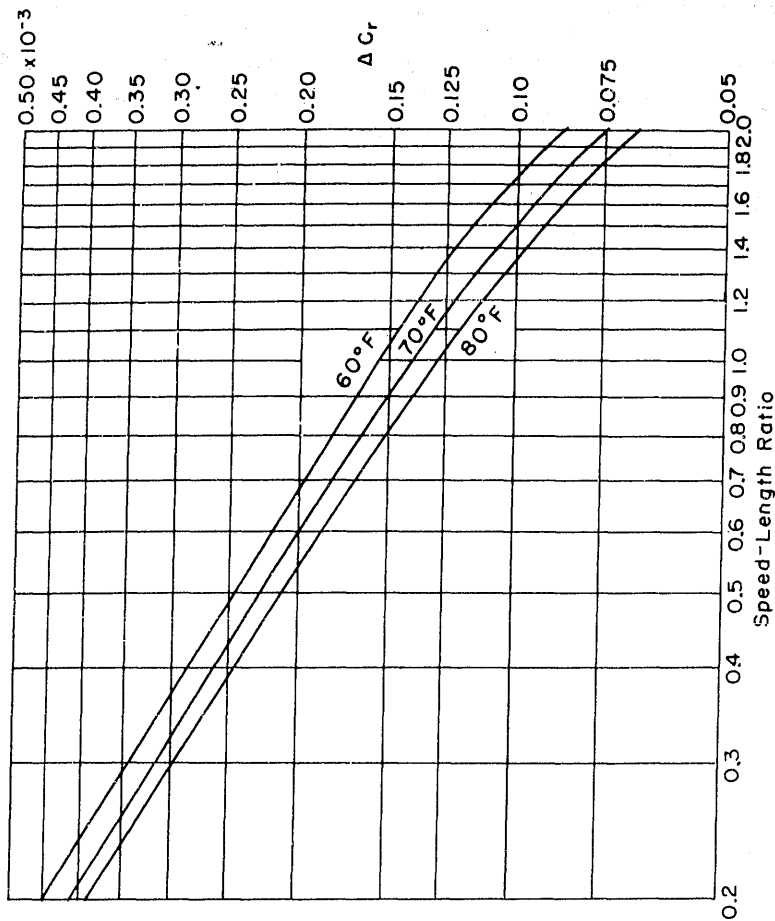


FIGURE 26.--Residual-resistance coefficient corrections
These values are added to the residual-resistance coefficients of the revised Taylor Series to convert from C_r based on the use of the Schoenherr Formula to C_r based on the use of the Gebers Formula

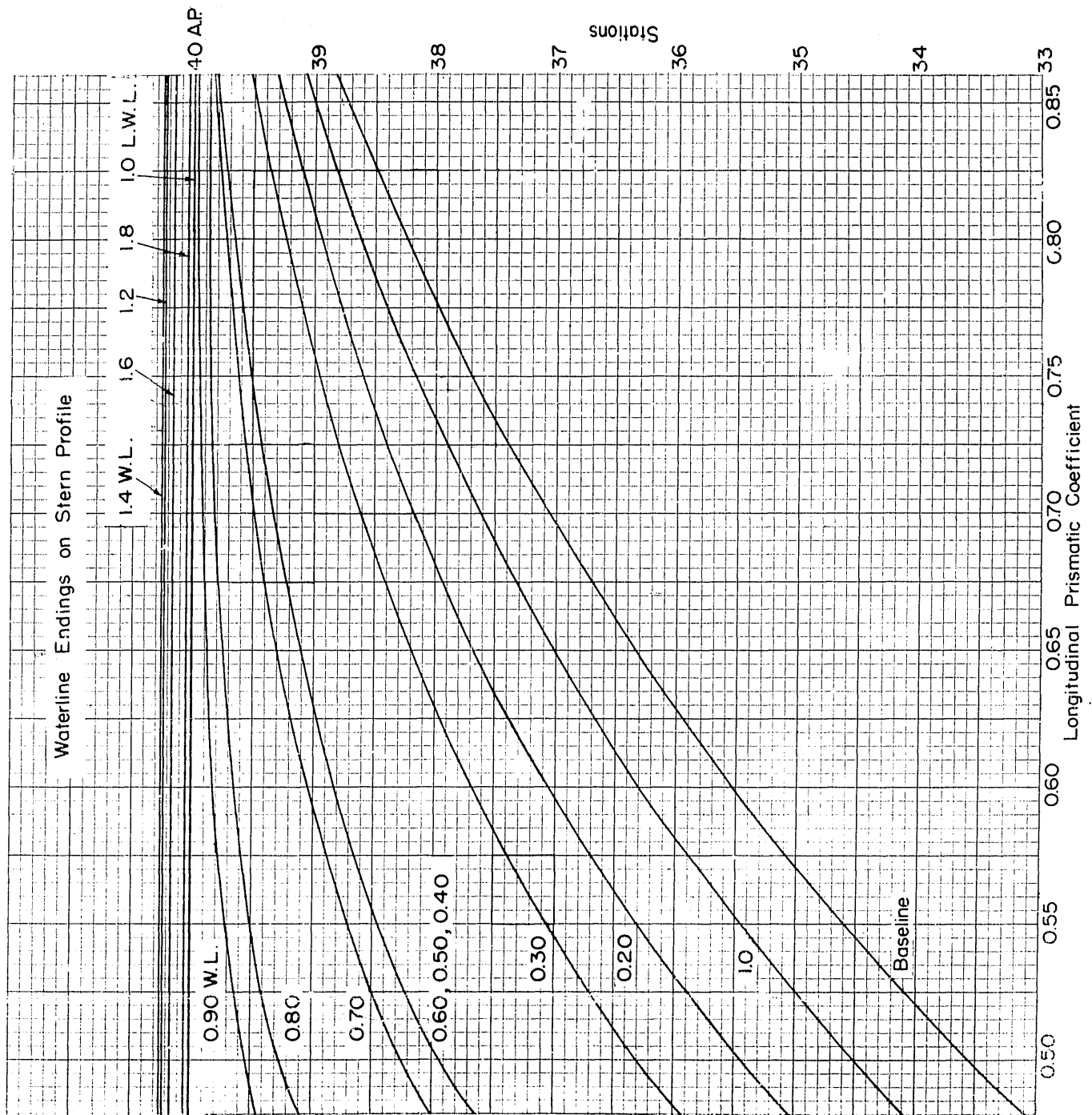
REFERENCES

1. Taylor, D. W., "The Speed and Power of Ships," Third Edition, U. S. Government Printing Office, 1943.
2. "Minutes of the Seventh Meeting of the American Towing Tank Conference," 7-8 October 1947.
3. Rossell, H. E. and Chapman, L. B., "Principles of Naval Architecture," Volume 2, Society of Naval Architects and Marine Engineers, 1939.
4. Todd, F. H. and Forest, F. X., "A Proposed New Basis for the Design of Single-Screw Merchant Ship Forms and Standard Series Lines," Transactions of the Society of Naval Architects and Marine Engineers, 1951.
5. Landweber, L. and Gertler, M., "Mathematical Formulation of Bodies of Revolution," TMB Report 719, September 1950.
6. Gertler, M., "The Prediction of the Effective Horsepower of Ships by Methods in Use at the David Taylor Model Basin," TMB Report 576, Second Edition, December 1947.
7. Landweber, L., "Tests of a Model in Restricted Channels," TMB Report 460, May 1939.
8. Gertler, M., "A Method for Converting the British© Coefficient Based on the Froude "O" Values to a© Coefficient Based on the Schoenherr Formula," TMB Report 657, Second Edition, June 1949.

APPENDIX 1

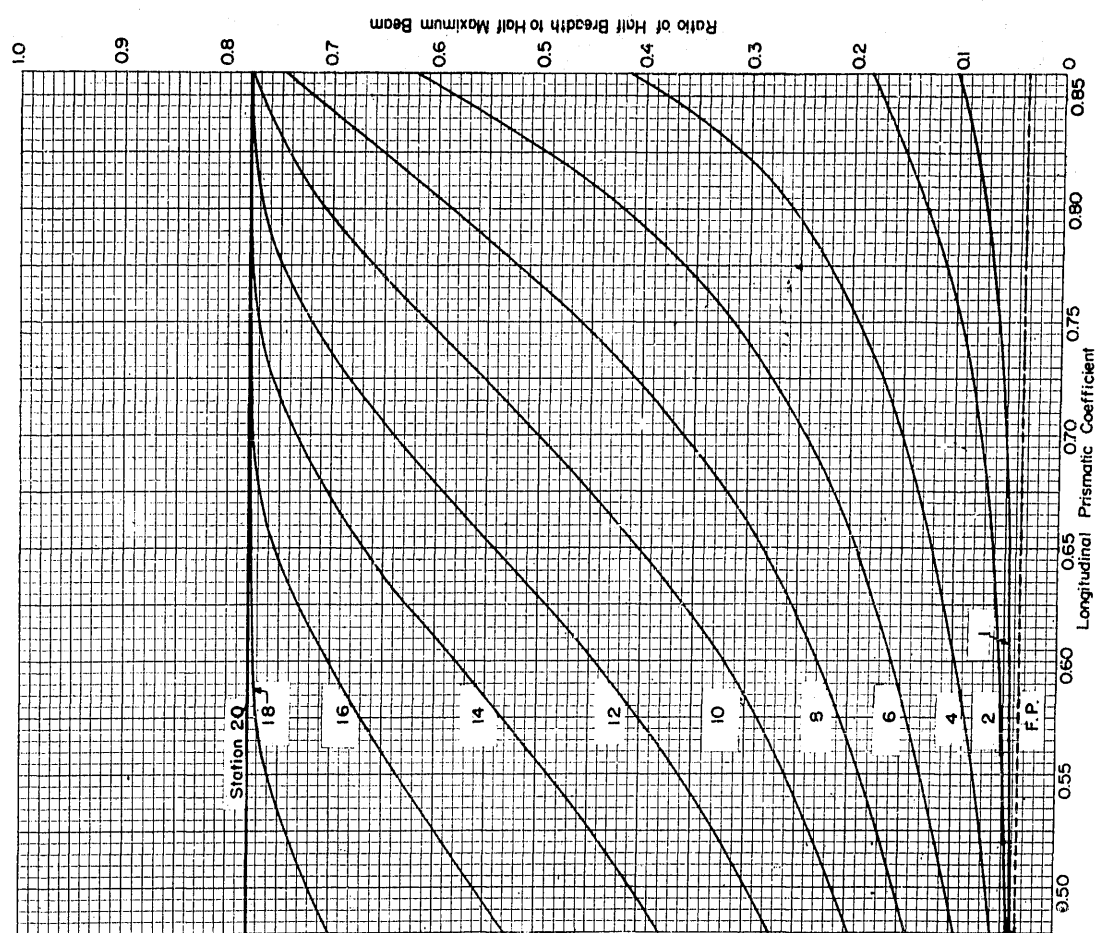
CURVES OF HALF-BREADTH AND WATERLINE ENDINGS VERSUS LONGITUDINAL PRISMATIC COEFFICIENT FOR DERIVED FORMS OF THE TAYLOR STANDARD SERIES

The half breadths are expressed as ratios to the half maximum beam at the load waterline.

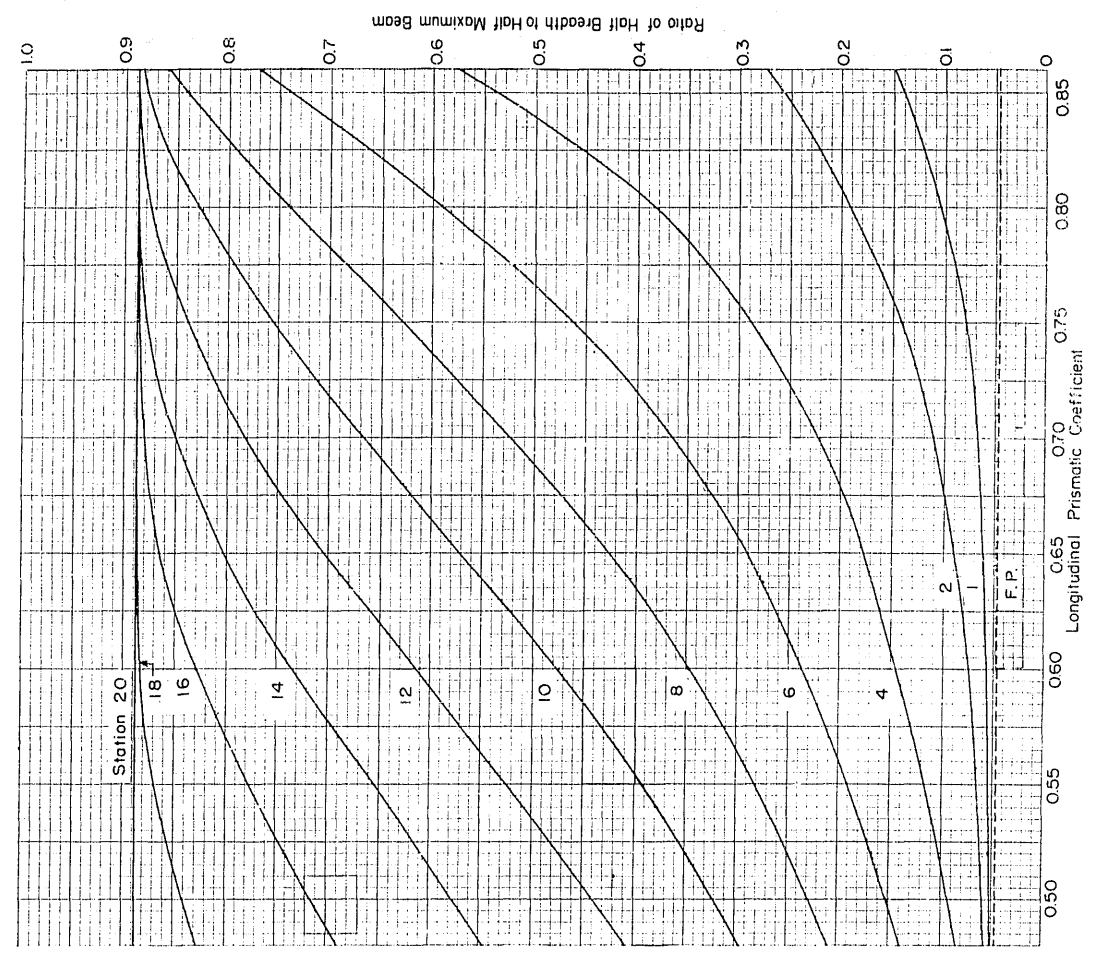
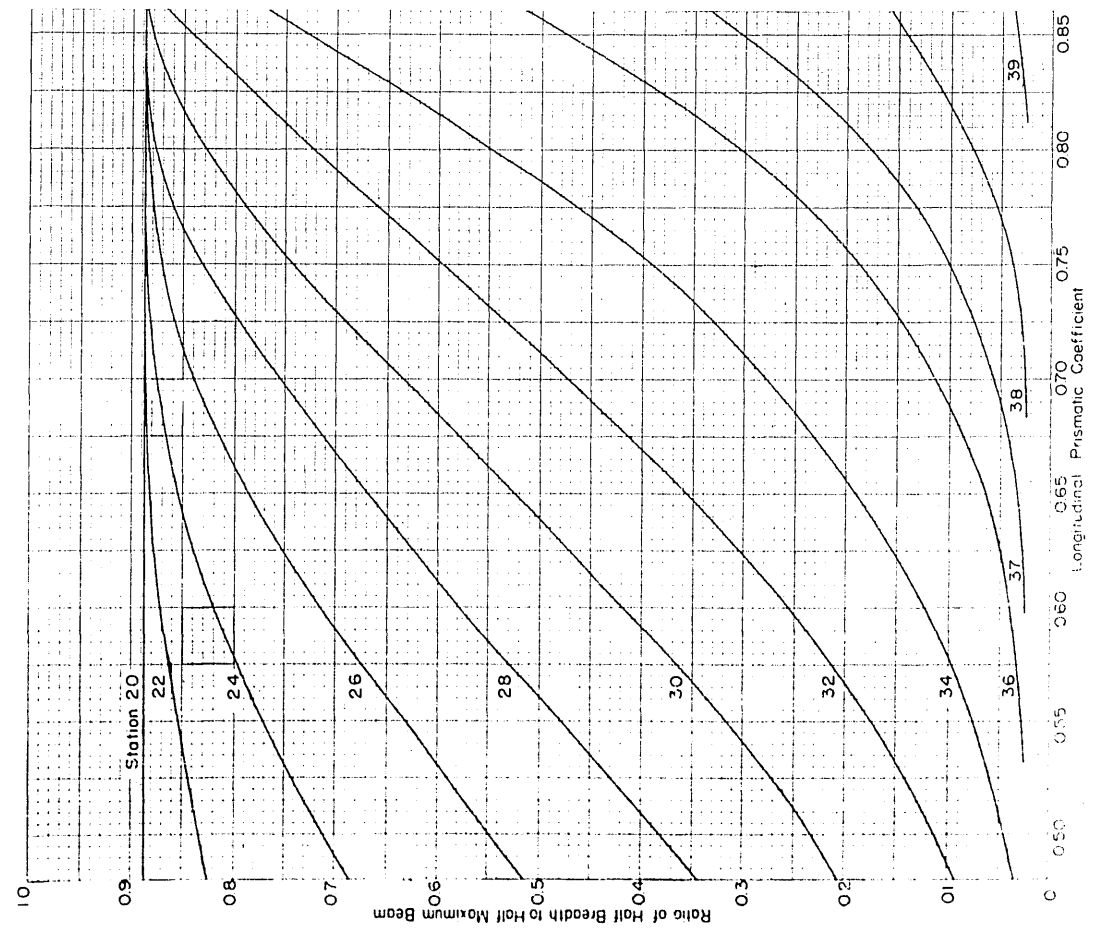


The graph plots the Ratio of Half Breadth to Half Maximum Beam (Y-axis, 0 to 1.0) against the Longitudinal Prismatic Coefficient (X-axis, 0.50 to 0.85). Multiple curves are shown, each labeled with a station number. The curves generally show a decreasing trend as the prismatic coefficient increases.

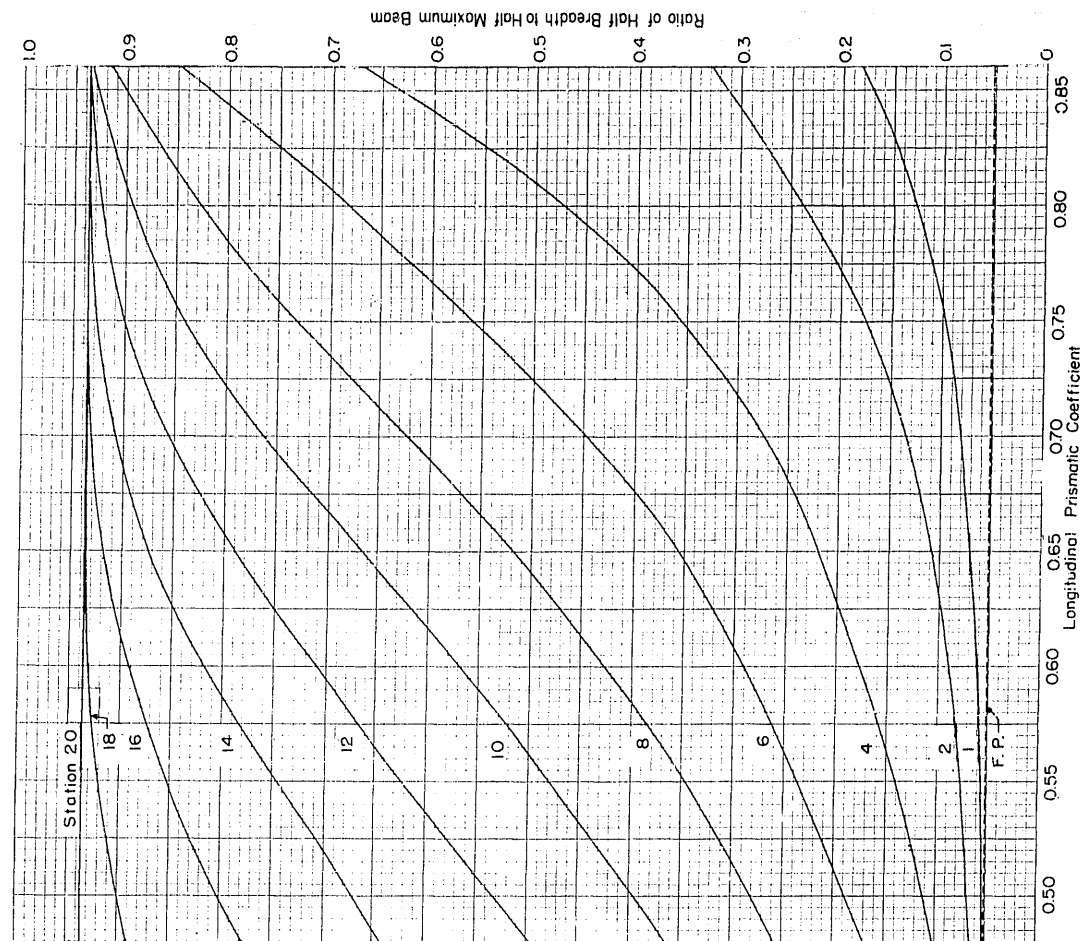
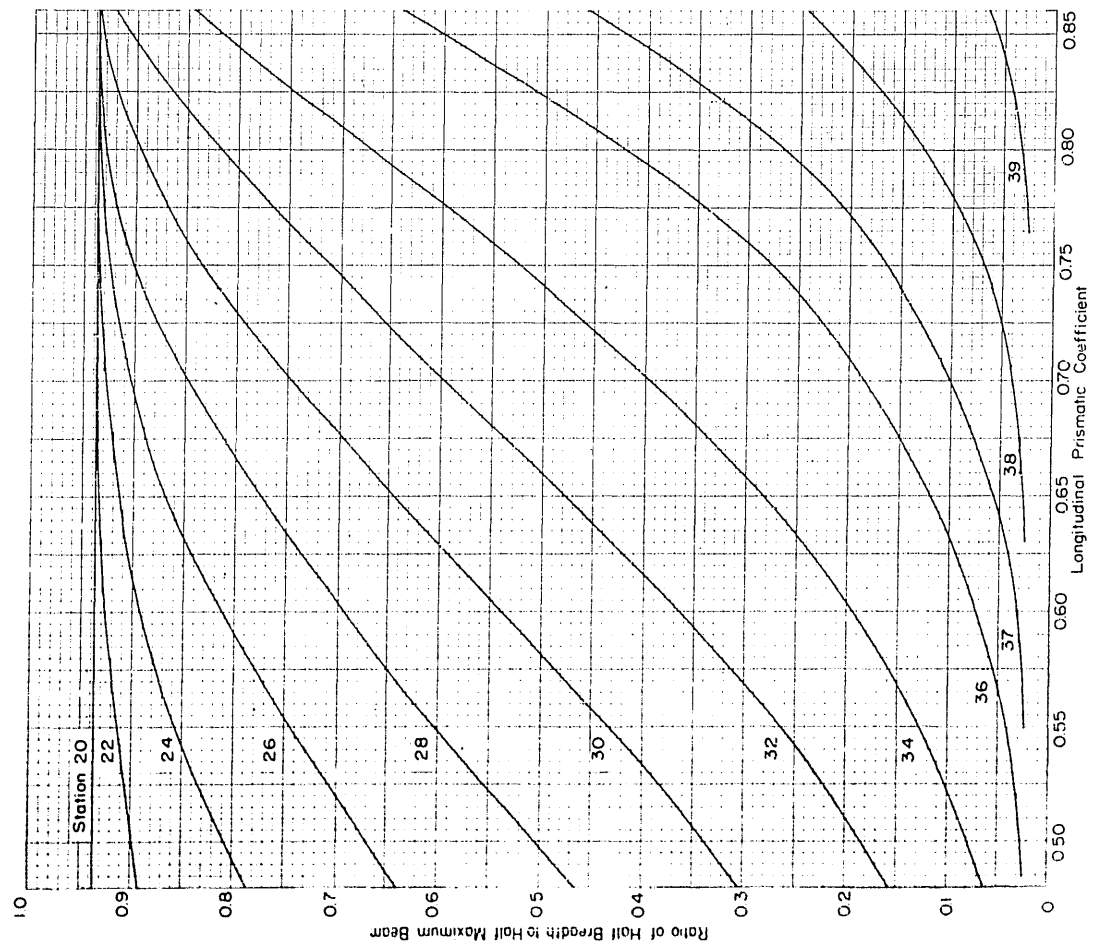
Station	Prismatic Coefficient	Ratio of Half Breadth to Half Maximum Beam
20	0.50	0.78
	0.85	0.75
22	0.50	0.75
	0.85	0.72
24	0.50	0.72
	0.85	0.69
26	0.50	0.69
	0.85	0.66
28	0.50	0.66
	0.85	0.63
30	0.50	0.63
	0.85	0.60
32	0.50	0.60
	0.85	0.57
34	0.50	0.57
	0.85	0.54
36	0.50	0.54
	0.85	0.51
37	0.50	0.51
	0.85	0.48
38	0.50	0.48
	0.85	0.45
39	0.50	0.45
	0.85	0.42



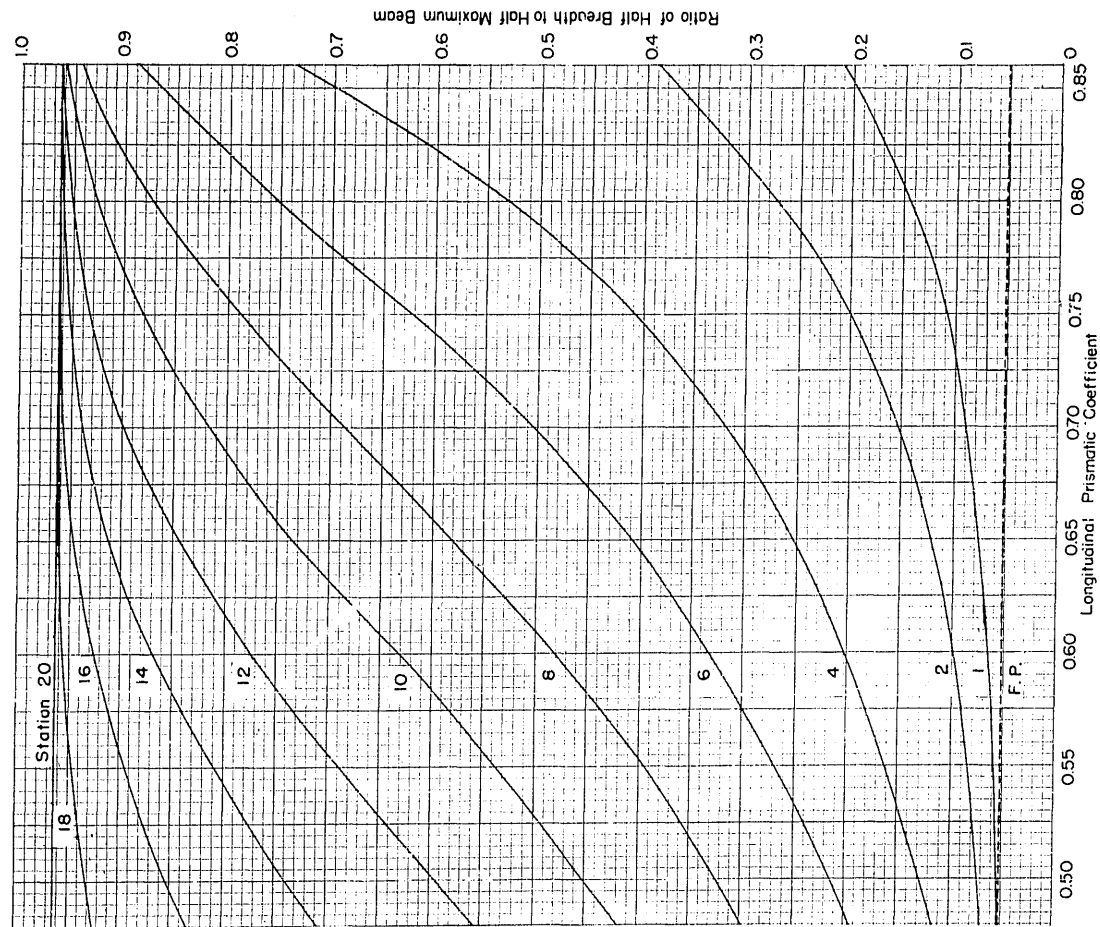
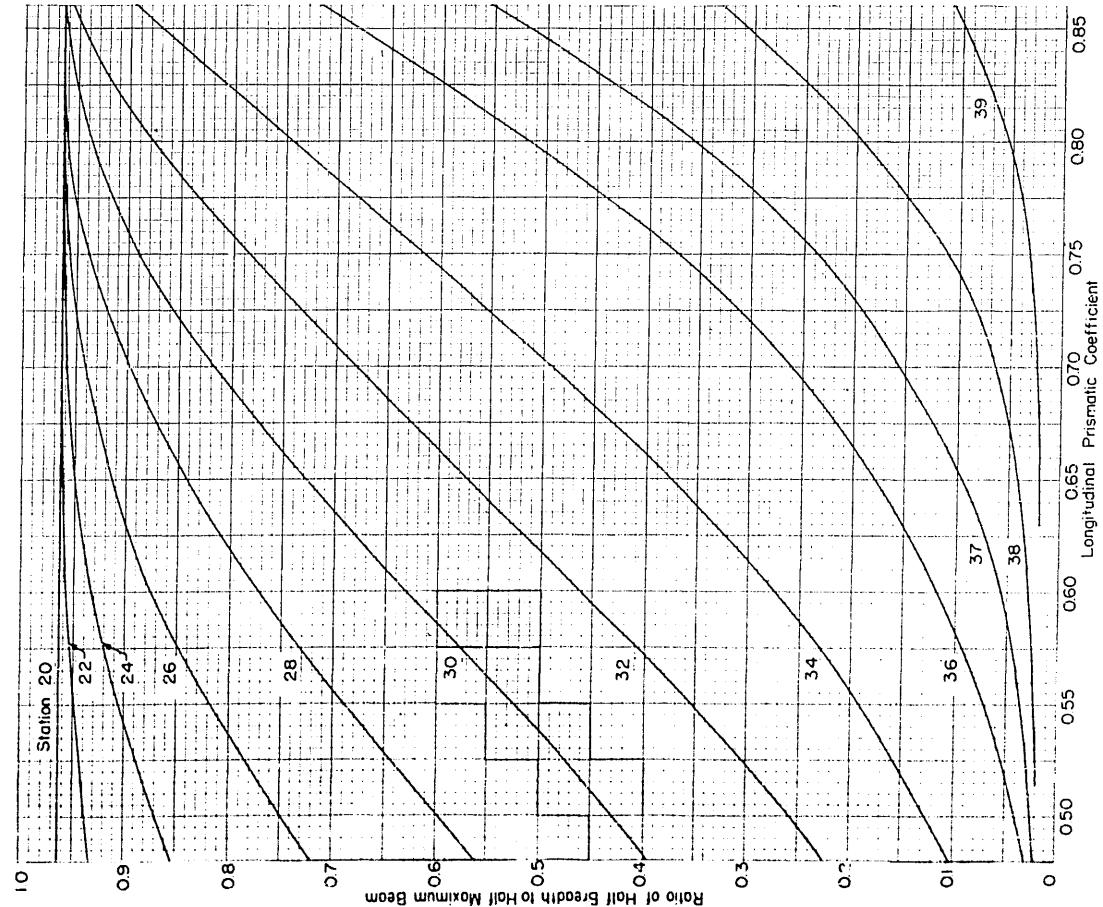
0.2 WL



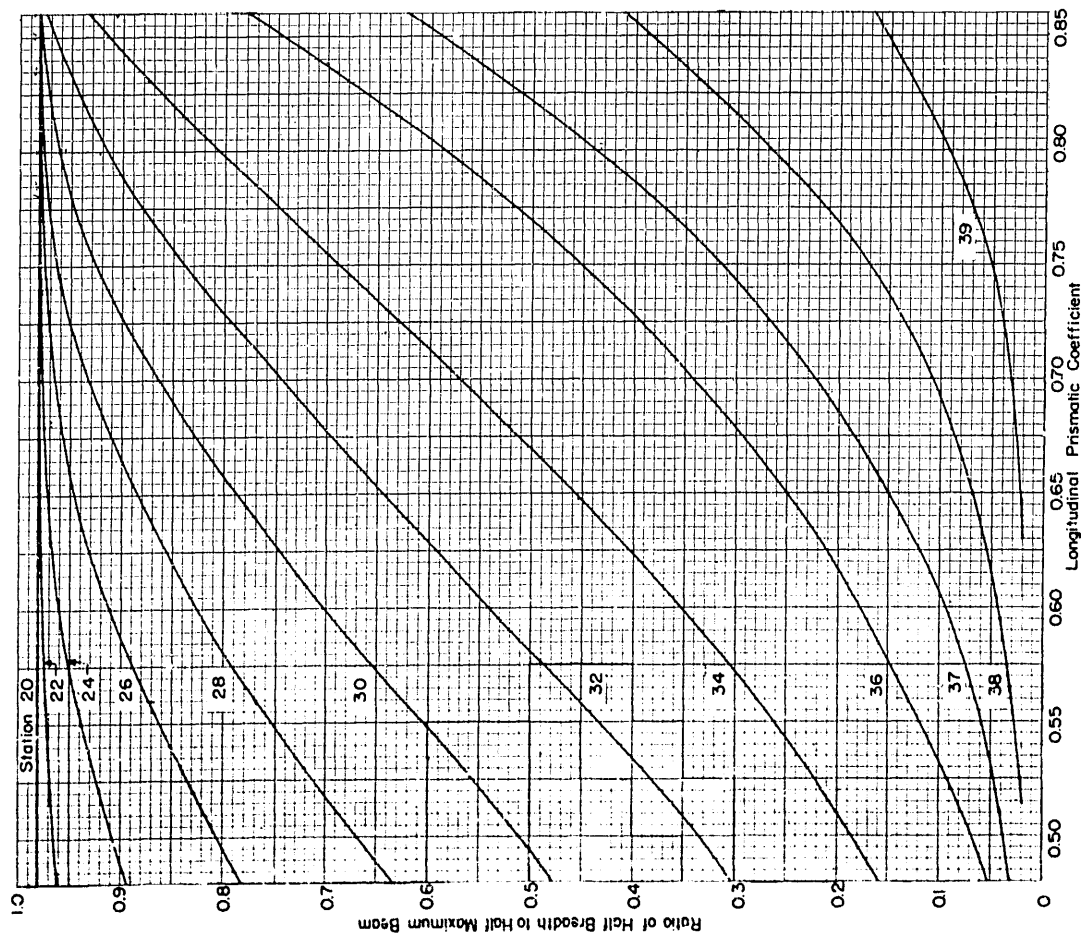
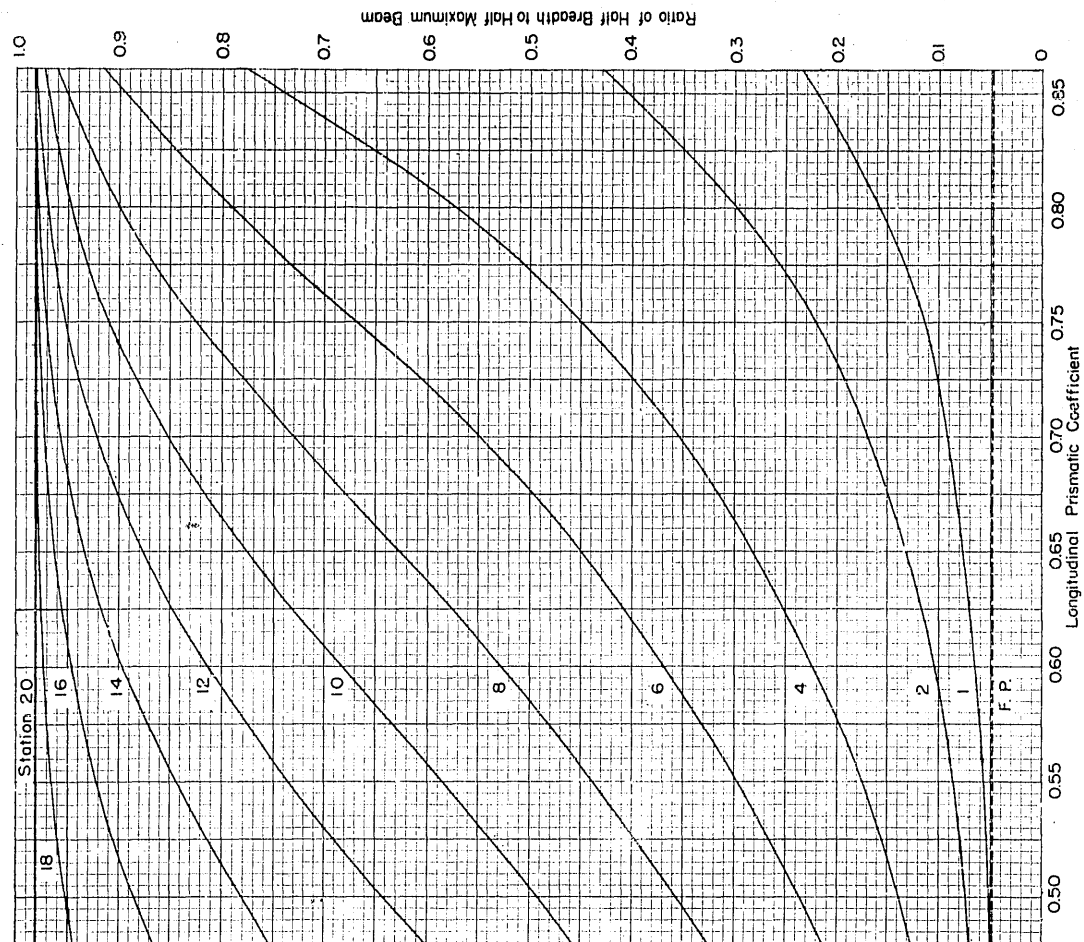
0.3 WL



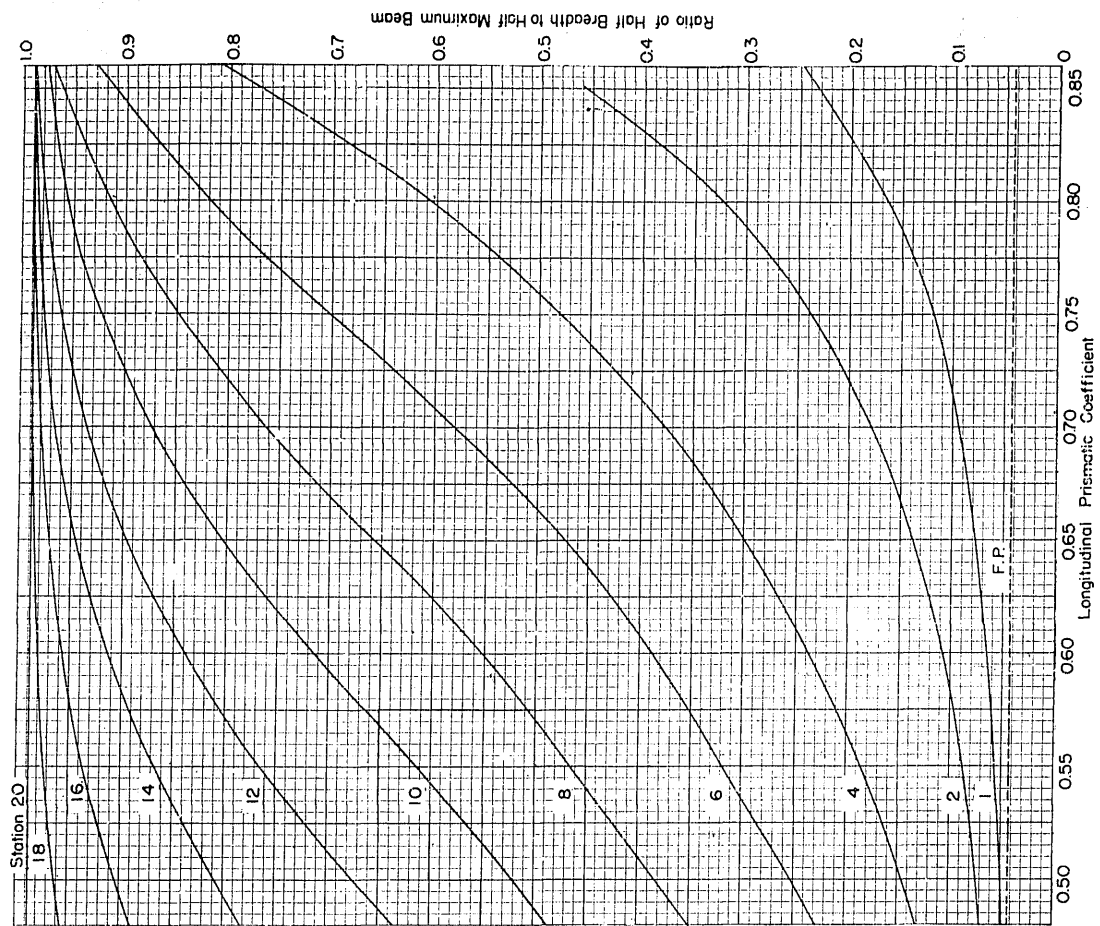
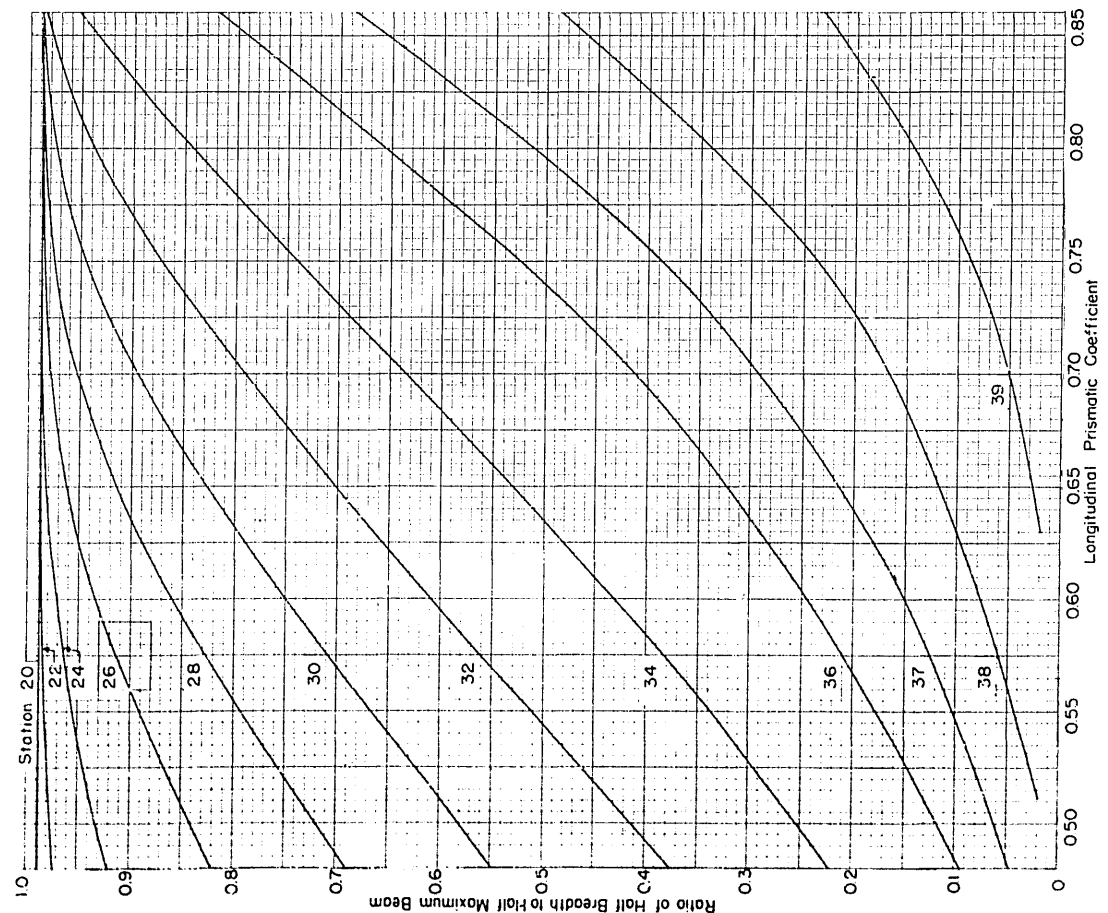
0.4 WL



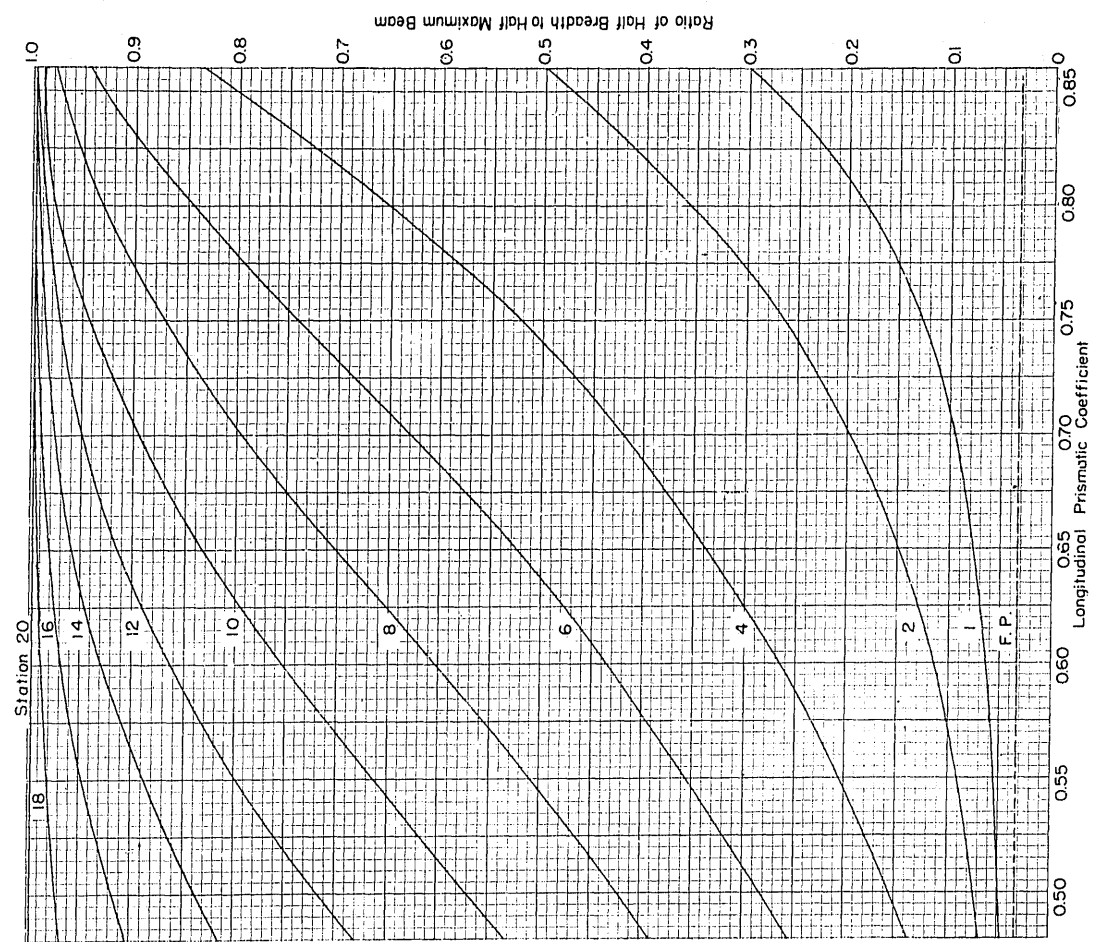
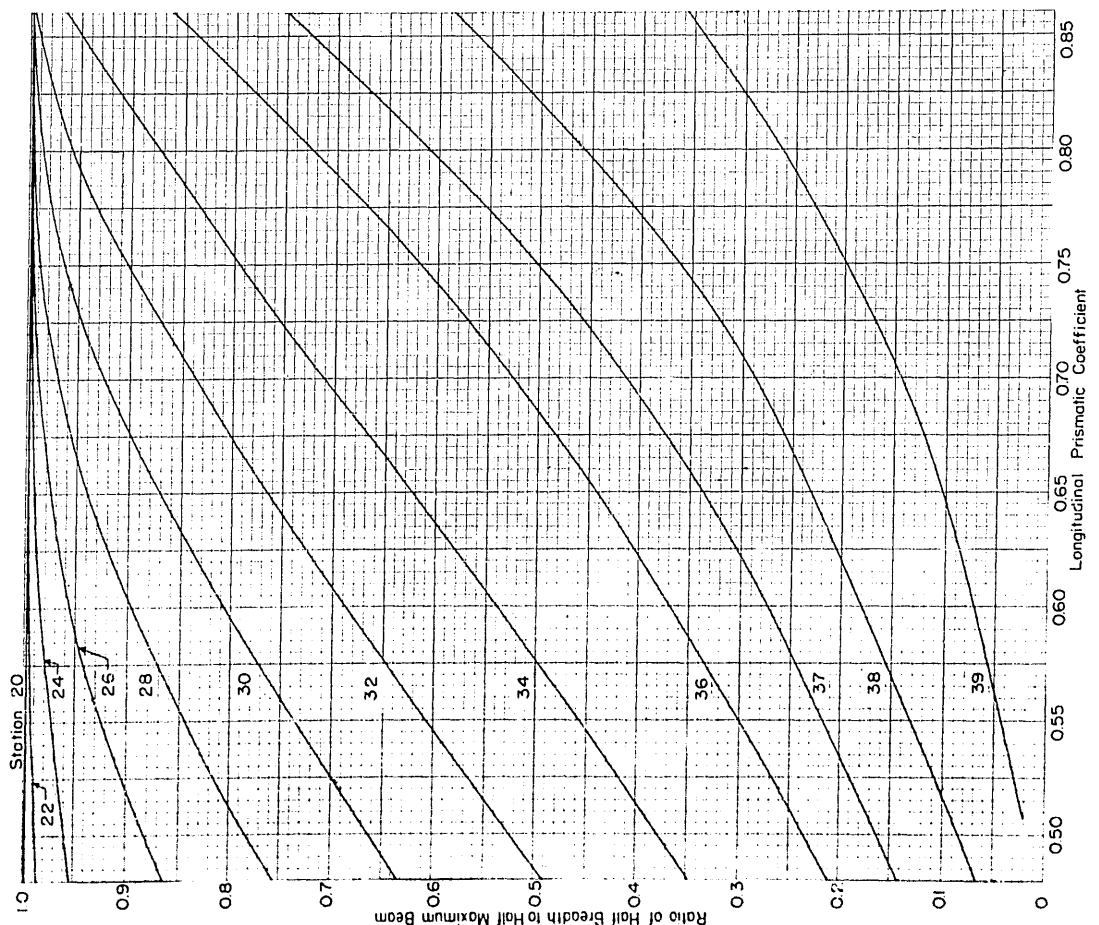
0.5 WL



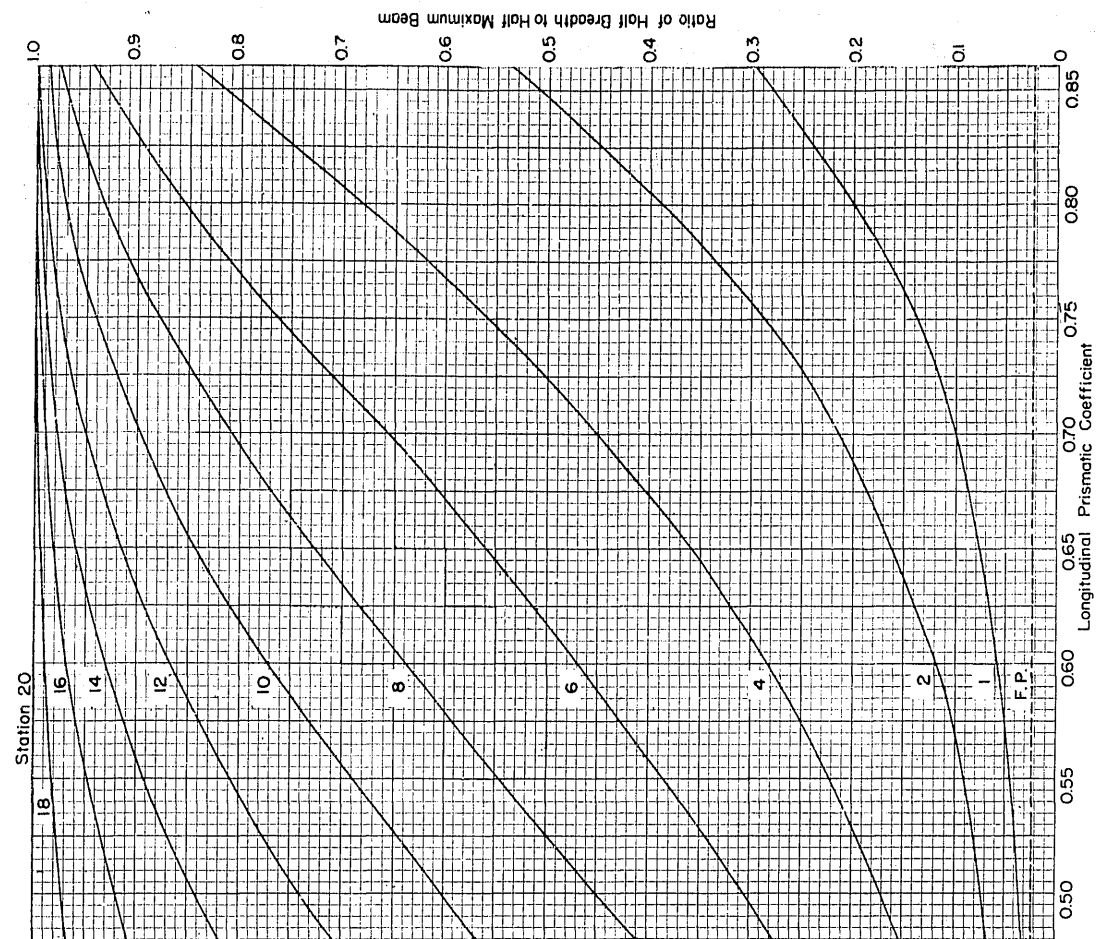
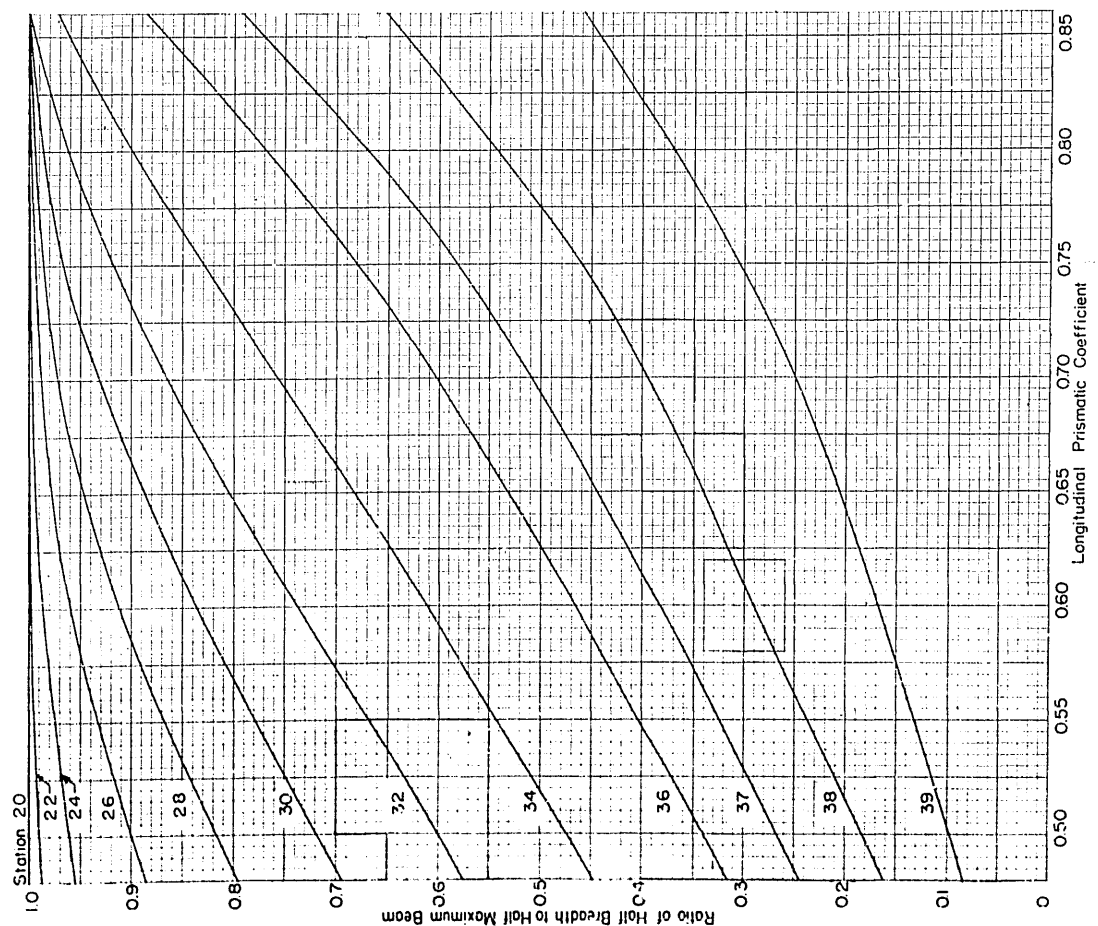
0.6 WL



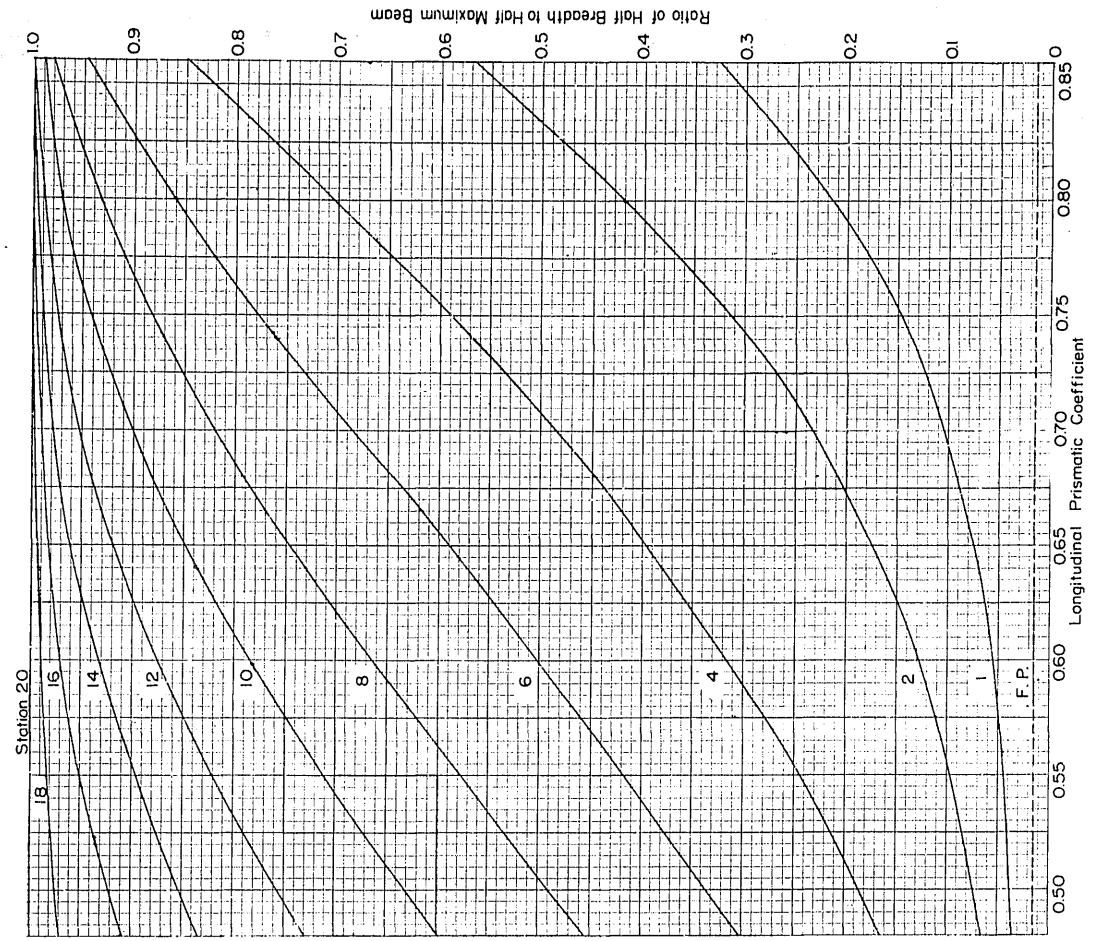
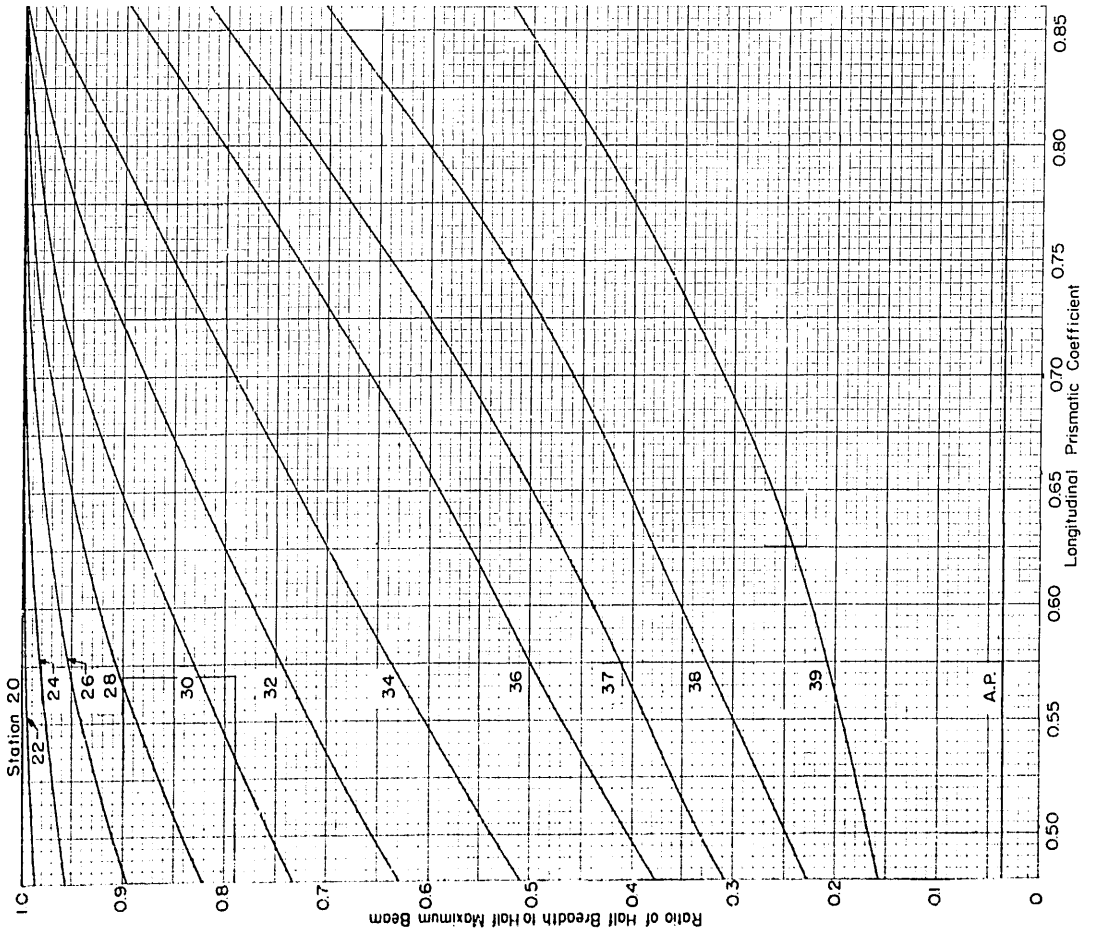
0.8 WL



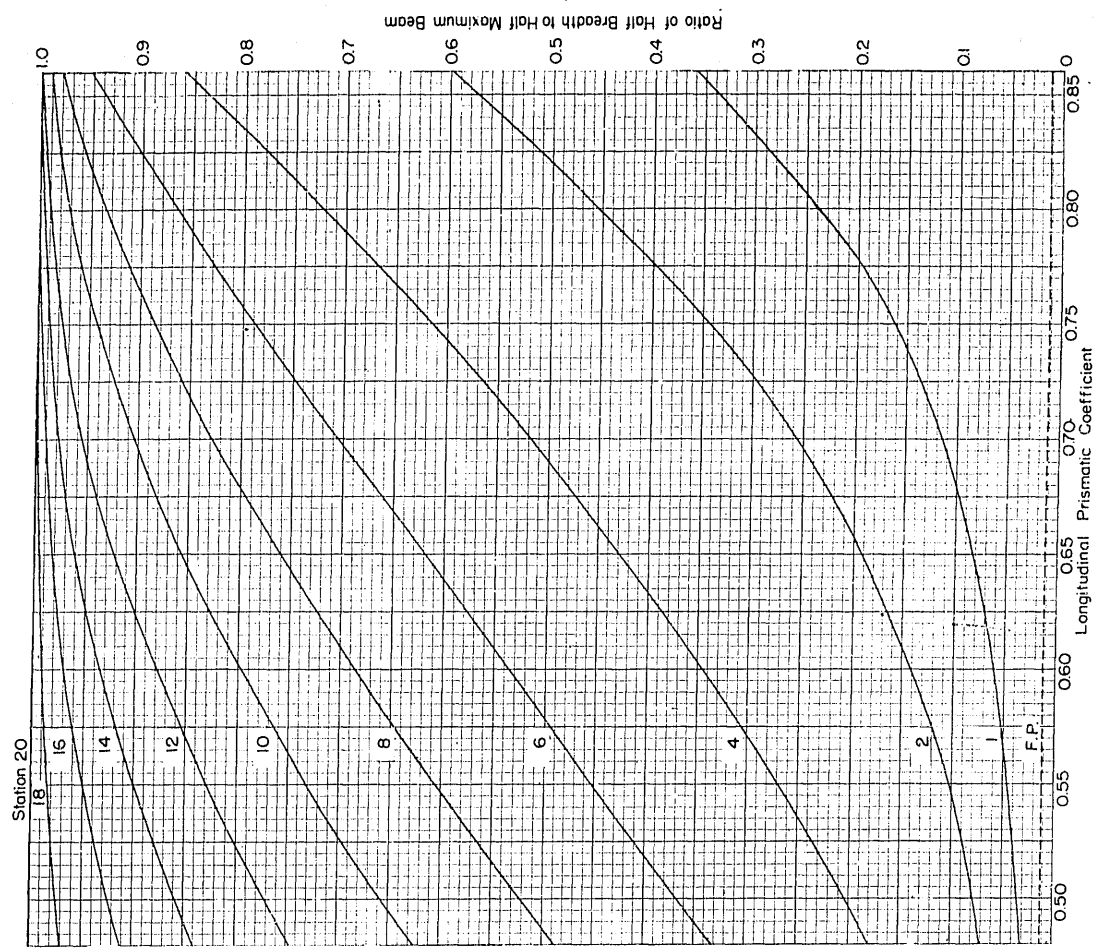
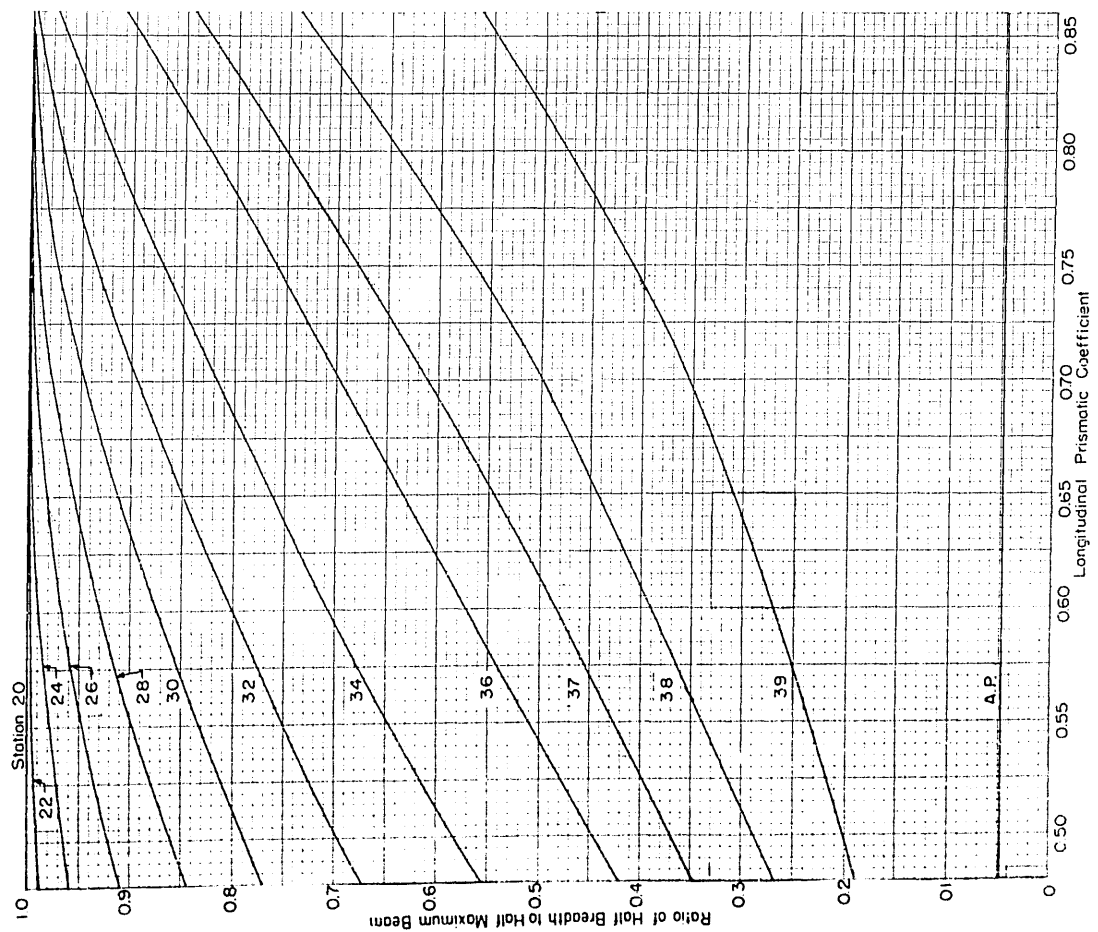
I.O WL



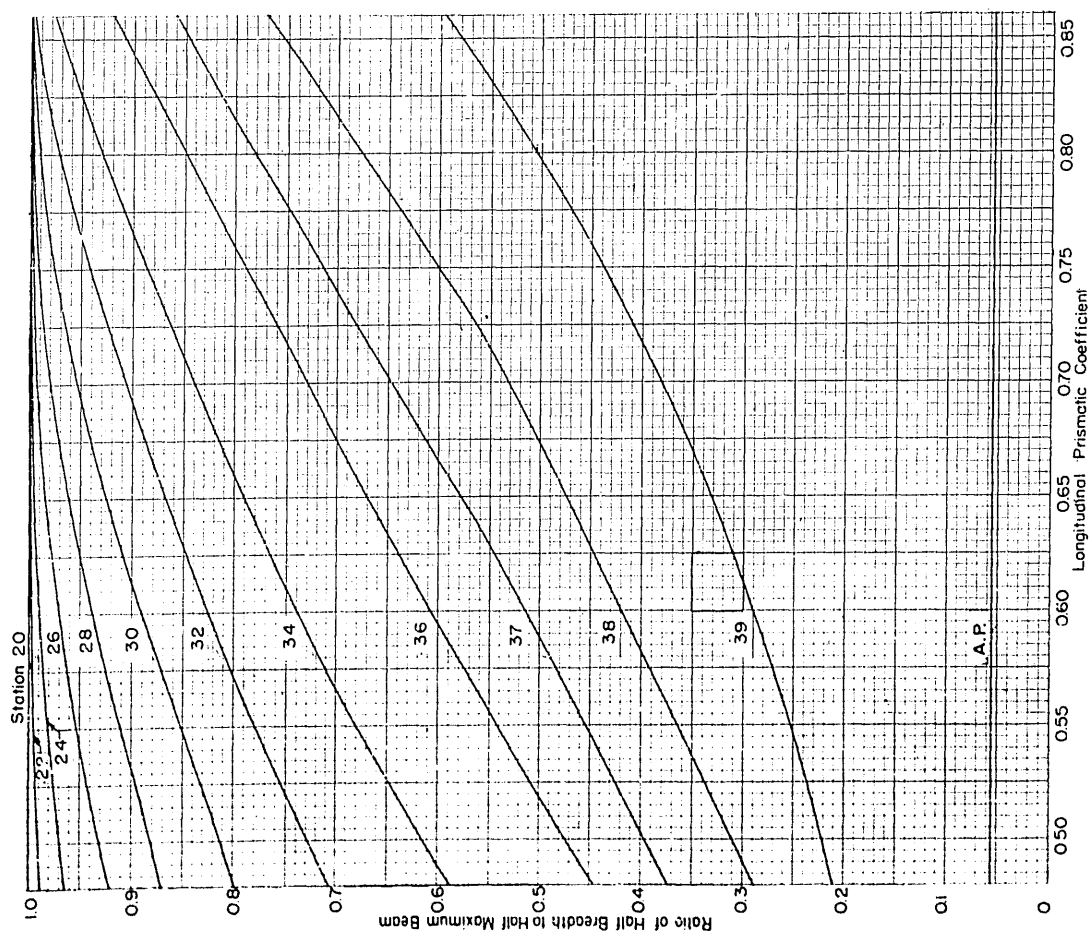
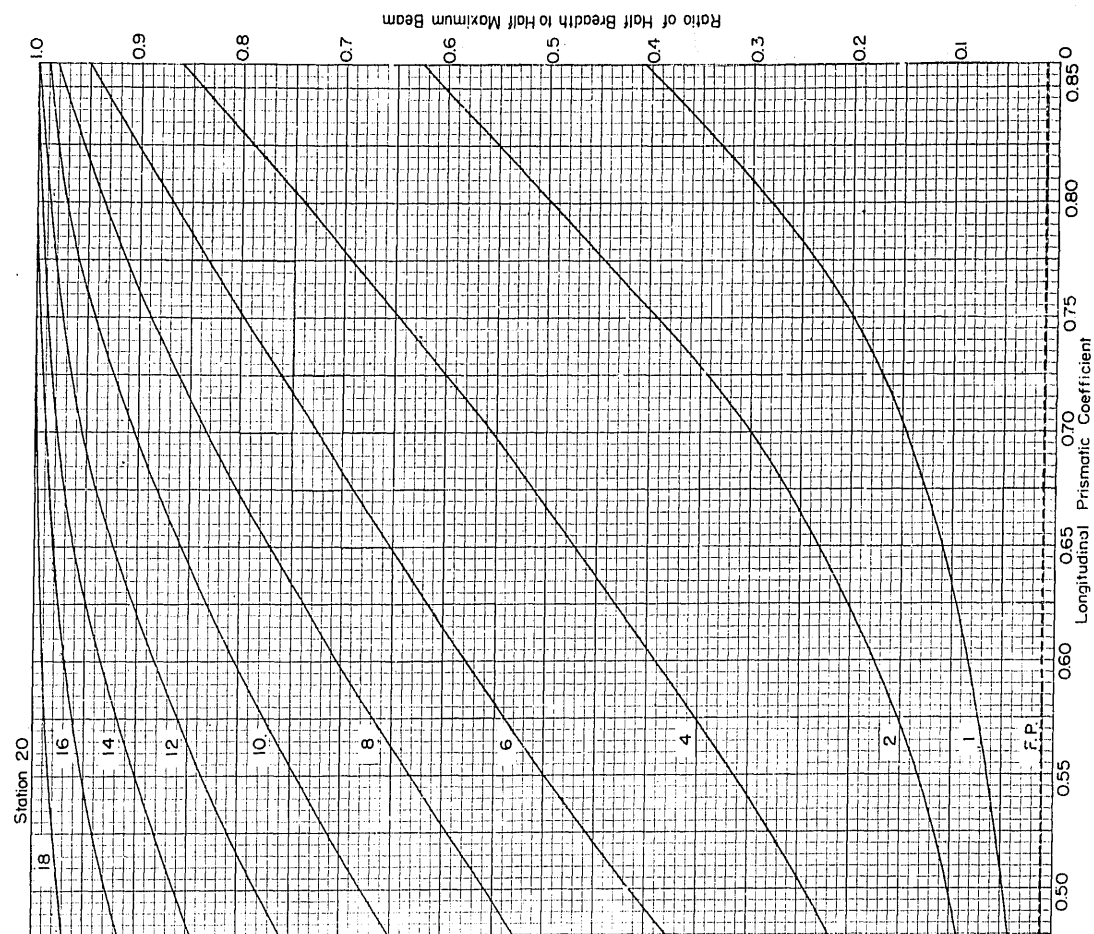
1.2 WL



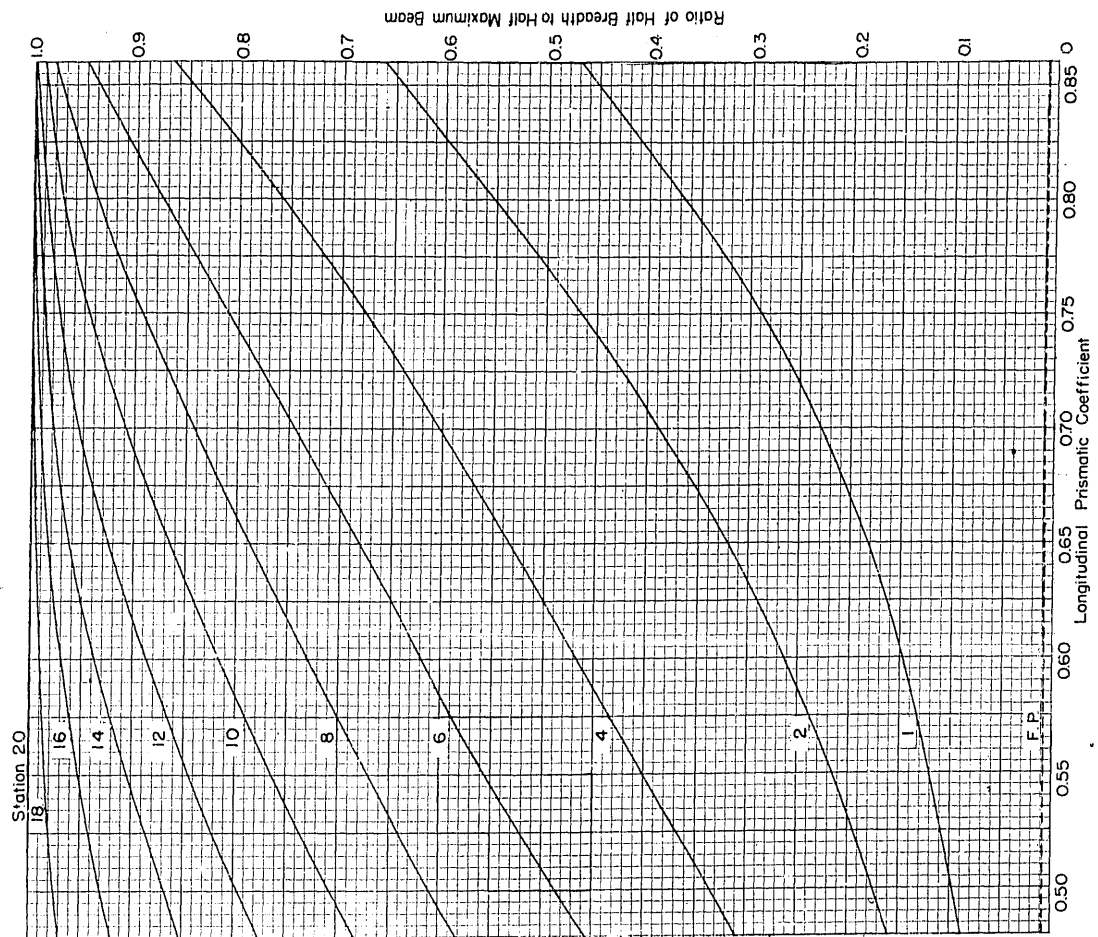
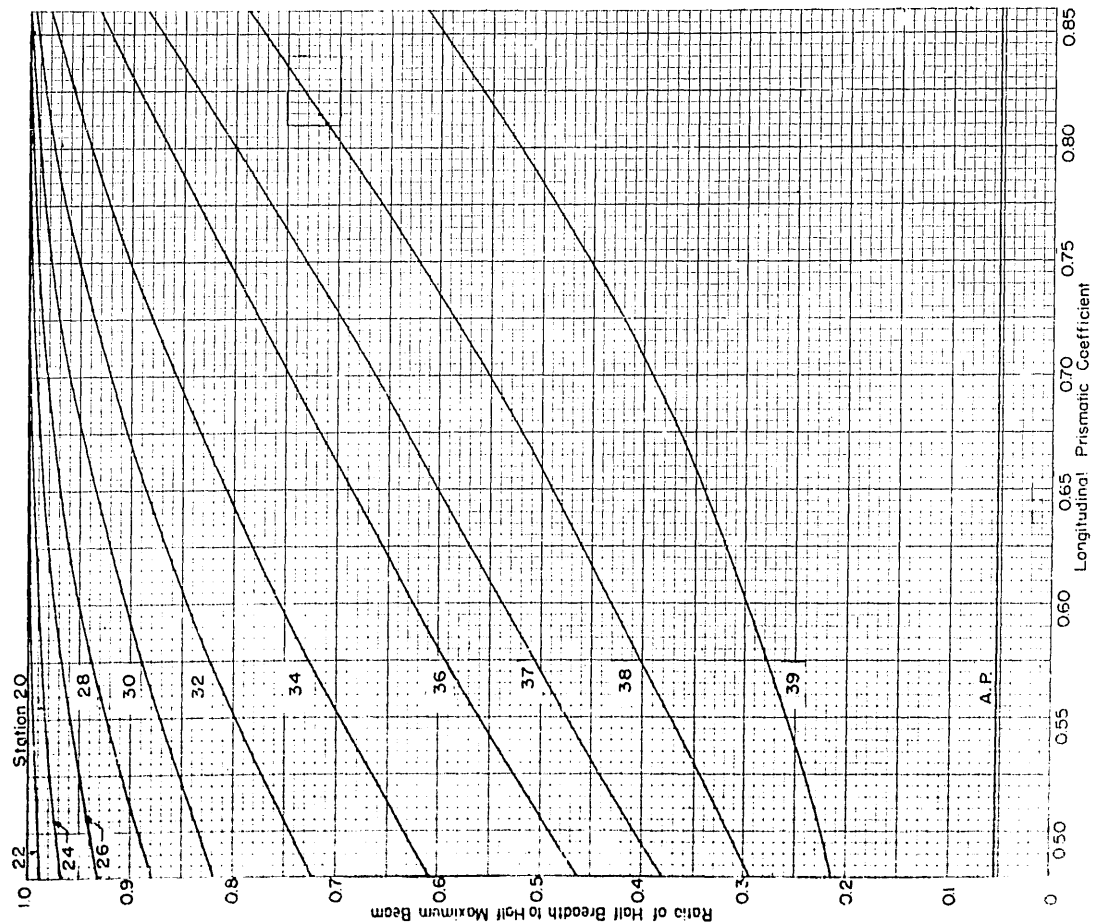
1.4 WL



1.6 WL



1.8 WL

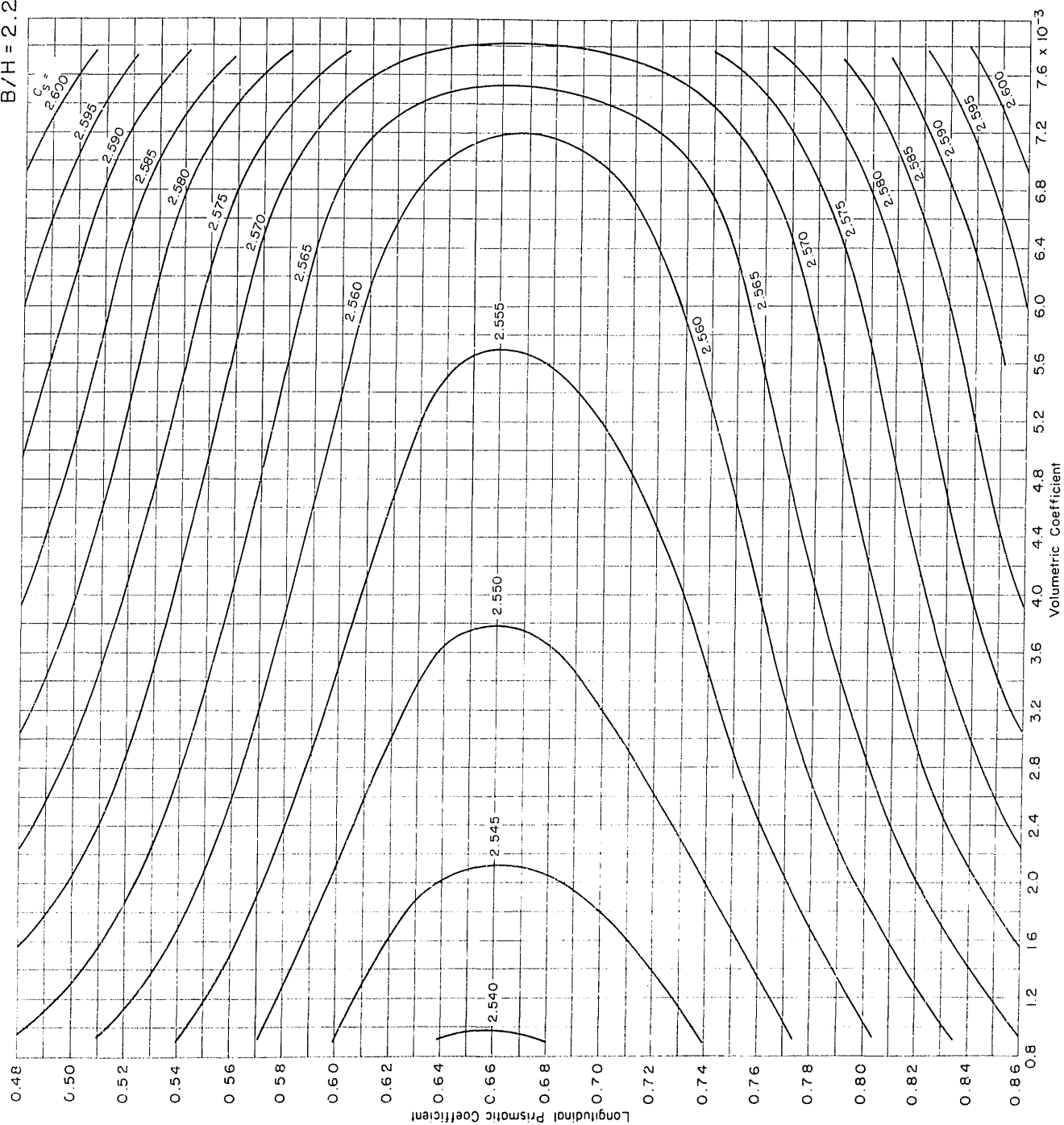


APPENDIX 2

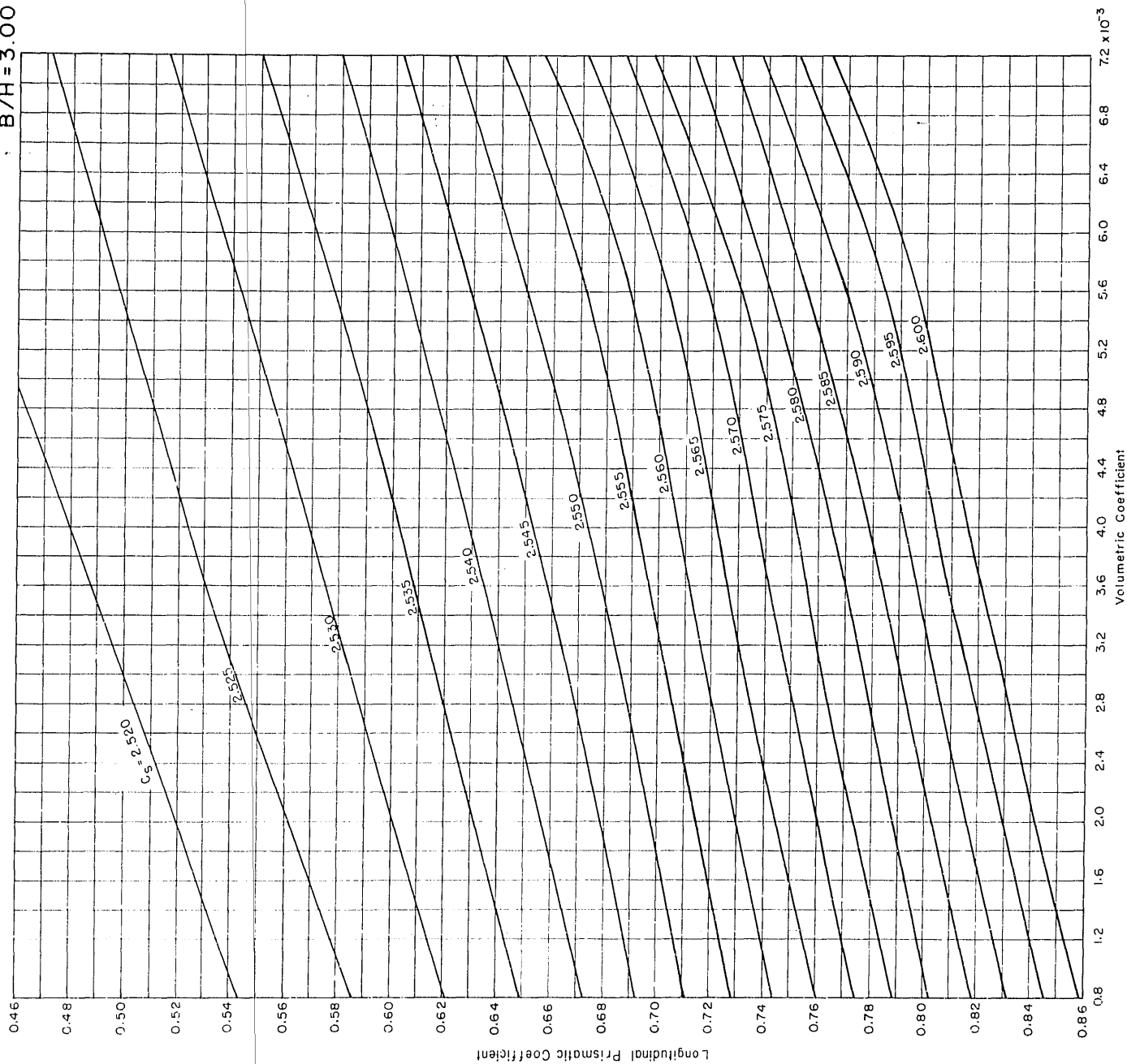
CONTOURS OF WETTED-SURFACE COEFFICIENTS FOR STANDARD SERIES VESSELS PLOTTED AGAINST PRISMATIC COEFFICIENT AND VOLUMETRIC COEFFICIENT

Separate sets of contours are given for beam-draft ratios of 2.25, 3.00 and 3.75.

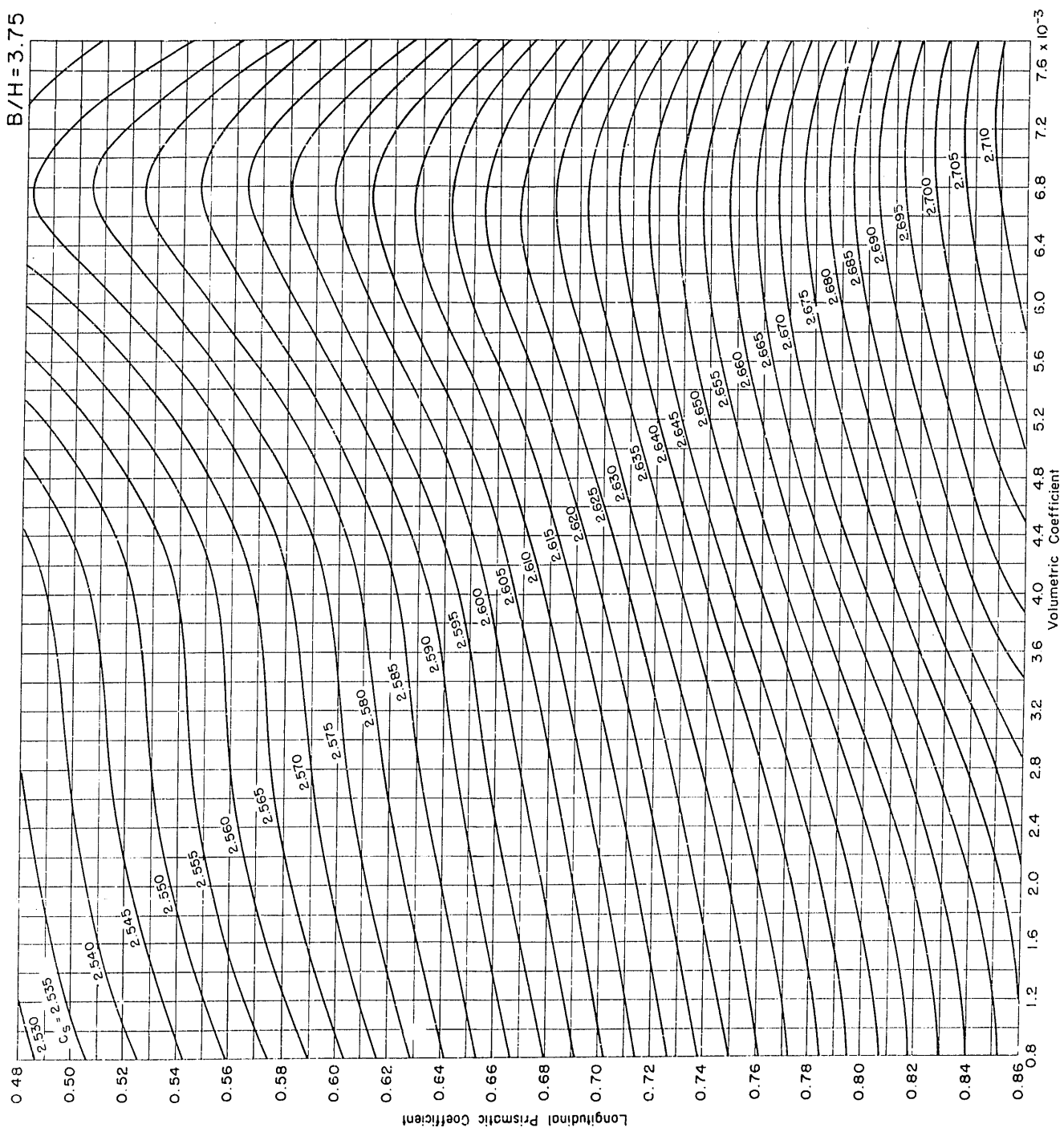
$B/H = 2.25$



$B/H = 3.00$



B/H = 3.75



APPENDIX 3

CURVES OF RESIDUAL-RESISTANCE COEFFICIENT VERSUS SPEED-LENGTH RATIO AND FROUDE NUMBER FOR STANDARD SERIES VESSELS HAVING A BEAM-DRAFT RATIO OF 2.25

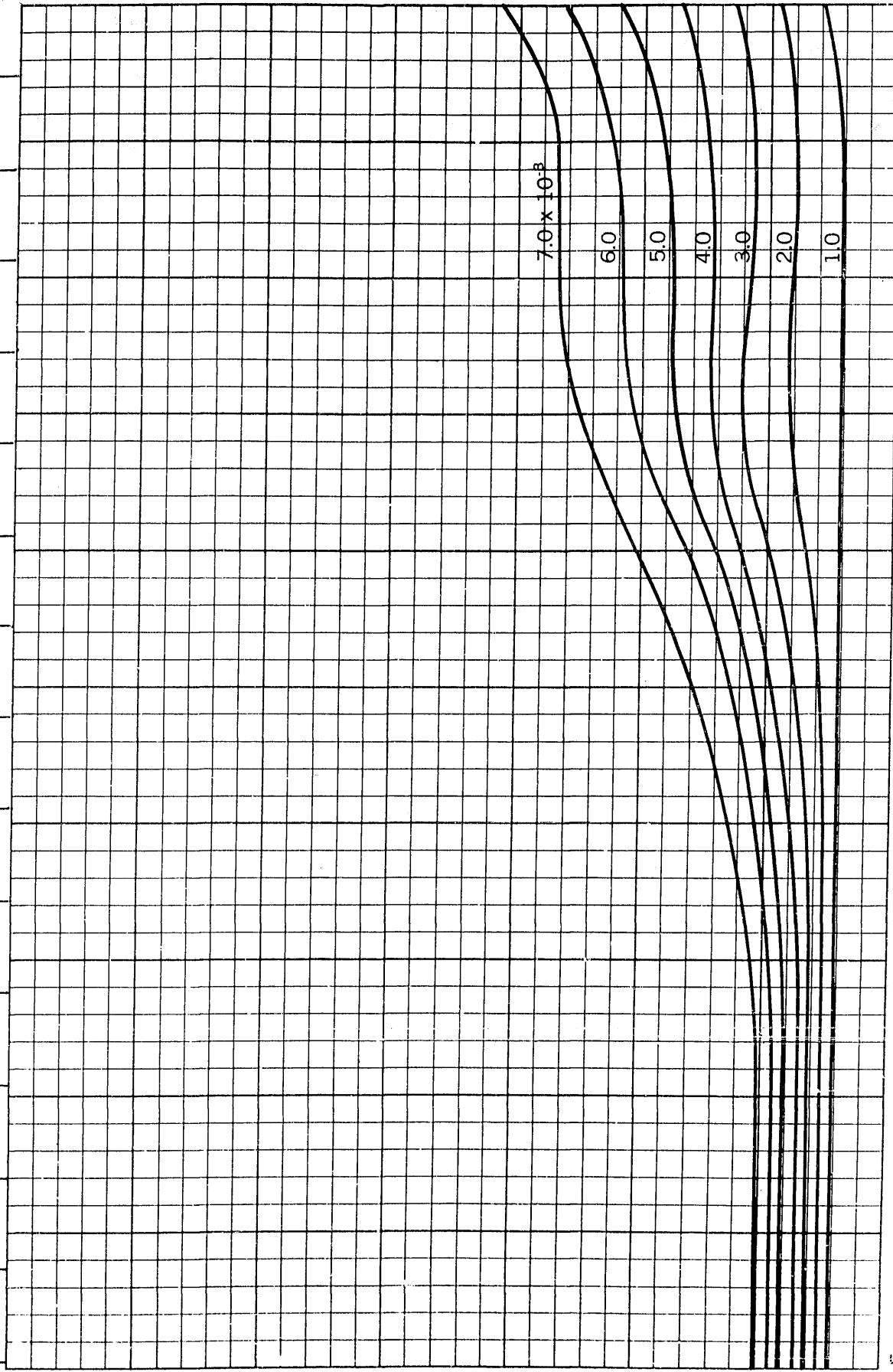
The curves of residual-resistance coefficients for even values of volumetric coefficient are presented separately for each longitudinal prismatic coefficient between 0.48 and 0.86 in increments of 0.01. For each family of curves, ranges of speed-length ratios of 0.5 to 1.0 and 1.0 to 2.0 are given on adjacent pages. The scale divisions, for both ordinate and abscissa, at the lower speed-length ratios are twice as large as those of the higher range to permit increased accuracy of reading.

A supplementary table of residual-resistance coefficients is given for those coefficients which are not constant below a speed-length ratio of 0.50.

$B/H=2.25$
 $C_p=0.48$

Froude Number $\frac{v}{\sqrt{gL}}$

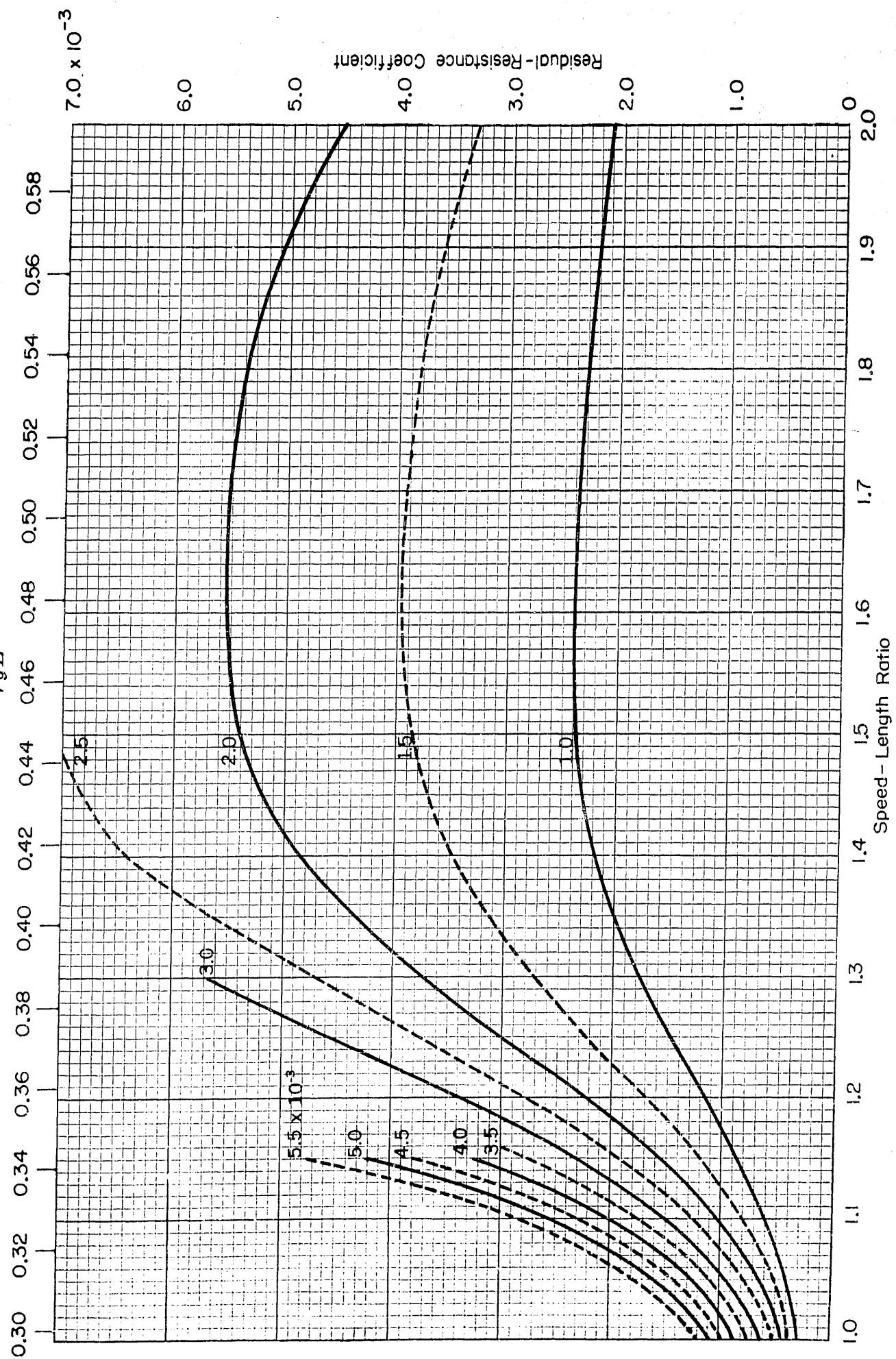
0.15 0.16 0.17 0.18 0.19 0.20 0.21 0.22 0.23 0.24 0.25 0.26 0.27 0.28 0.29



Residual-Resistance Coefficient

3.0×10^{-3}

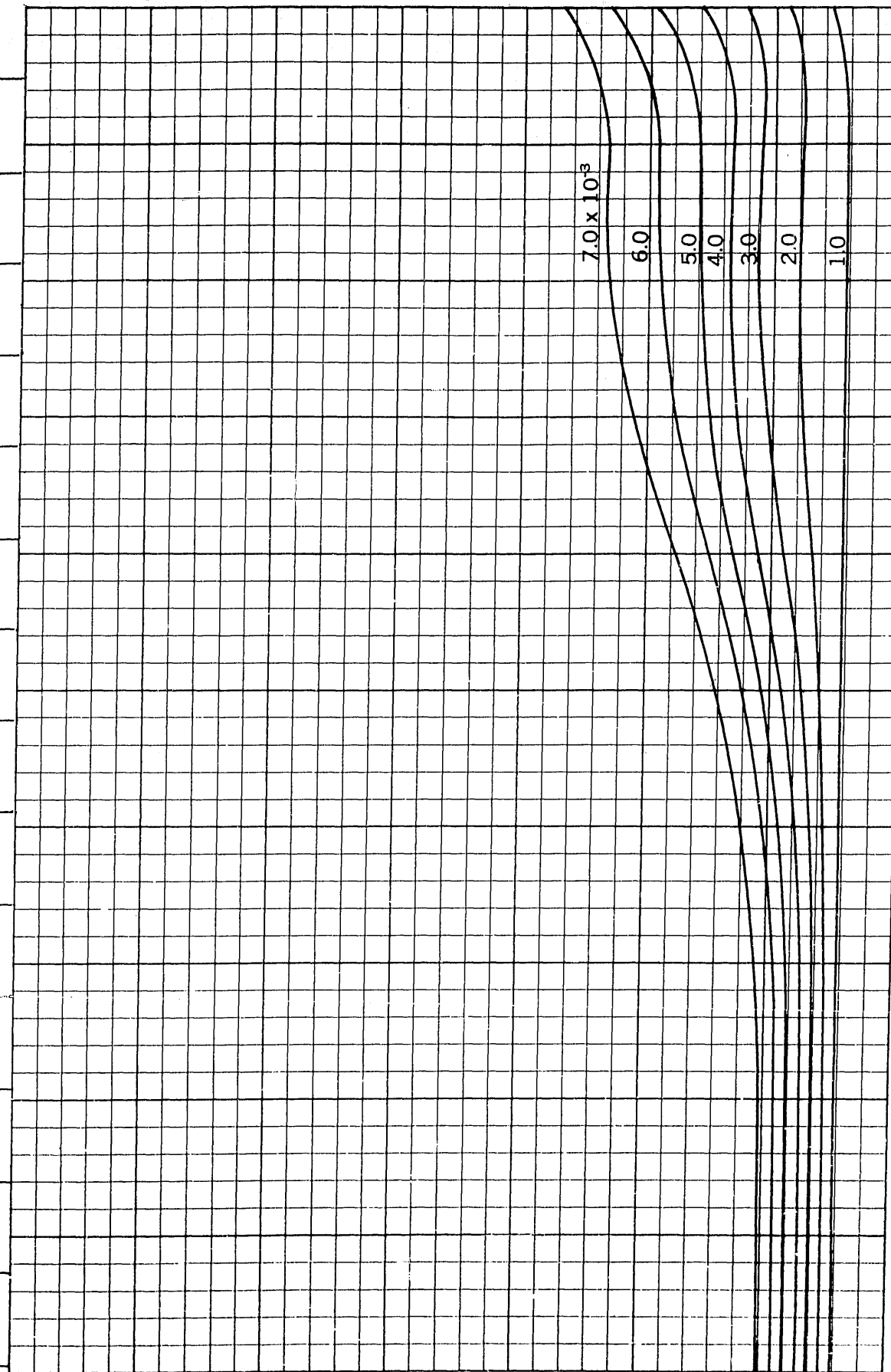
0.5 0.6 0.7 0.8 0.9 1.0

$$\frac{v}{\sqrt{gL}}$$


$B/H=2.25$
 $C_p=0.49$

Froude Number $\frac{v}{\sqrt{gL}}$

0.15 0.16 0.17 0.18 0.19 0.20 0.21 0.22 0.23 0.24 0.25 0.26 0.27 0.28 0.29



3.0 $\times 10^{-3}$
2.0
1.0

0.5

0.6

0.7

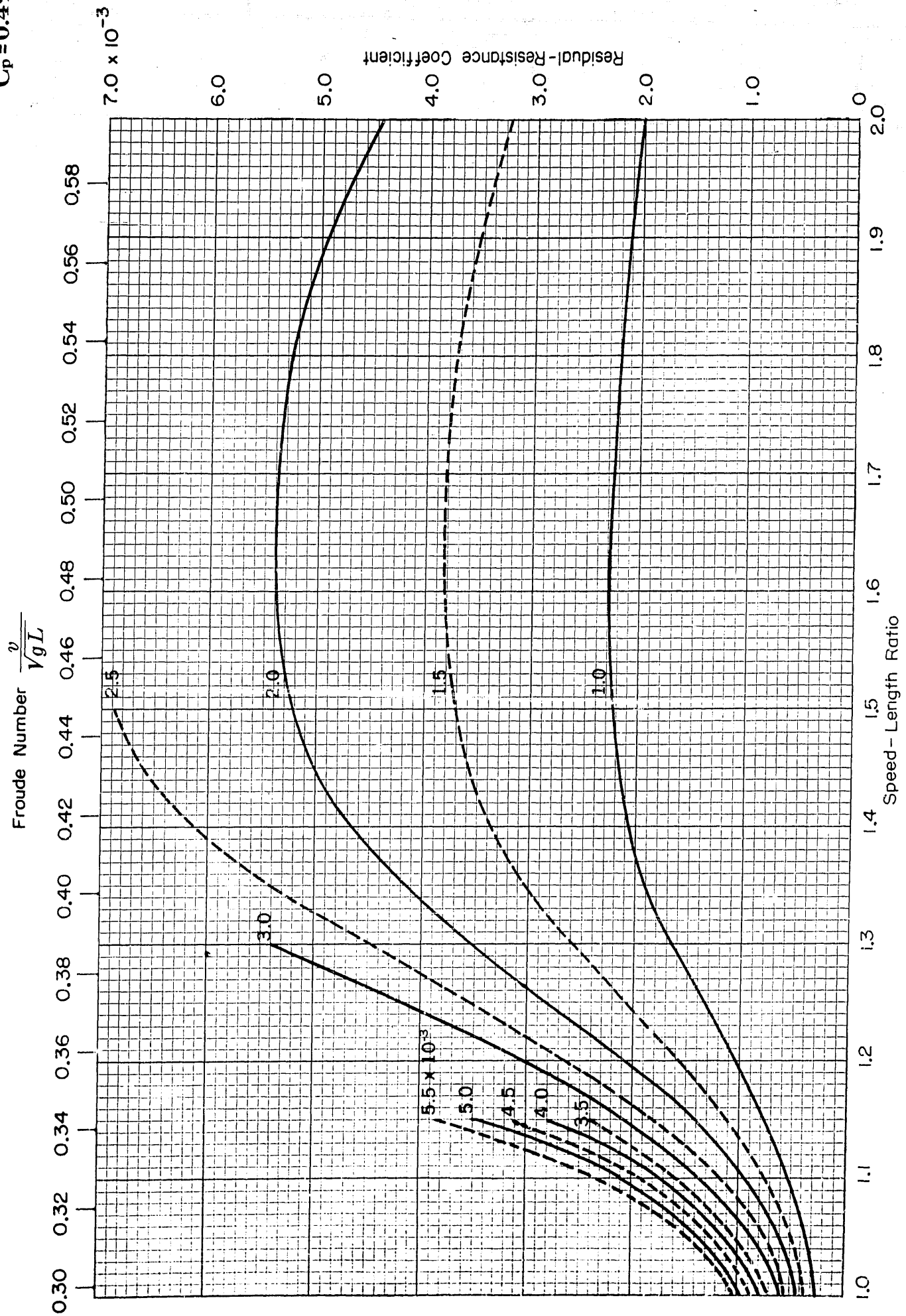
0.8

0.9

1.0

Speed - Length Ratio

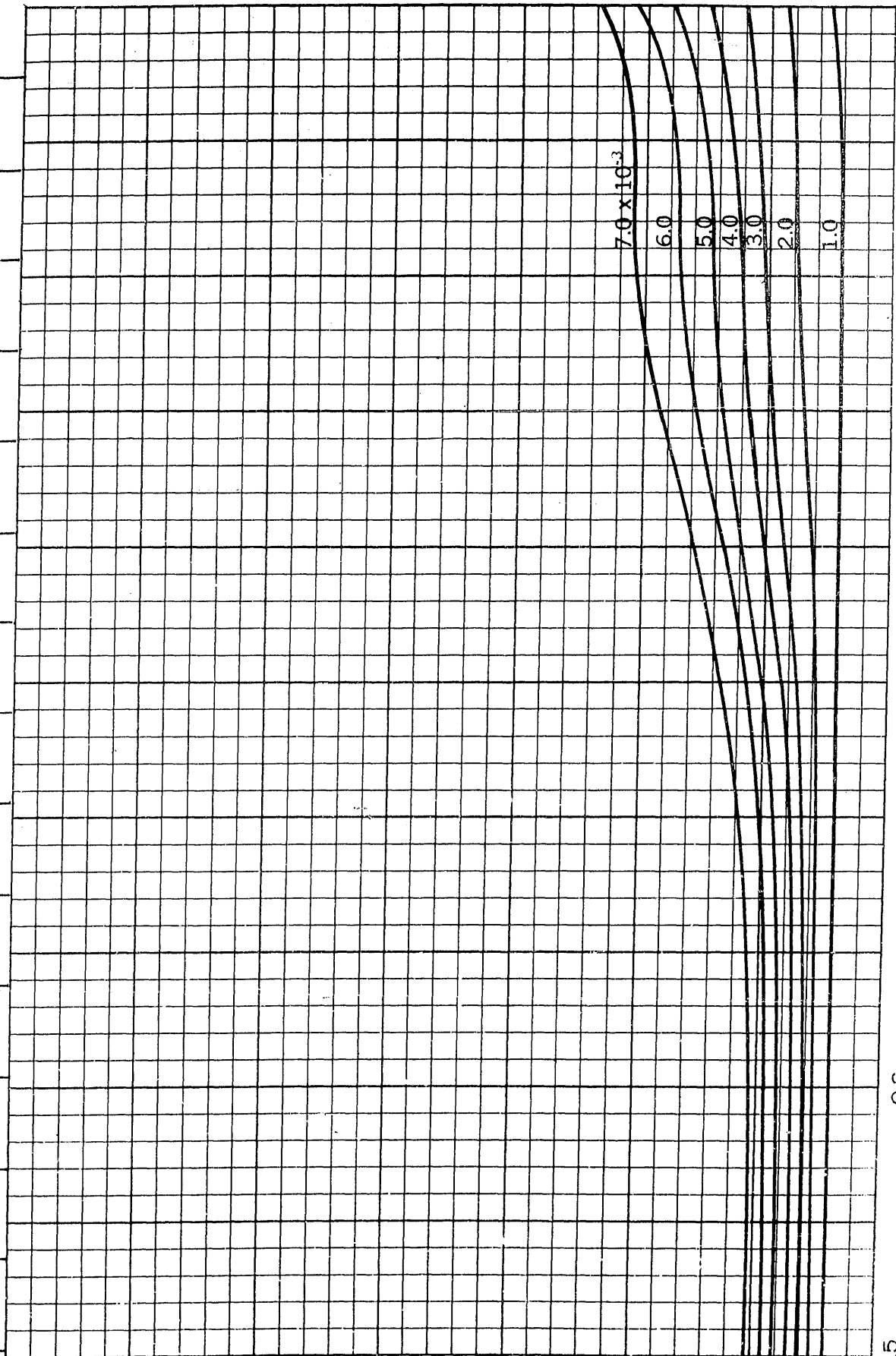
$B/H=2.25$
 $C_p=0.49$



$B/H = 2.25$
 $C_p = 0.50$

Froude Number $\frac{v}{\sqrt{gL}}$

0.15 0.16 0.17 0.18 0.19 0.20 0.21 0.22 0.23 0.24 0.25 0.26 0.27 0.28 0.29



Residual-Resistance Coefficient

3.0×10^{-3}

0.5

0.6

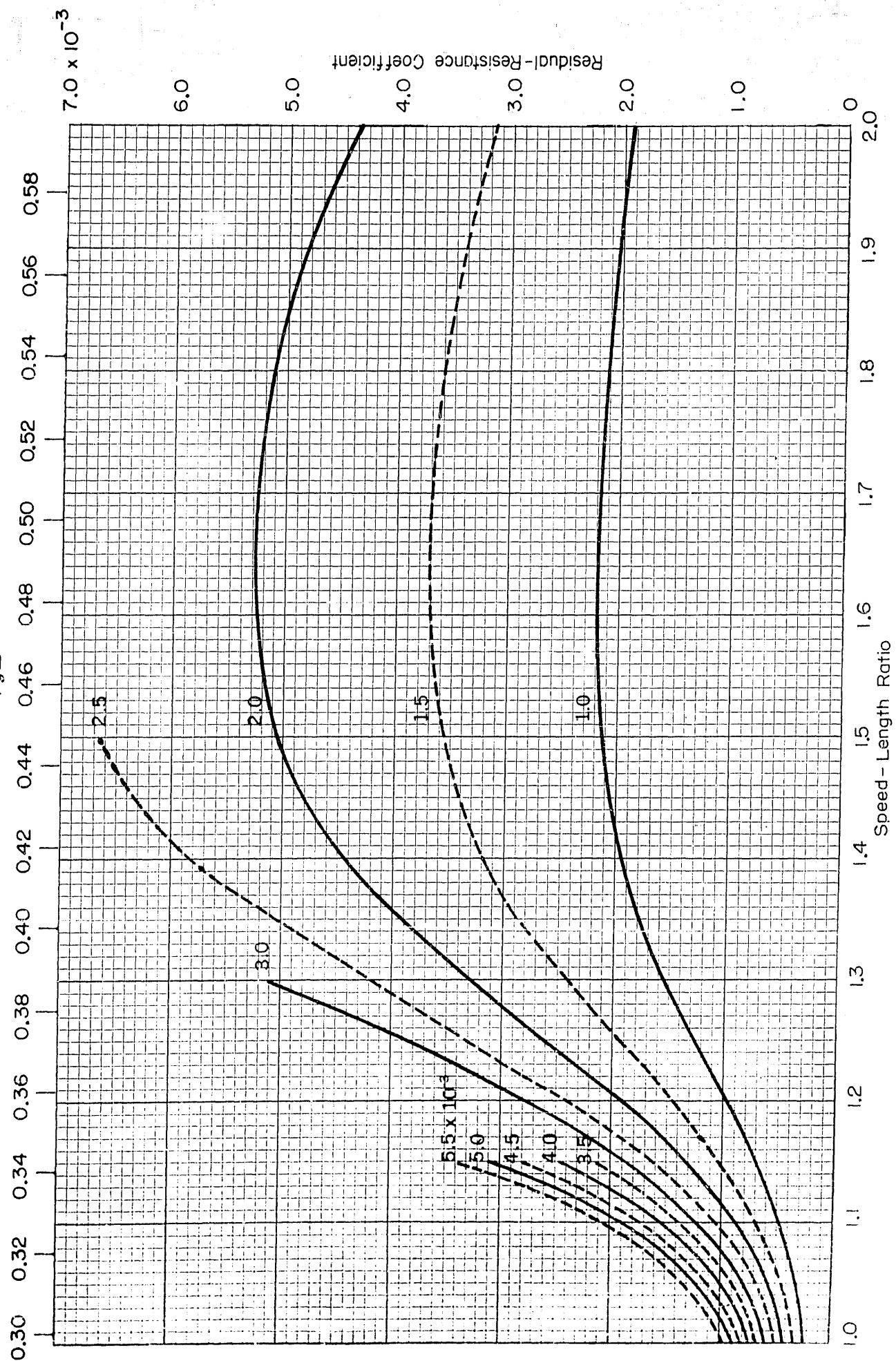
0.7

0.8

0.9

1.0

Speed - Length Ratio

Froude Number $\frac{v}{\sqrt{gL}}$ 

$B/H=2.25$
 $C_p=0.51$

Froude Number $\frac{v}{\sqrt{gL}}$

0.15 0.16 0.17 0.18 0.19 0.20 0.21 0.22 0.23 0.24 0.25 0.26 0.27 0.28 0.29

0.5

0.6

0.7

0.8

0.9

1.0

Speed - Length Ratio

Residual-Resistance Coefficient

2.0

1.0

3.0×10^{-3}

7.0×10^{-3}

6.0

5.0

4.0

3.0

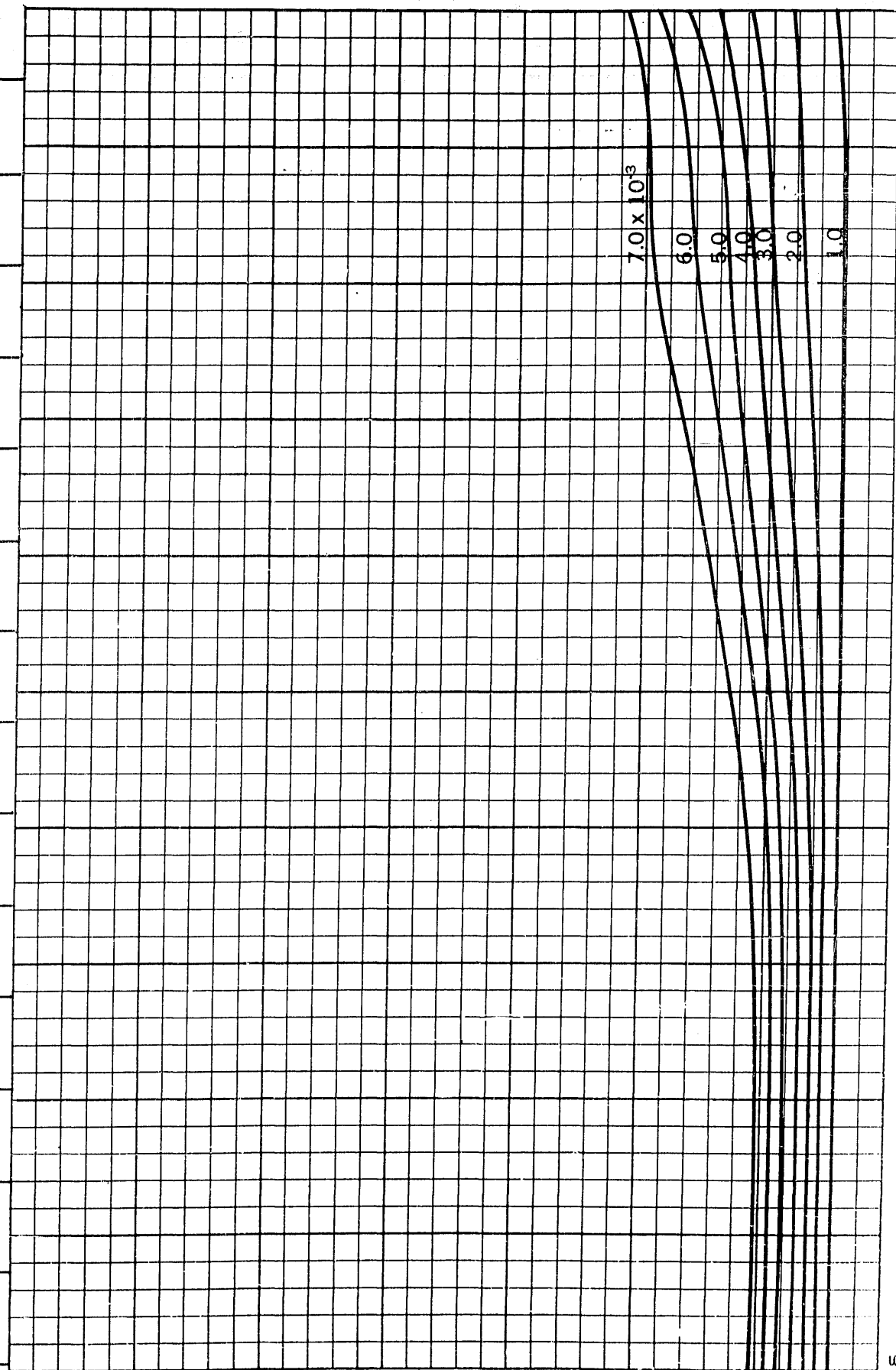
2.0

1.0

$B/H = 2.25$
 $C_p = 0.51$

Froude Number $\frac{v}{\sqrt{gL}}$

0.15 0.16 0.17 0.18 0.19 0.20 0.21 0.22 0.23 0.24 0.25 0.26 0.27 0.28 0.29



Residual-Resistance Coefficient

3.0×10^{-3}

0

1.0

0.9

0.8

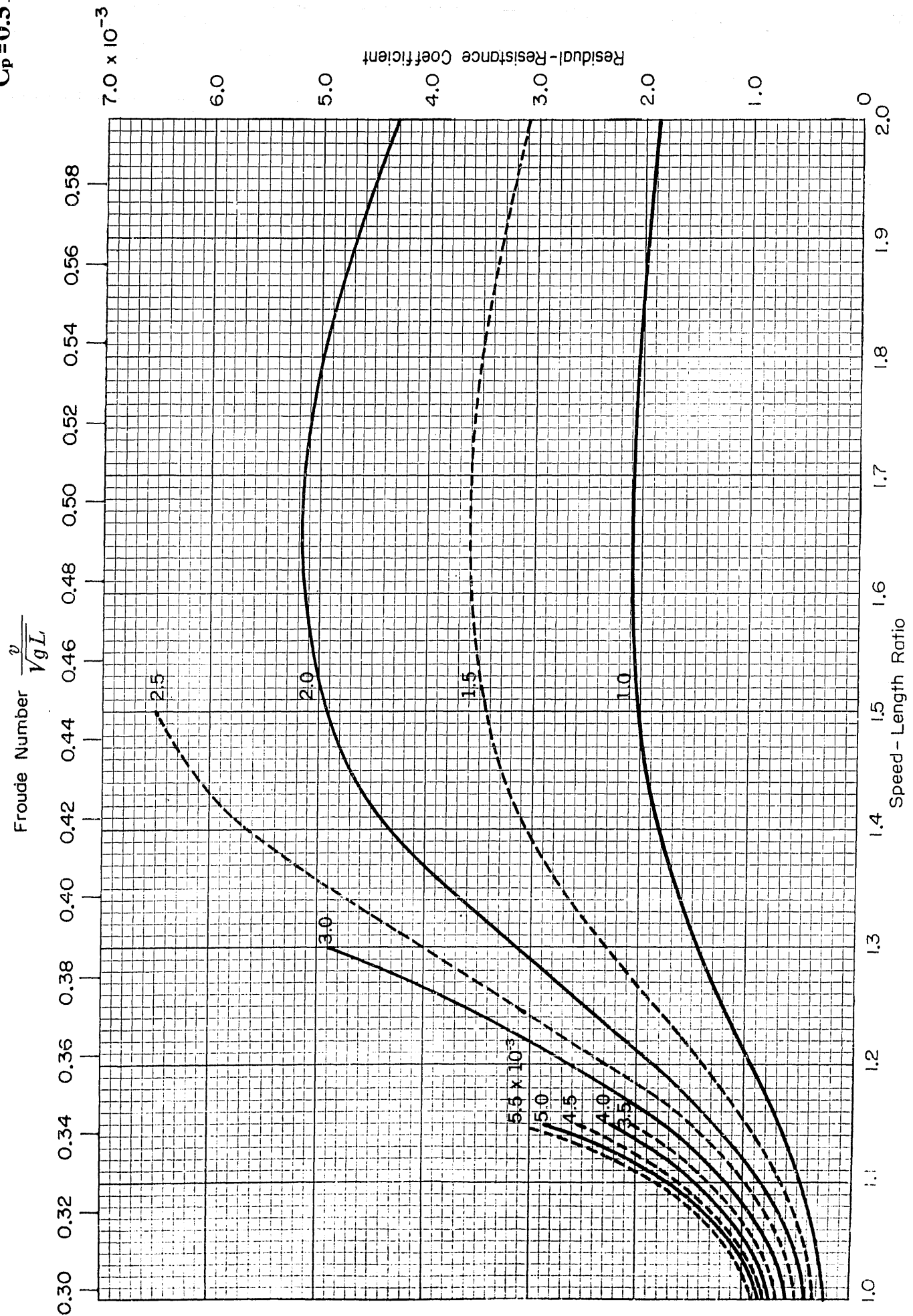
Speed - Length Ratio

0.7

0.6

0.5

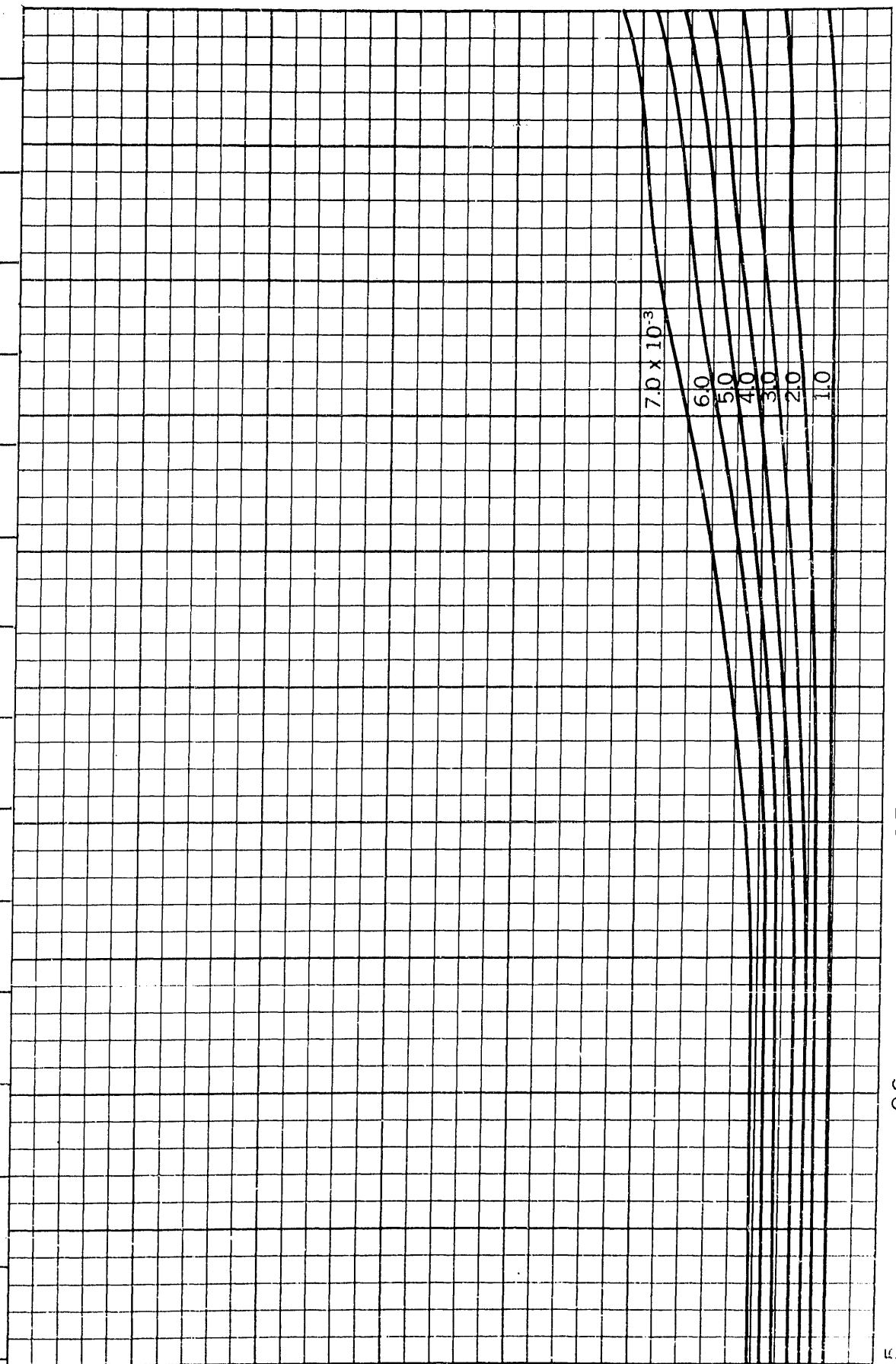
$B/H=2.25$
 $C_p=0.51$



$B/H=2.25$
 $C_p=0.52$

Froude Number $\frac{v}{\sqrt{gL}}$

0.15 0.16 0.17 0.18 0.19 0.20 0.21 0.22 0.23 0.24 0.25 0.26 0.27 0.28 0.29



Residual-Resistance Coefficient

0

0.9

0.8

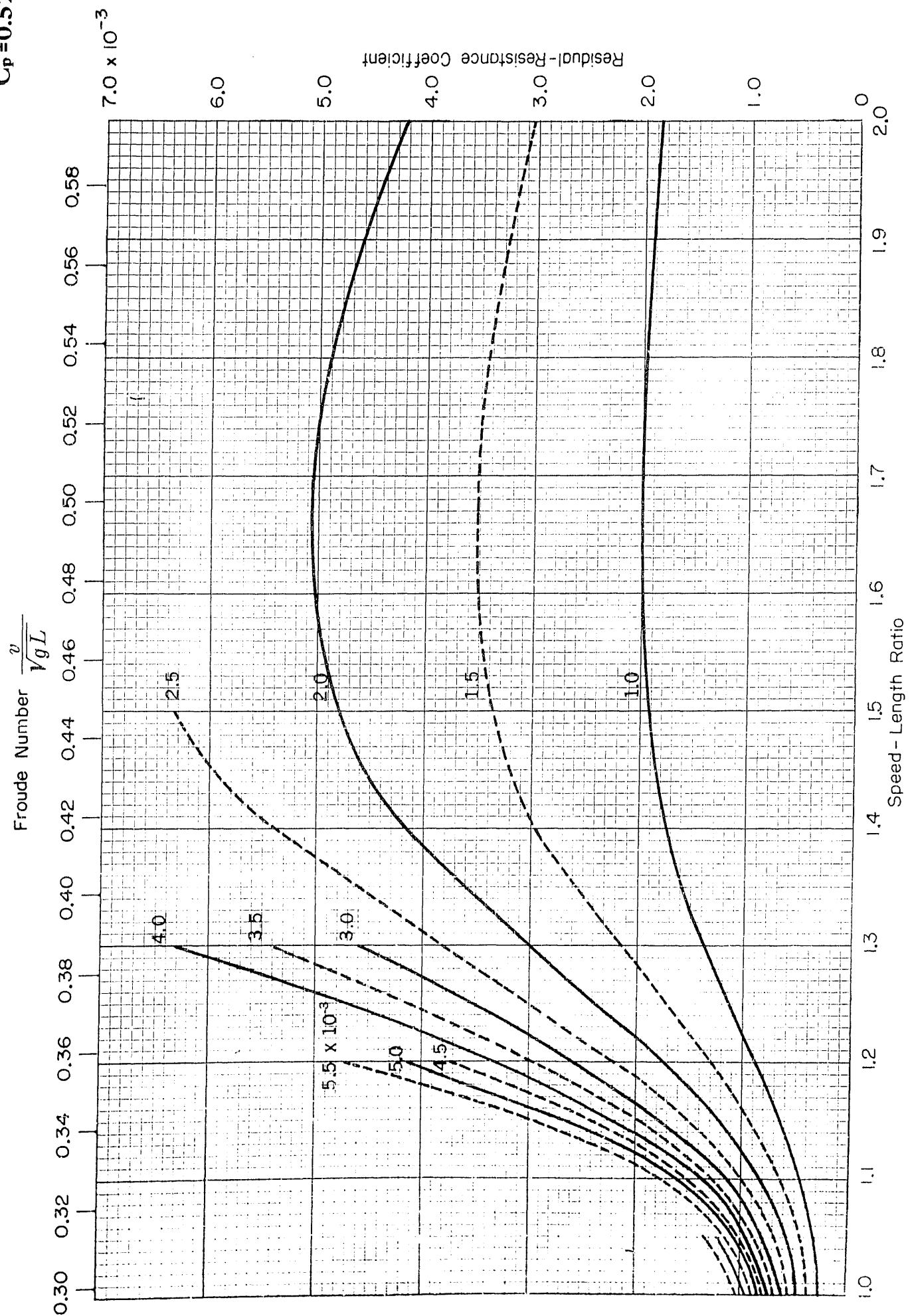
0.7

0.6

0.5

Speed - Length Ratio

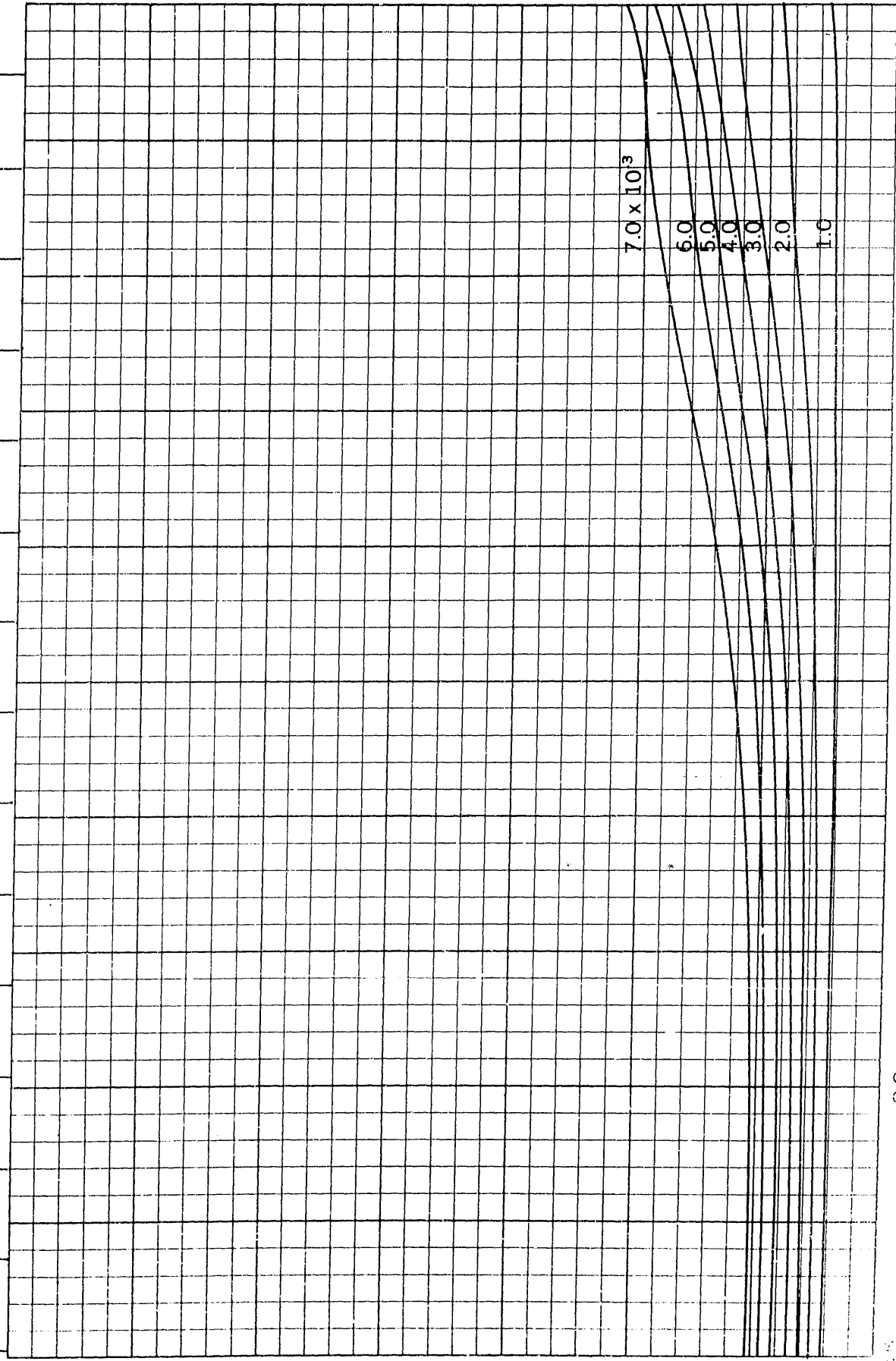
$B/H=2.25$
 $C_p=0.52$



$B/H = 2.25$
 $C_p = 0.53$

Froude Number $\frac{v}{\sqrt{gL}}$

0.15 0.16 0.17 0.18 0.19 0.20 0.21 0.22 0.23 0.24 0.25 0.26 0.27 0.28 0.29



Residual-Resistance Coefficient

3.0×10^{-3}

0

0.9

0.8

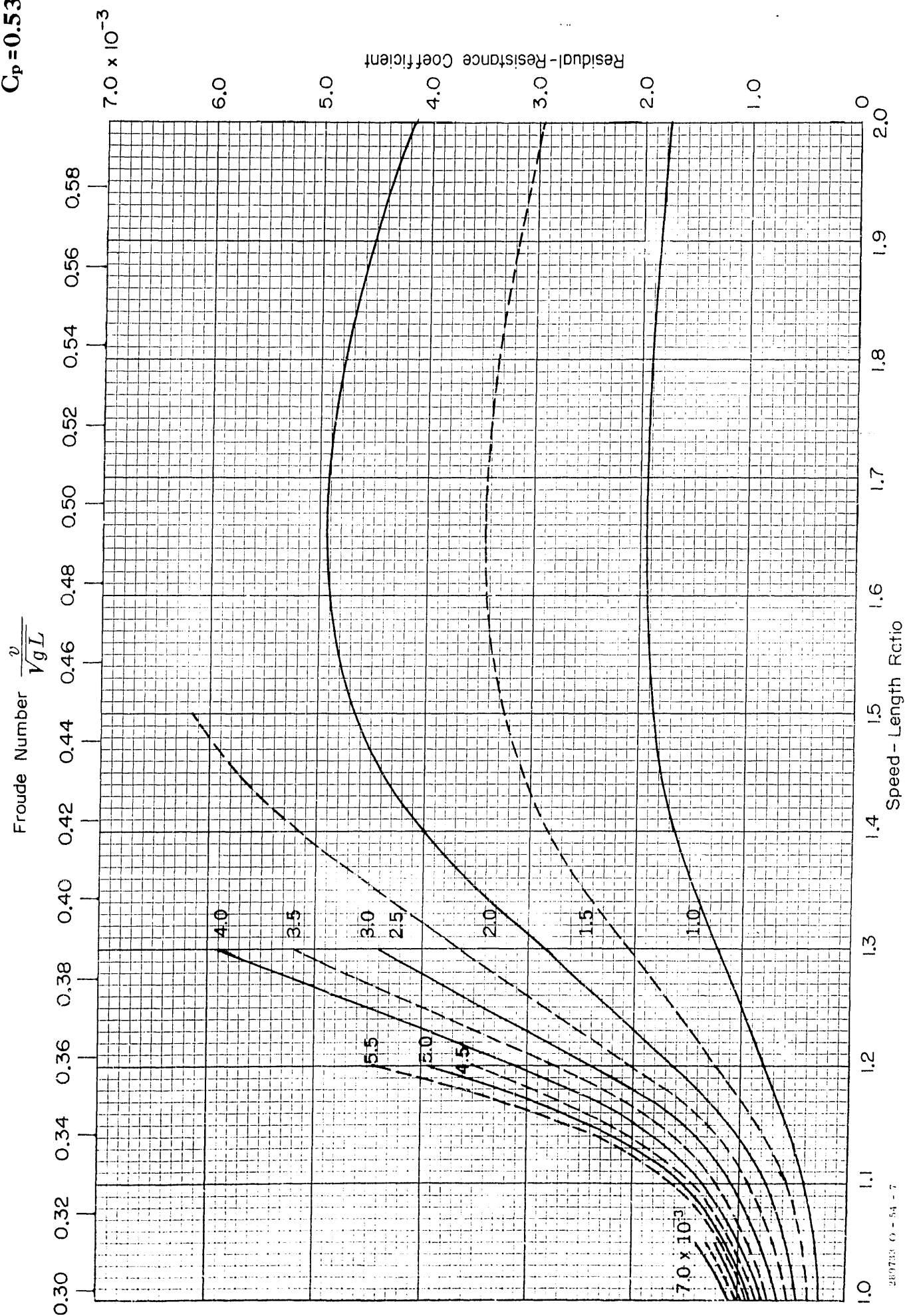
0.7

0.6

0.5

Speed - Length Ratio

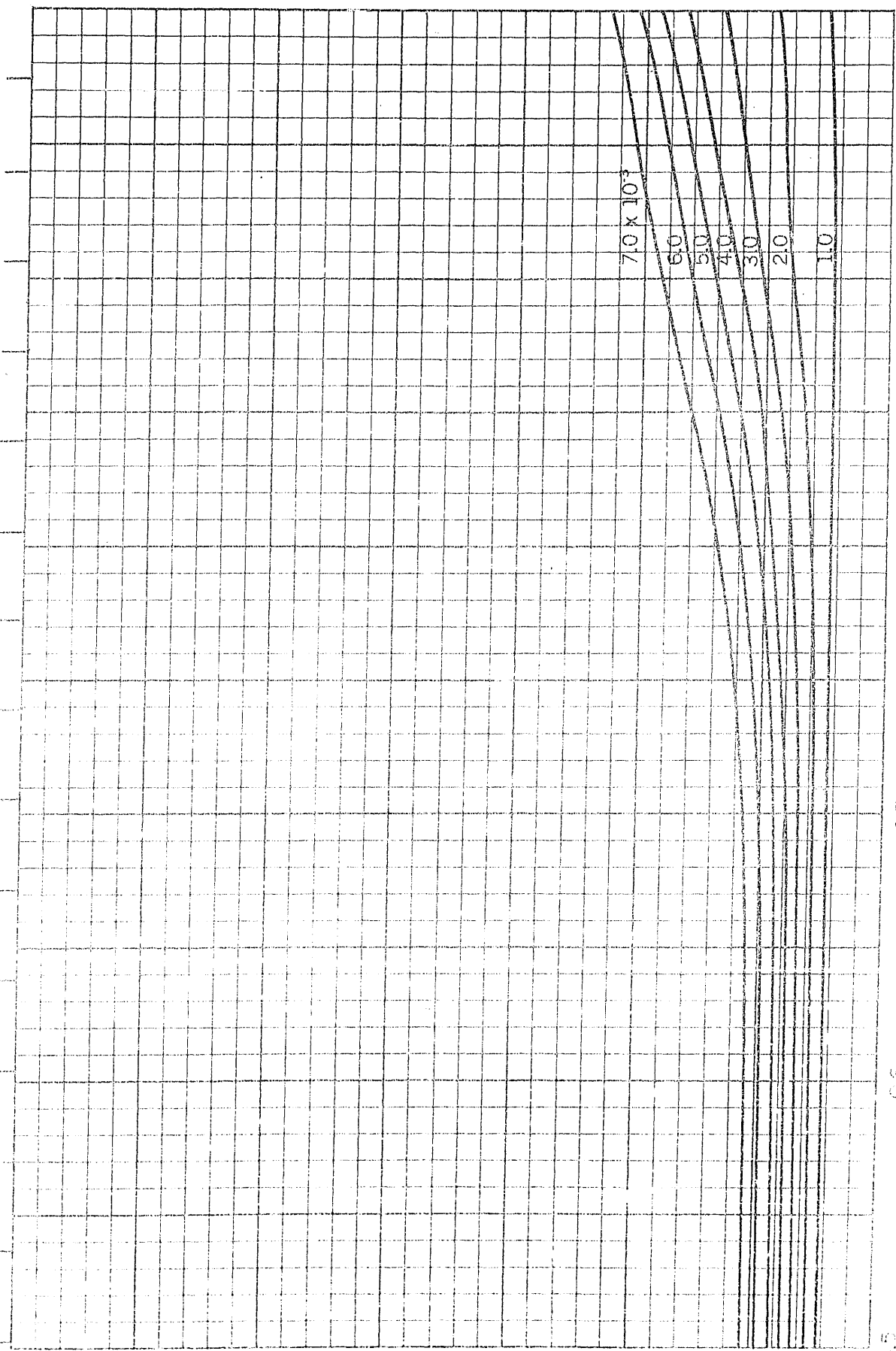
$B/H=2.25$
 $C_p=0.53$



B/H=2.25
C_p=0.54

Froude Number $\frac{v}{\sqrt{gL}}$

0.15 0.16 0.17 0.18 0.19 0.20 0.21 0.22 0.23 0.24 0.25 0.26 0.27 0.28 0.29



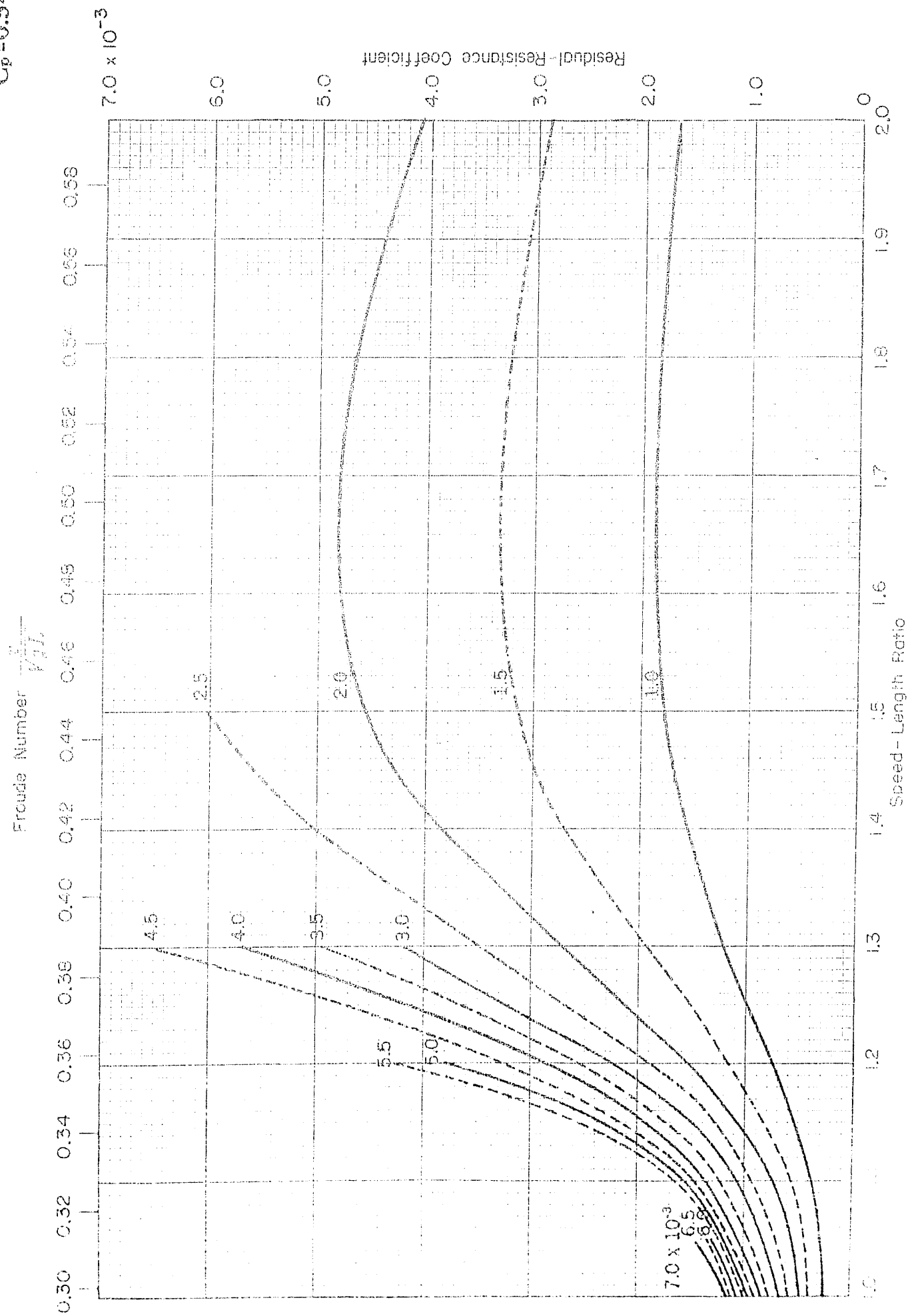
Residual-Resistance Coefficient
2.0
1.0
0

$\times 10^{-3}$

0
1.0

Speed-Length Ratio
0.5 0.6 0.7 0.8 0.9 1.0

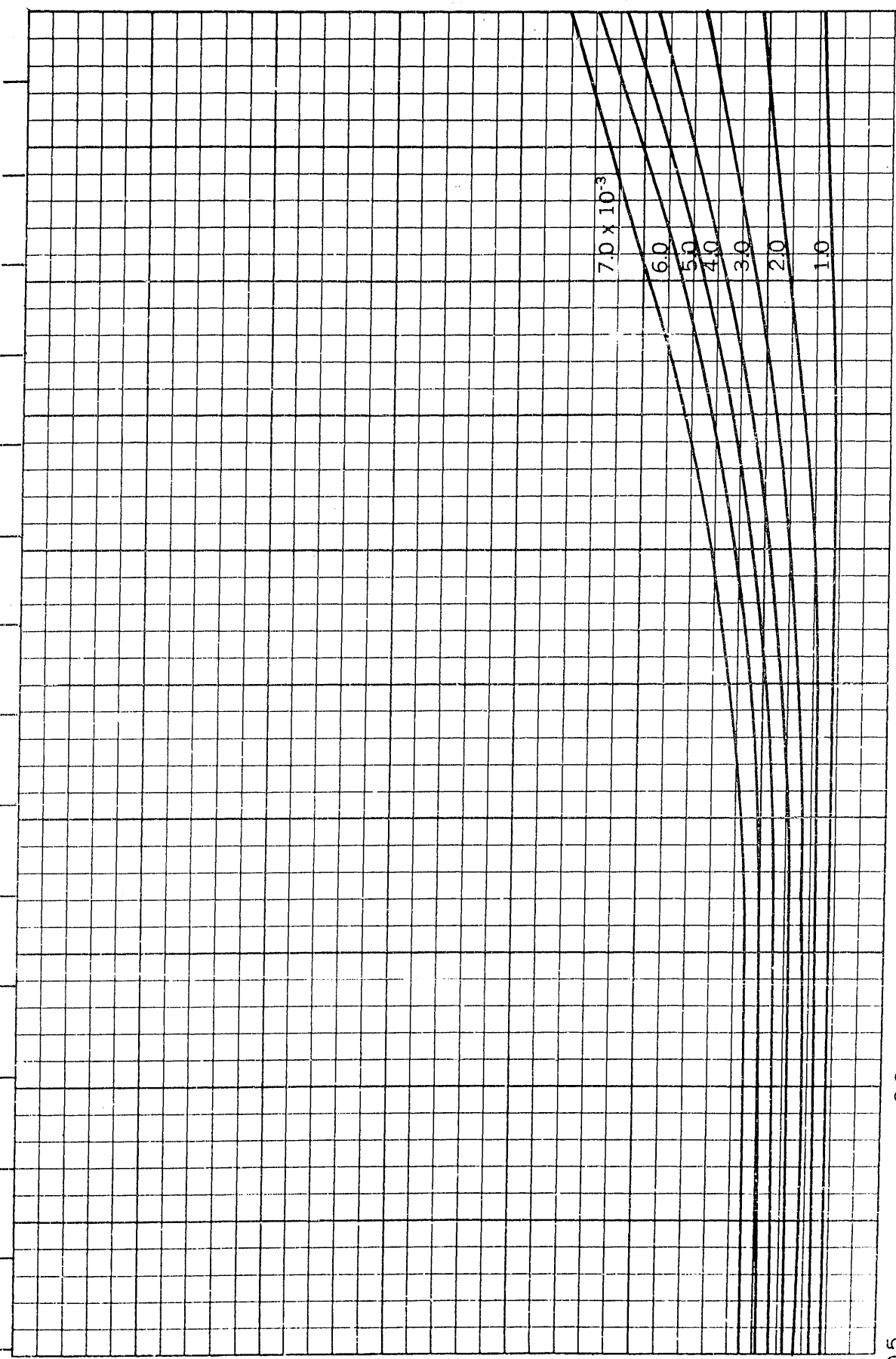
$B/H=2.25$
 $C_p=0.54$



$B/H = 2.25$
 $C_p = 0.55$

Froude Number $\frac{v}{\sqrt{gL}}$

0.15 0.16 0.17 0.18 0.19 0.20 0.21 0.22 0.23 0.24 0.25 0.26 0.27 0.28 0.29



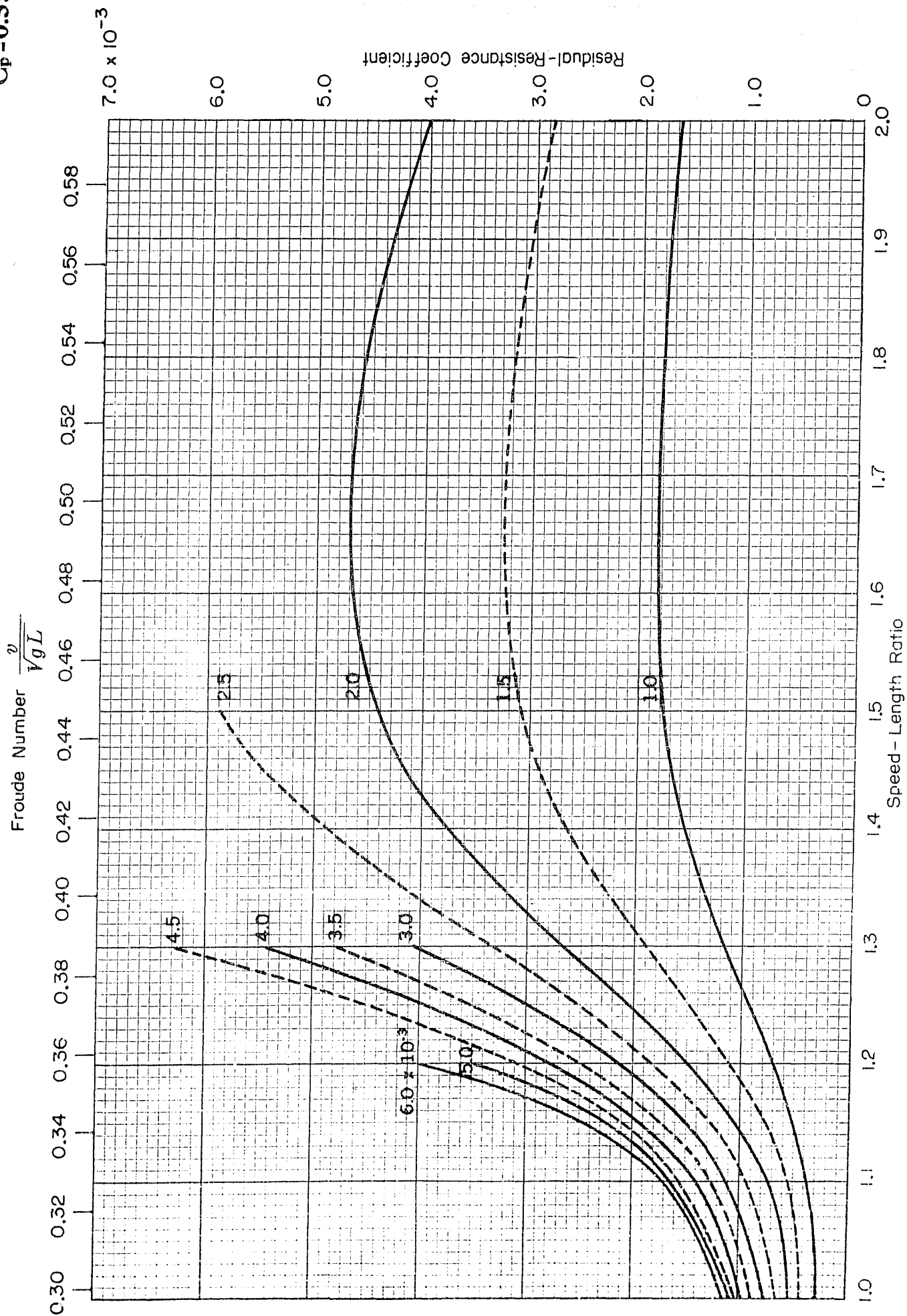
Residual-Resistance Coefficient

3.0×10^{-3}

0.5 0.6 0.7 0.8 0.9 1.0

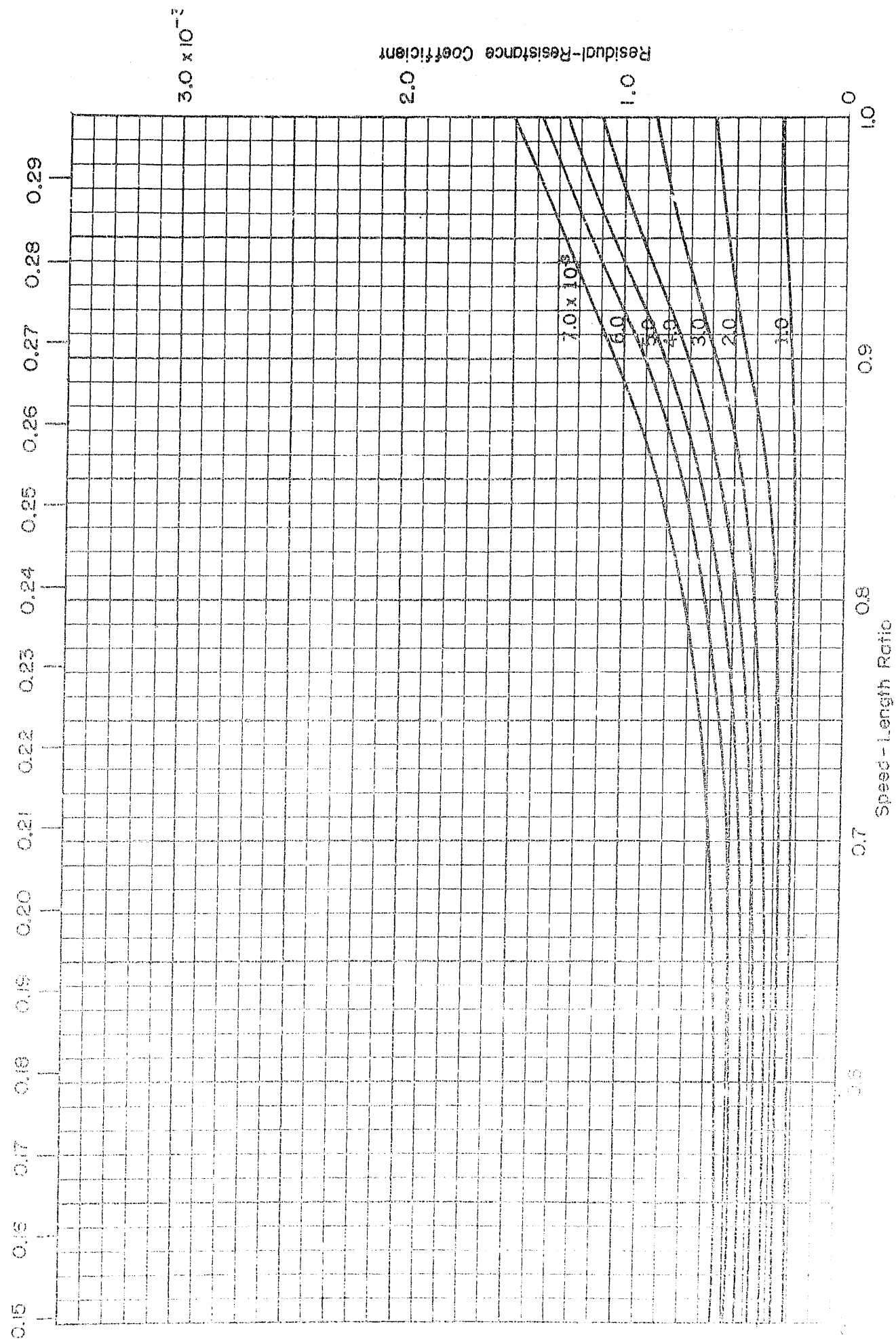
Speed - Length Ratio

$B/H=2.25$
 $C_p=0.55$

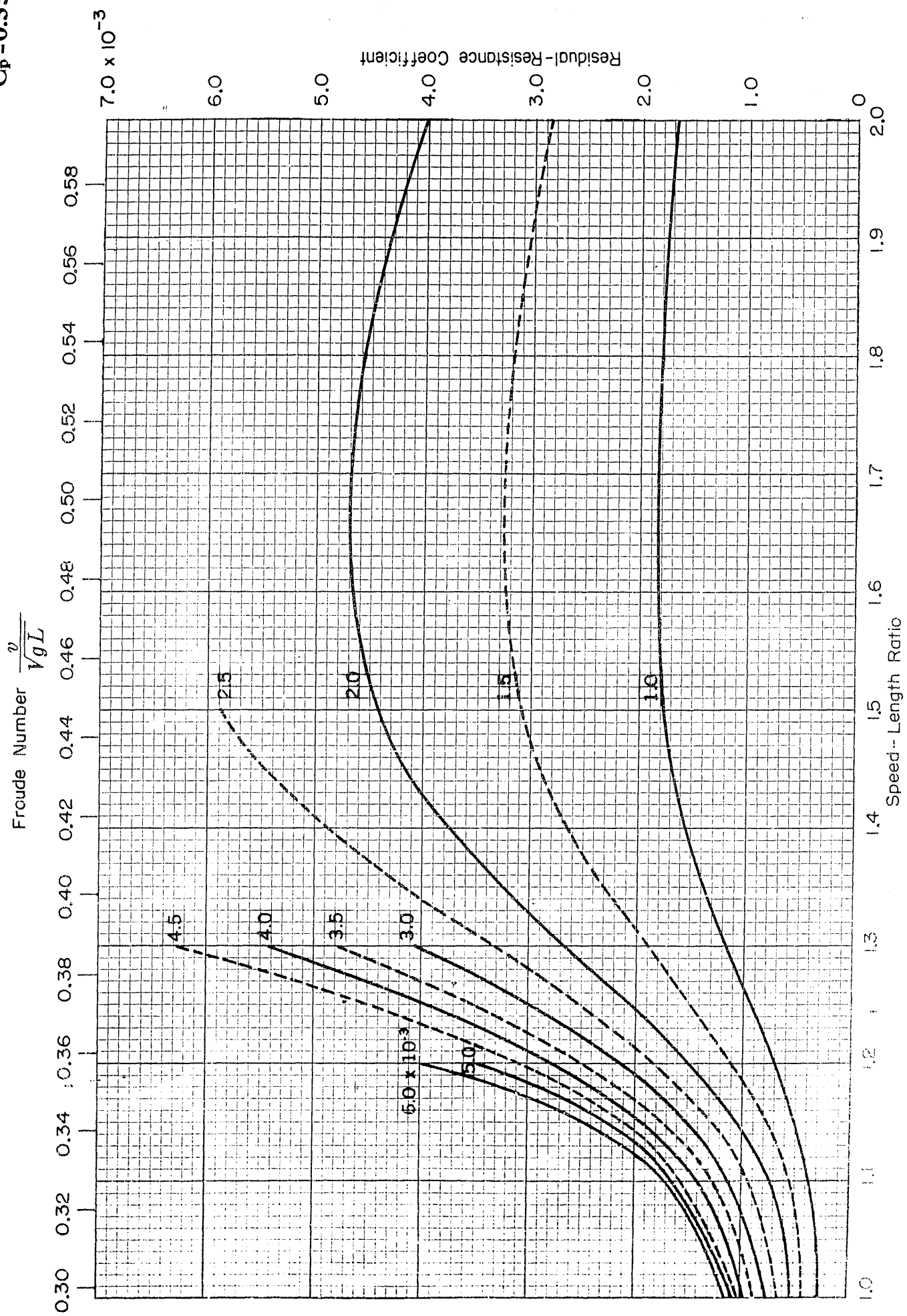


B/H=2.25
C_p=0.56

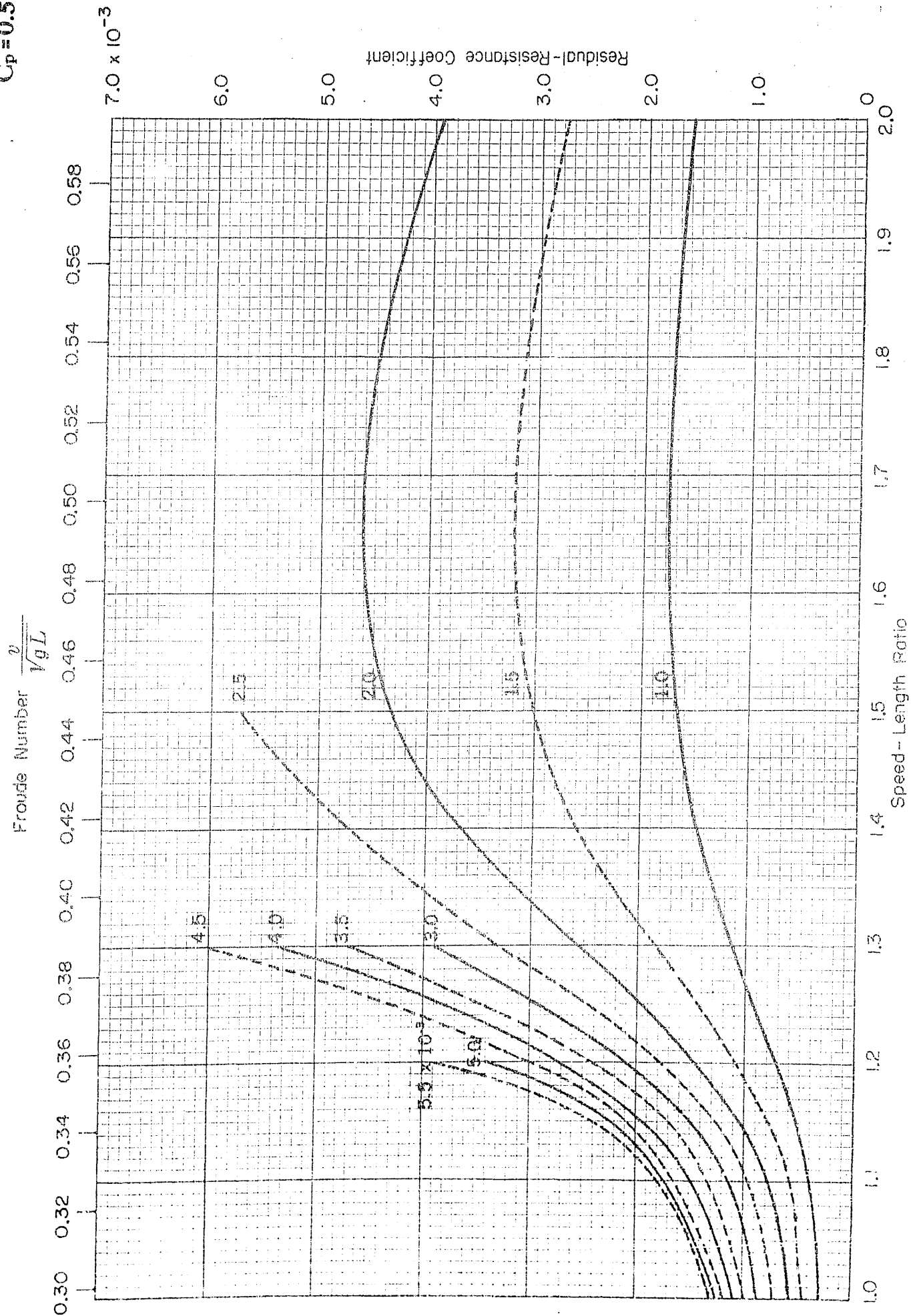
Froude Number $\frac{v}{\sqrt{gL}}$



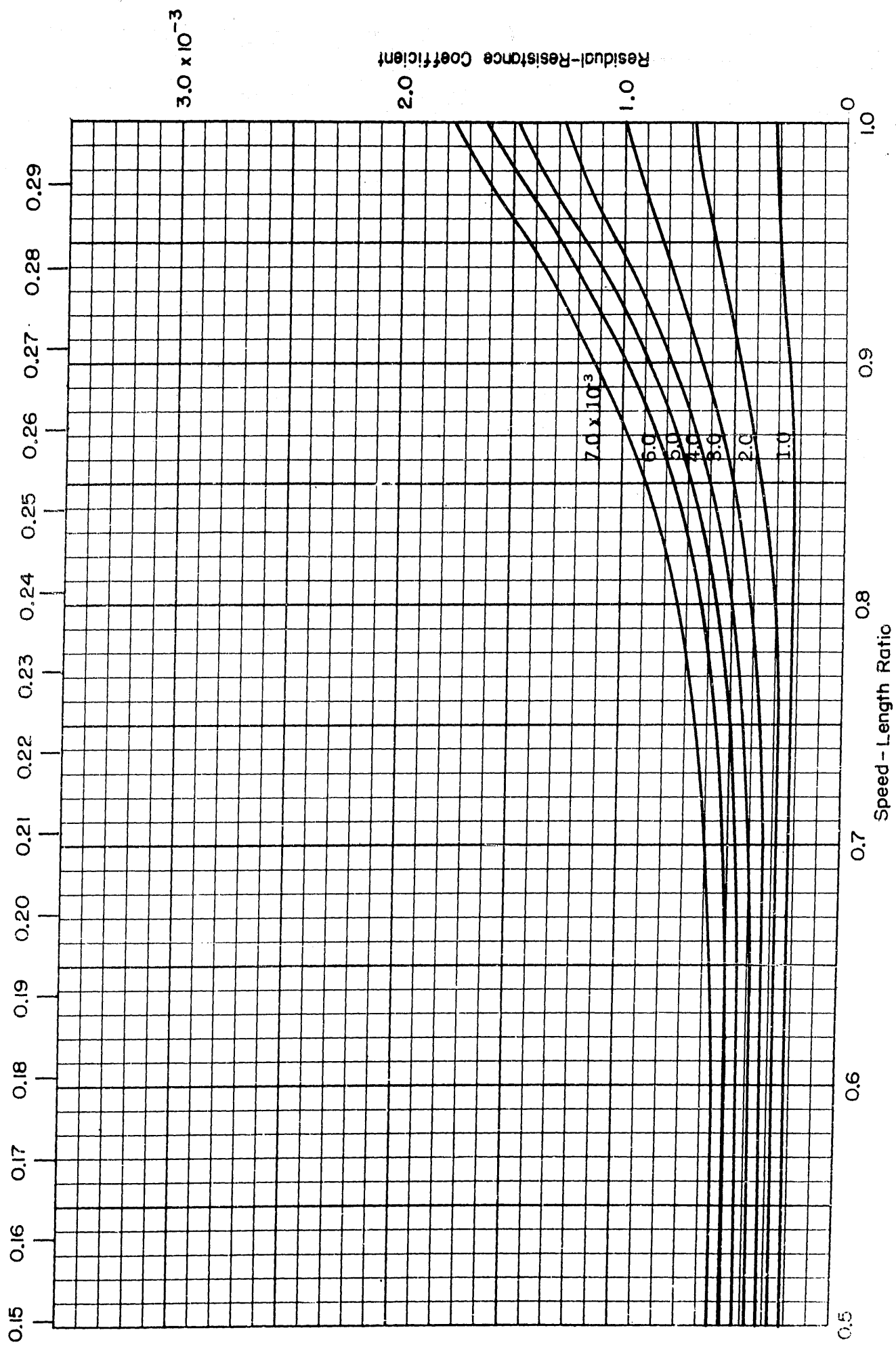
$B/H=2.25$
 $C_p=0.55$

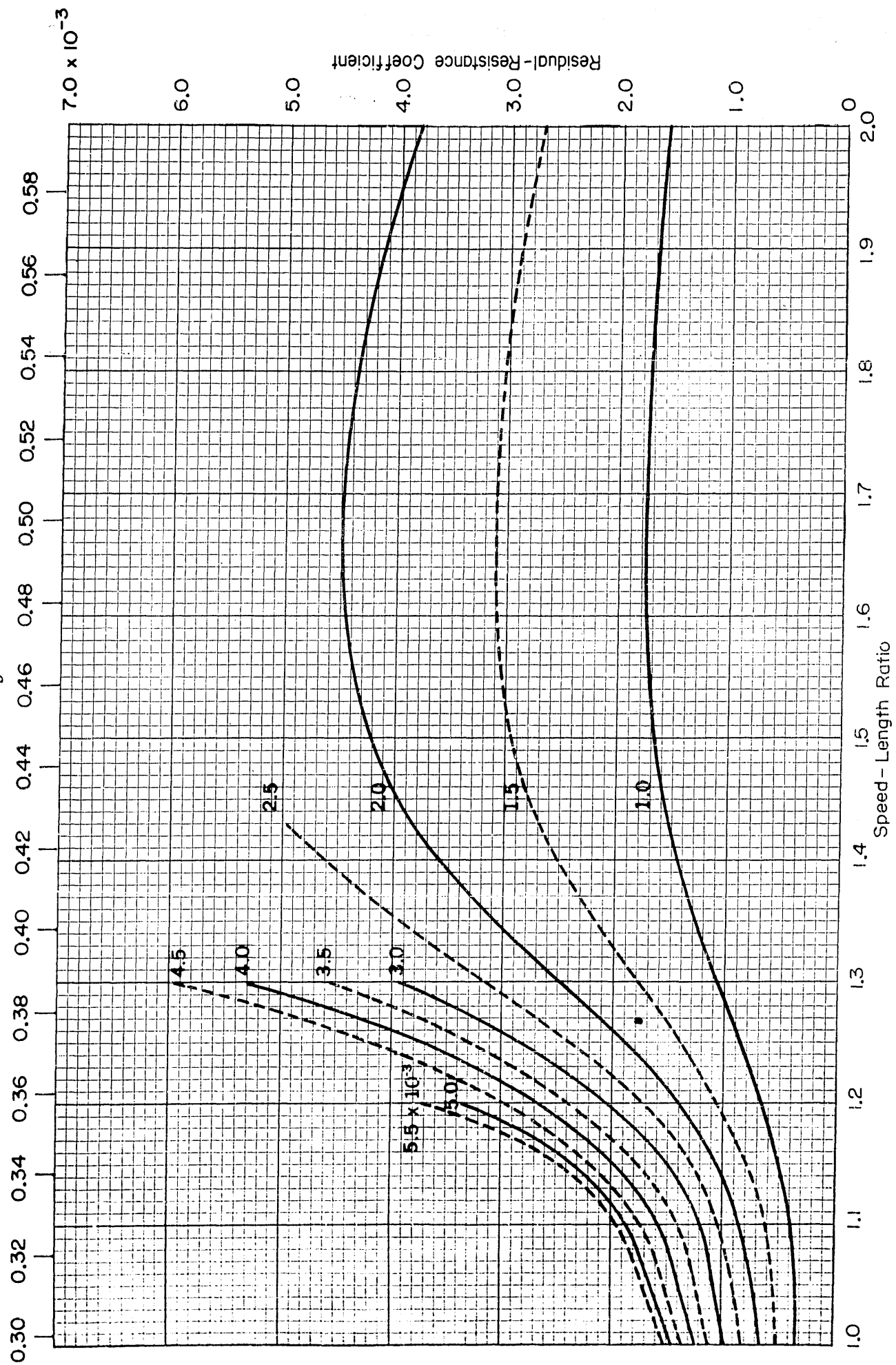


$B/H=2.25$
 $C_p=0.56$



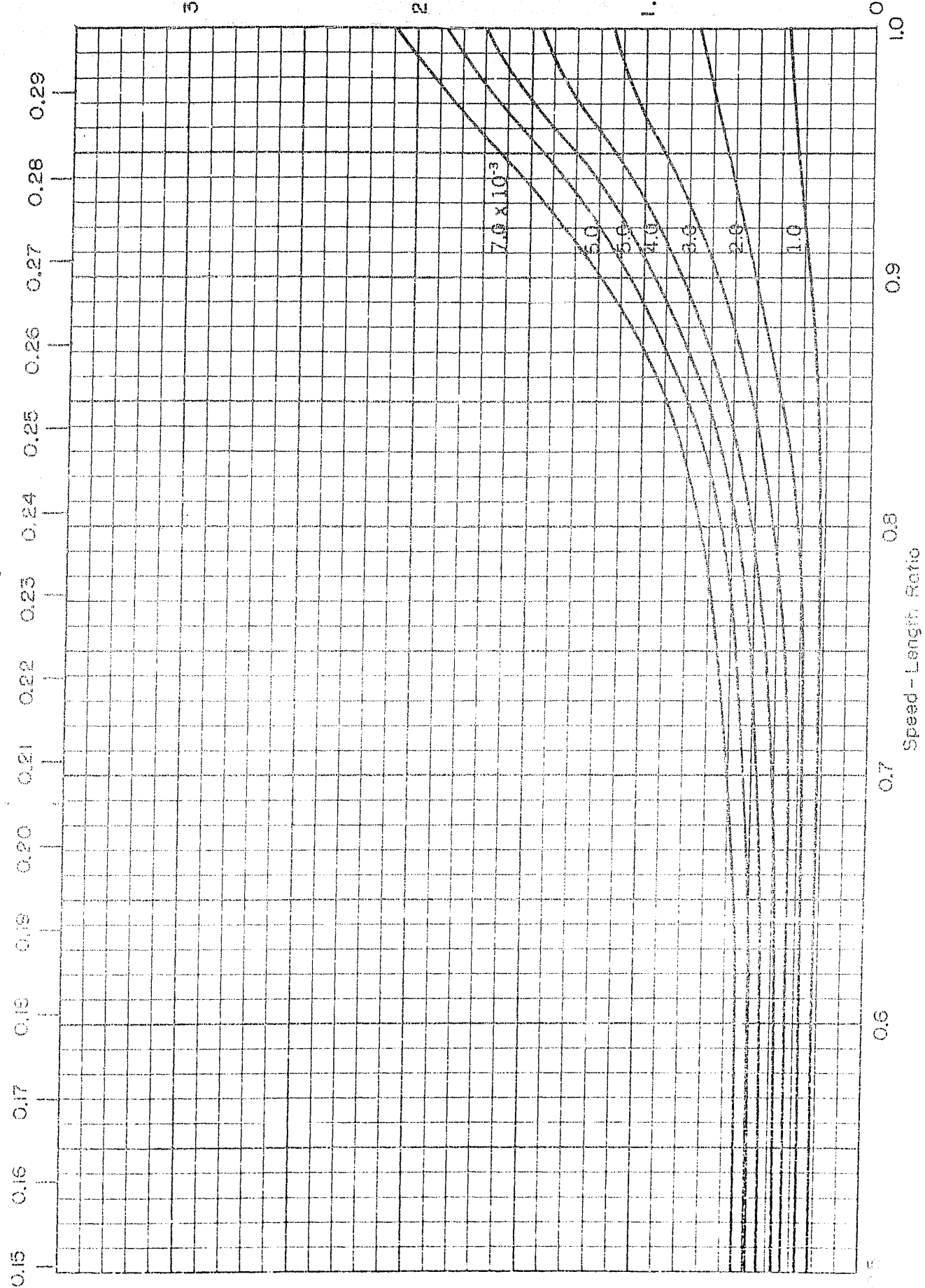
Froude Number $\frac{v}{\sqrt{gL}}$



$$\frac{v}{\sqrt{gL}}$$


$B/H=2.25$
 $C_p=0.58$

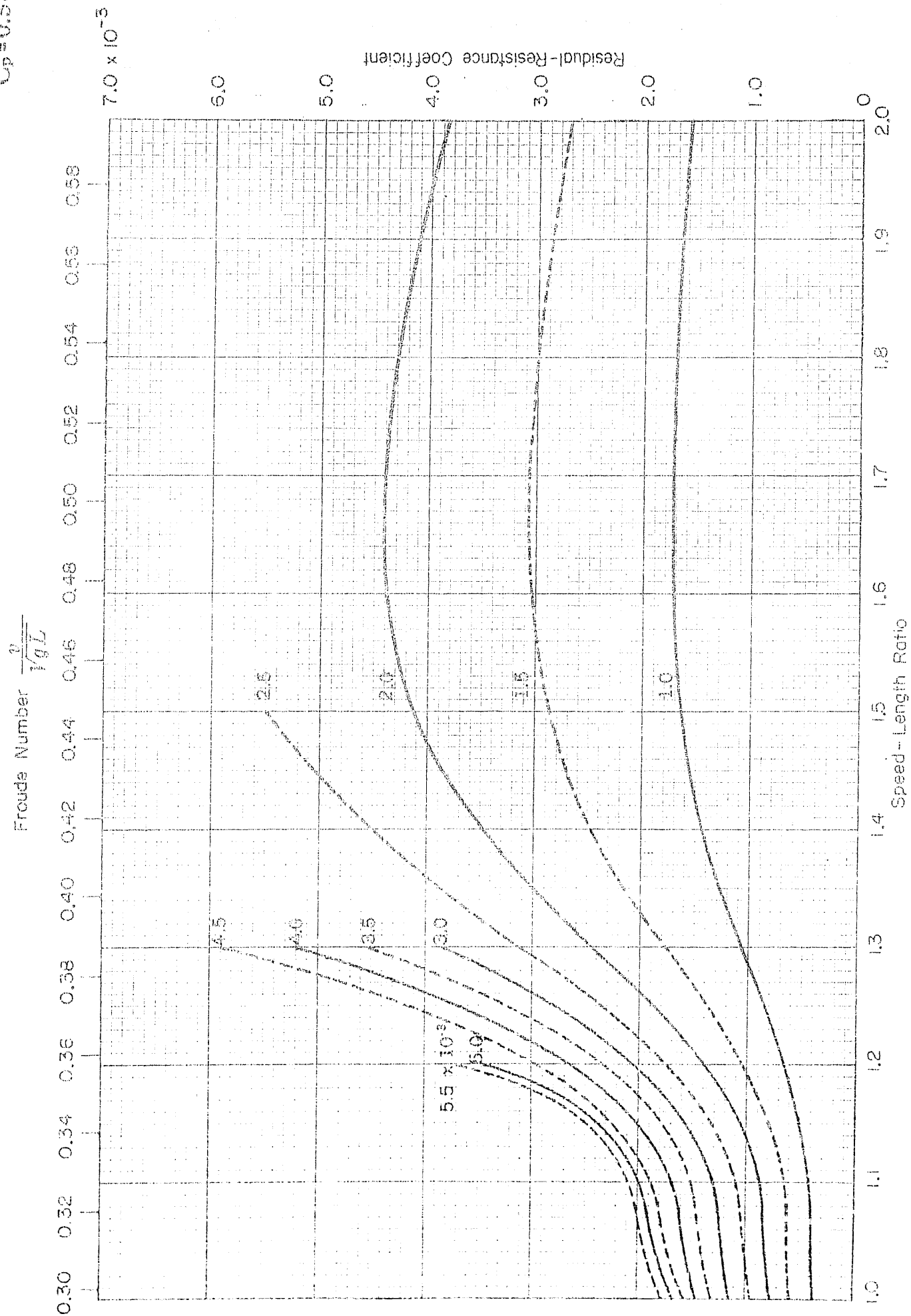
Froude Number $\frac{v}{\sqrt{gL}}$



Residual-Resistance Coefficient

3.0×10^{-3}

15 00
12 00
24 00
11 00
13 00
10 00



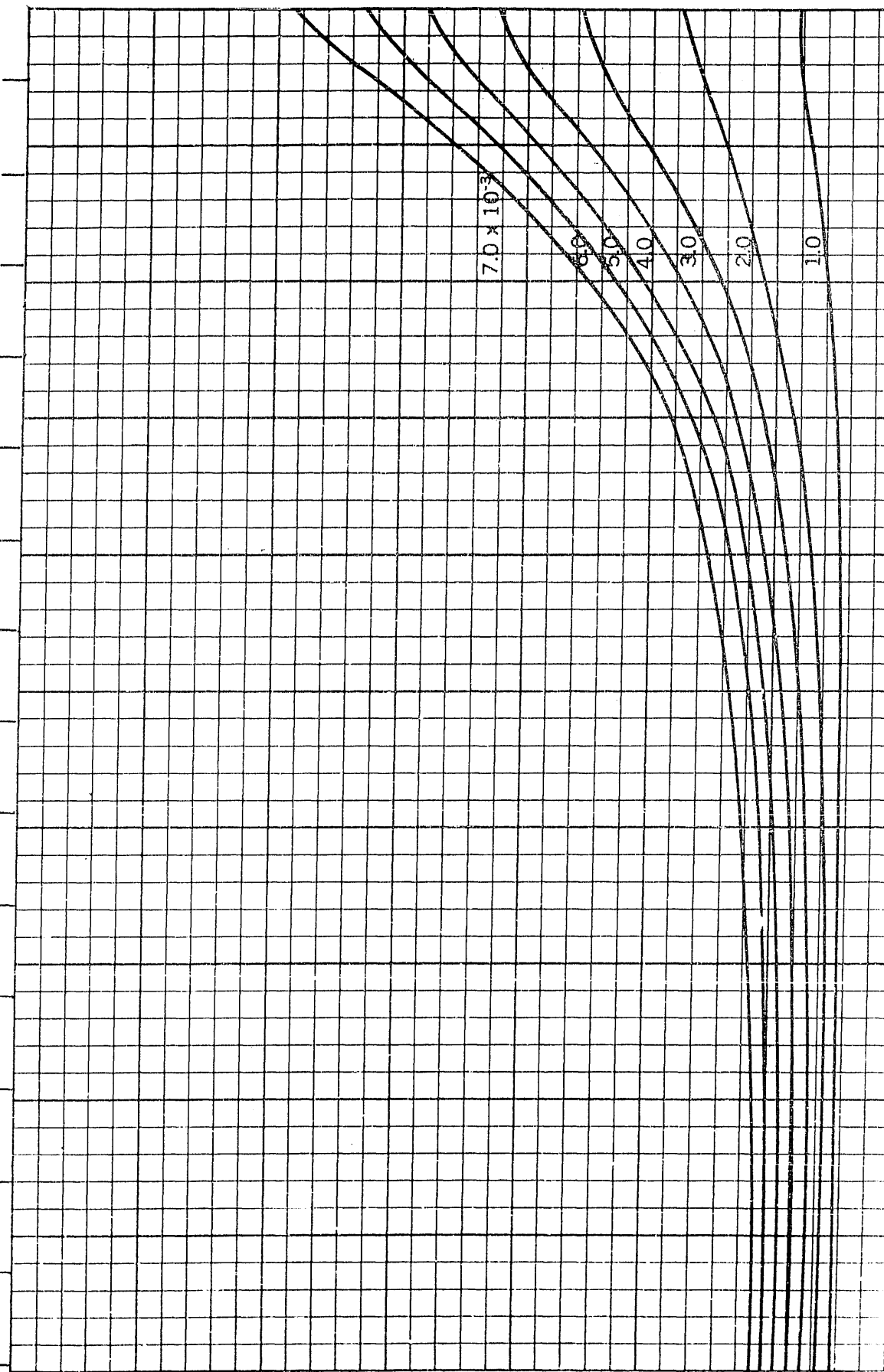
$B/H=2.25$
 $C_p=0.59$

Froude Number $\frac{v}{\sqrt{gL}}$

0.15 0.16 0.17 0.18 0.19 0.20 0.21 0.22 0.23 0.24 0.25 0.26 0.27 0.28 0.29

0.5 0.6 0.7 0.8 0.9 1.0

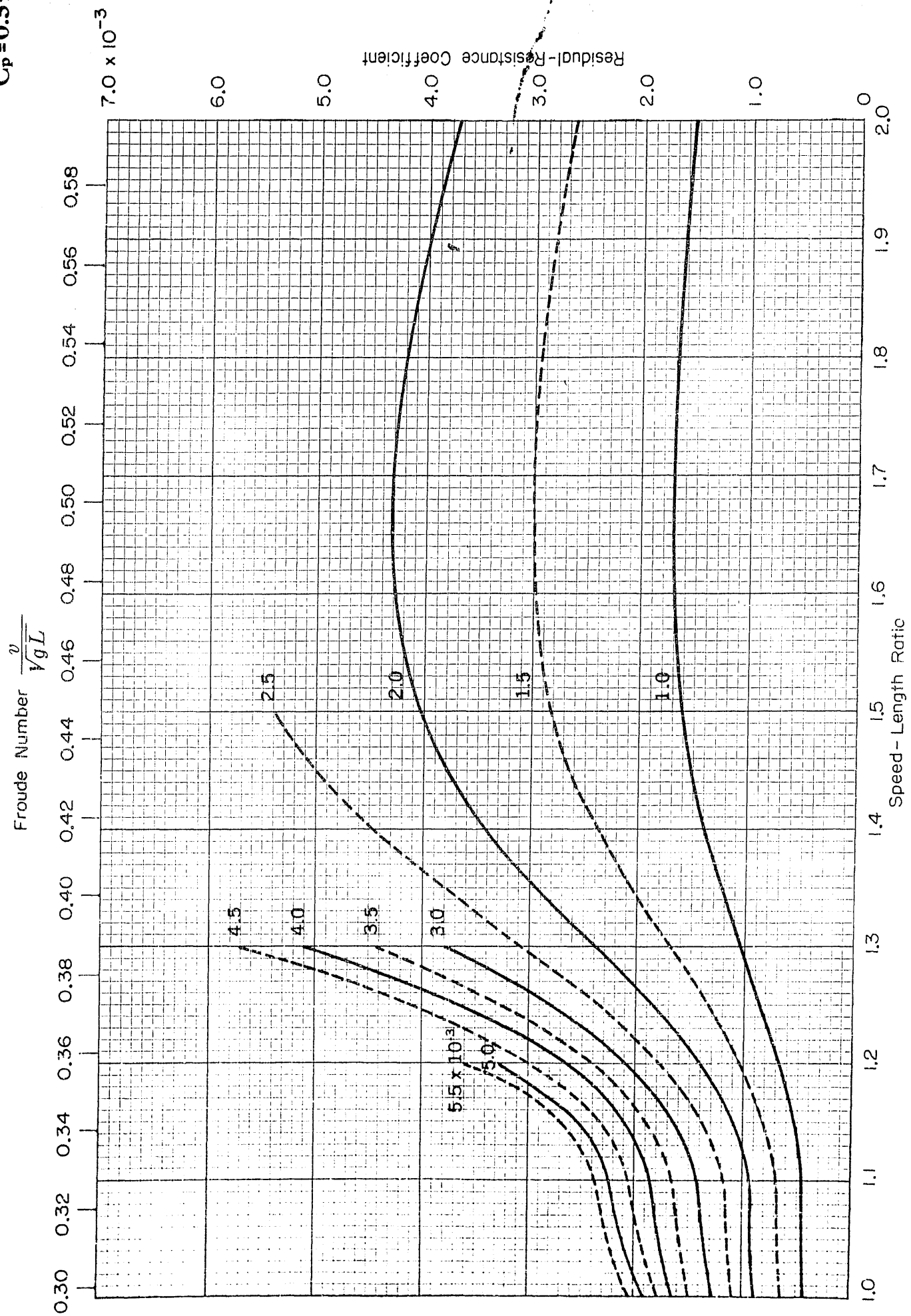
Speed - Length Ratio

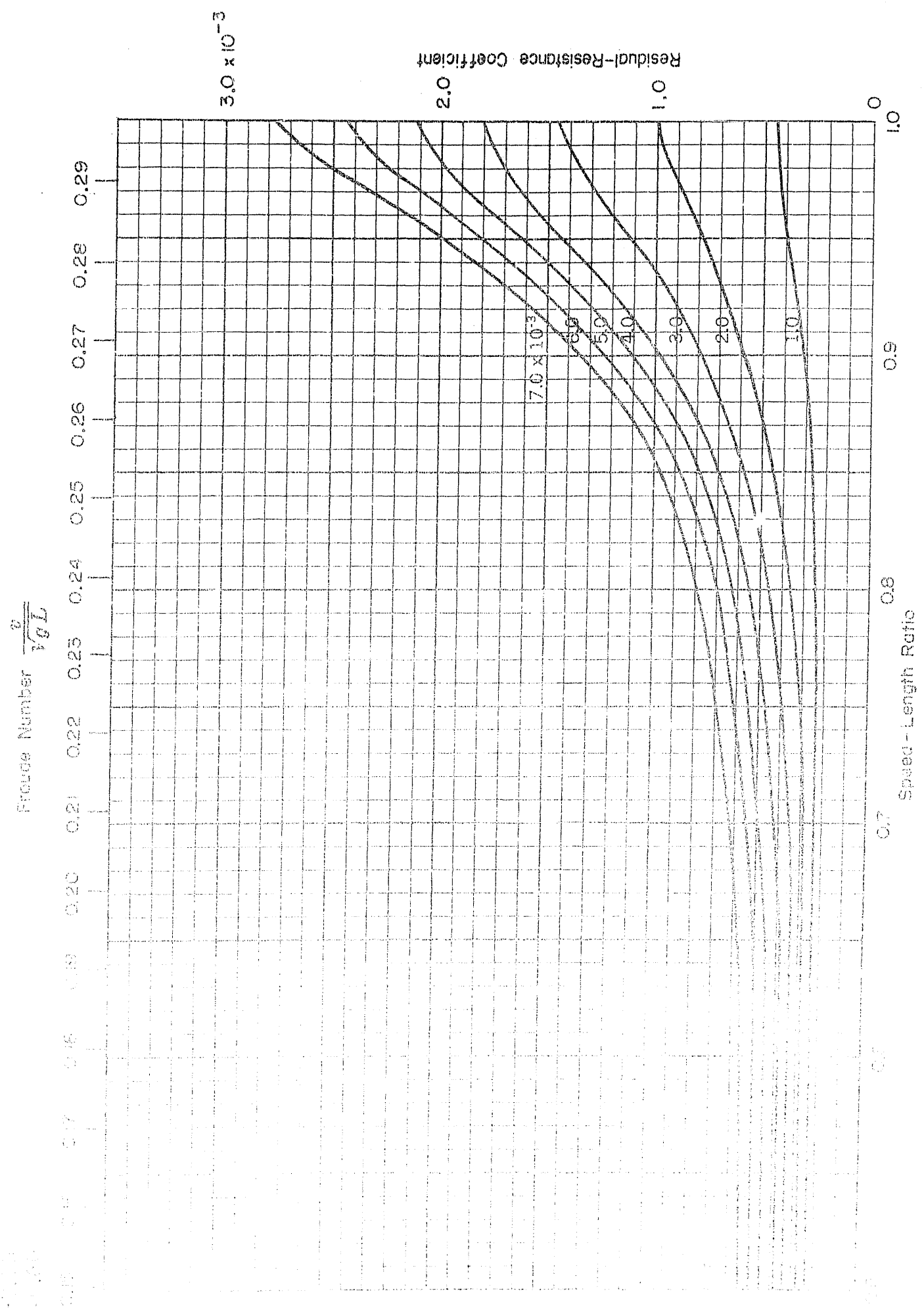


Residual-Resistance Coefficient

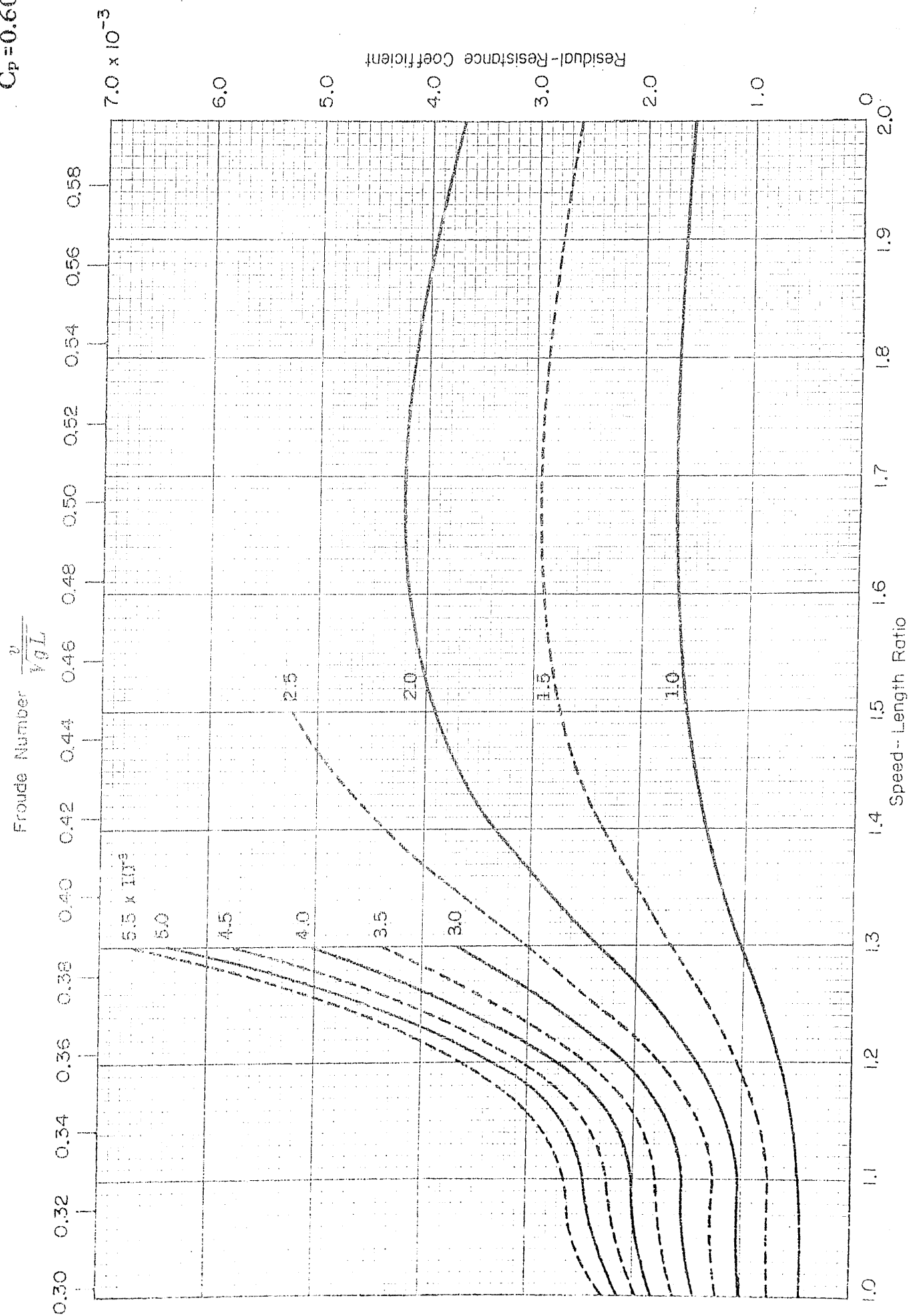
3.0×10^{-3}

$B/H=2.25$
 $C_p=0.59$



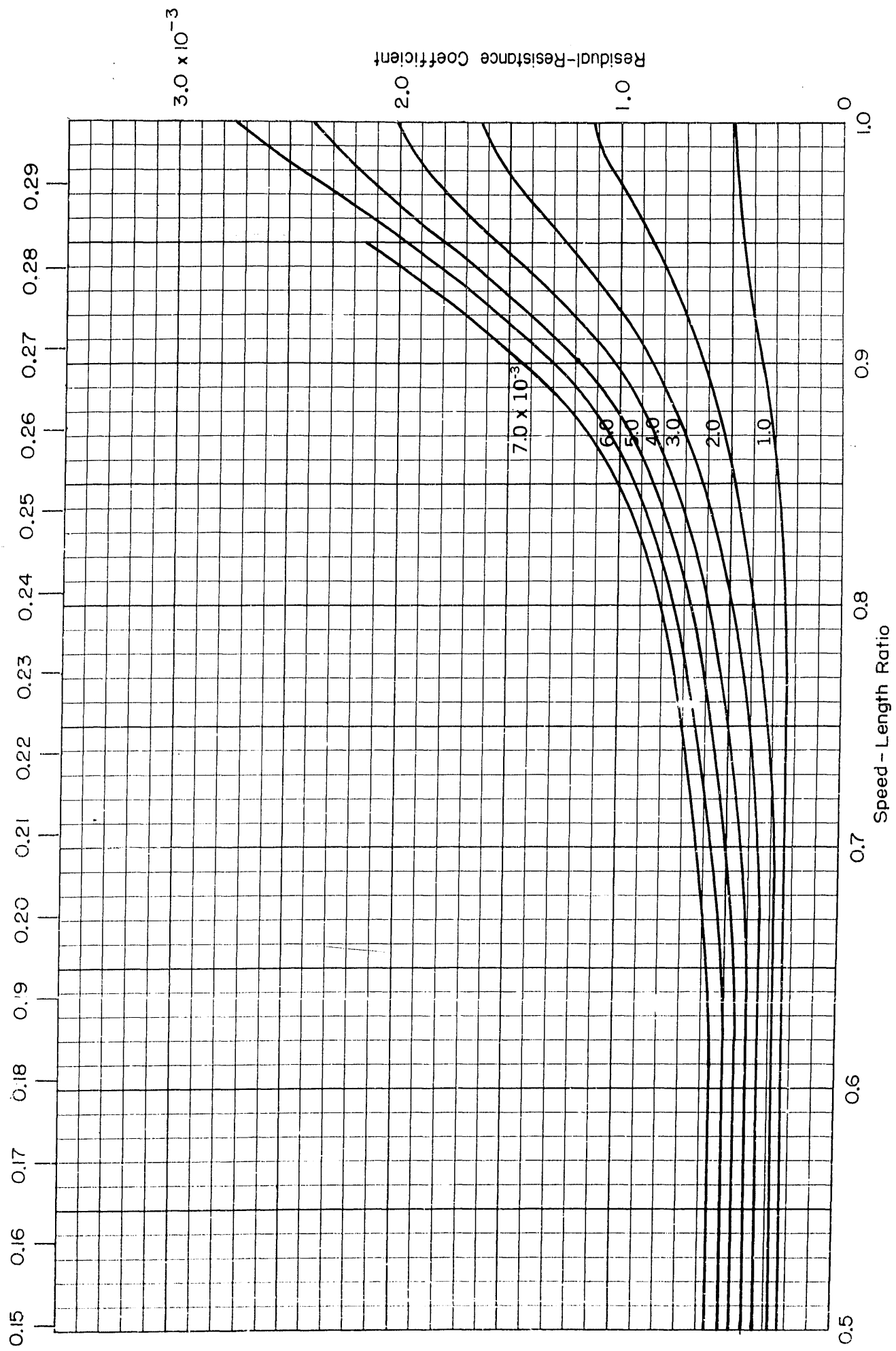


$B/H=2.25$
 $C_p=0.60$

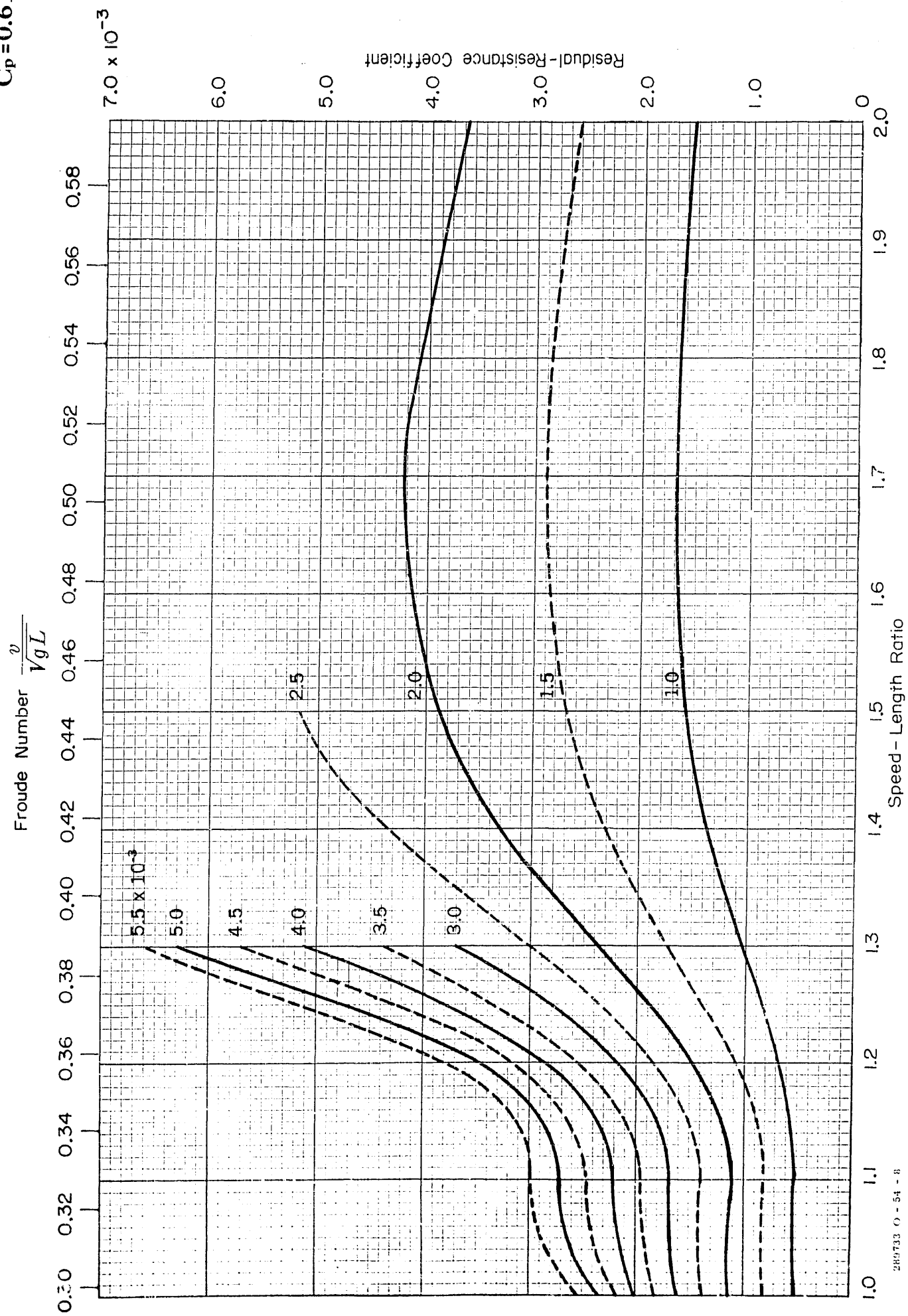


$B/H=2.25$
 $C_p=0.61$

Froude Number $\frac{v}{\sqrt{gL}}$

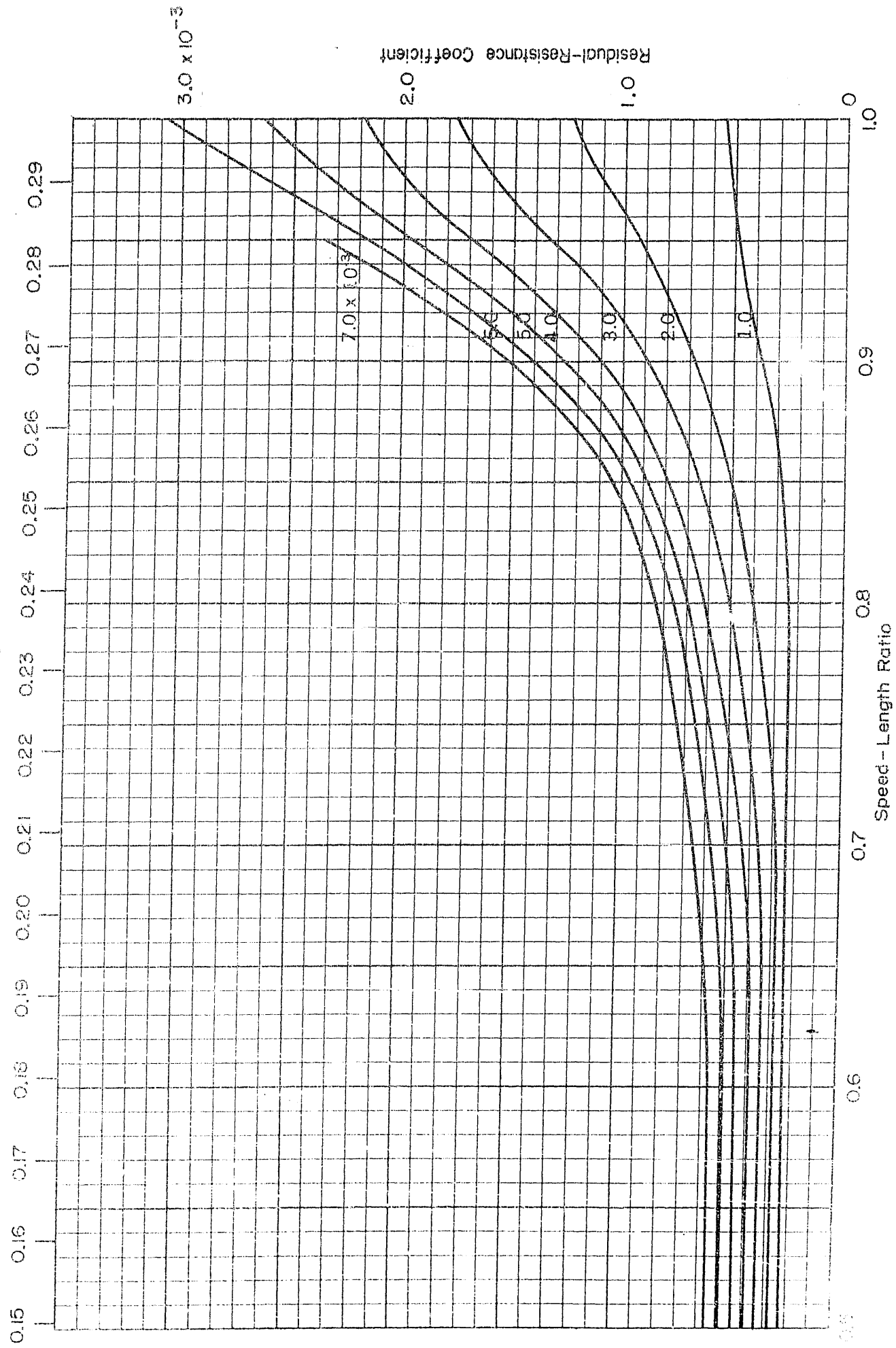


$B/H=2.25$
 $C_p=0.61$

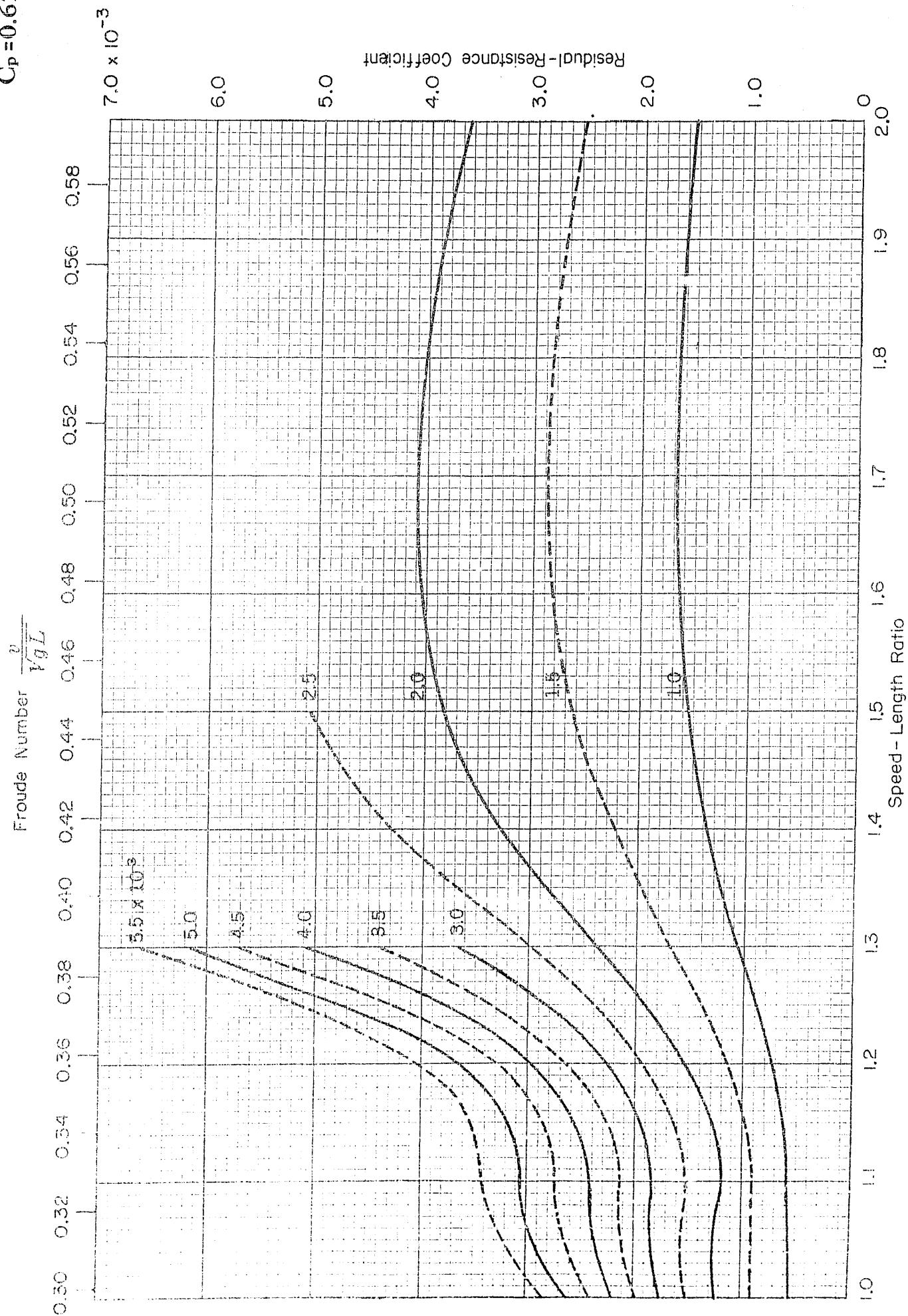


$B/H = 2.25$
 $C_p = 0.62$

Froude Number $\frac{v}{\sqrt{gL}}$



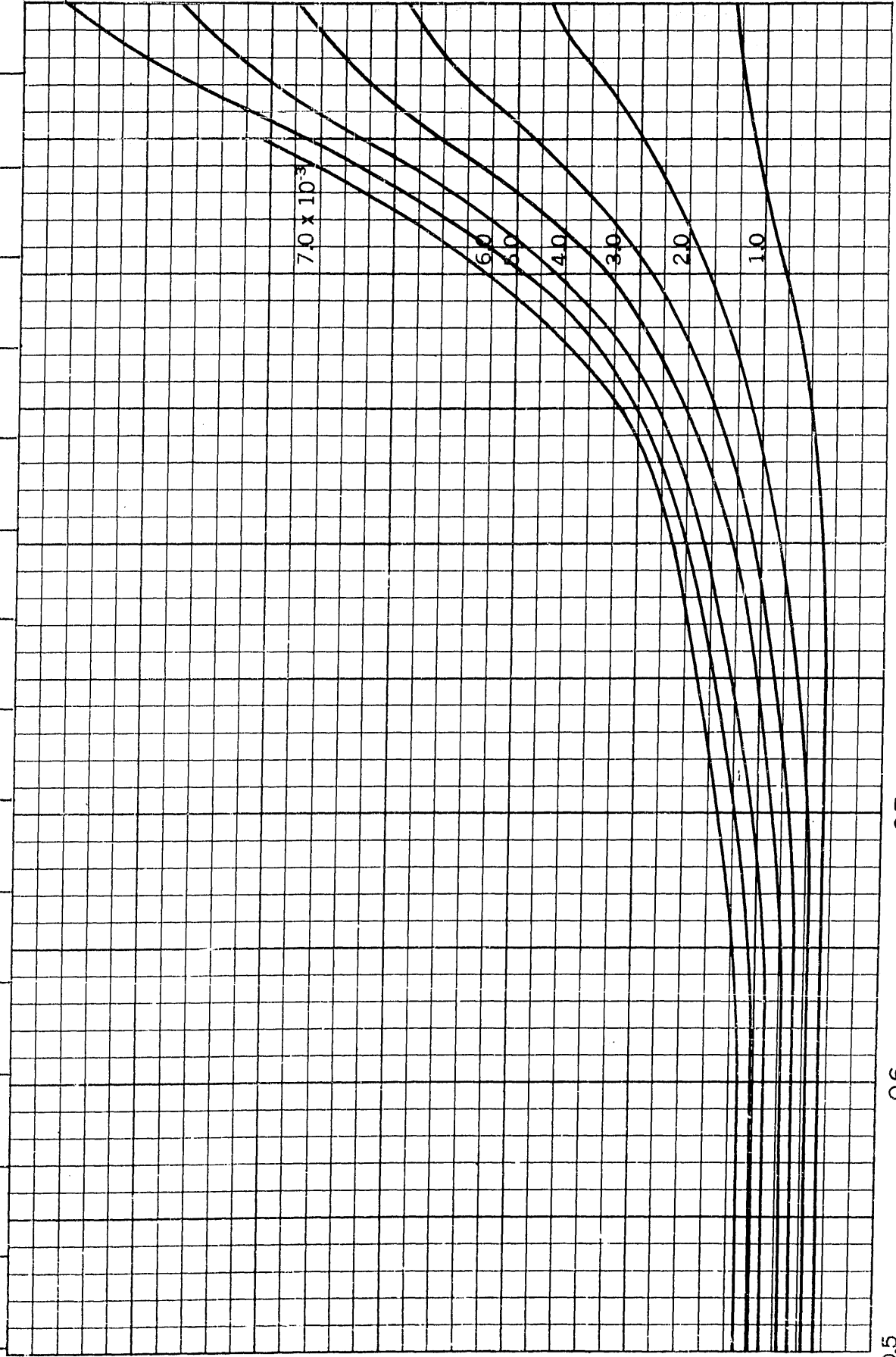
$B/H=2.25$
 $C_p=0.62$



$B/H=2.25$
 $C_p=0.63$

Froude Number $\frac{v}{\sqrt{gL}}$

0.15 0.16 0.17 0.18 0.19 0.20 0.21 0.22 0.23 0.24 0.25 0.26 0.27 0.28 0.29



Residual-Resistance Coefficient

3.0×10^{-3}

7.0×10^{-3}

6.0

5.0

4.0

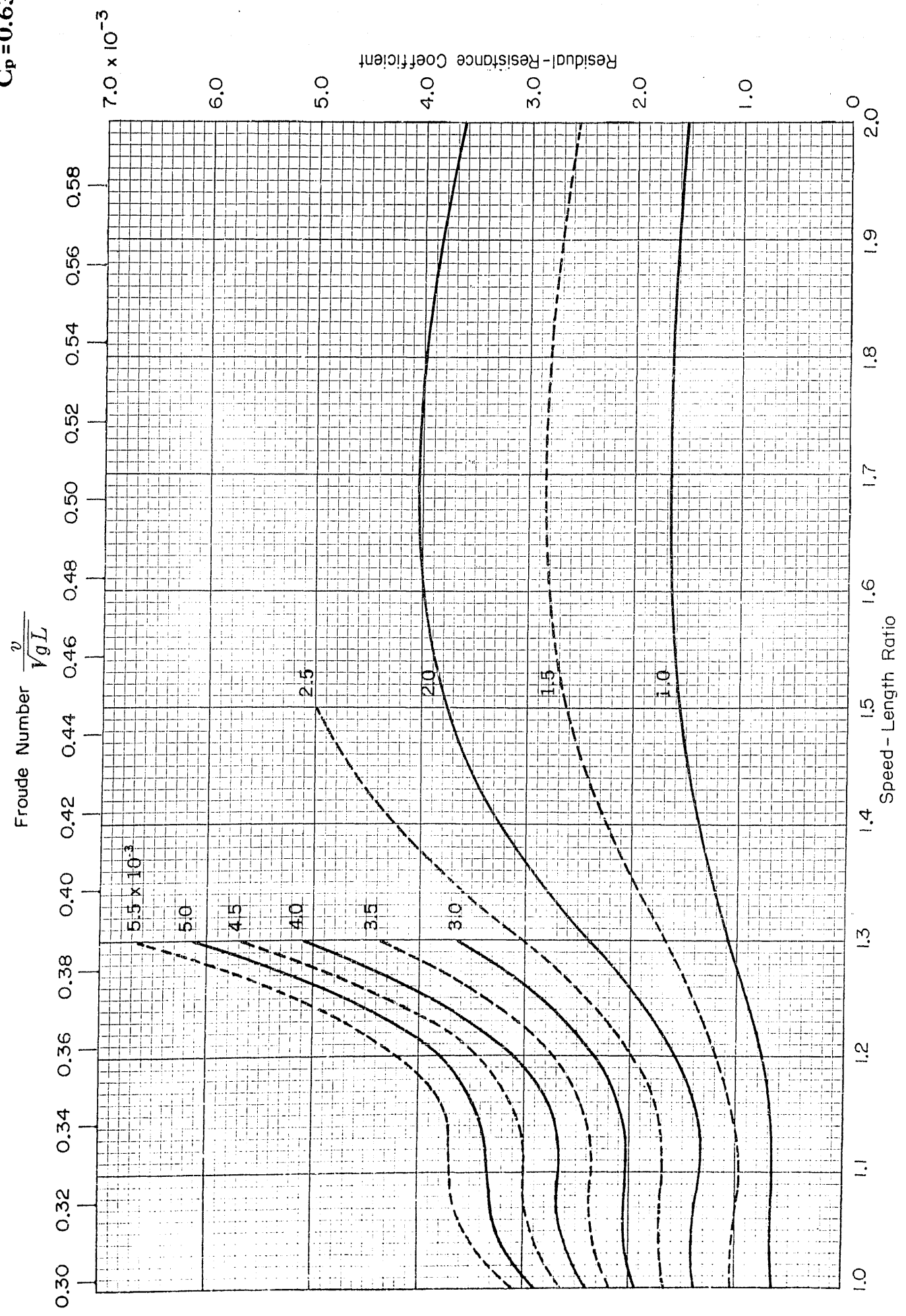
3.0

2.0

1.0

Speed-Length Ratio

$B/H=2.25$
 $C_p=0.63$



Residual-Resistance Coefficient

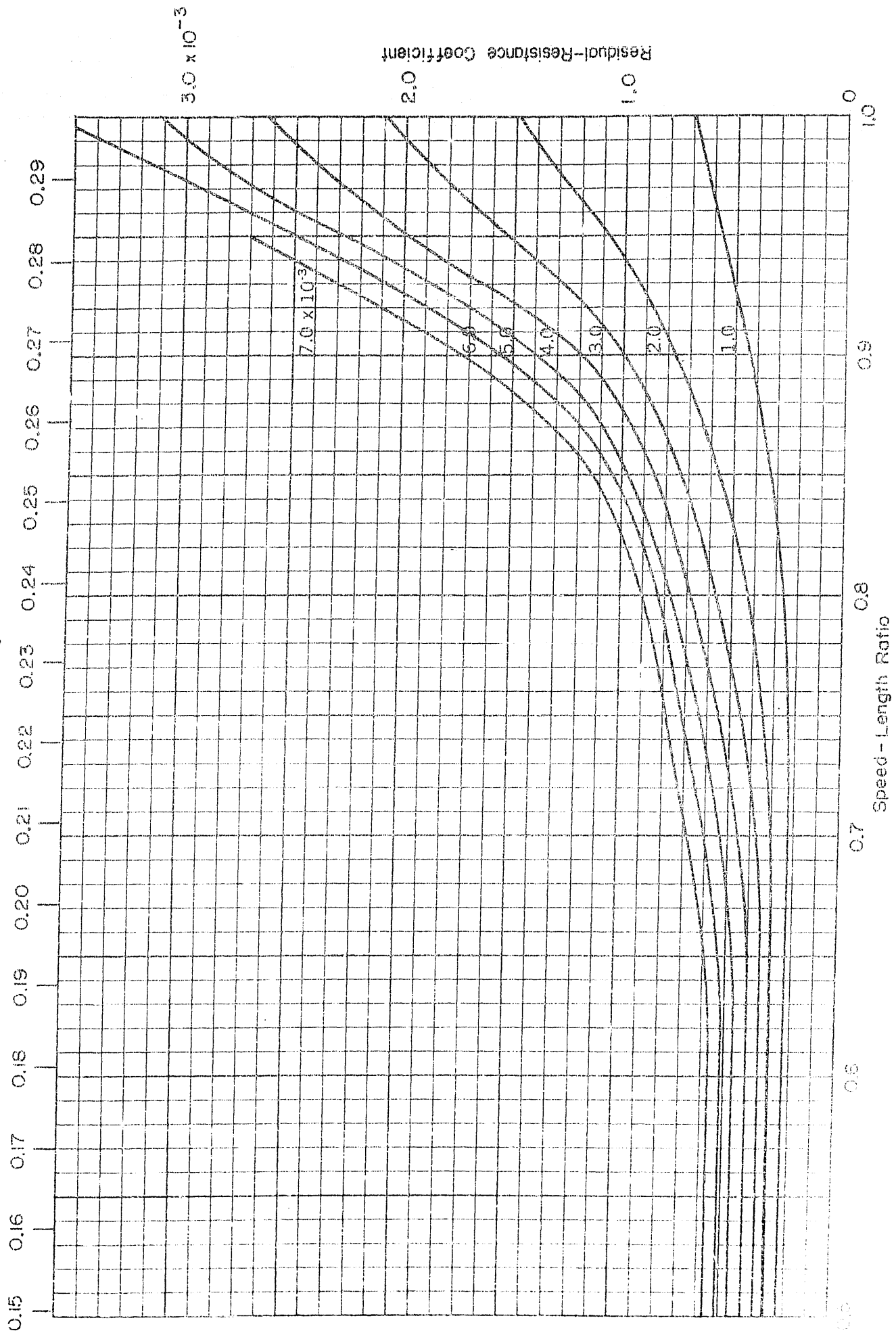
7.0×10^{-3}

Froude Number $\frac{v}{\sqrt{gL}}$

Speed - Length Ratio

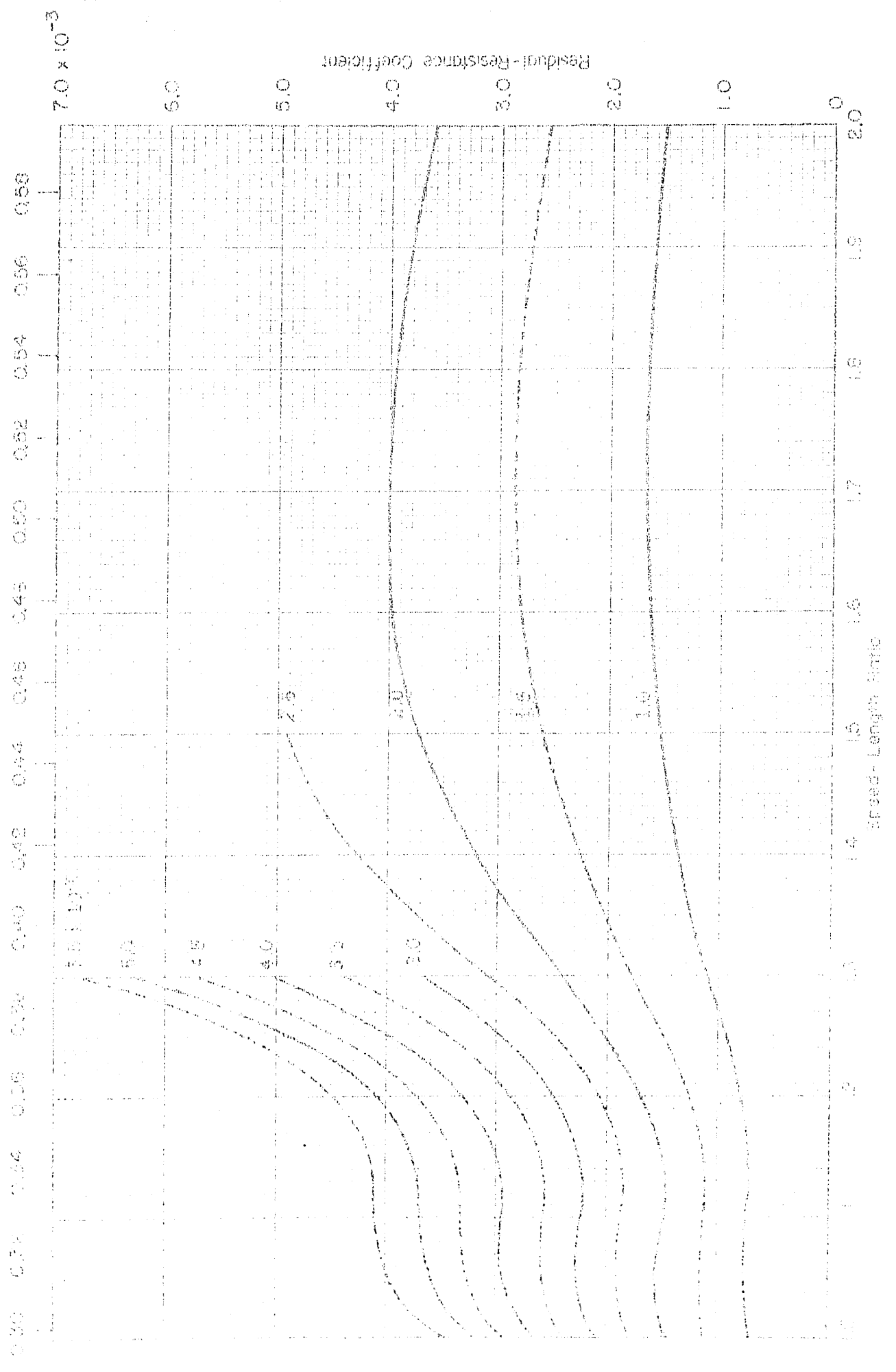
B/H=2.25
C_p=0.64

Froude Number $\frac{v}{\sqrt{gL}}$



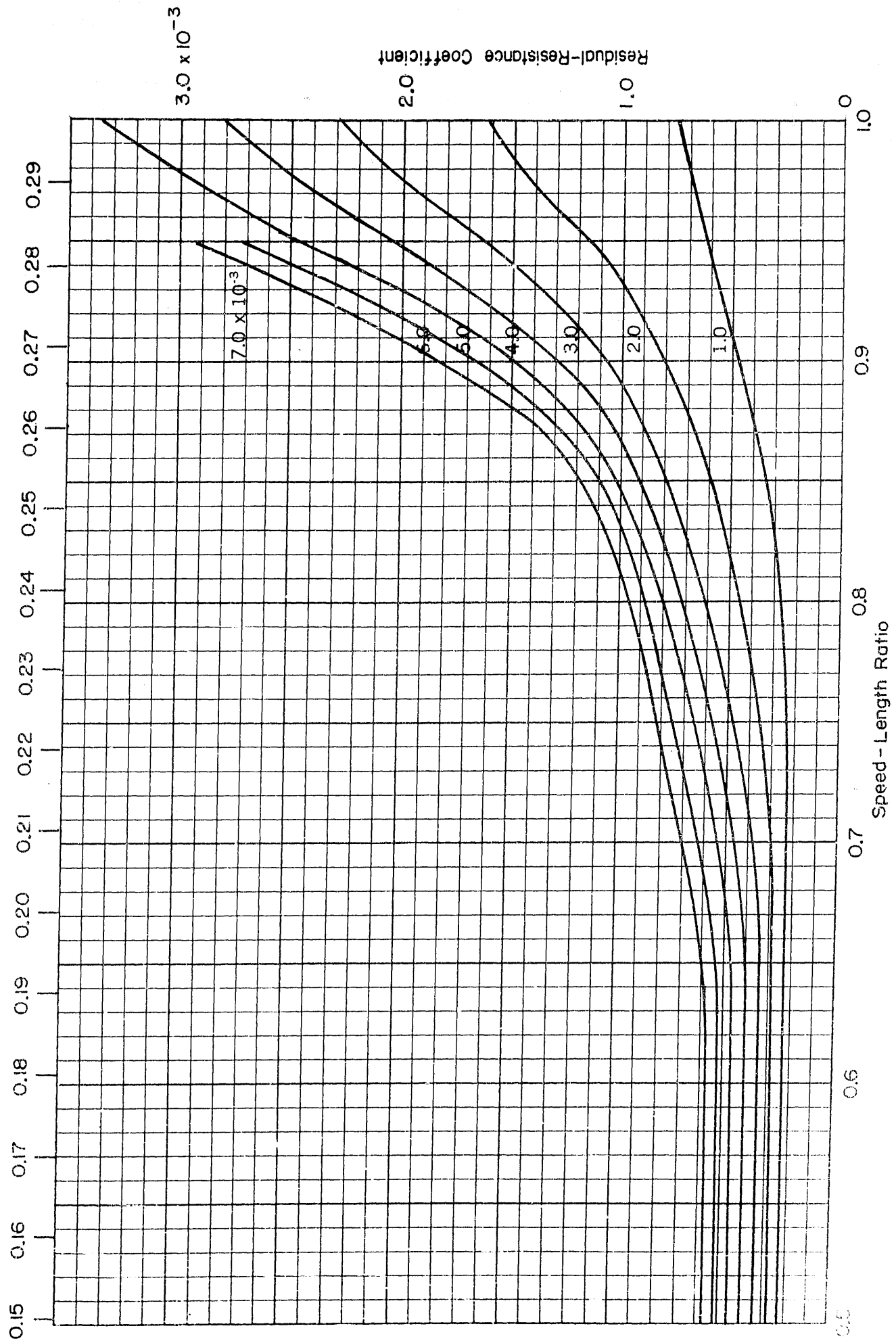
$R/H=2.25$
 $C_p=0.54$

Probe Number $\frac{2}{107}$

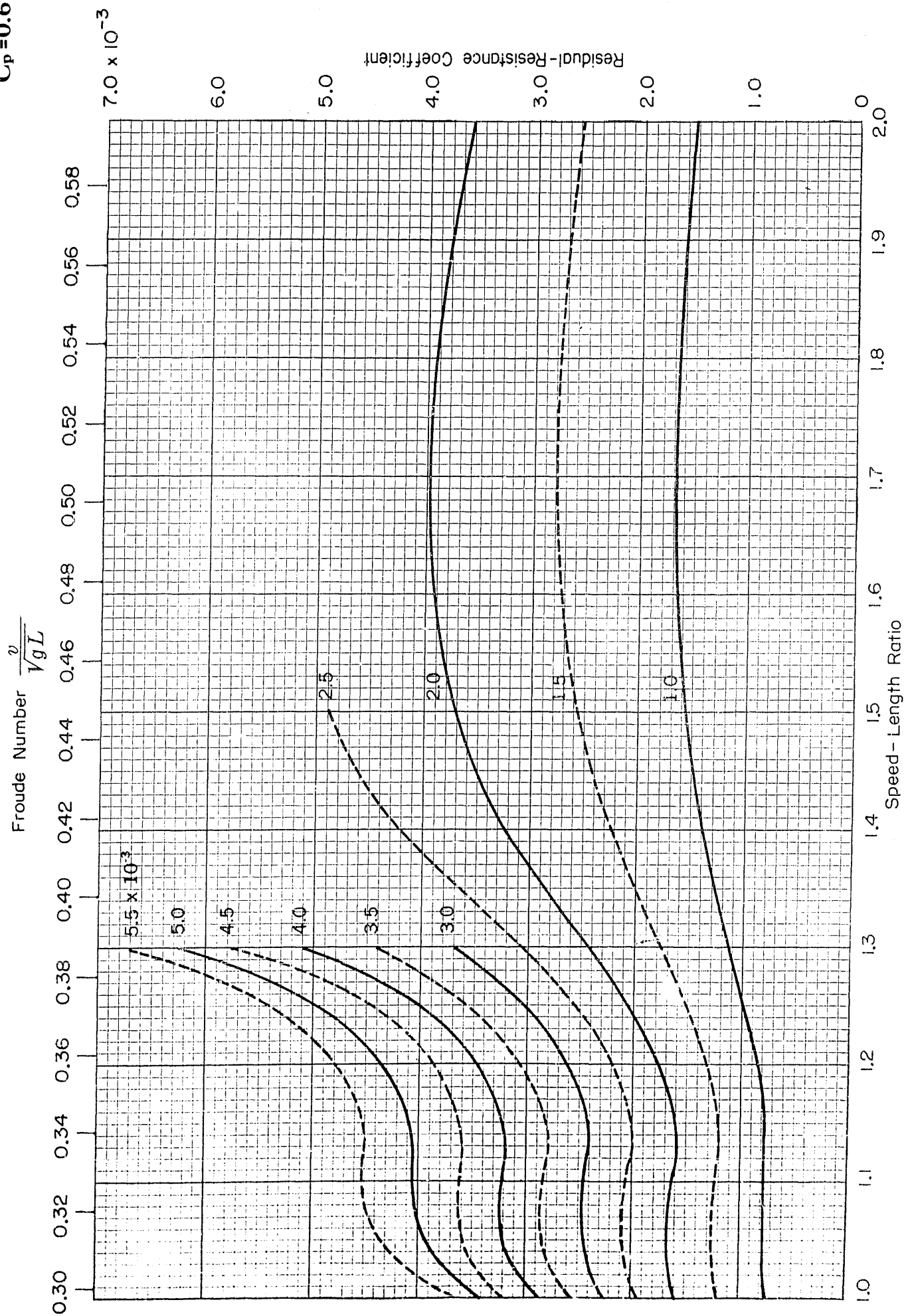


$B/H=2.25$
 $C_p=0.65$

Froude Number $\frac{V}{\sqrt{gL}}$

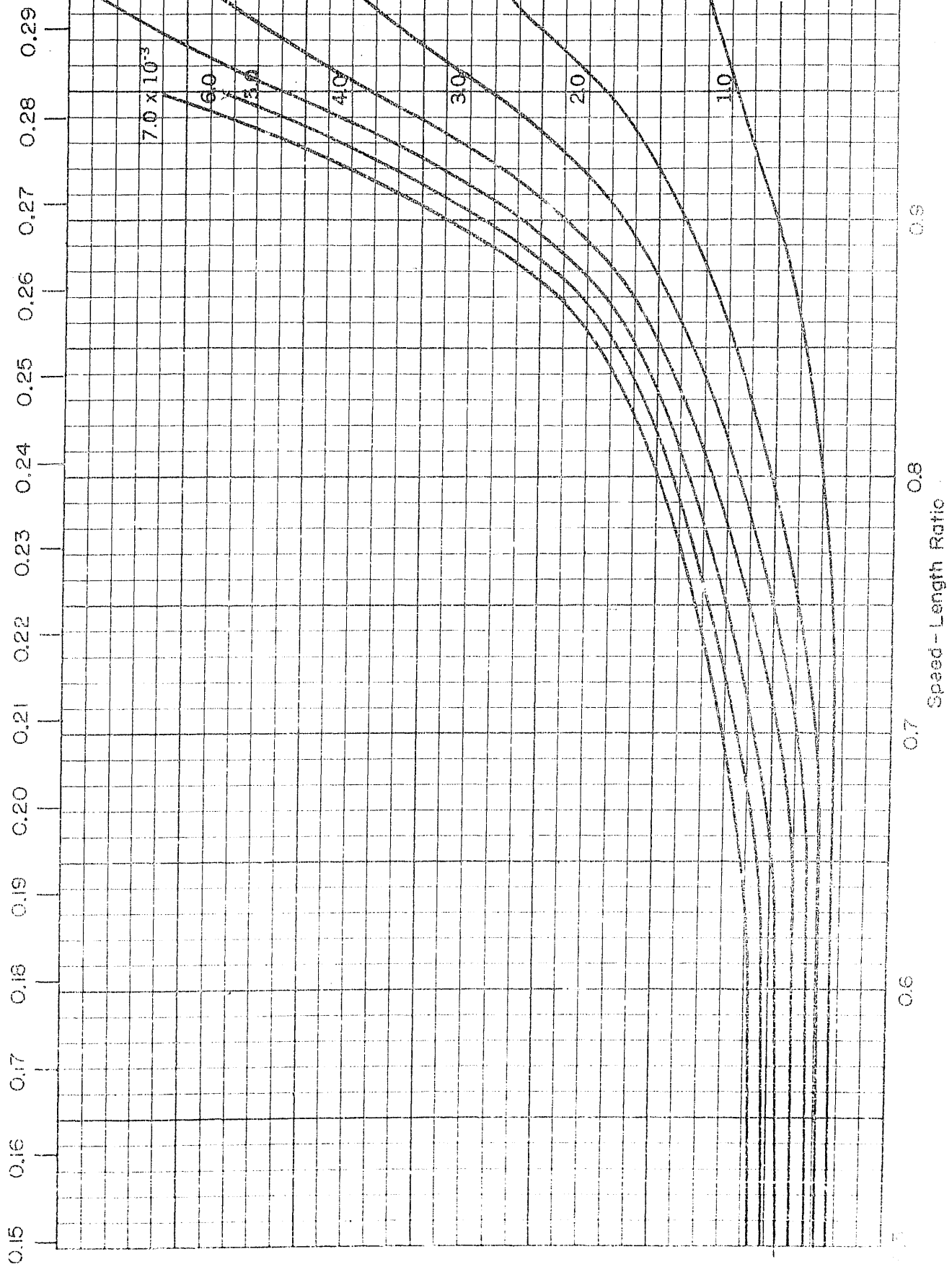


$B/H=2.25$
 $C_p=0.65$



$B/H = 2.25$
 $C_p = 0.66$

Froude Number $\frac{v}{\sqrt{gL}}$



Residual-Resistance Coefficient

3.0×10^{-3}

7.0×10^{-3}

60

50

40

30

20

10

0

1.0

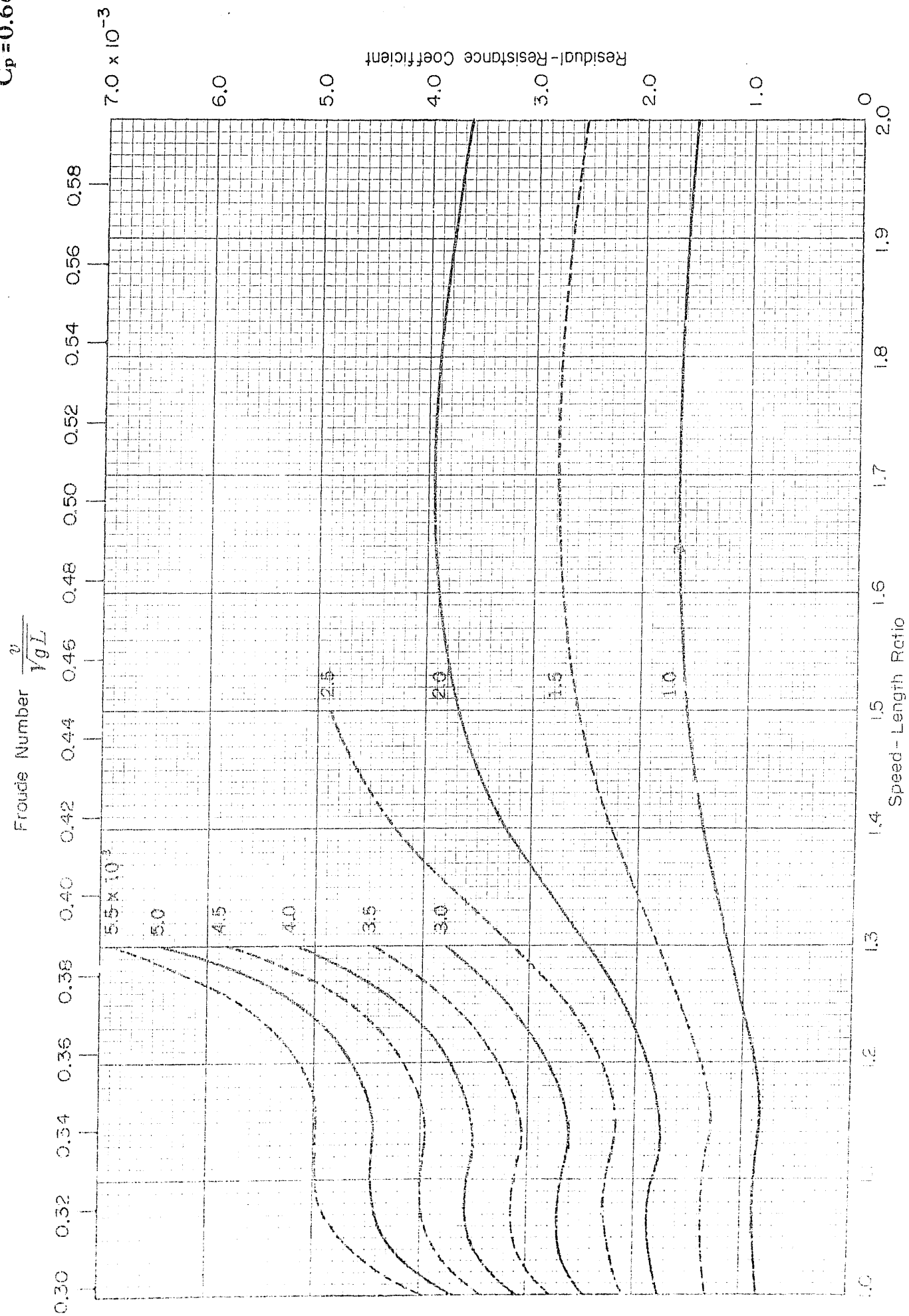
0.8

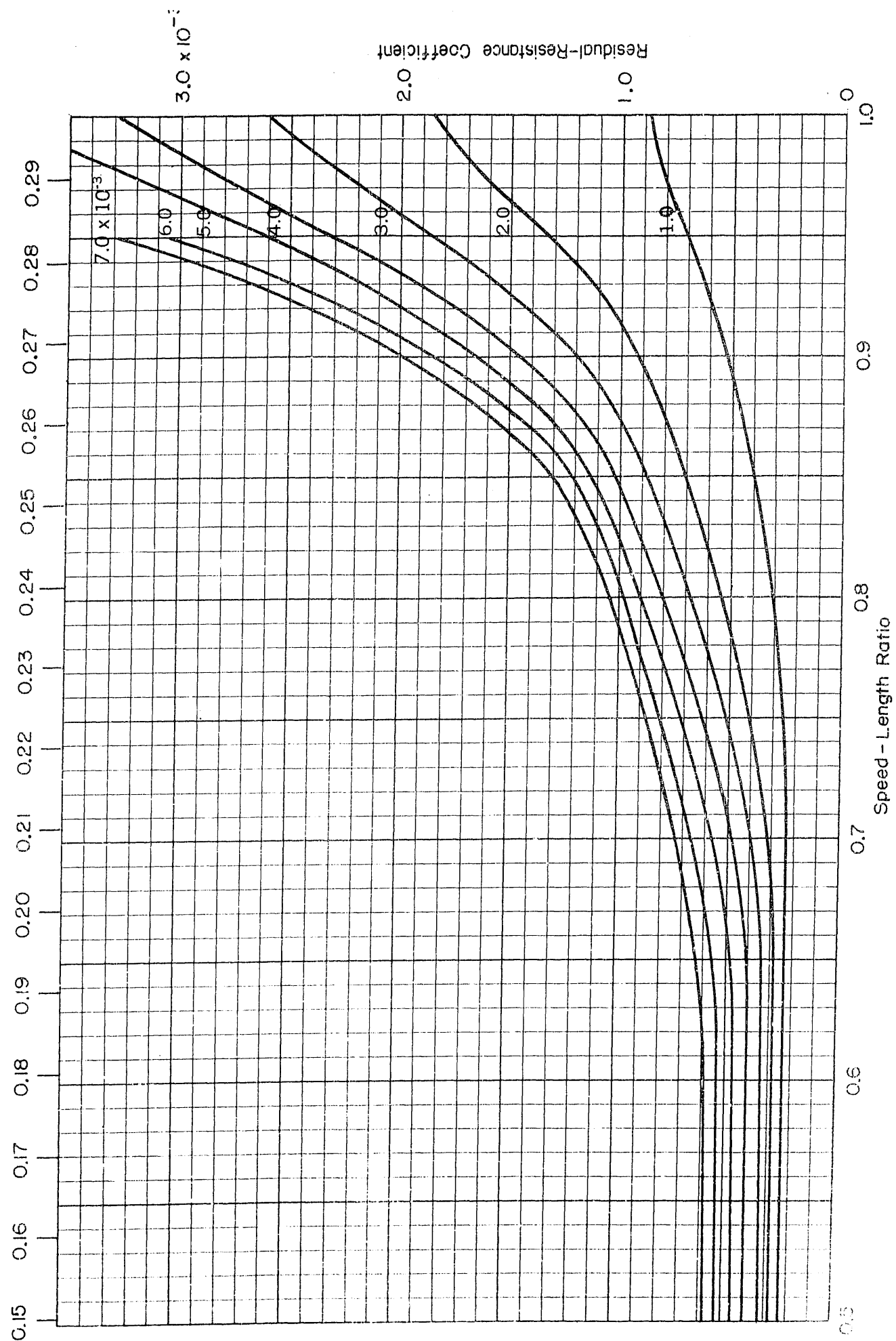
Speed-Length Ratio

0.7

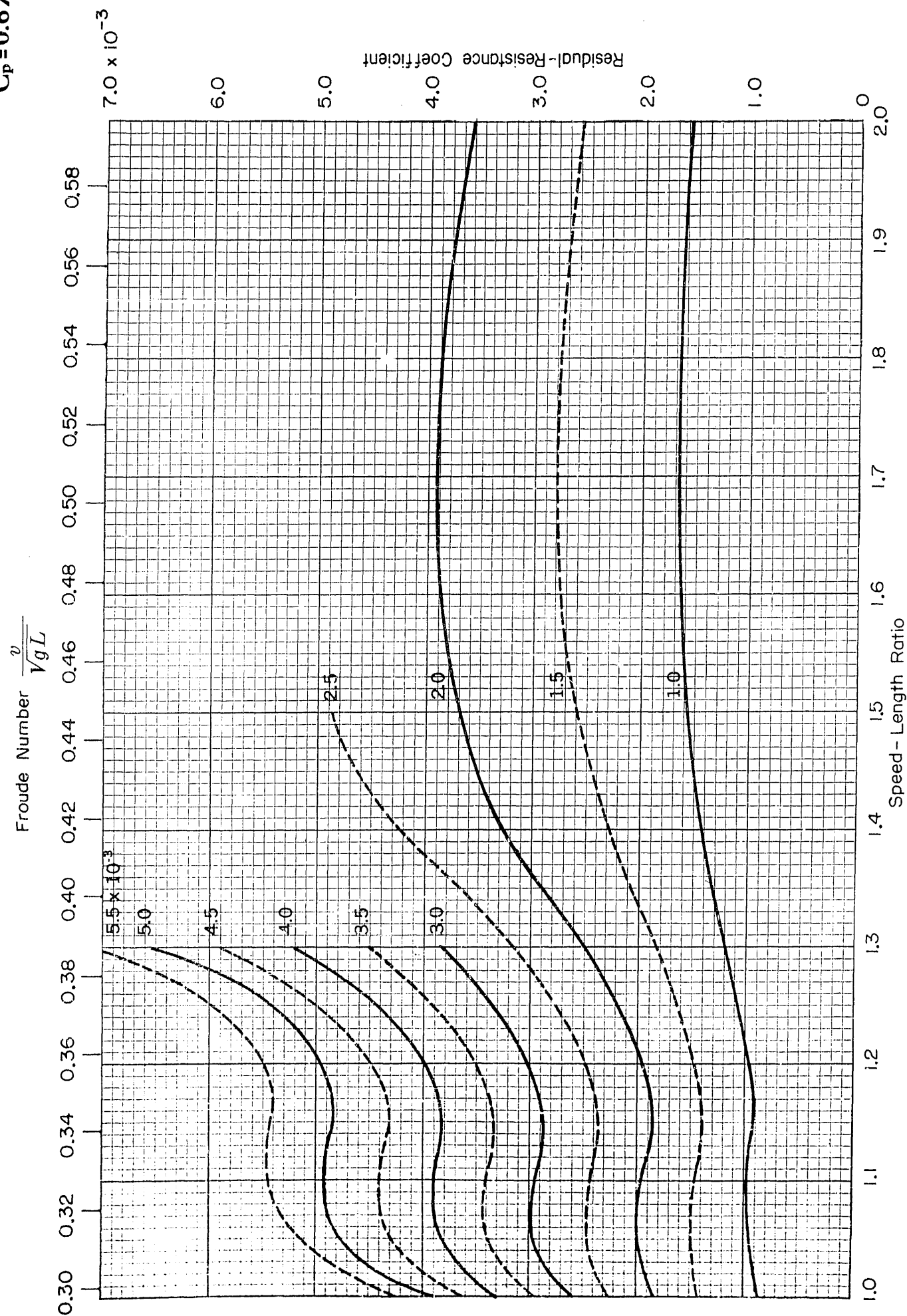
0.6

$B/H=2.25$
 $C_p=0.66$



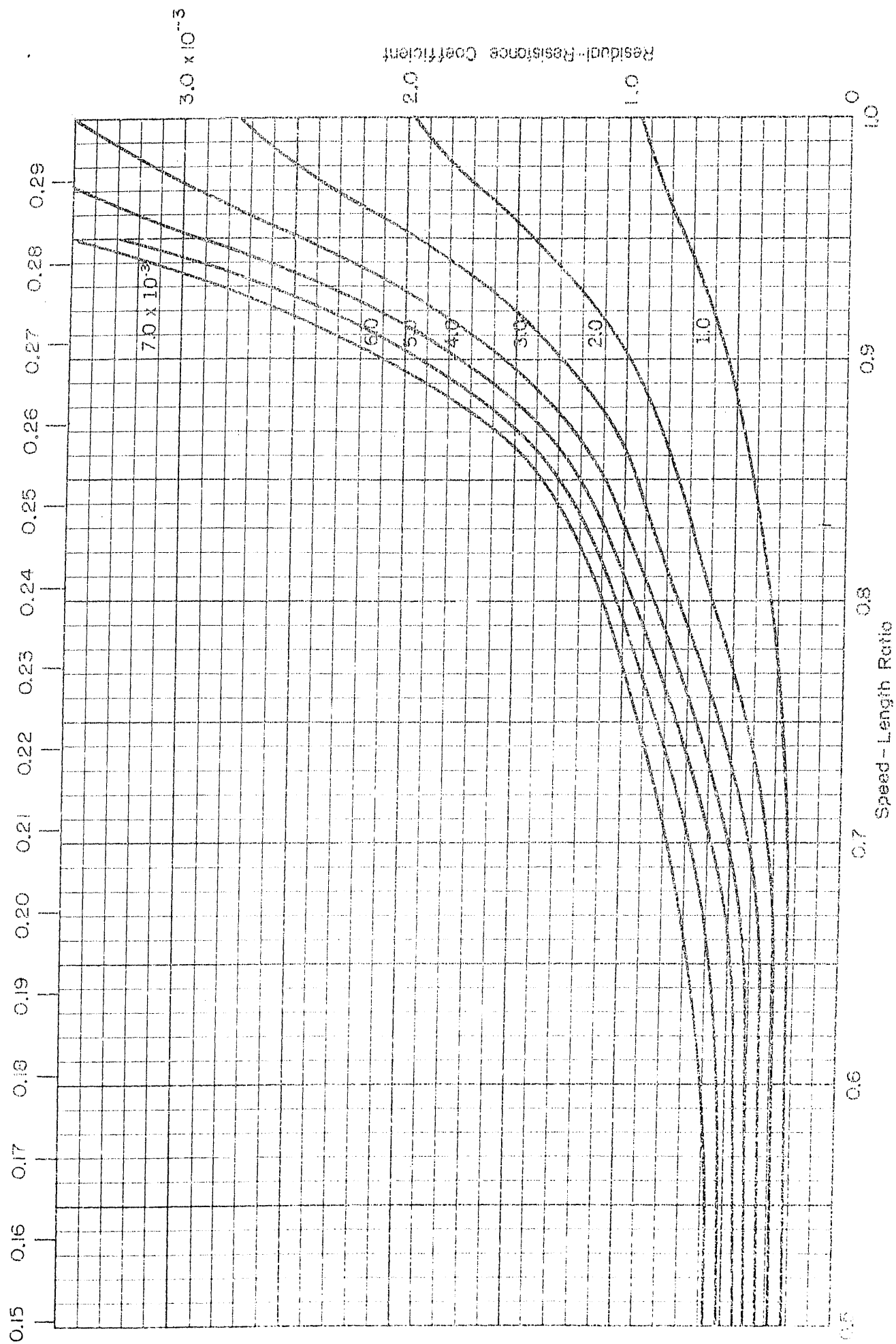
$$\frac{v}{\sqrt{gL}}$$


$B/H = 2.25$
 $C_p = 0.67$



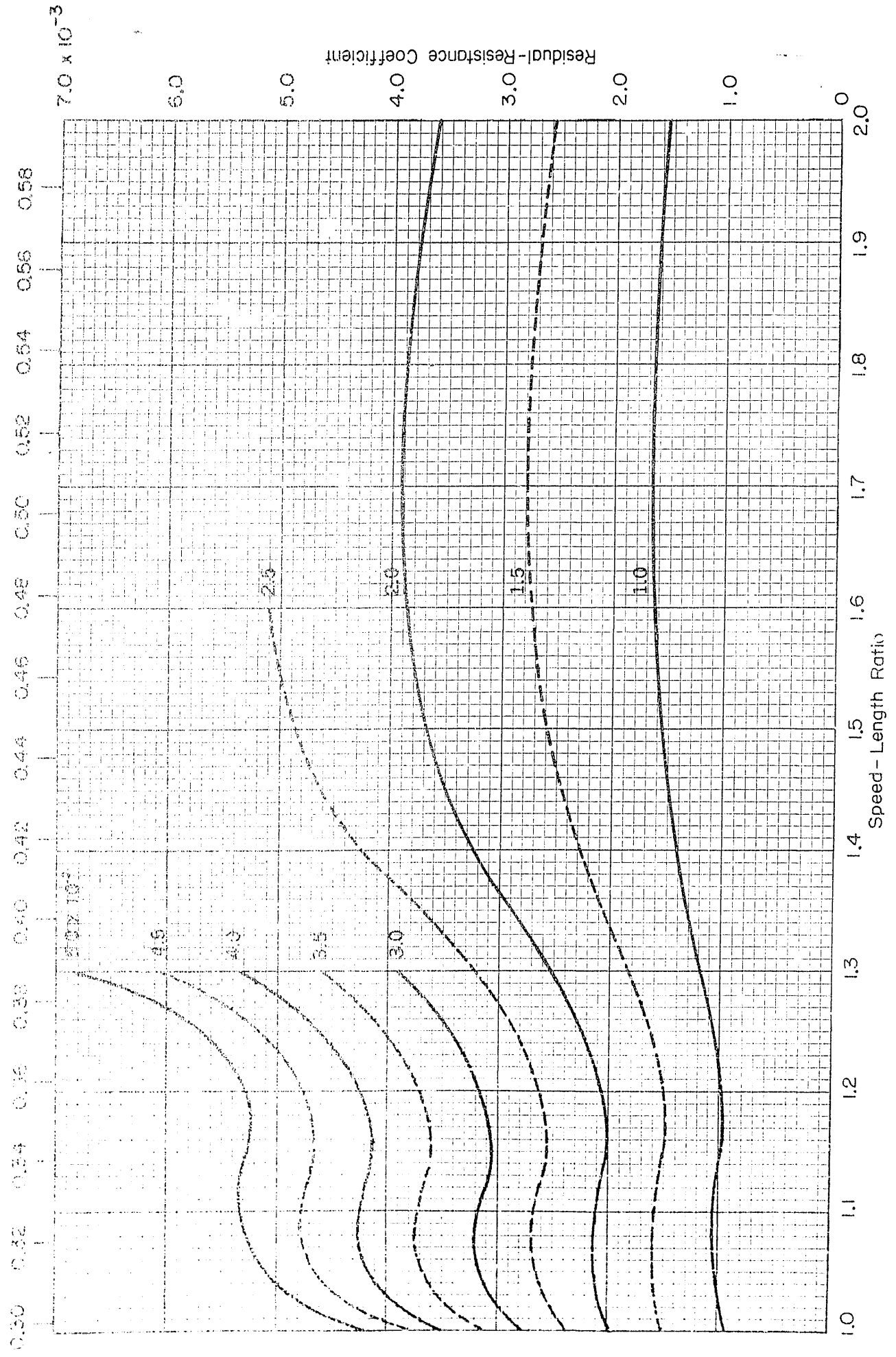
$B/H=2.25$
 $C_p=0.68$

Froude Number $\frac{v}{\sqrt{gL}}$



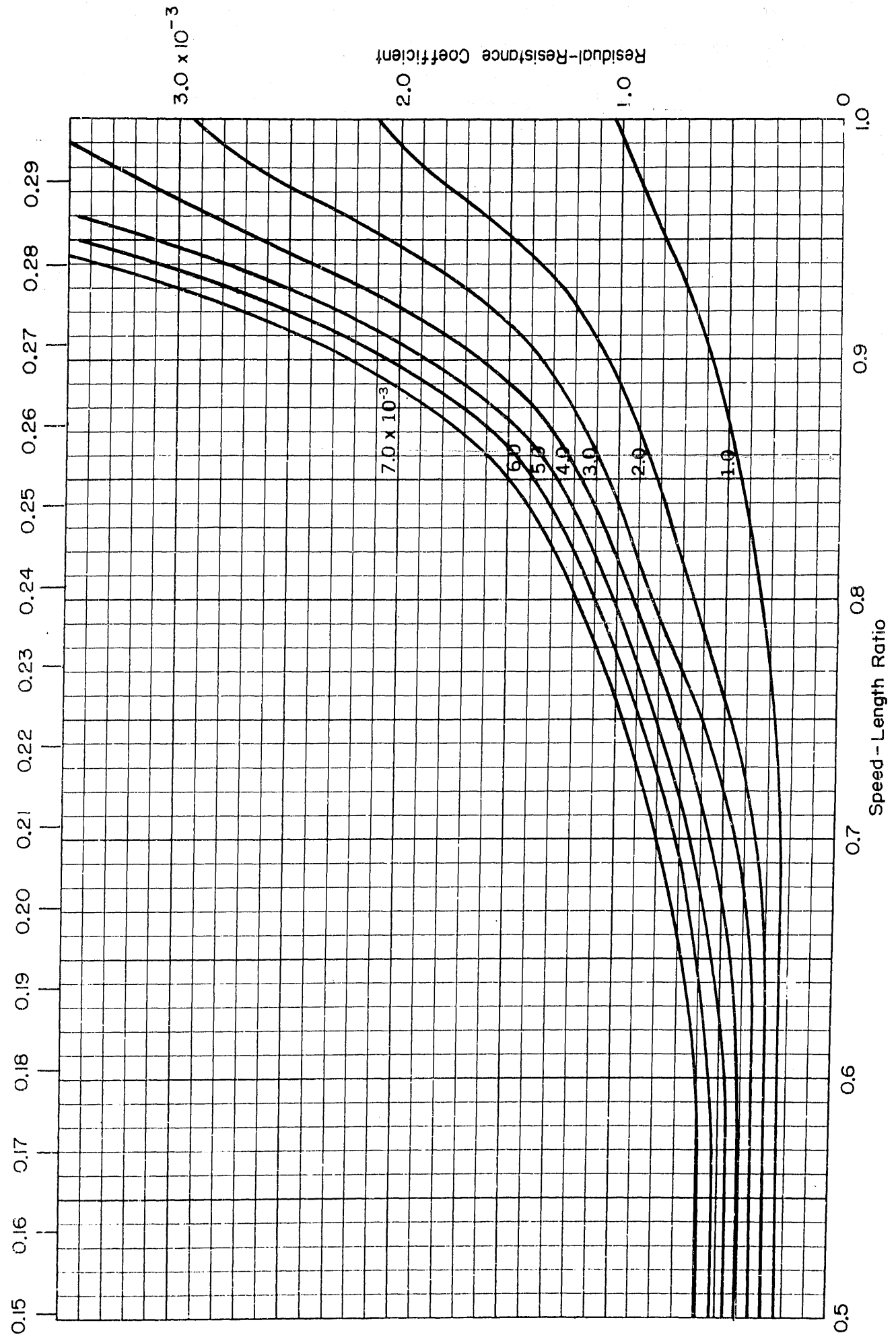
$B/H=2.25$
 $C_p=0.68$

Froude Number $\frac{V}{\sqrt{gH}}$

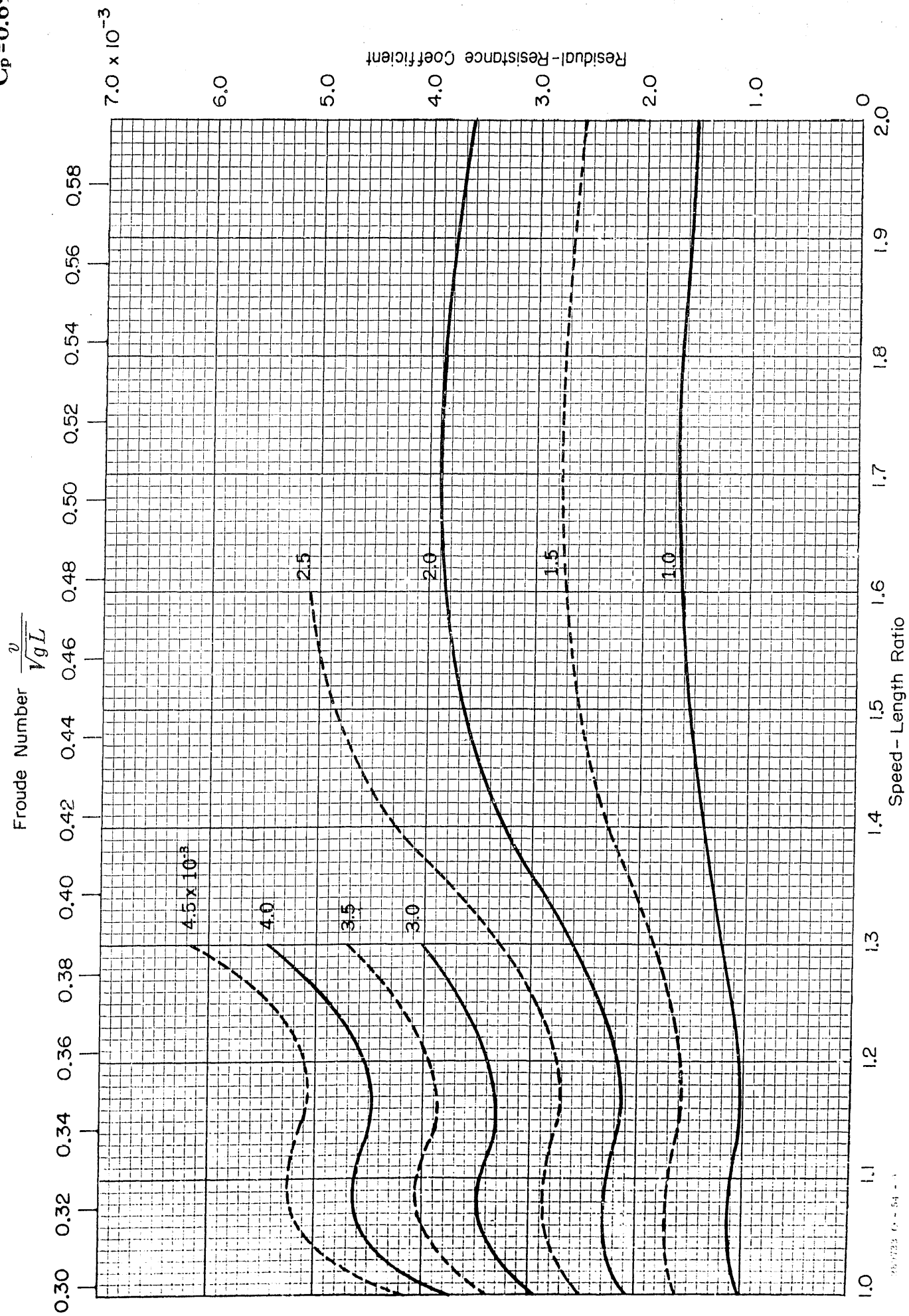


$B/H = 2.25$
 $C_p = 0.69$

Froude Number $\frac{v}{\sqrt{gL}}$



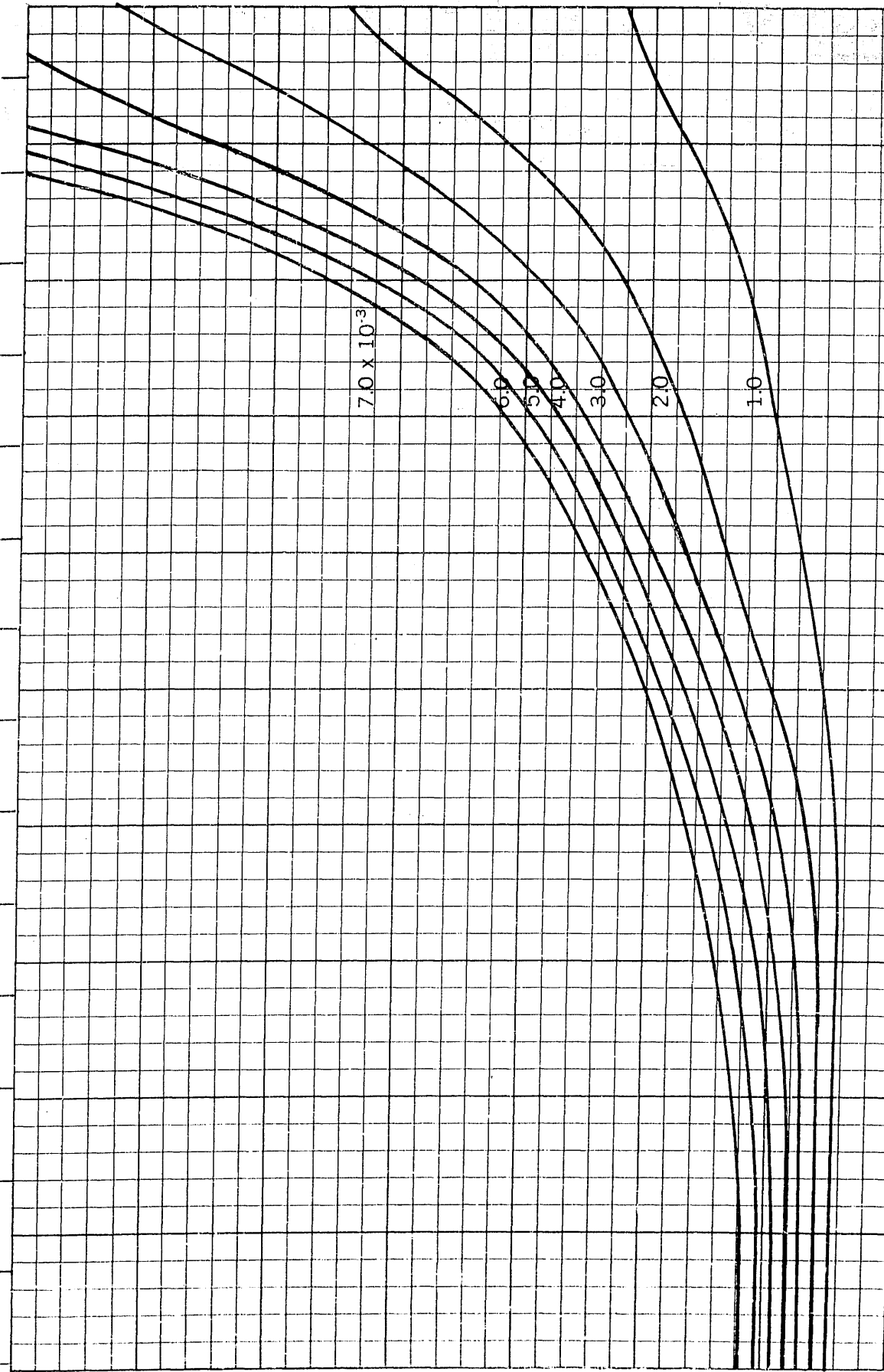
$B/H=2.25$
 $C_p=0.69$



$B/H = 2.25$
 $C_p = 0.70$

Froude Number $\frac{v}{\sqrt{gL}}$

0.15 0.16 0.17 0.18 0.19 0.20 0.21 0.22 0.23 0.24 0.25 0.26 0.27 0.28 0.29



Residual-Resistance Coefficient

3.0×10^{-3}

2.0

1.0

7.0×10^{-3}

6.0

5.0

4.0

3.0

2.0

1.0

0.5

0.6

0.7

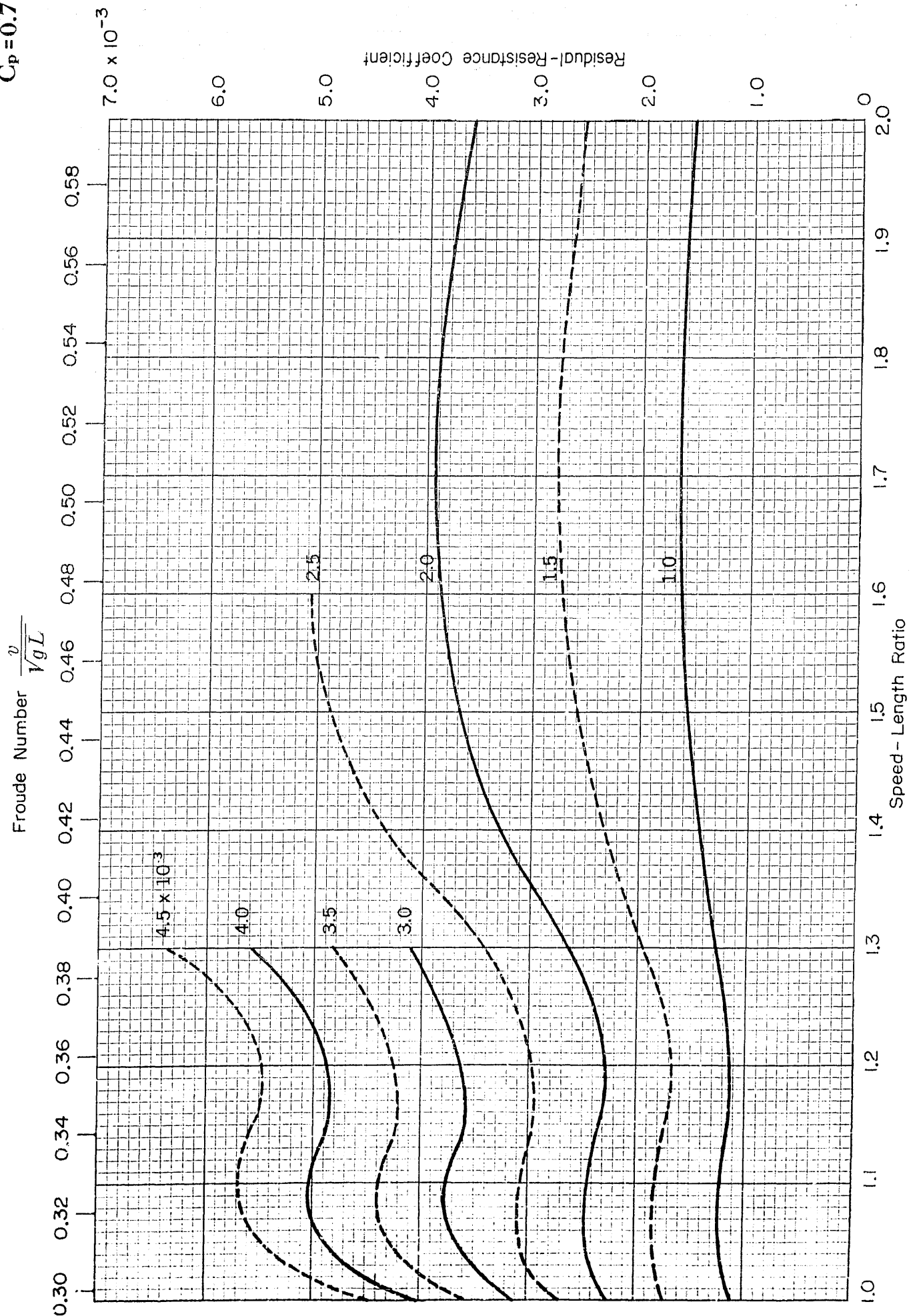
0.8

0.9

1.0

Speed - Length Ratio

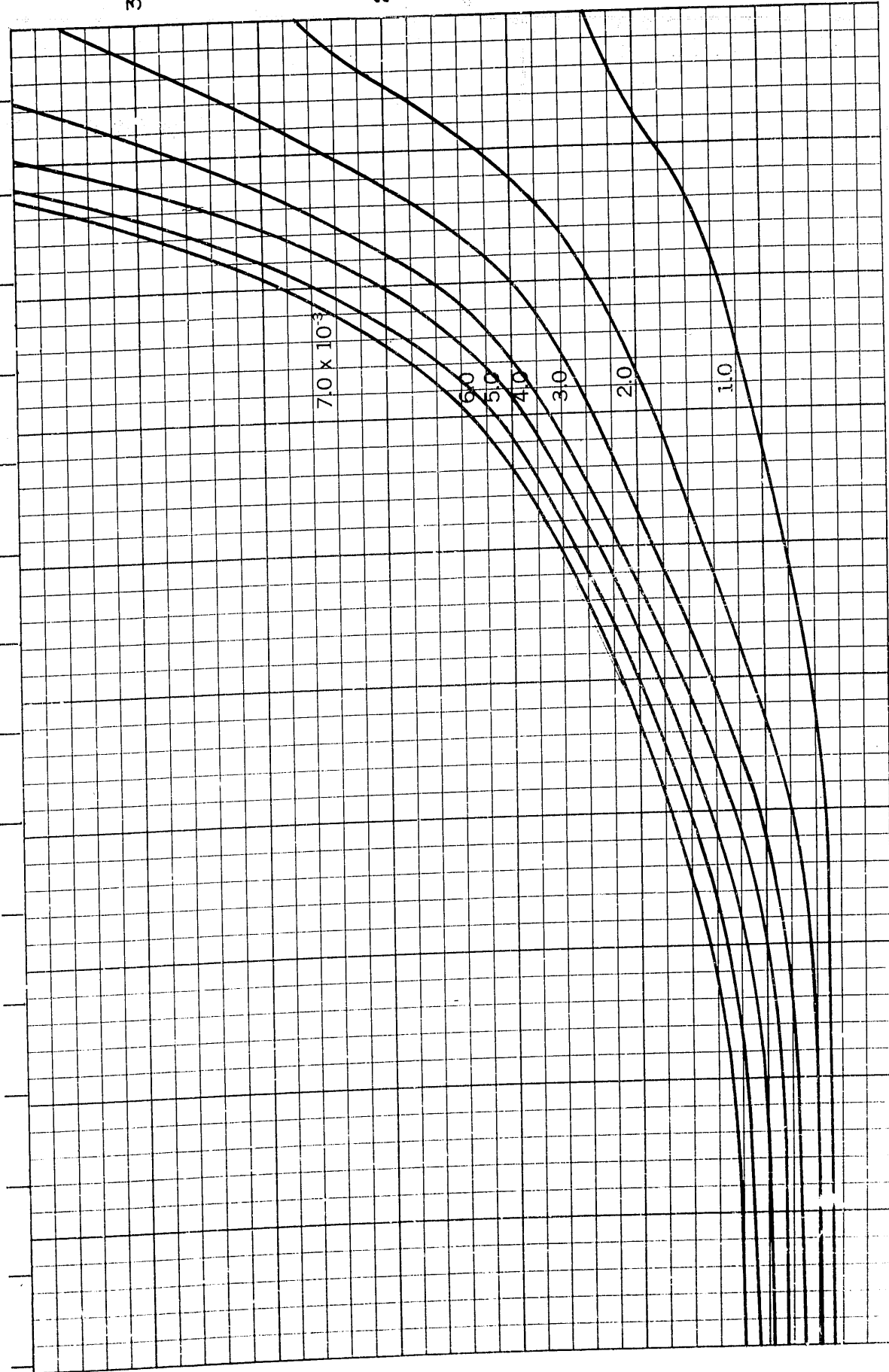
$B/H=2.25$
 $C_p=0.70$



$B/H=2.25$
 $C_p=0.71$

Froude Number $\frac{v}{\sqrt{gL}}$

0.15 0.16 0.17 0.18 0.19 0.20 0.21 0.22 0.23 0.24 0.25 0.26 0.27 0.28 0.29



Residual-Resistance Coefficient

1.0

0.9

0.8

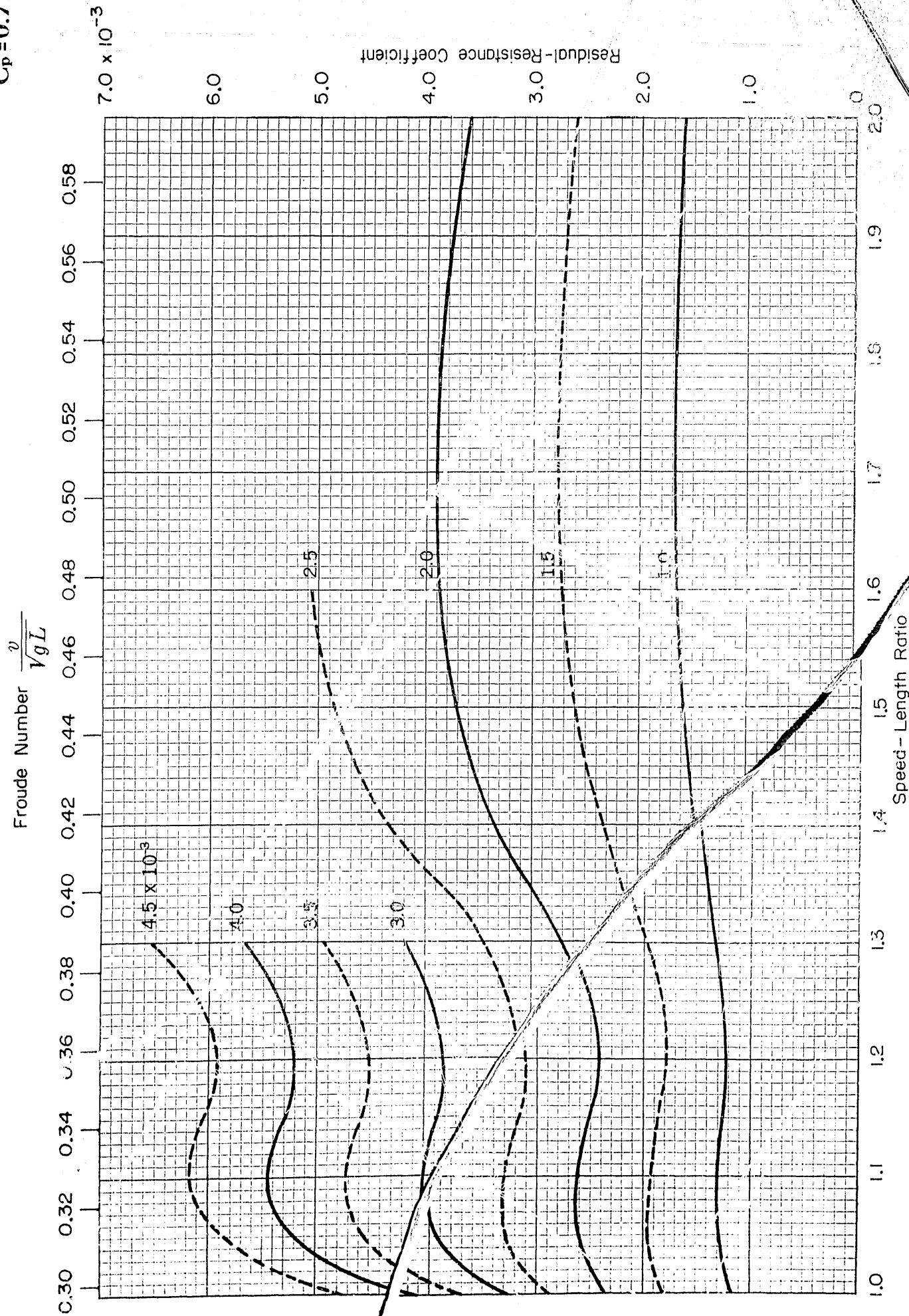
Speed-Length Ratio

0.7

0.6

0.5

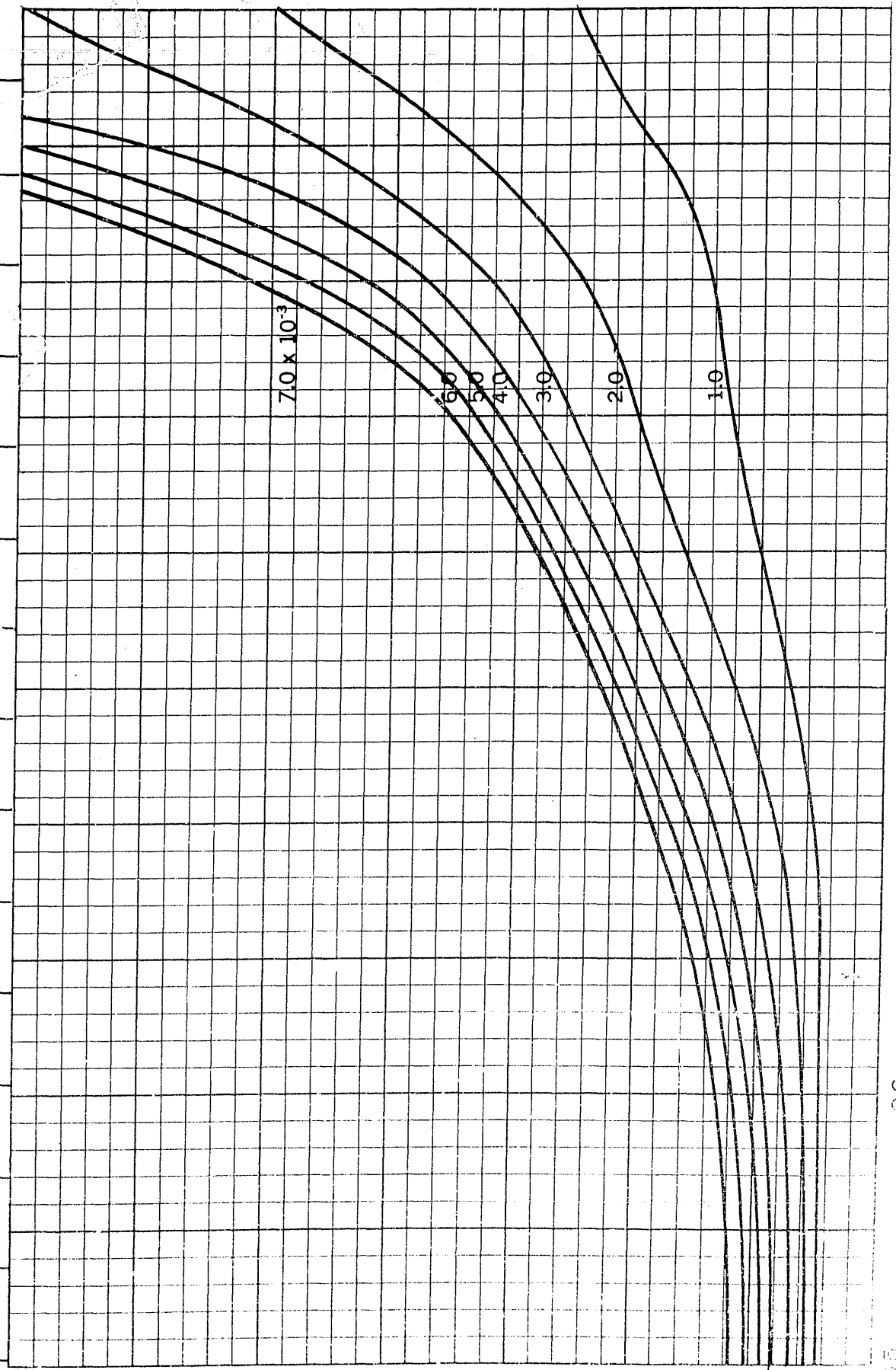
$B/H=2.25$
 $C_p=0.71$



$B/H = 2.25$
 $C_p = 0.72$

Froude Number $\frac{v}{\sqrt{gL}}$

0.15 0.16 0.17 0.18 0.19 0.20 0.21 0.22 0.23 0.24 0.25 0.26 0.27 0.28 0.29



Residual-Resistance Coefficient

3.0×10^{-2}

7.0×10^{-3}

6.0

5.0

4.0

3.0

2.0

1.0

0.6

0.7

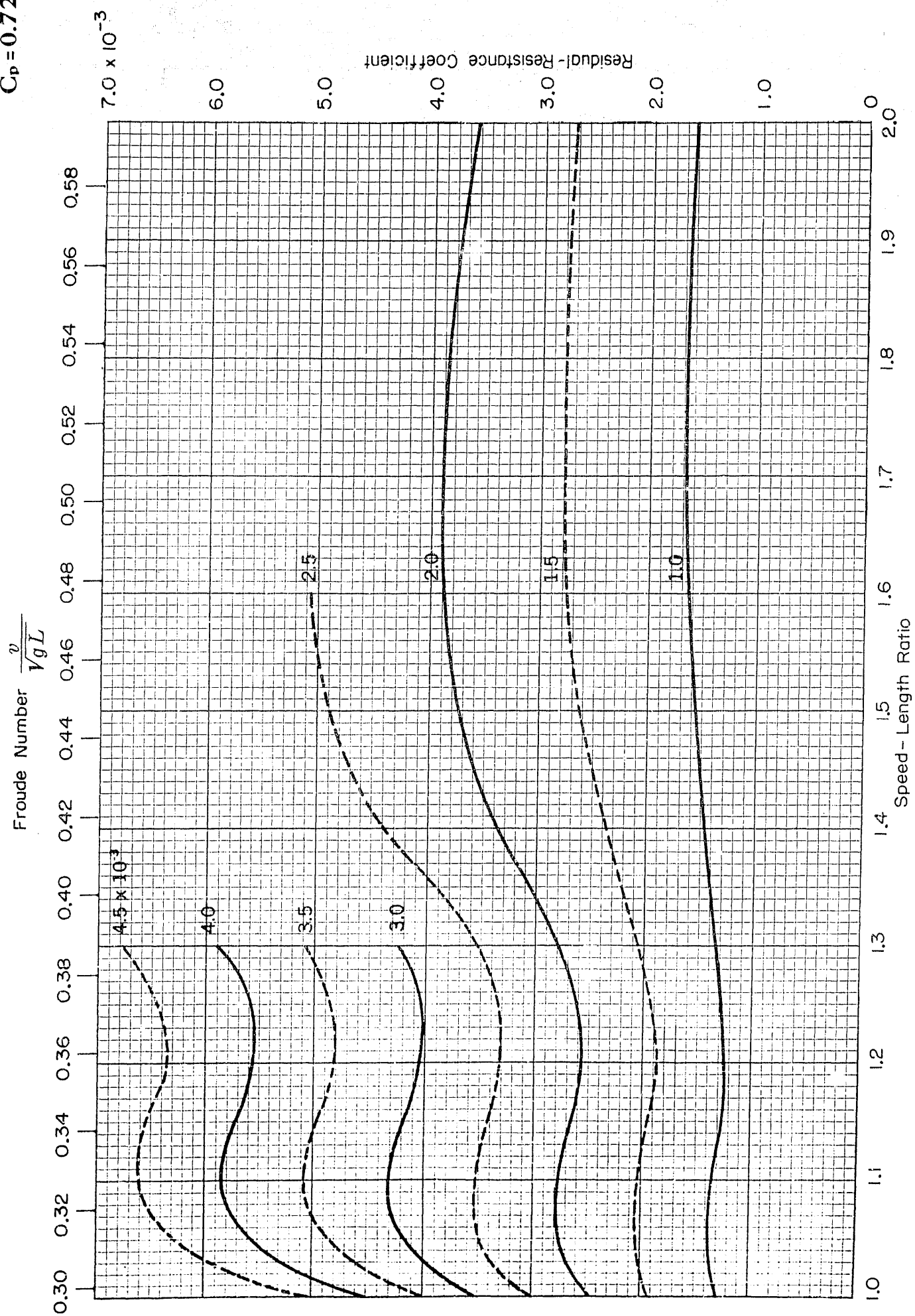
0.8

0.9

1.0

Speed - Length Ratio

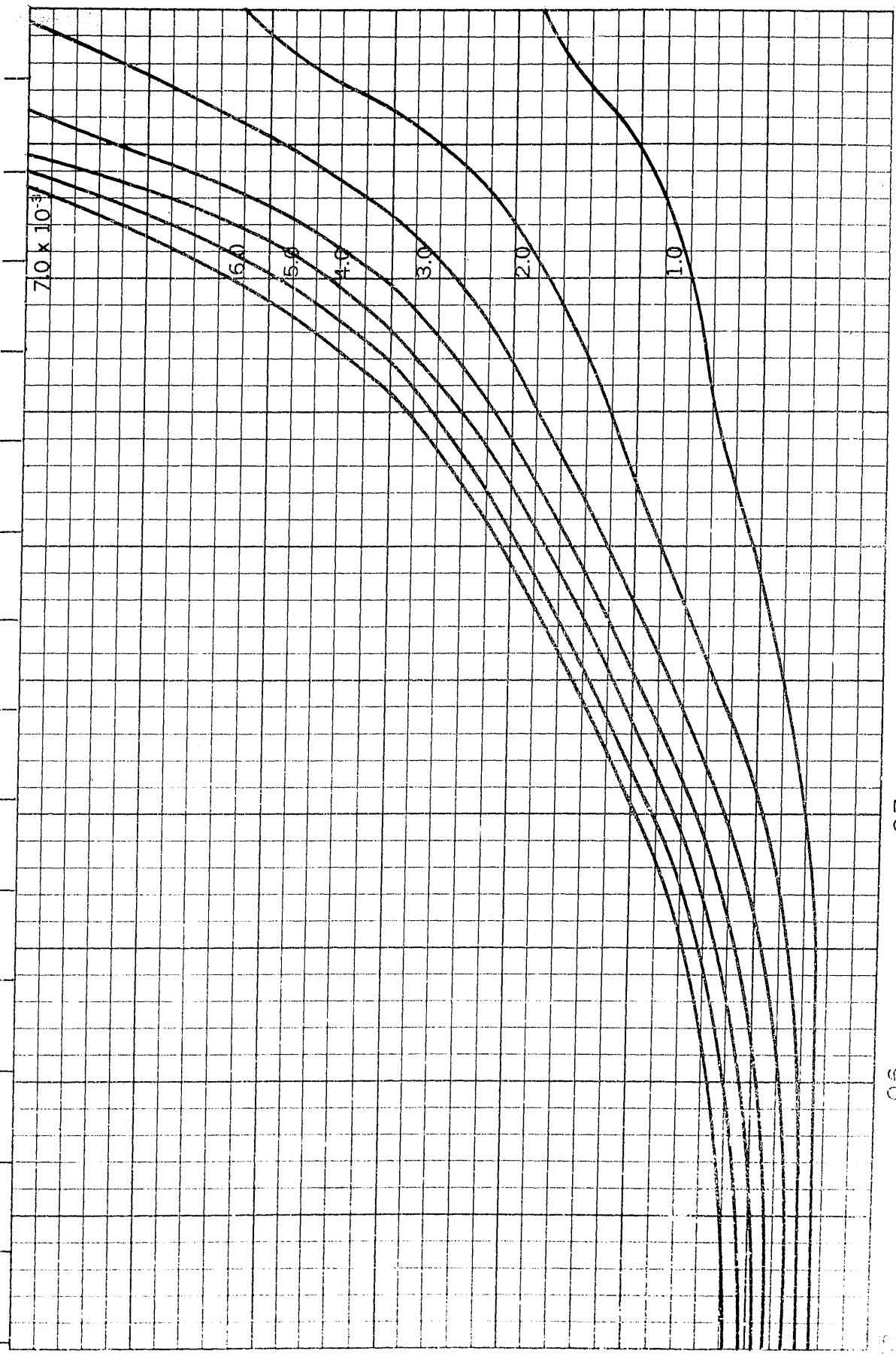
$B/H = 2.25$
 $C_D = 0.72$



$B/H=2.25$
 $C_p=0.73$

Froude Number $\frac{v}{\sqrt{gL}}$

0.15 0.16 0.17 0.18 0.19 0.20 0.21 0.22 0.23 0.24 0.25 0.26 0.27 0.28 0.29



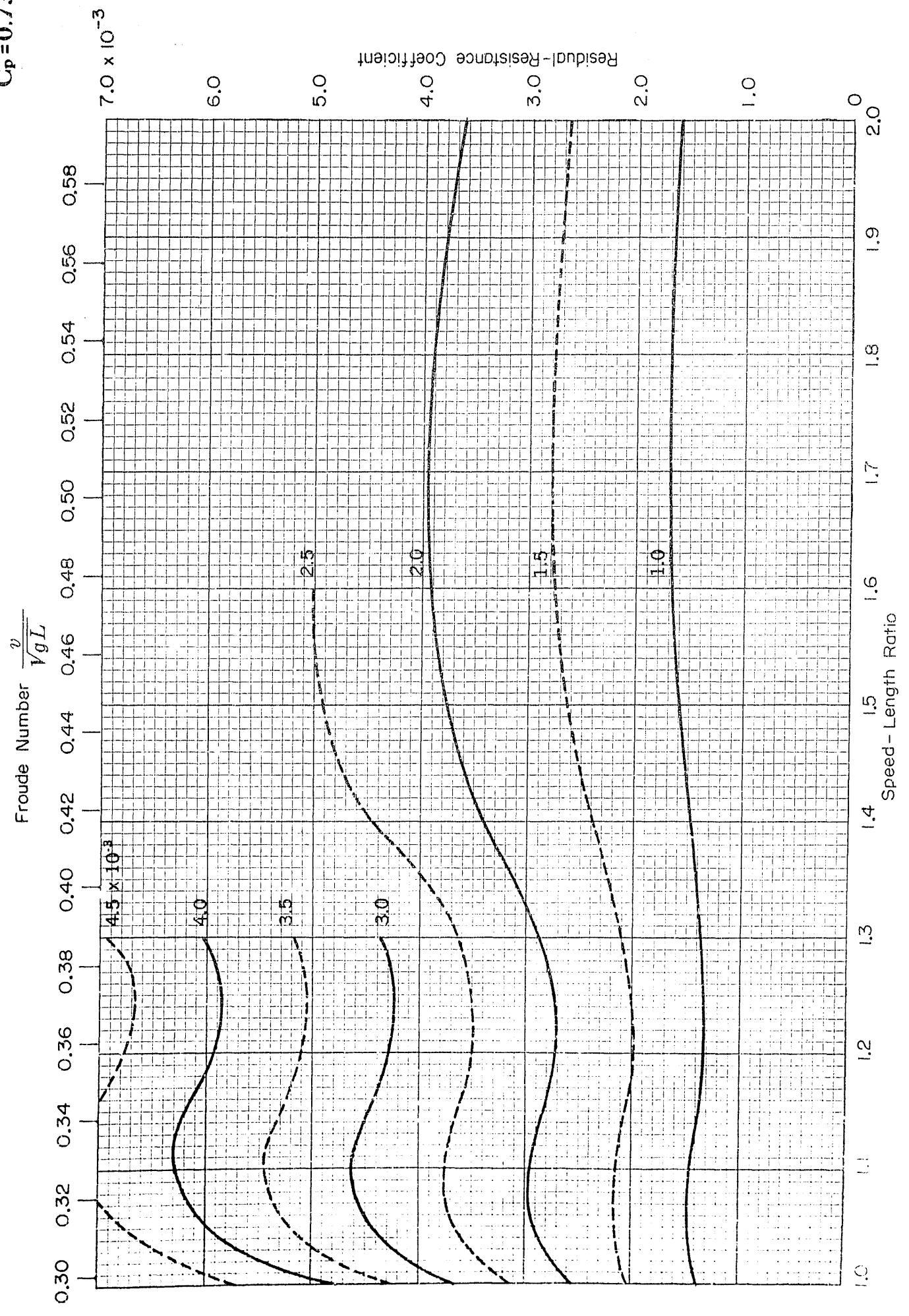
Residual-Resistance Coefficient

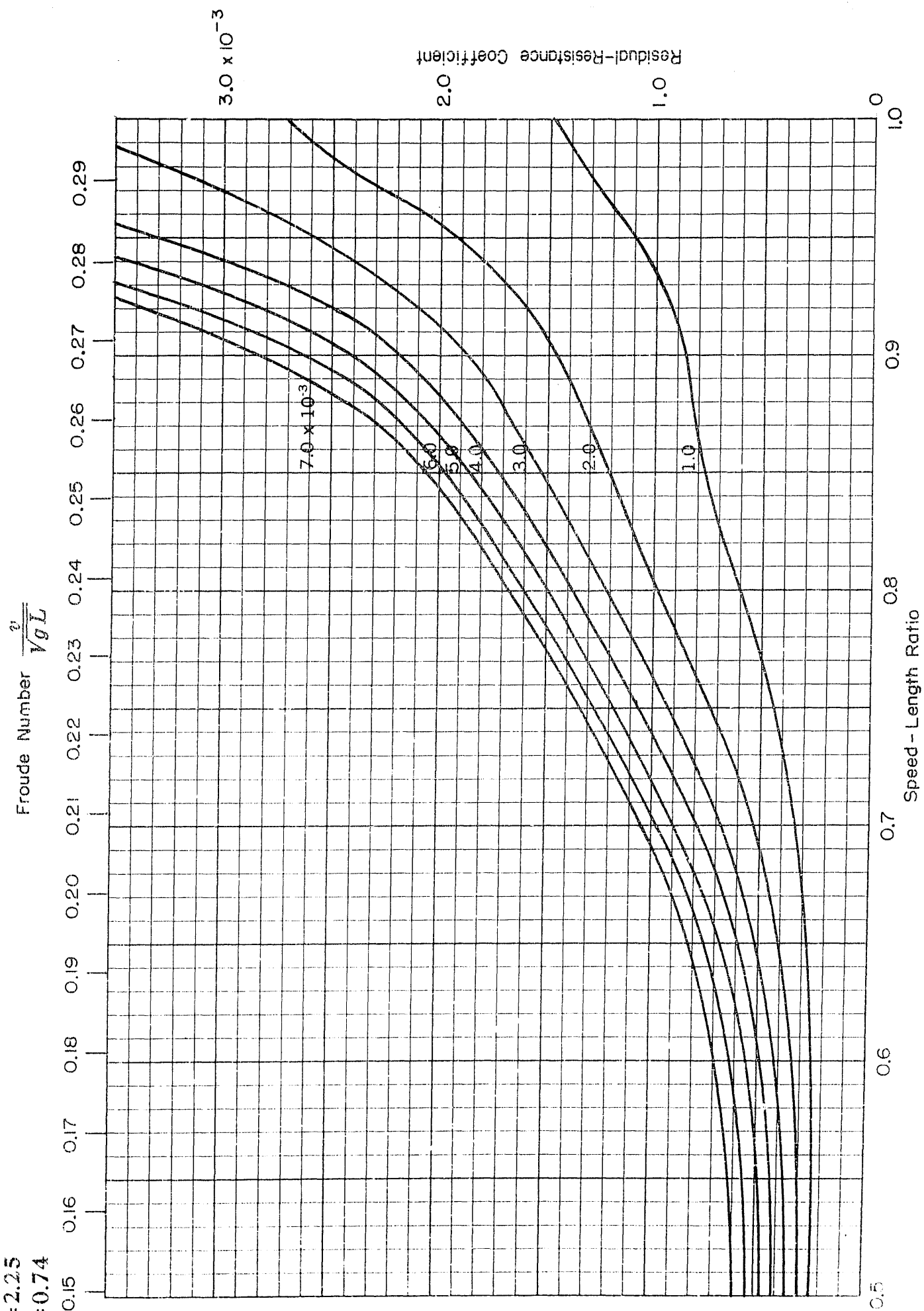
3.0×10^{-3}

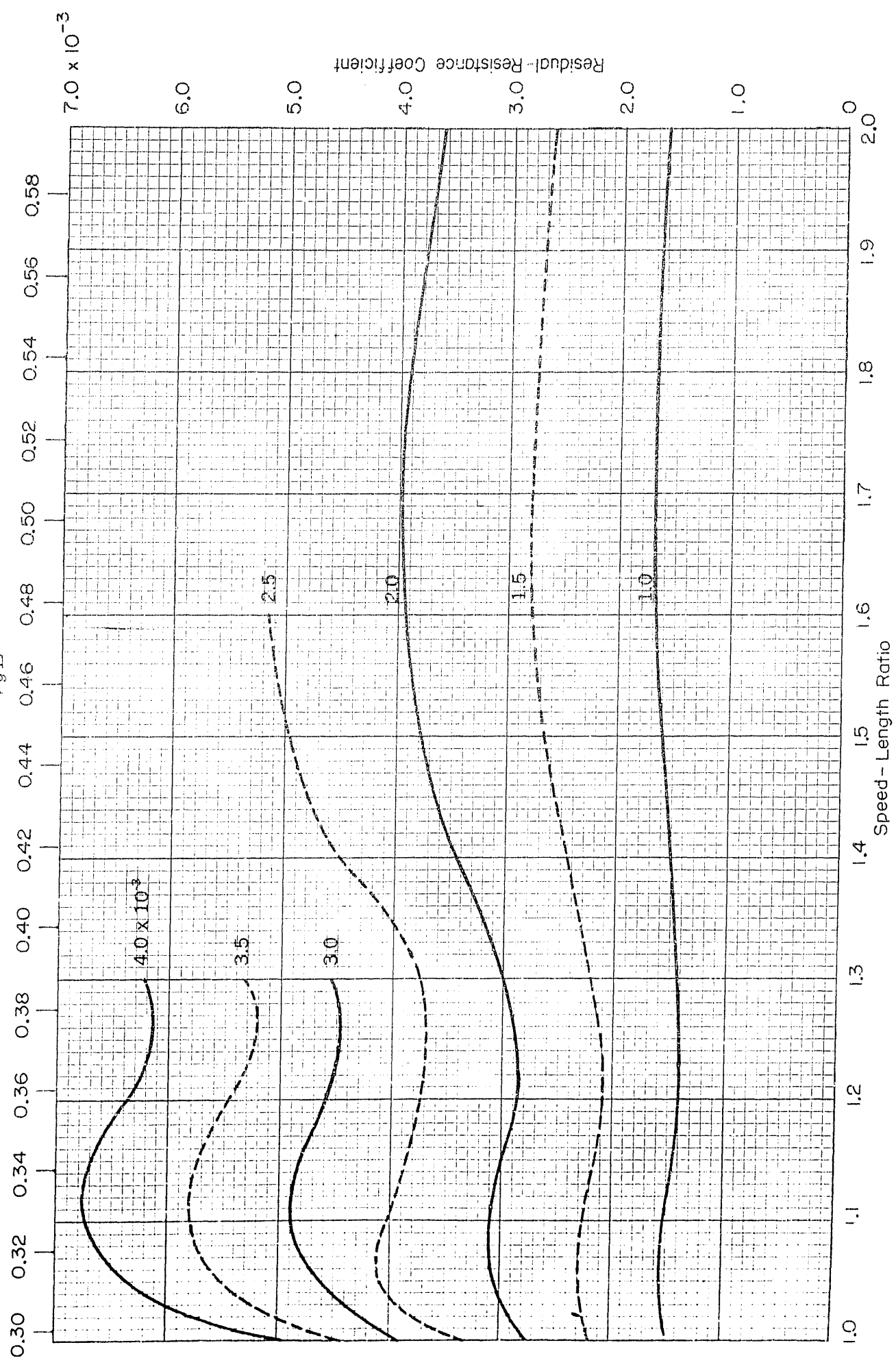
7.0×10^{-3}

Speed-Length Ratio

$B/H = 2.25$
 $C_p = 0.73$



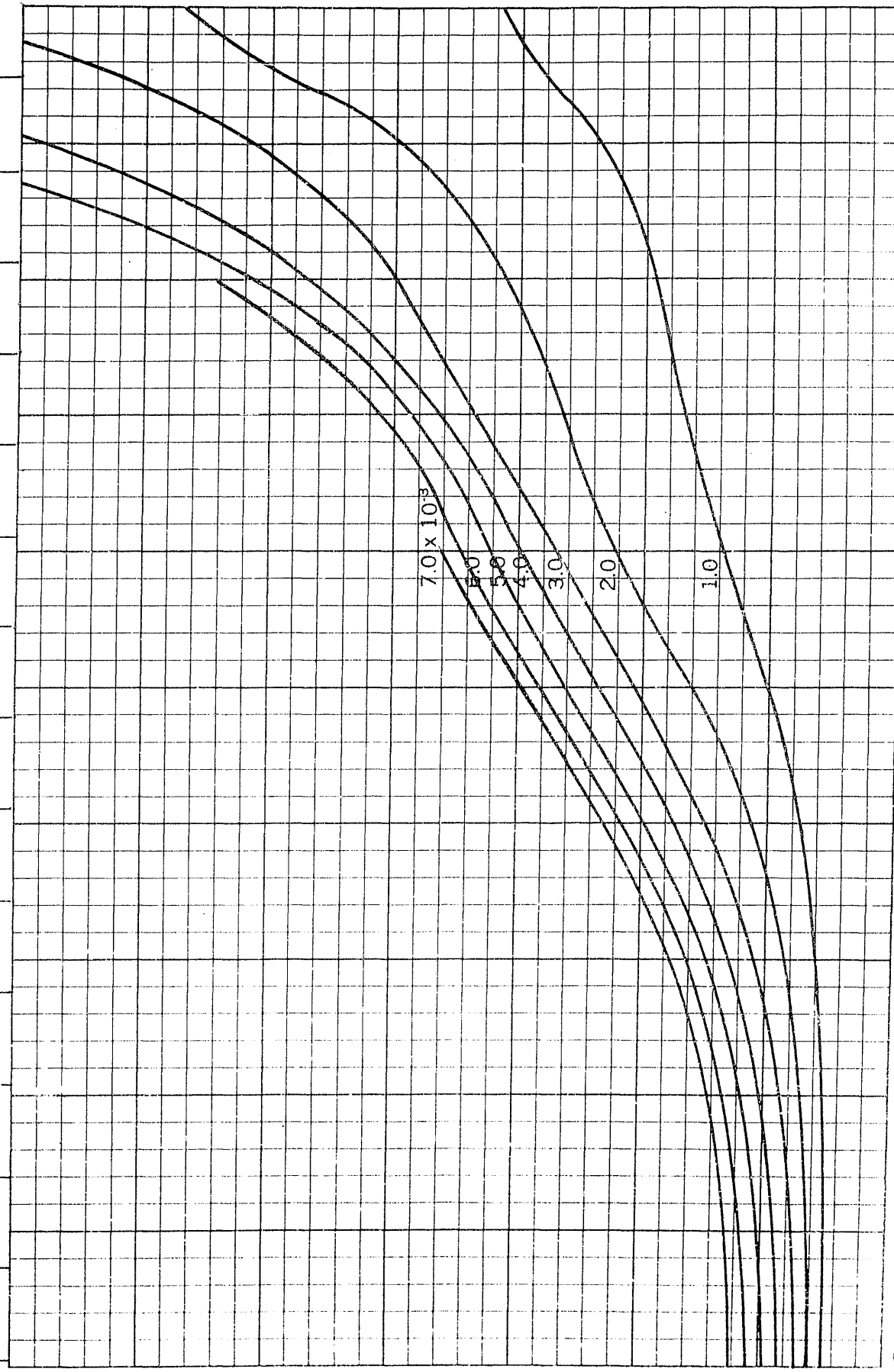
Froude Number $\frac{U^2}{gD}$ 

$$\frac{v}{\sqrt{gL}}$$


$B/H = 2.25$
 $C_p = 0.75$

Froude Number $\frac{v}{\sqrt{gL}}$

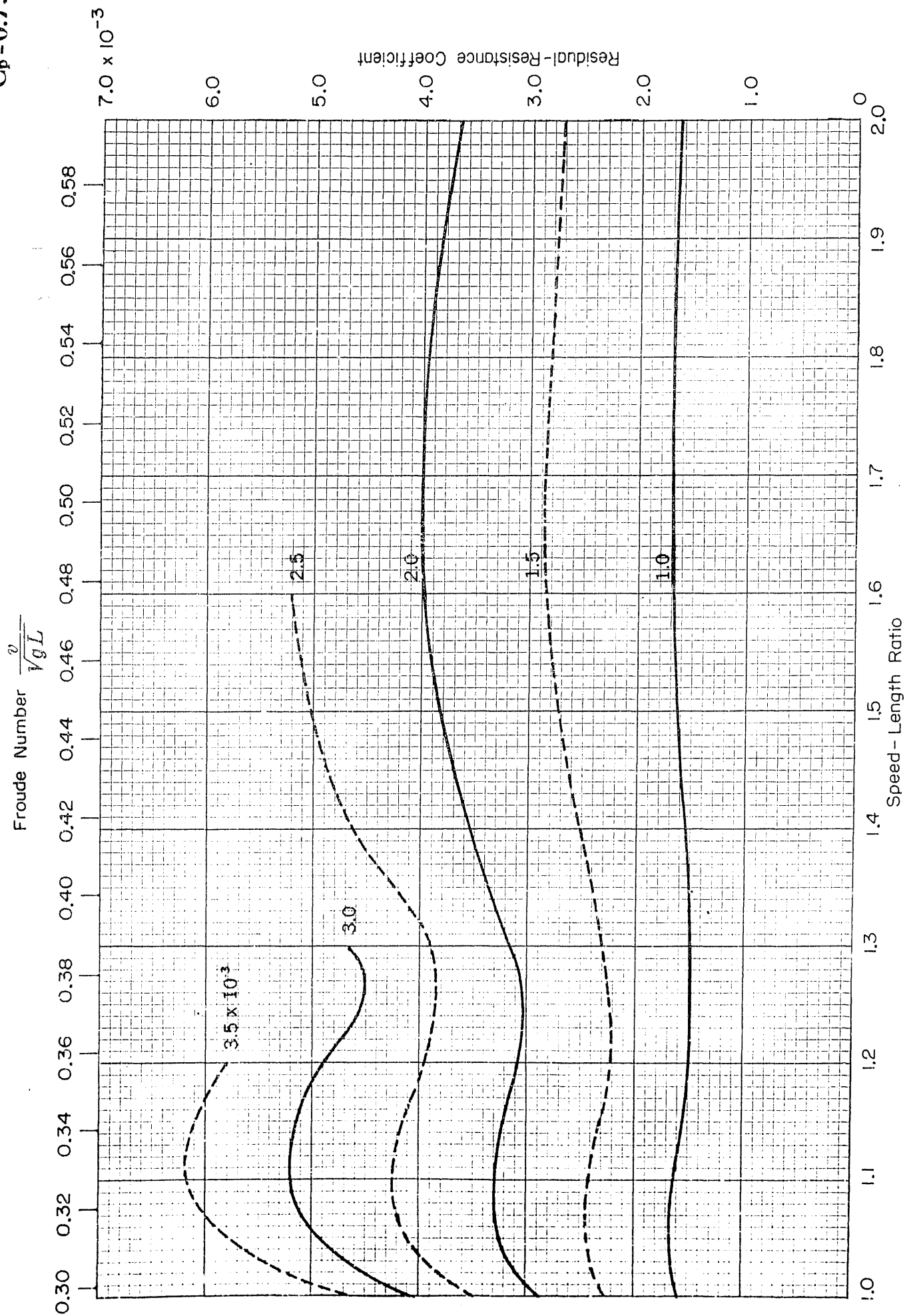
0.15 0.16 0.17 0.18 0.19 0.20 0.21 0.22 0.23 0.24 0.25 0.26 0.27 0.28 0.29



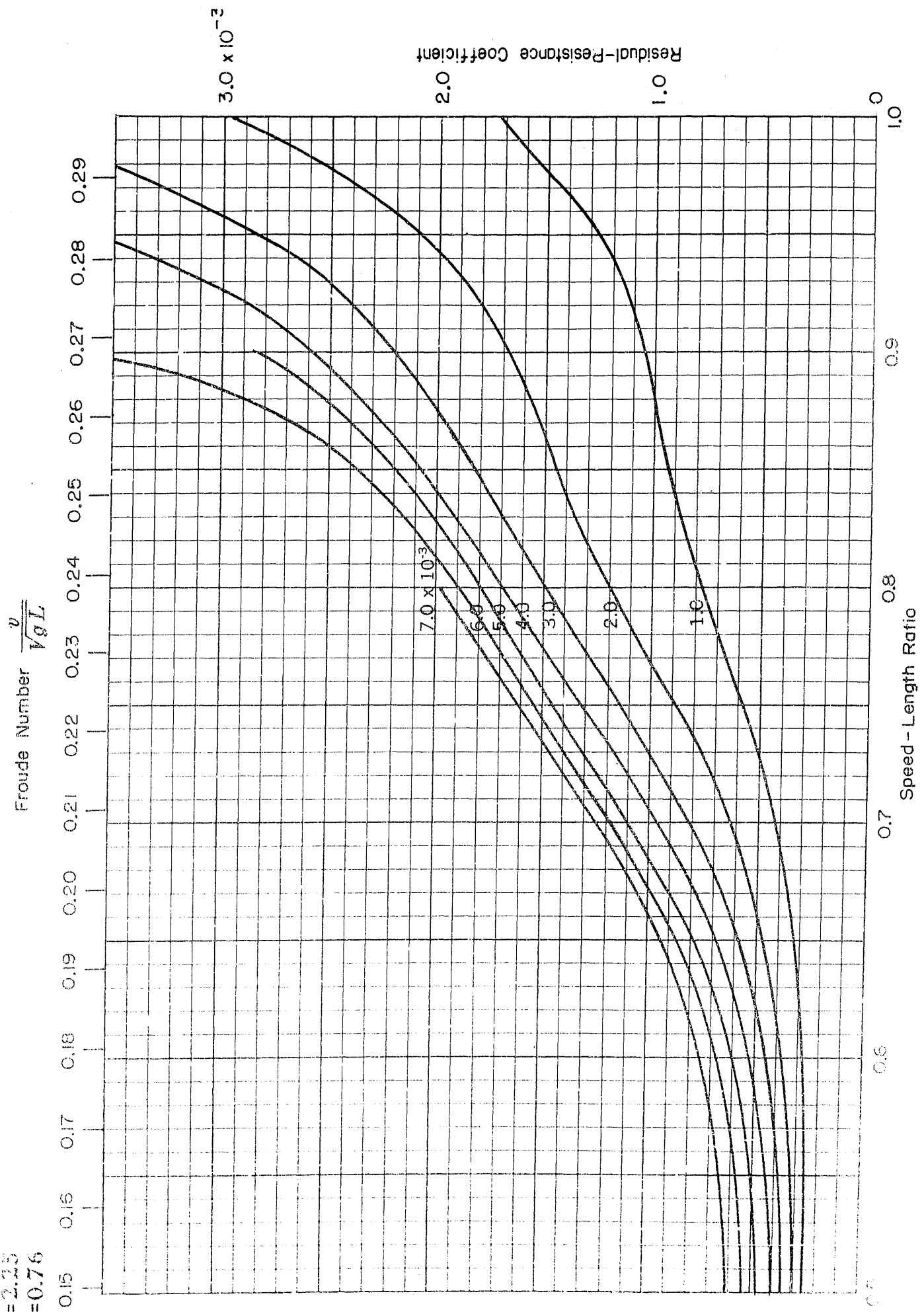
3.0 $\times 10^{-3}$
 2.0
 1.0
 0

0.5 0.6 0.7 0.8 0.9 1.0
 Speed - Length Ratio

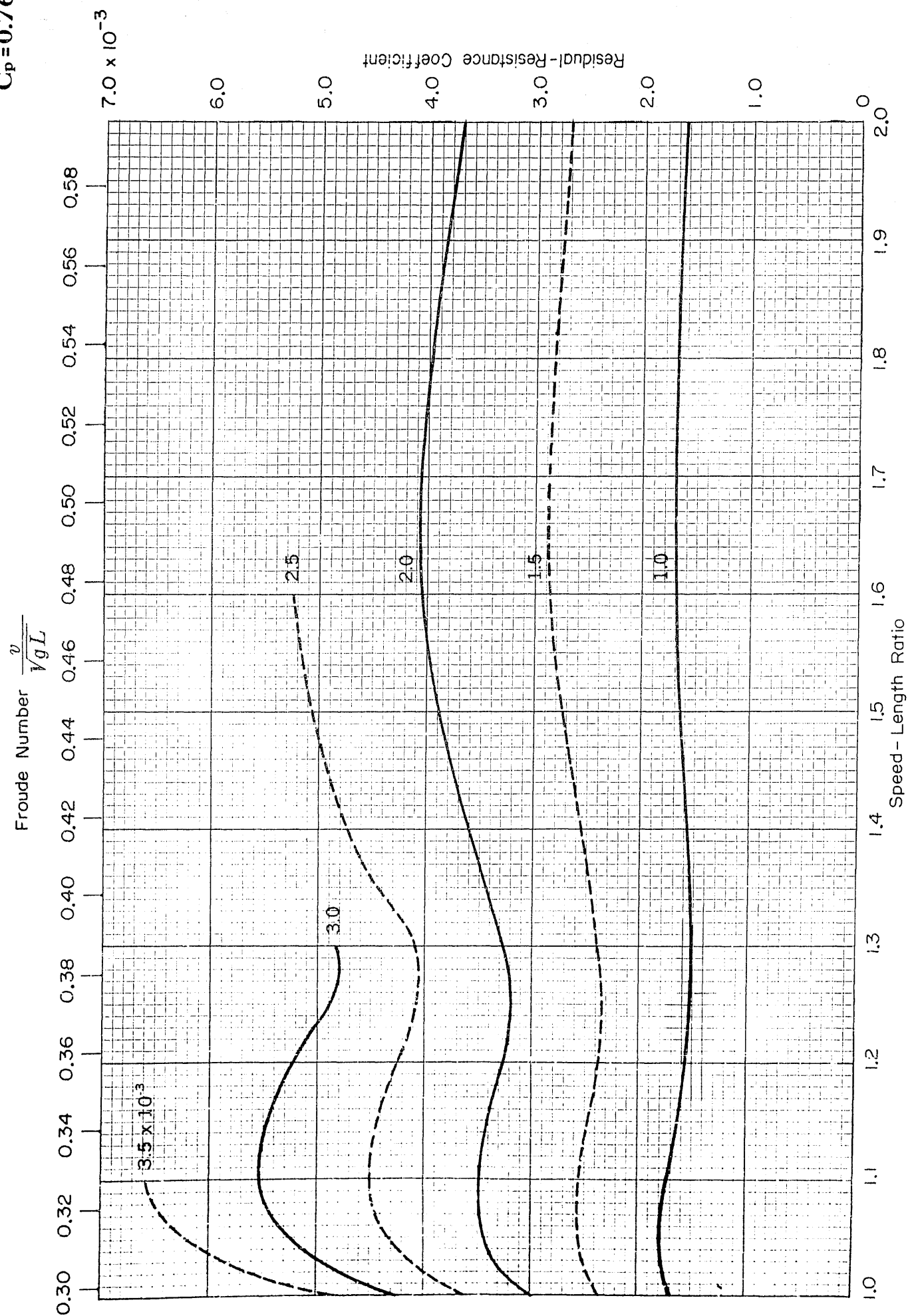
$B/H=2.25$
 $C_p=0.75$



$B/H = 2.25$
 $C_p = 0.76$



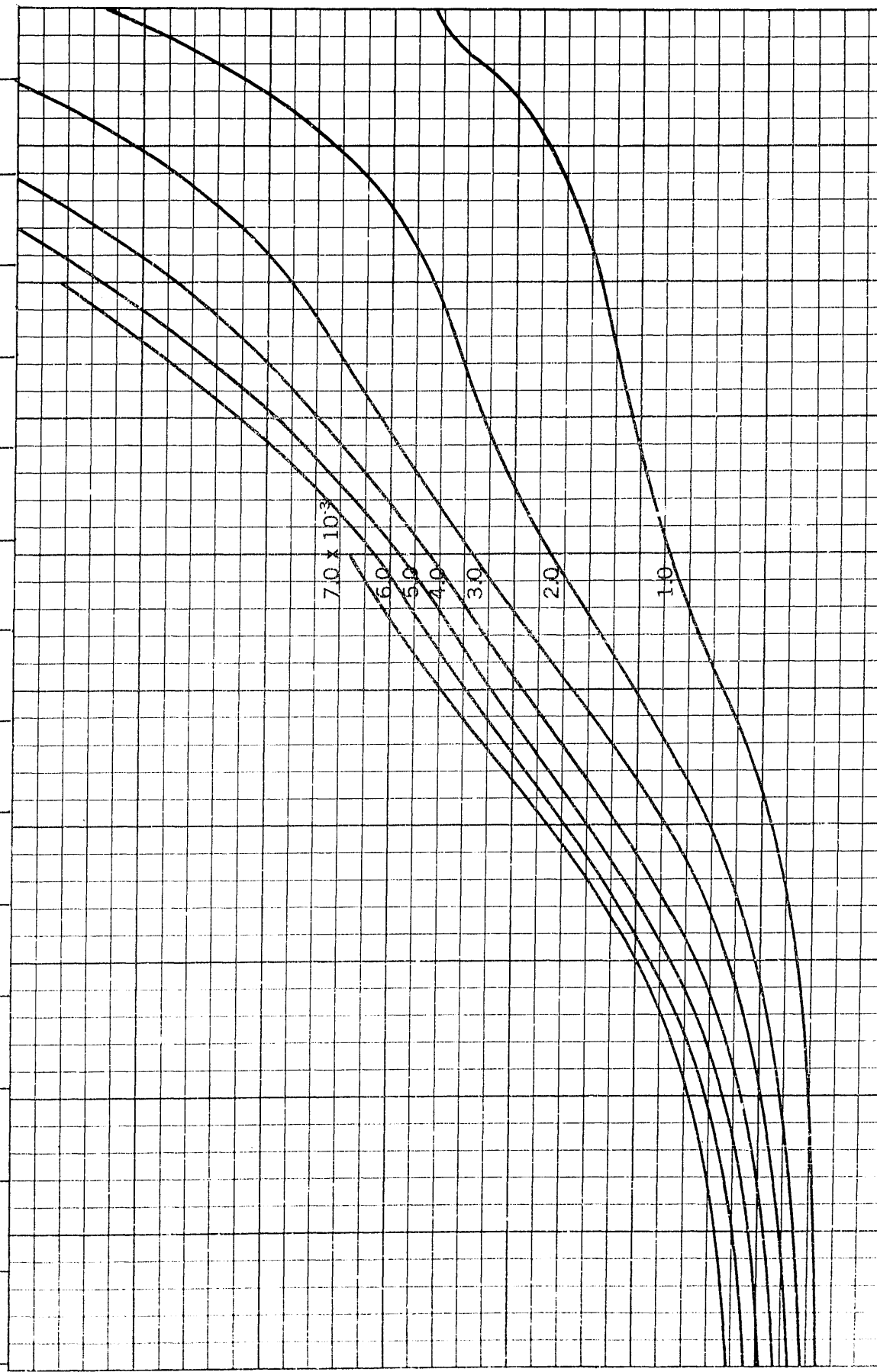
$B/H=2.25$
 $C_p=0.76$



$B/H=2.25$
 $C_p=0.77$

Froude Number $\frac{v}{\sqrt{gL}}$

0.15 0.16 0.17 0.18 0.19 0.20 0.21 0.22 0.23 0.24 0.25 0.26 0.27 0.28 0.29

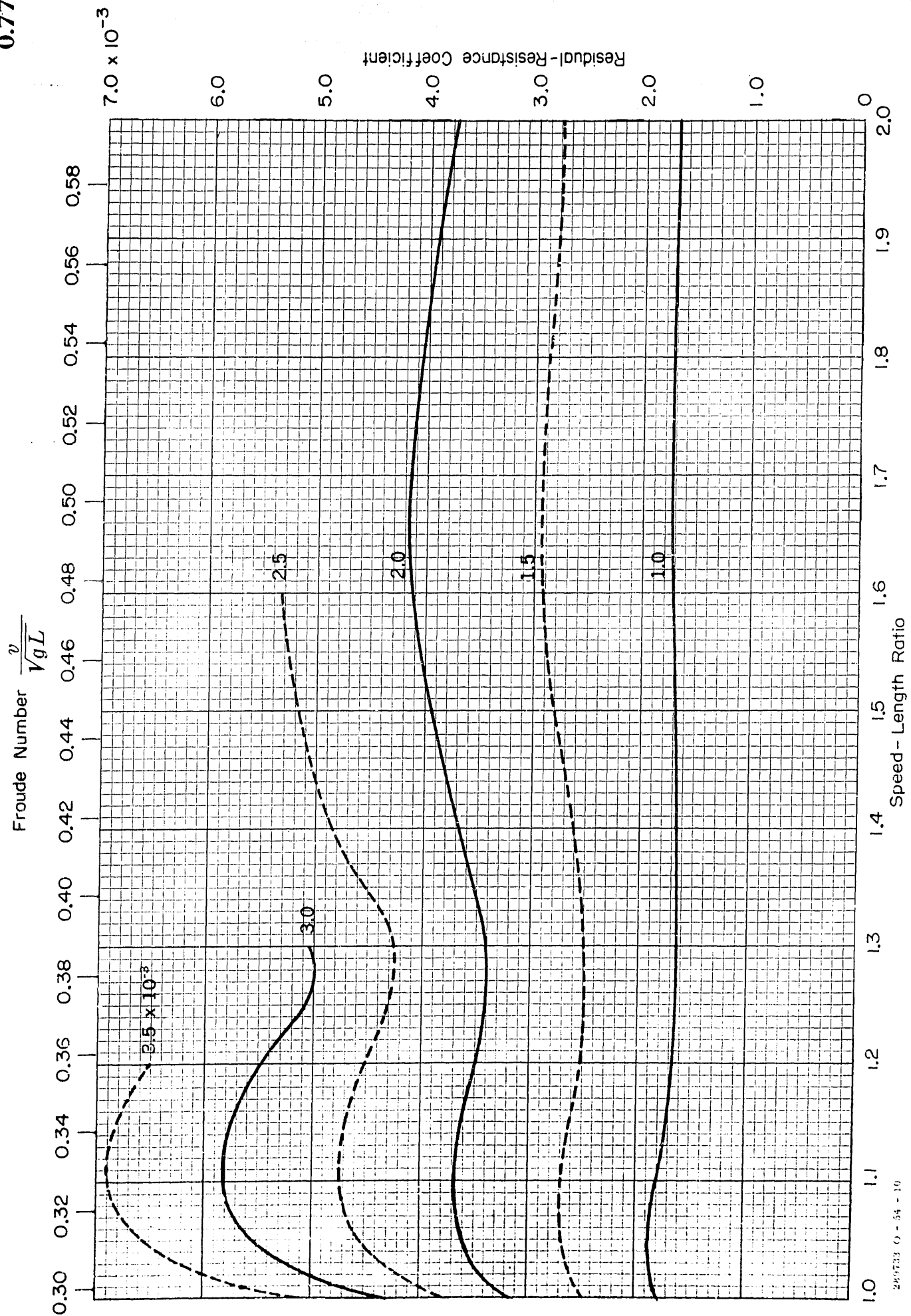


Residual-Resistance Coefficient

0 1.0 0.9 0.8 0.7 0.6 0.5

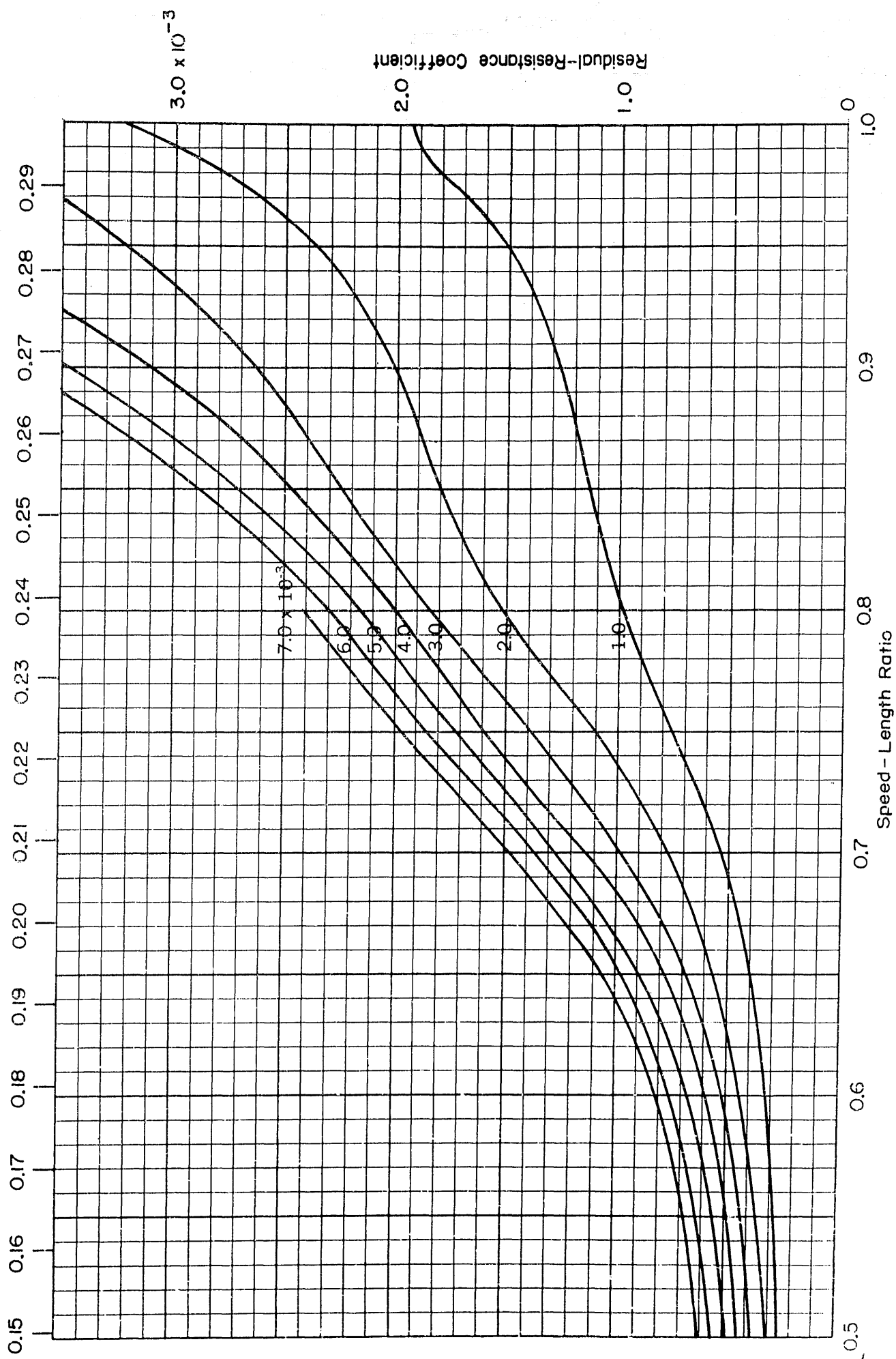
Speed-Length Ratio

$B/H=2.25$
0.77

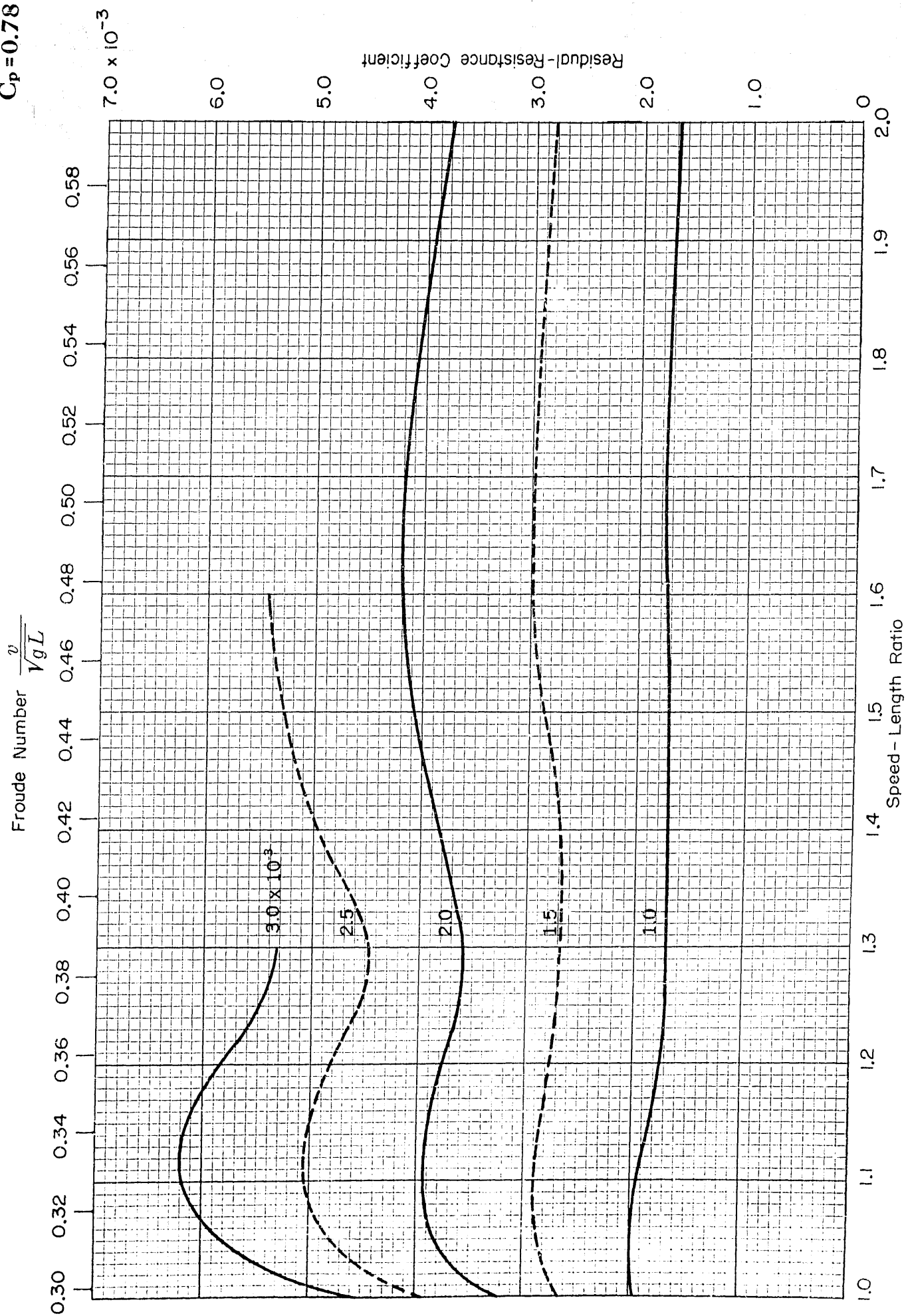


$B/H=2.25$
 $C_p=0.78$

Froude Number $\frac{v}{\sqrt{gL}}$

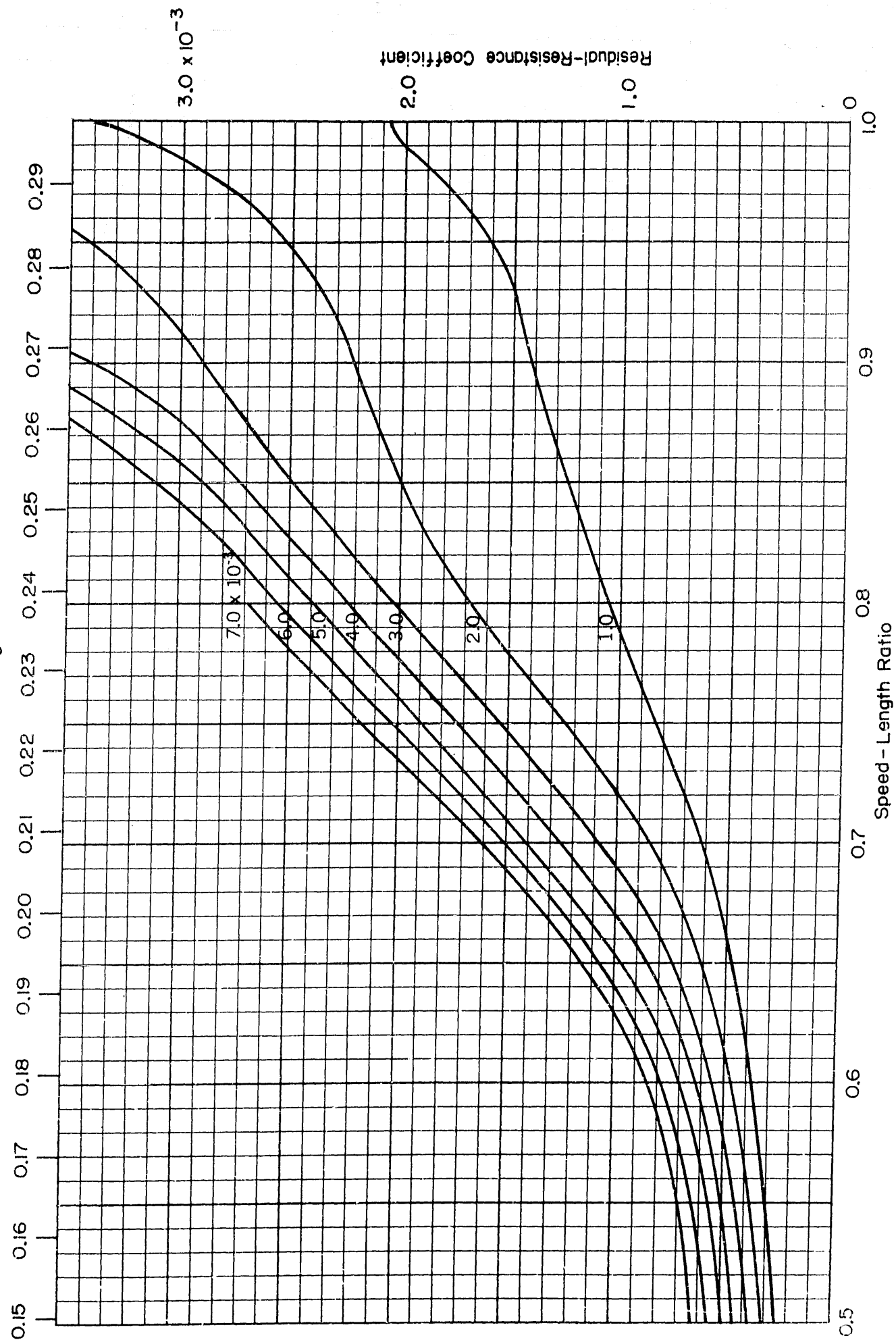


$B/H = 2.25$
 $C_p = 0.78$

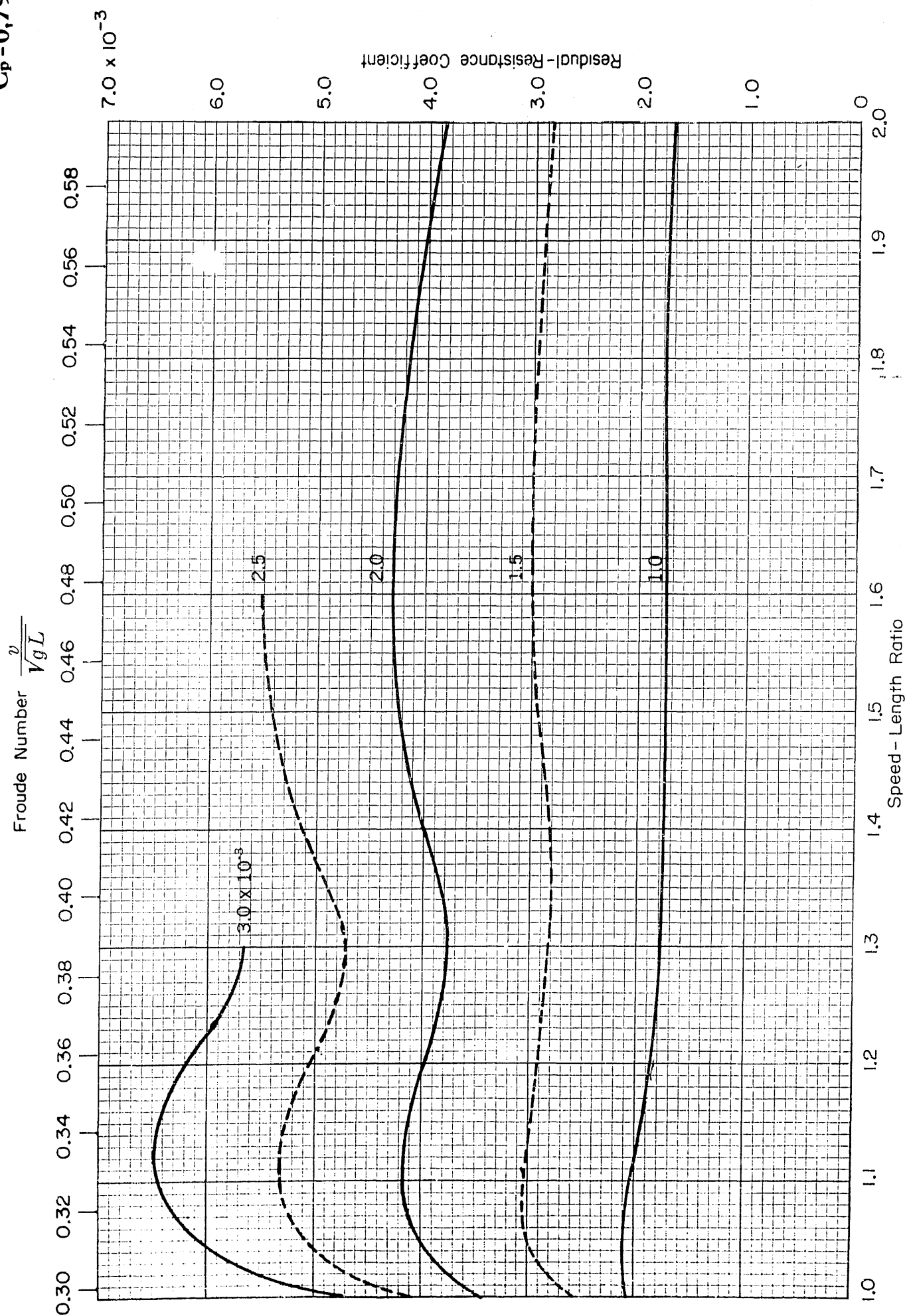


$B/H=2.25$
 $C_p=0.79$

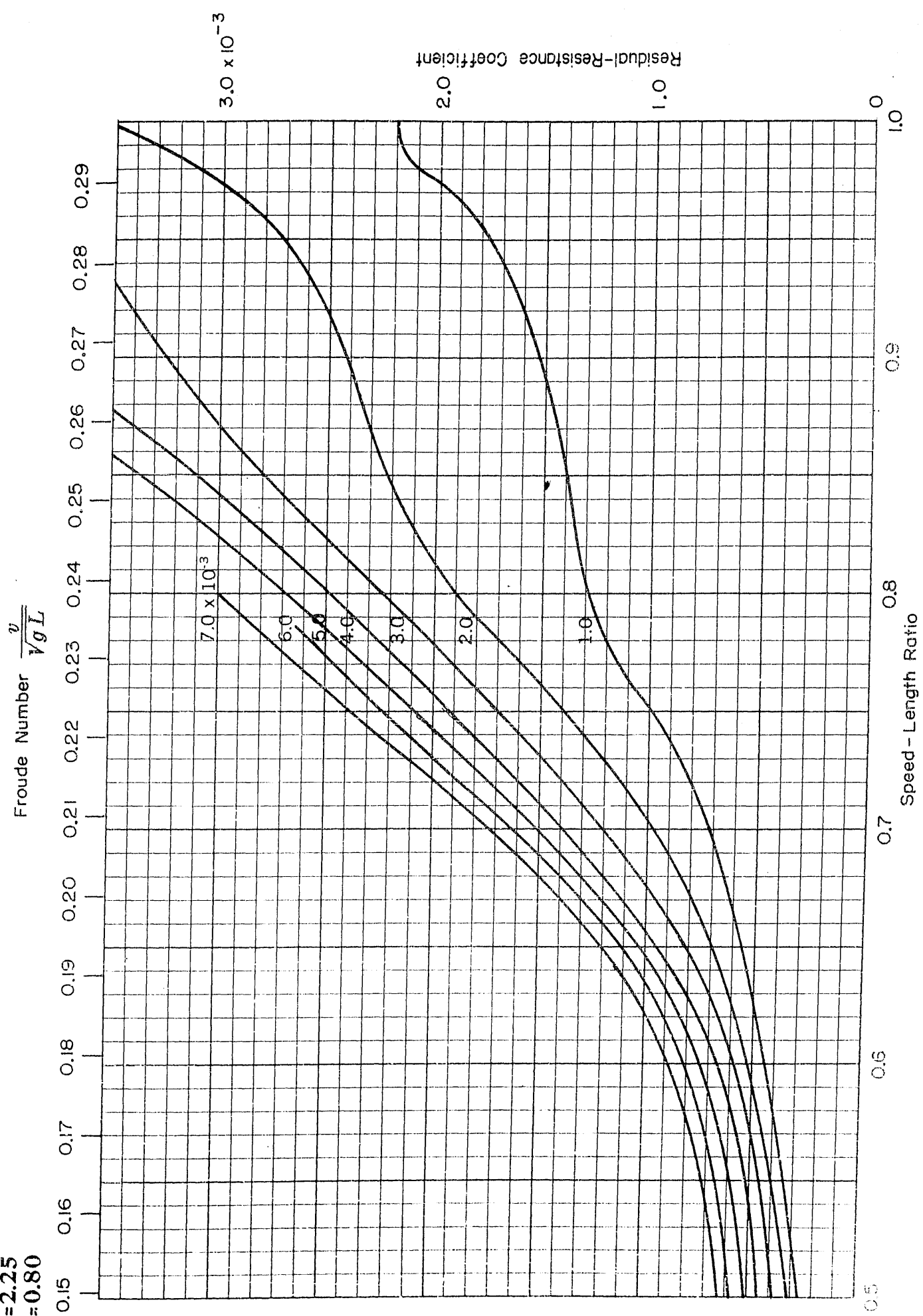
Froude Number $\frac{v}{\sqrt{gL}}$



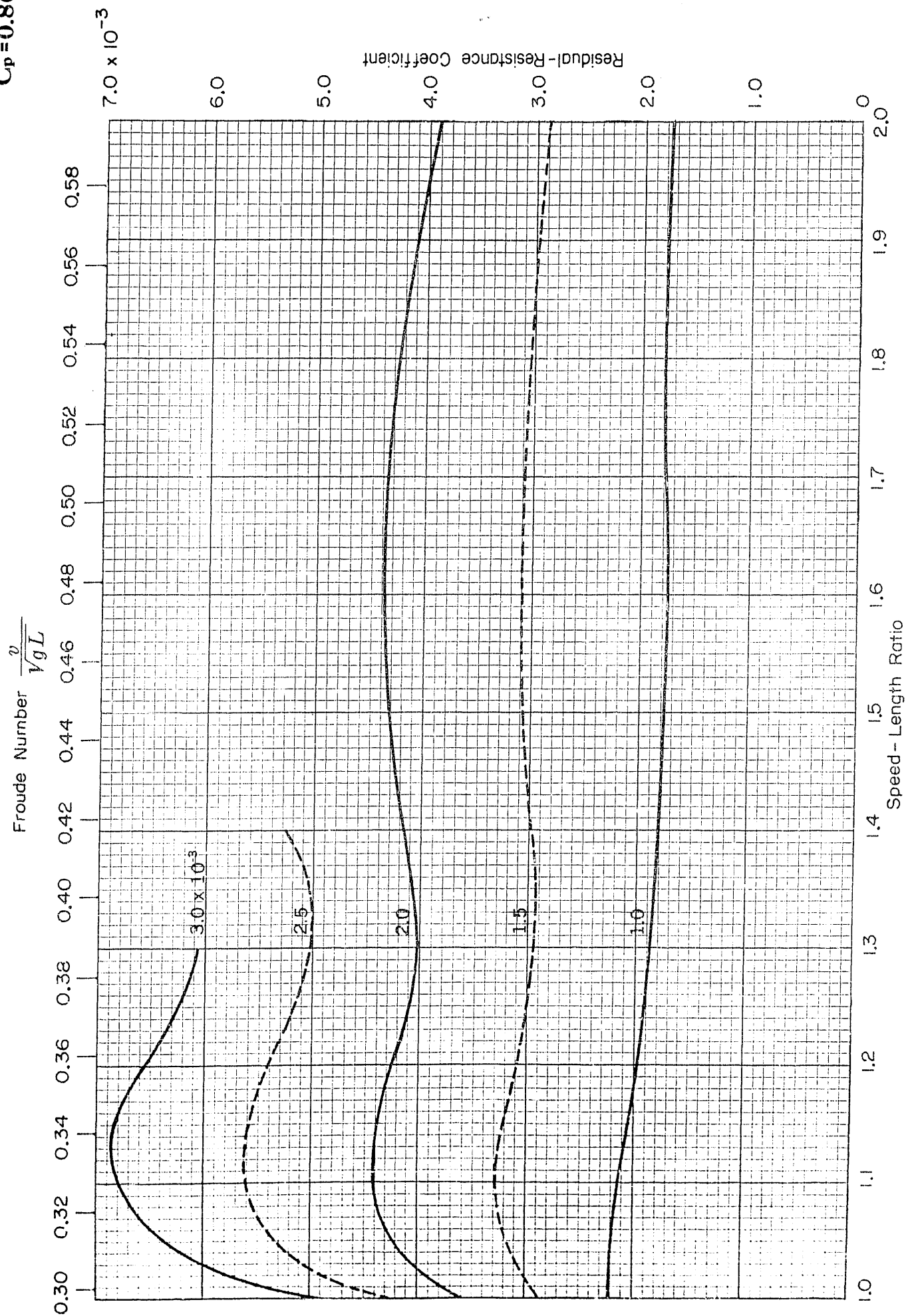
$B/H=2.25$
 $C_p=0.79$

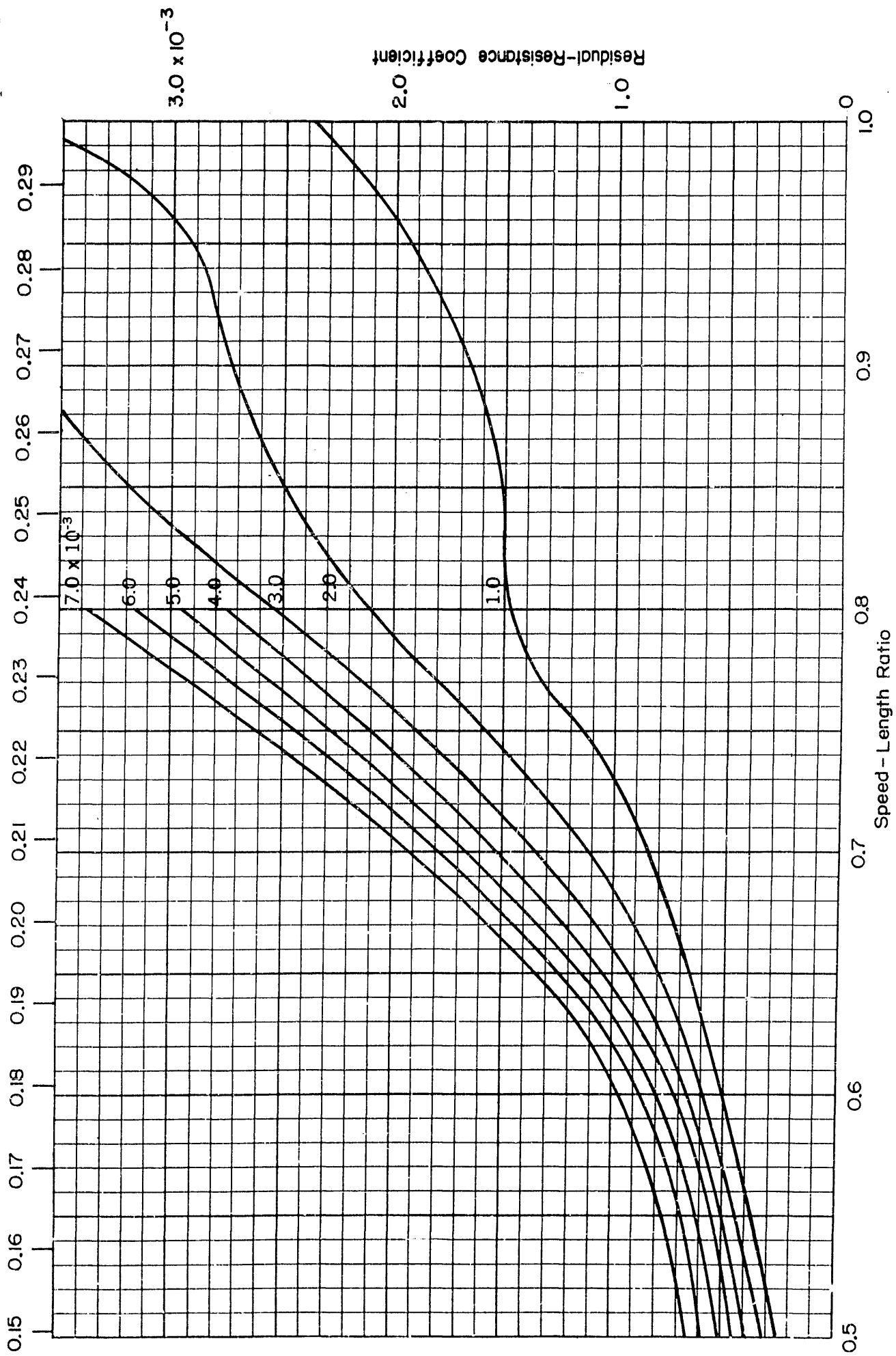


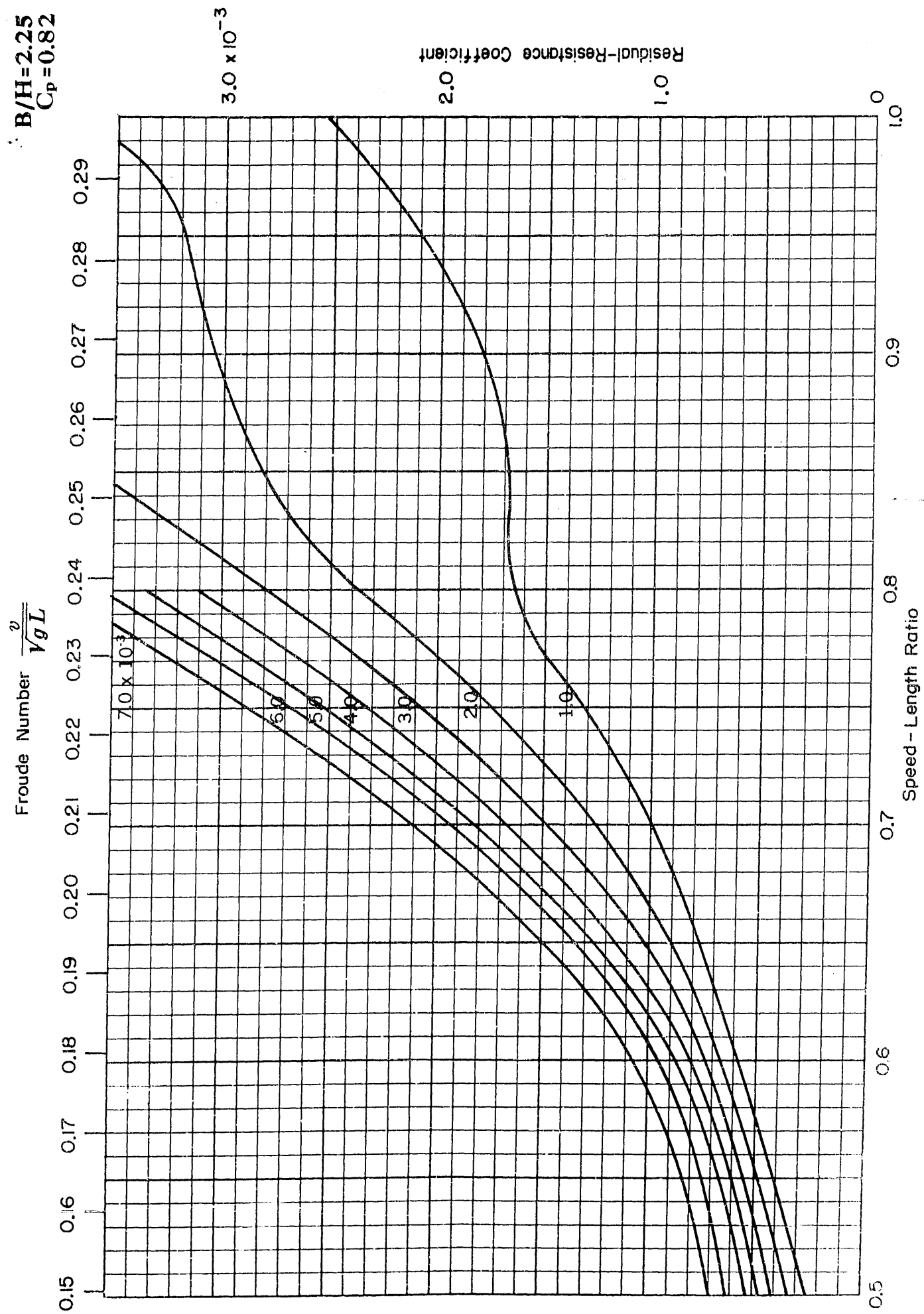
$B/H=2.25$
 $C_p=0.80$



$B/H=2.25$
 $C_p=0.80$

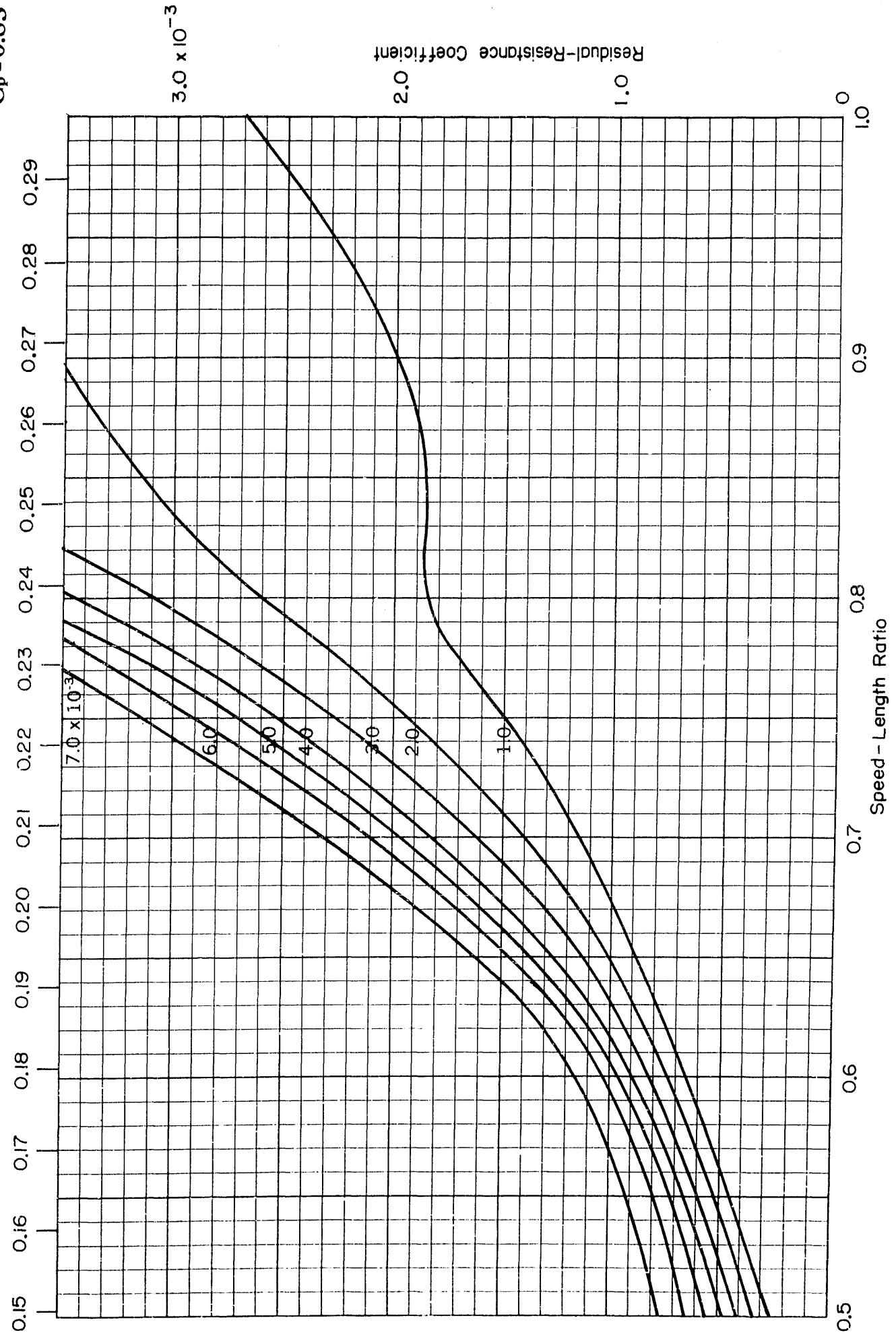


$$\frac{v}{\sqrt{gL}}$$


$$\frac{v}{\sqrt{g L}}$$


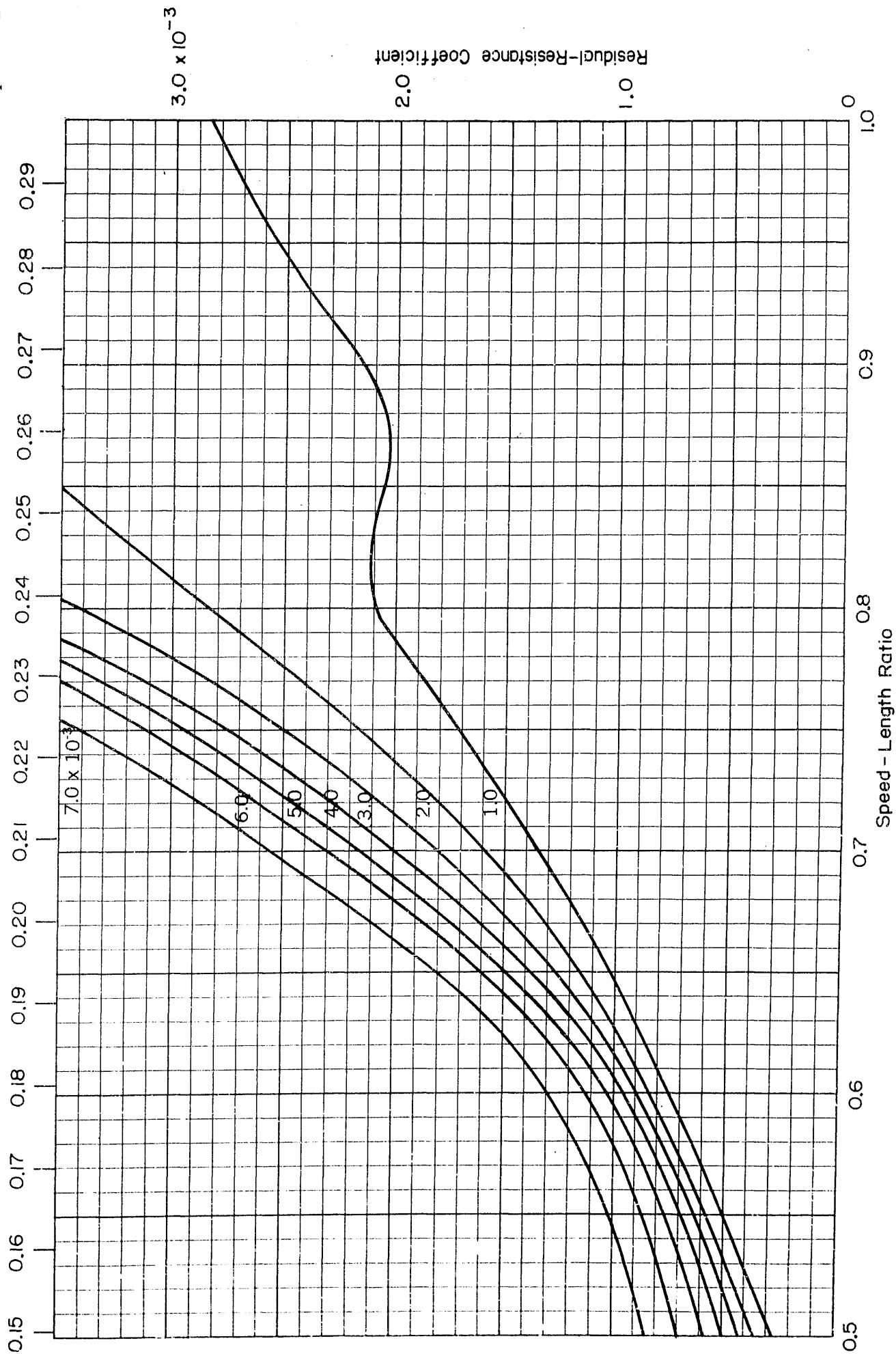
$B/H = 2.25$
 $C_p = 0.83$

Froude Number $\frac{v}{\sqrt{gL}}$



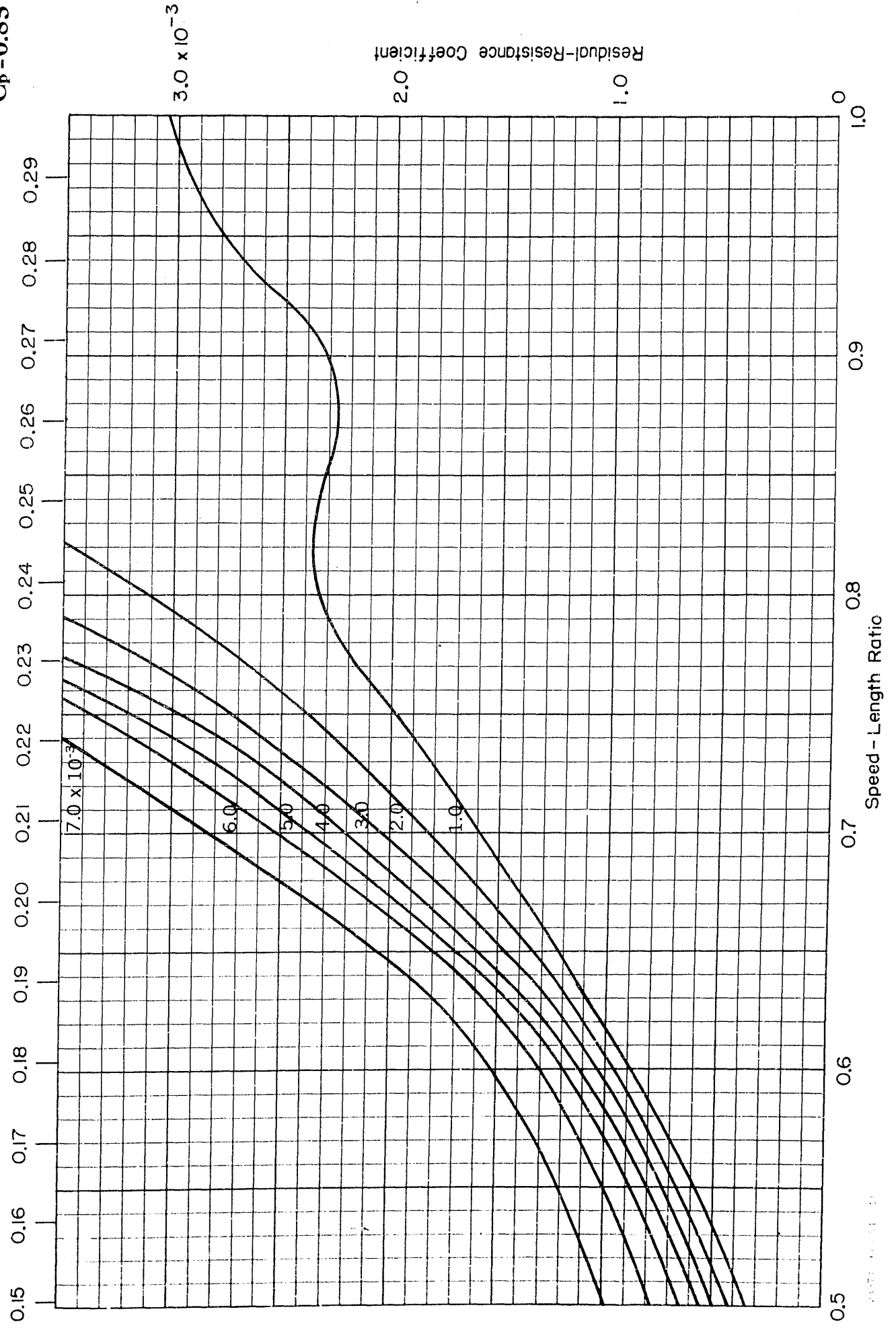
$B/H = 2.25$
 $C_p = 0.84$

Froude Number $\frac{v}{\sqrt{gL}}$

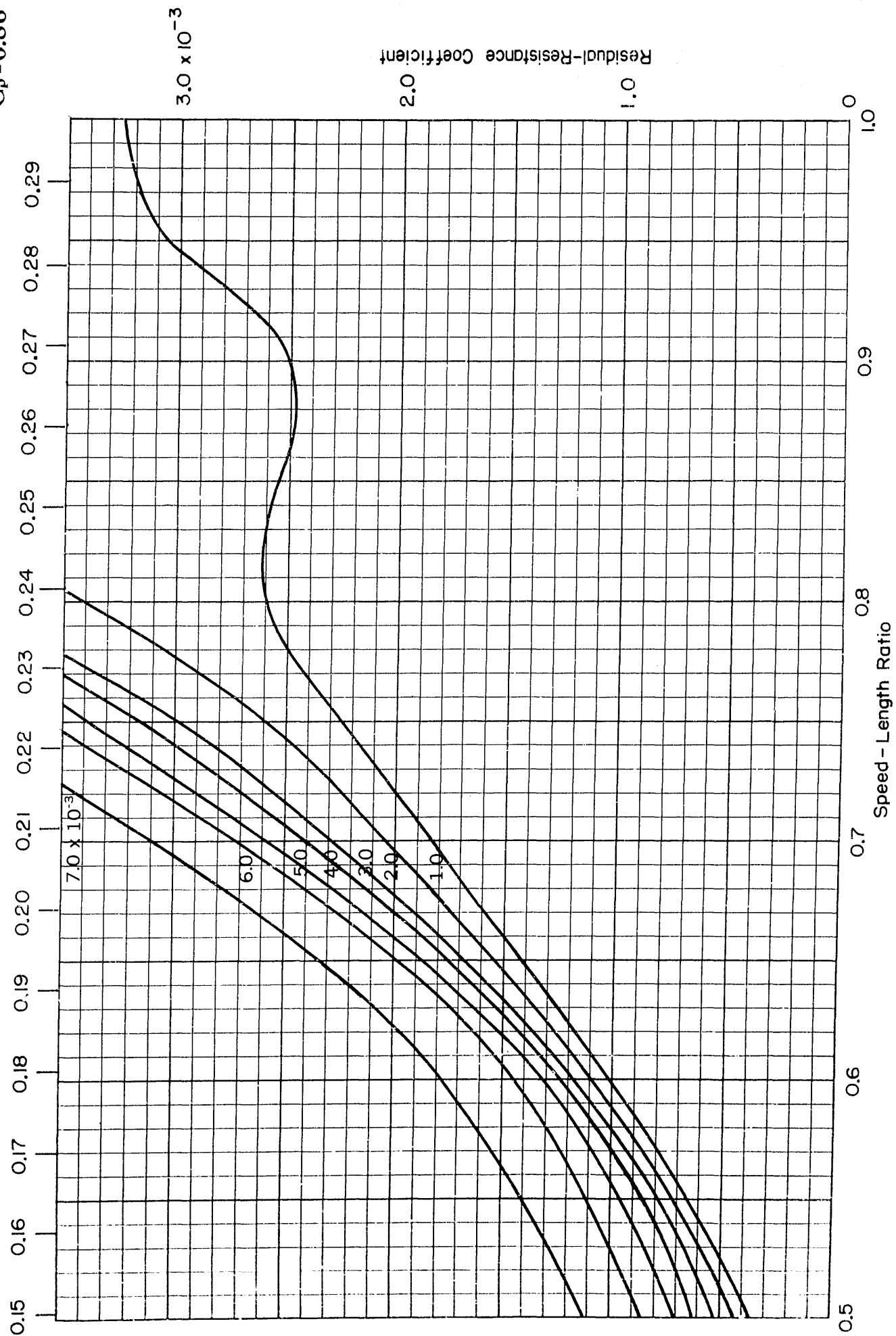


$B/H=2.25$
 $C_p=0.85$

Froude Number $\frac{v}{\sqrt{gL}}$



Residual-Resistance Coefficient

Froude Number $\frac{v}{\sqrt{gL}}$ 

APPENDIX 4

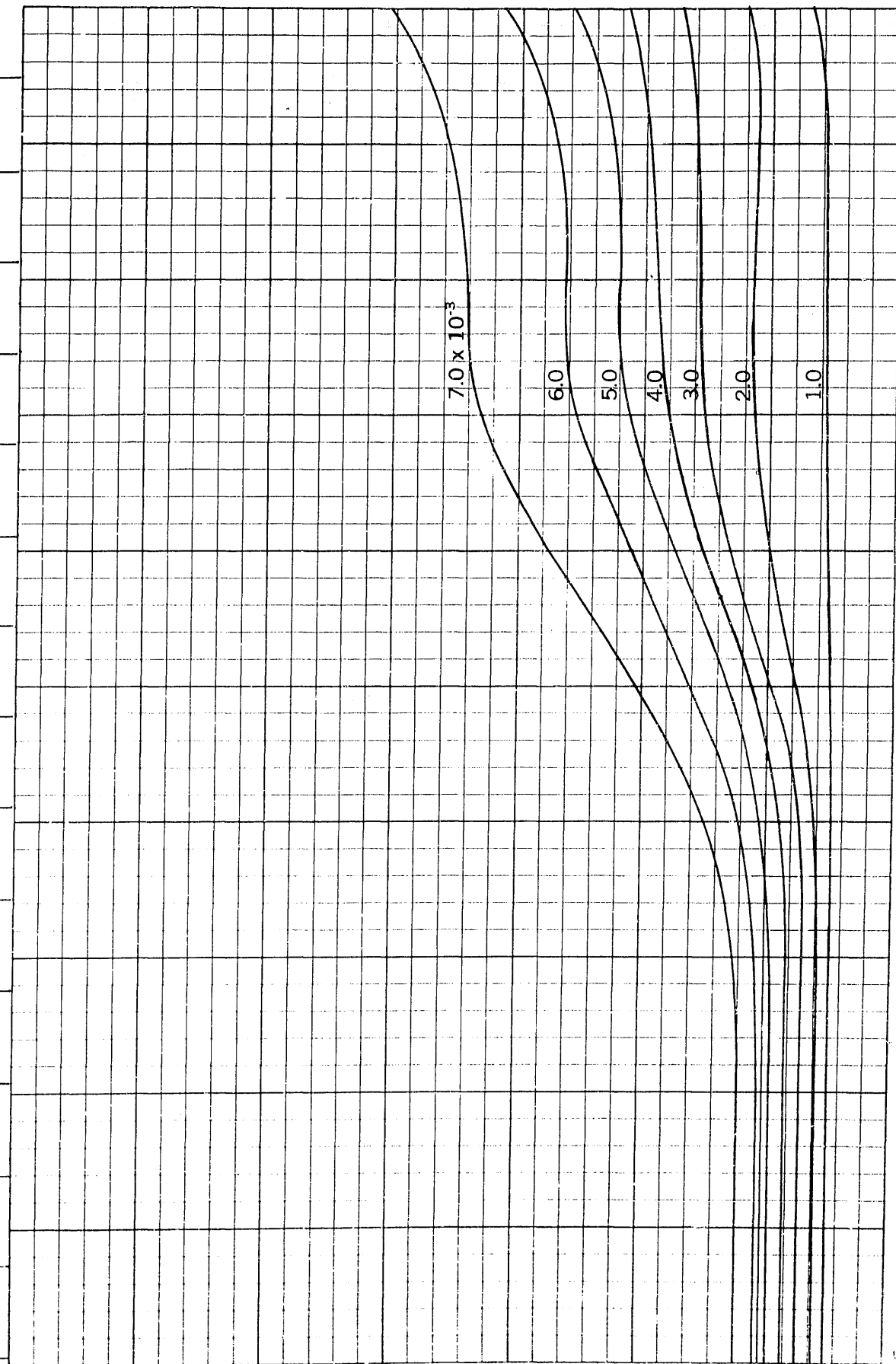
CURVES OF RESIDUAL-RESISTANCE COEFFICIENT VERSUS SPEED-LENGTH RATIO AND FROUDE NUMBER FOR STANDARD SERIES VESSELS HAVING A BEAM-DRAFT RATIO OF 3.00

The curves of residual-resistance coefficients for even values of volumetric coefficient are presented separately for each longitudinal prismatic coefficient between 0.48 and 0.80 in increments of 0.01. For each family of curves, ranges of speed-length ratios of 0.5 to 1.0 and 1.0 to 2.0 are given on adjacent pages. The scale divisions, for both ordinate and abscissa, at the lower speed-length ratios are twice as large as those of the higher range to permit increased accuracy of reading.

$B/H=3.00$
 $C_p=0.48$

Froude Number $\frac{v}{\sqrt{gL}}$

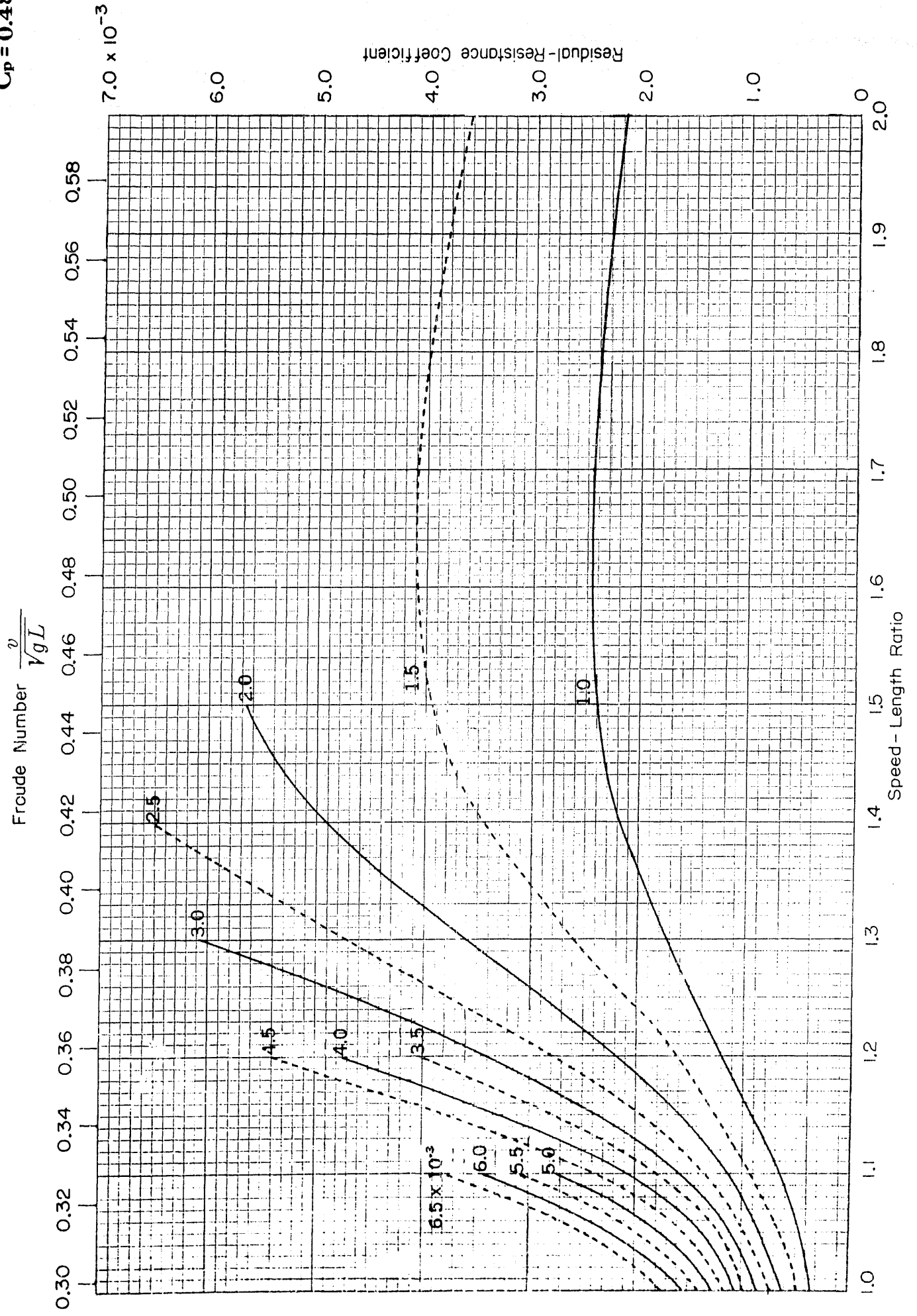
0.15 0.16 0.17 0.18 0.19 0.20 0.21 0.22 0.23 0.24 0.25 0.26 0.27 0.28 0.29

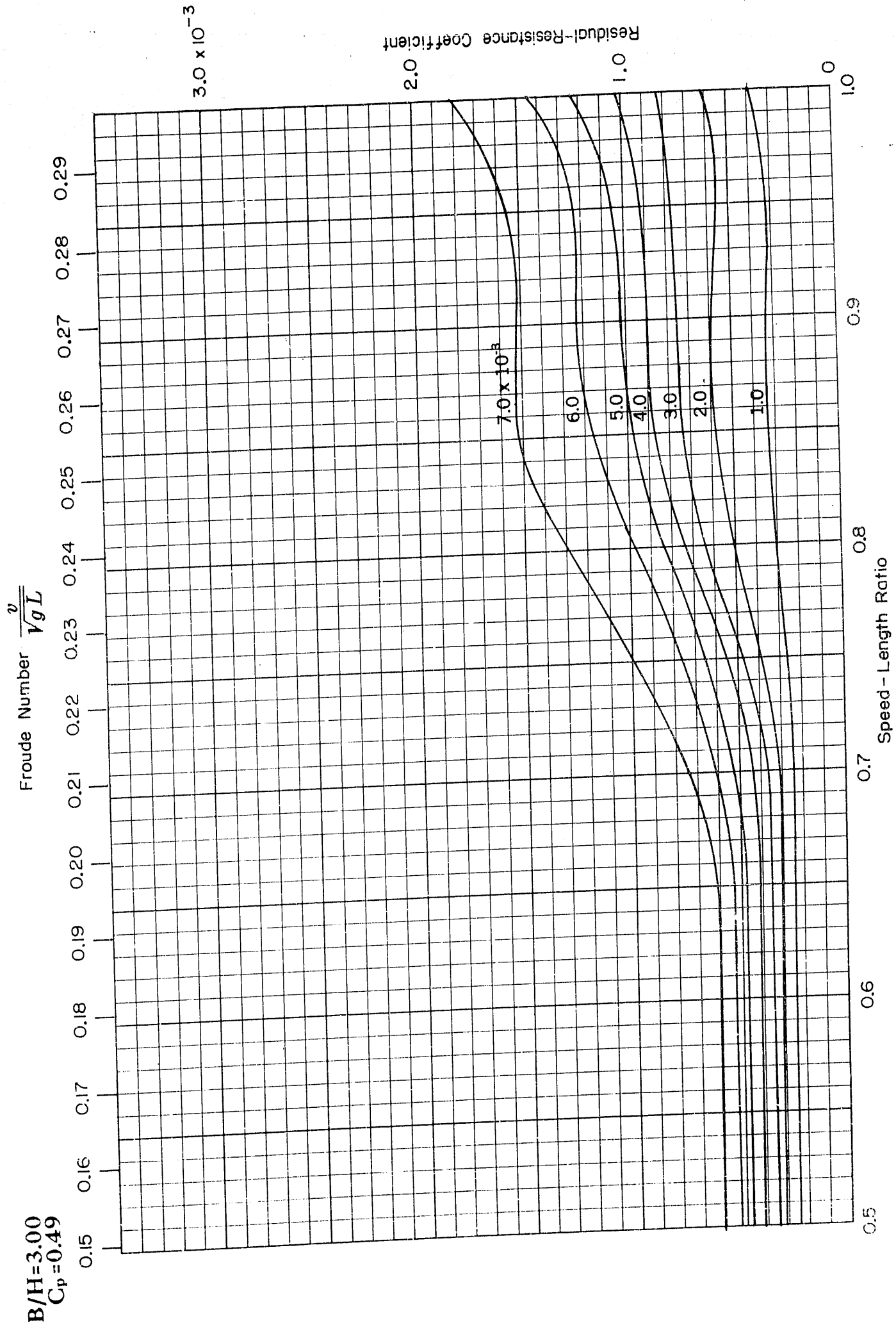


2.0
1.0
Residual-Resistance Coefficient
 3.0×10^{-3}

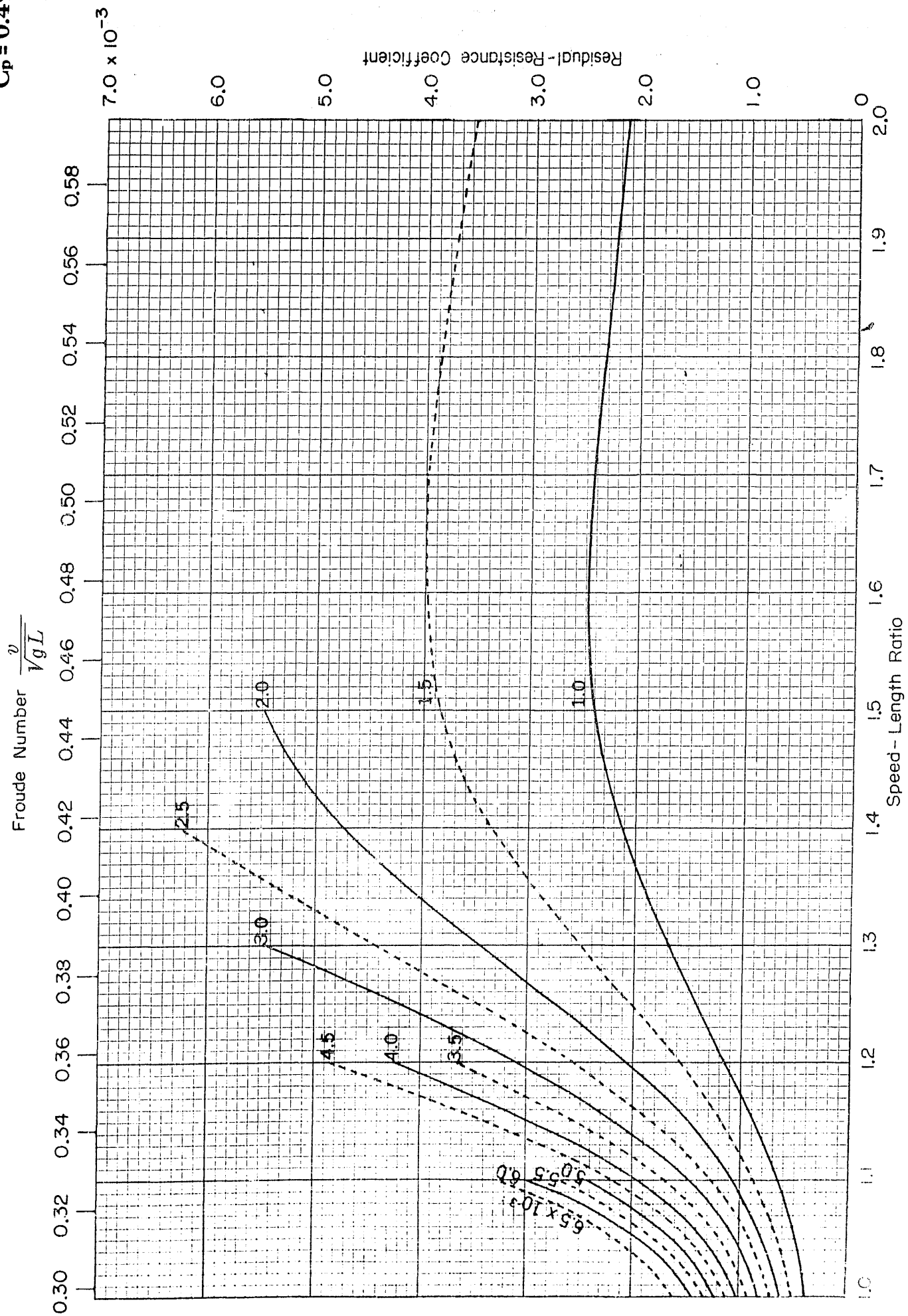
0.5 0.6 0.7 0.8 0.9 1.0
Speed - Length Ratio

$B/H=3.00$
 $C_p=0.48$





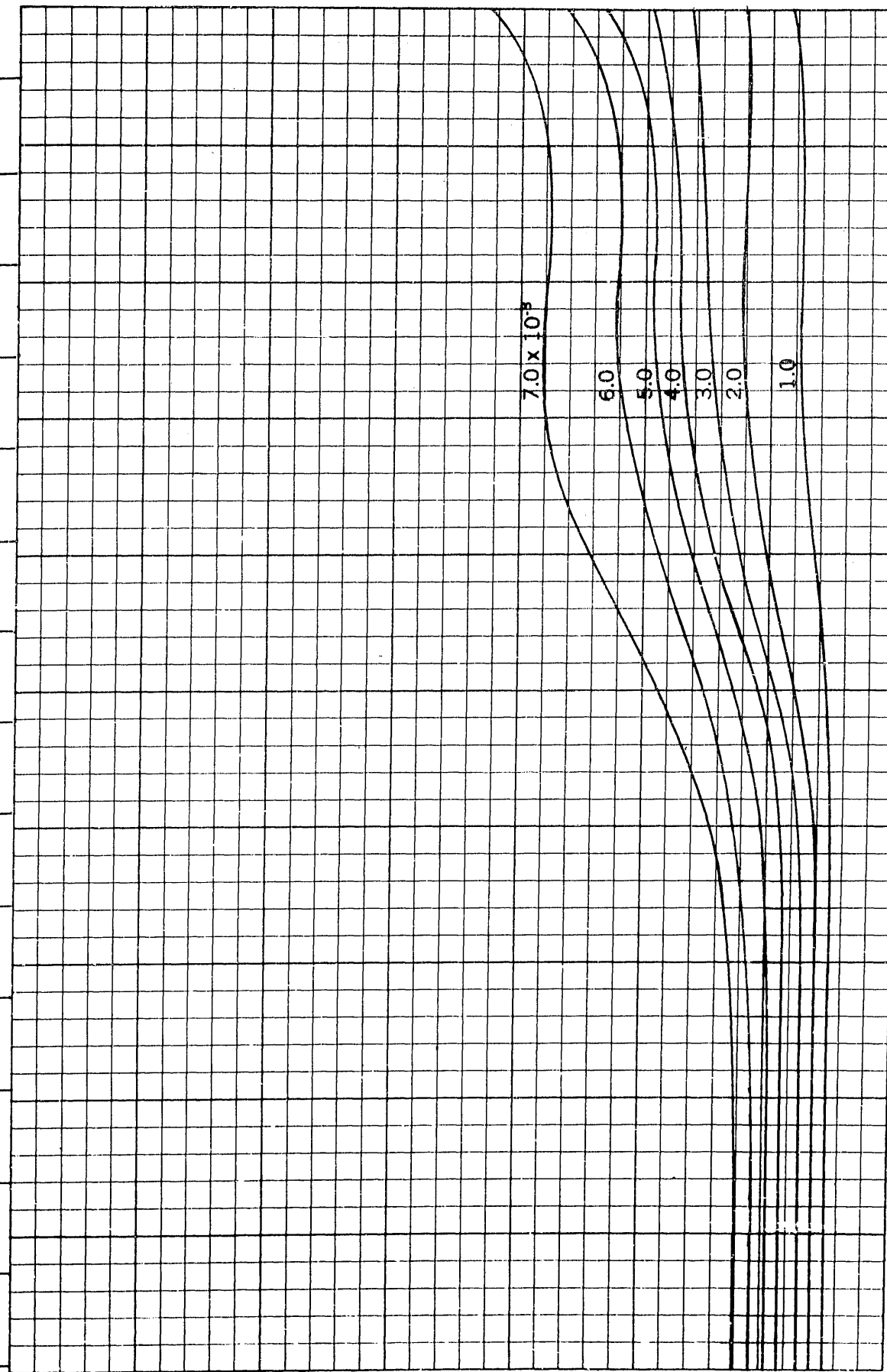
$B/H=3.00$
 $C_p=0.49$



$B/H=3.00$
 $C_p=0.50$

Froude Number $\frac{v}{\sqrt{gL}}$

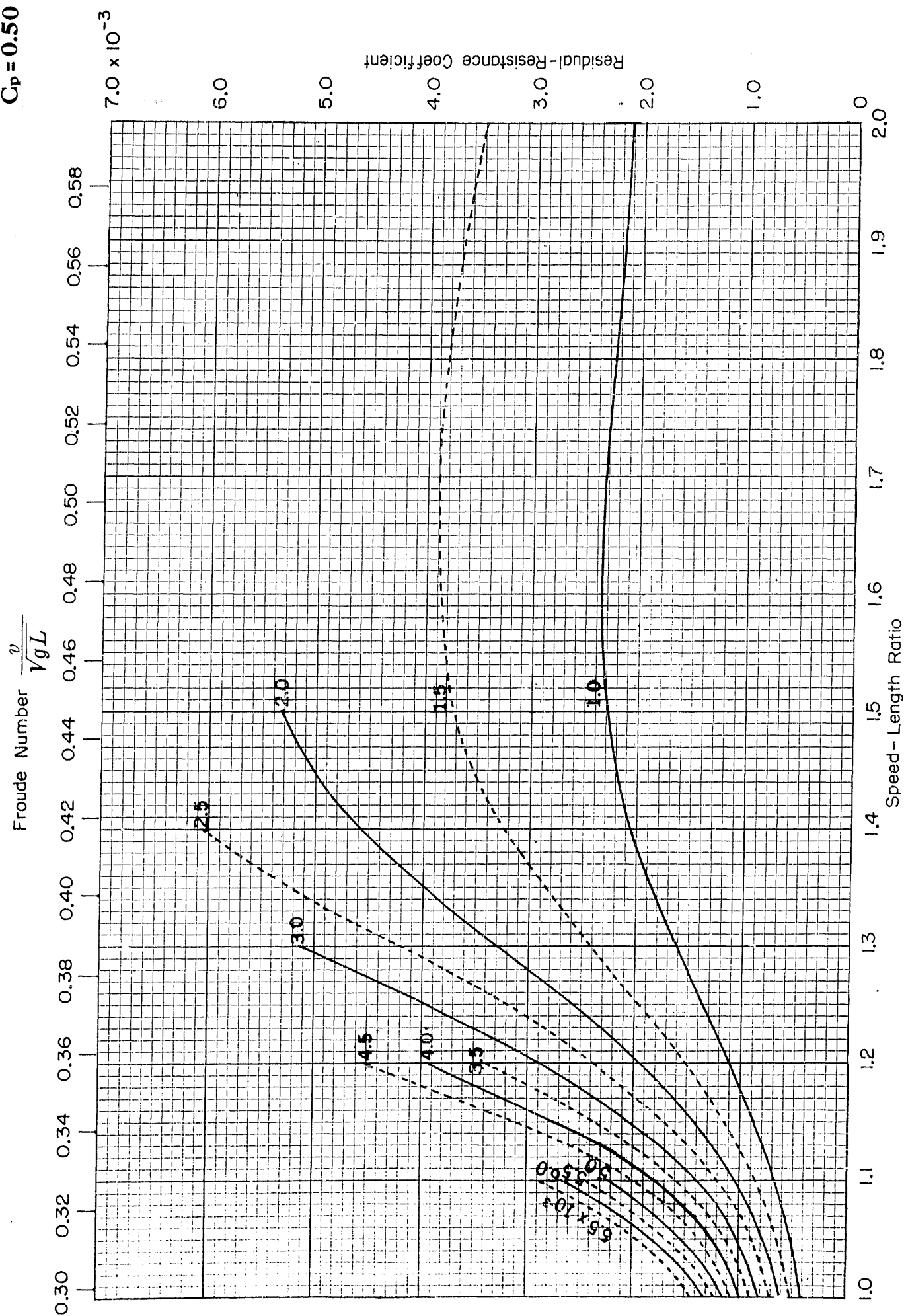
0.15 0.16 0.17 0.18 0.19 0.20 0.21 0.22 0.23 0.24 0.25 0.26 0.27 0.28 0.29



Residual-Resistance Coefficient

3.0×10^{-3}

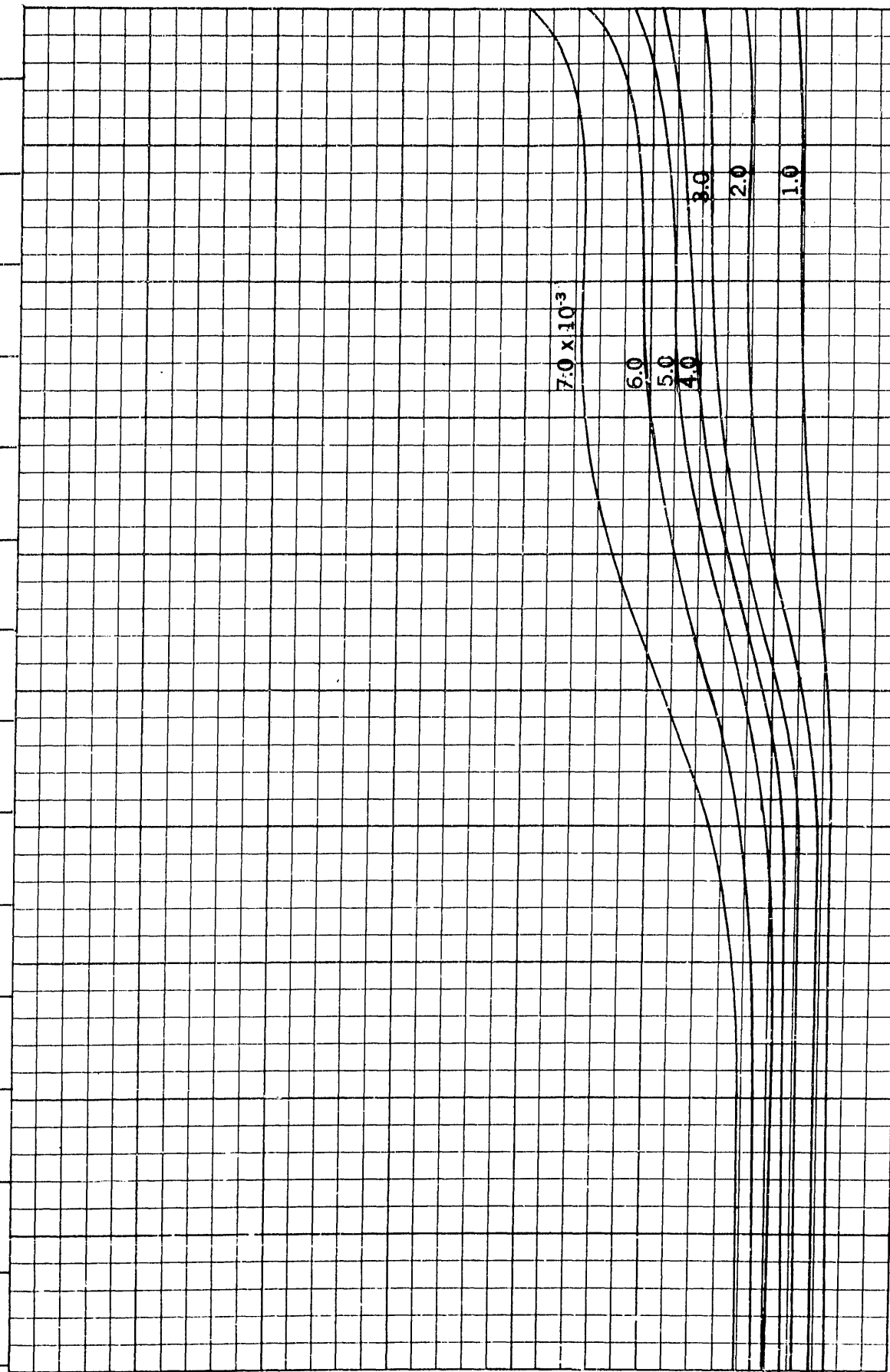
$B/H=3.00$
 $C_p=0.50$



$B/H=3.00$
 $C_v=0.51$

Froude Number $\frac{v}{\sqrt{gL}}$

0.15 0.16 0.17 0.18 0.19 0.20 0.21 0.22 0.23 0.24 0.25 0.26 0.27 0.28 0.29



Residual-Resistance Coefficient

3.0×10^{-3}

7.0×10^{-3}

6.0

5.0

4.0

3.0

2.0

1.0

0.5

0.6

0.7

0.8

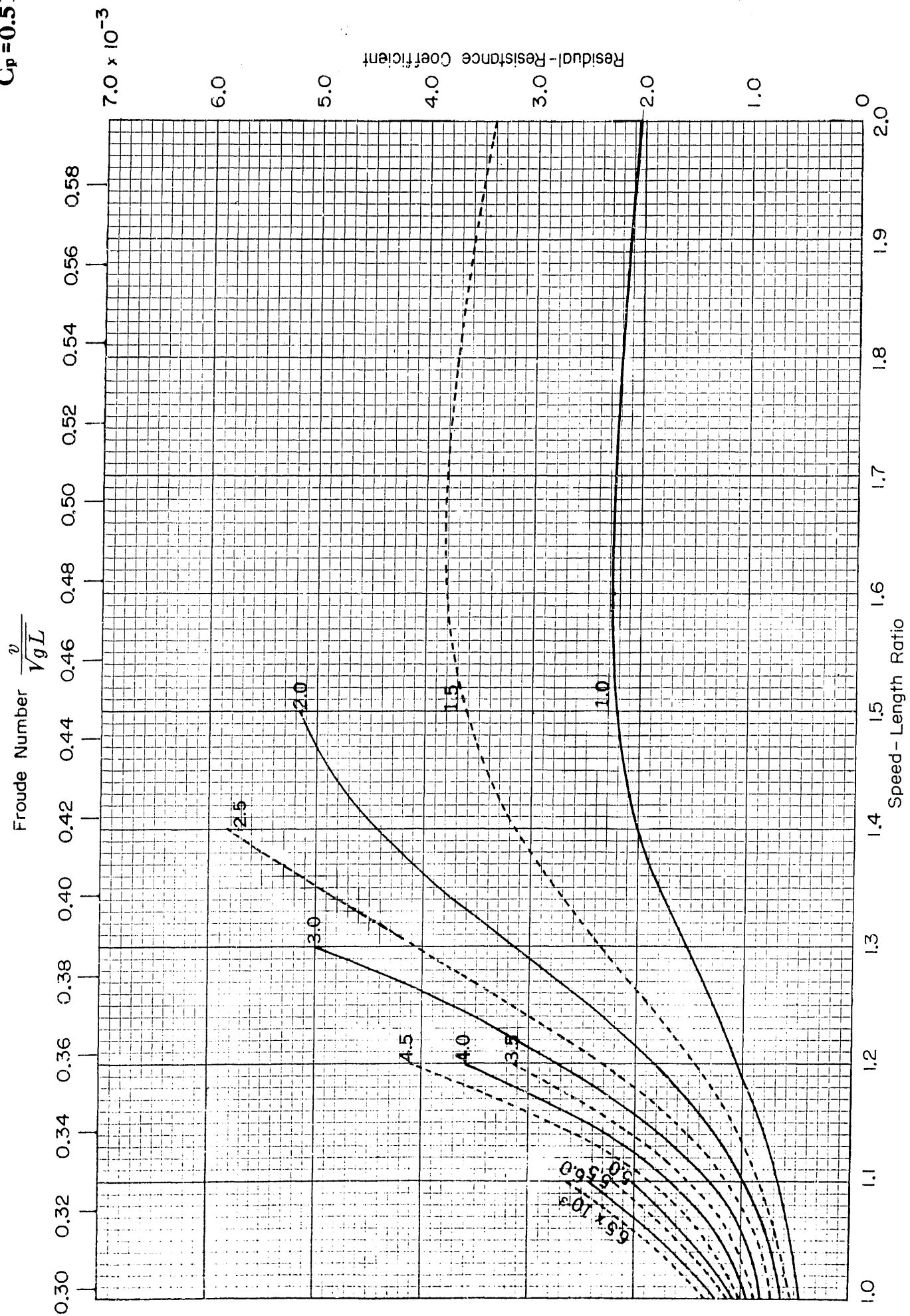
0.9

1.0

0

Speed - Length Ratio

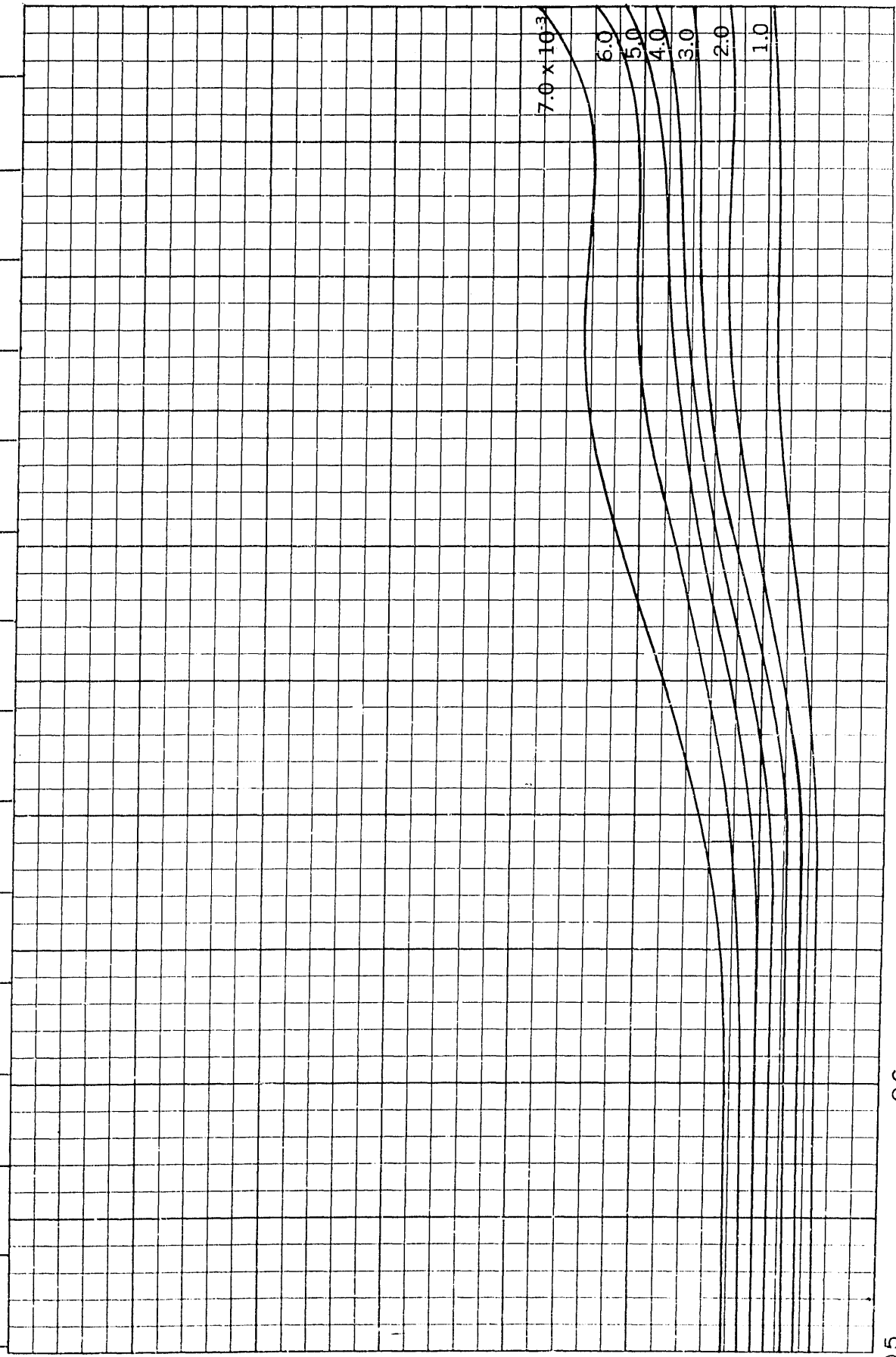
$B/H=3.00$
 $C_p=0.51$



$B/H=3.00$
 $C_p=0.52$

Froude Number $\frac{v}{\sqrt{gL}}$

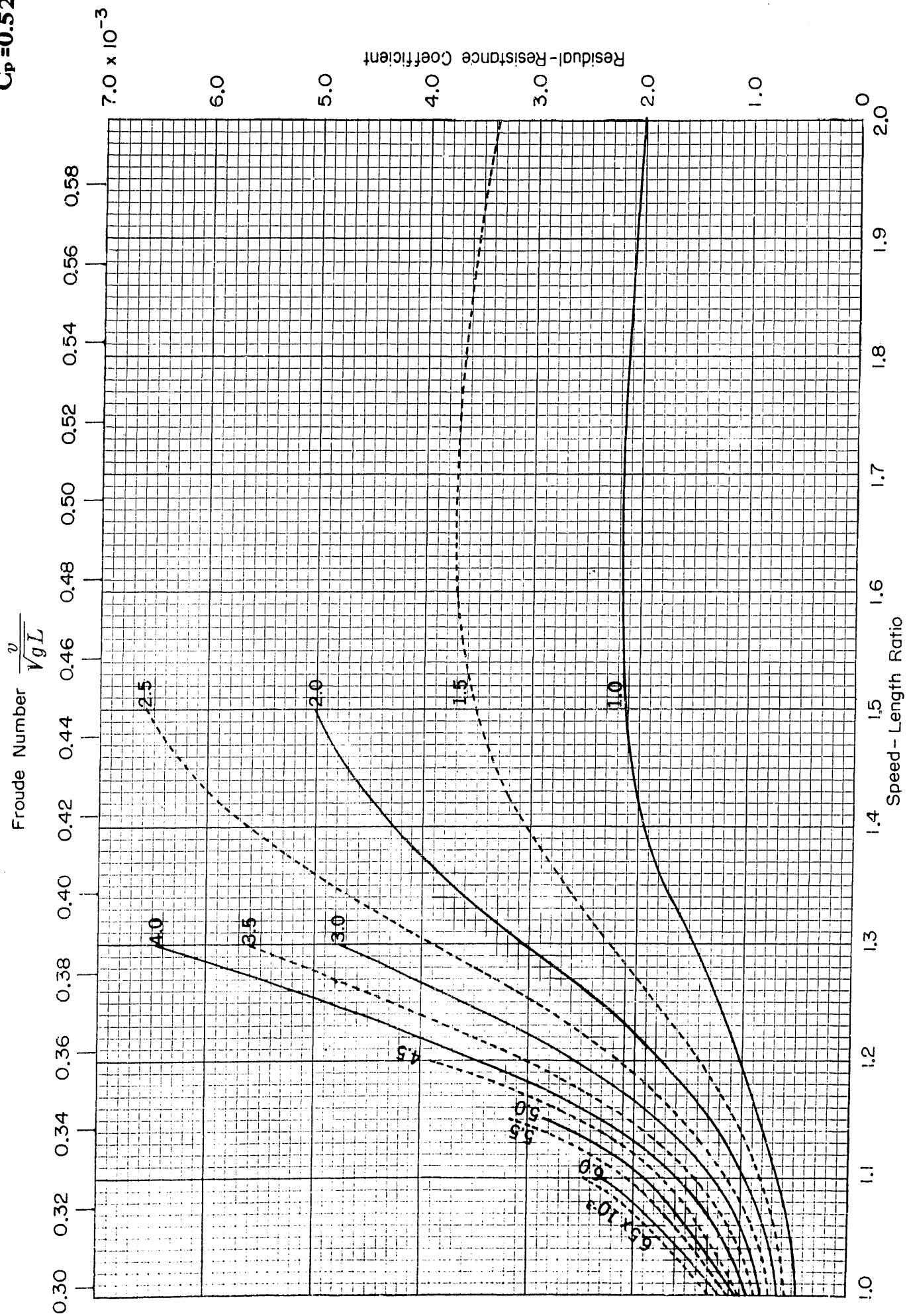
0.15 0.16 0.17 0.18 0.19 0.20 0.21 0.22 0.23 0.24 0.25 0.26 0.27 0.28 0.29



Residual-Resistance Coefficient
2.0
1.0
 3.0×10^{-3}

0.5 0.6 0.7 0.8 0.9 1.0
Speed - Length Ratio

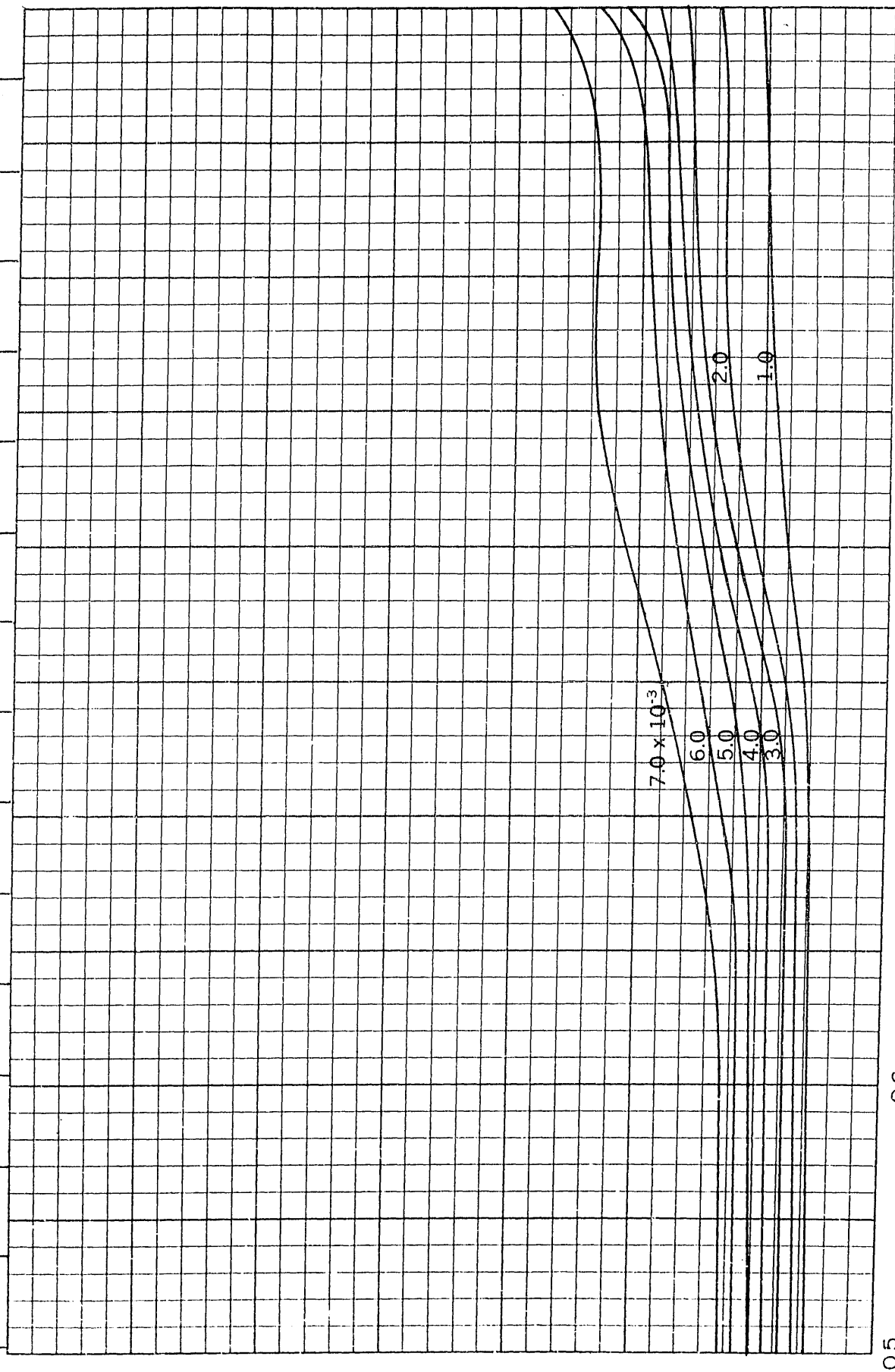
$B/H=3.00$
 $C_p=0.52$



$B/H=3.00$
 $C_p=0.53$

Froude Number $\frac{v}{\sqrt{gL}}$

0.15 0.16 0.17 0.18 0.19 0.20 0.21 0.22 0.23 0.24 0.25 0.26 0.27 0.28 0.29



Residual-Resistance Coefficient

0

Speed - Length Ratio

0.5

0.6

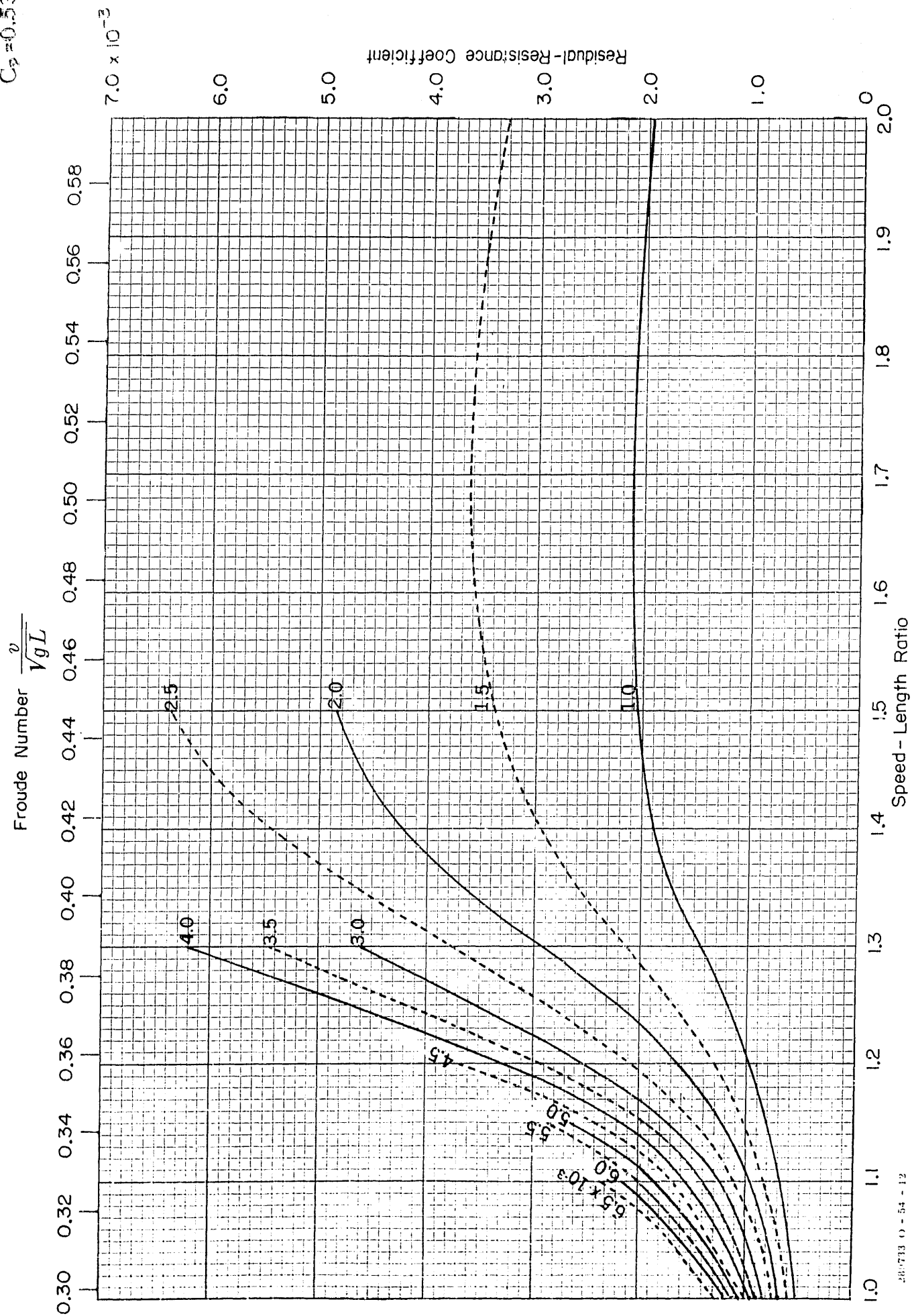
0.7

0.8

0.9

1.0

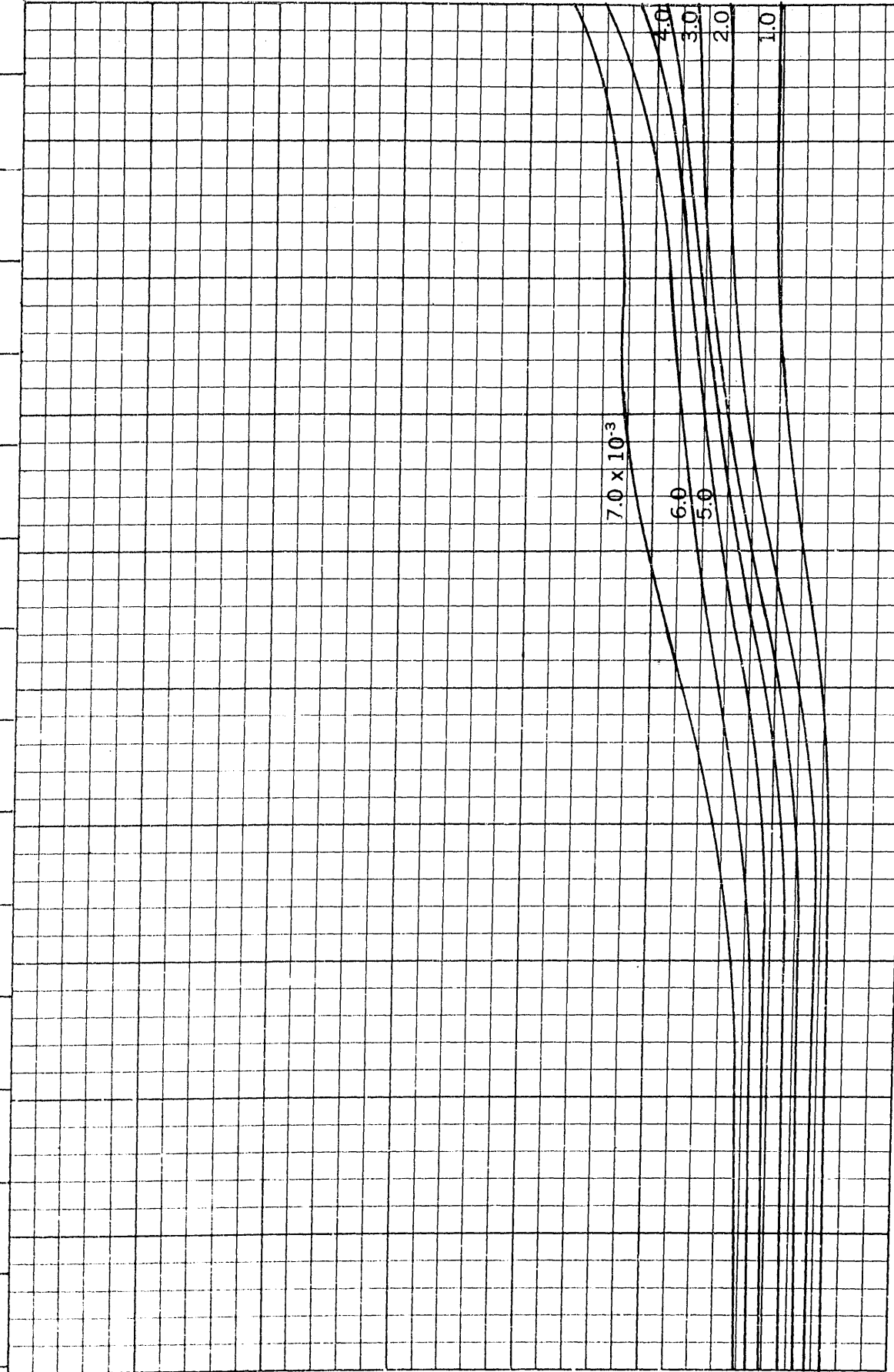
$B/H=3.00$
 $C_p=0.53$



$B/H=3.00$
 $C_p=0.54$

Froude Number $\frac{v}{\sqrt{gL}}$

0.15 0.16 0.17 0.18 0.19 0.20 0.21 0.22 0.23 0.24 0.25 0.26 0.27 0.28 0.29

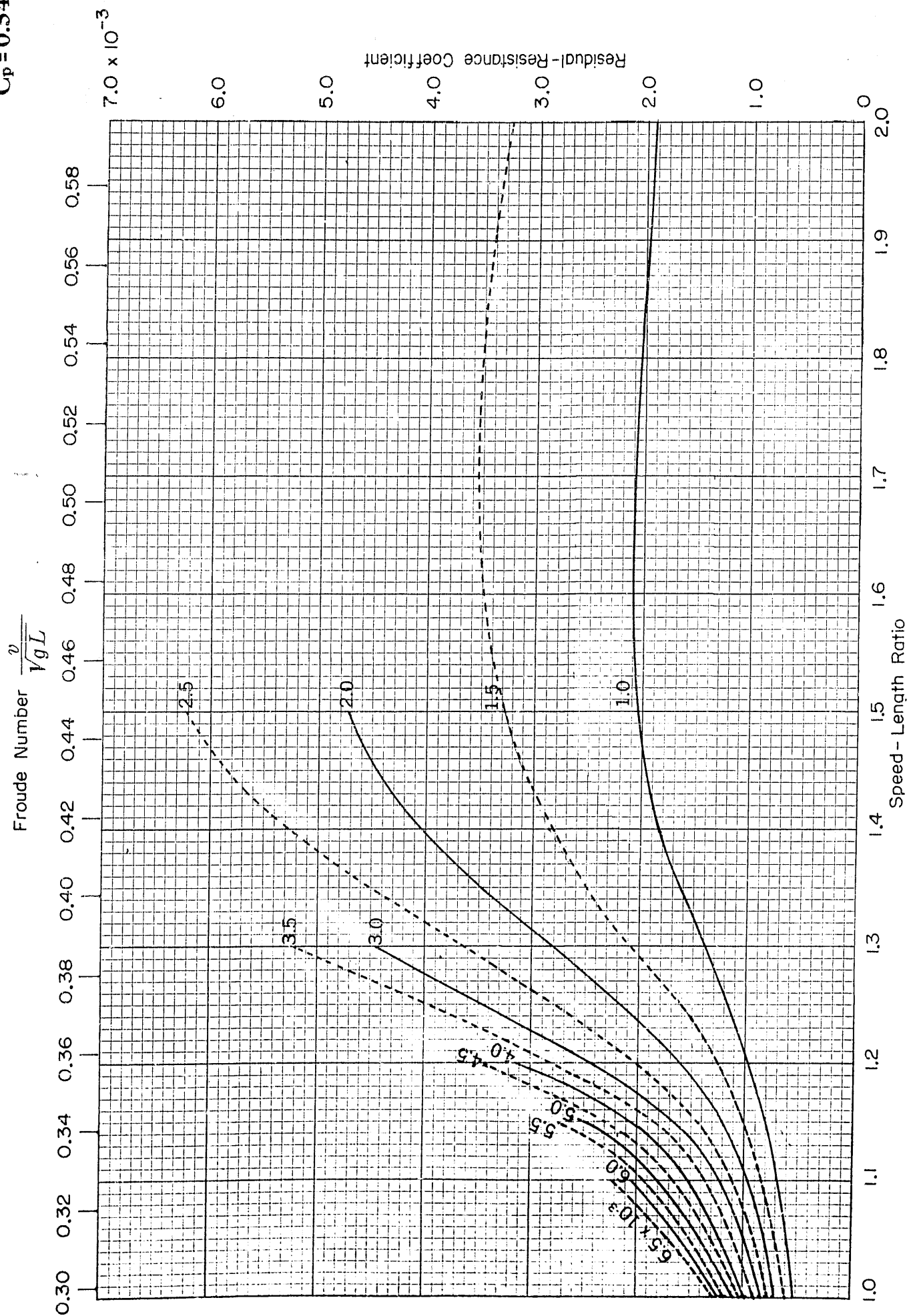


Residual-Resistance Coefficient

0.5 0.6 0.7 0.8 0.9 1.0

Speed - Length Ratio

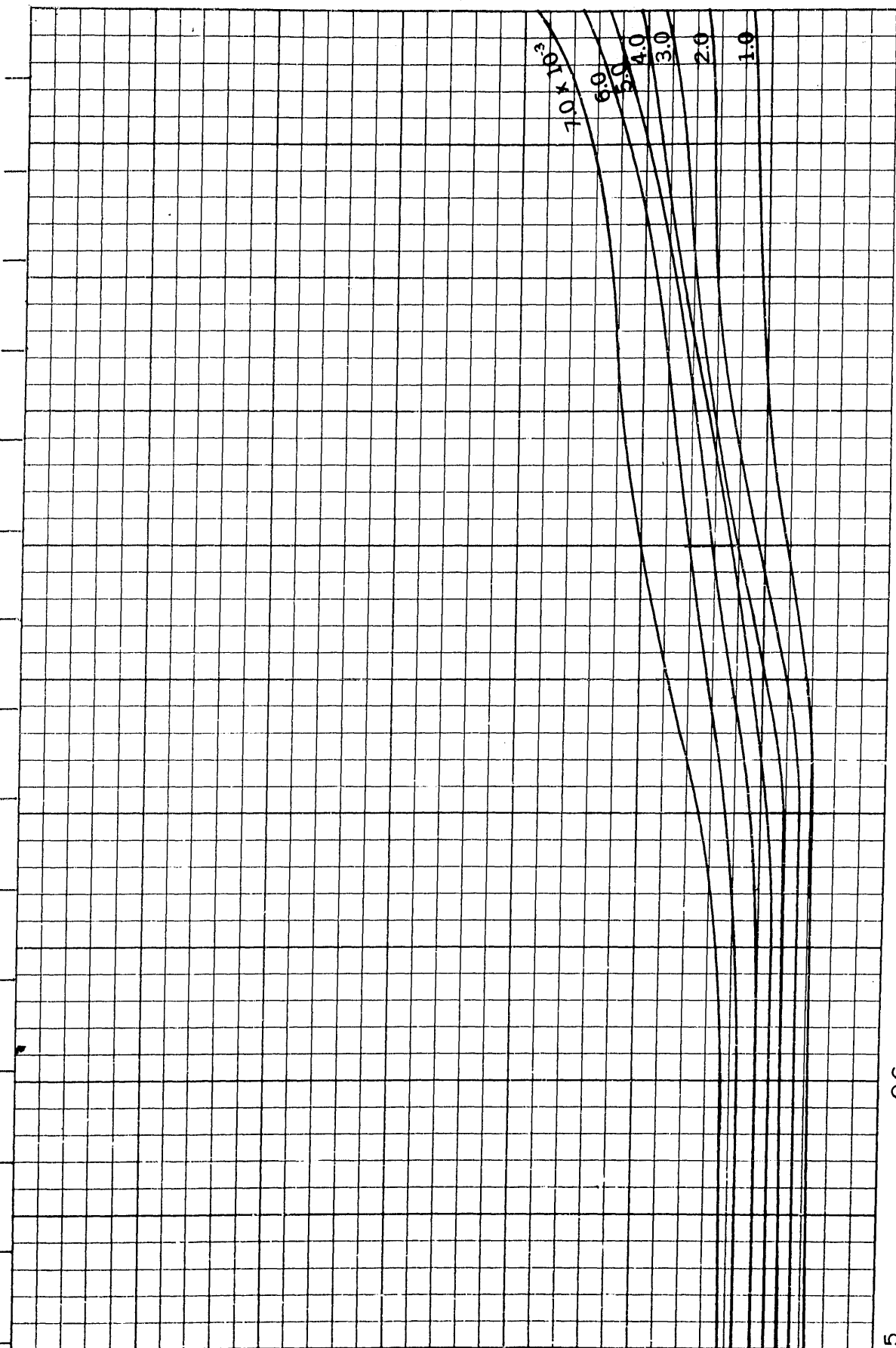
$B/H=3.00$
 $C_p=0.54$



$B/H=3.00$
 $C_n=0.55$

Froude Number $\frac{v}{\sqrt{gL}}$

0.15 0.16 0.17 0.18 0.19 0.20 0.21 0.22 0.23 0.24 0.25 0.26 0.27 0.28 0.29



Residual-Resistance Coefficient

3.0×10^{-3}

0.5

0.6

0.7

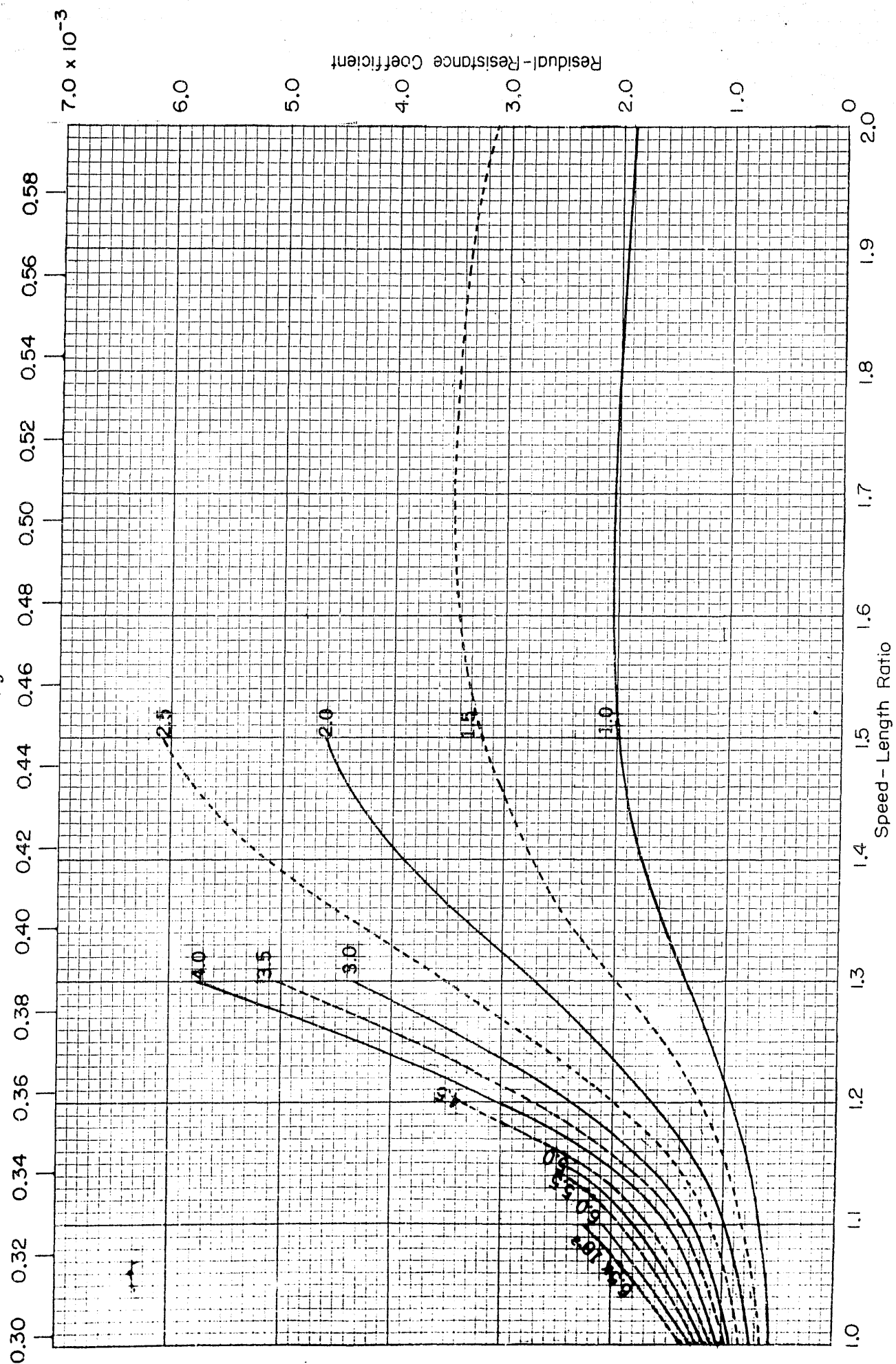
0.8

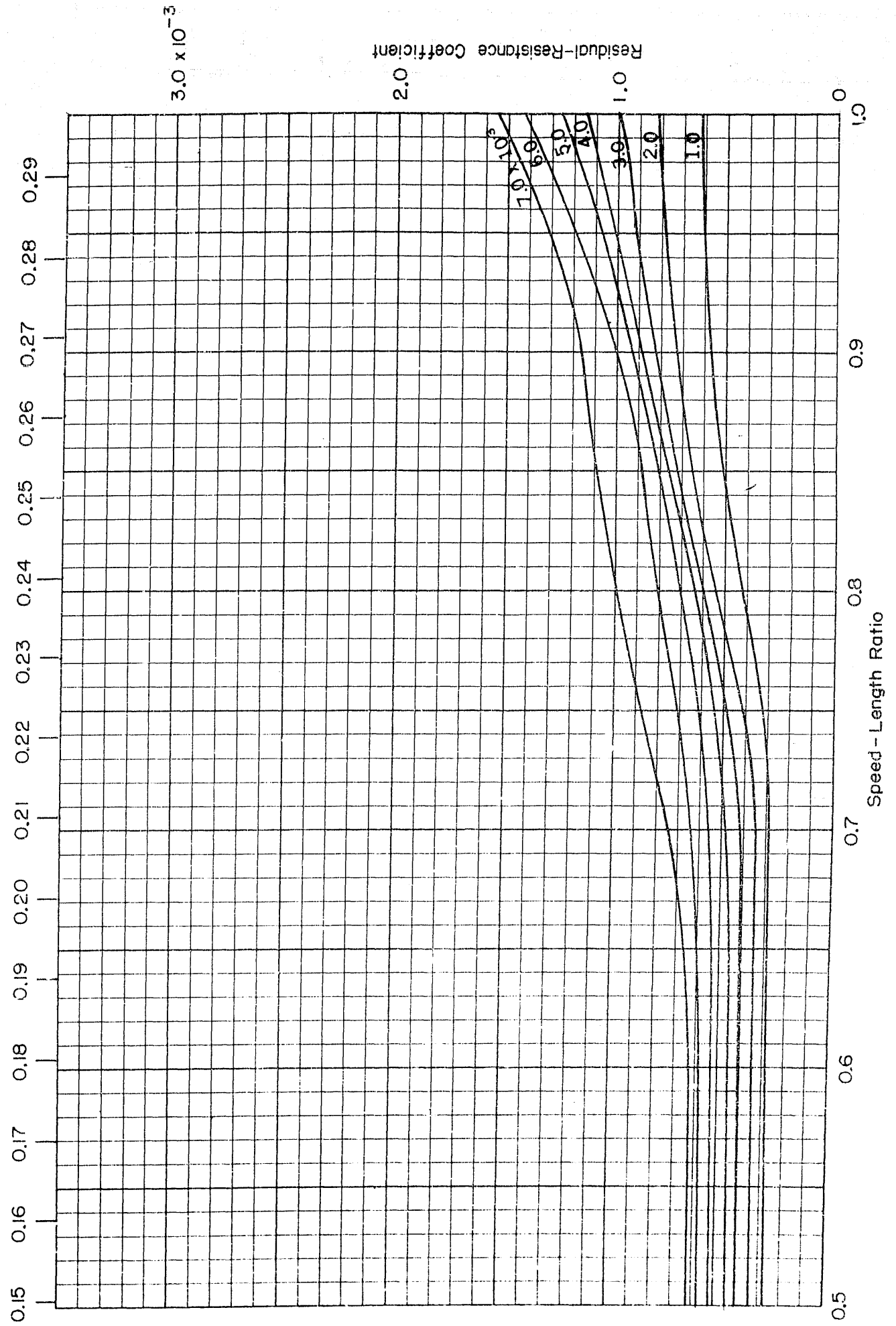
0.9

1.0

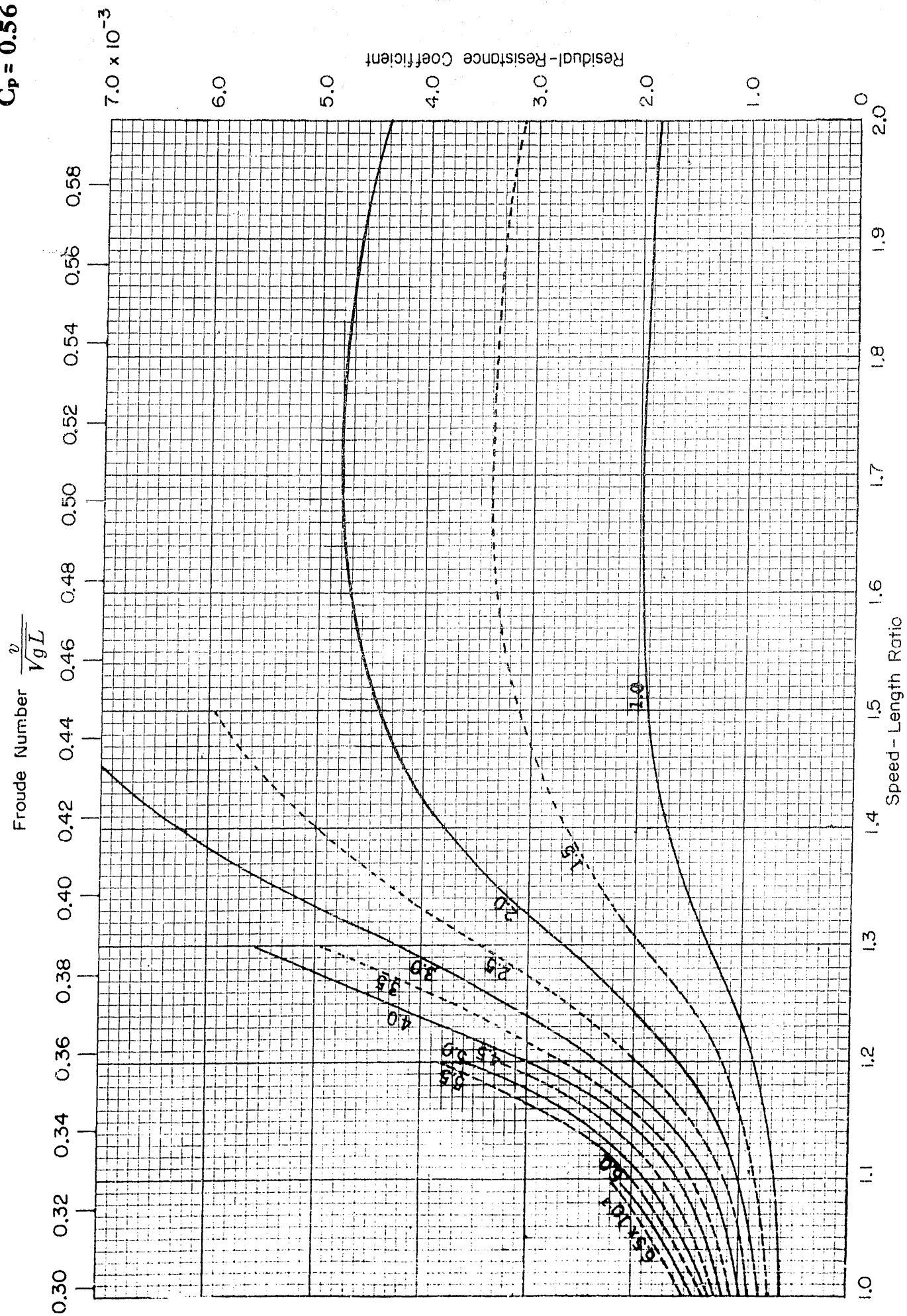
0

Speed - Length Ratio

$$\frac{v}{\sqrt{g L}}$$


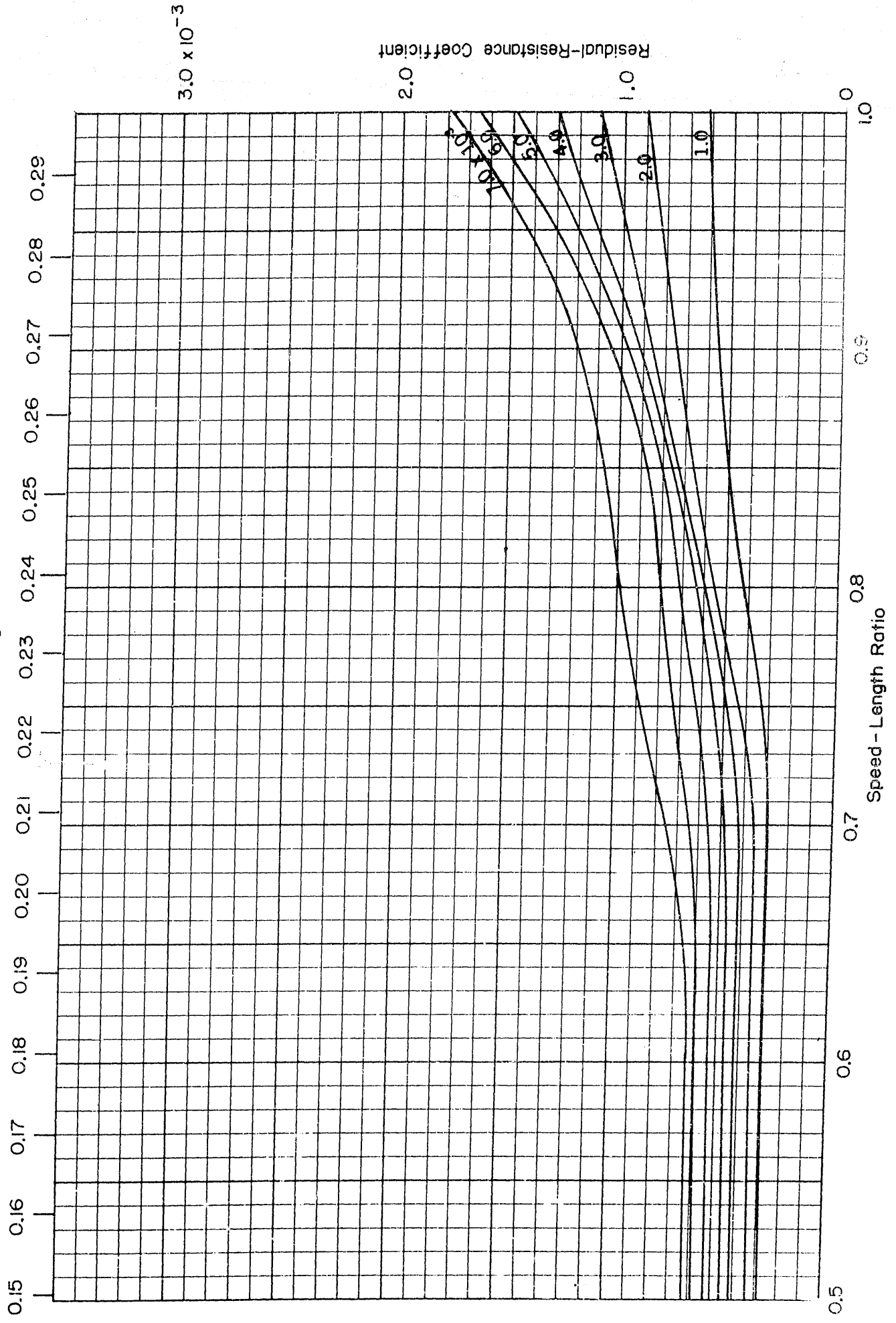
$$\frac{v}{\sqrt{gL}}$$


$B/H=3.00$
 $C_p=0.56$

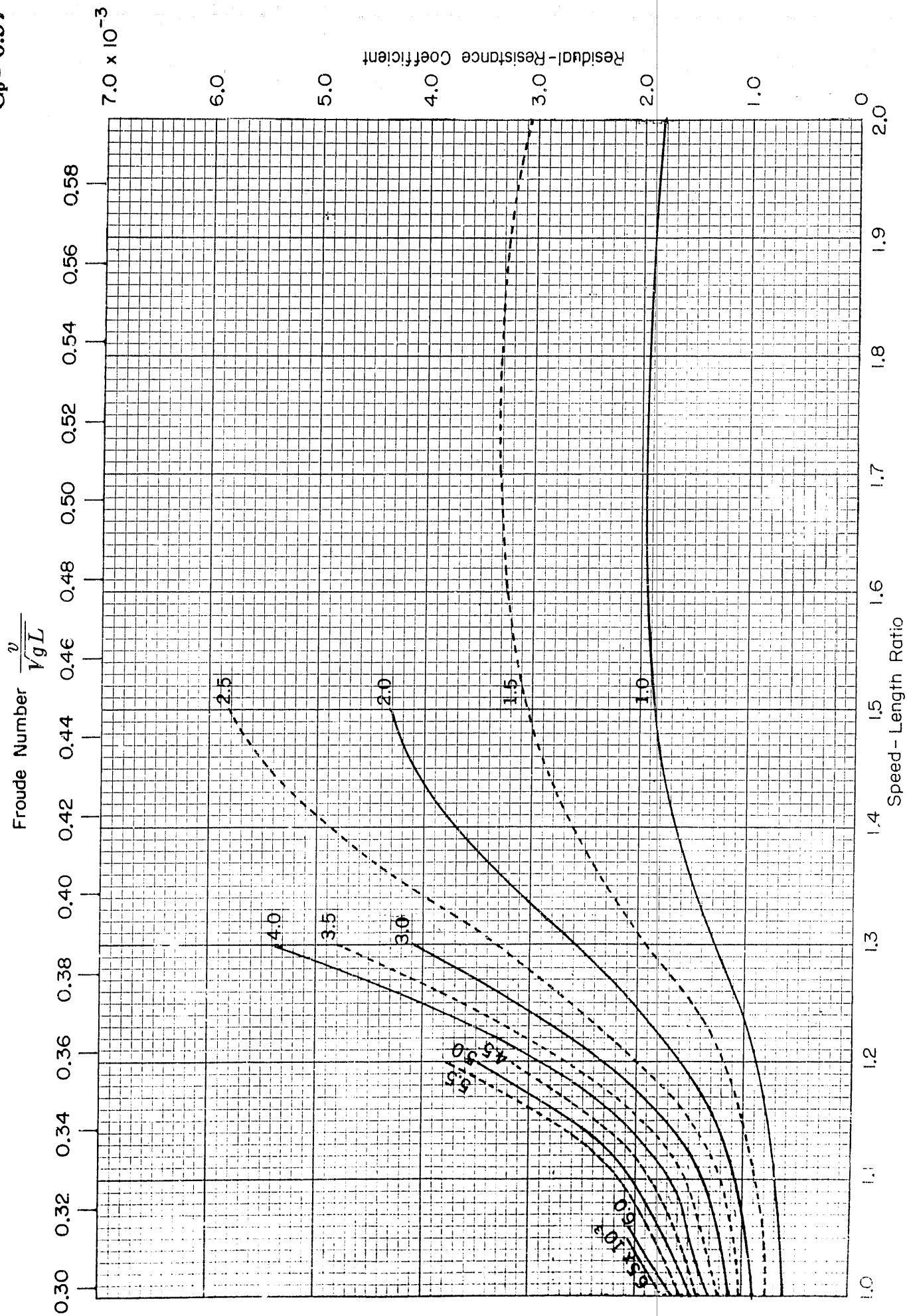


$B/H=3.00$
 $C_p=0.57$

Froude Number $\frac{v}{\sqrt{gL}}$



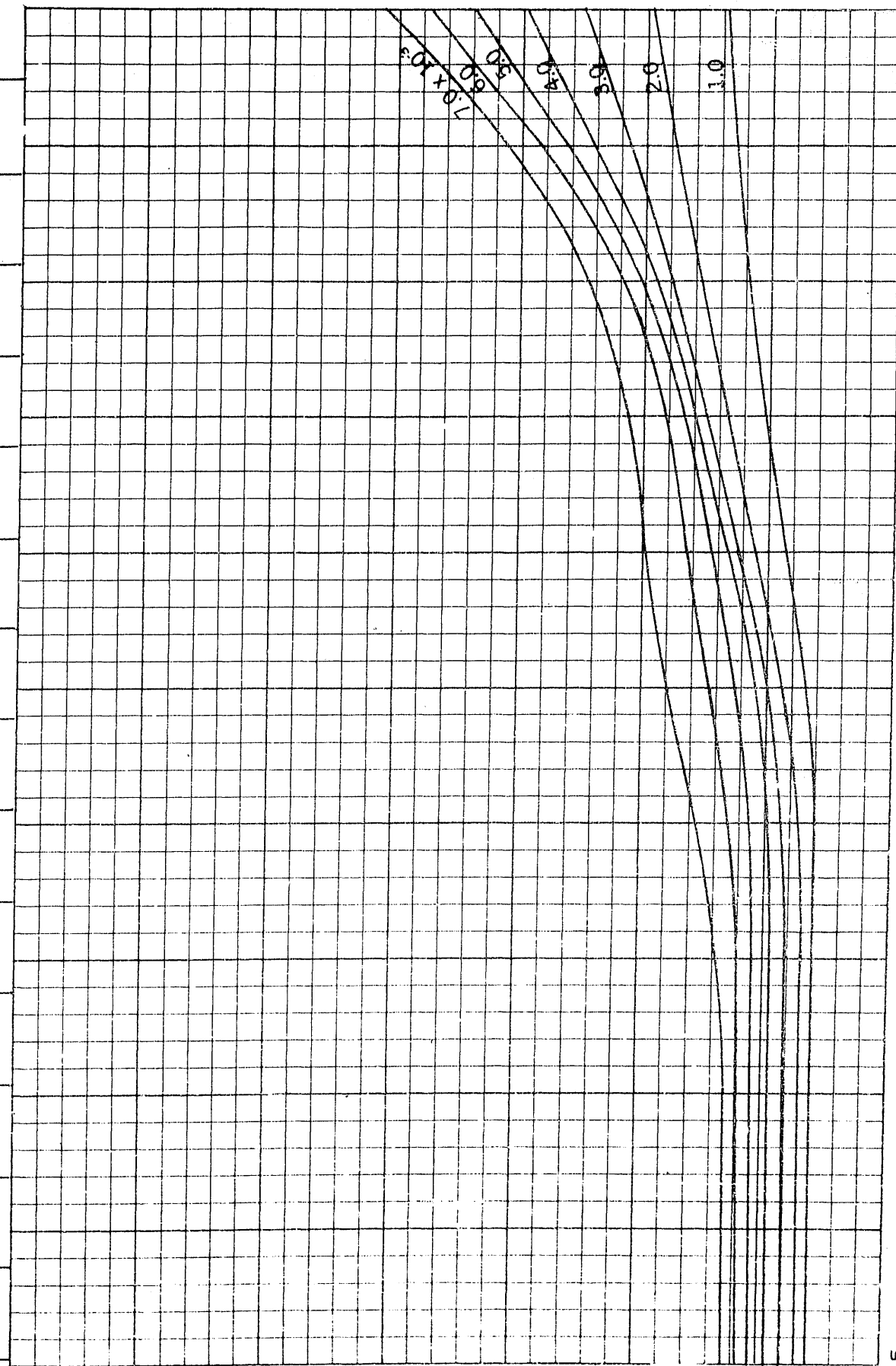
$B/H=3.00$
 $C_p=0.57$



$B/H=3.00$
 $C_p=0.58$

Froude Number $\frac{v}{\sqrt{gL}}$

0.15 0.16 0.17 0.18 0.19 0.20 0.21 0.22 0.23 0.24 0.25 0.26 0.27 0.28 0.29



Residual-Resistance Coefficient

0.5

0.6

0.7

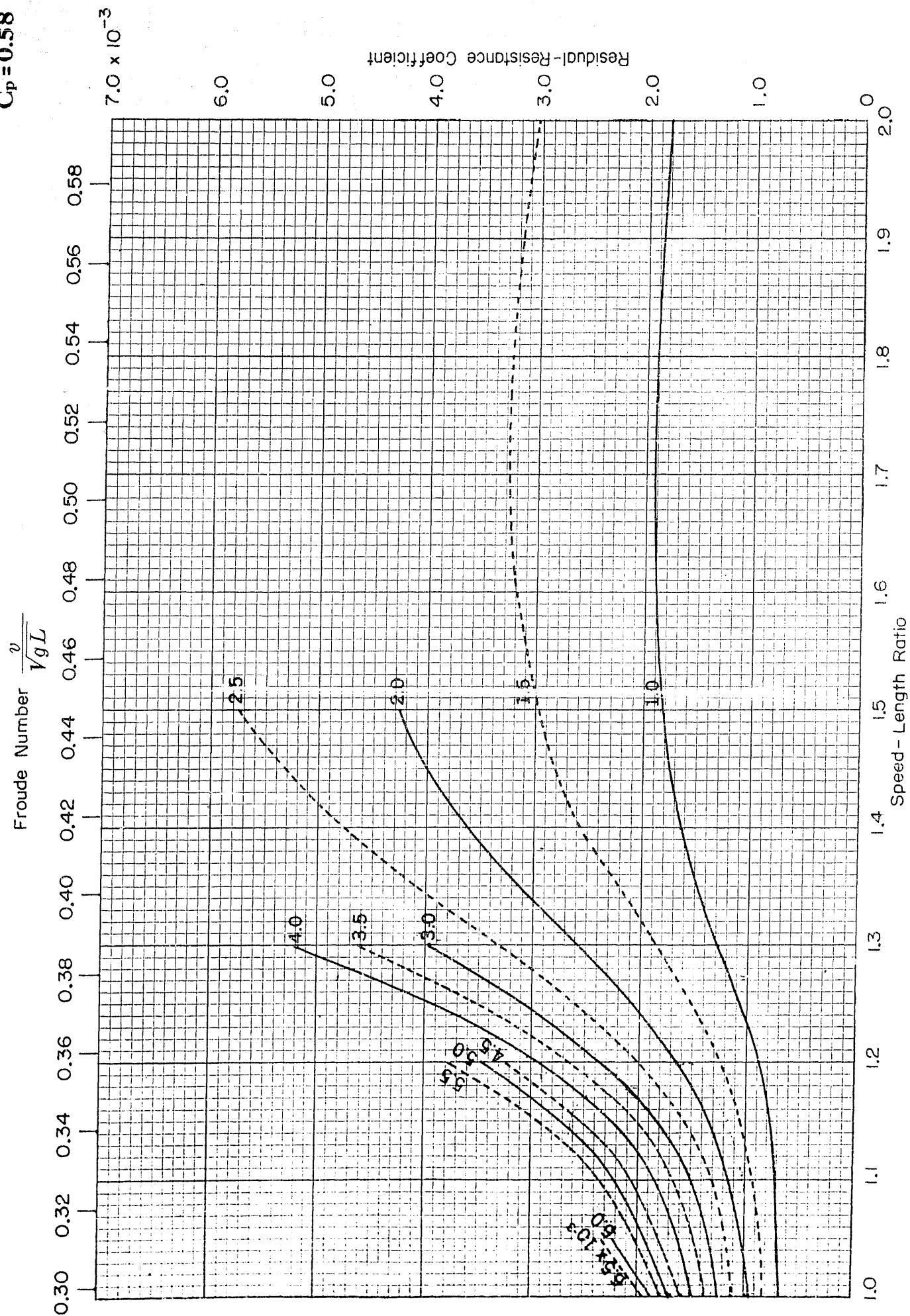
0.8

0.9

1.0

Speed-Length Ratio

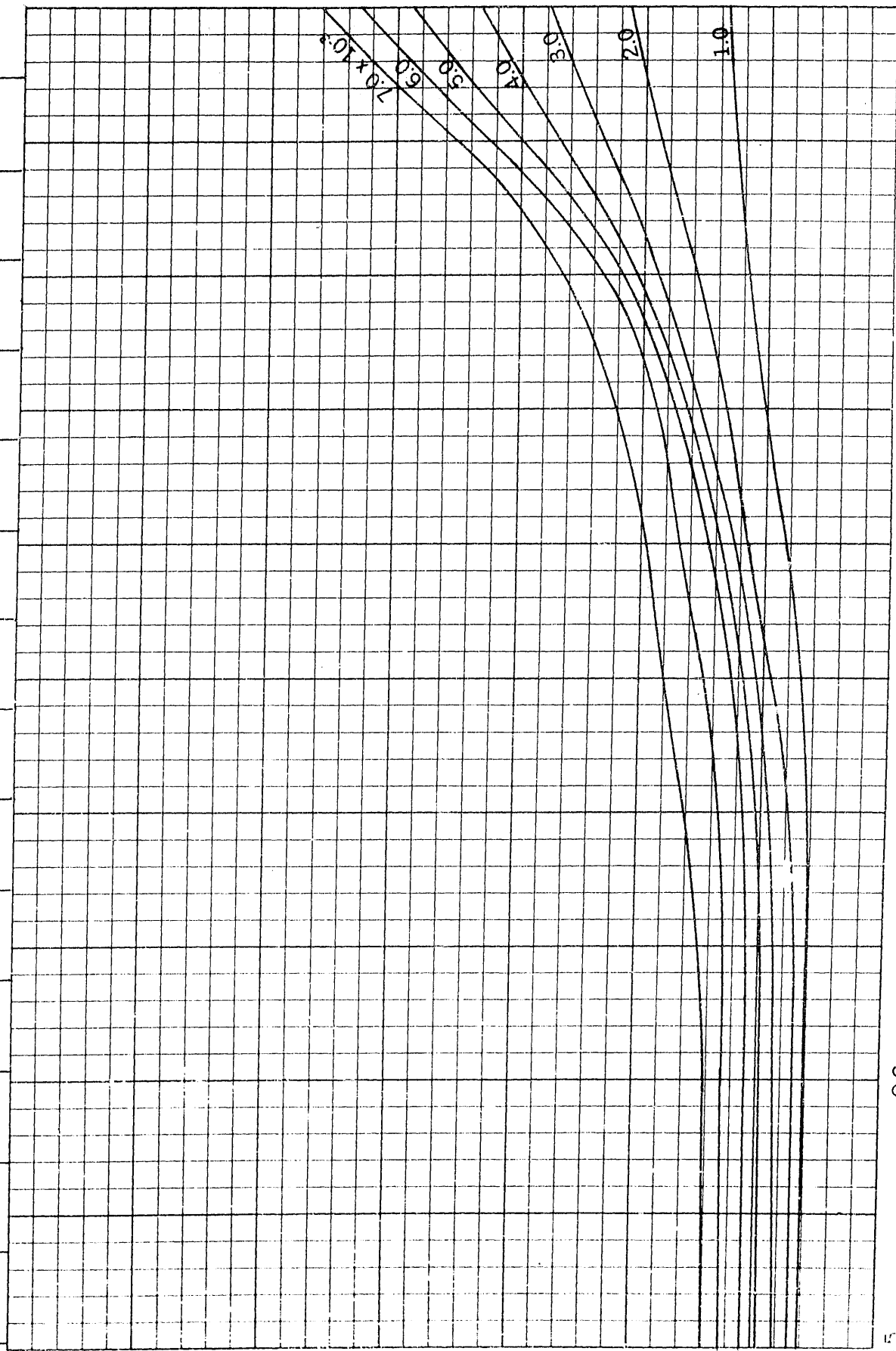
$B/H=3.00$
 $C_p=0.58$



$B/H = 3.00$
 $C_p = 0.59$

Froude Number $\frac{v}{\sqrt{gL}}$

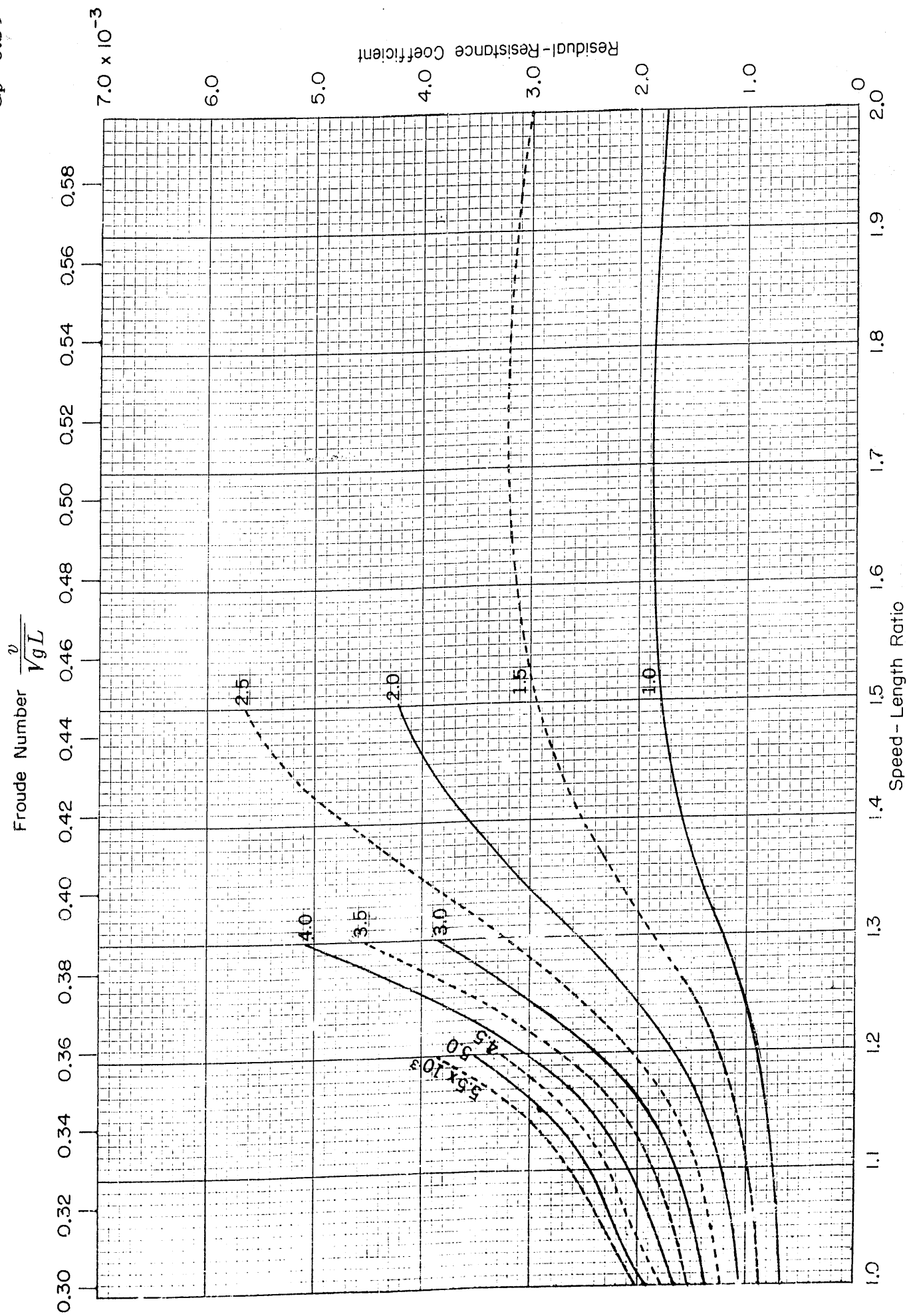
0.15 0.16 0.17 0.18 0.19 0.20 0.21 0.22 0.23 0.24 0.25 0.26 0.27 0.28 0.29

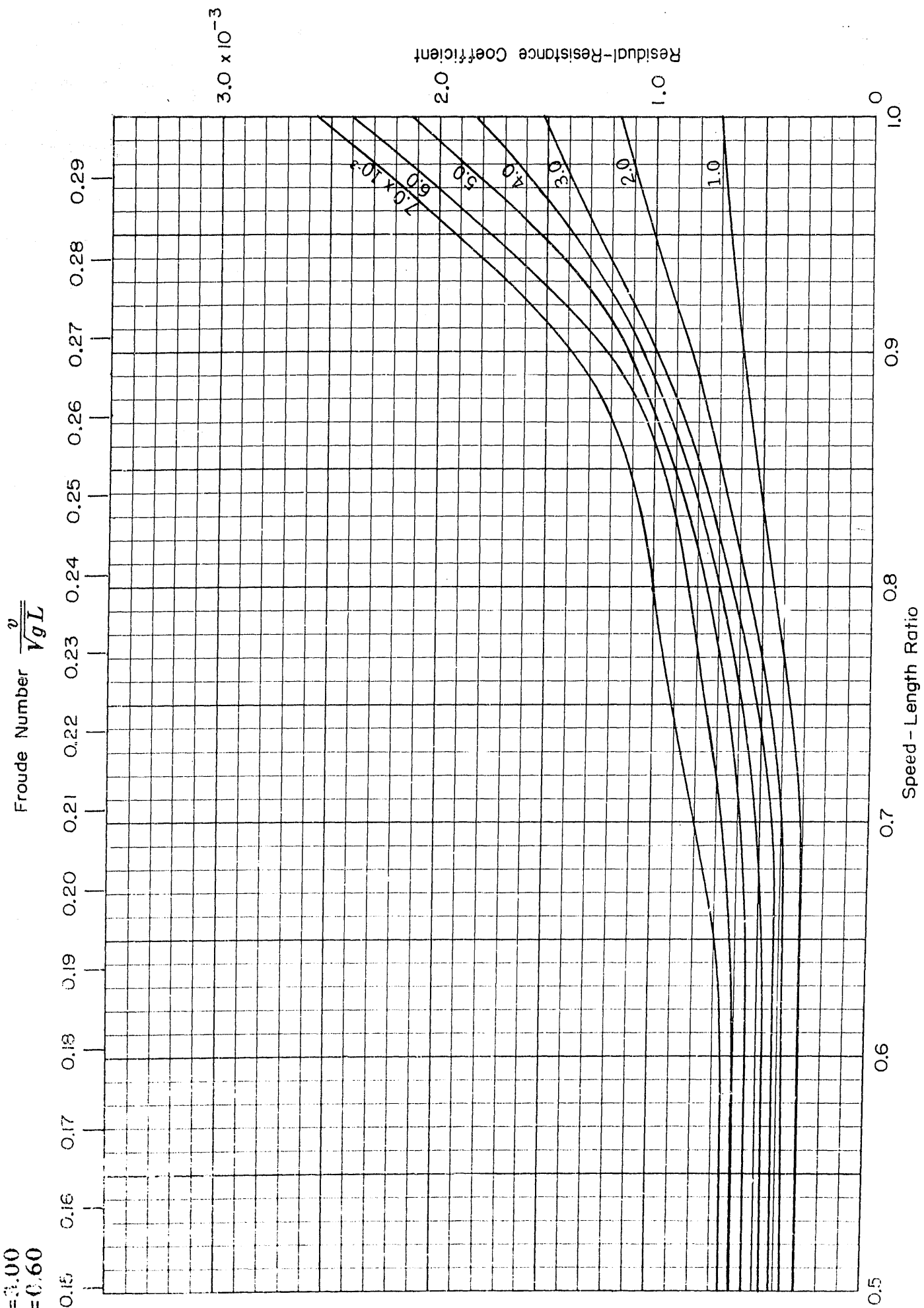


Residual-Resistance Coefficient

3.0×10^{-3}

$B/H=3.00$
 $C_p=0.59$



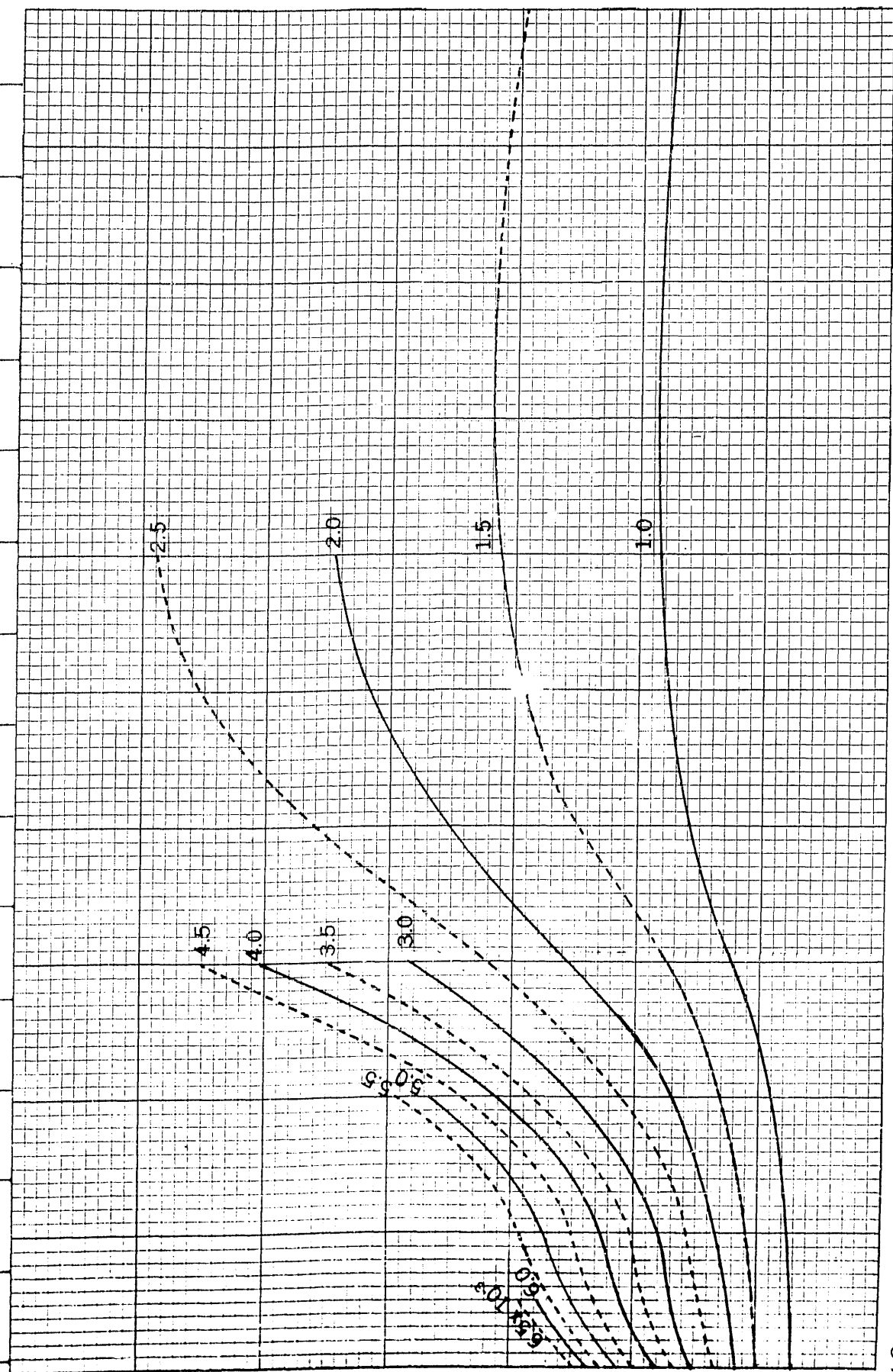
$$\frac{v}{\sqrt{g L}}$$


$B/H=3.00$
 $C_p=0.60$

Froude Number $\frac{v}{\sqrt{gL}}$

0.30 0.32 0.34 0.36 0.38 0.40 0.42 0.44 0.46 0.48 0.50 0.52 0.54 0.56 0.58

7.0×10^{-3}



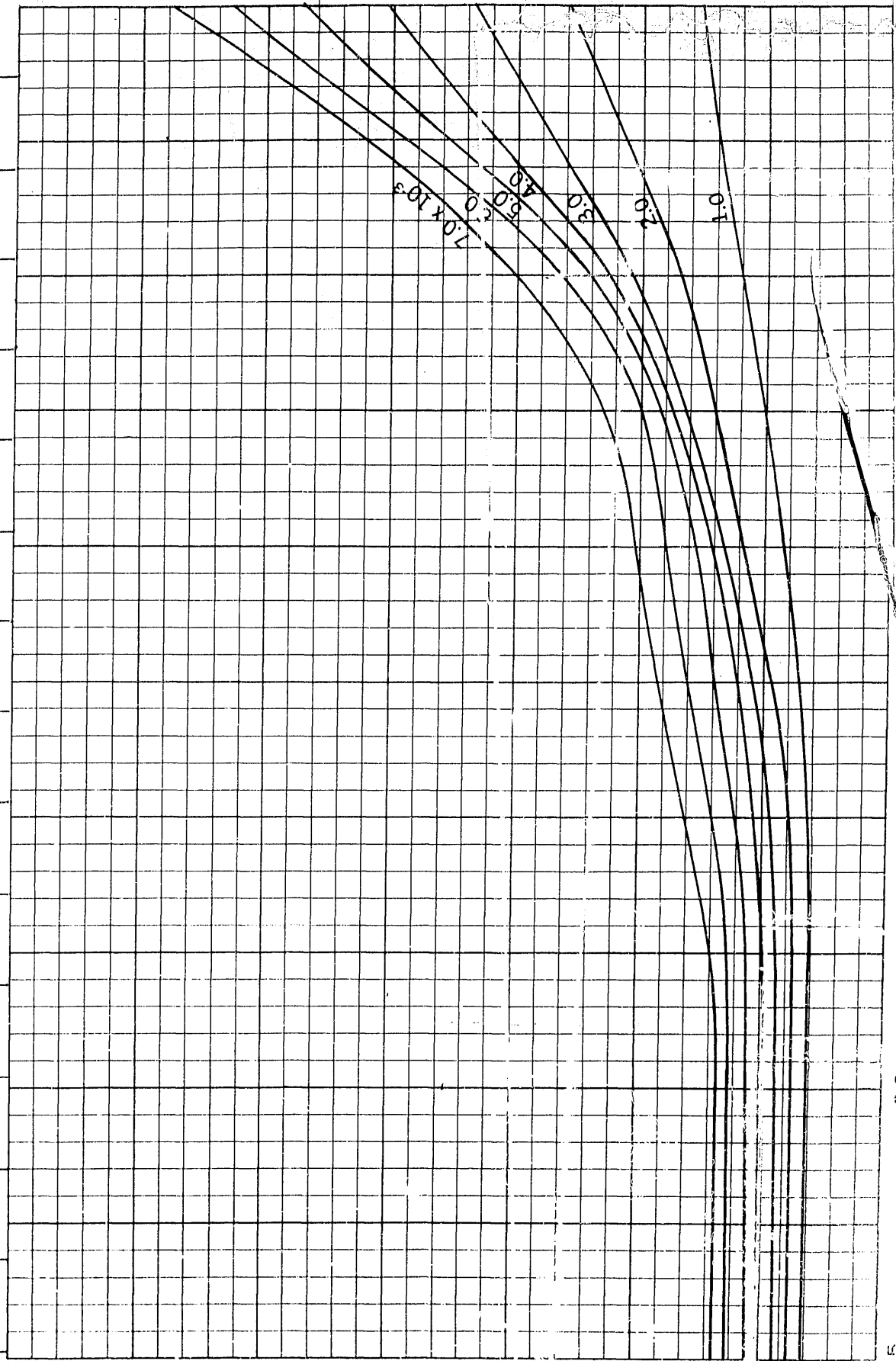
Residual-Resistance Coefficient

0 1.0 2.0
 1.0 1.1 1.2 1.3 1.4 1.5 1.6 1.7 1.8 1.9 2.0
 Speed-Length Ratio

$B/H=3.00$
 $C_p=0.61$

Froude Number $\frac{v}{\sqrt{gL}}$

0.15 0.16 0.17 0.18 0.19 0.20 0.21 0.22 0.23 0.24 0.25 0.26 0.27 0.28 0.29



Residual-Resistance Coefficient

3.0×10^{-3}

Speed Length Ratio

0.5 0.6 0.7 0.8 0.9 1.0

$B/H=3.00$
 $C_p=0.61$

Froude Number $\frac{v}{\sqrt{gL}}$

0.30 0.32 0.34 0.36 0.38 0.40 0.42 0.44 0.46 0.48 0.50 0.52 0.54 0.56 0.58

7.0×10^{-3}

6.0

5.0

4.0

3.0

2.0

1.0

0 2.0

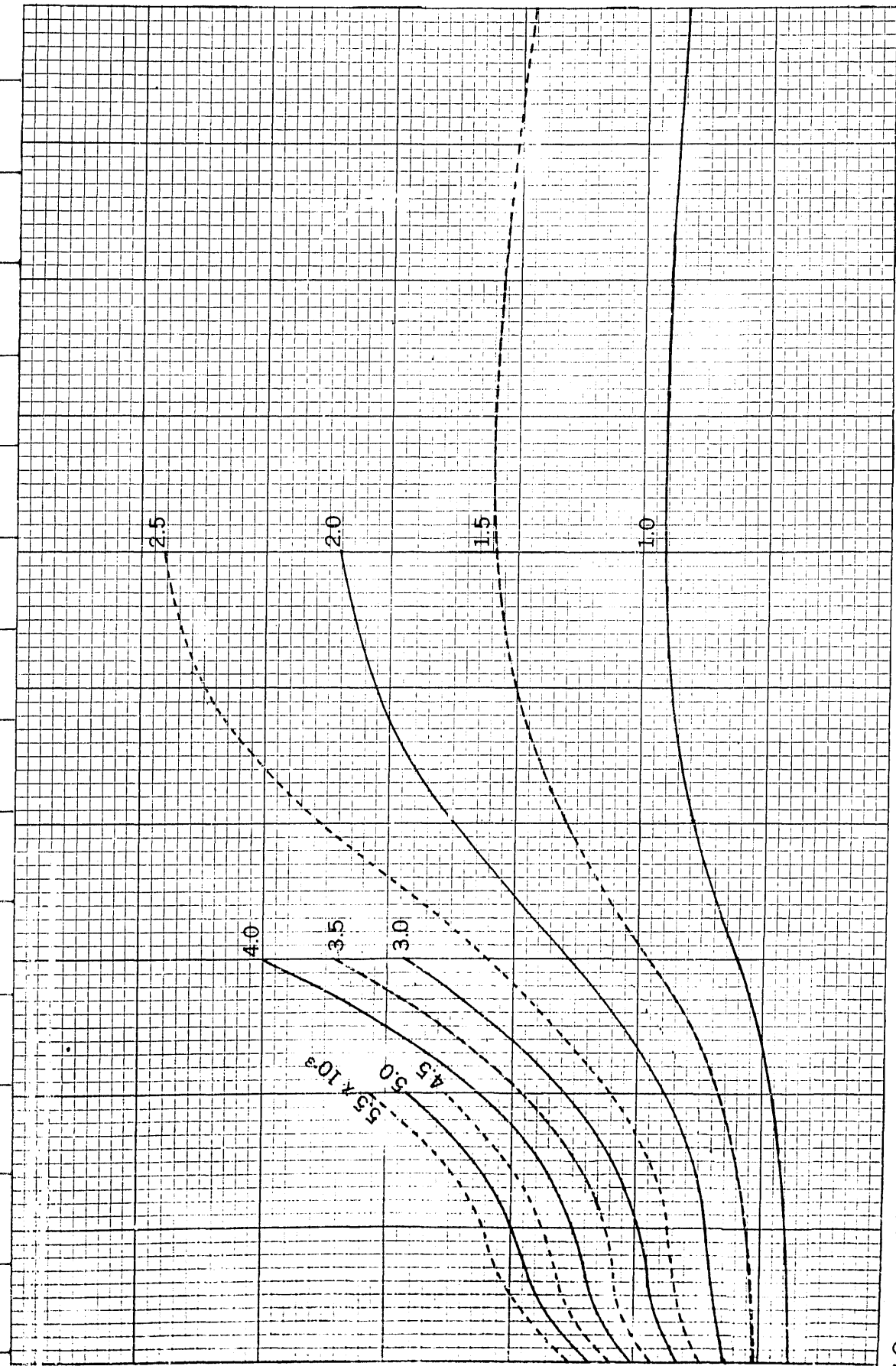
Speed - Length Ratio

1.3

1.2

1.1

1.0



Residual-Resistance Coefficient

$B/H=3.00$
 $C_p=0.62$

Froude Number $\frac{v}{\sqrt{gL}}$

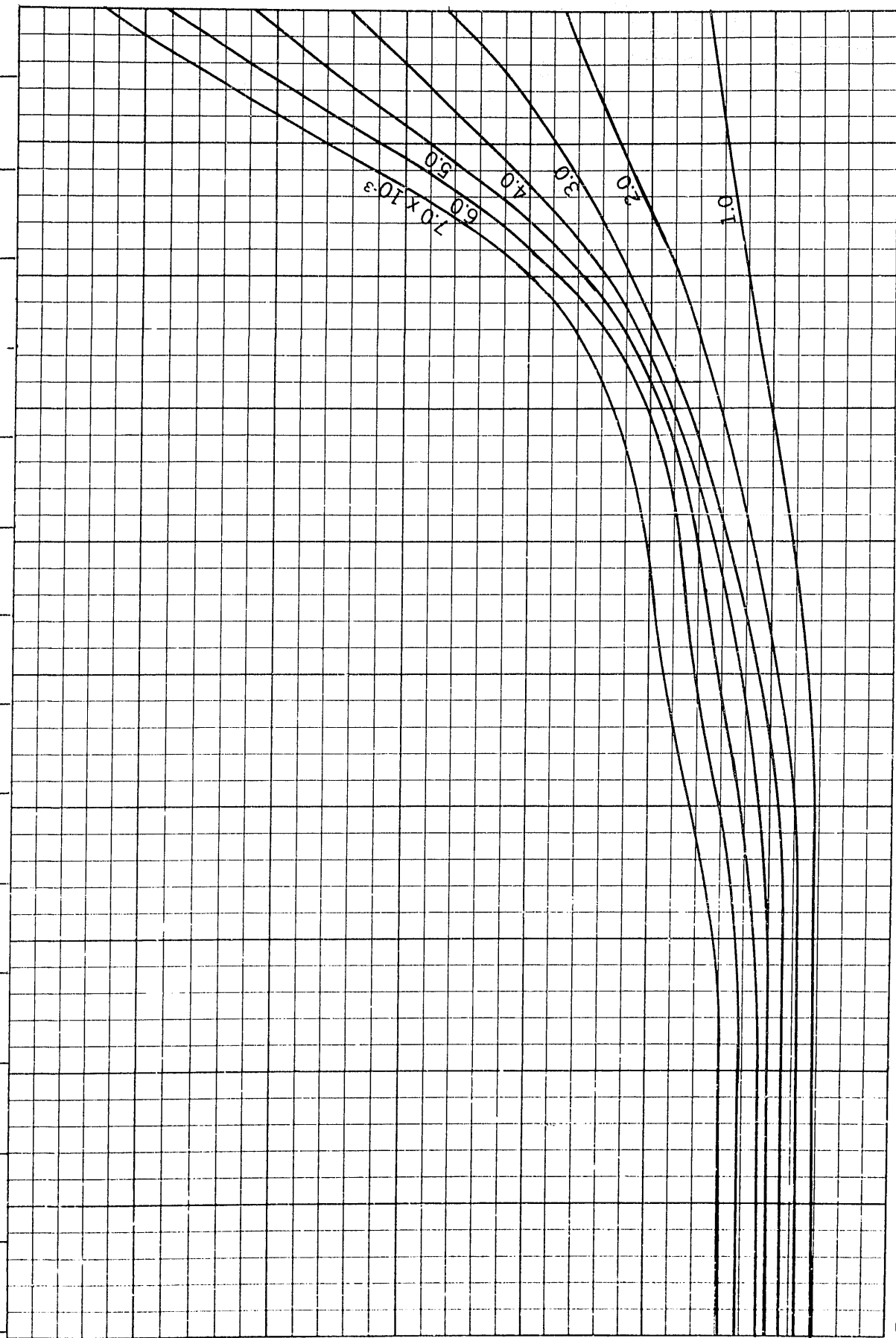
0.15 0.16 0.17 0.18 0.19 0.20 0.21 0.22 0.23 0.24 0.25 0.26 0.27 0.28 0.29

0.5 0.6 0.7 0.8 0.9 1.0

Speed - Length Ratio

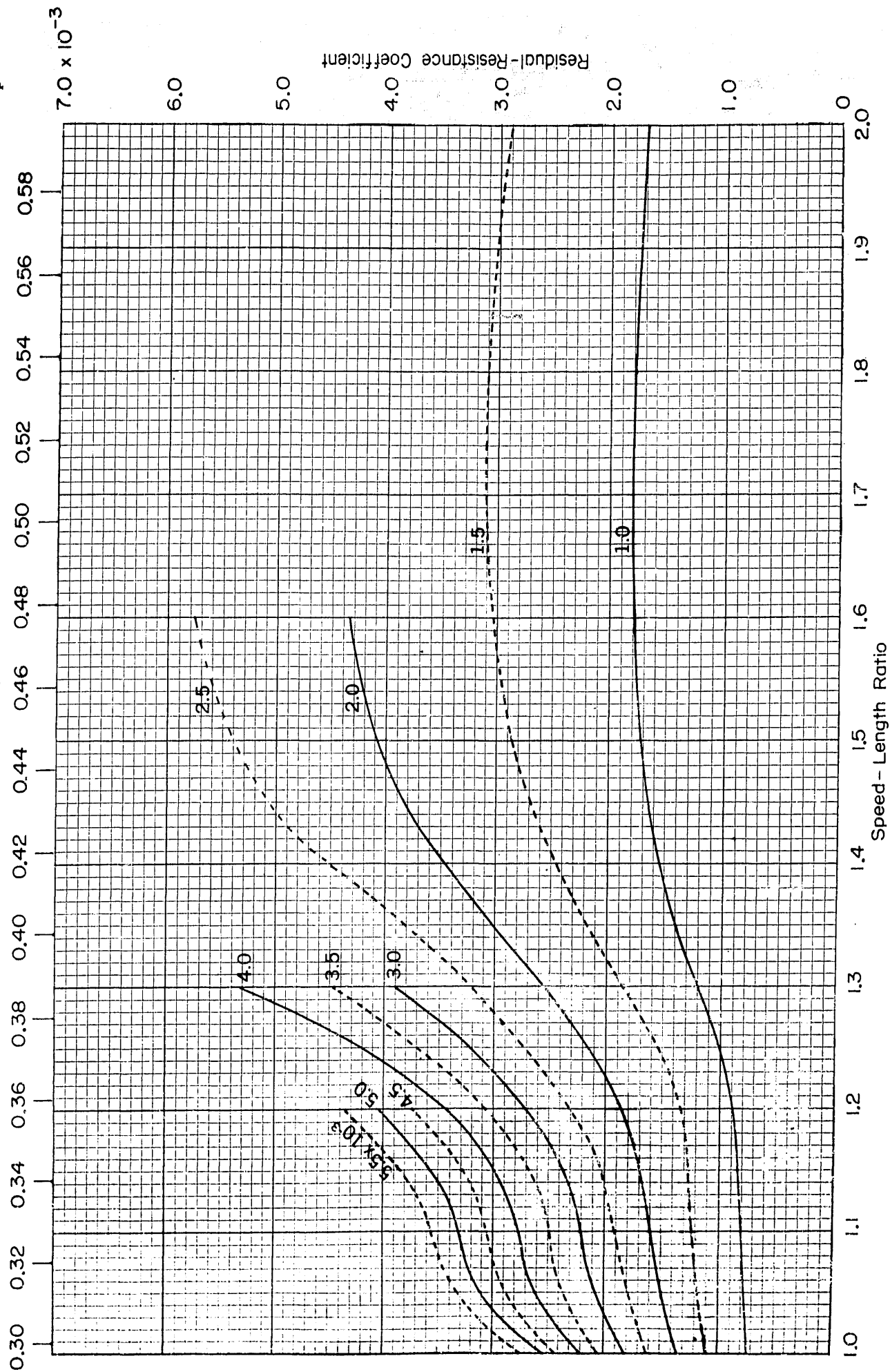
Residual-Resistance Coefficient
 3.0×10^{-3}
2.0
1.0

1.0
2.0
3.0
4.0
5.0
 7.0×10^{-3}



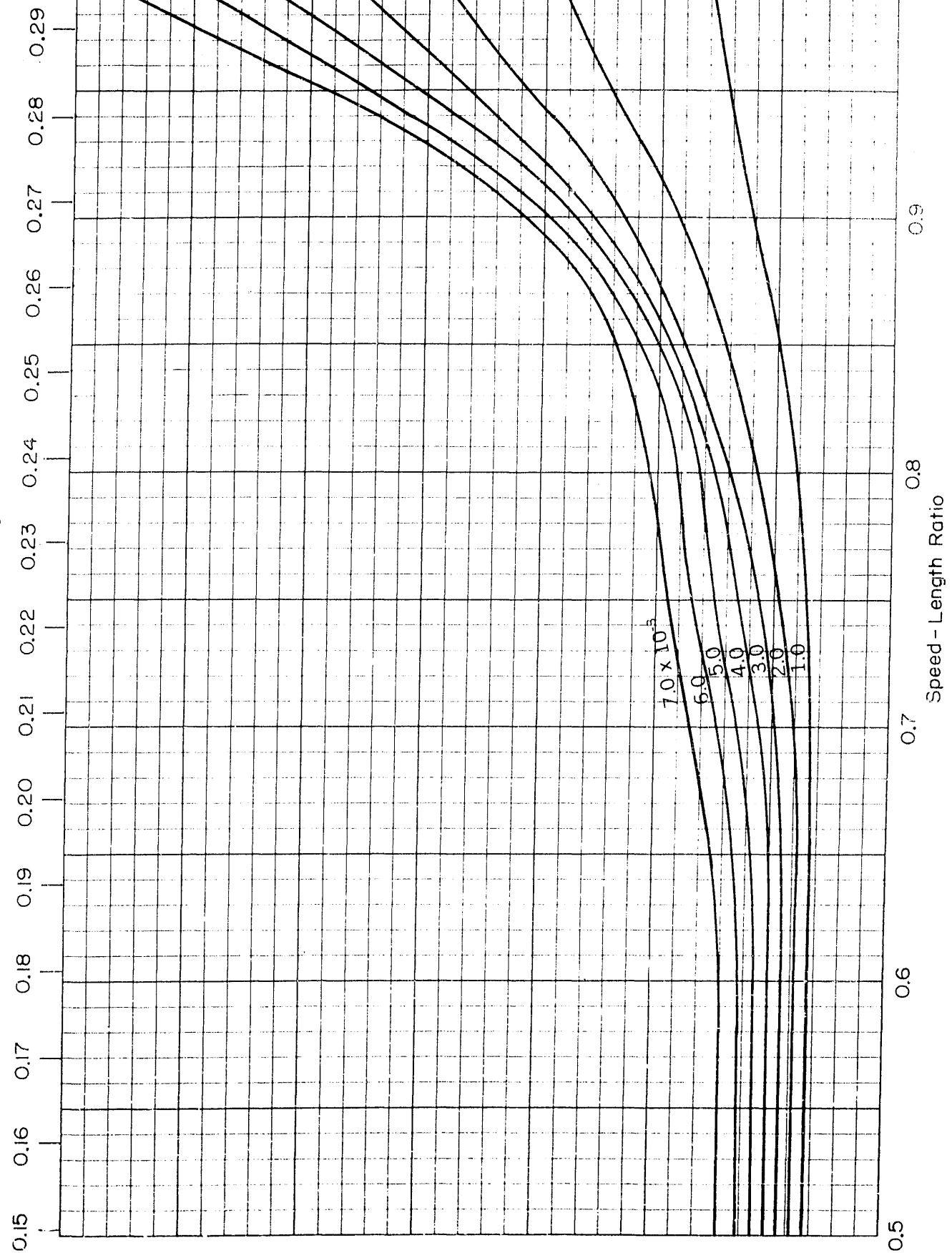
$B/H=3.00$
 $C_p=0.62$

Froude Number $\frac{v}{\sqrt{gL}}$

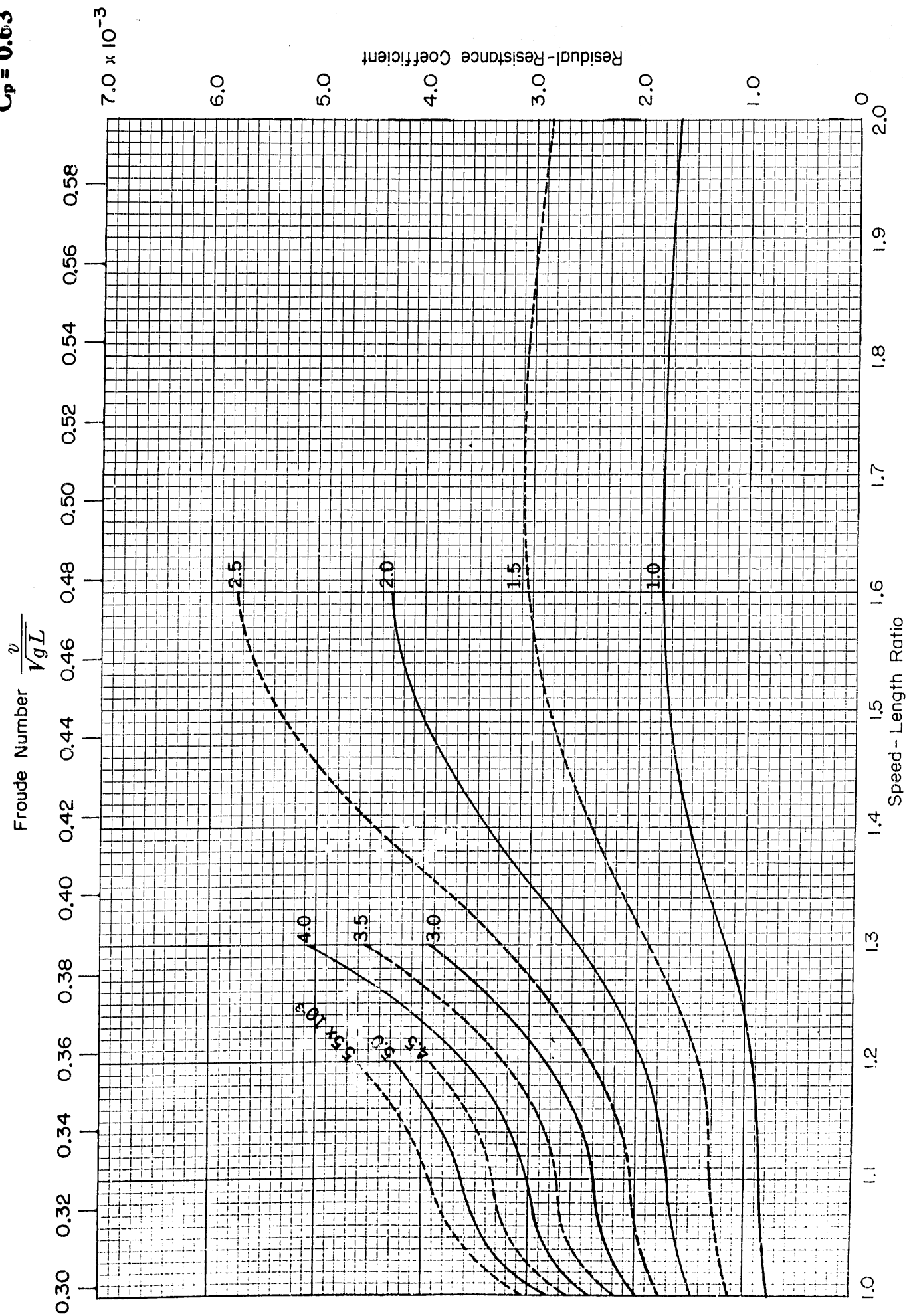


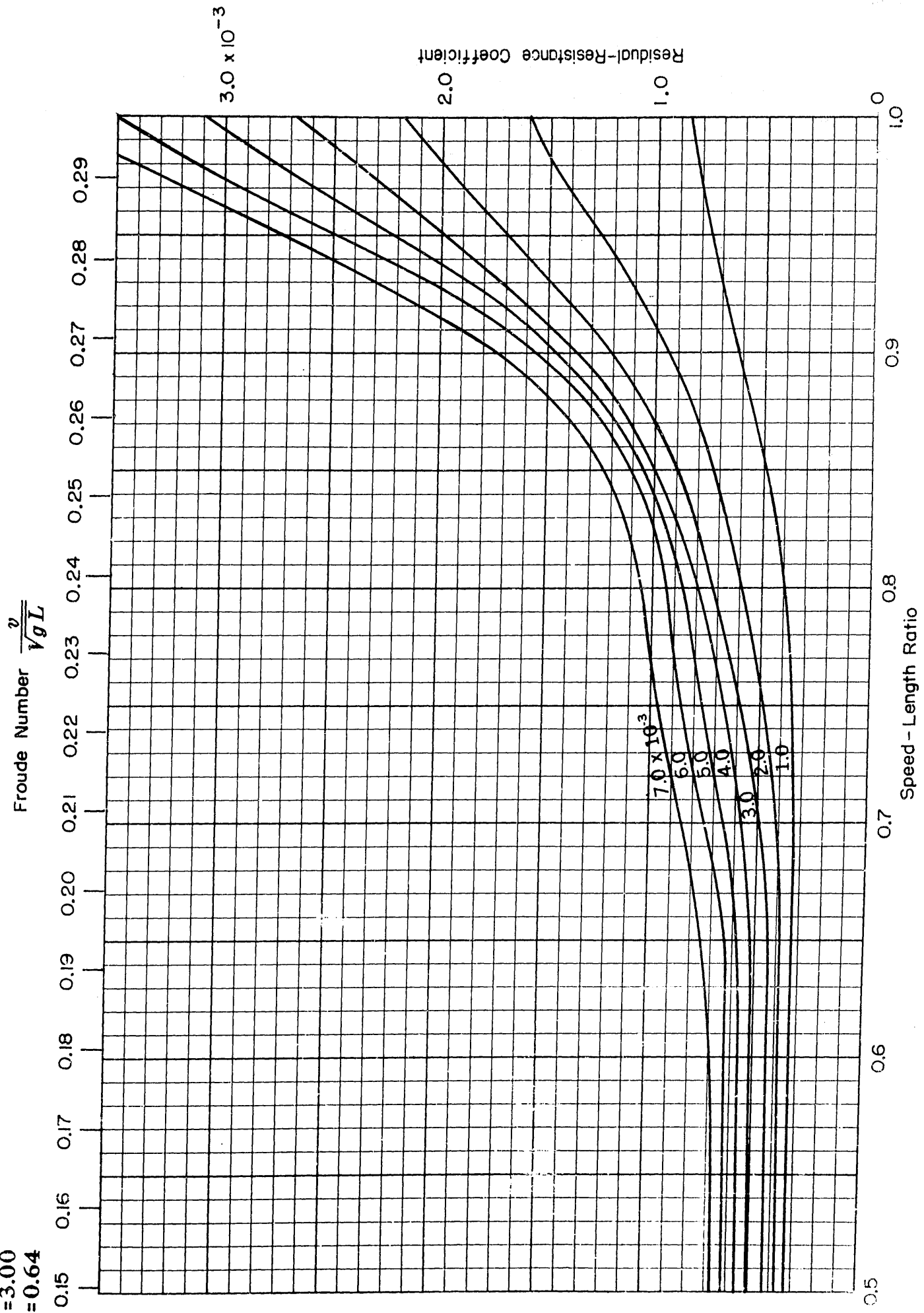
$B/H=3.00$
 $C_p=0.63$

Froude Number $\frac{v}{\sqrt{gL}}$

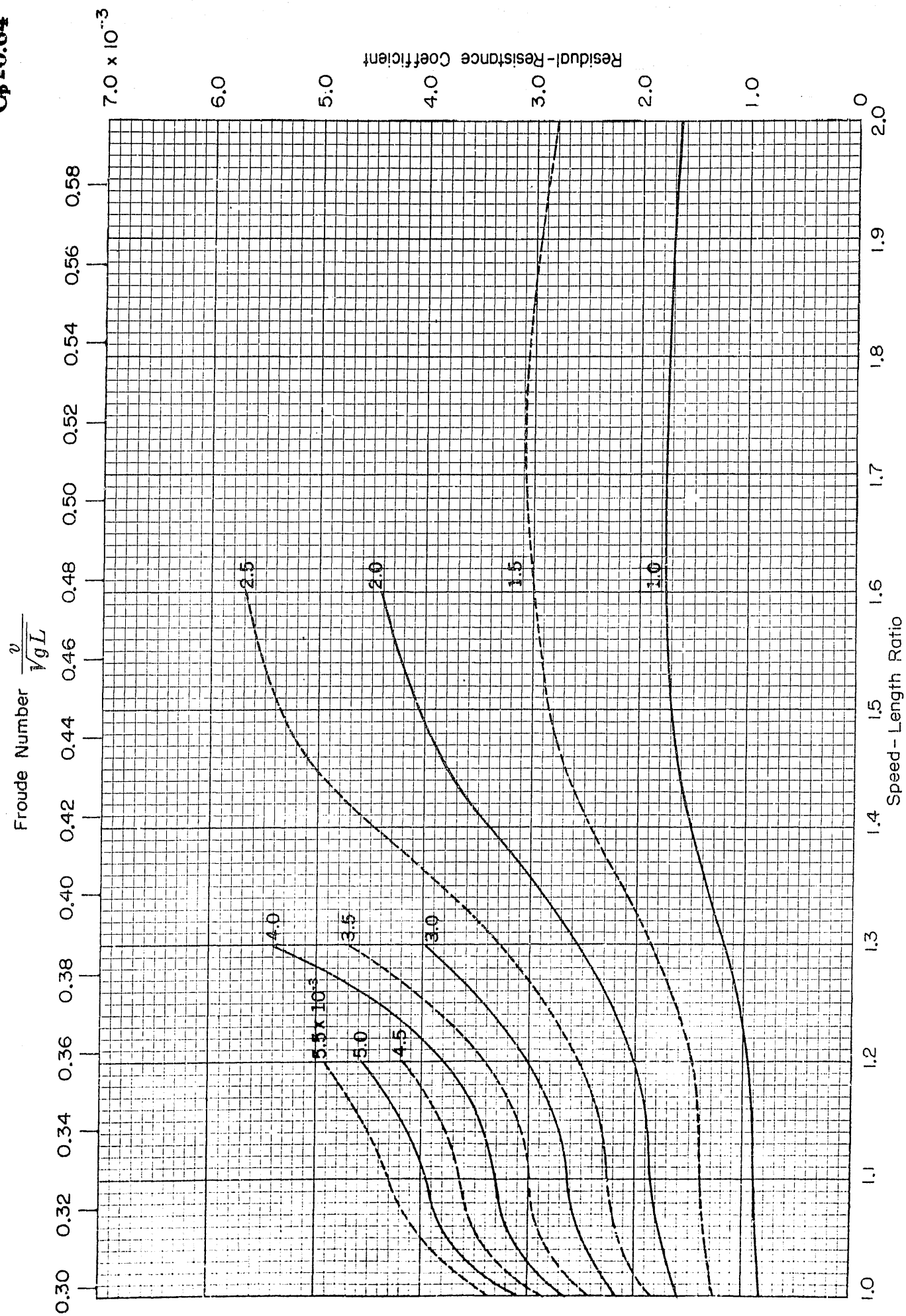


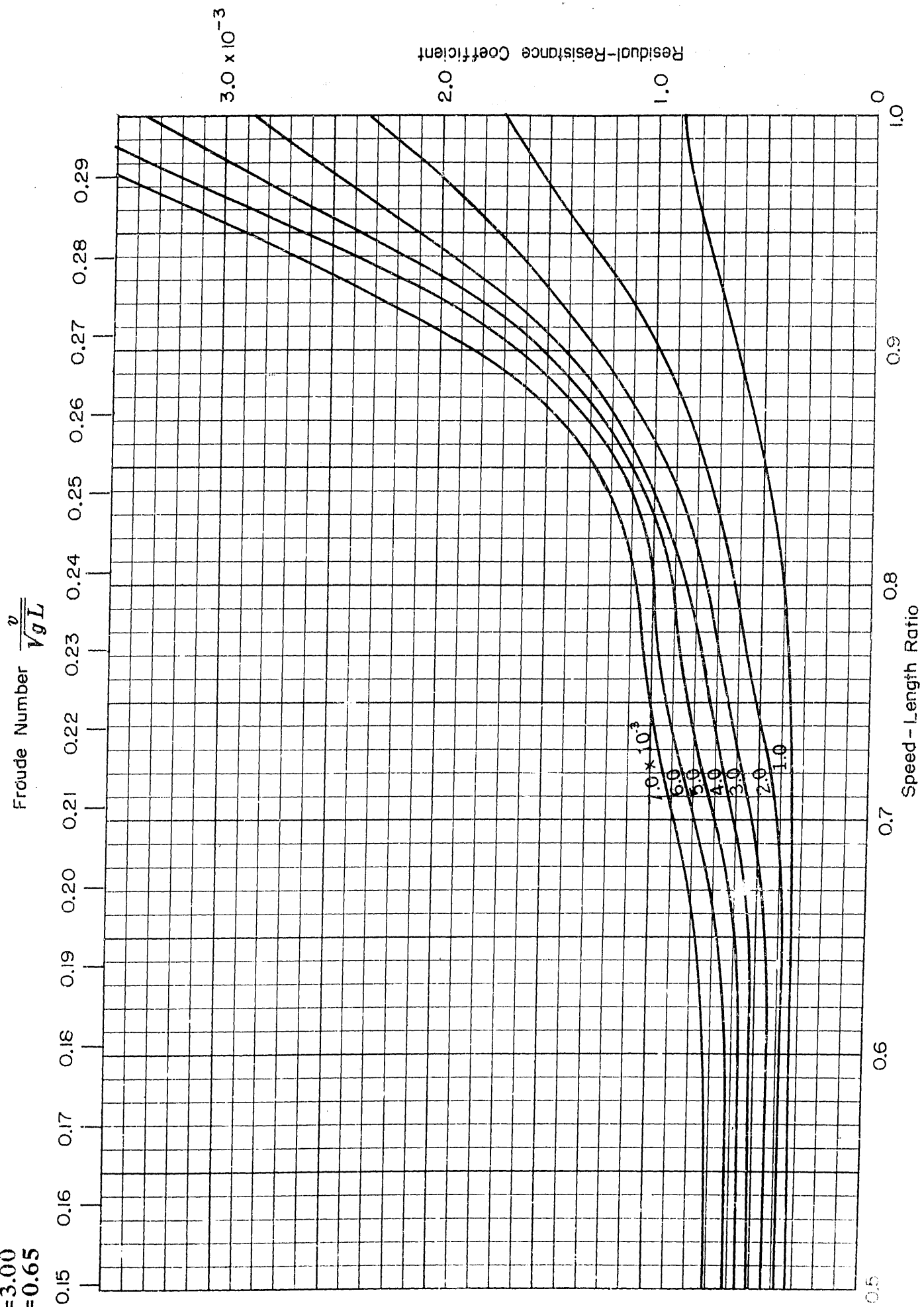
B/H=3.00
C_p = 0.63



$$\frac{v}{\sqrt{gL}}$$


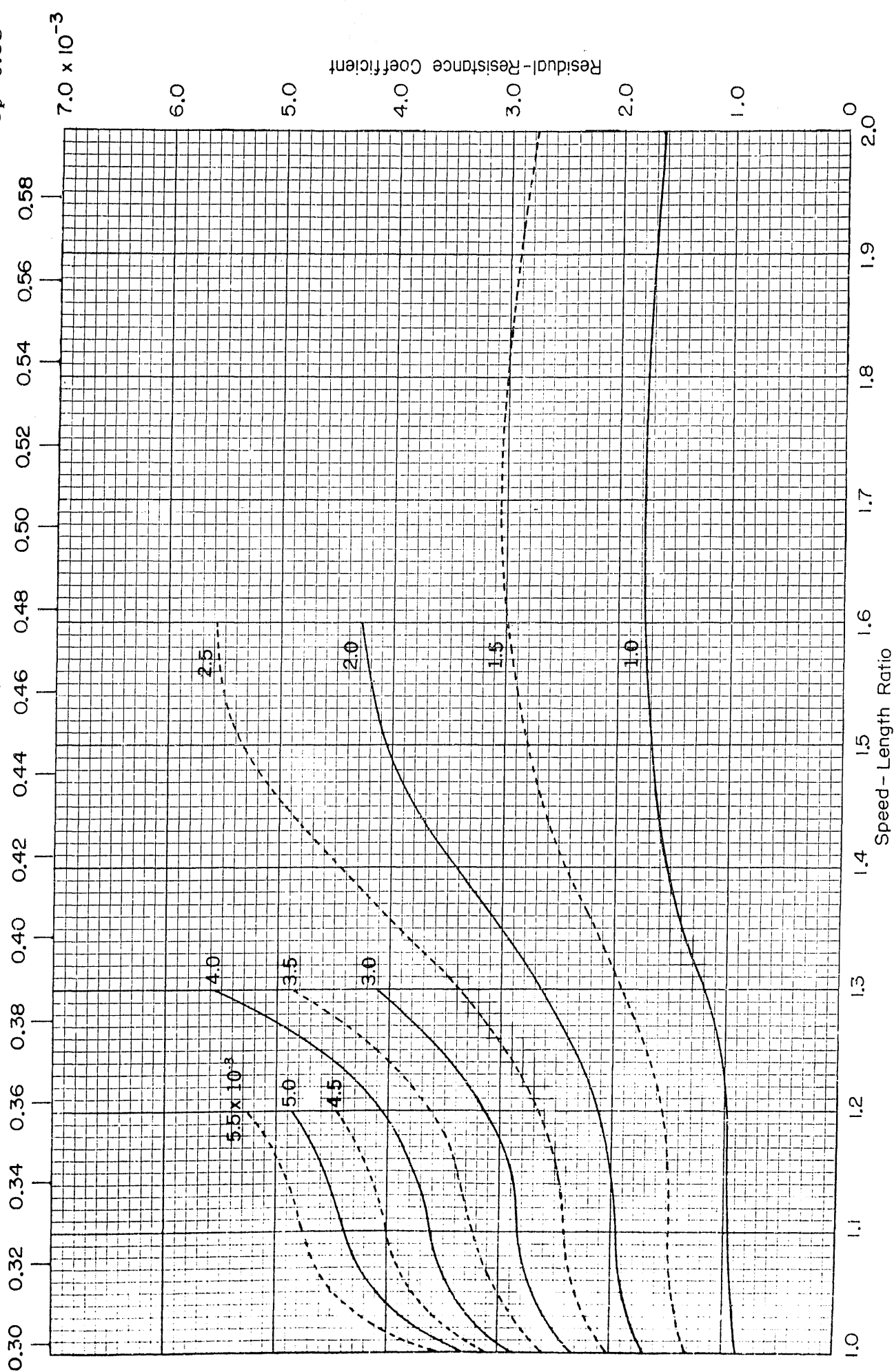
$B/H=3.00$
 $C_p=0.64$



$$\frac{v}{\sqrt{g L}}$$


$B/H=3.00$
 $C_p=0.65$

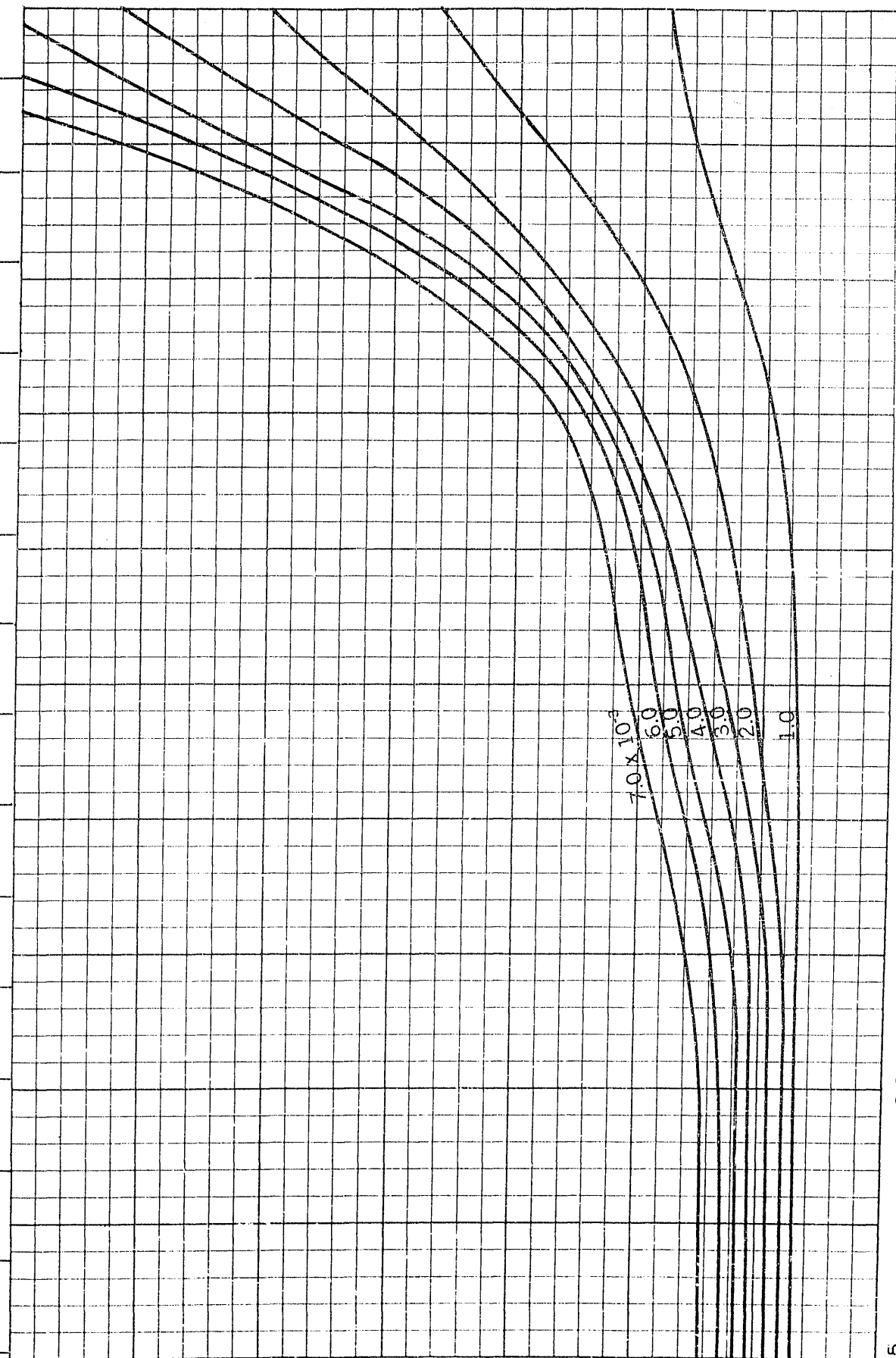
Froude Number $\frac{v}{\sqrt{gL}}$



$B/H=3.00$
 $C_p=0.66$

Froude Number $\frac{v}{\sqrt{gL}}$

0.15 0.16 0.17 0.18 0.19 0.20 0.21 0.22 0.23 0.24 0.25 0.26 0.27 0.28 0.29



1.0
2.0
 3.0×10^{-3}

0.5 0.6 0.7 0.8 0.9 1.0

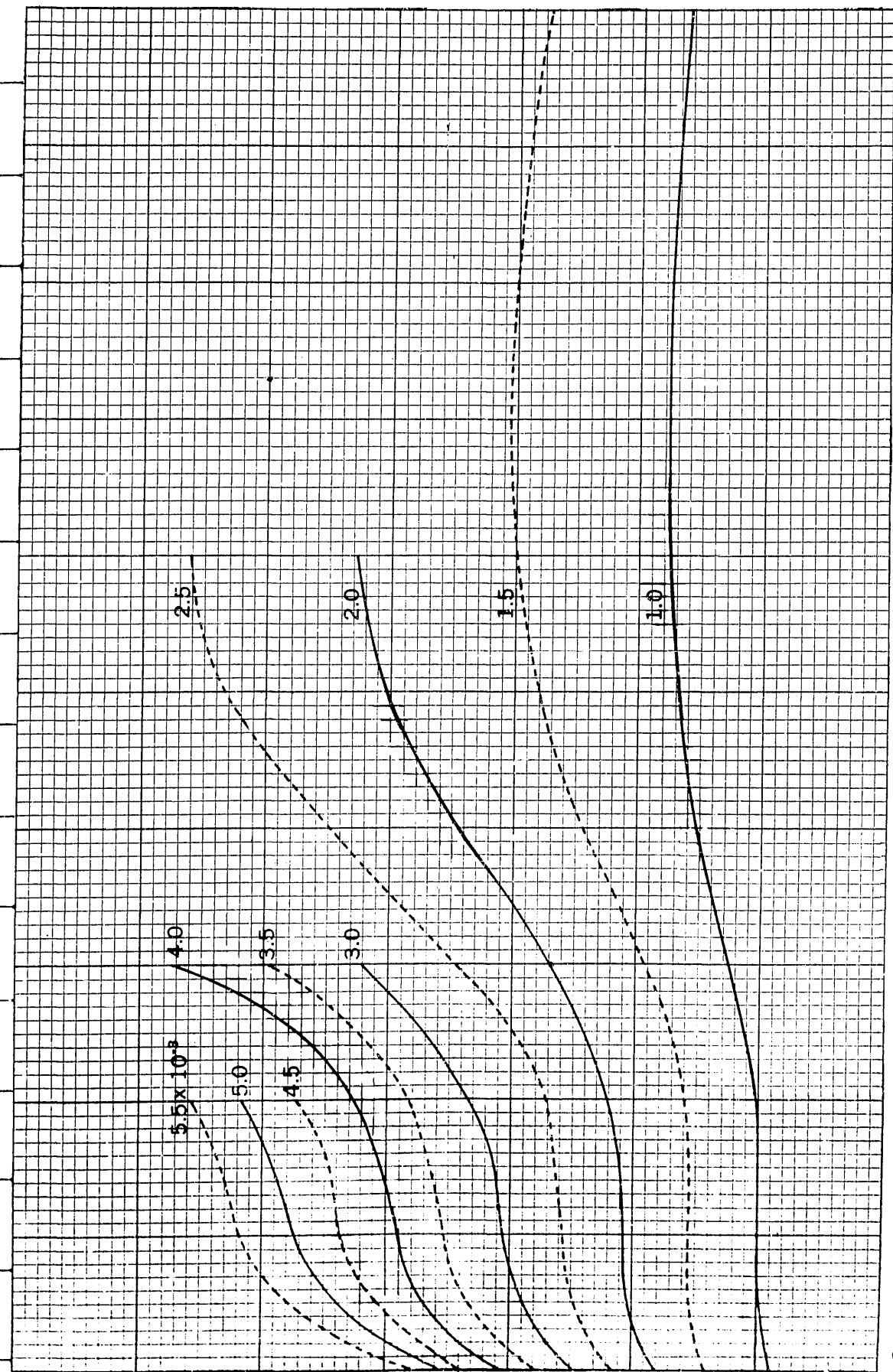
Speed - Length Ratio

$B/H=3.00$
 $C_p=0.66$

Froude Number $\frac{v}{\sqrt{gL}}$

0.30 0.32 0.34 0.36 0.38 0.40 0.42 0.44 0.46 0.48 0.50 0.52 0.54 0.56 0.58

7.0×10^{-3}



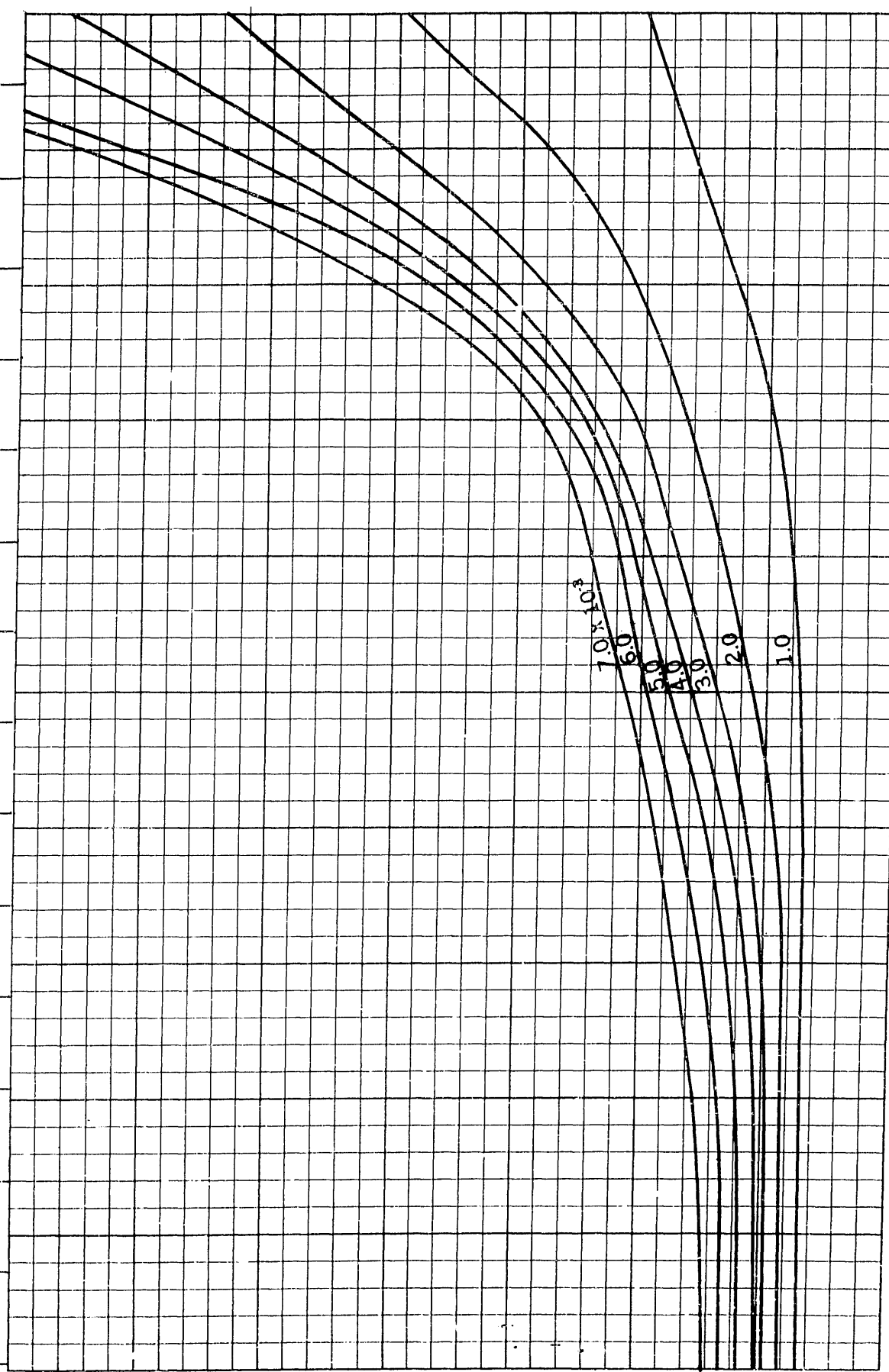
1.0 1.1 1.2 1.3 1.4 1.5 1.6 1.7 1.8 1.9 2.0

Speed - Length Ratio

$B/H=3.00$
 $C_p=0.67$

Froude Number $\frac{v}{\sqrt{gL}}$

0.15 0.16 0.17 0.18 0.19 0.20 0.21 0.22 0.23 0.24 0.25 0.26 0.27 0.28 0.29



Residual-Resistance Coefficient
3.0 x 10⁻³
2.0
1.0

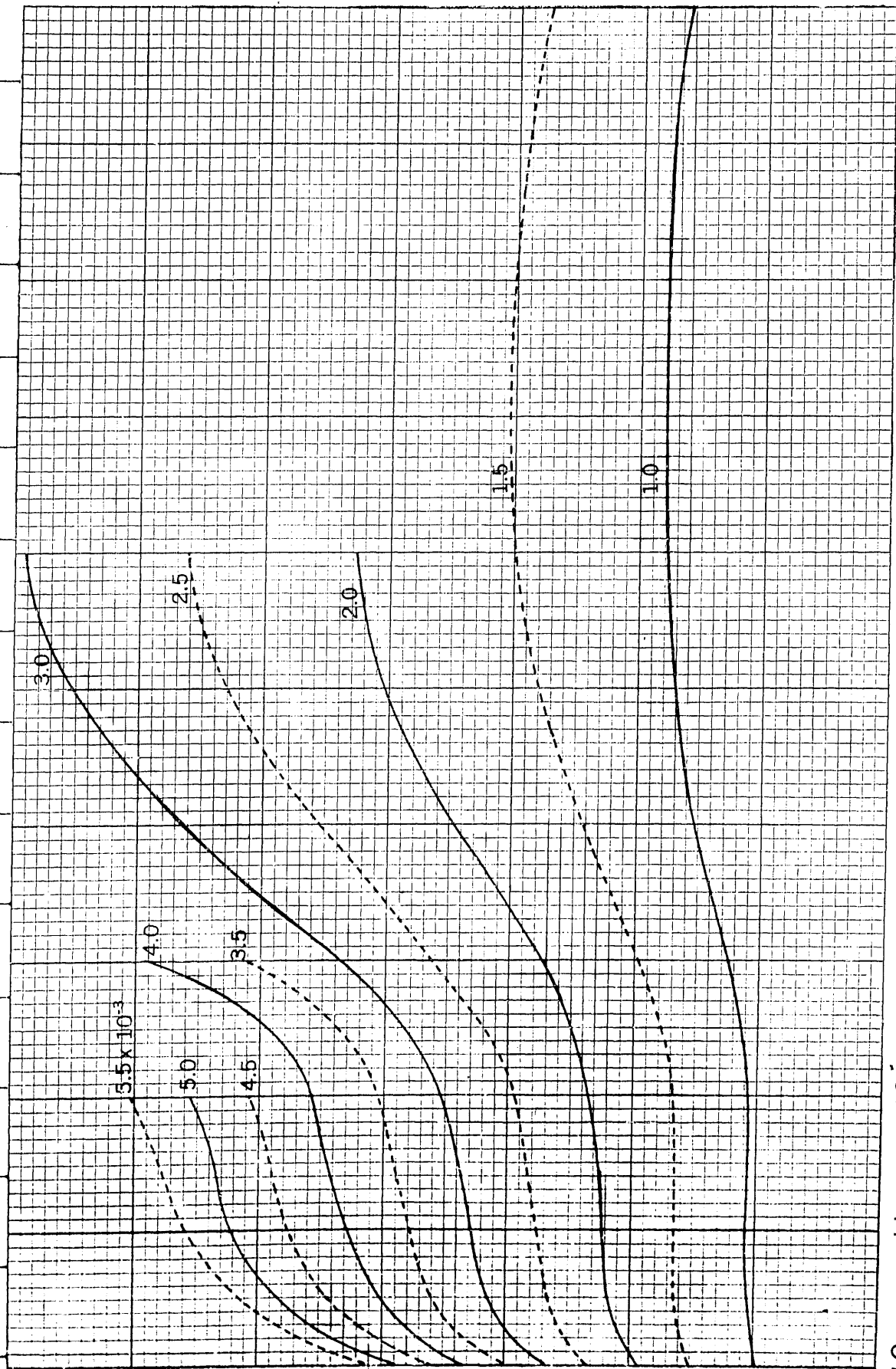
0
1.0

0.5 0.6 0.7 0.8 0.9 1.0
Speed - Length Ratio

$B/H=3.00$
 $C_p=0.67$

Froude Number $\frac{v}{\sqrt{gL}}$

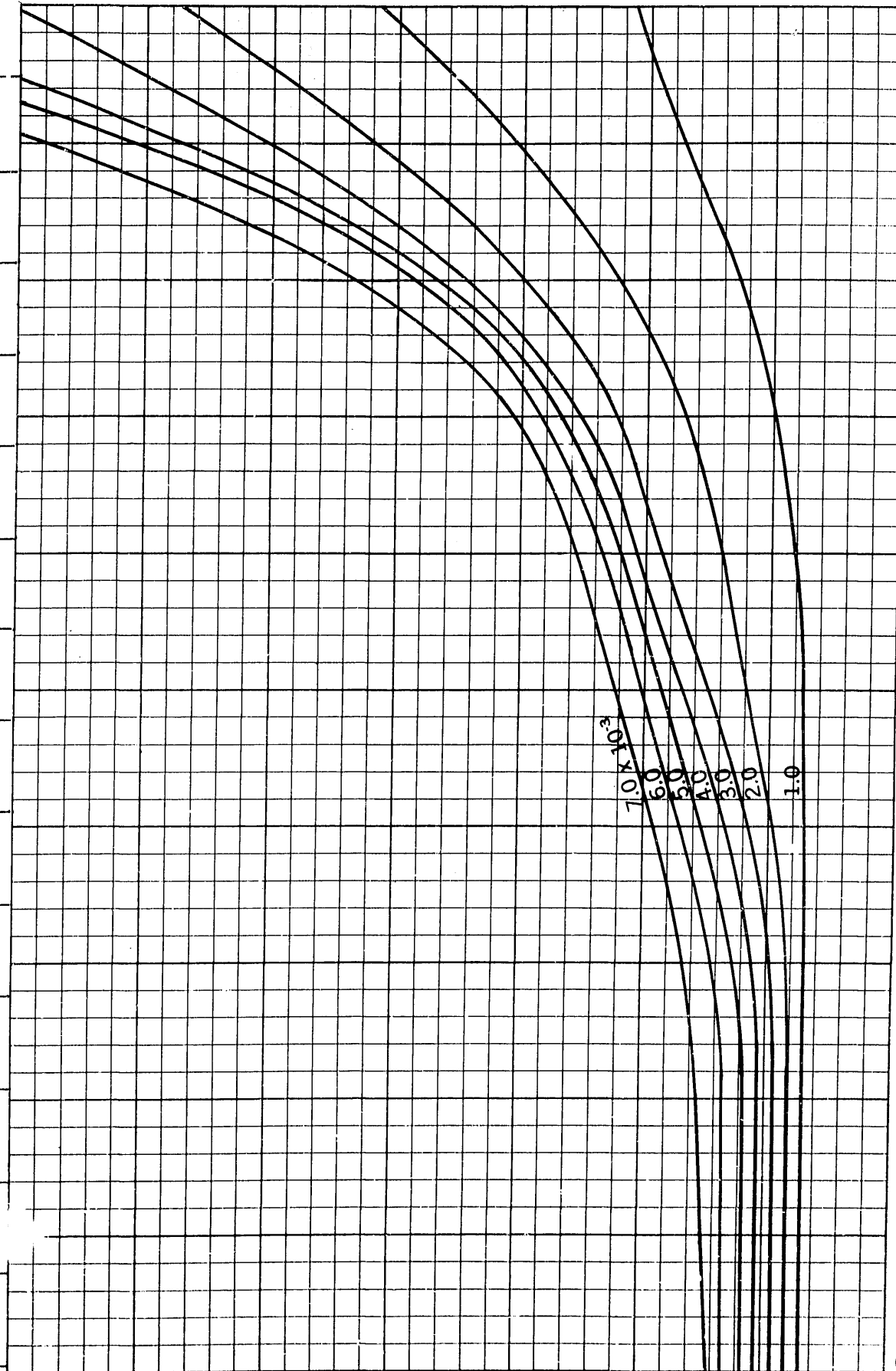
0.30 0.32 0.34 0.36 0.38 0.40 0.42 0.44 0.46 0.48 0.50 0.52 0.54 0.56 0.58



$B/H=3.00$
 $C_p=0.68$

Froude Number $\frac{v}{\sqrt{gL}}$

0.15 0.16 0.17 0.18 0.19 0.20 0.21 0.22 0.23 0.24 0.25 0.26 0.27 0.28 0.29



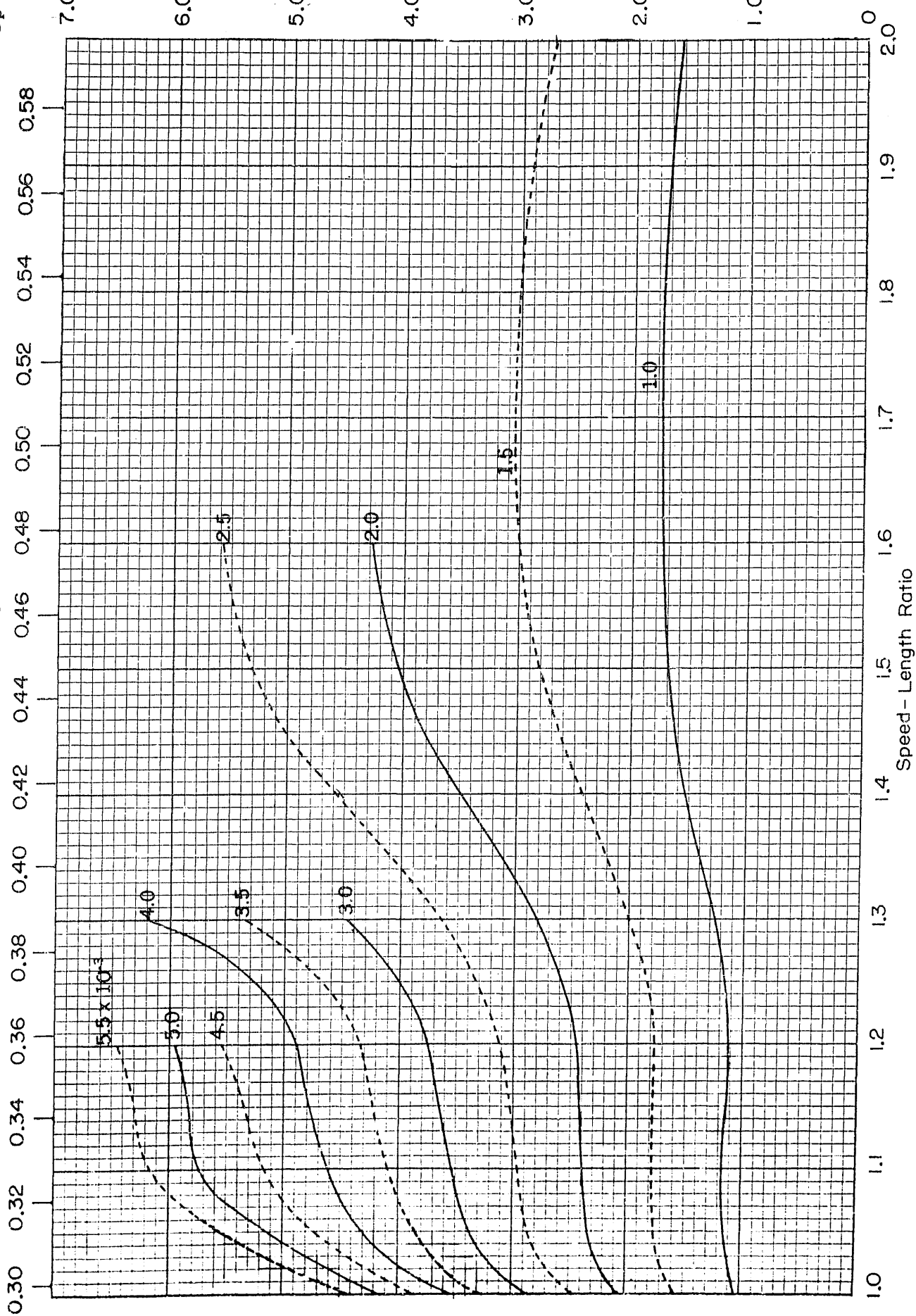
1.0
 2.0
 3.0 $\times 10^{-3}$

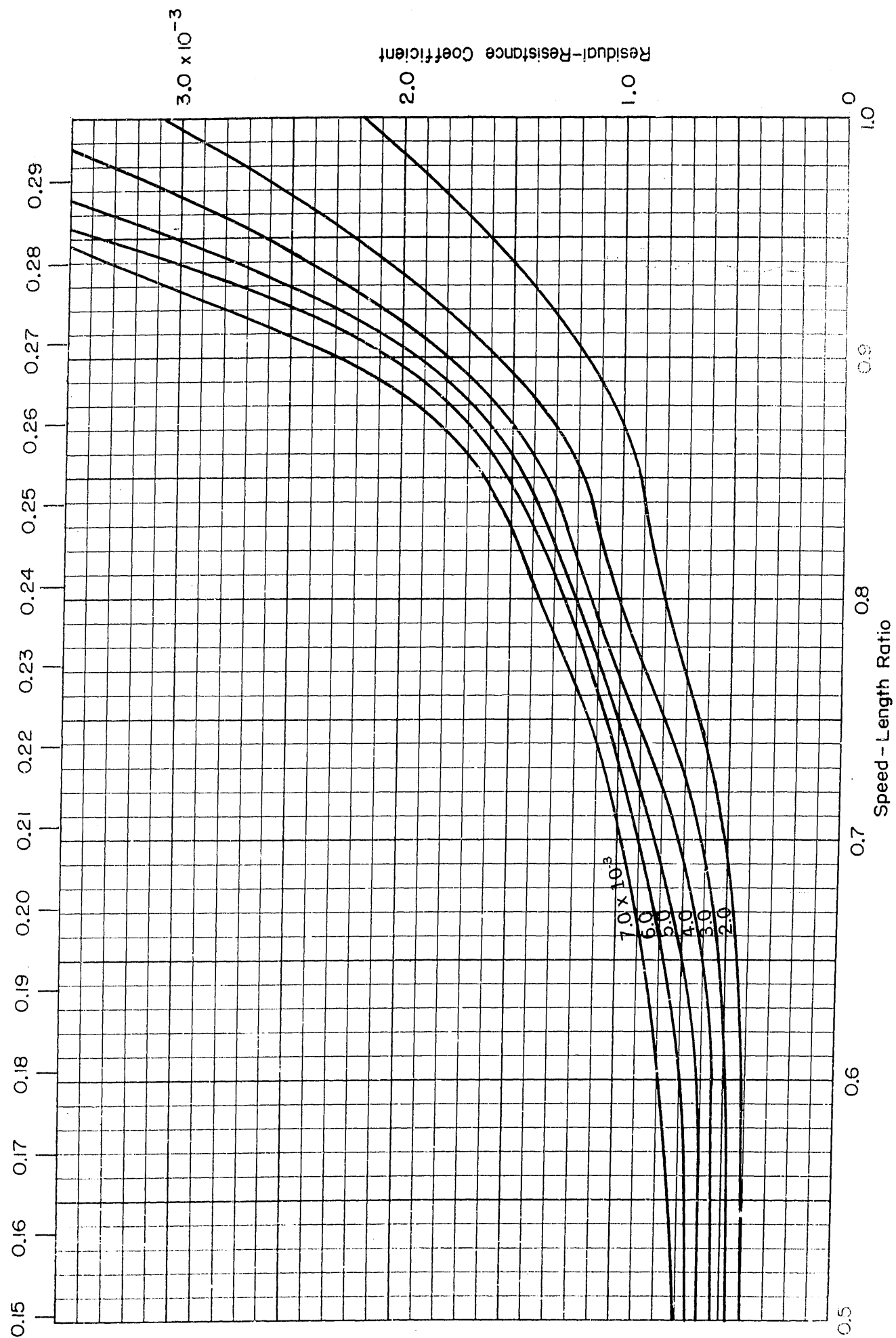
0.5 0.6 0.7 0.8 0.9 1.0

Speed - Length Ratio

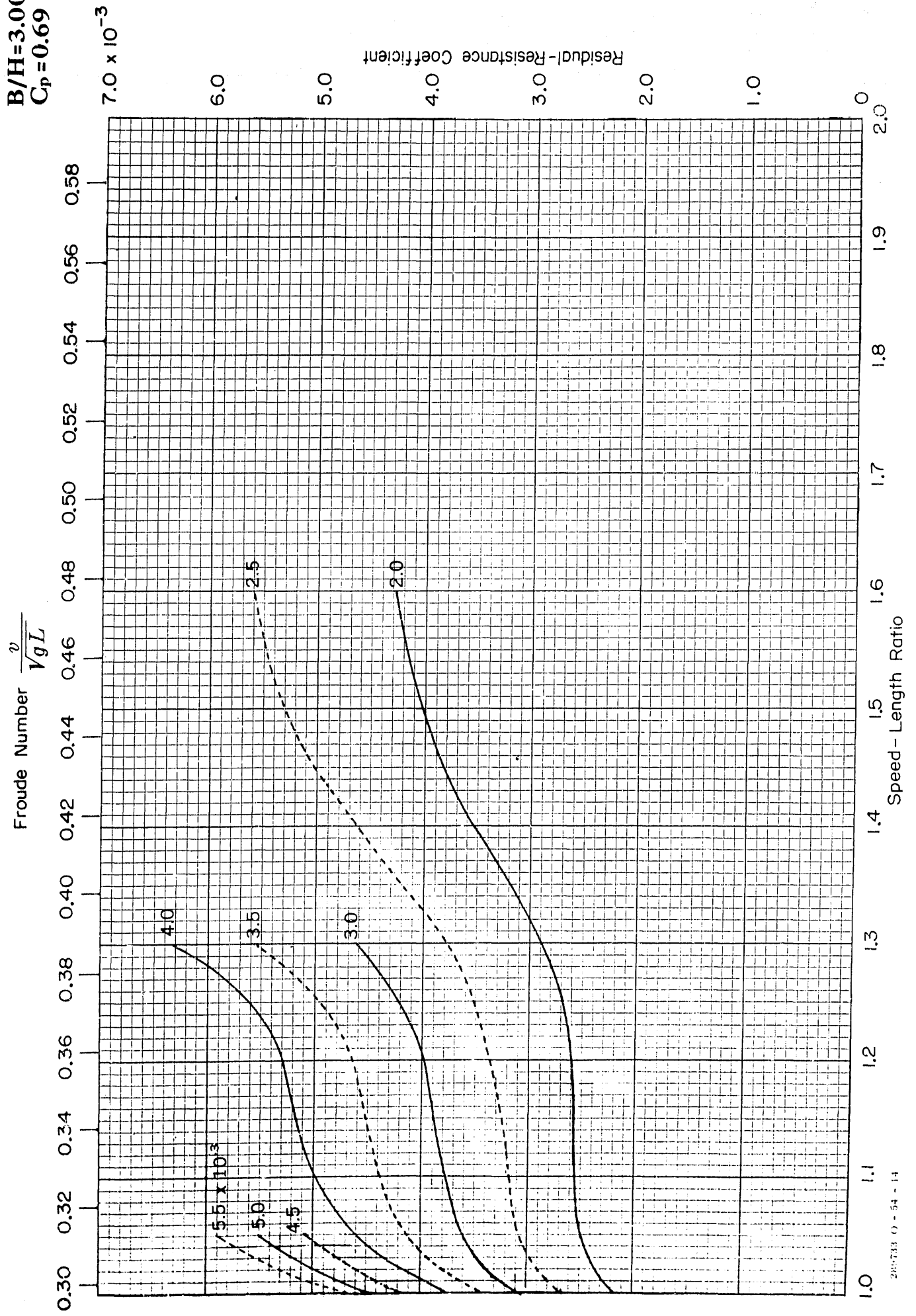
$B/H=3.00$
 $C_p = 0.68$

Froude Number $\frac{v}{\sqrt{gL}}$

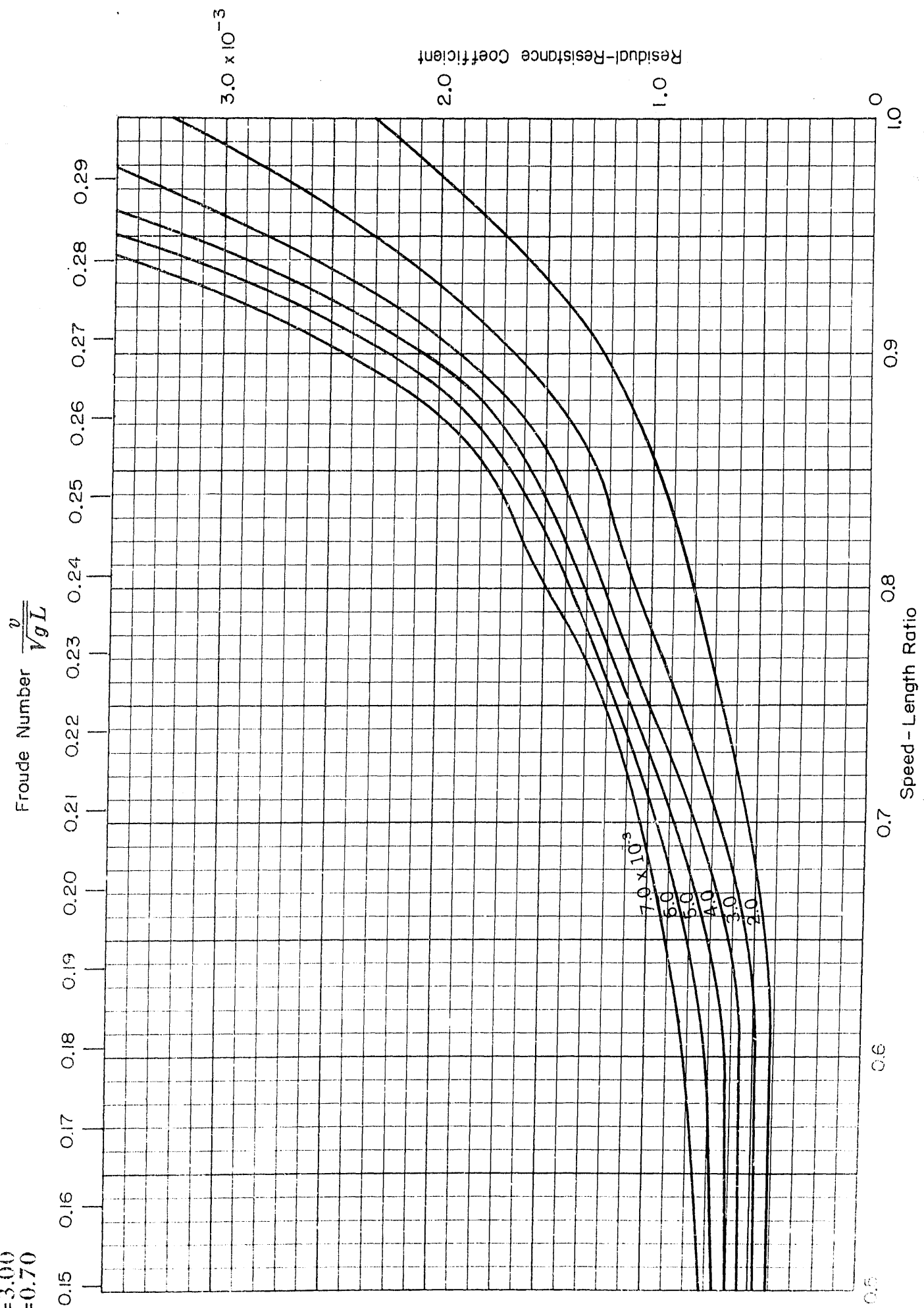


$$\frac{v}{\sqrt{g L}}$$


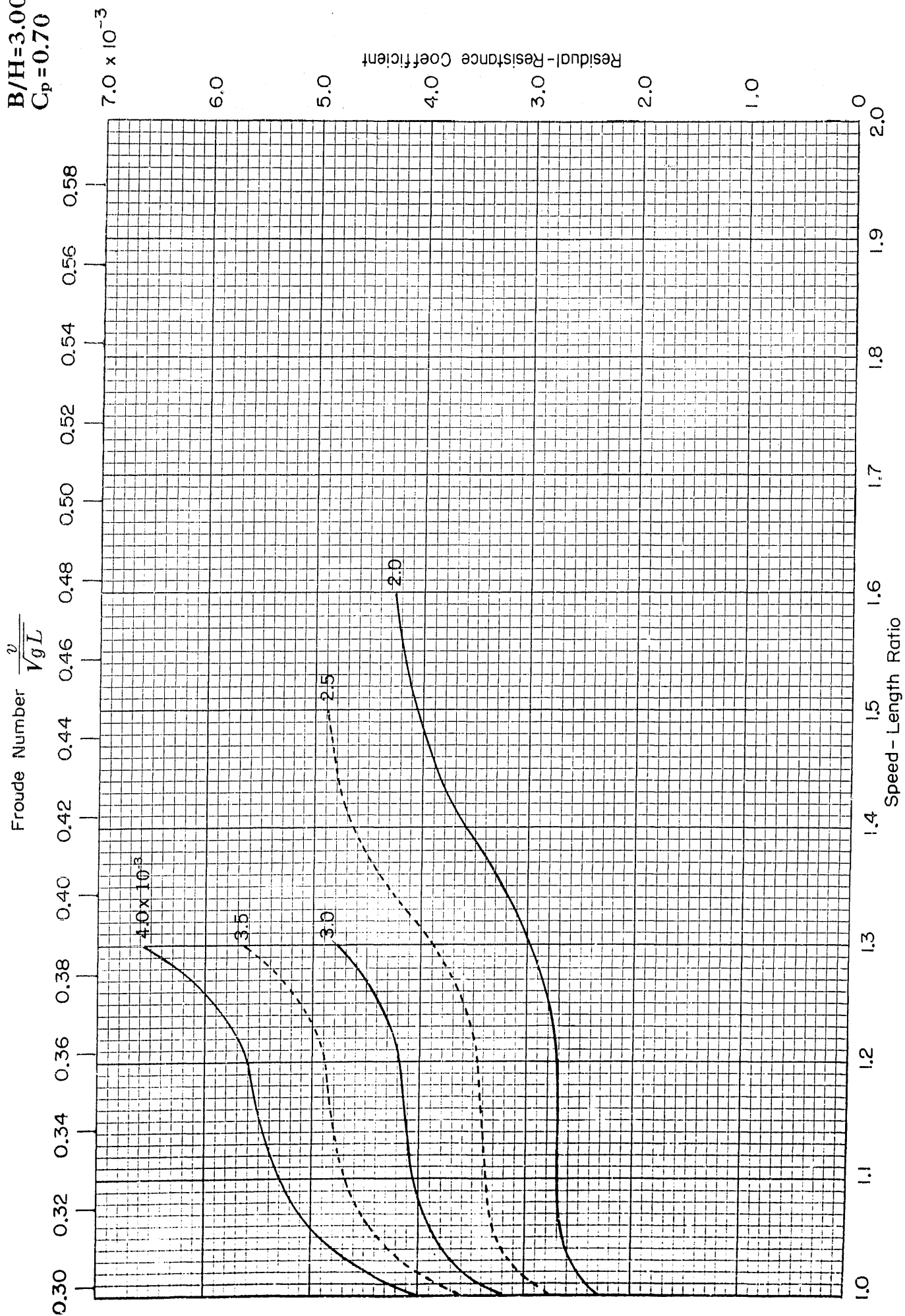
$B/H=3.00$
 $C_p=0.69$



$B/H=3.00$
 $C_p=0.70$



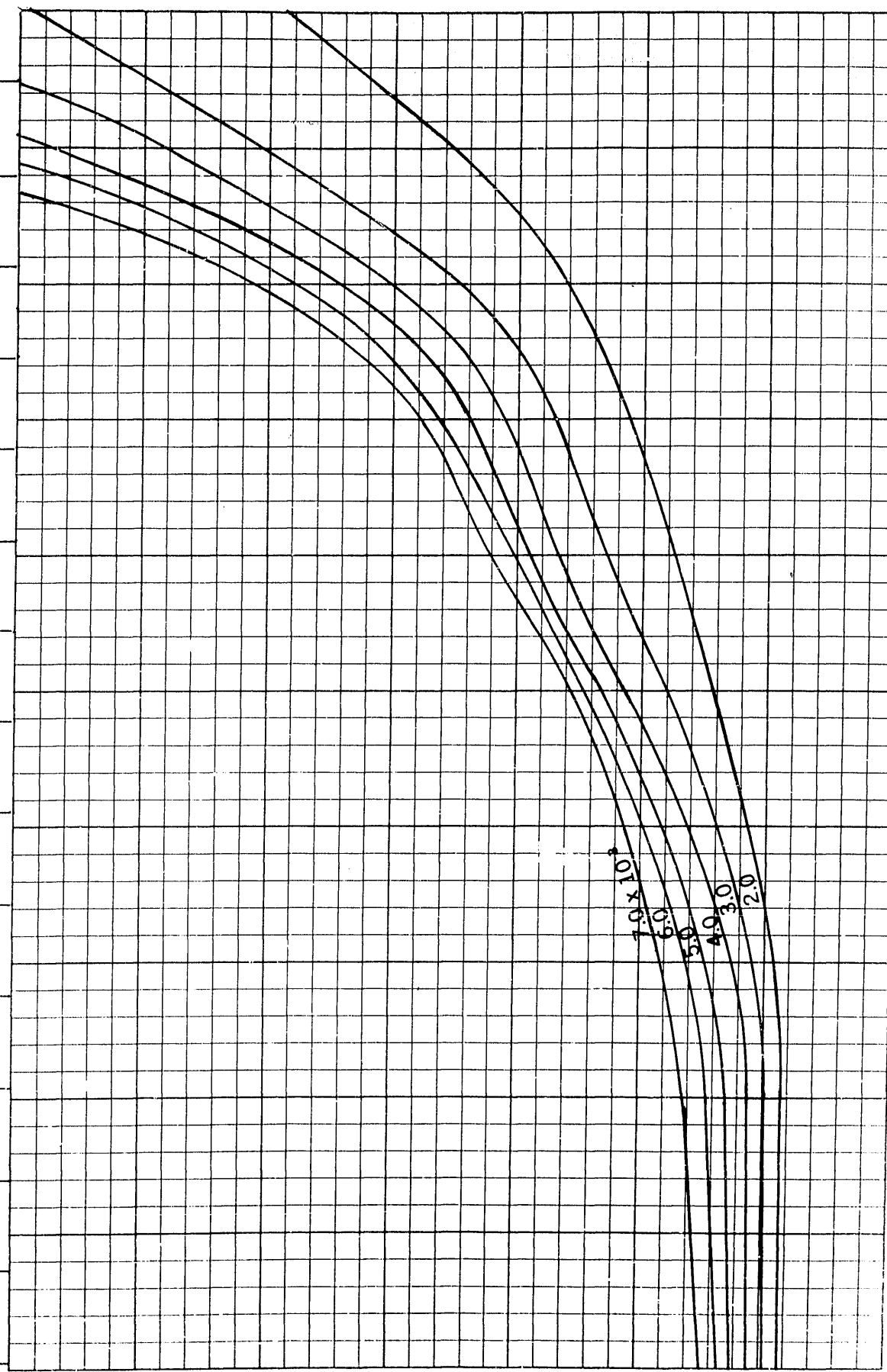
$B/H=3.00$
 $C_p=0.70$



$B/H=3.00$
 $C_p=0.71$

Froude Number $\frac{v}{\sqrt{gL}}$

0.15 0.16 0.17 0.18 0.19 0.20 0.21 0.22 0.23 0.24 0.25 0.26 0.27 0.28 0.29

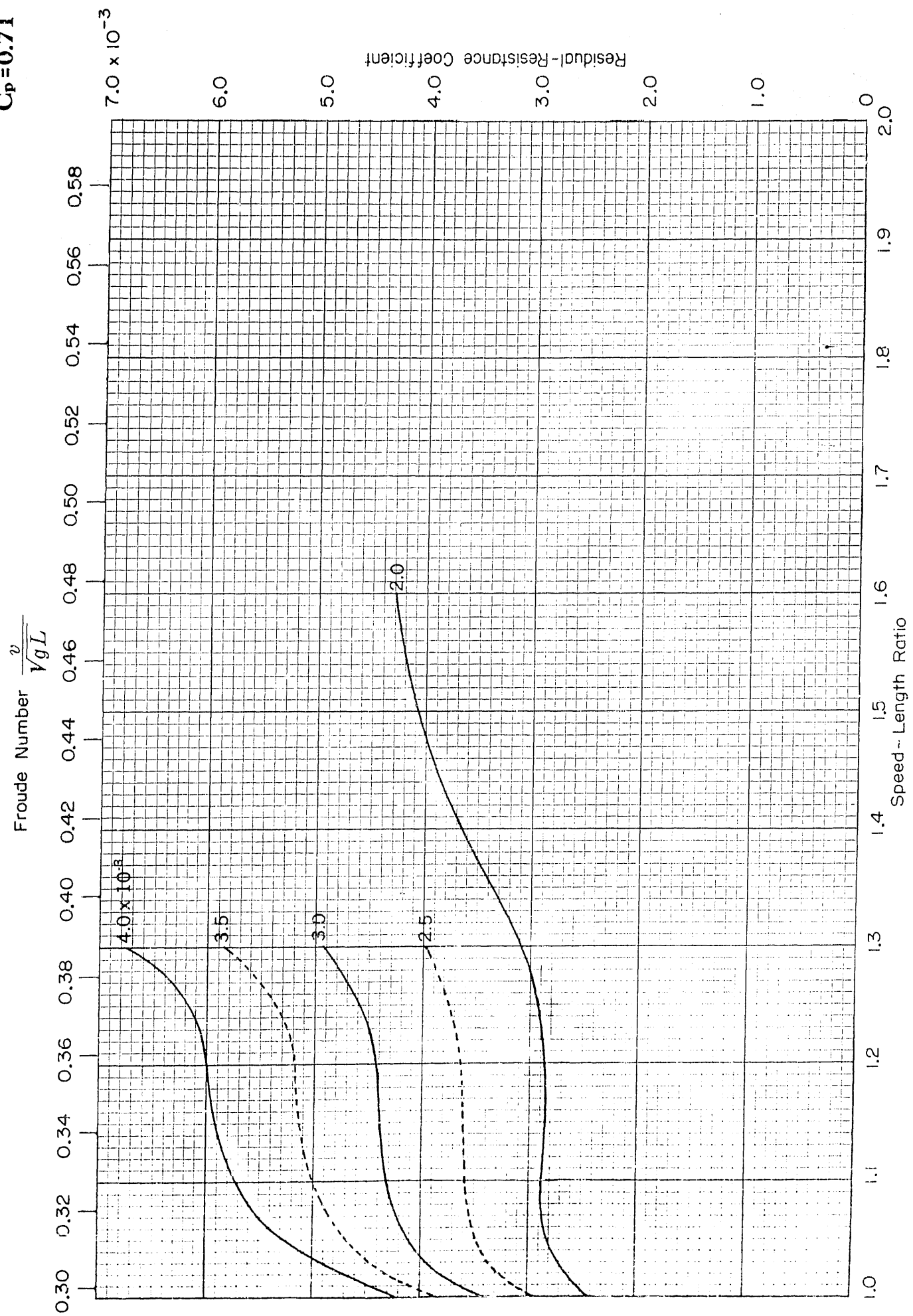


Residual-Resistance Coefficient
 3.0×10^{-3}
 2.0
 1.0

0 1.0 0.9 0.8 0.7 0.6 0.5

Speed - Length Ratio

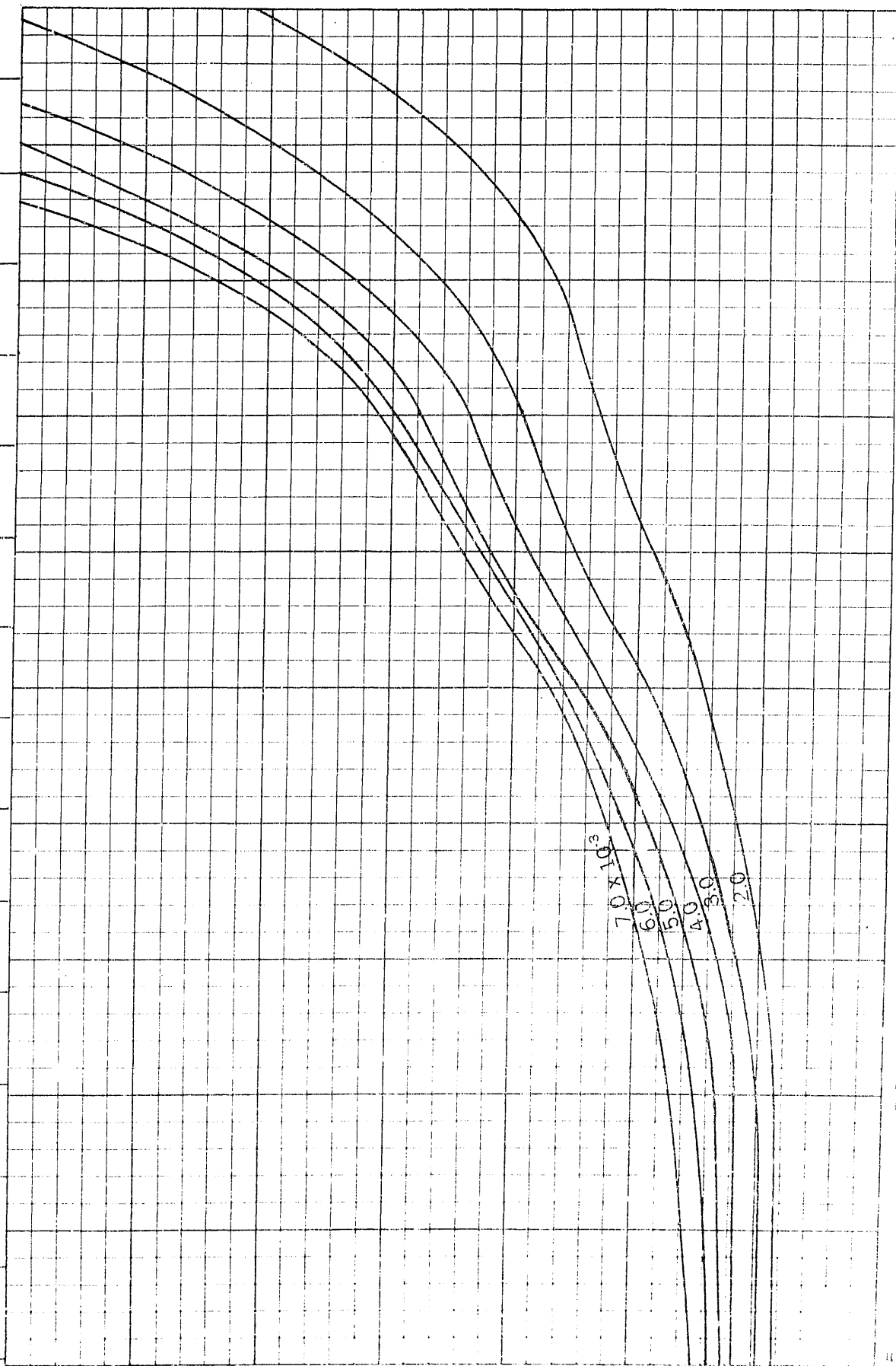
$B/H=3.00$
 $C_p=0.71$



$B/H=3.00$
 $C_p=0.72$

Froude Number $\frac{v}{\sqrt{gL}}$

0.15 0.16 0.17 0.18 0.19 0.20 0.21 0.22 0.23 0.24 0.25 0.26 0.27 0.28 0.29



Residual-Resistance Coefficient

3.0×10^{-3}

0

0.9

0.8

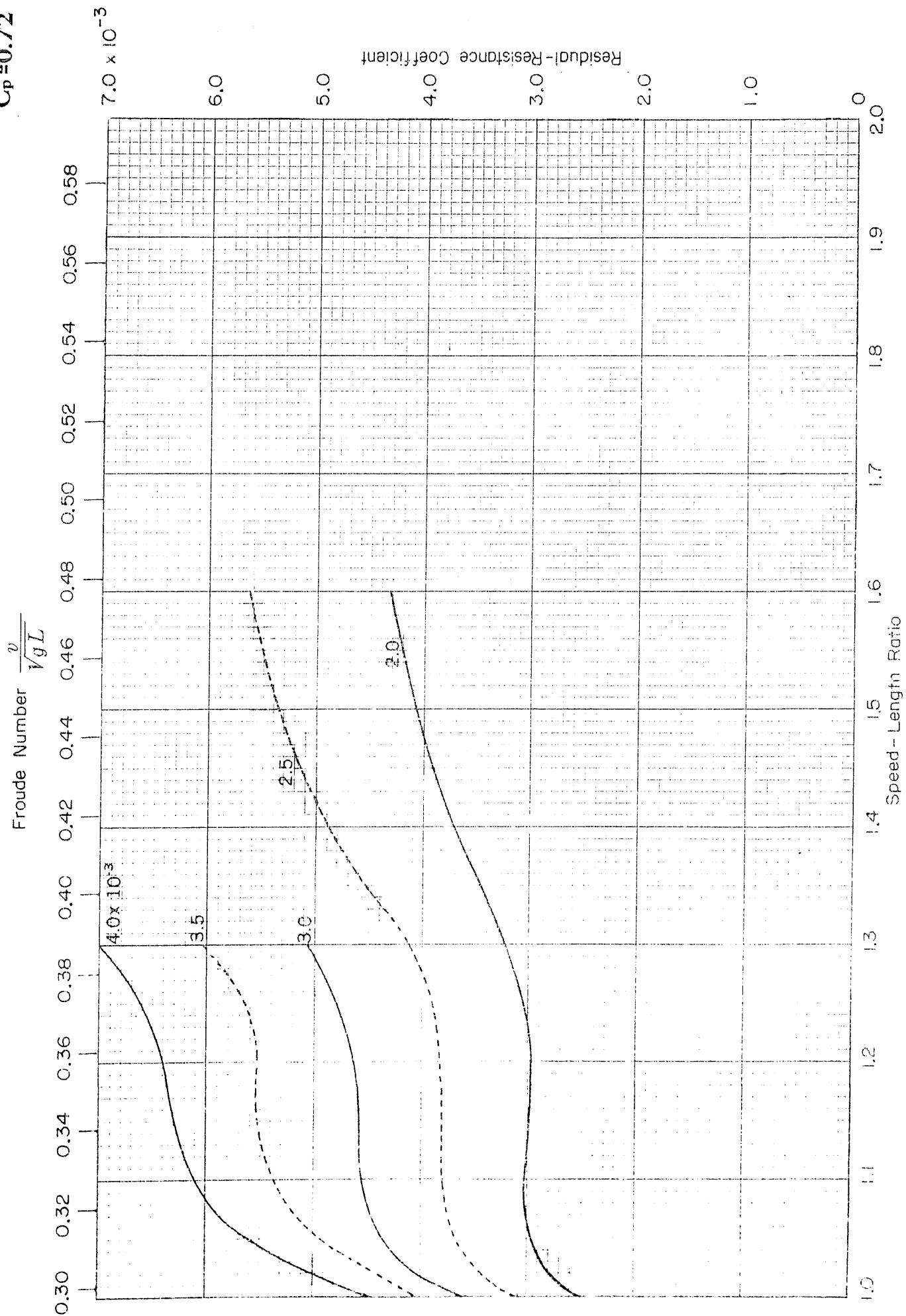
0.7

0.6

0.5

Speed-Length Ratio

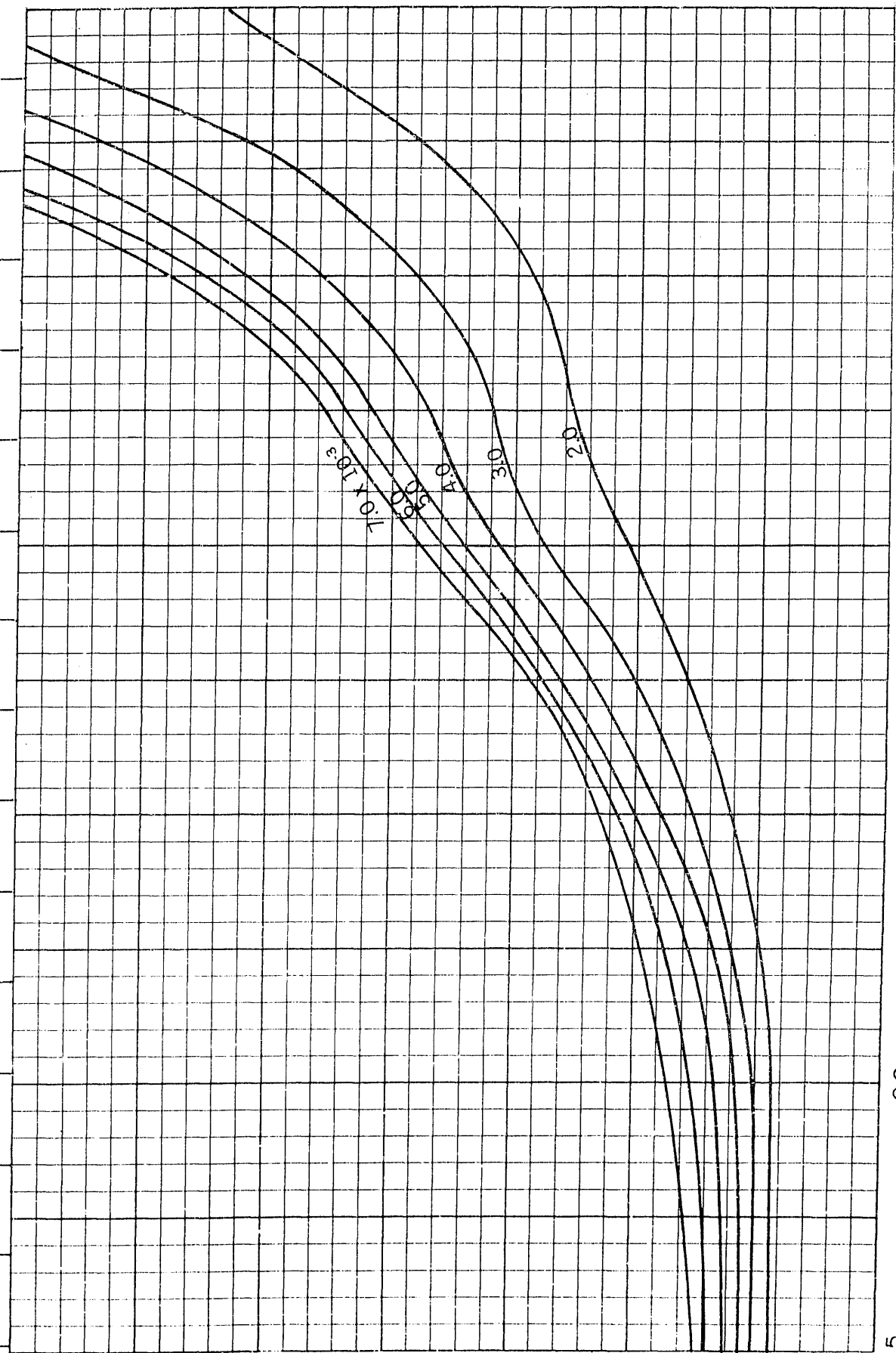
$B/H=3.00$
 $C_p=0.72$



$B/H=3.00$
 $C_p=0.73$

Froude Number $\frac{v}{\sqrt{gL}}$

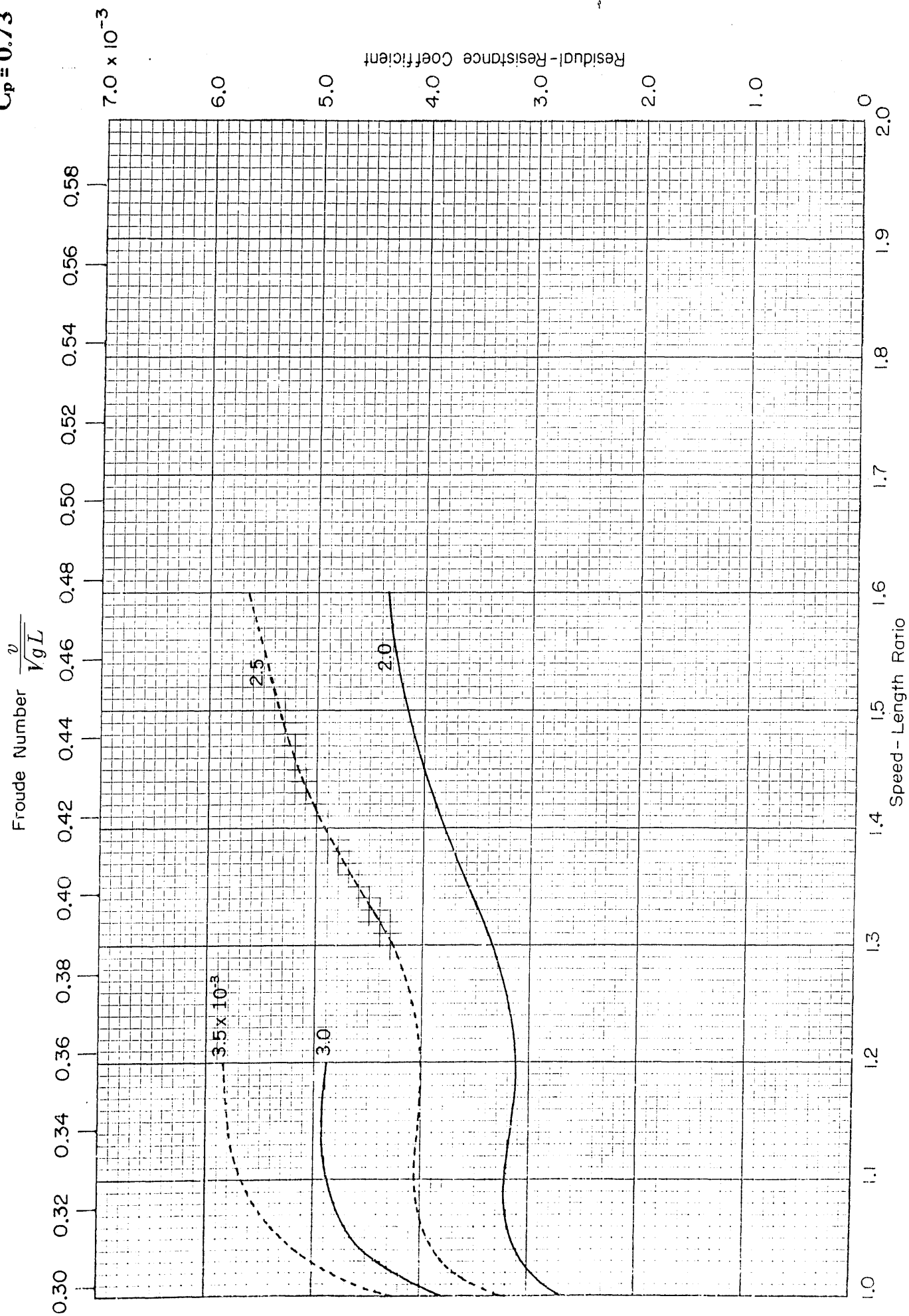
0.15 0.16 0.17 0.18 0.19 0.20 0.21 0.22 0.23 0.24 0.25 0.26 0.27 0.28 0.29



Residual-Resistance Coefficient

0.5 0.6 0.7 0.8 0.9 1.0

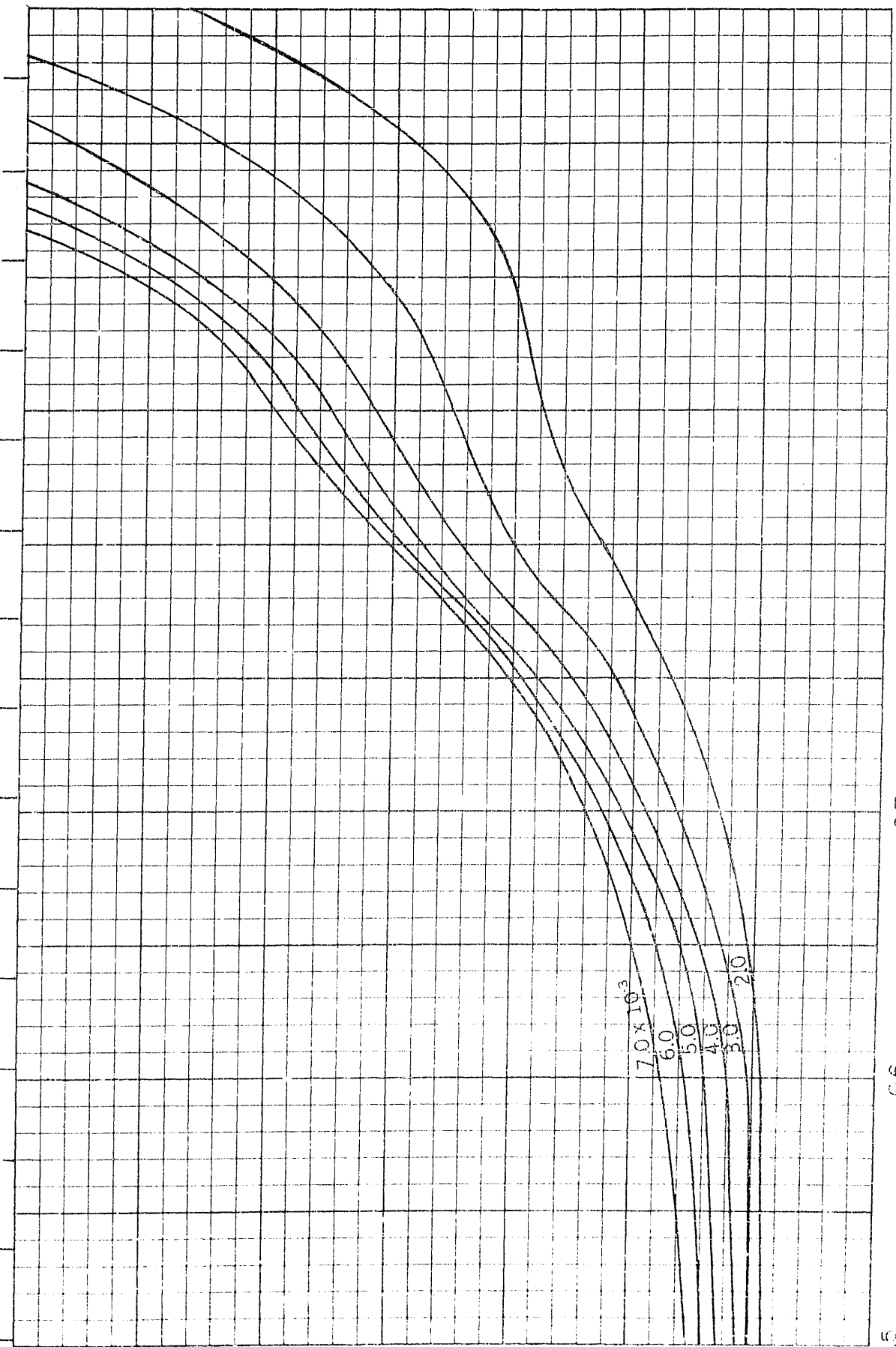
$B/H=3.00$
 $C_p=0.73$



$B/H=3.00$
 $C_p=0.74$

Froude Number $\frac{v}{\sqrt{gL}}$

0.15 0.16 0.17 0.18 0.19 0.20 0.21 0.22 0.23 0.24 0.25 0.26 0.27 0.28 0.29

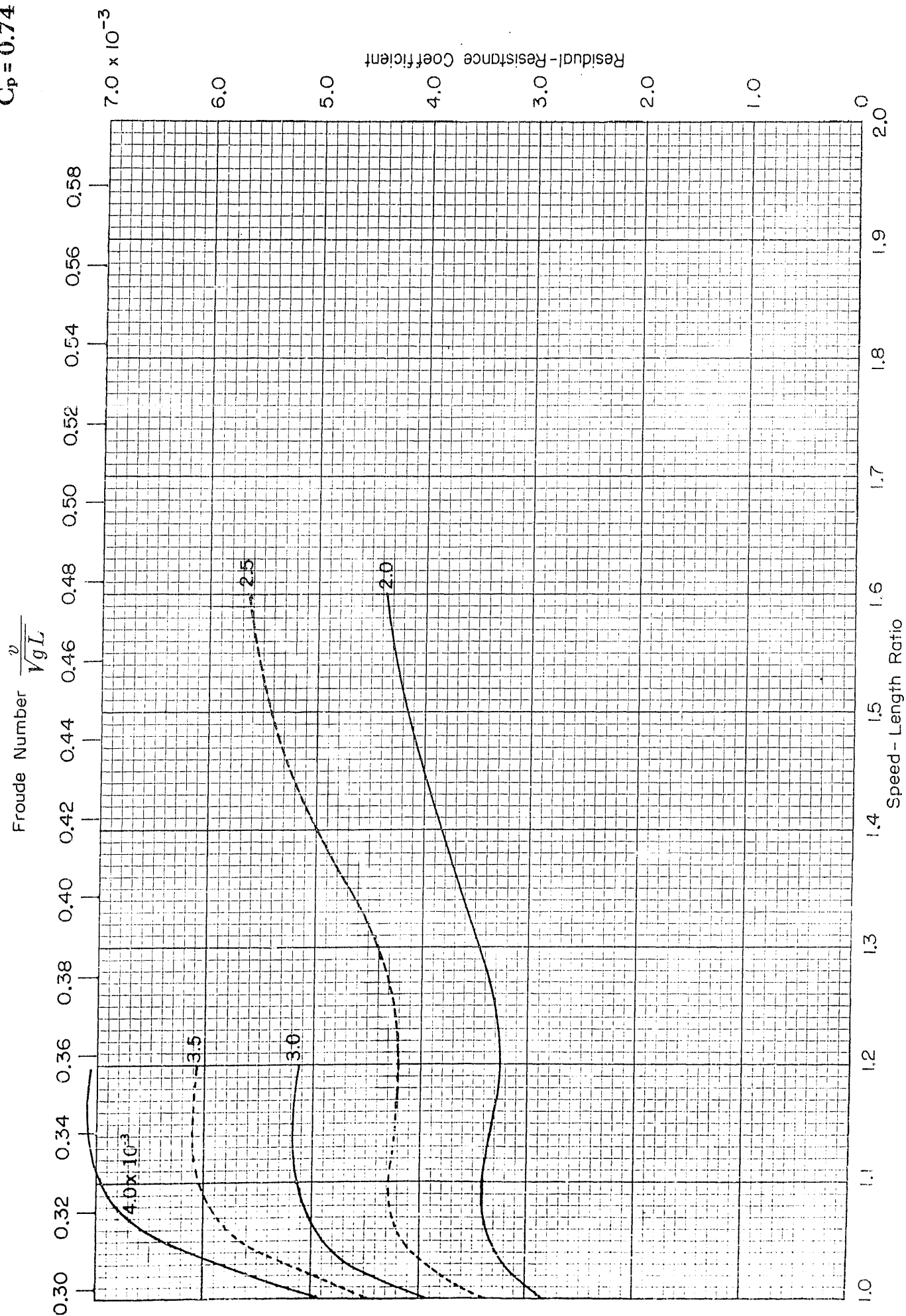


Residual-Resistance Coefficient

0.5 0.6 0.7 0.8 0.9 1.0

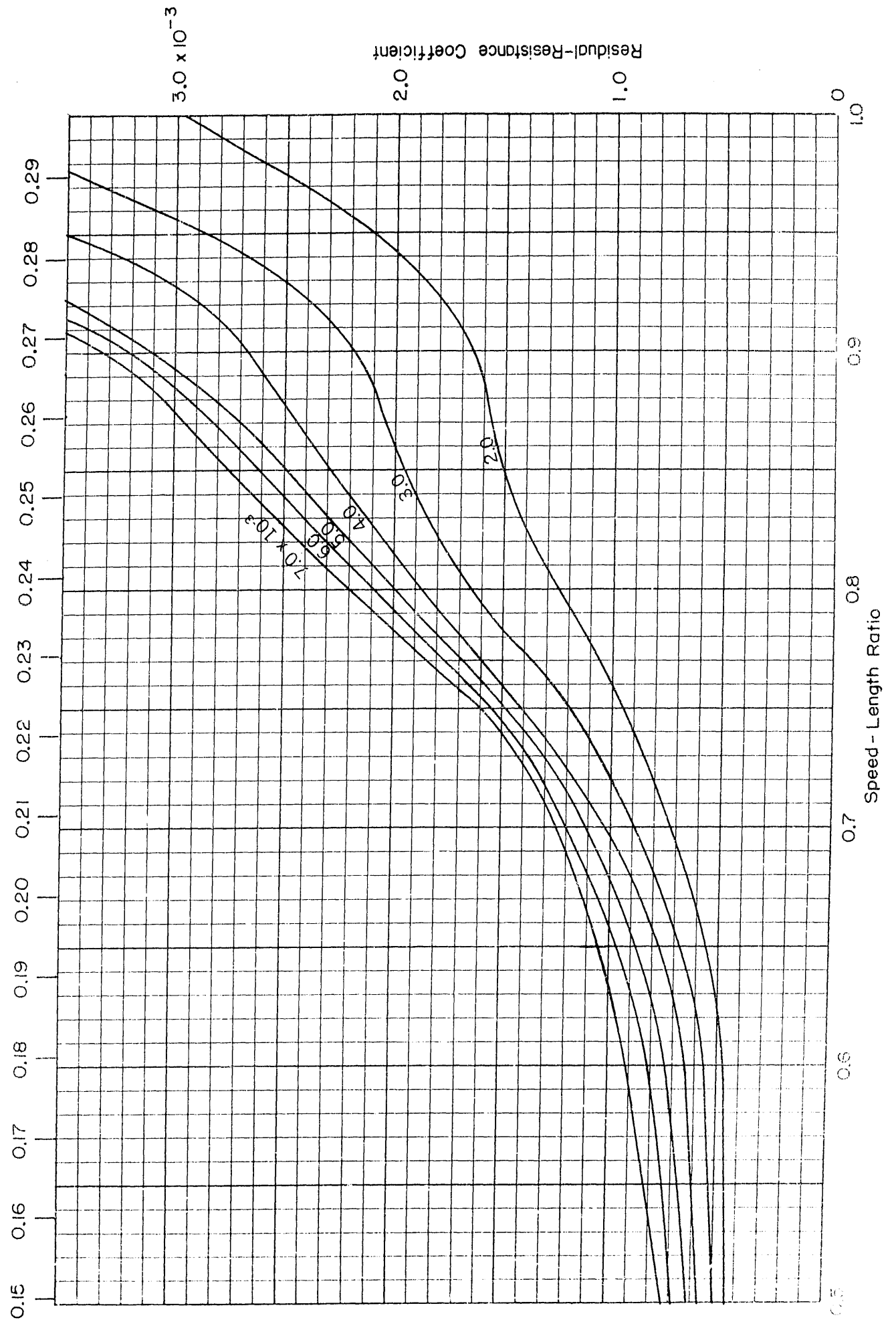
Speed - Length Ratio

$B/H=3.00$
 $C_p=0.74$

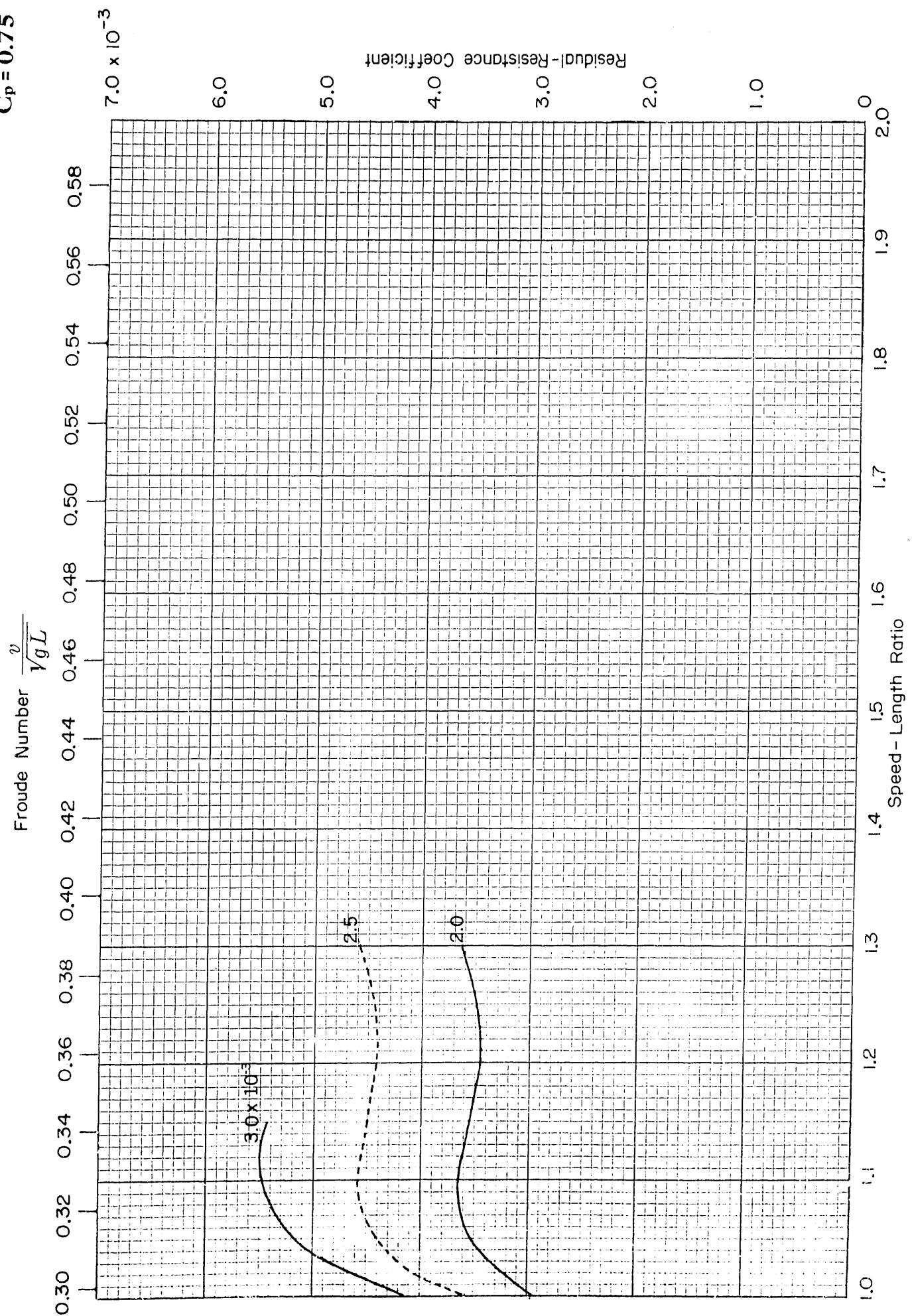


$B/H=3.00$
 $C_p=0.75$

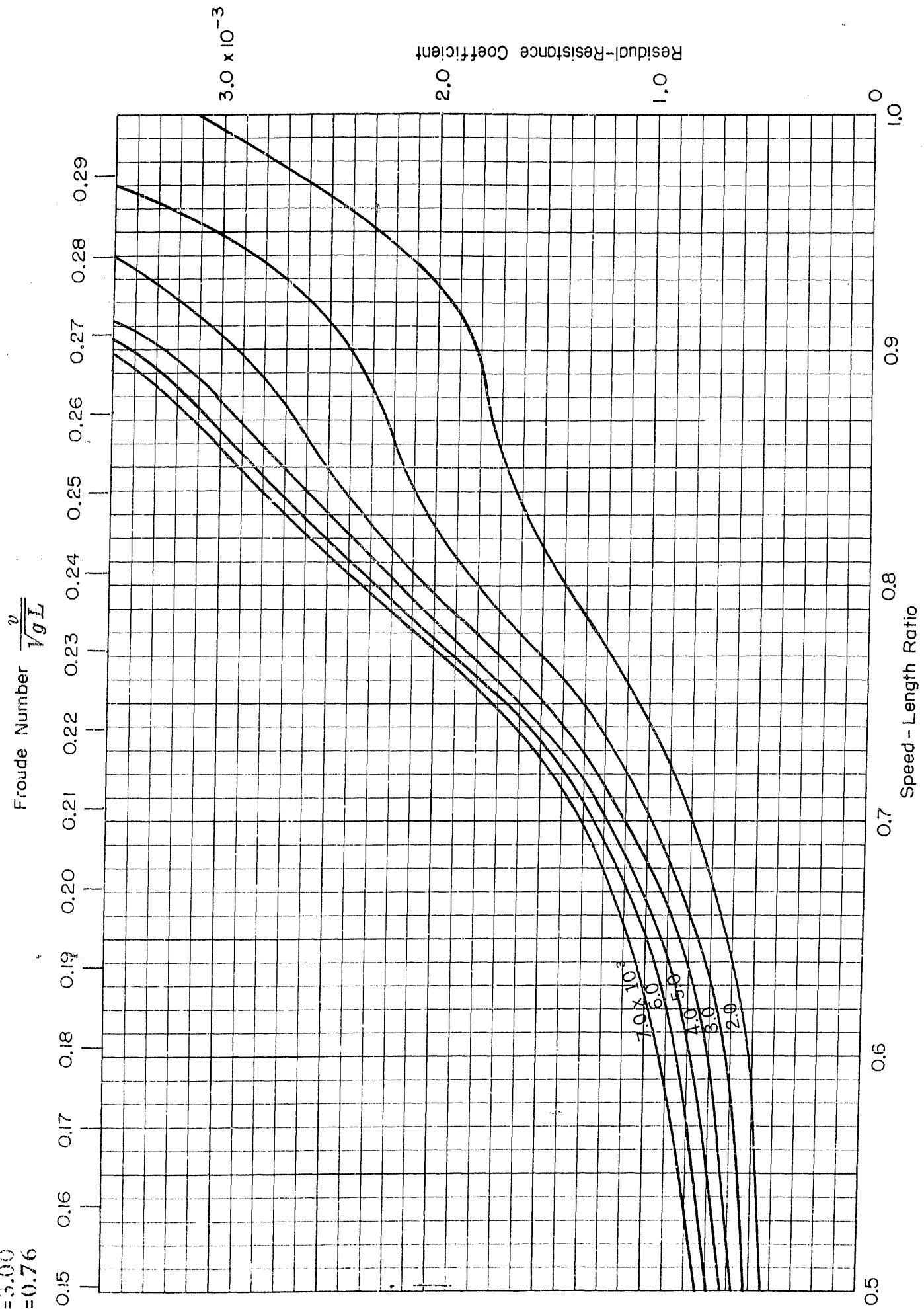
Froude Number $\frac{v}{\sqrt{gL}}$



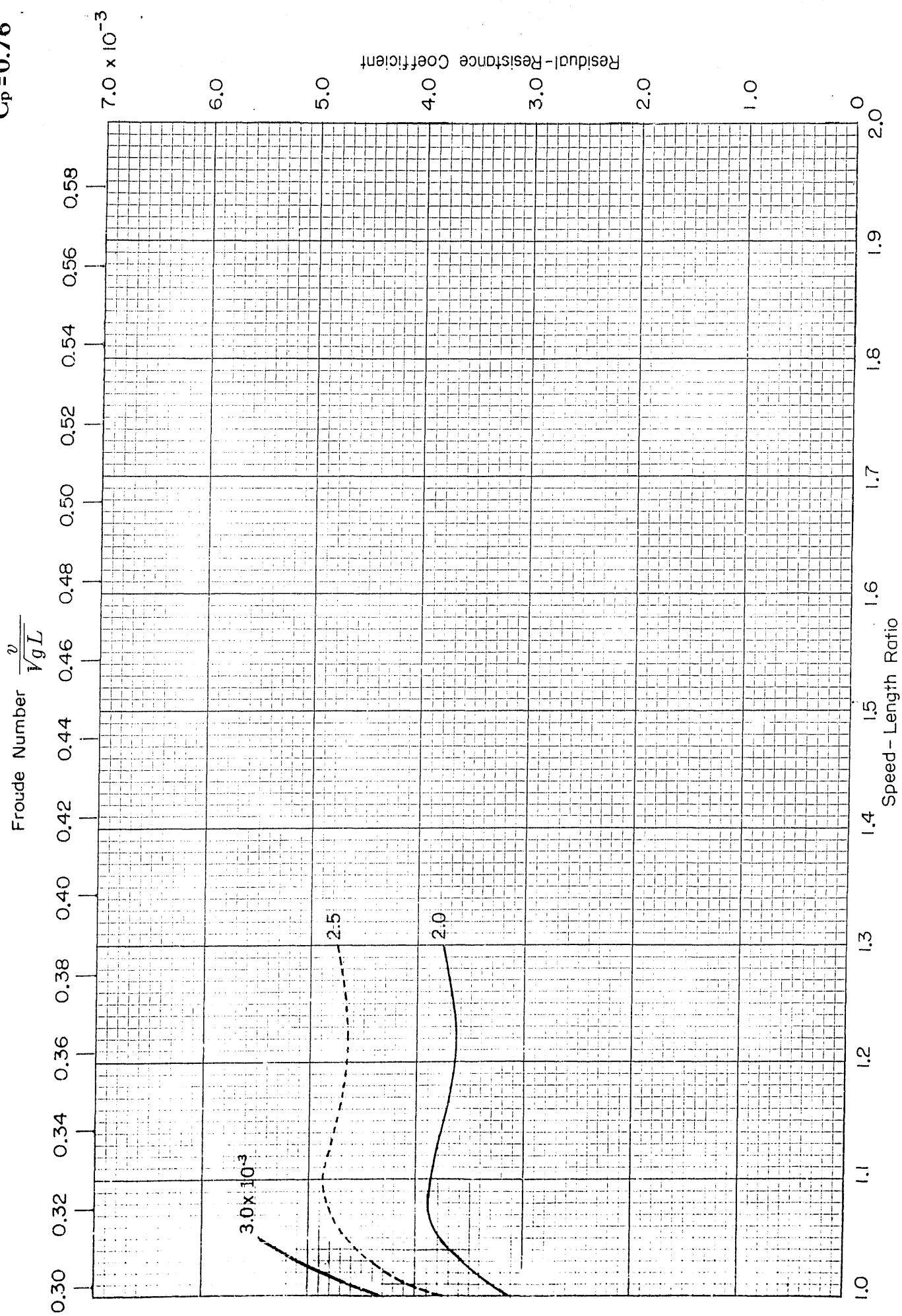
$B/H=3.00$
 $C_p=0.75$



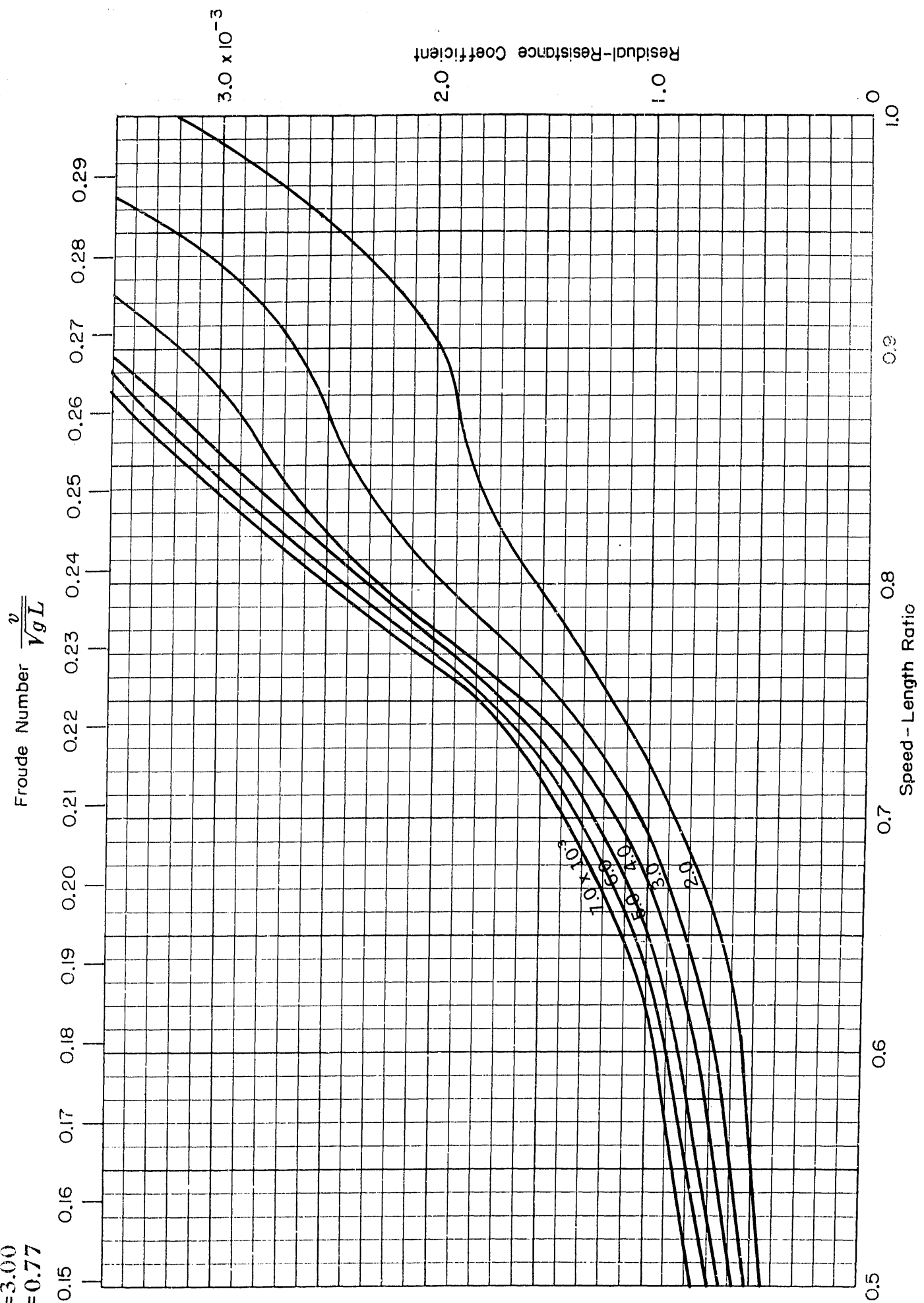
$B/H=3.00$
 $C_p=0.76$



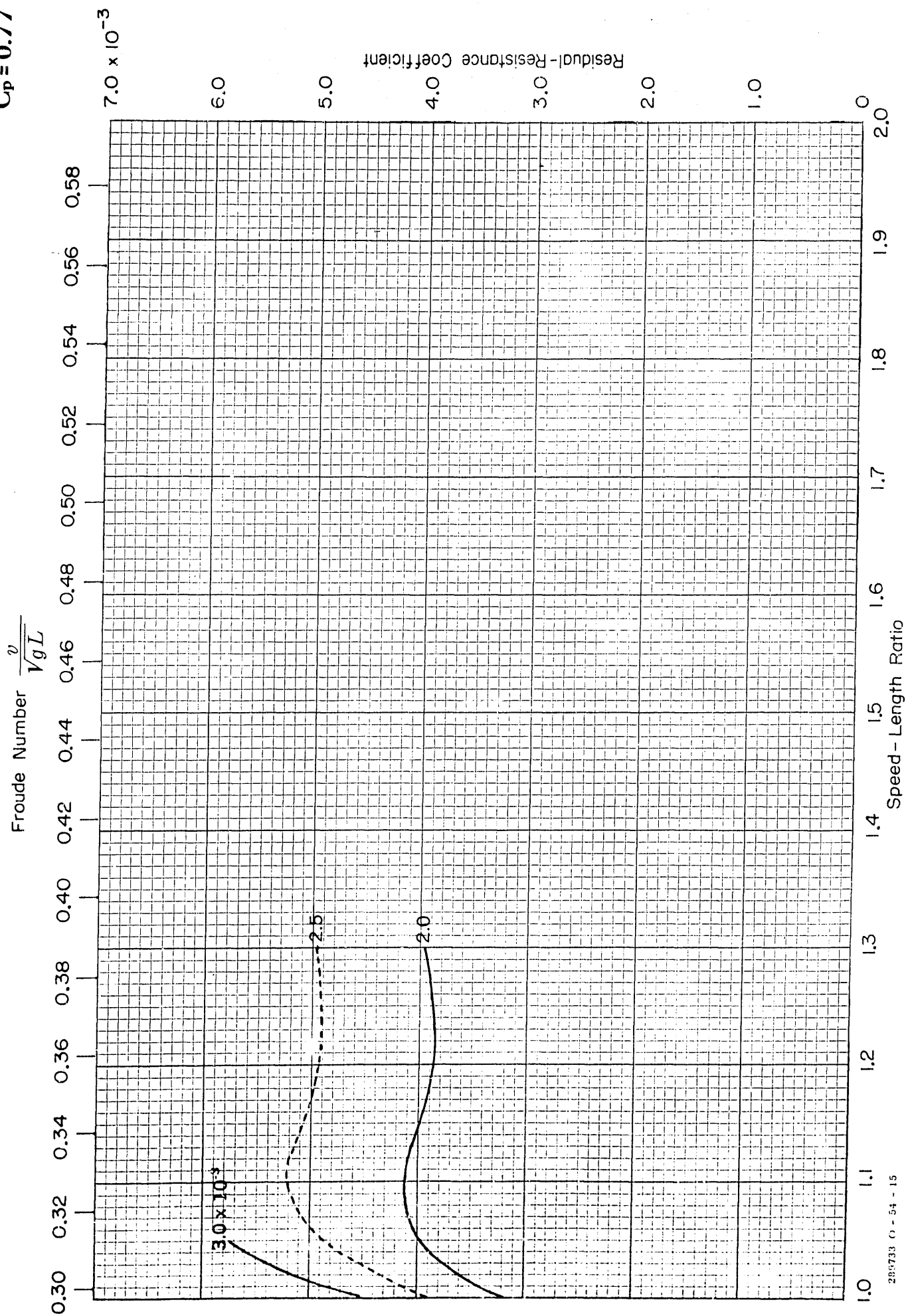
$B/H=3.00$
 $C_p=0.76$



$B/H=3.00$
 $C_p=0.77$



$B/H = 3.00$
 $C_p = 0.77$



$B/H=3.00$
 $C_p=0.78$

Froude Number $\frac{v}{\sqrt{gL}}$

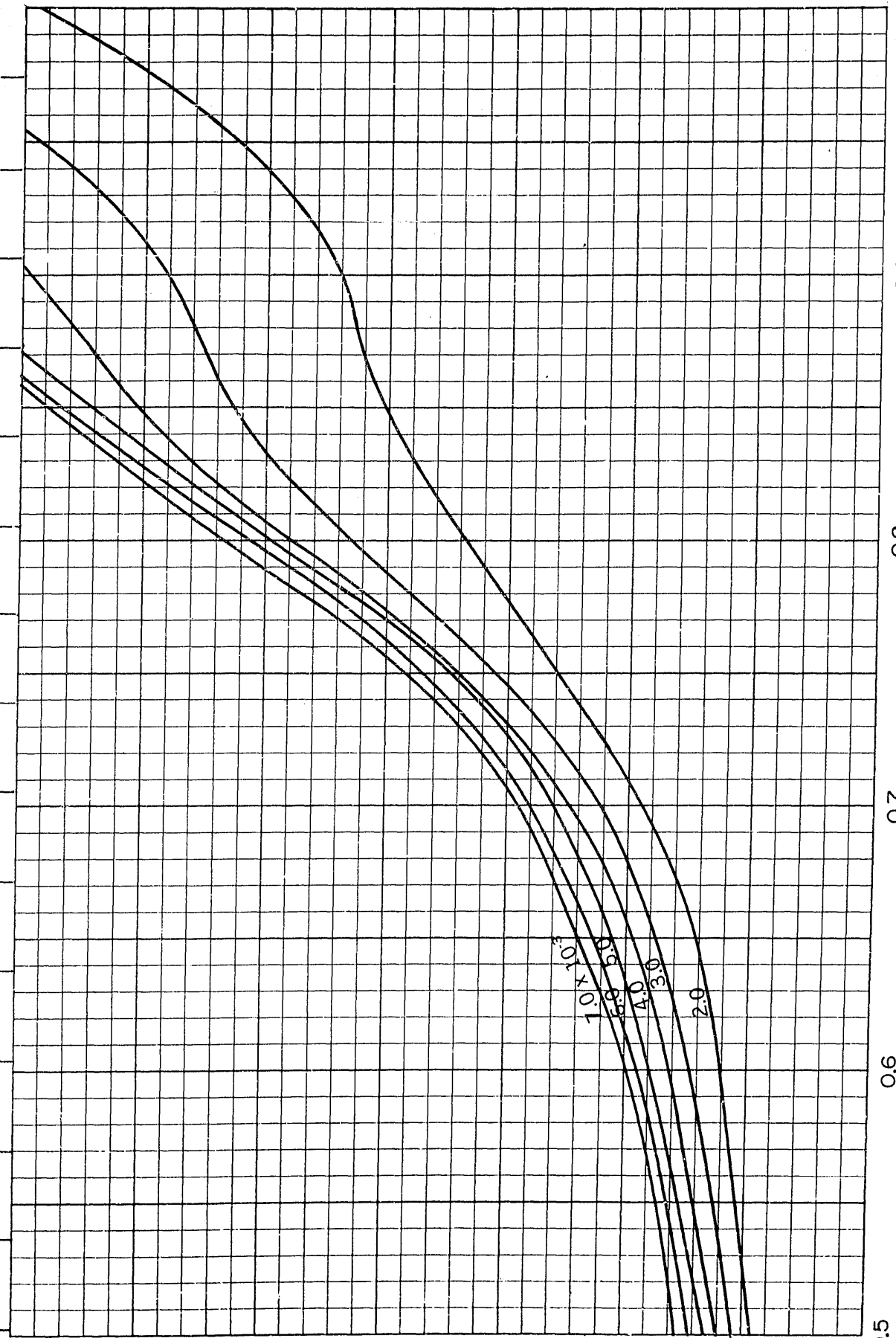
0.15 0.16 0.17 0.18 0.19 0.20 0.21 0.22 0.23 0.24 0.25 0.26 0.27 0.28 0.29

0.5 0.6 0.7 0.8 0.9 1.0

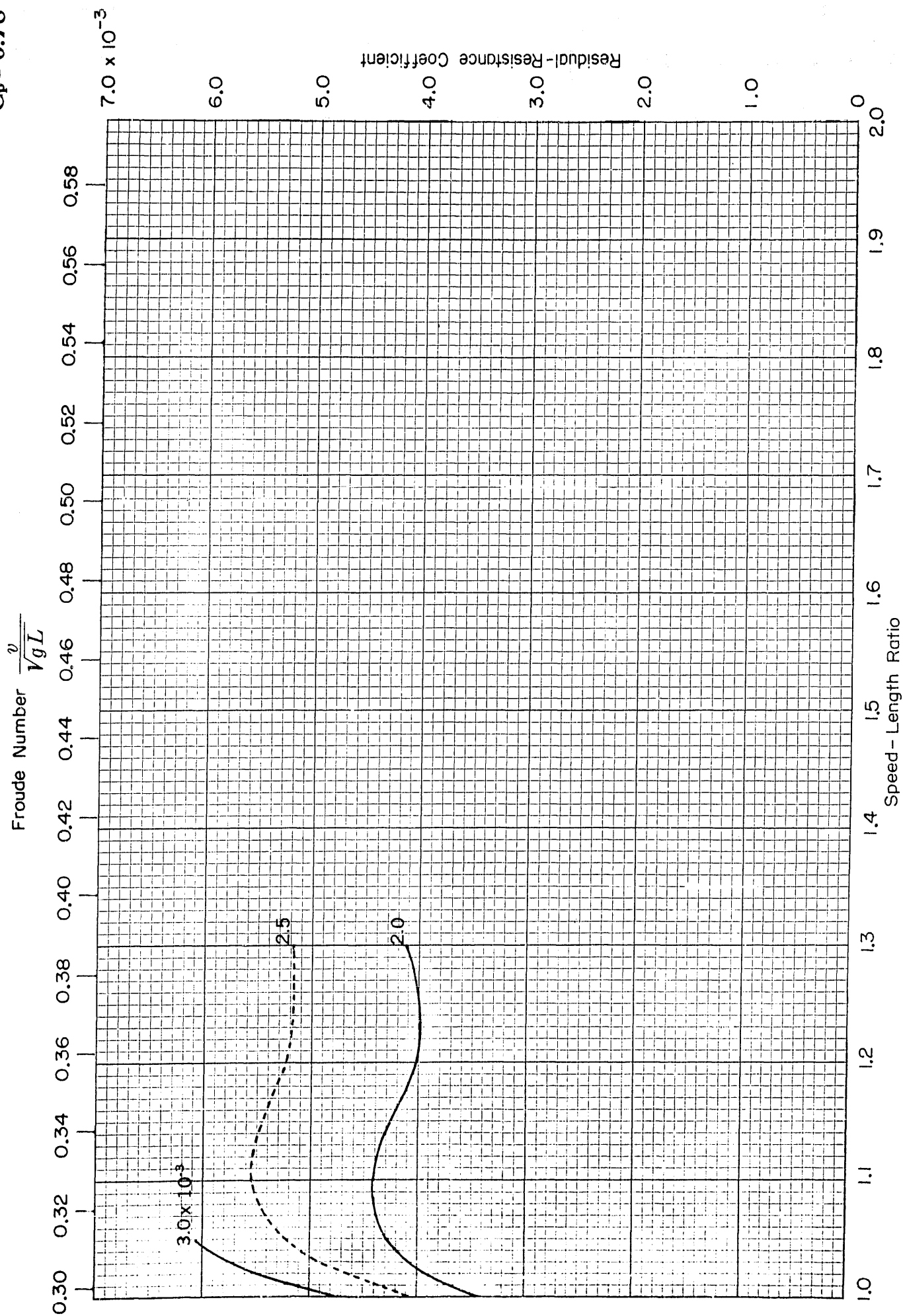
Speed - Length Ratio

Residual-Resistance Coefficient

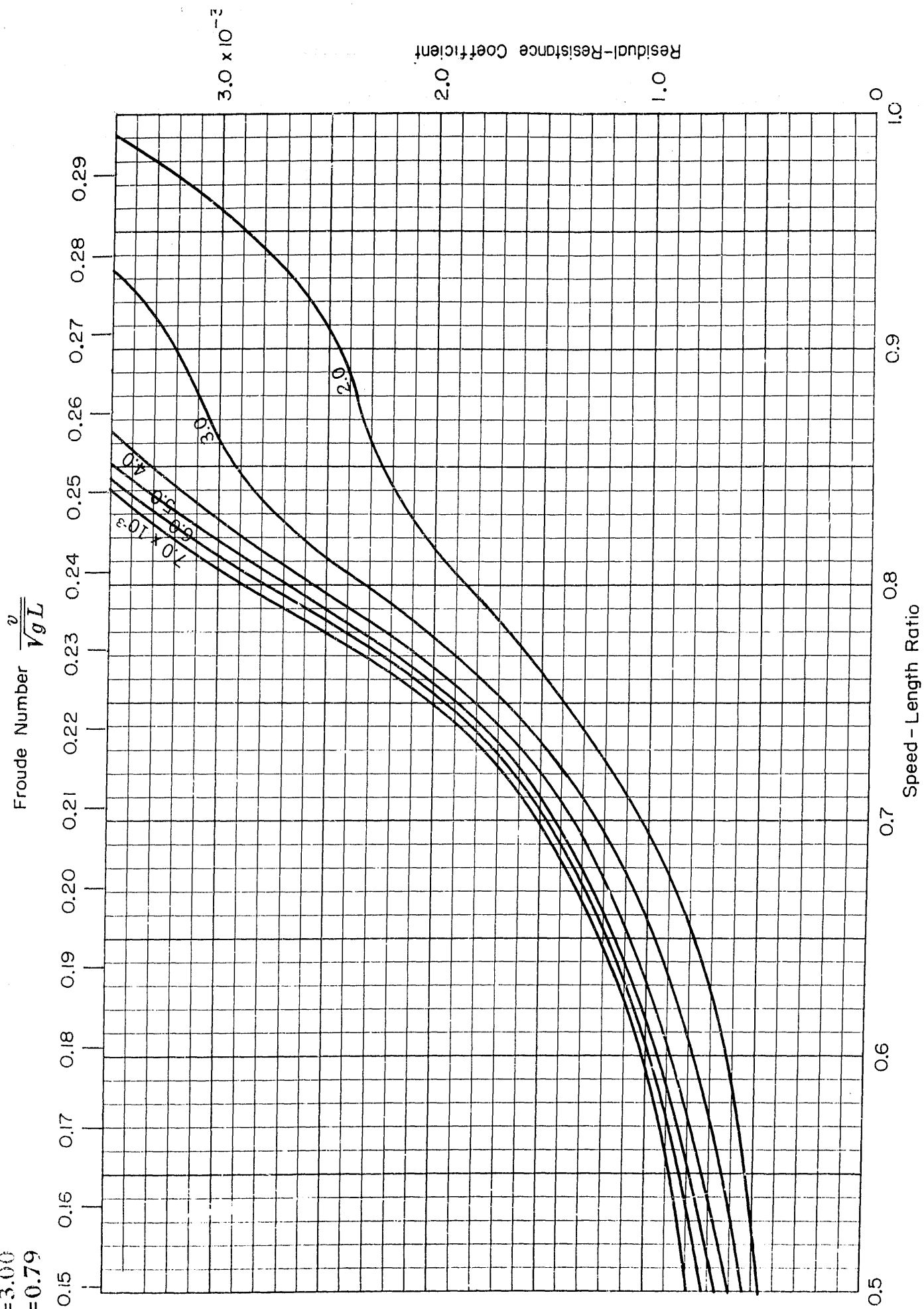
3.0×10^{-3}



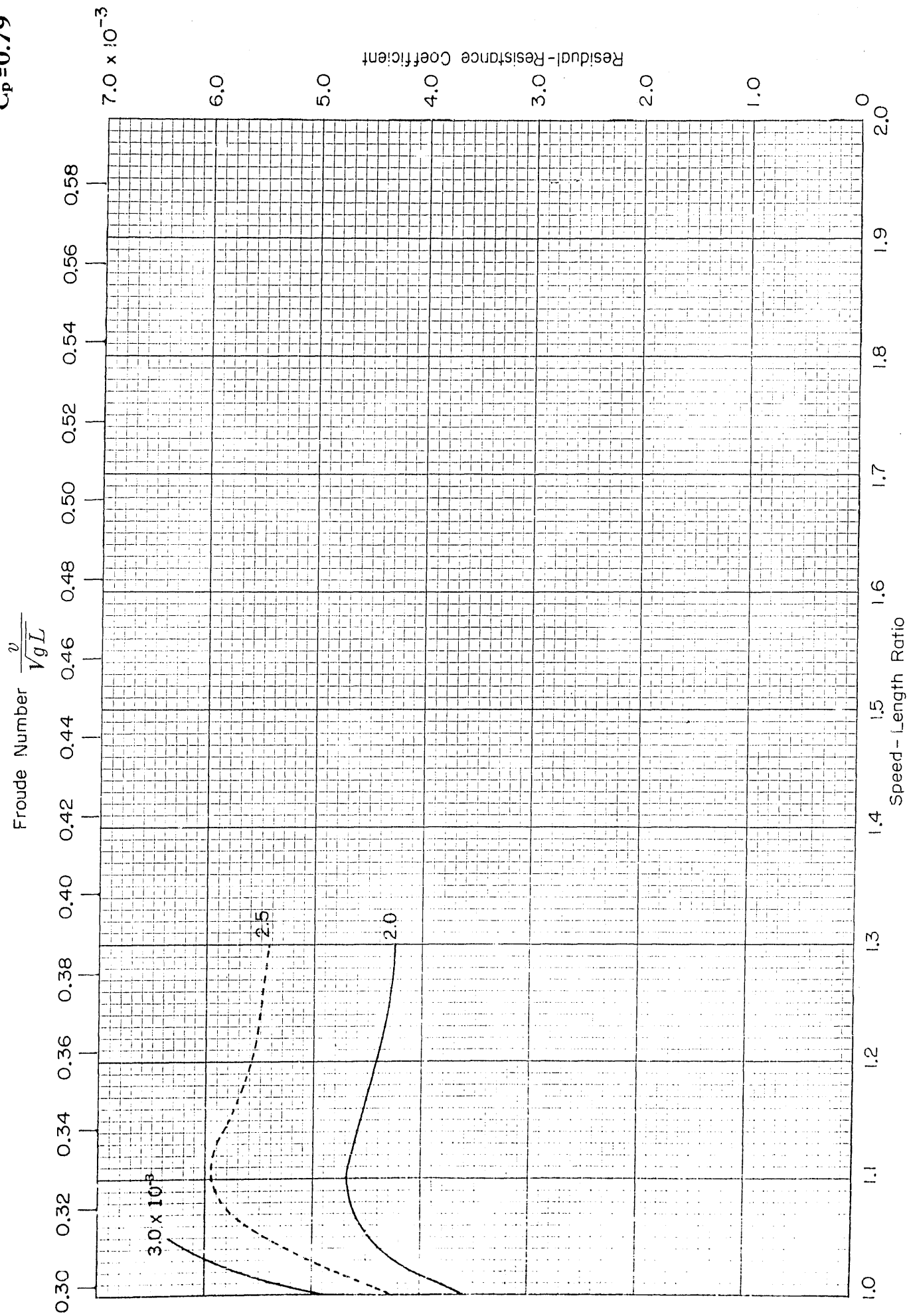
$B/H=3.00$
 $C_p=0.78$



$B/H = 3.00$
 $C_p = 0.79$



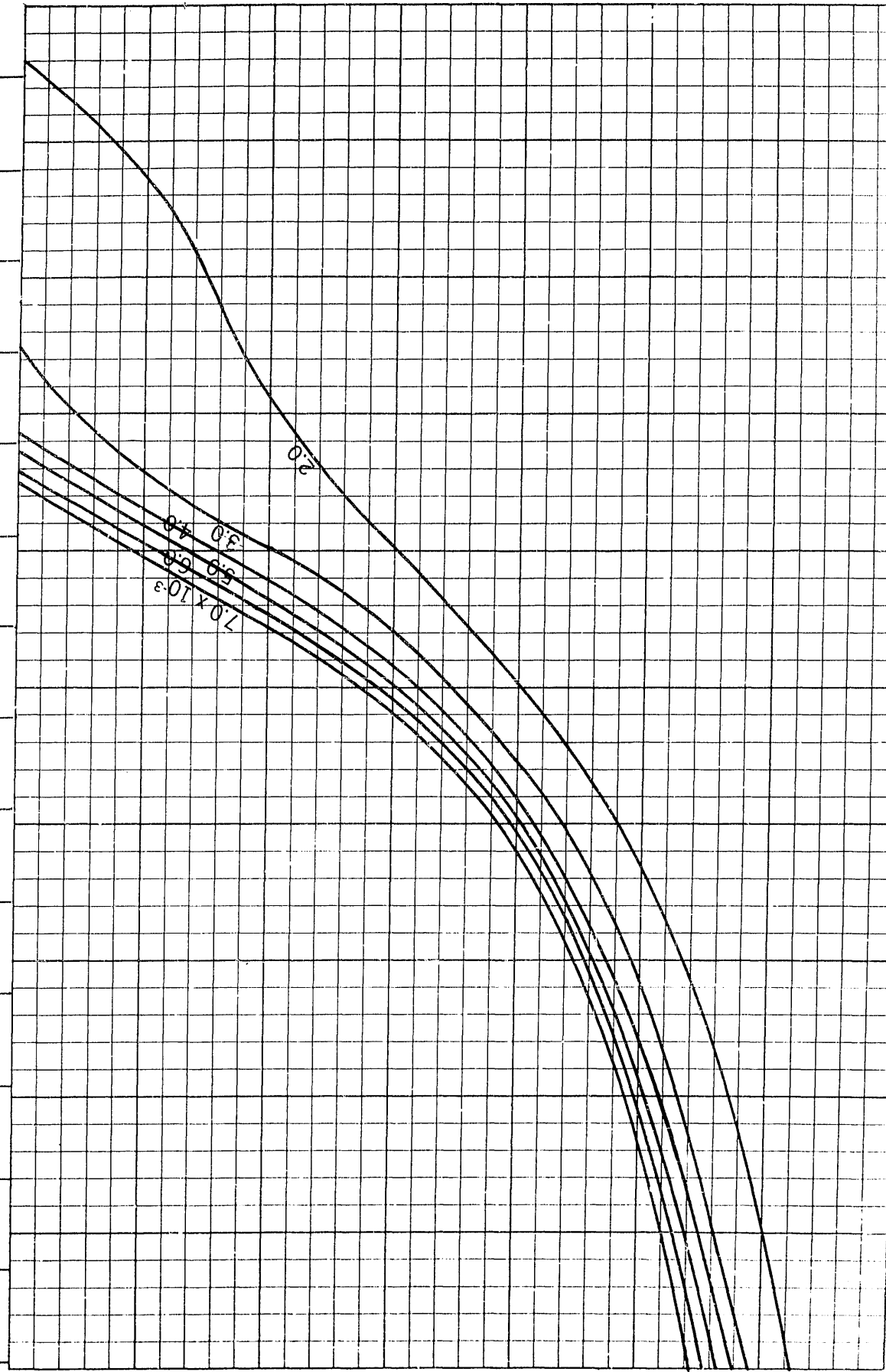
$B/H=3.00$
 $C_p=0.79$



$B/H=3.00$
 $C_p=0.80$

Froude Number $\frac{v}{\sqrt{gL}}$

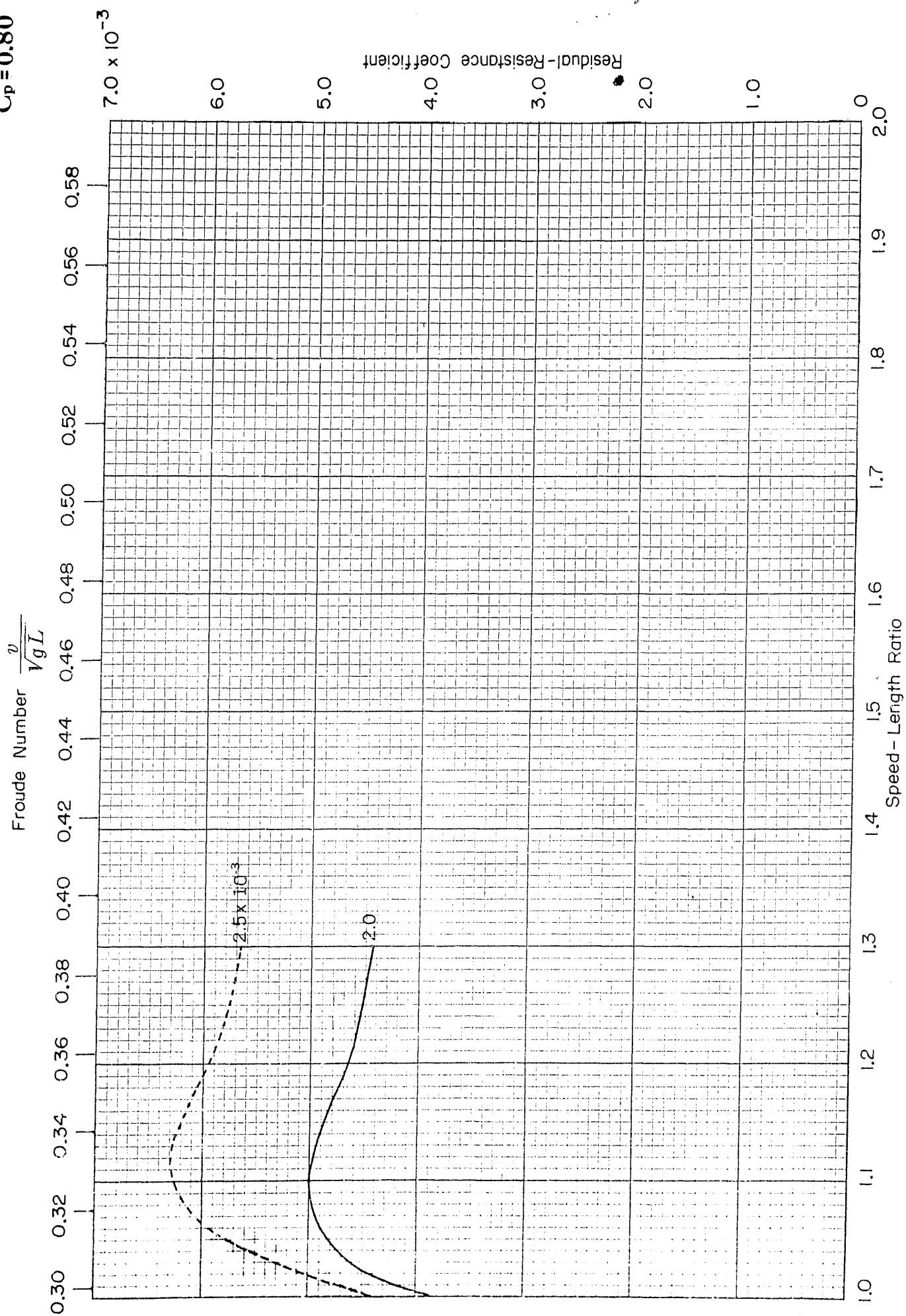
0.15 0.16 0.17 0.18 0.19 0.20 0.21 0.22 0.23 0.24 0.25 0.26 0.27 0.28 0.29



0.5 0.6 0.7 0.8 0.9 1.0

3.0 x 10⁻³
2.0
1.0

$B/H=3.00$
 $C_p=0.80$



APPENDIX 5

CURVES OF RESIDUAL-RESISTANCE COEFFICIENT VERSUS SPEED-LENGTH RATIO AND FROUDE NUMBER FOR STANDARD SERIES VESSELS HAVING A BEAM-DRAFT RATIO OF 3.75

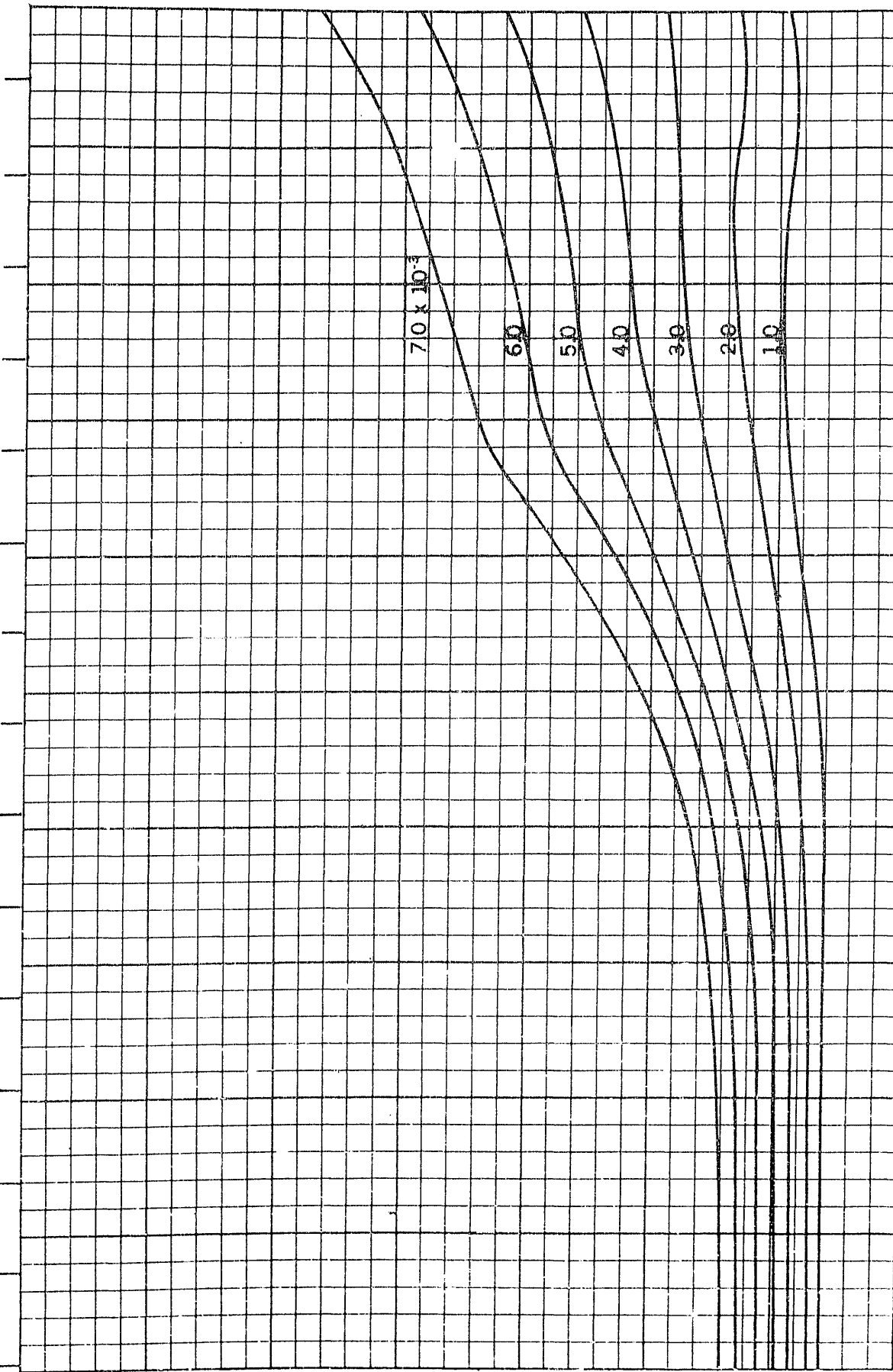
The curves of residual-resistance coefficients for even values of volumetric coefficient are presented separately for each longitudinal prismatic coefficient between 0.48 and 0.86 in increments of 0.01. For each family of curves, ranges of speed-length ratios of 0.5 to 1.0 and 1.0 to 2.0 are given on adjacent pages. The scale divisions, for both ordinate and abscissa, at the lower speed-length ratios are twice as large as those of the higher range to permit increased accuracy of reading.

A supplementary table of residual-resistance coefficients is given for those coefficients which are not constant below a speed-length ratio of 0.50.

$B/H=3.75$
 $C_p=0.48$

Froude Number $\frac{v}{\sqrt{gL}}$

0.15 0.16 0.17 0.18 0.19 0.20 0.21 0.22 0.23 0.24 0.25 0.26 0.27 0.28 0.29



Residual-Resistance Coefficient

3.0×10^{-3}

0.5 0.6 0.7 0.8 0.9 1.0

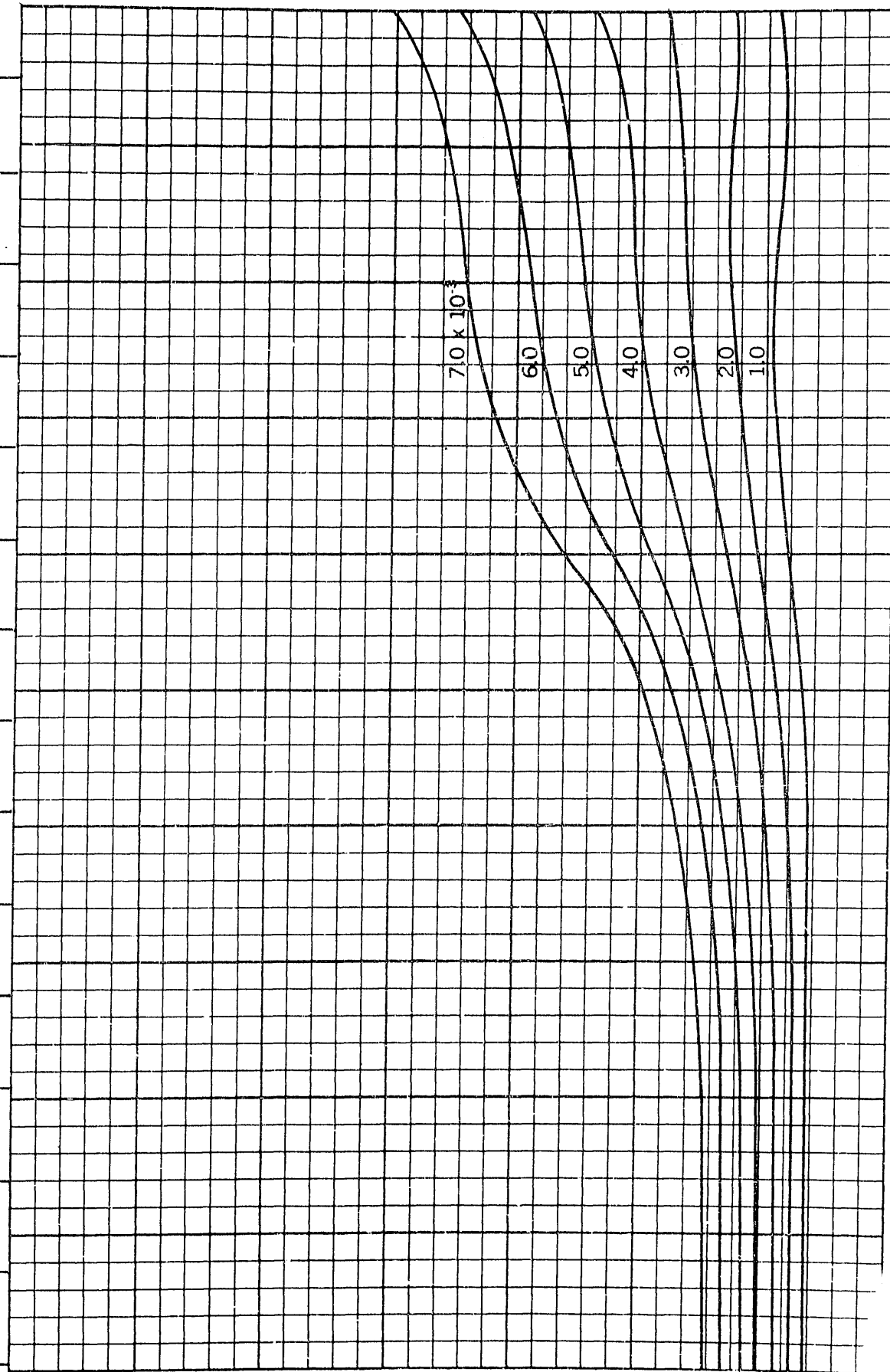
Speed-Length Ratio

This graph plots the Froude Number ($\frac{v}{\sqrt{gL}}$) on the vertical axis against the Speed-Length Ratio on the horizontal axis. The vertical axis ranges from 0.30 to 0.70 with major ticks every 0.02 and minor ticks every 0.005. The horizontal axis ranges from 1.0 to 2.0 with major ticks every 0.1 and minor ticks every 0.02. A series of curves are plotted, each corresponding to a specific Residual-Resistance Coefficient. The curves are labeled with their respective values: 1.0, 1.5, 2.0, 2.5, 3.0, 3.5, 4.0, 4.5, 5.0, 5.5, 6.0, 6.5, 7.0, and 7.5. The curves show that for a given speed-length ratio, the Froude number decreases as the residual-resistance coefficient increases. Conversely, for a given Froude number, the speed-length ratio increases with a higher residual-resistance coefficient.

$B/H=3.75$
 $C_p=0.49$

Froude Number $\frac{v}{\sqrt{gL}}$

0.15 0.16 0.17 0.18 0.19 0.20 0.21 0.22 0.23 0.24 0.25 0.26 0.27 0.28 0.29



Residual-Resistance Coefficient

3.0×10^{-3}

70×10^{-3}

60

50

40

30

20

10

0.6

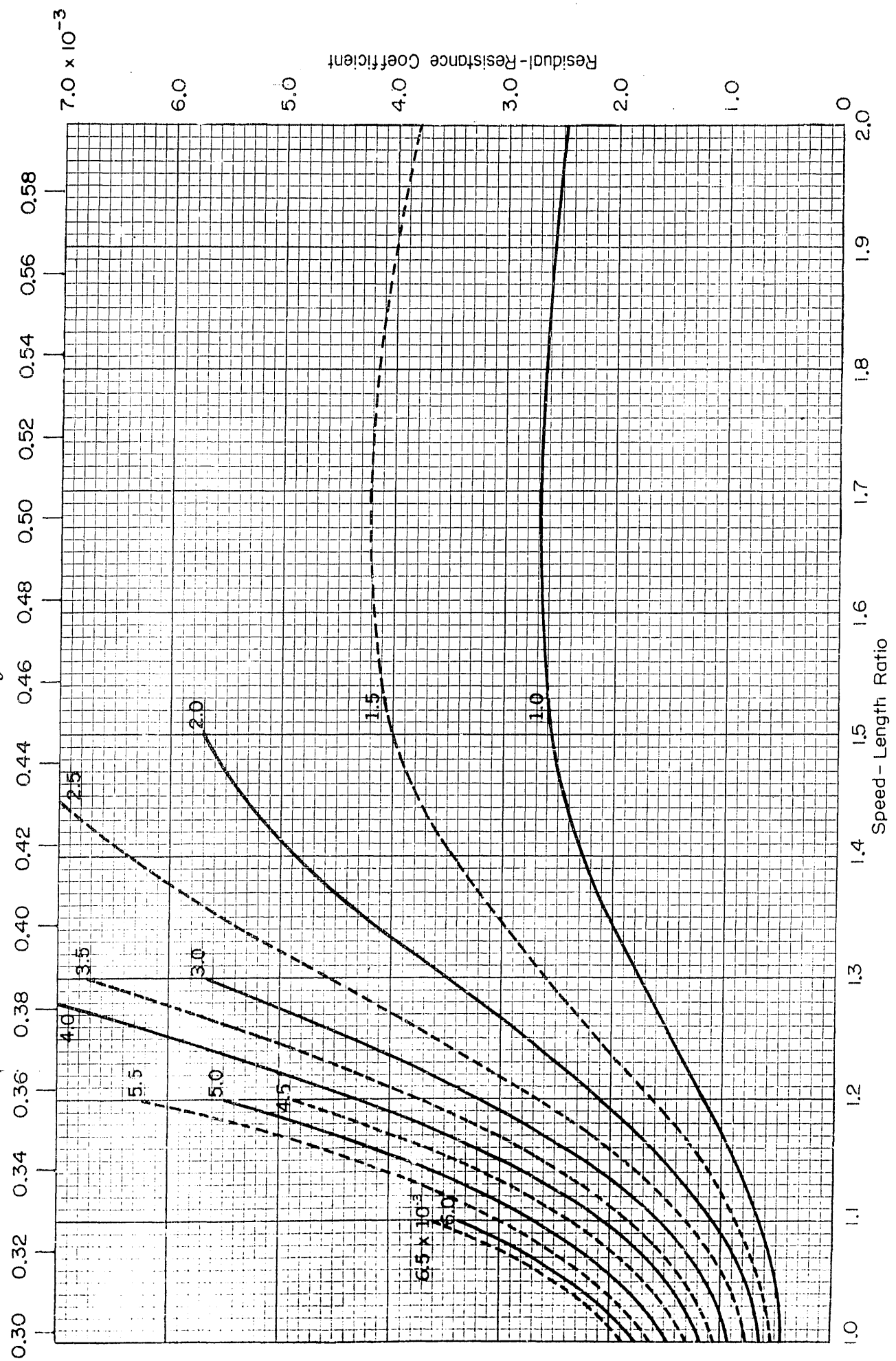
0.7

0.8

0.9

1.0

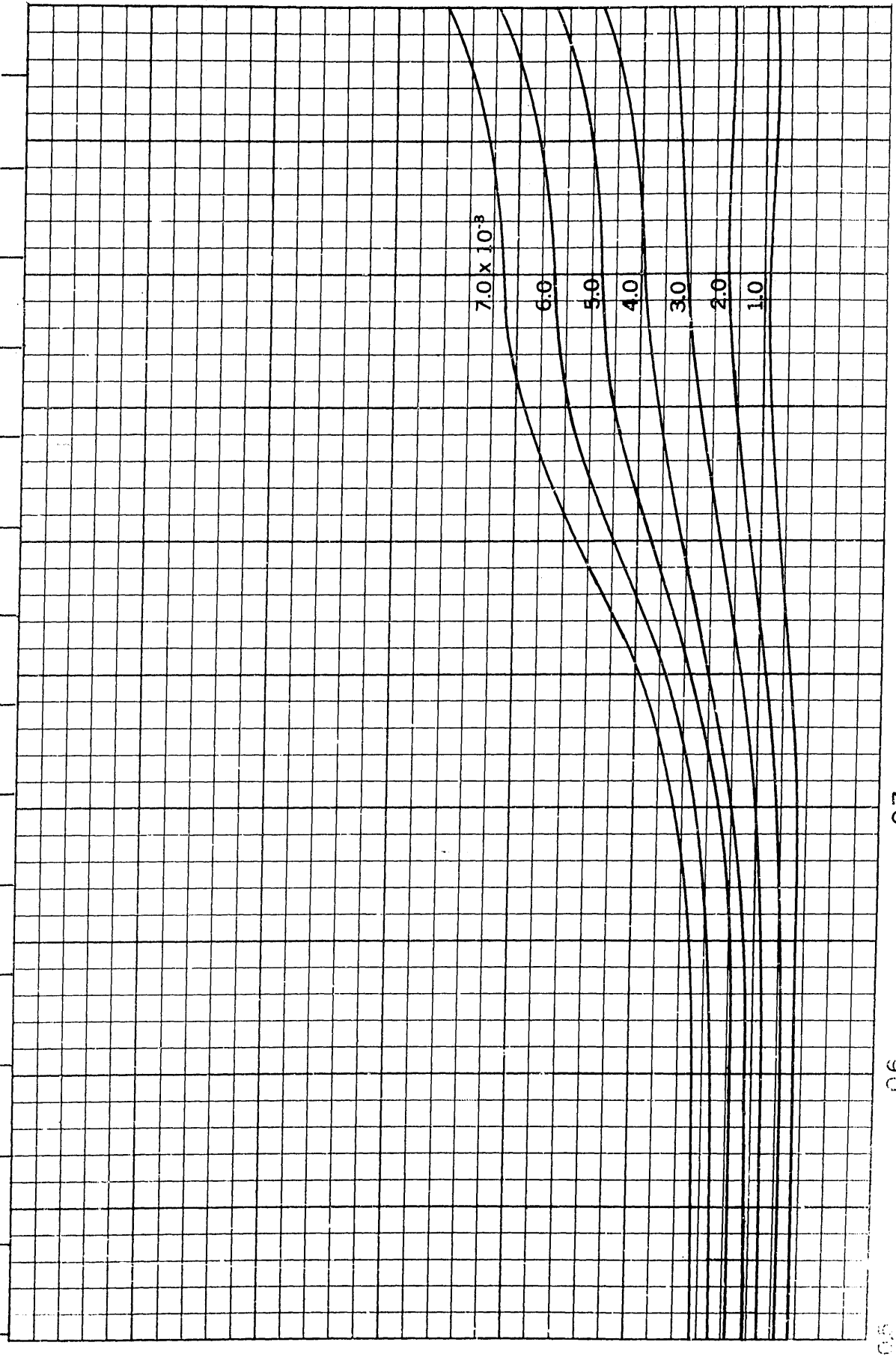
Speed - Length Ratio

$$\frac{v}{\sqrt{gL}}$$


$B/H=3.75$
 $C_p=0.50$

Froude Number $\frac{v}{\sqrt{gL}}$

0.15 0.16 0.17 0.18 0.19 0.20 0.21 0.22 0.23 0.24 0.25 0.26 0.27 0.28 0.29



Residual-Resistance Coefficient

3.0×10^{-3}

7.0×10^{-3}

6.0

5.0

4.0

3.0

2.0

1.0

Speed - Length Ratio

1.0

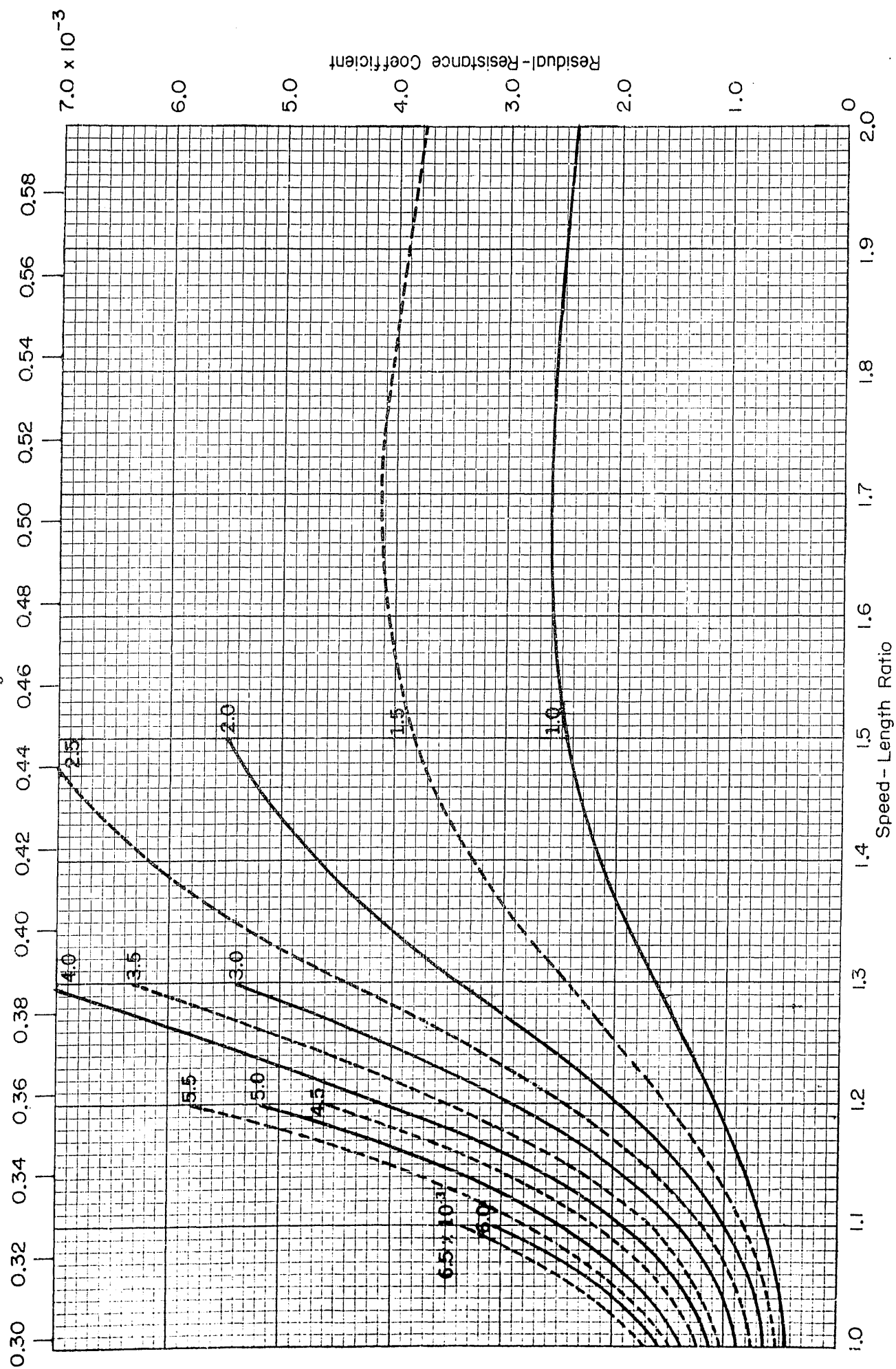
0.9

0.8

0.7

0.6

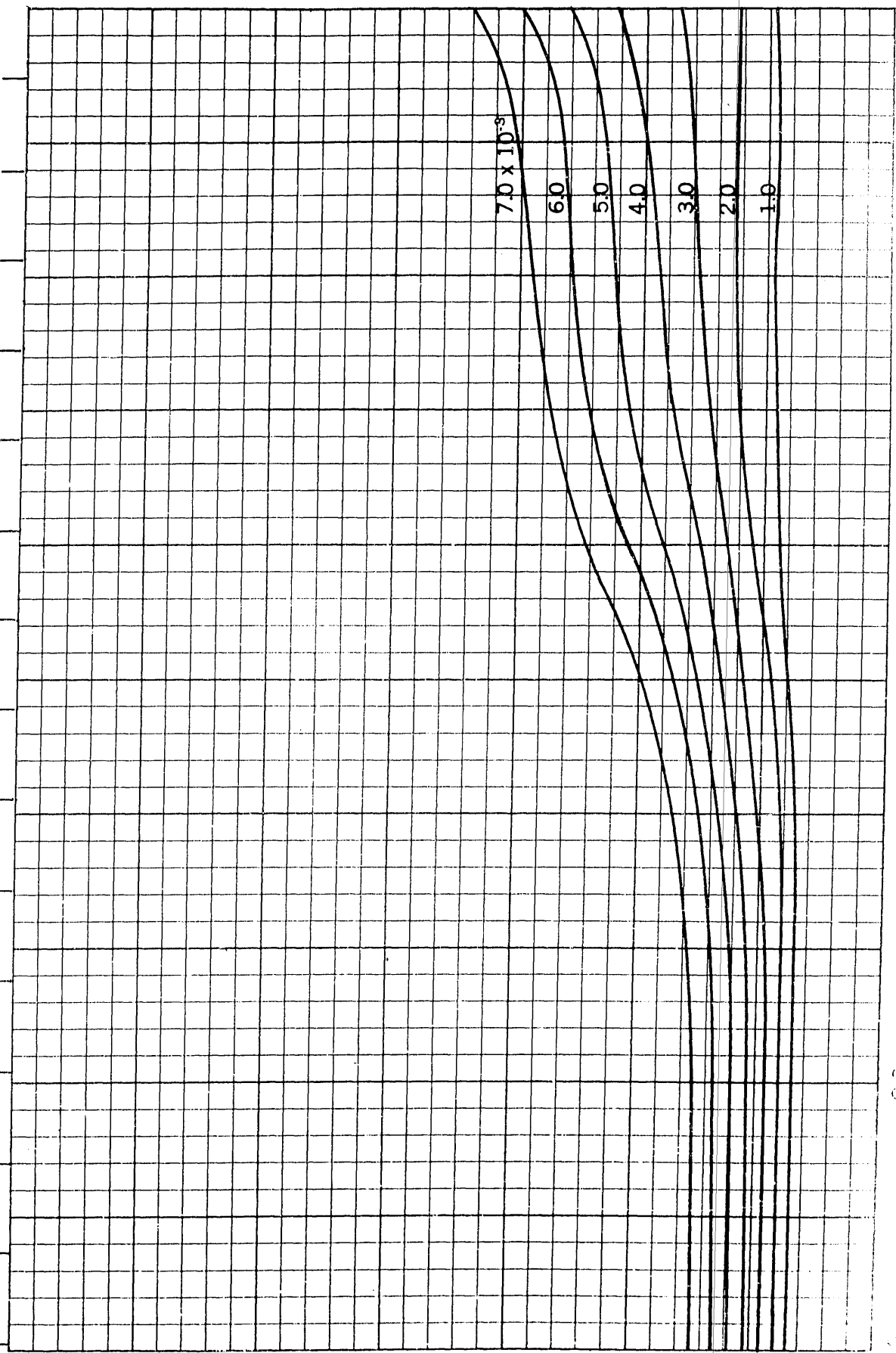
0.5

$$\frac{v}{\sqrt{gL}}$$


$B/H=3.75$
 $C_p=0.51$

Froude Number $\frac{v}{\sqrt{gL}}$

0.15 0.16 0.17 0.18 0.19 0.20 0.21 0.22 0.23 0.24 0.25 0.26 0.27 0.28 0.29



Residual-Resistance Coefficient

3.0×10^{-3}

7.0×10^{-3}

6.0

5.0

4.0

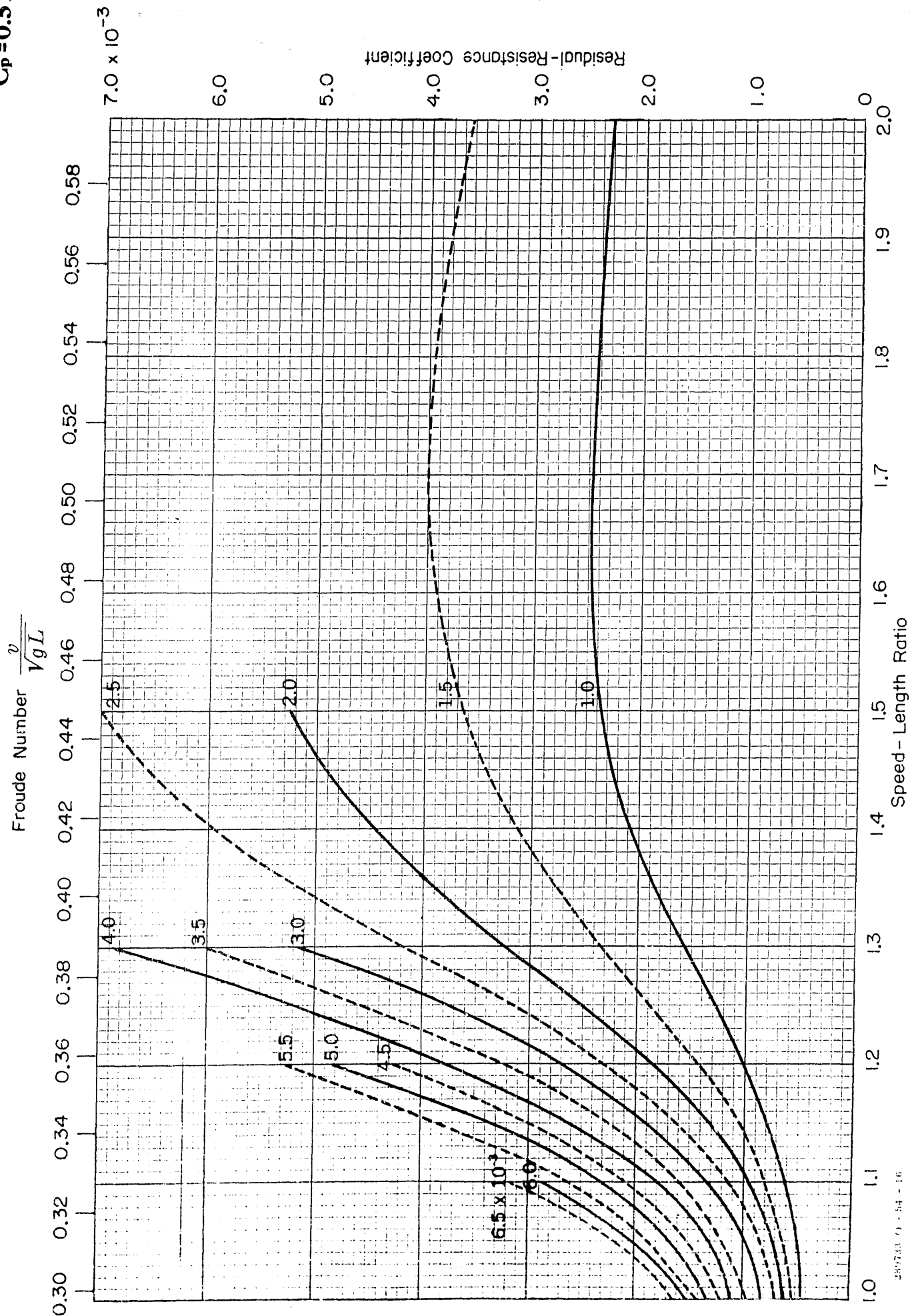
3.0

2.0

1.0

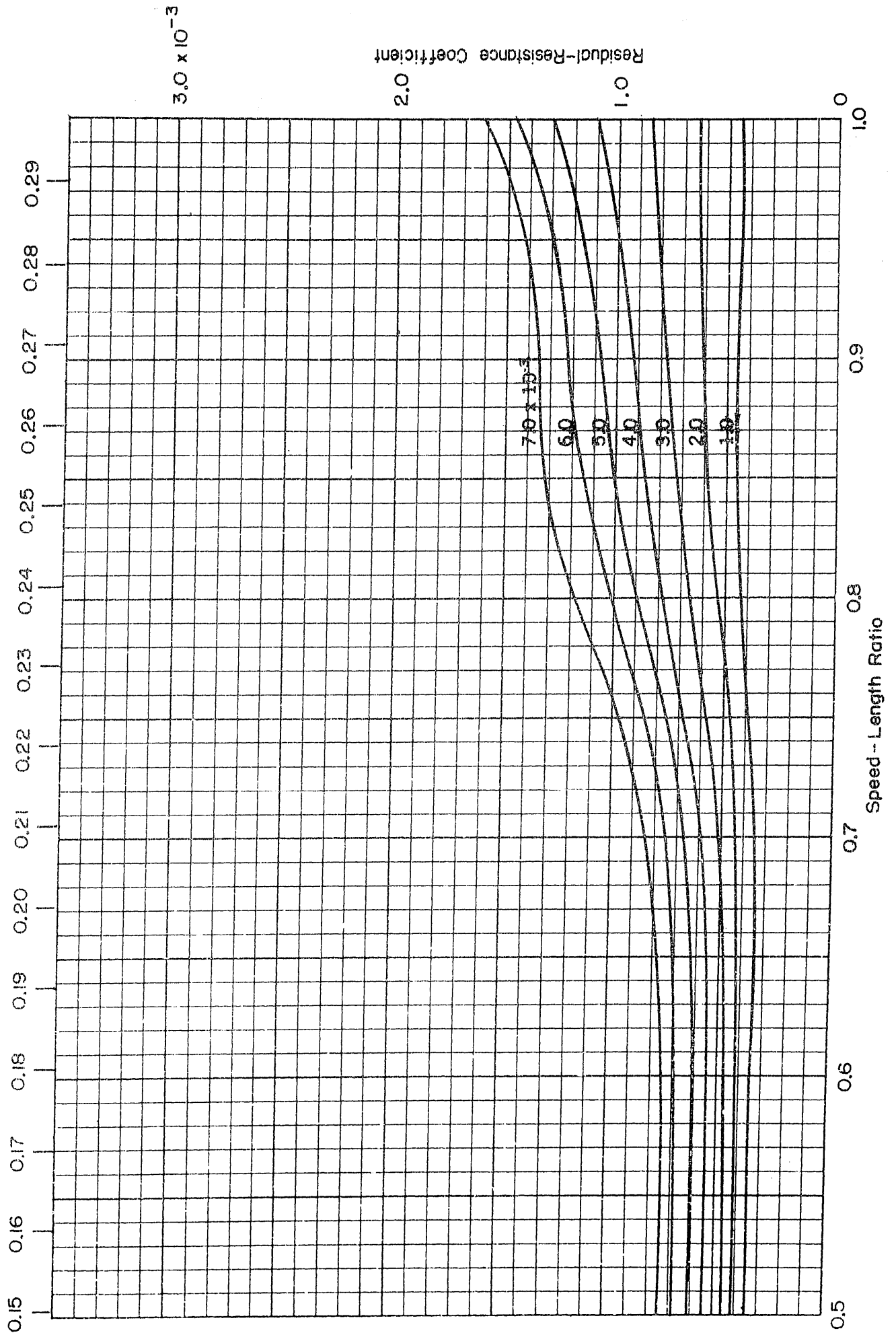
Speed - Length Ratio

B/H=3.75
C_p=0.51

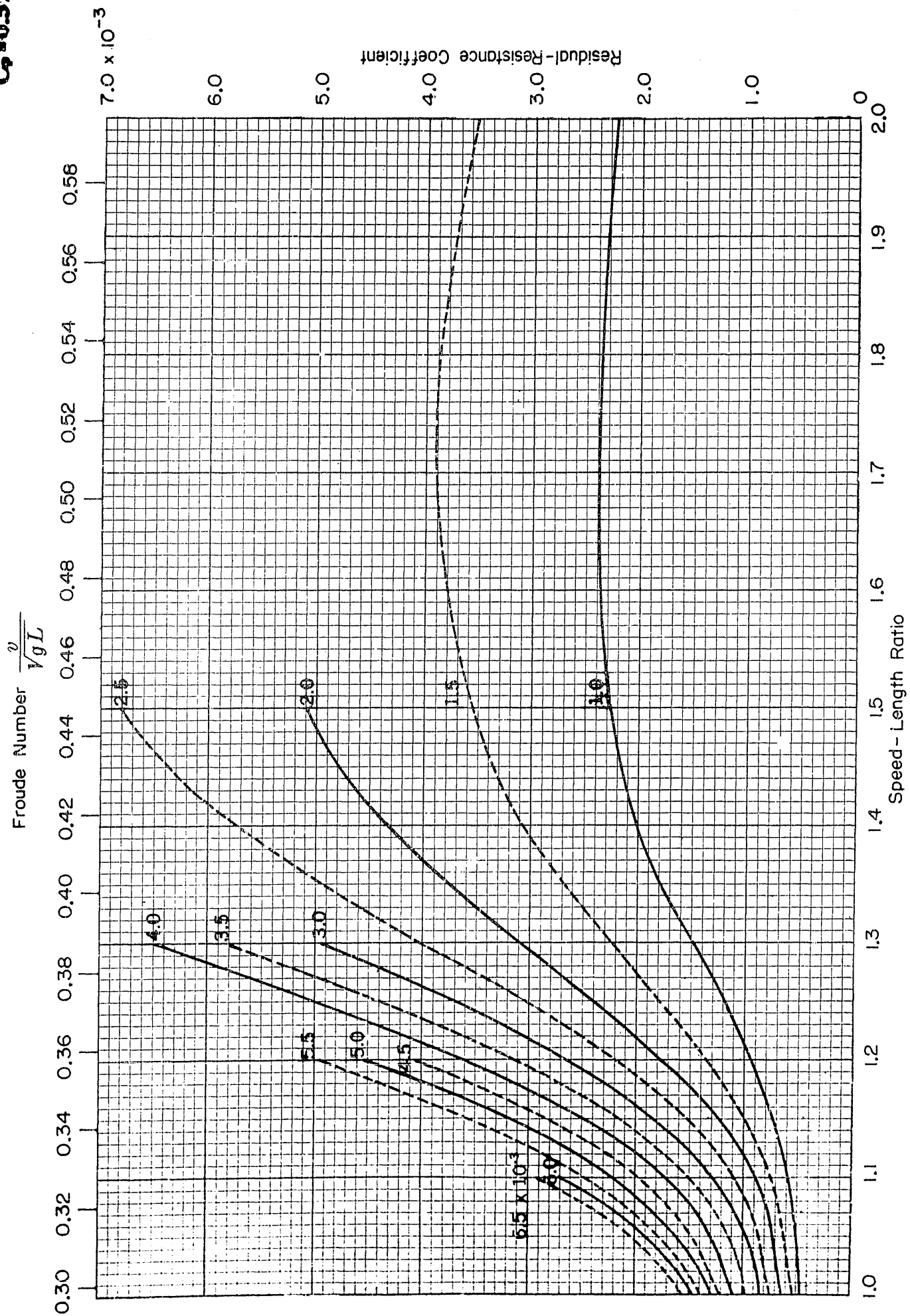


$B/H=3.75$
 $C_p=0.52$

Froude Number $\frac{v}{\sqrt{gL}}$



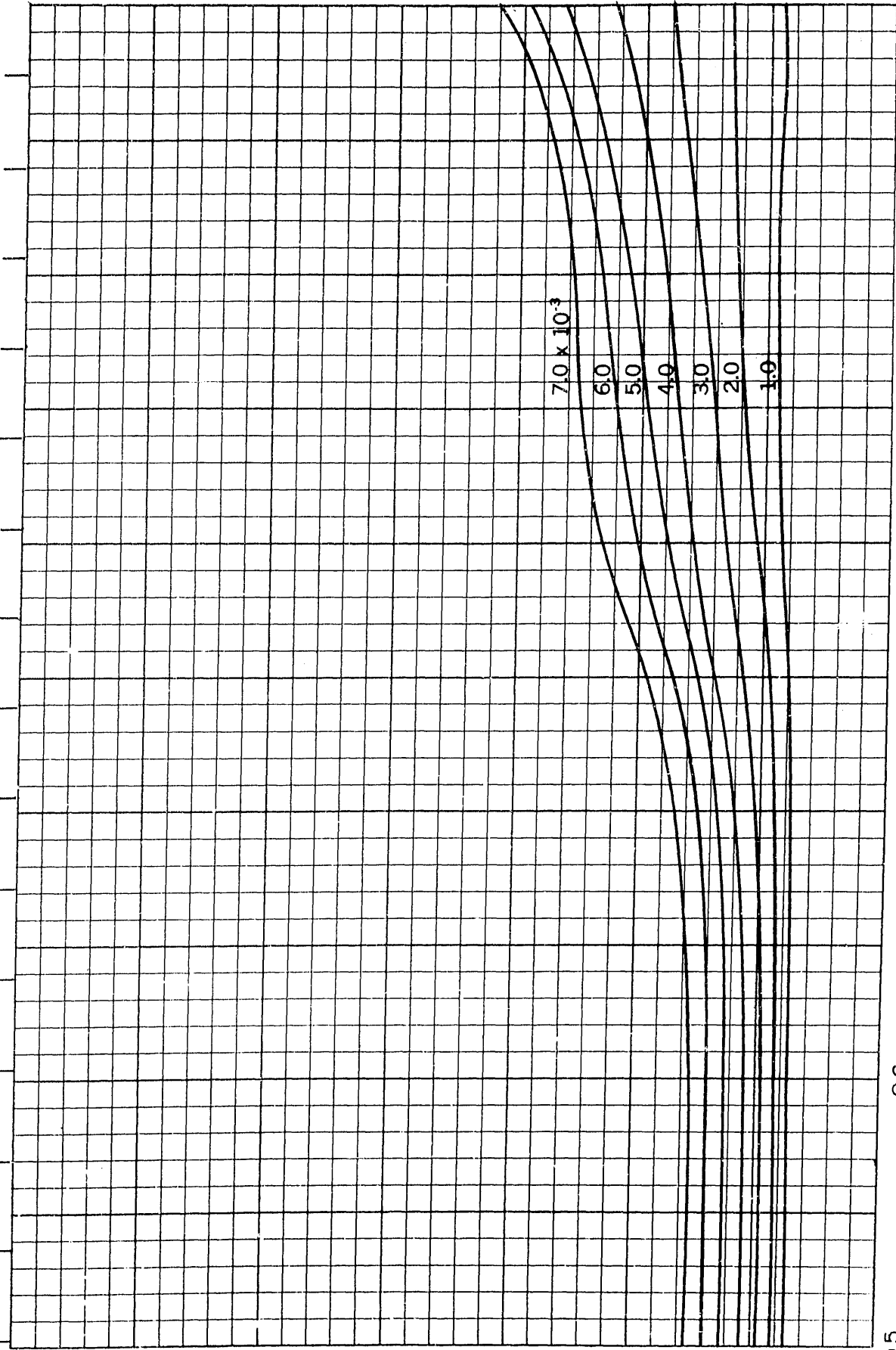
B/H=3.75
C_p=0.52



$B/H=3.75$
 $C_p=0.53$

Froude Number $\frac{v}{\sqrt{gL}}$

0.15 0.16 0.17 0.18 0.19 0.20 0.21 0.22 0.23 0.24 0.25 0.26 0.27 0.28 0.29



Residual-Resistance Coefficient

3.0 x 10^-3

0

1.0

0.9

0.8

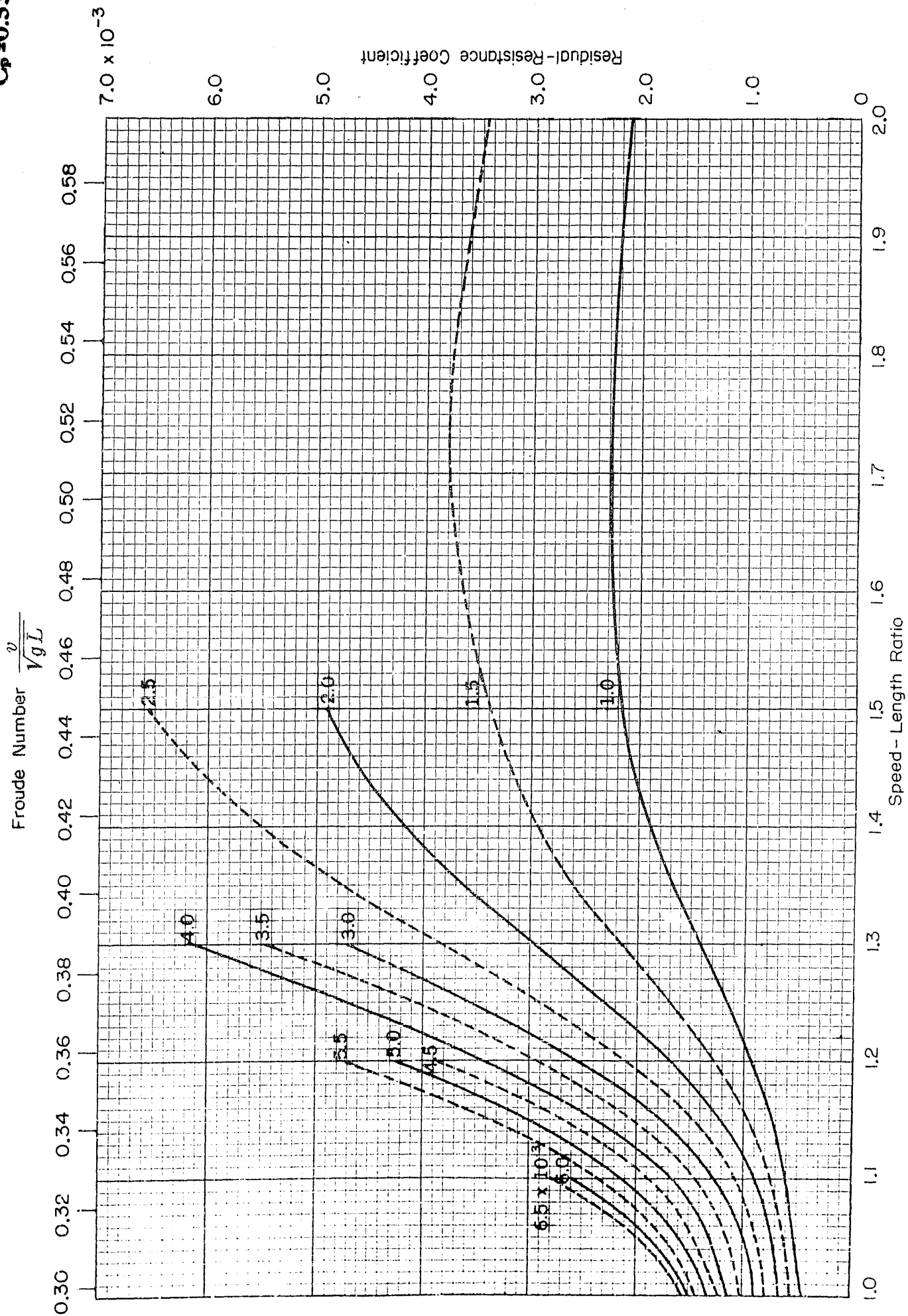
0.7

0.6

0.5

Speed - Length Ratio

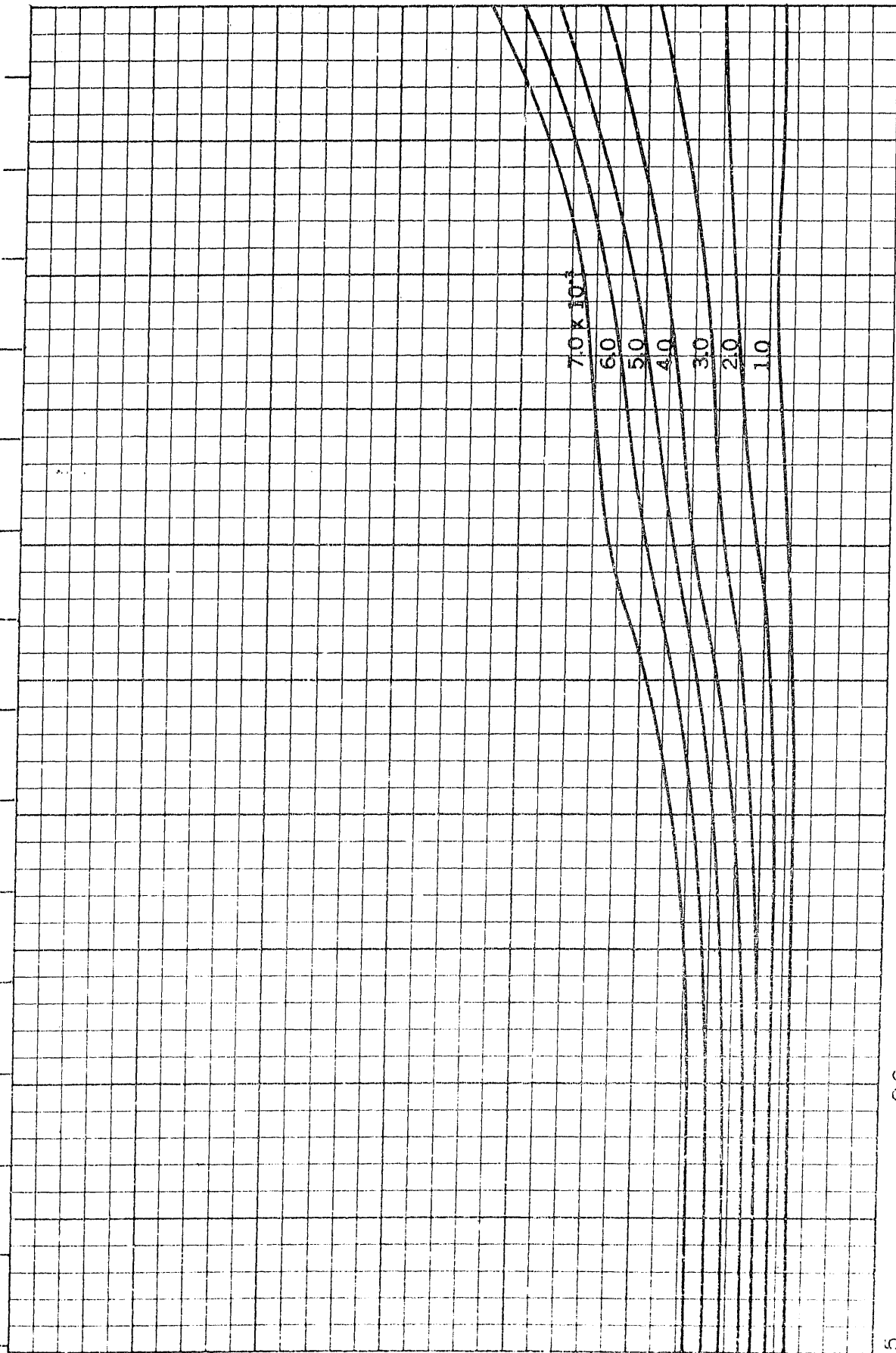
$B/H=3.75$
 $C_p=0.53$



$B/H=3.75$
 $C_p=0.54$

Froude Number $\frac{v}{\sqrt{gL}}$

0.15 0.16 0.17 0.18 0.19 0.20 0.21 0.22 0.23 0.24 0.25 0.26 0.27 0.28 0.29



Residual-Resistance Coefficient

3.0×10^{-3}

0

0.9

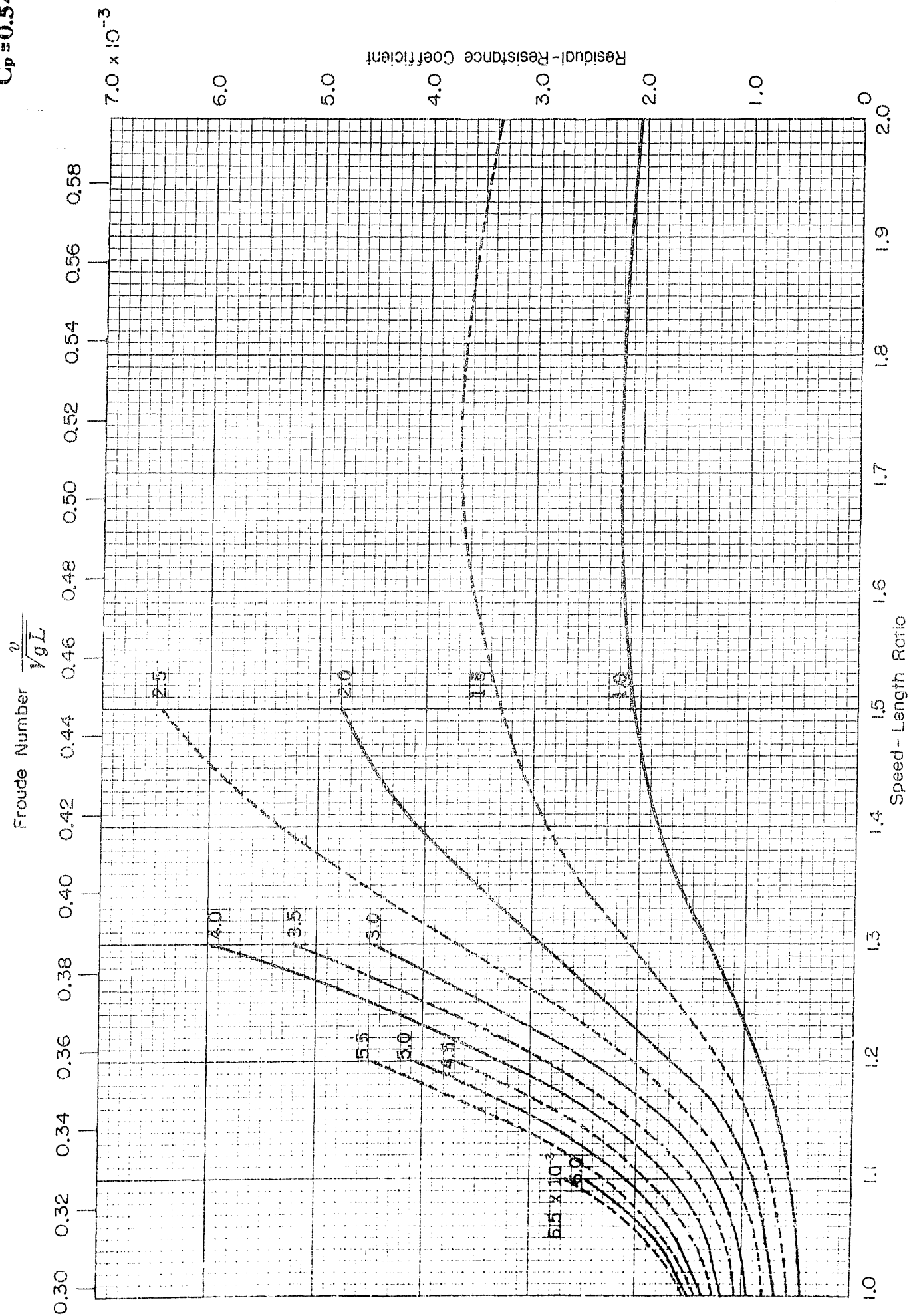
Speed - Length Ratio

0.7

0.6

0.5

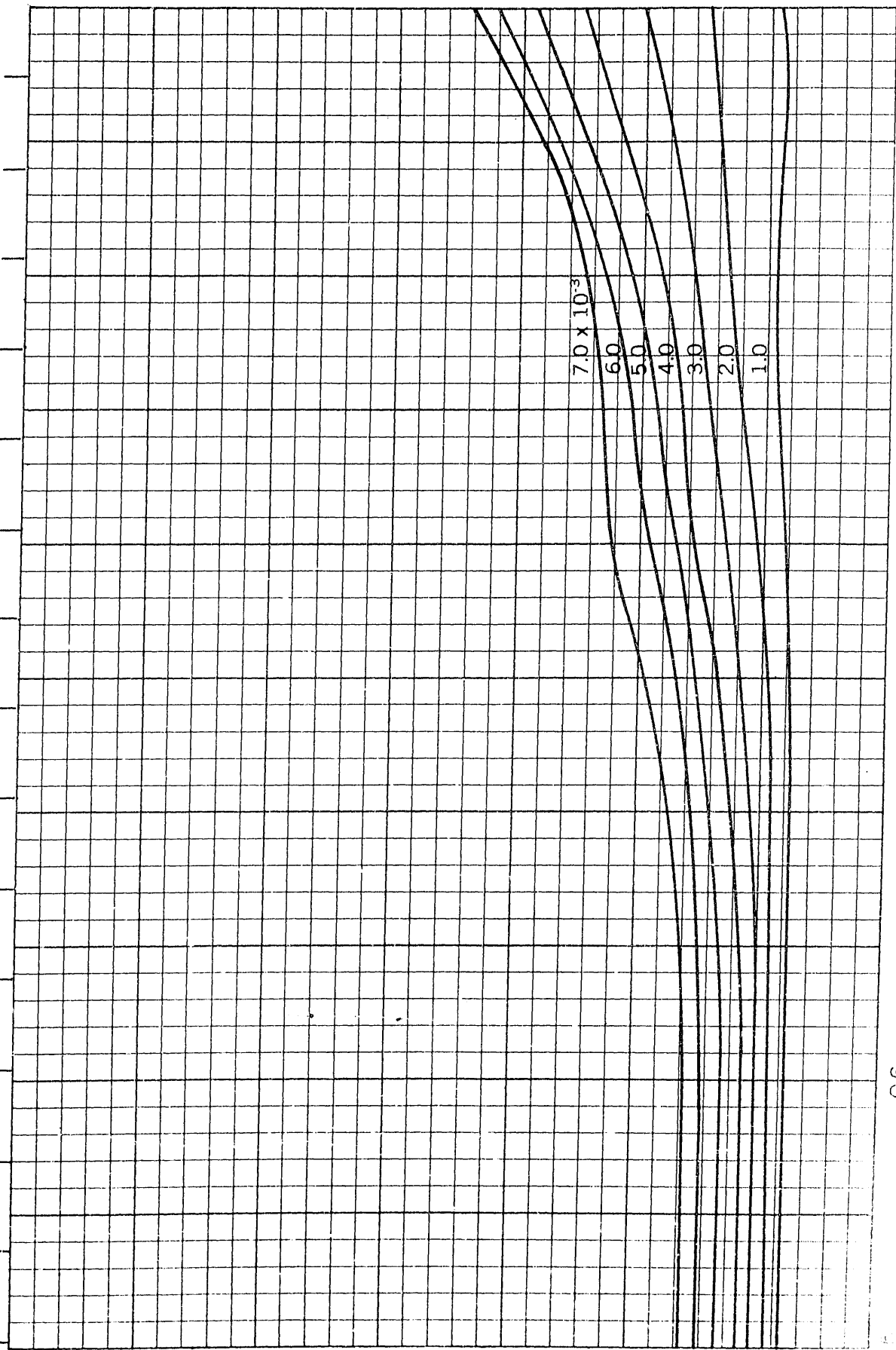
$B/H=3.75$
 $C_p=0.54$



$B/H=3.75$
 $C_p=0.55$

Froude Number $\frac{v}{\sqrt{gL}}$

0.15 0.16 0.17 0.18 0.19 0.20 0.21 0.22 0.23 0.24 0.25 0.26 0.27 0.28 0.29



Residual-Resistance Coefficient

3.0×10^{-3}

7.0×10^{-3}

6.0

5.0

4.0

3.0

2.0

1.0

Speed-Length Ratio

0.5

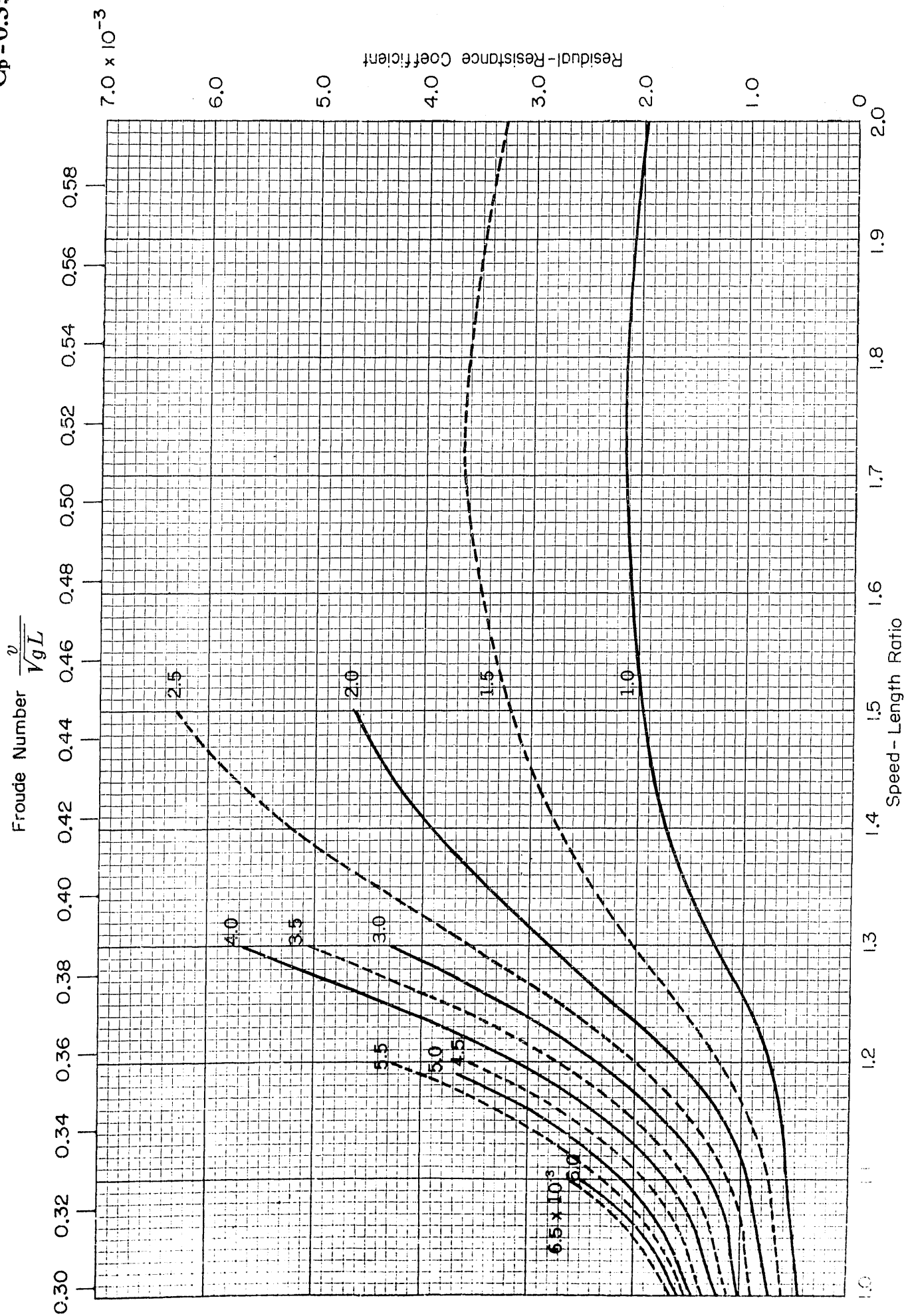
0.7

0.8

0.9

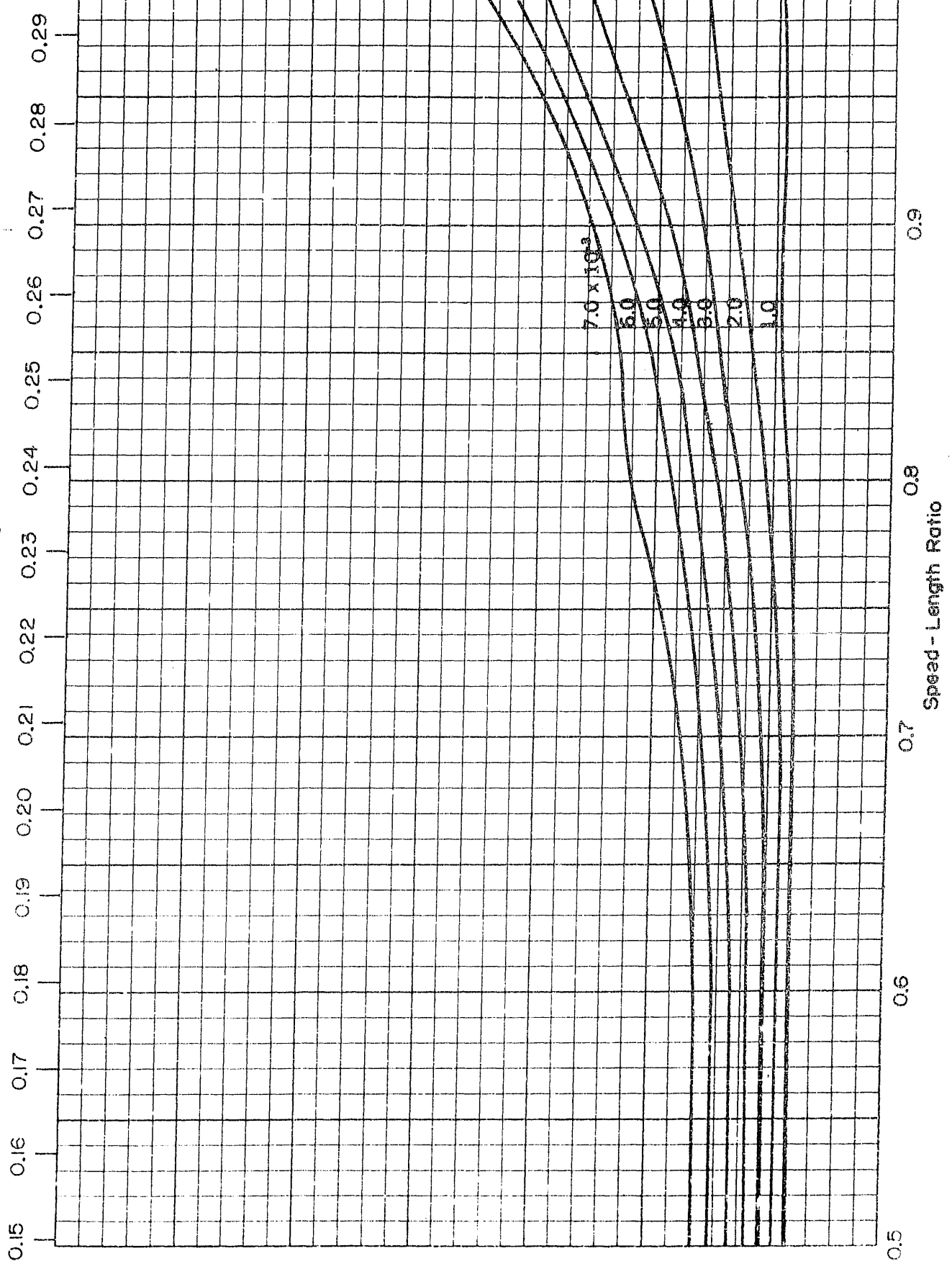
1.0

$B/H=3.75$
 $C_p=0.55$



$B/H=3.75$
 $C_p=0.56$

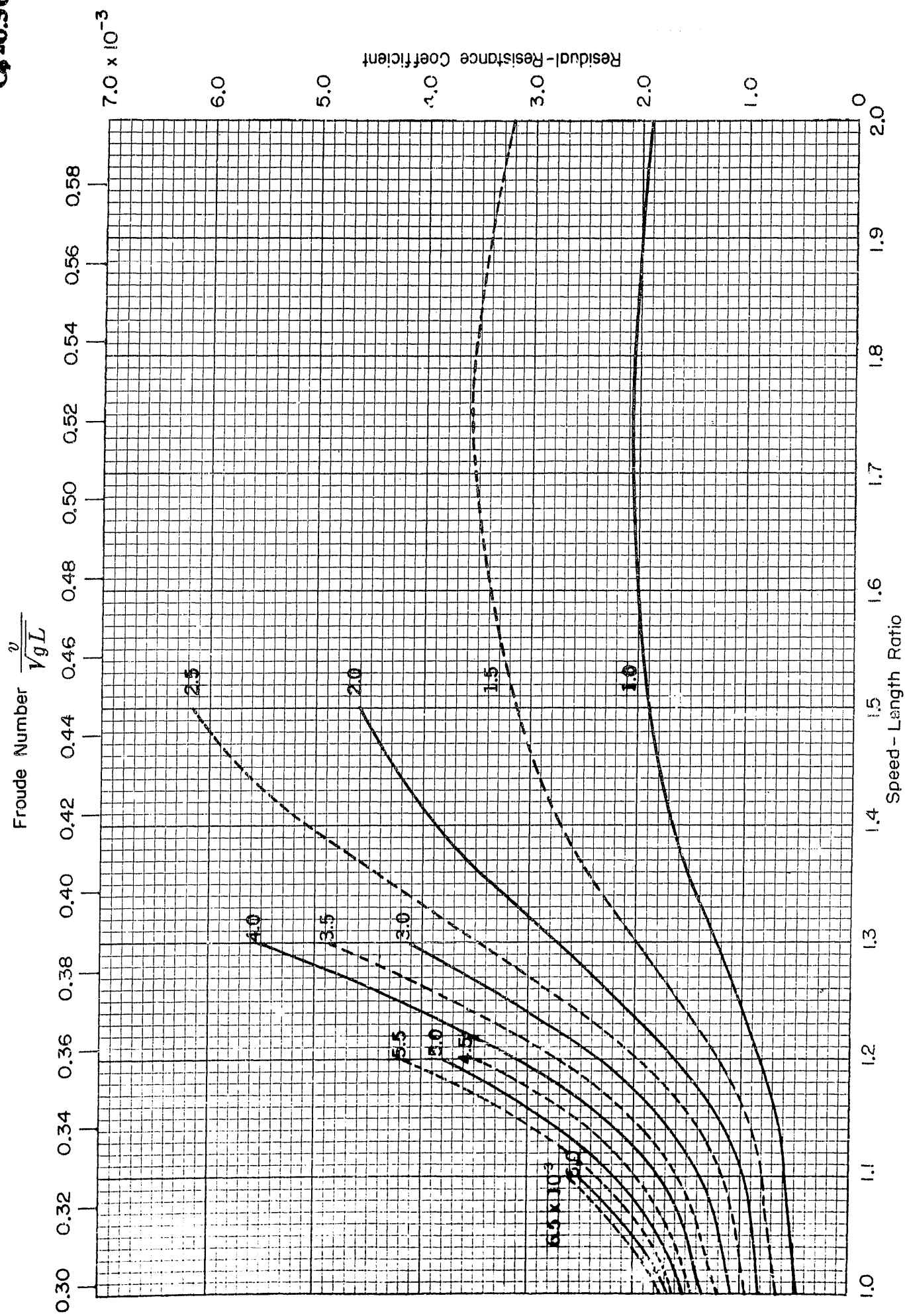
Froude Number $\frac{v}{\sqrt{gL}}$

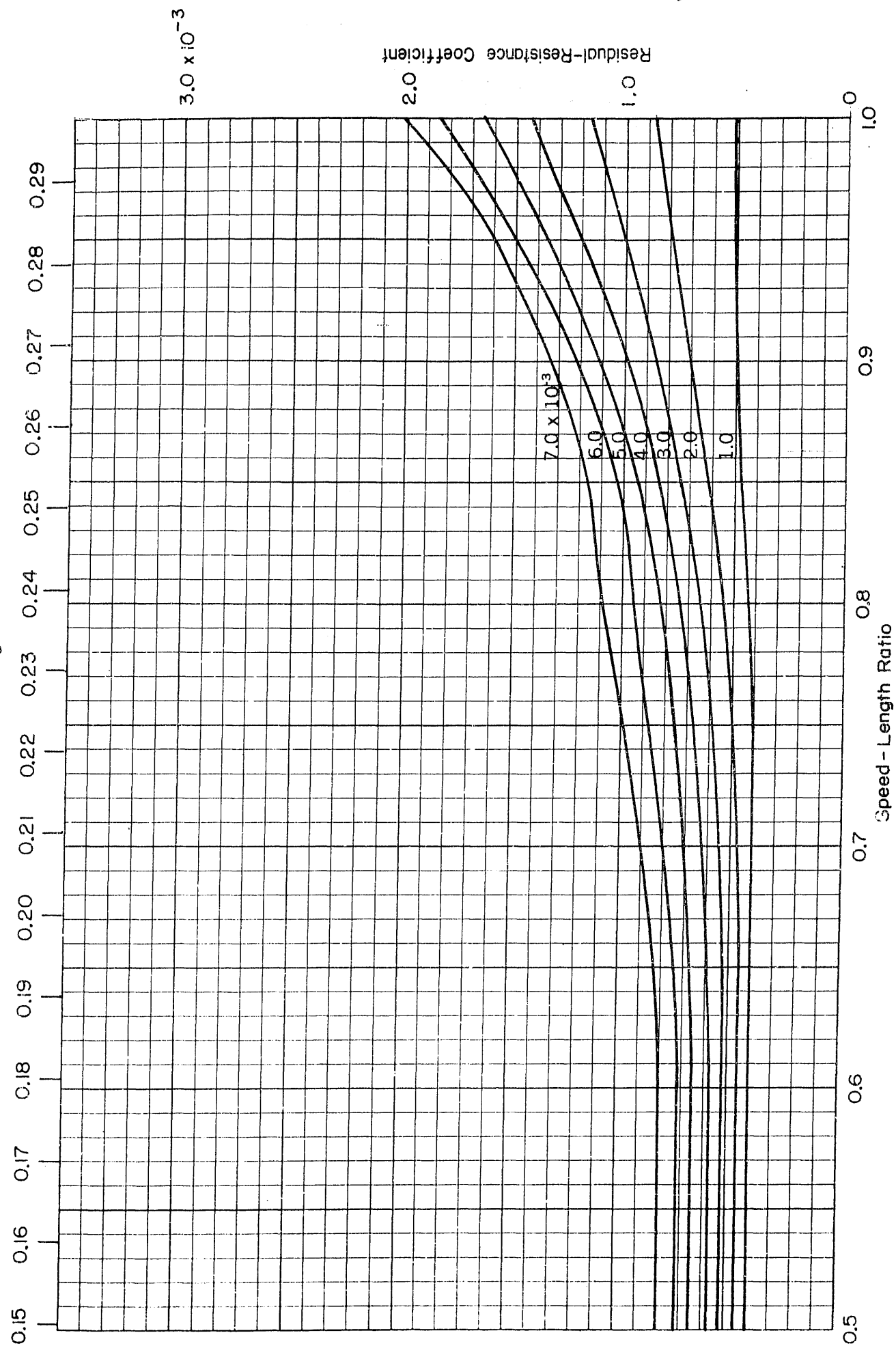


Residual-Resistance Coefficient

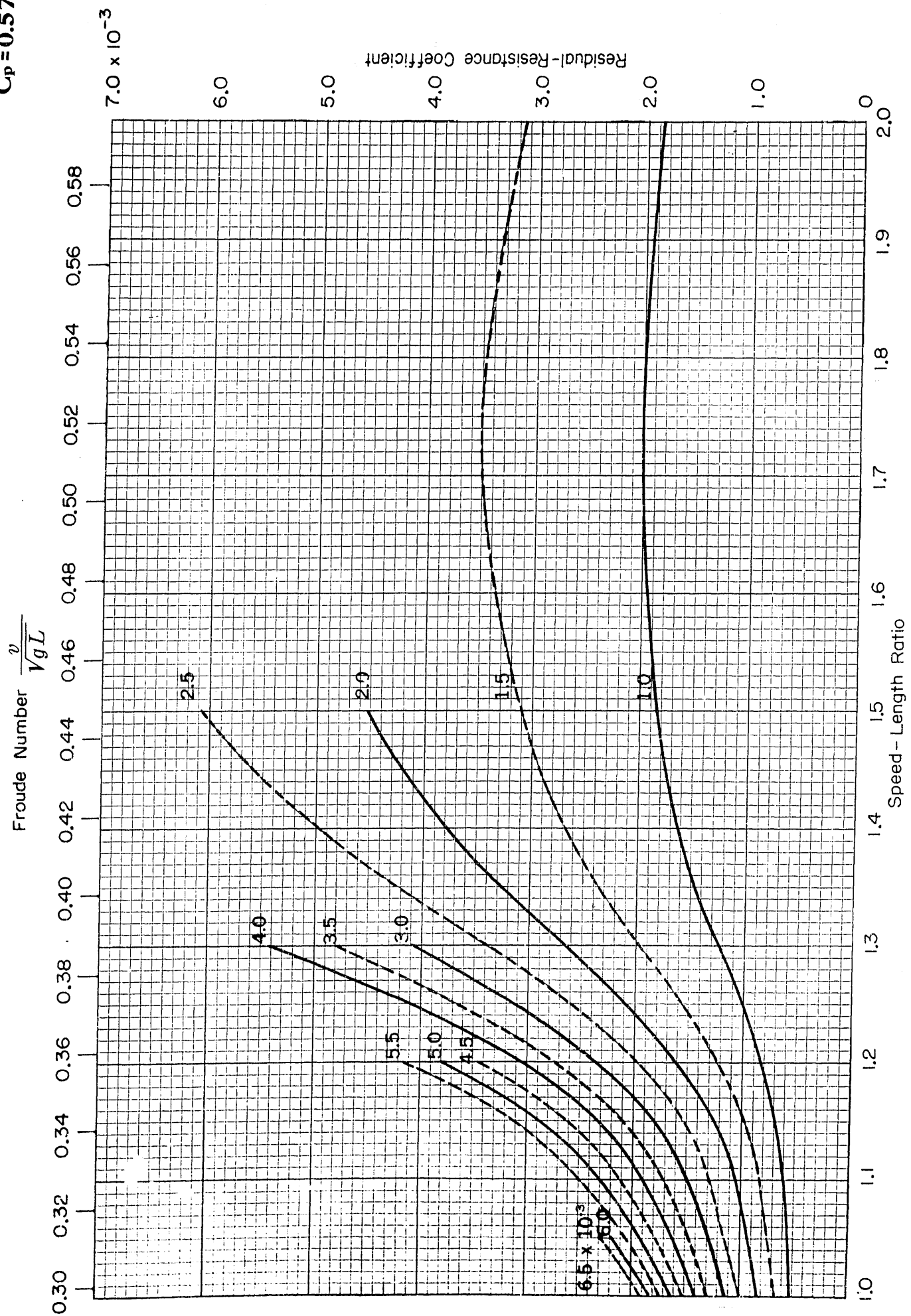
3.0×10^{-3}

B/H=3.75
C_p=0.56



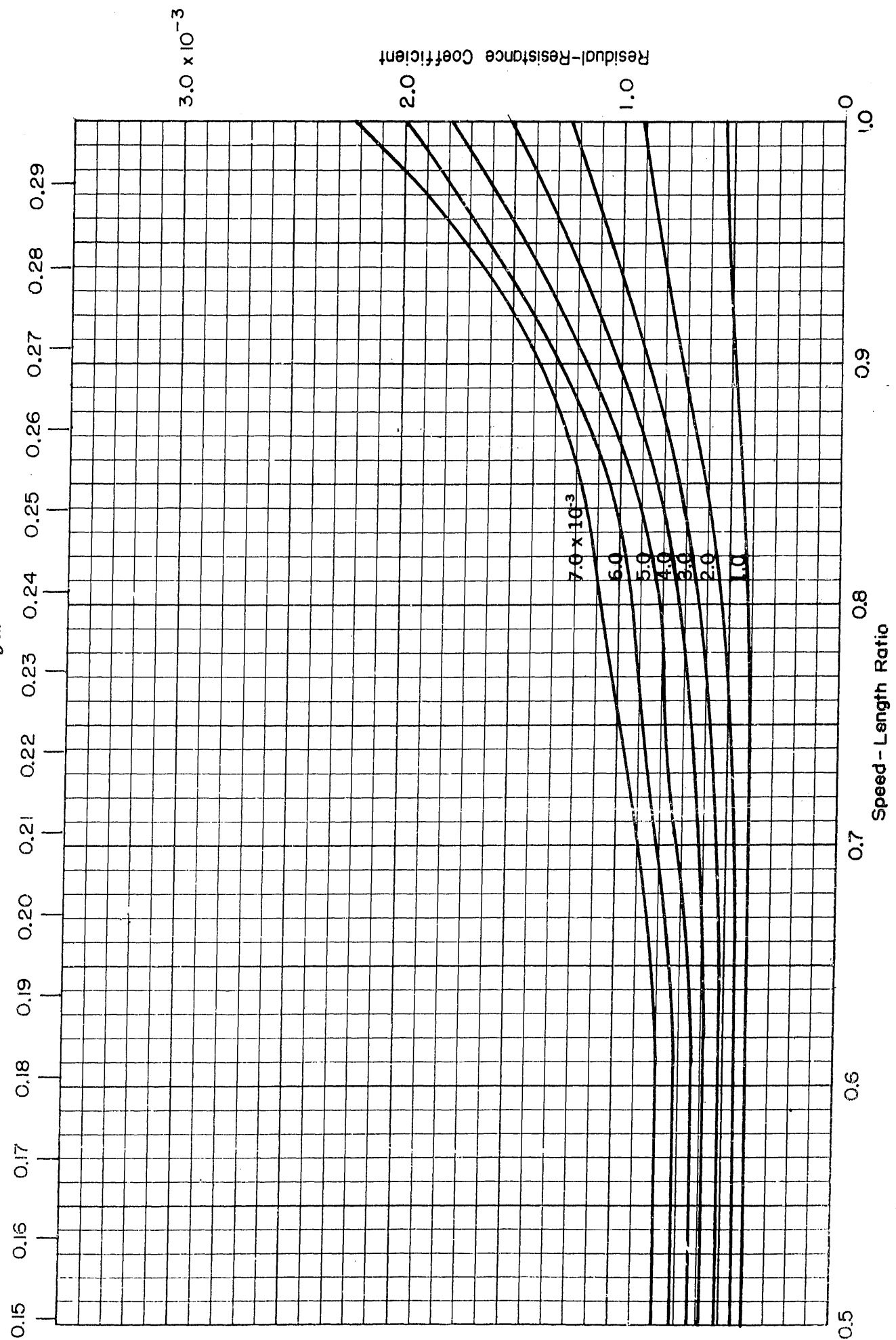
$$\frac{v}{\sqrt{g L}}$$


$B/H=3.75$
 $C_p=0.57$

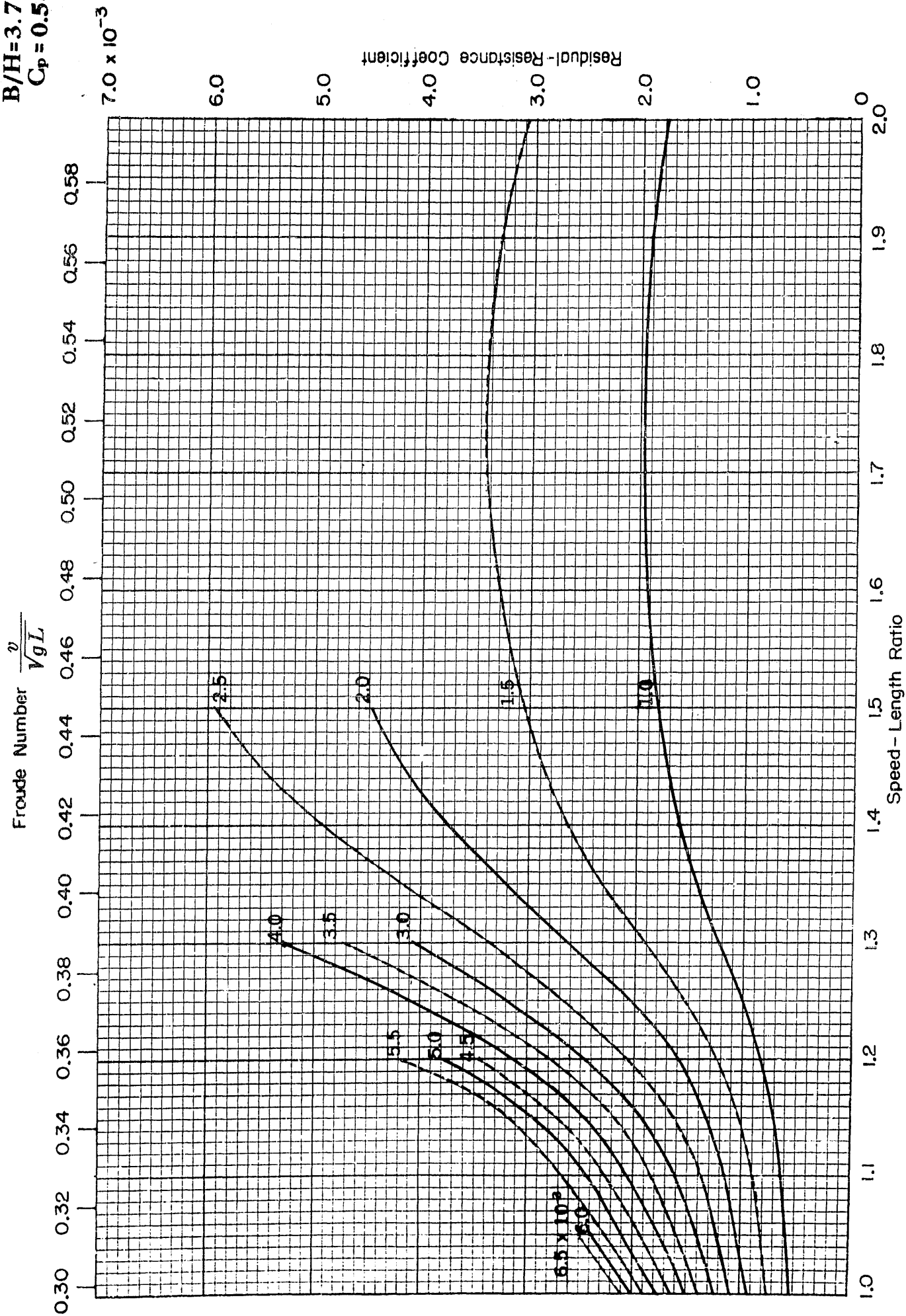


$B/H=3.75$
 $C_p=0.58$

Froude Number $\frac{v}{\sqrt{gL}}$

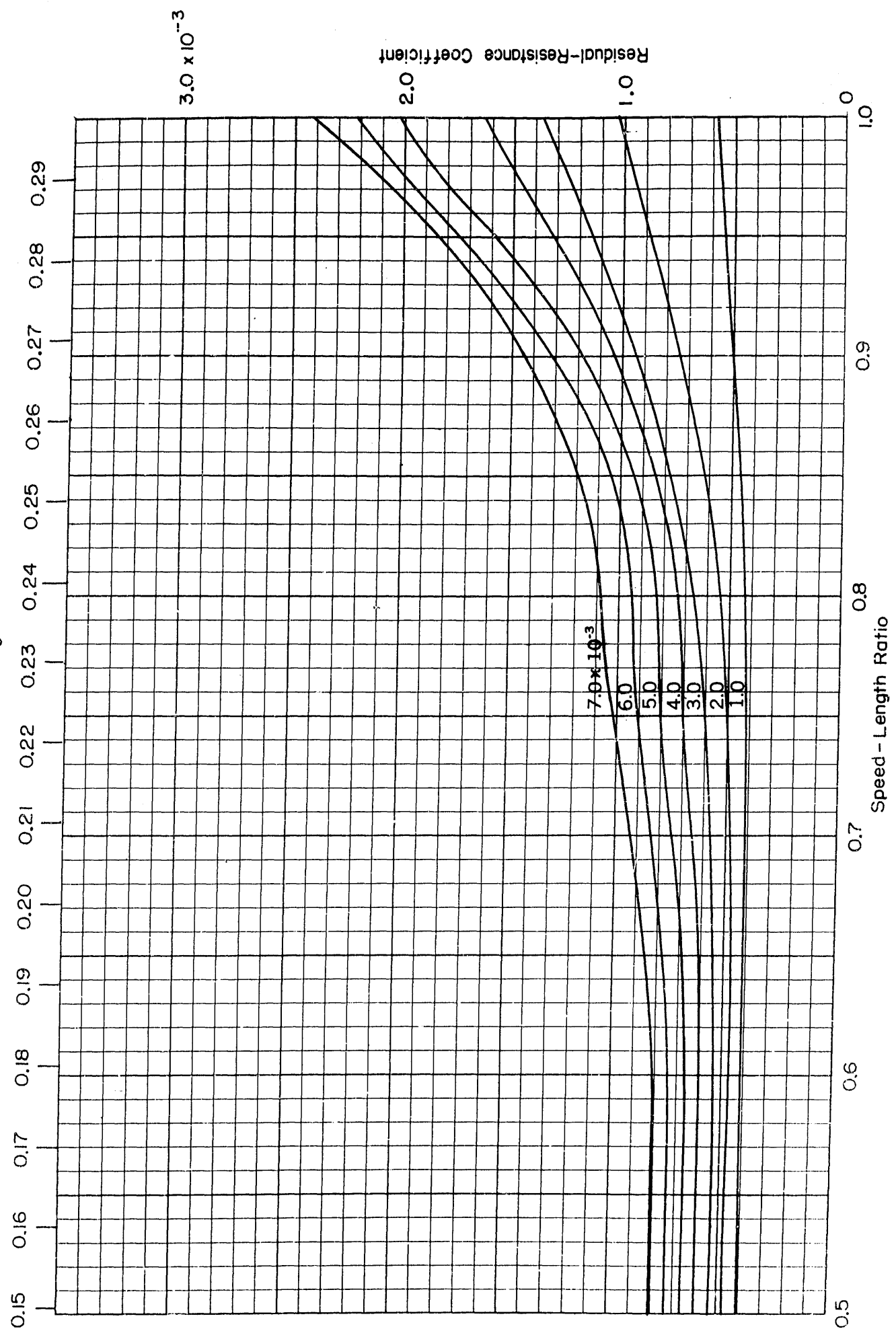


$B/H=3.75$
 $C_p=0.58$

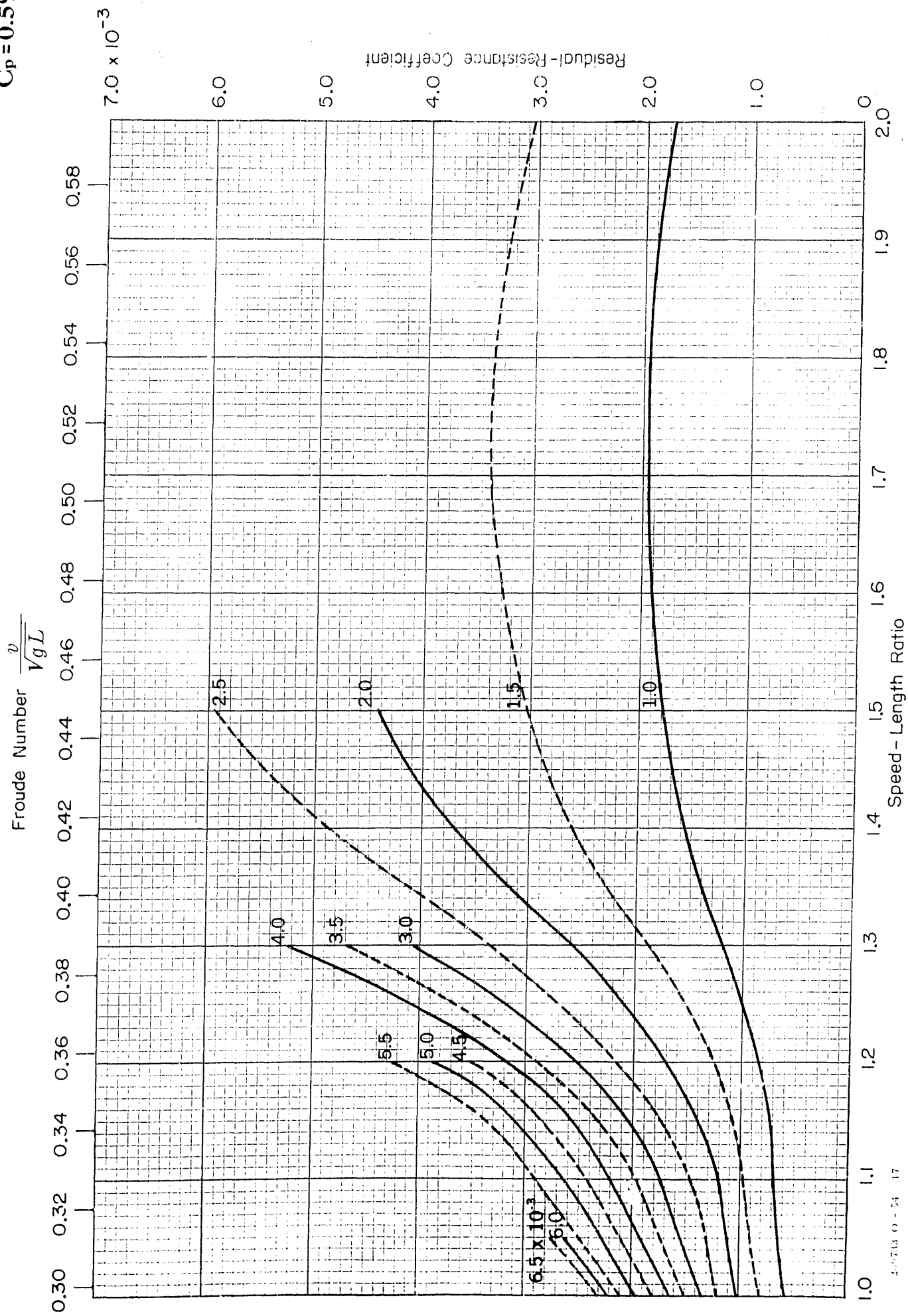


$B/H=3.75$
 $C_p=0.59$

Froude Number $\frac{v}{\sqrt{gL}}$



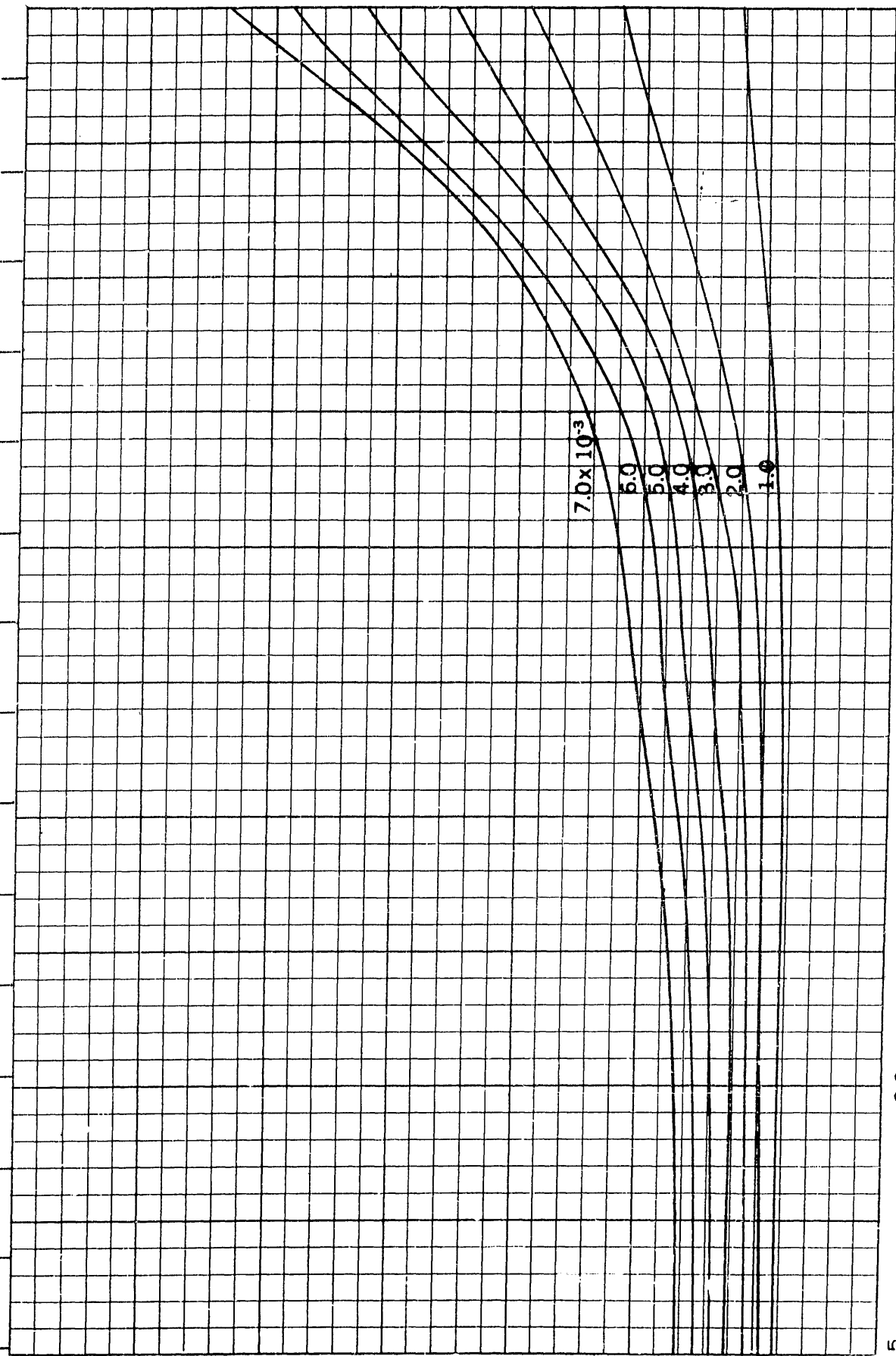
$B/H=3.75$
 $C_p=0.59$



$B/H=3.75$
 $C_p=0.60$

Froude Number $\frac{v}{\sqrt{gL}}$

0.15 0.16 0.17 0.18 0.19 0.20 0.21 0.22 0.23 0.24 0.25 0.26 0.27 0.28 0.29



0.5

0.6

0.7

0.8

0.9

1.0

Speed - Length Ratio

Residual-Resistance Coefficient

3.0×10^{-3}

7.0×10^{-3}

6.0

5.0

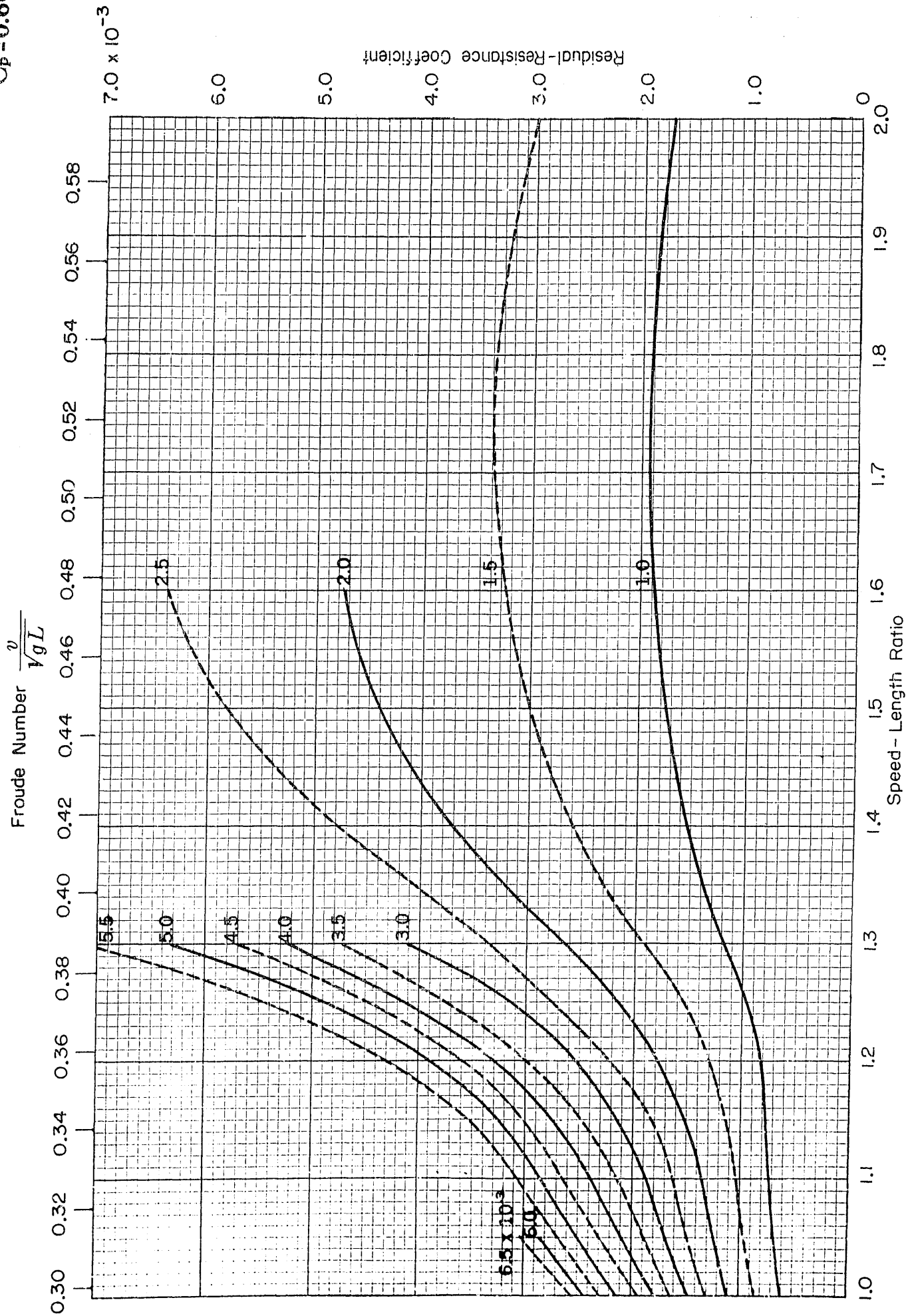
4.0

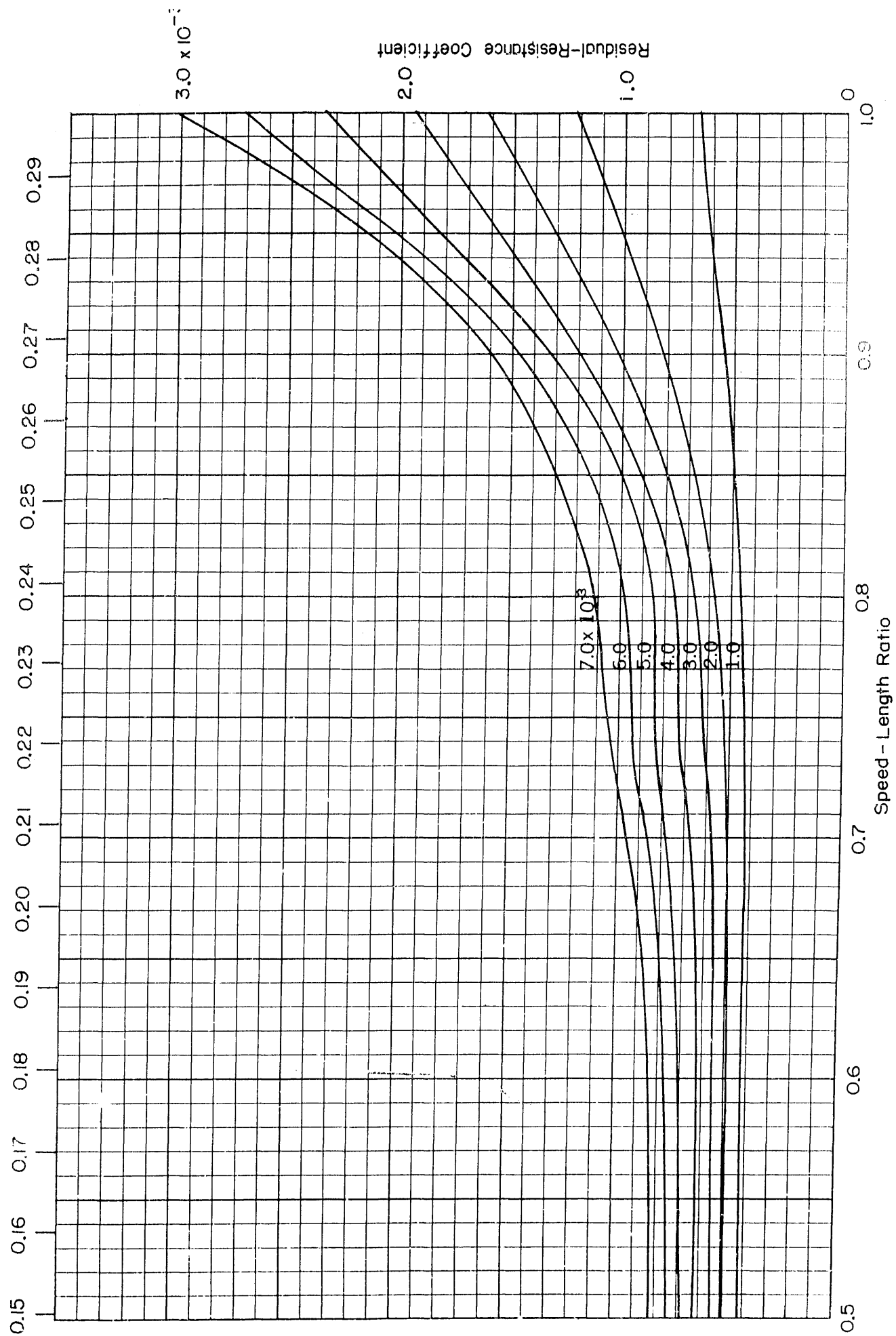
3.0

2.0

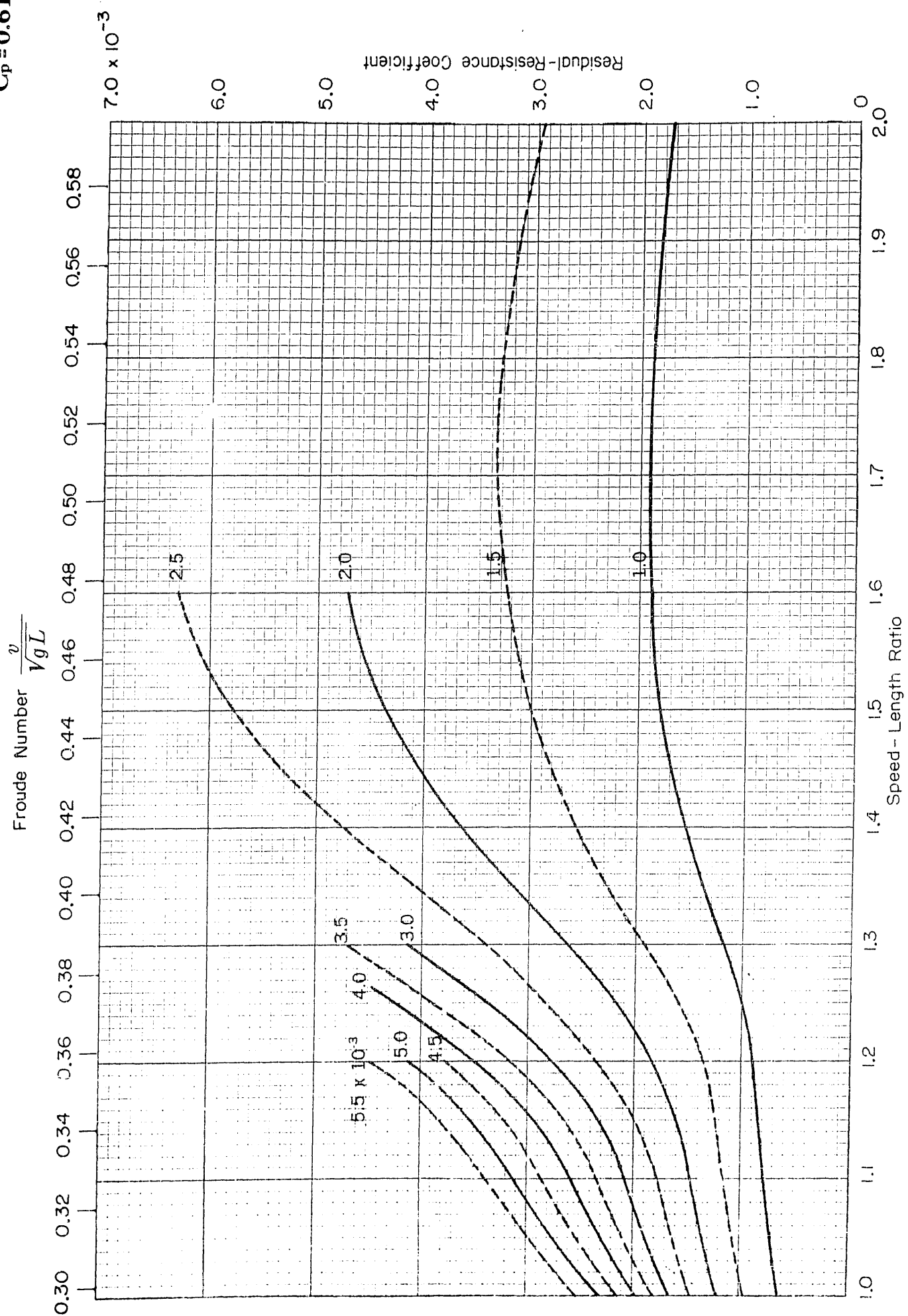
1.0

$B/H=3.75$
 $C_p=0.60$



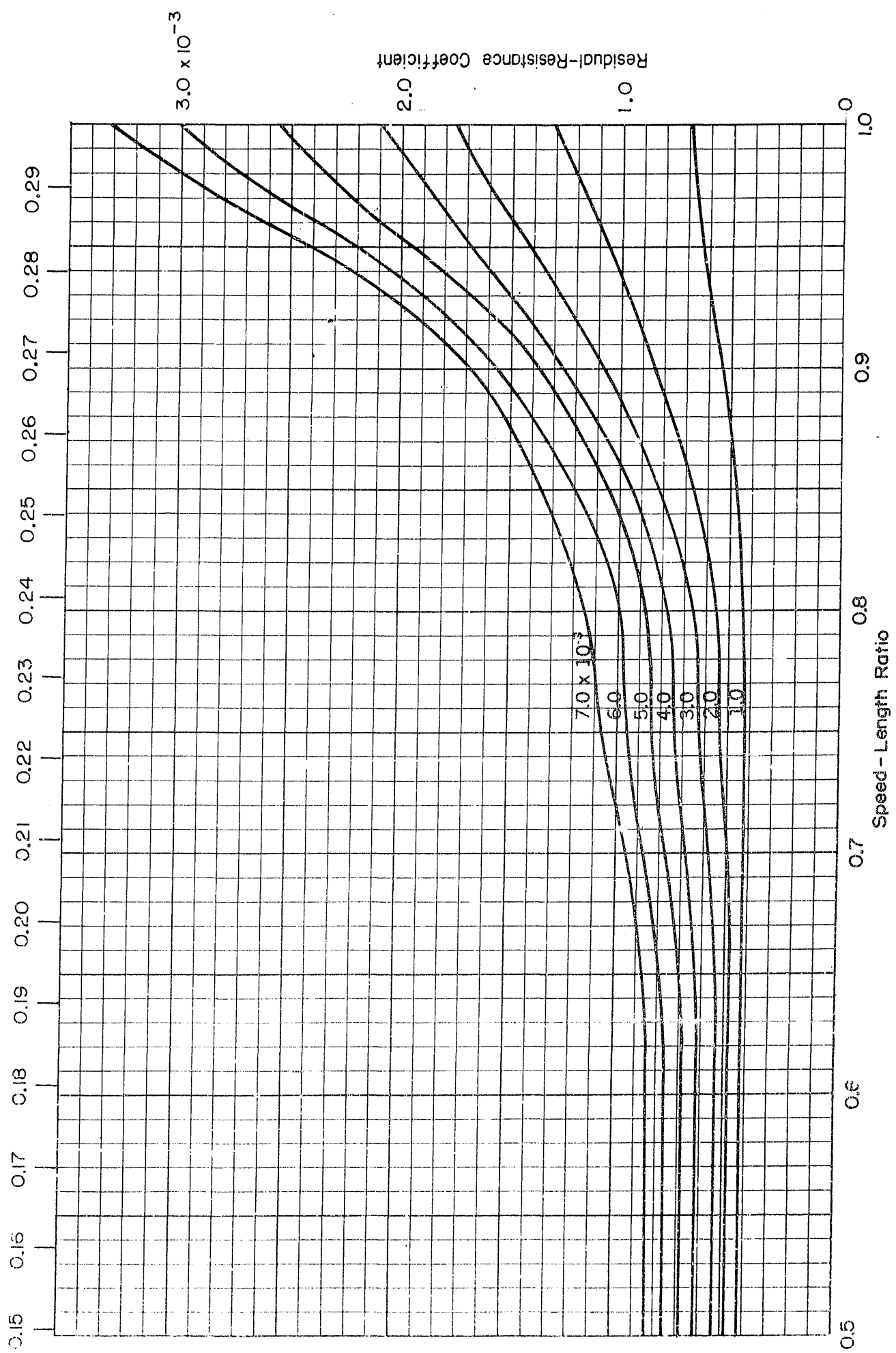
$$\frac{v}{\sqrt{gL}}$$


$B/H=3.75$
 $C_p=0.61$

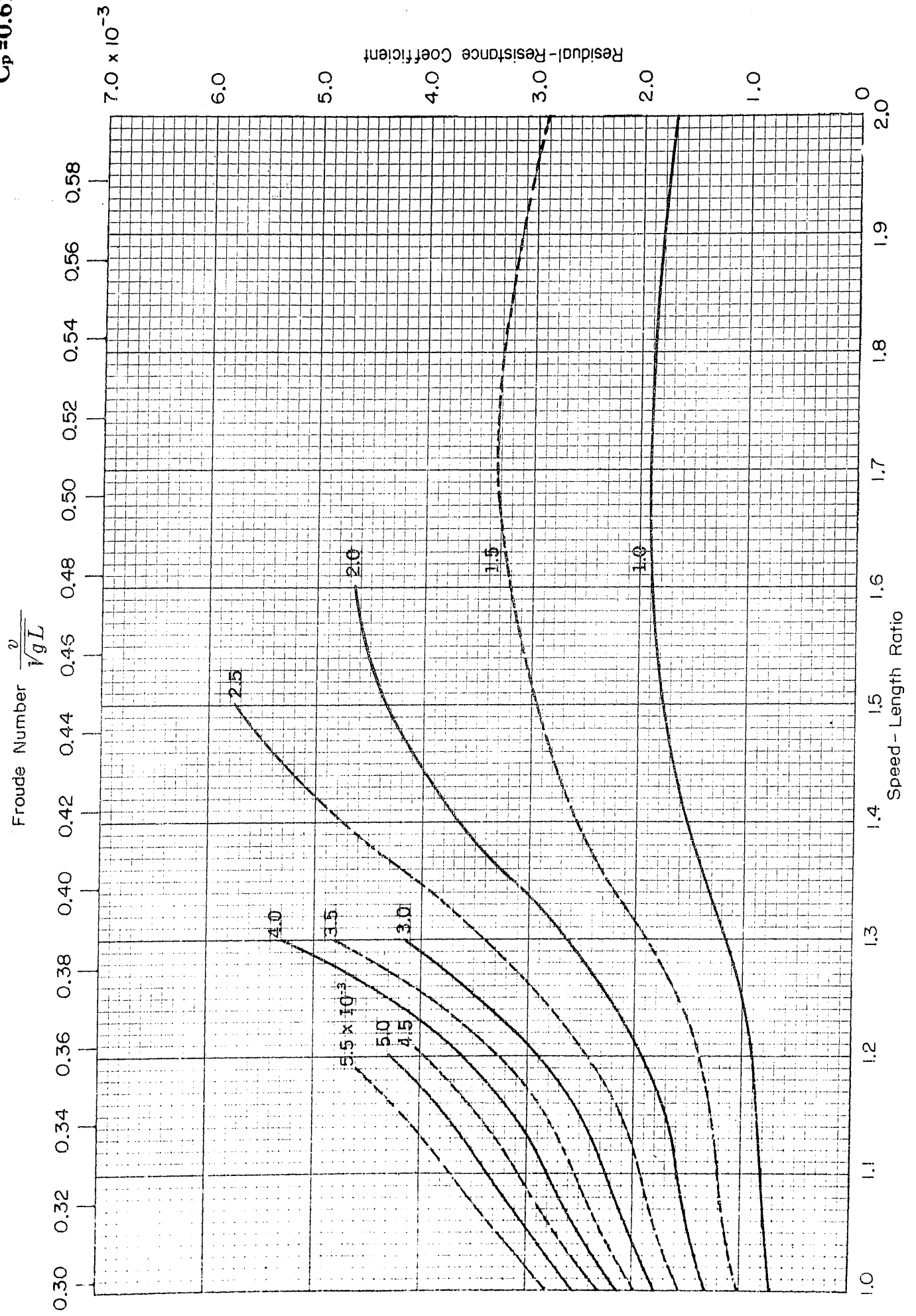


$B/H=3.75$
 $C_p=0.62$

Froude Number $\frac{v}{\sqrt{gL}}$

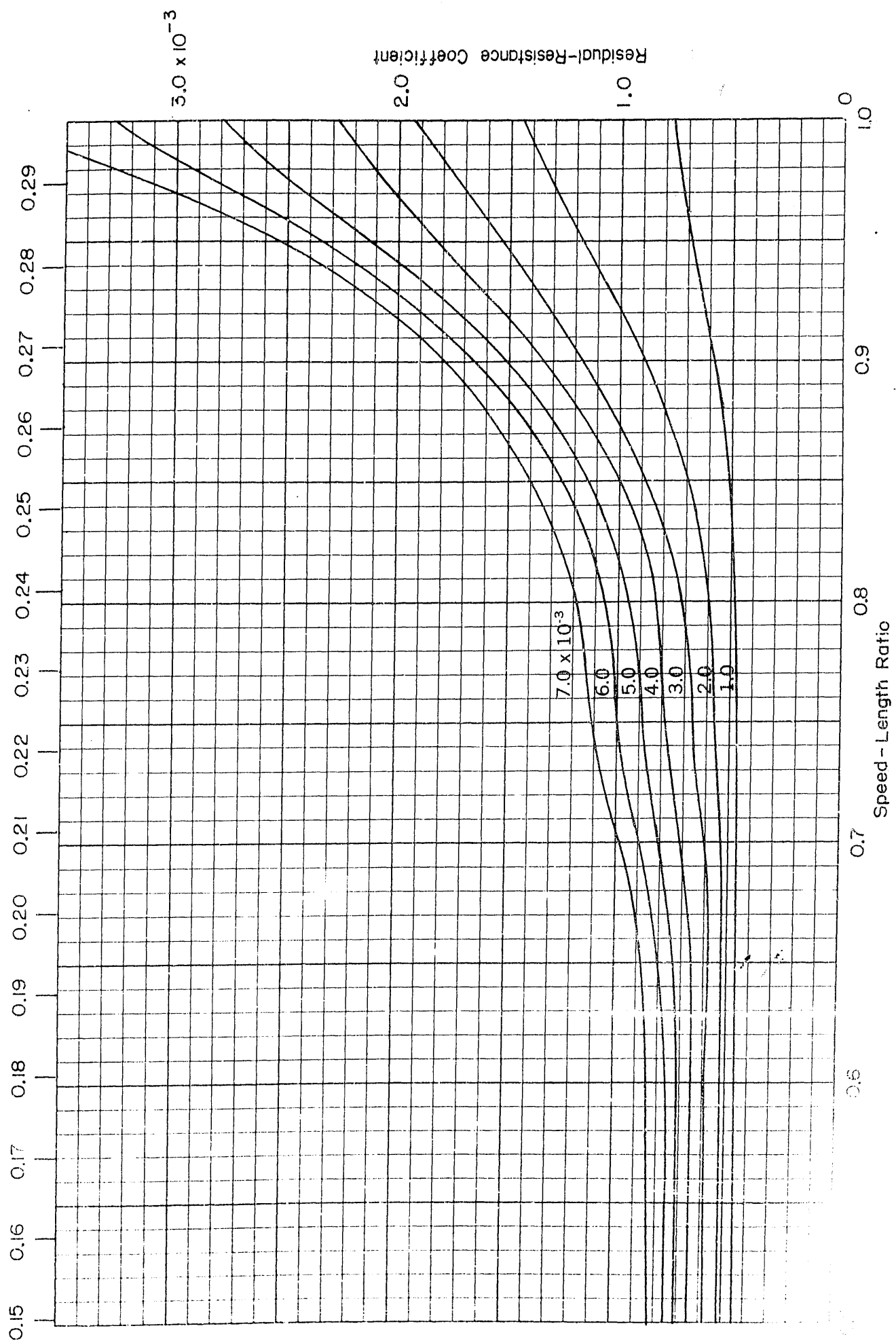


$B/H=3.75$
 $C_p=0.62$

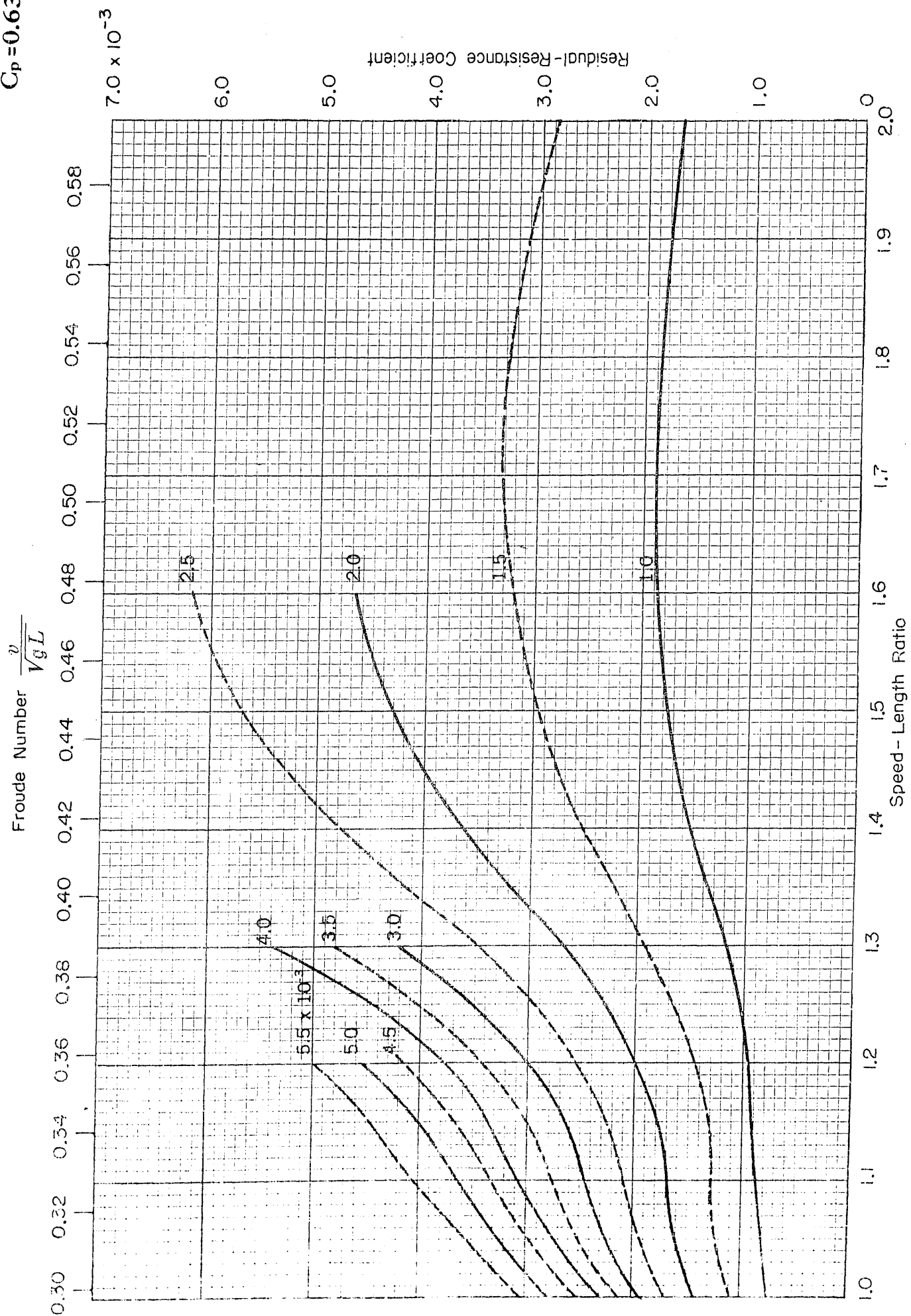


$B/H=3.75$
 $C_p=0.63$

Froude Number $\frac{v}{\sqrt{gL}}$

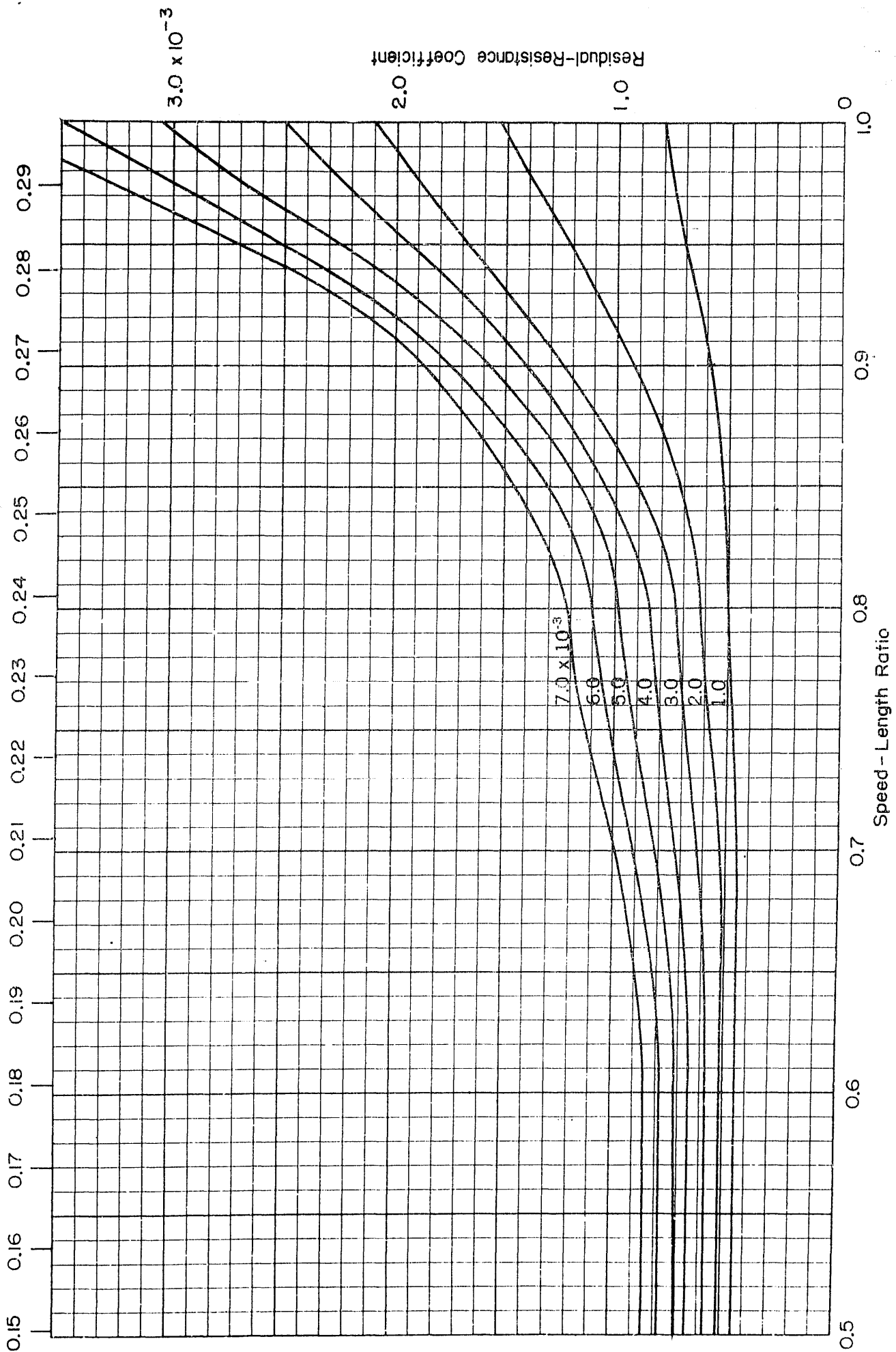


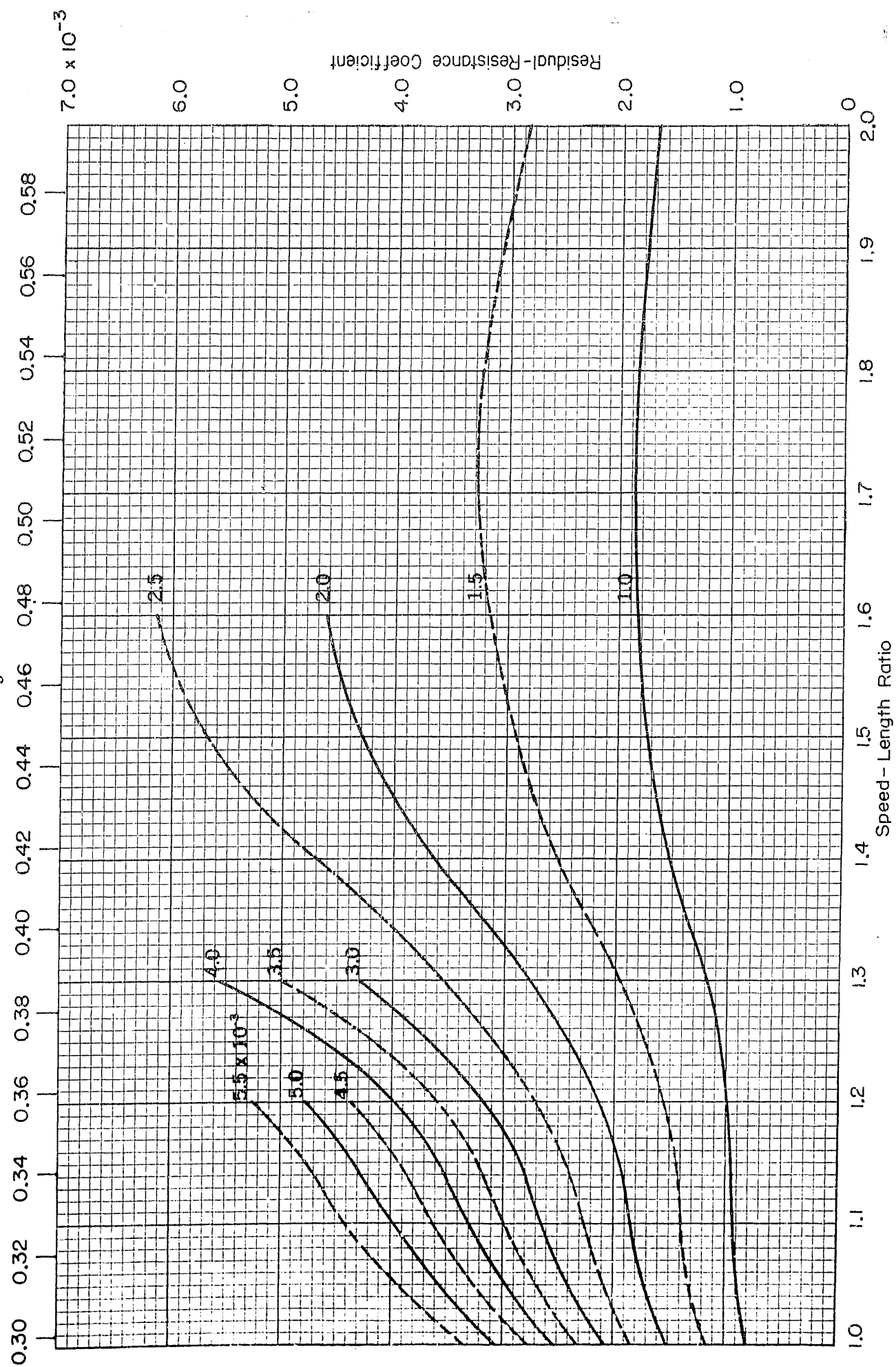
$B/H=3.75$
 $C_p=0.63$



$B/H=3.75$
 $C_p=0.64$

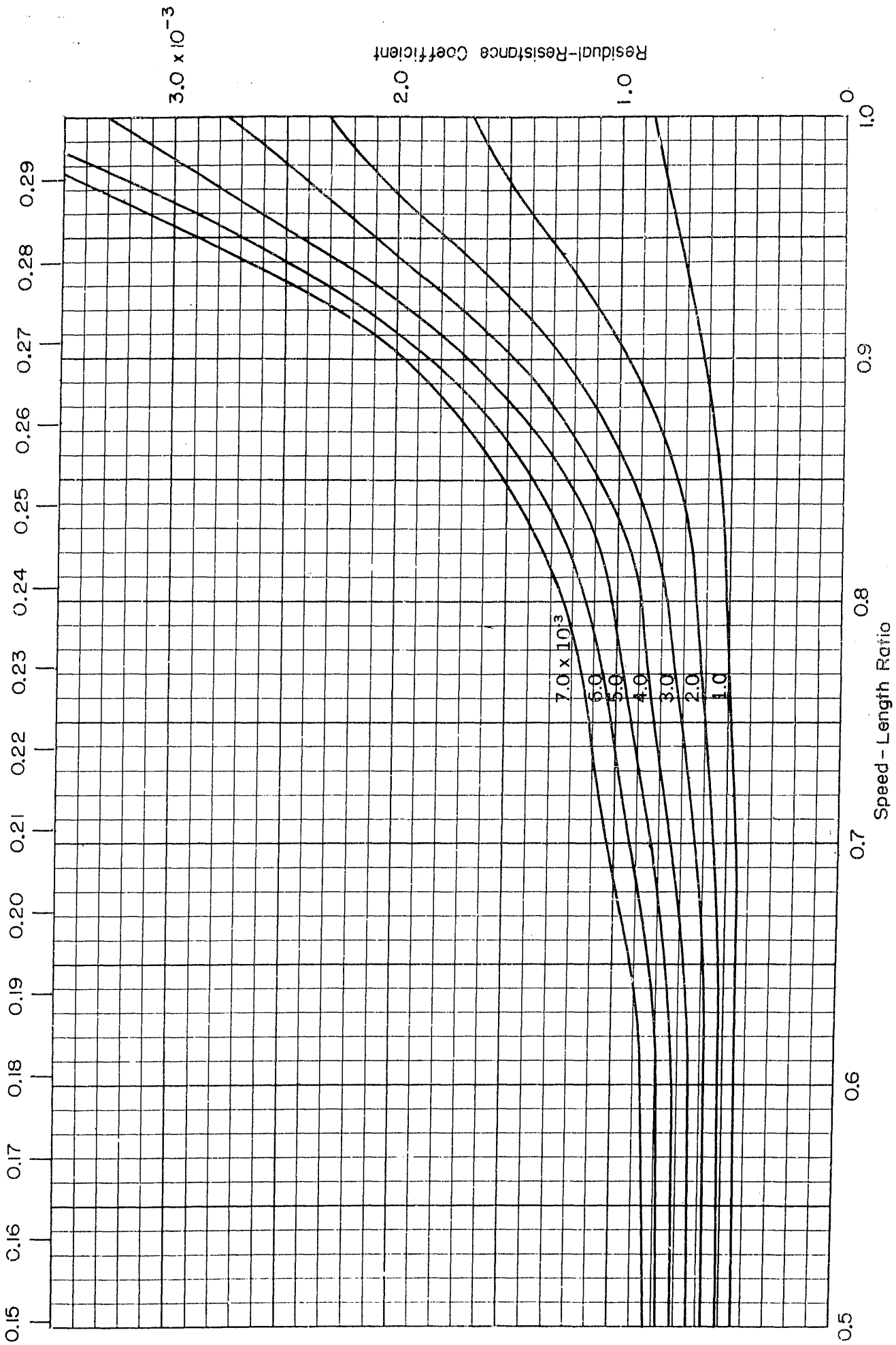
Froude Number $\frac{v}{\sqrt{gL}}$

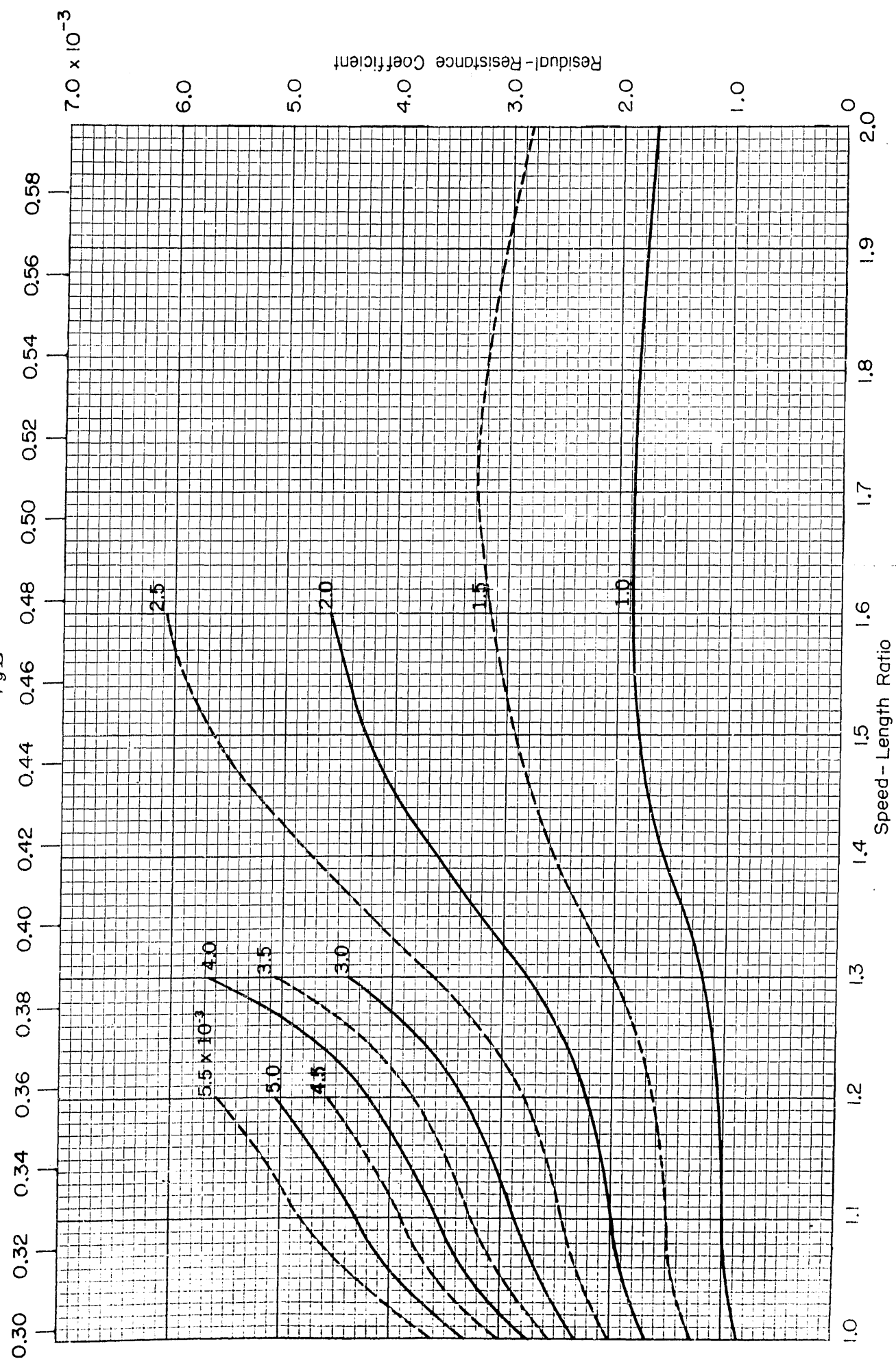


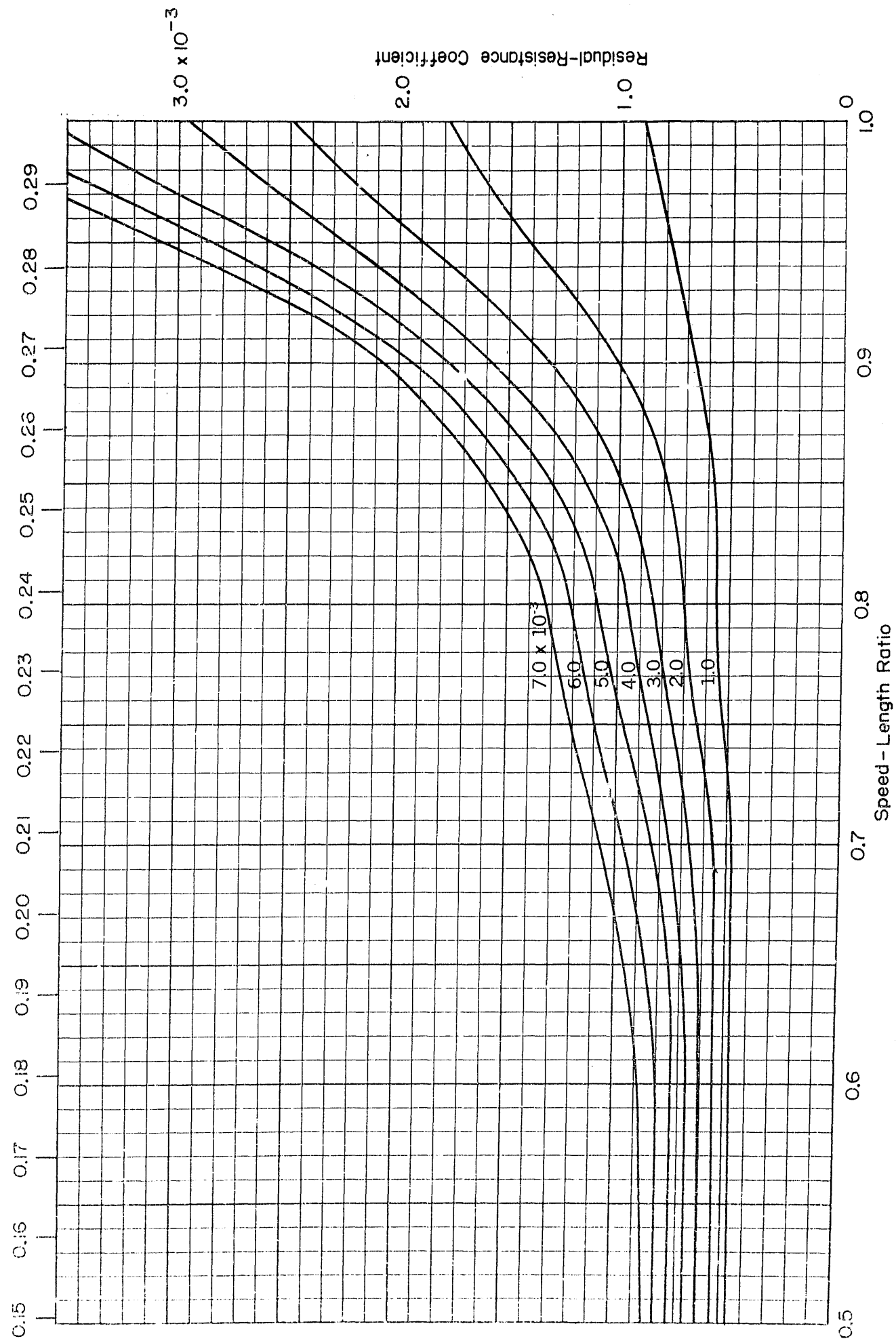
Froude Number $\frac{v}{\sqrt{gL}}$ 

$B/H=3.75$
 $C_p=0.65$

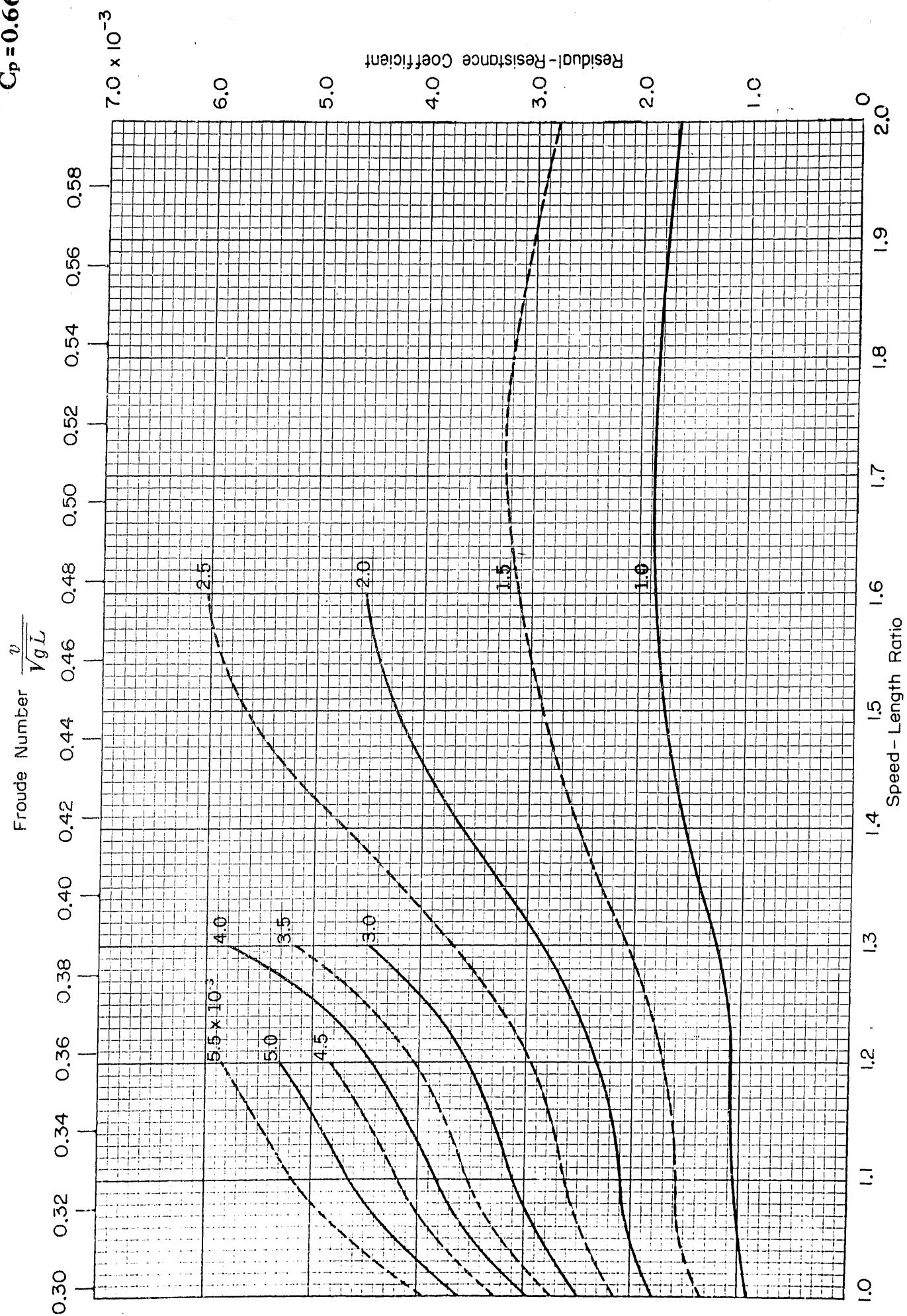
Froude Number $\frac{v}{\sqrt{gL}}$



$$\frac{v}{\sqrt{gL}}$$


$$\frac{v}{\sqrt{gL}}$$


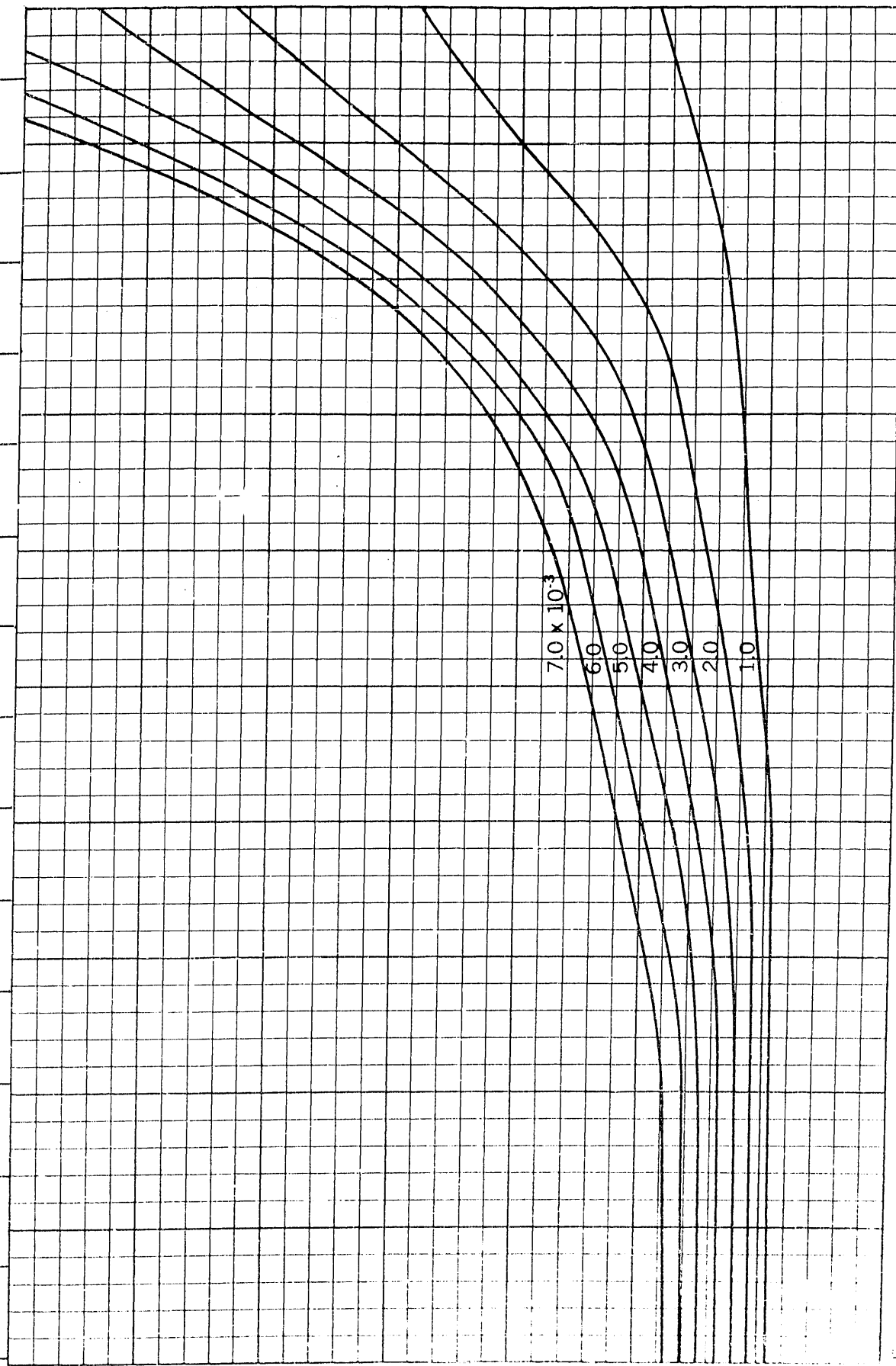
$B/H=3.75$
 $C_p=0.66$



$B/H=3.75$
 $C_p=0.67$

Froude Number $\frac{v}{\sqrt{gL}}$

0.15 0.16 0.17 0.18 0.19 0.20 0.21 0.22 0.23 0.24 0.25 0.26 0.27 0.28 0.29



Residual-Resistance Coefficient

3.0×10^{-3}

7.0×10^{-3}

6.0

5.0

4.0

3.0

2.0

1.0

0.5

0.6

0.7

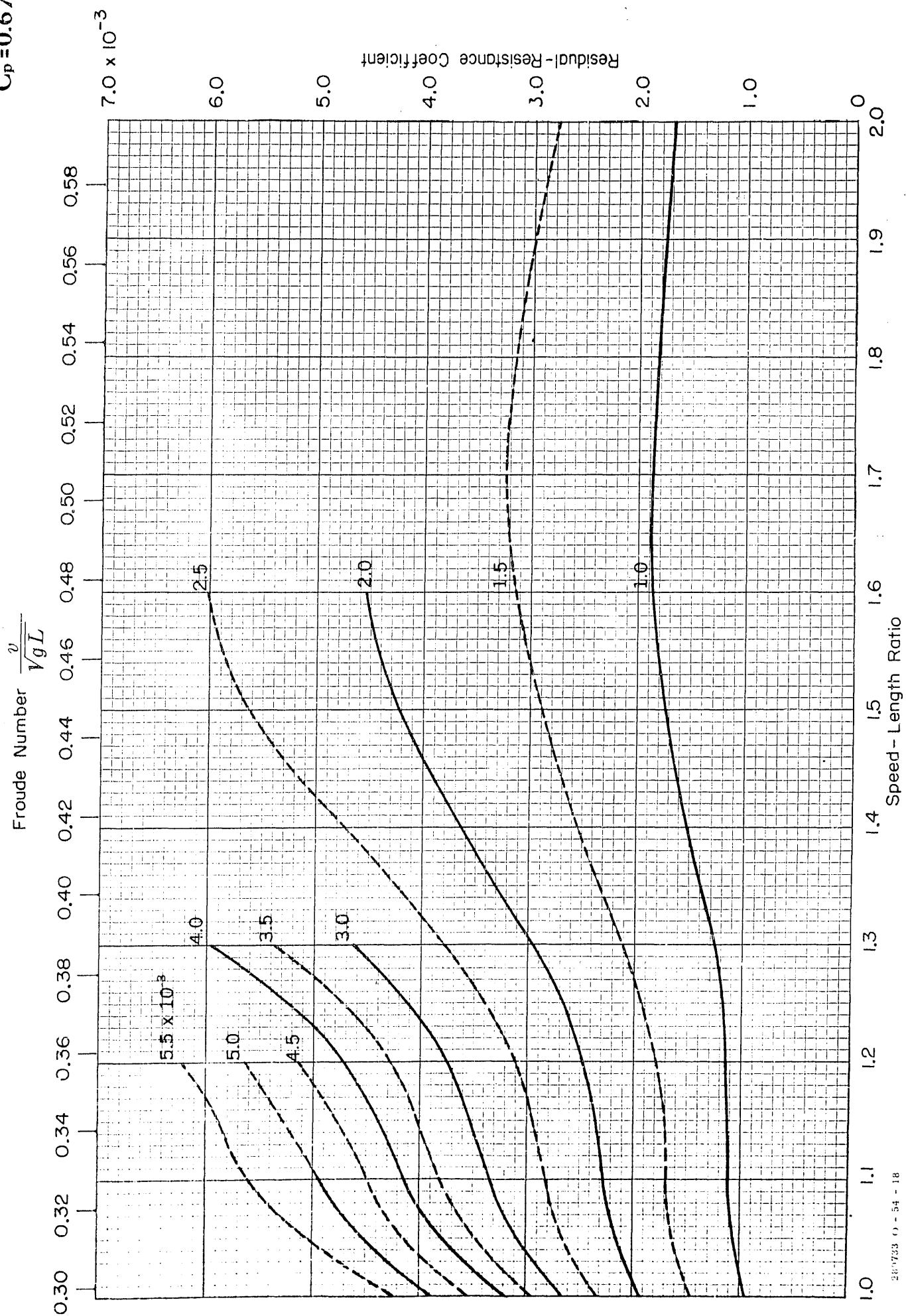
0.8

0.9

1.0

Speed - Length Ratio

$B/H=3.75$
 $C_p=0.67$



$B/H=3.75$
 $C_p=0.68$

Froude Number $\frac{v}{\sqrt{gL}}$

0.15 0.16 0.17 0.18 0.19 0.20 0.21 0.22 0.23 0.24 0.25 0.26 0.27 0.28 0.29

0.5

0.6

0.7

0.8

0.9

1.0

Speed - Length Ratio

Residual-Resistance Coefficient

2.0

1.0

3.0×10^{-3}

7.0×10^{-3}

6.0

5.0

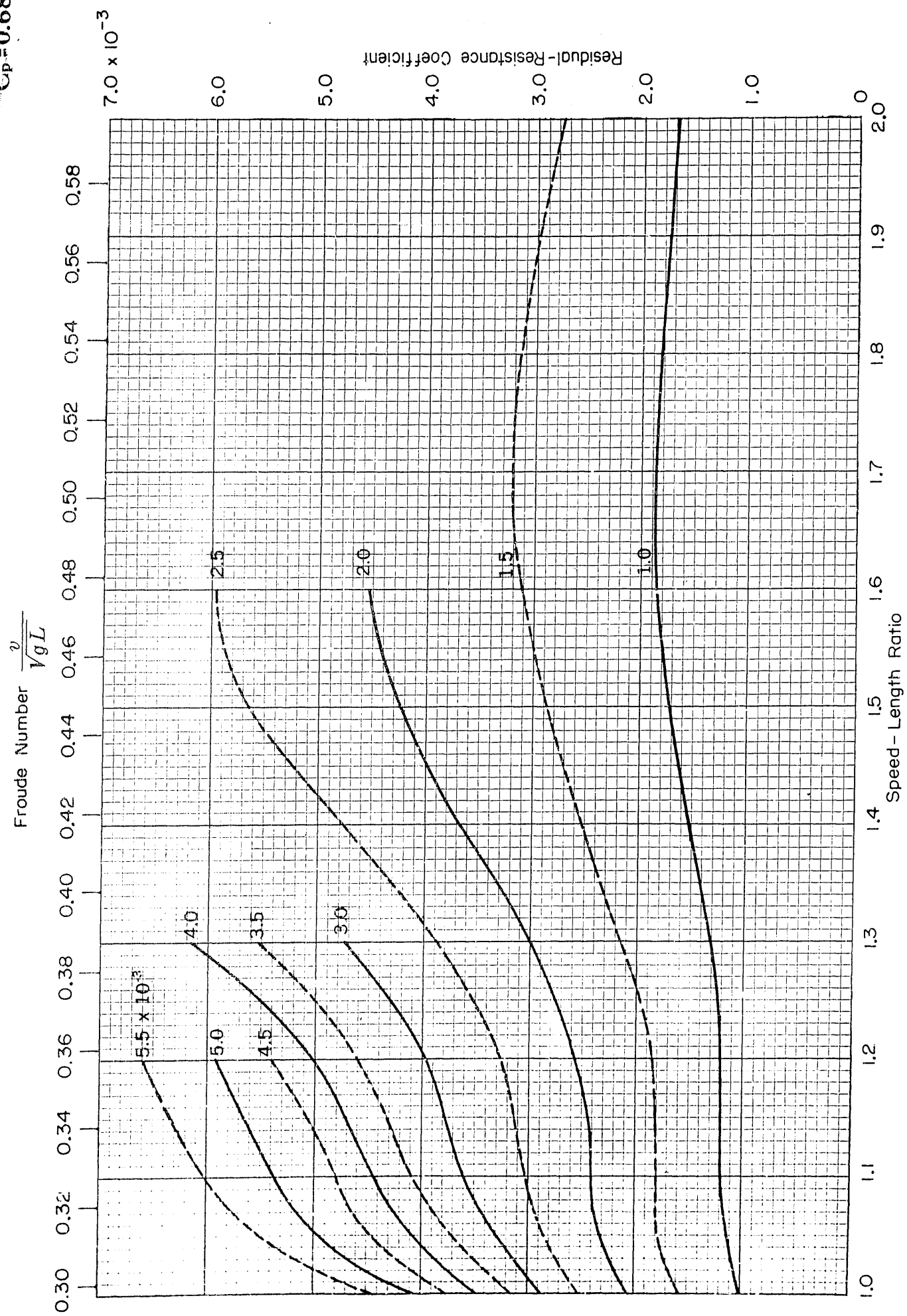
4.0

3.0

2.0

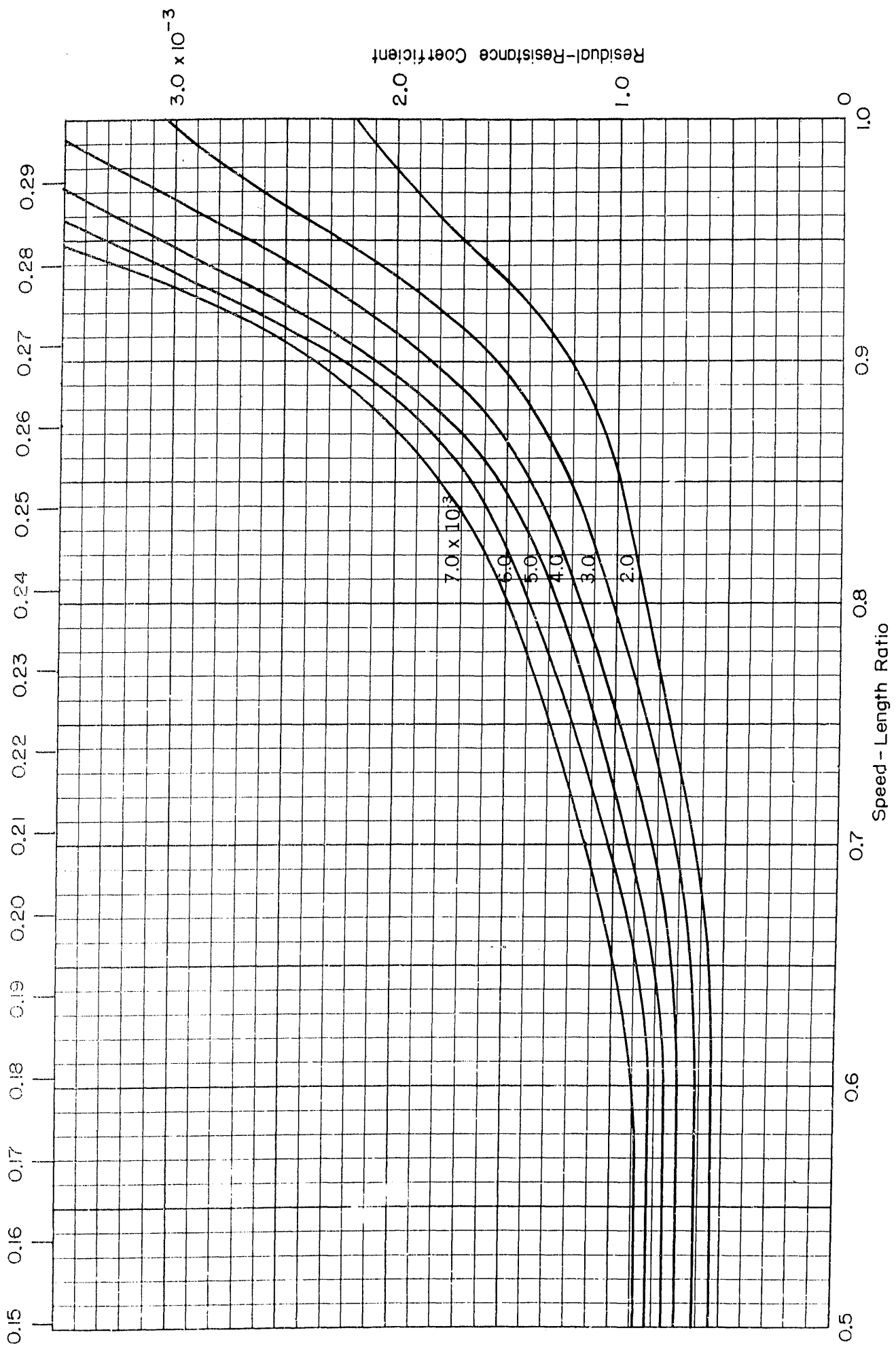
1.0

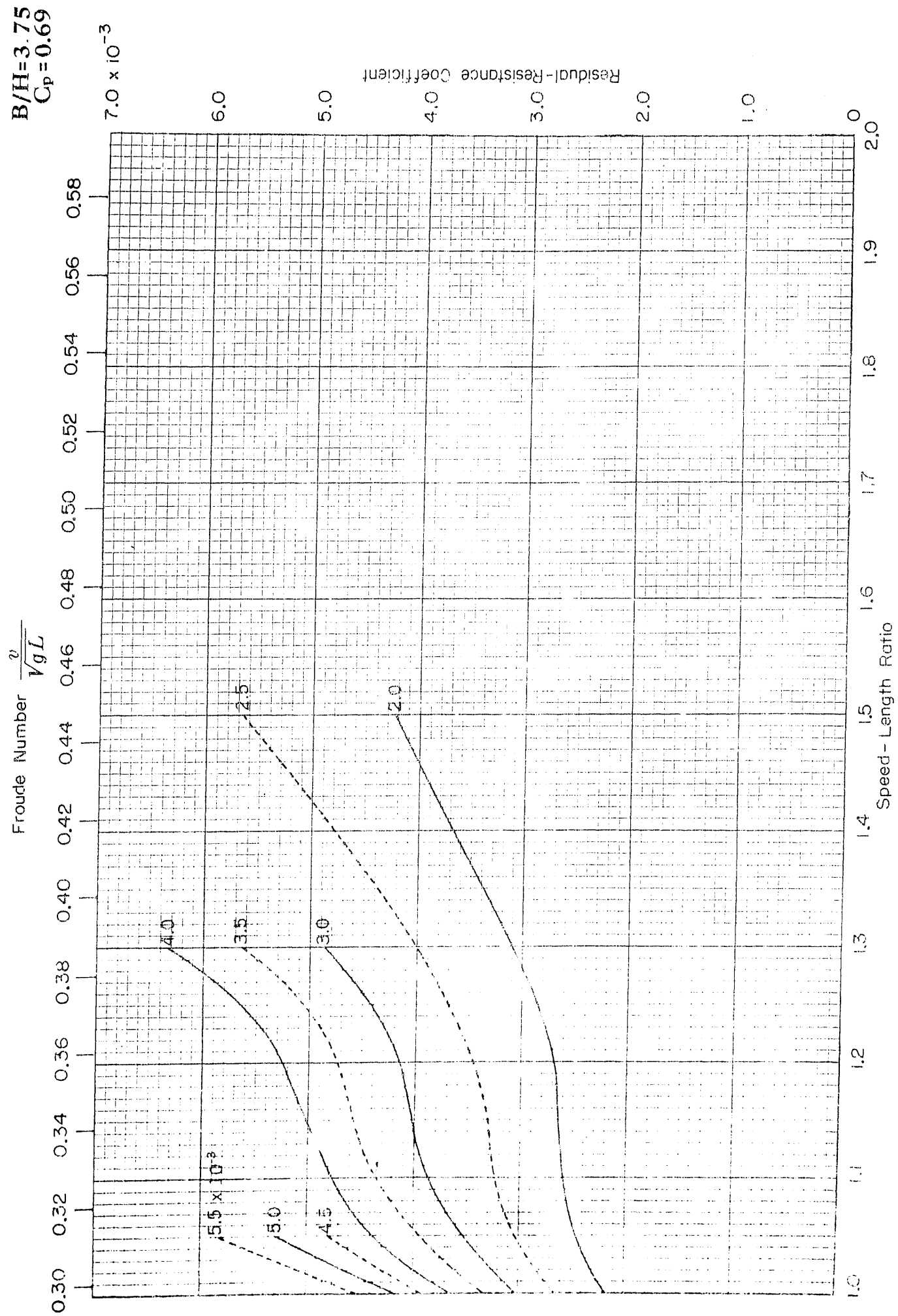
$B/H=3.75$
 $C_p=0.68$



$B/H = 2.75$
 $C_p = 0.69$

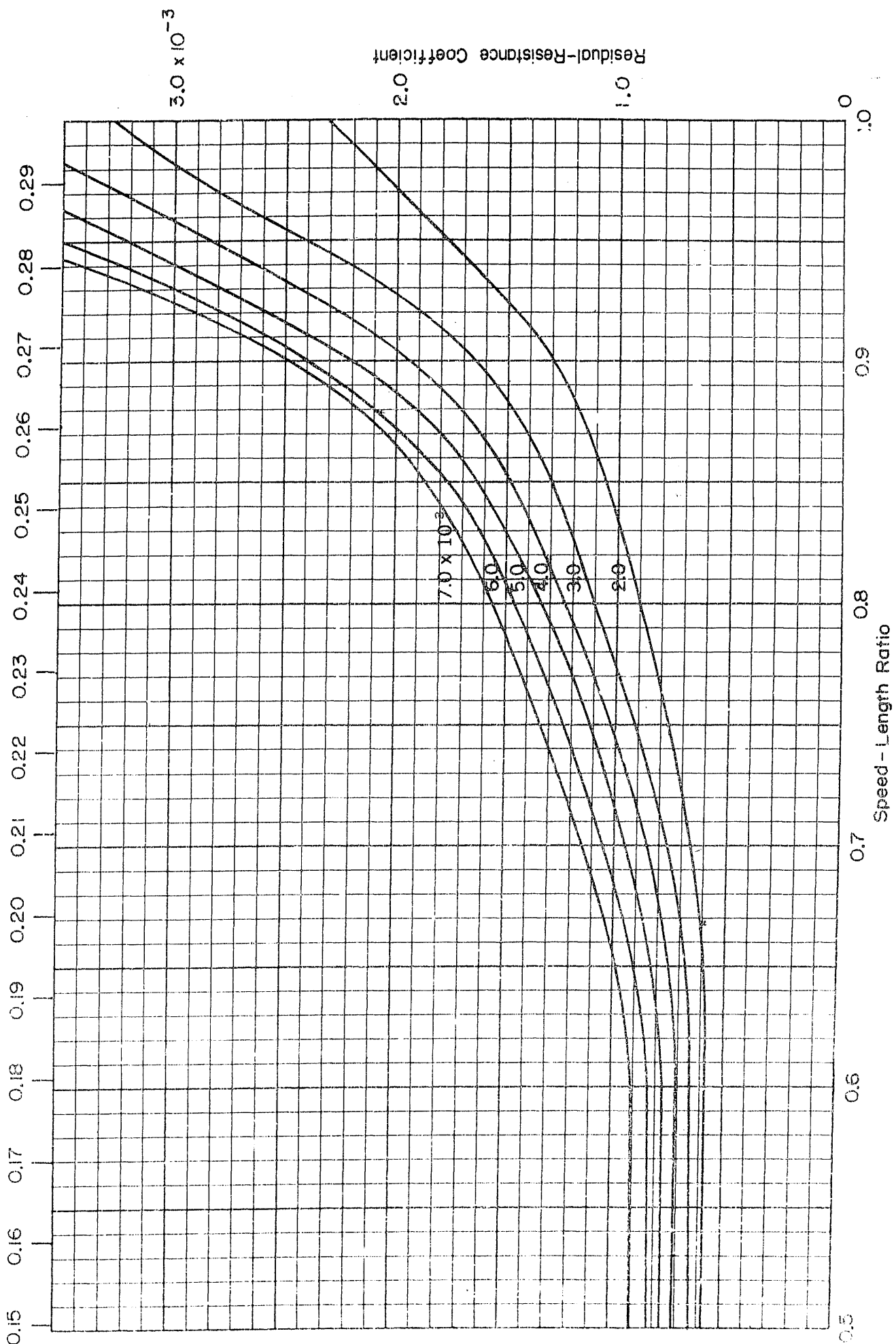
Froude Number $\frac{v}{\sqrt{gL}}$



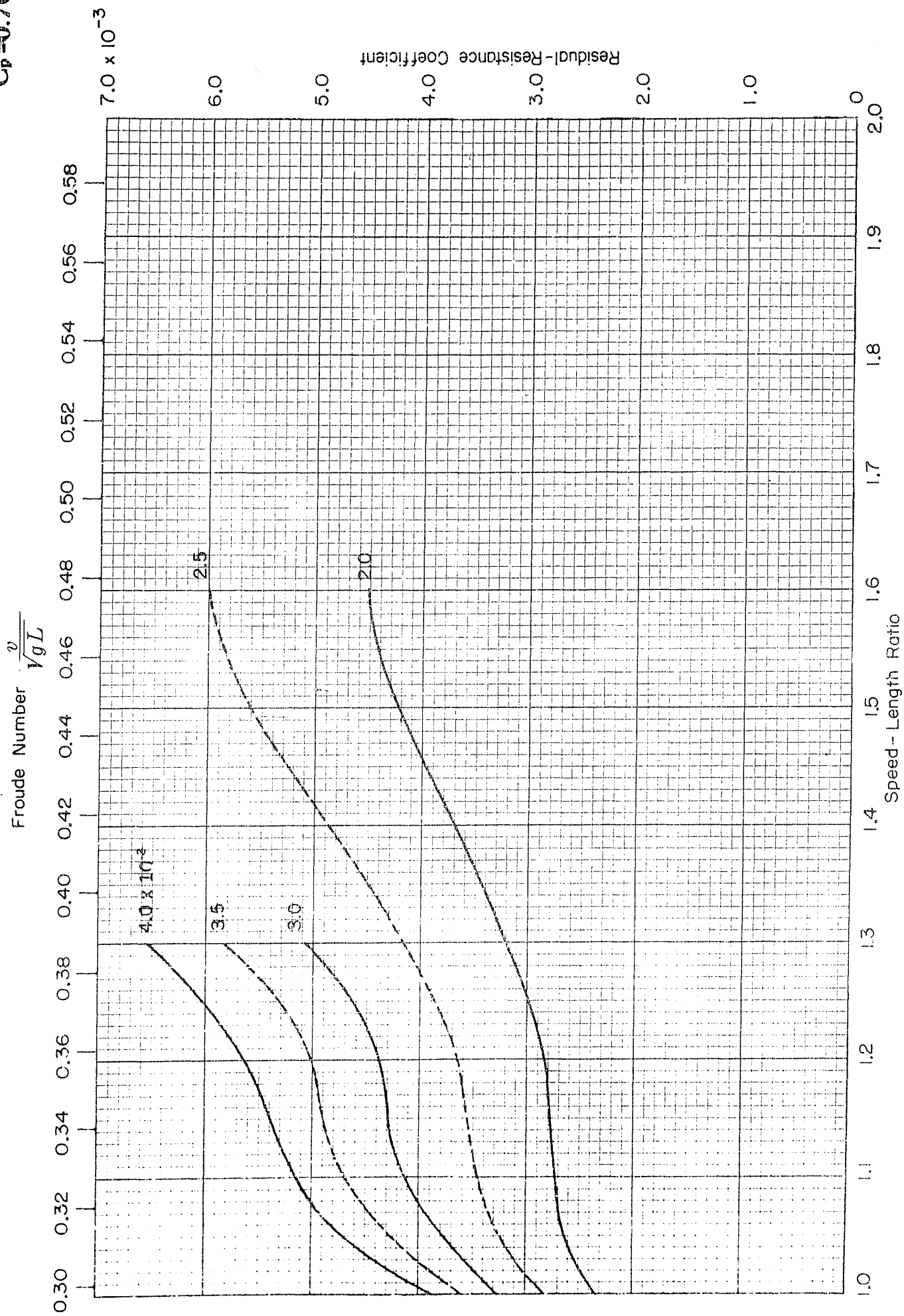
$$\frac{\text{Froude Number}}{\sqrt{gL}}$$


$B/H = 3.78$
 $C_p = 0.70$

Froude Number $\frac{v}{\sqrt{gL}}$

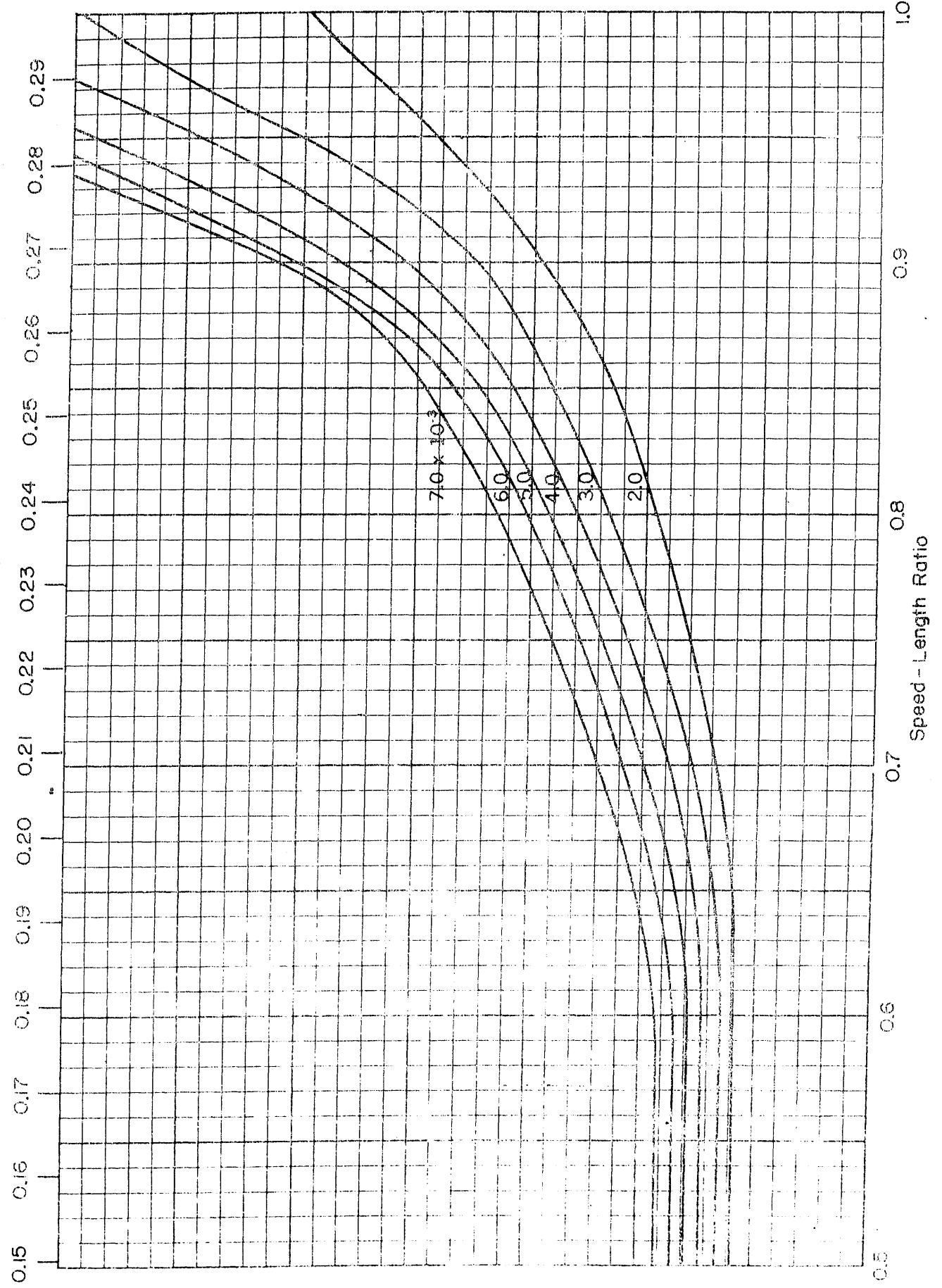


$B/H=3.75$
 $C_p=0.70$



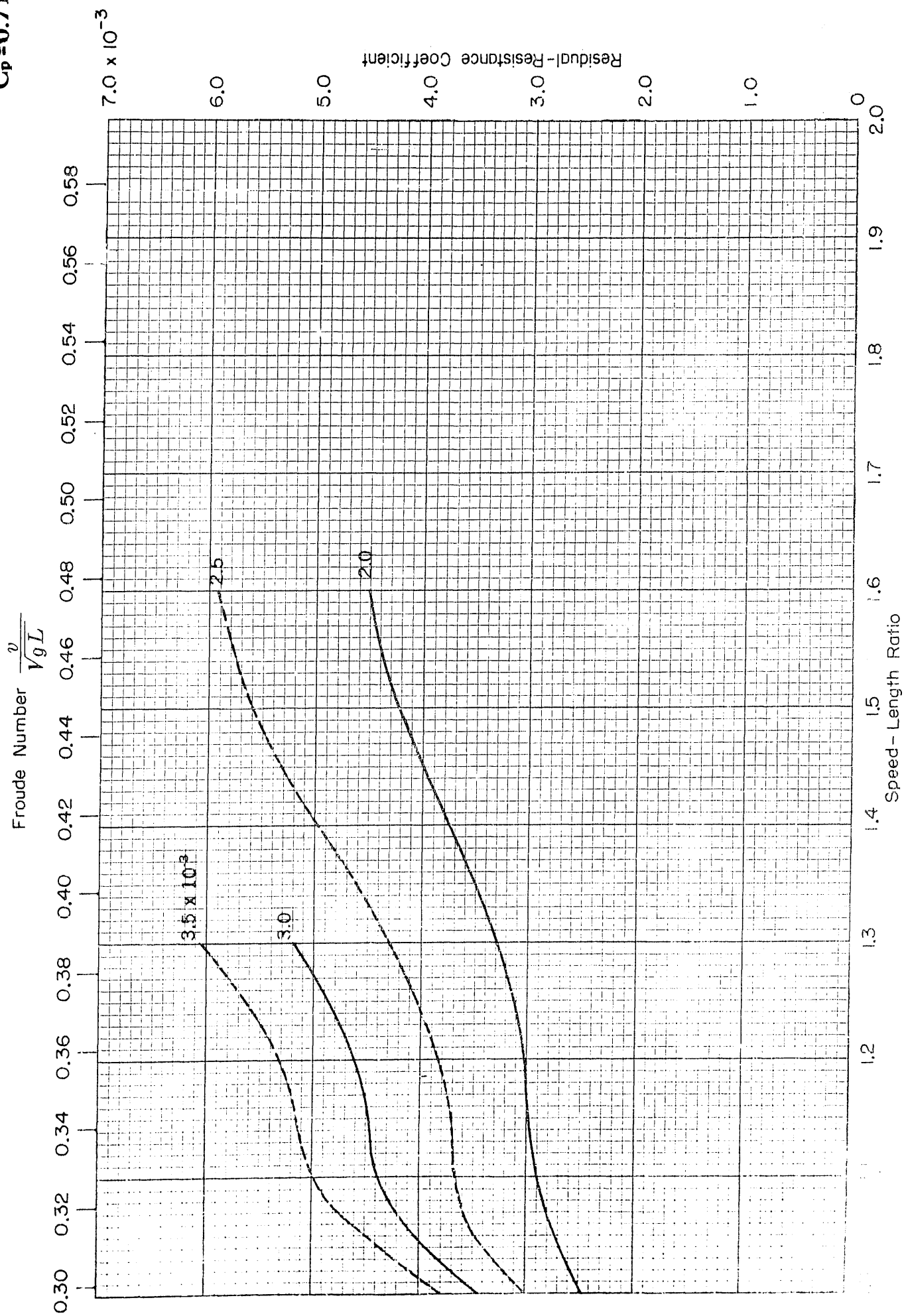
B/H=3.75
Cp=0.71

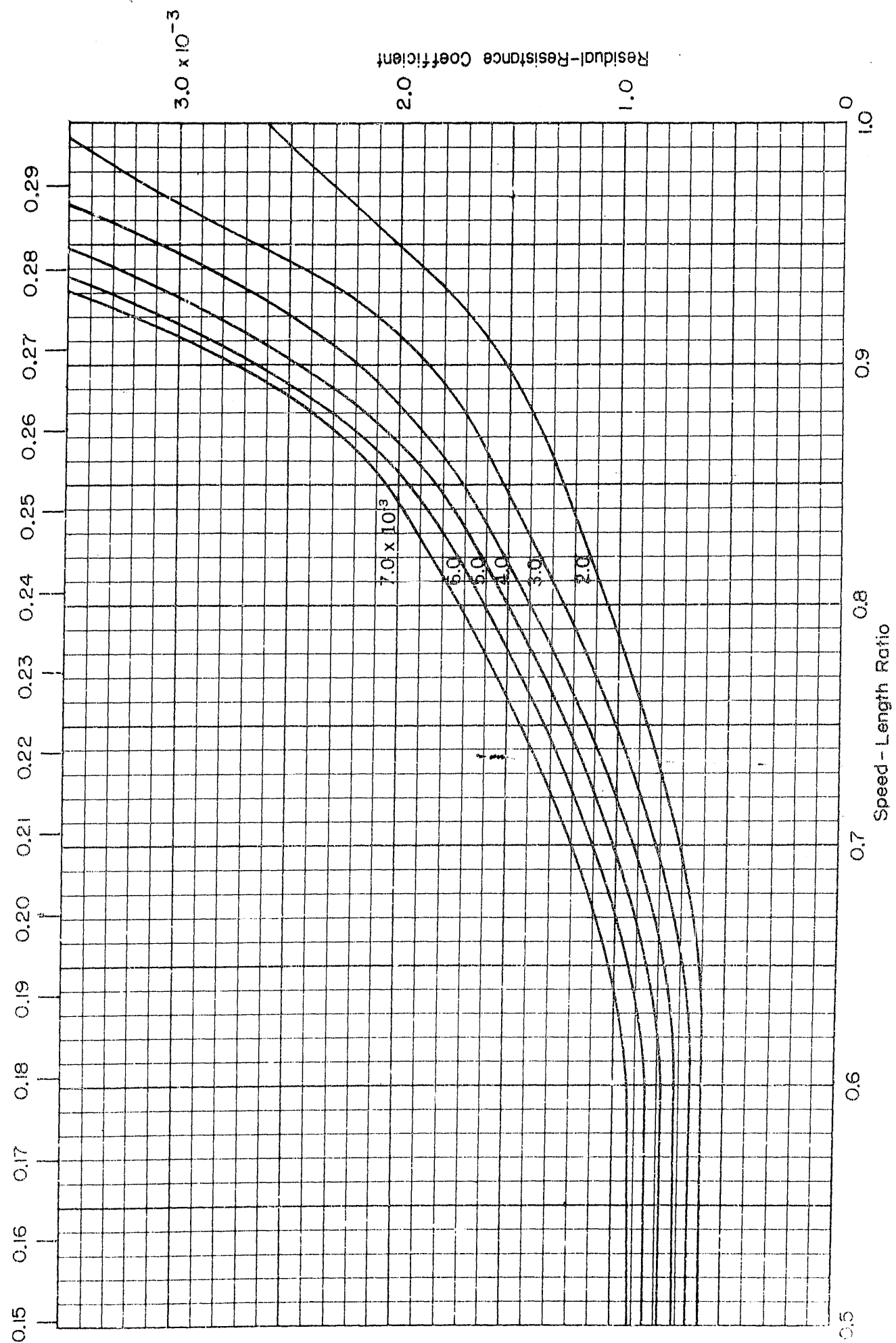
Froude Number $\frac{v}{\sqrt{gL}}$



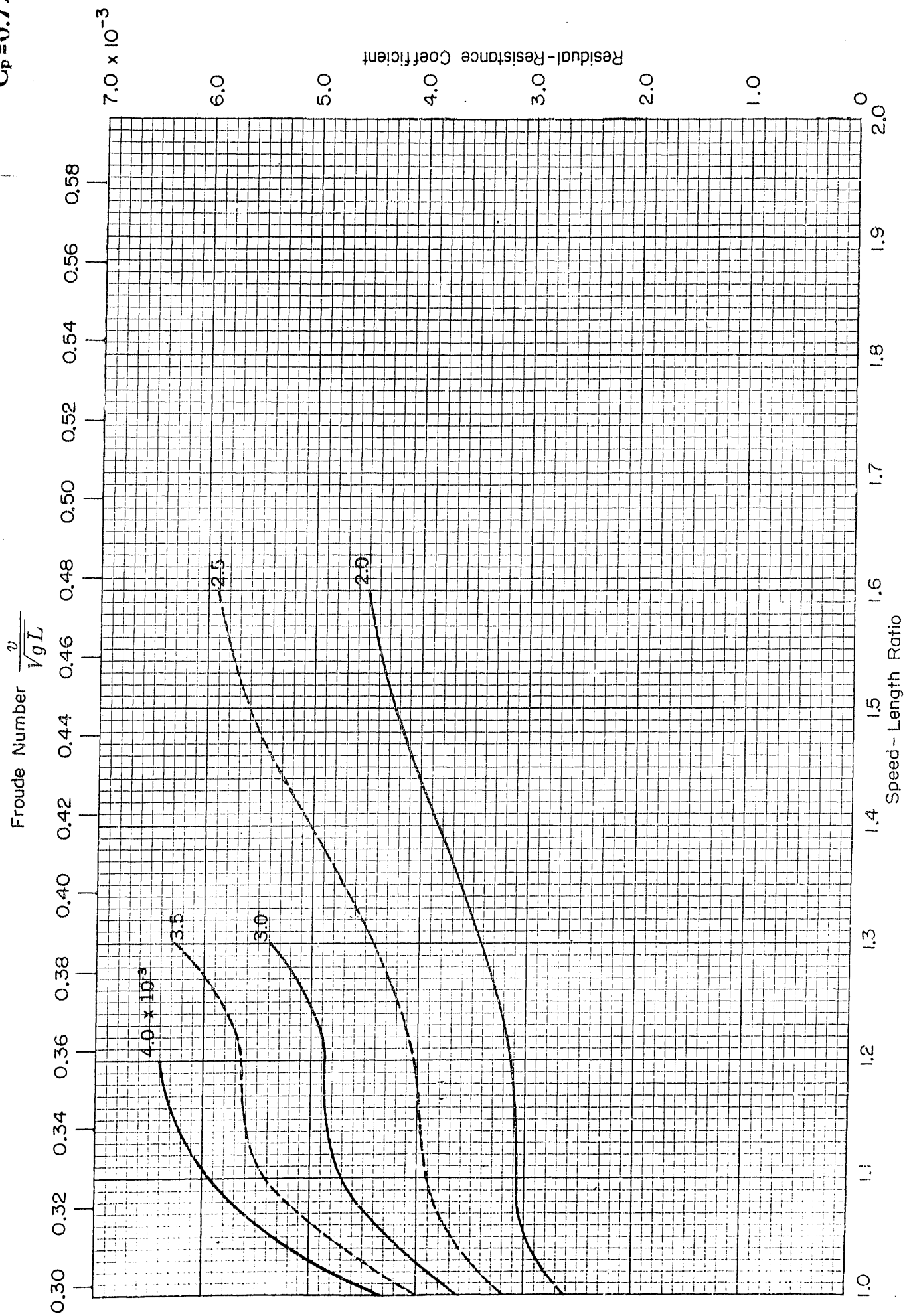
Residual-Resistance Coefficient

$B/H=3.75$
 $C_p=0.71$



$$\frac{v}{\sqrt{gL}}$$


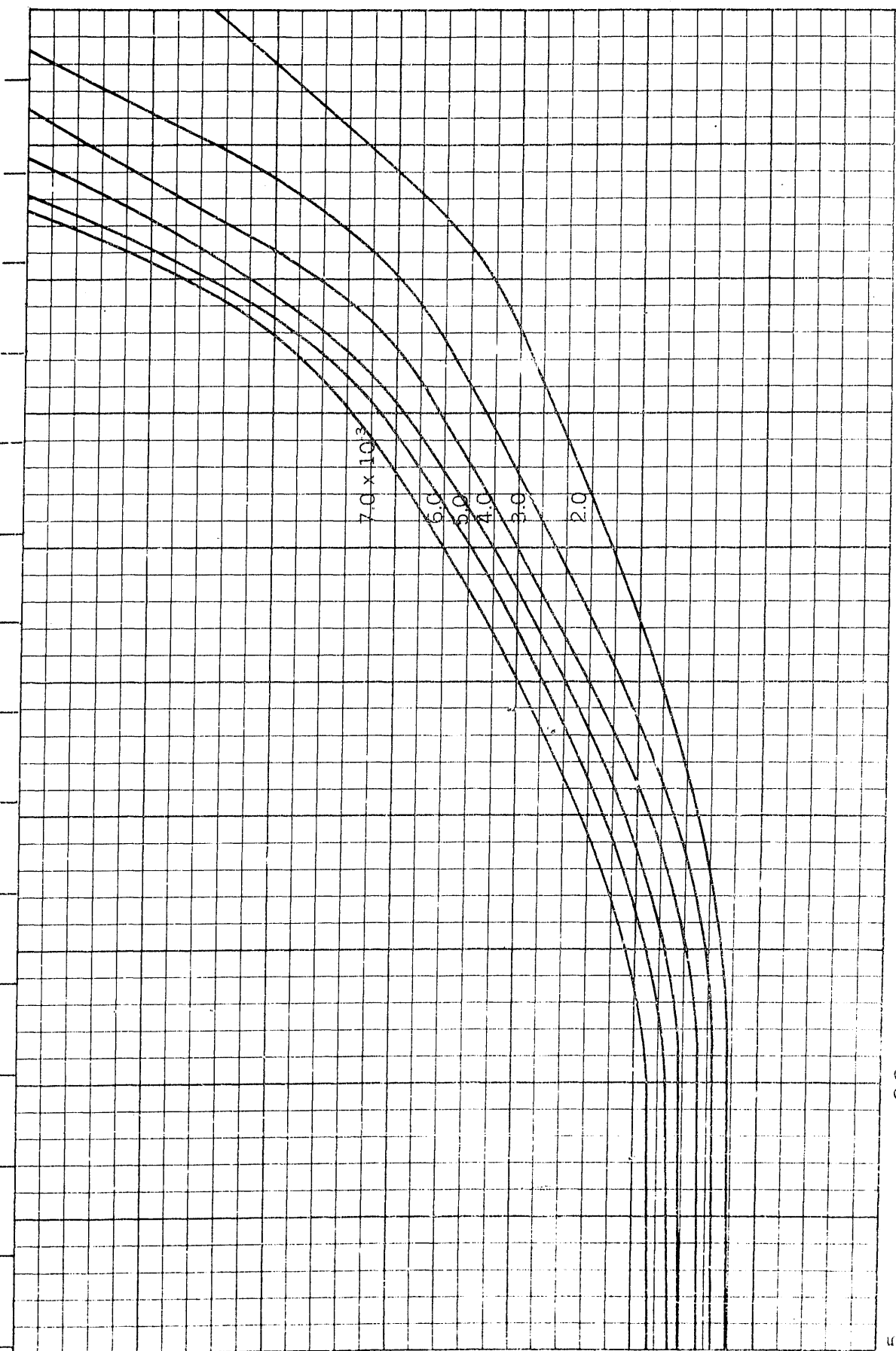
$B/H=3.75$
 $C_p=0.72$



$B/H=3.75$
 $C_p=0.73$

Froude Number $\frac{v}{\sqrt{gL}}$

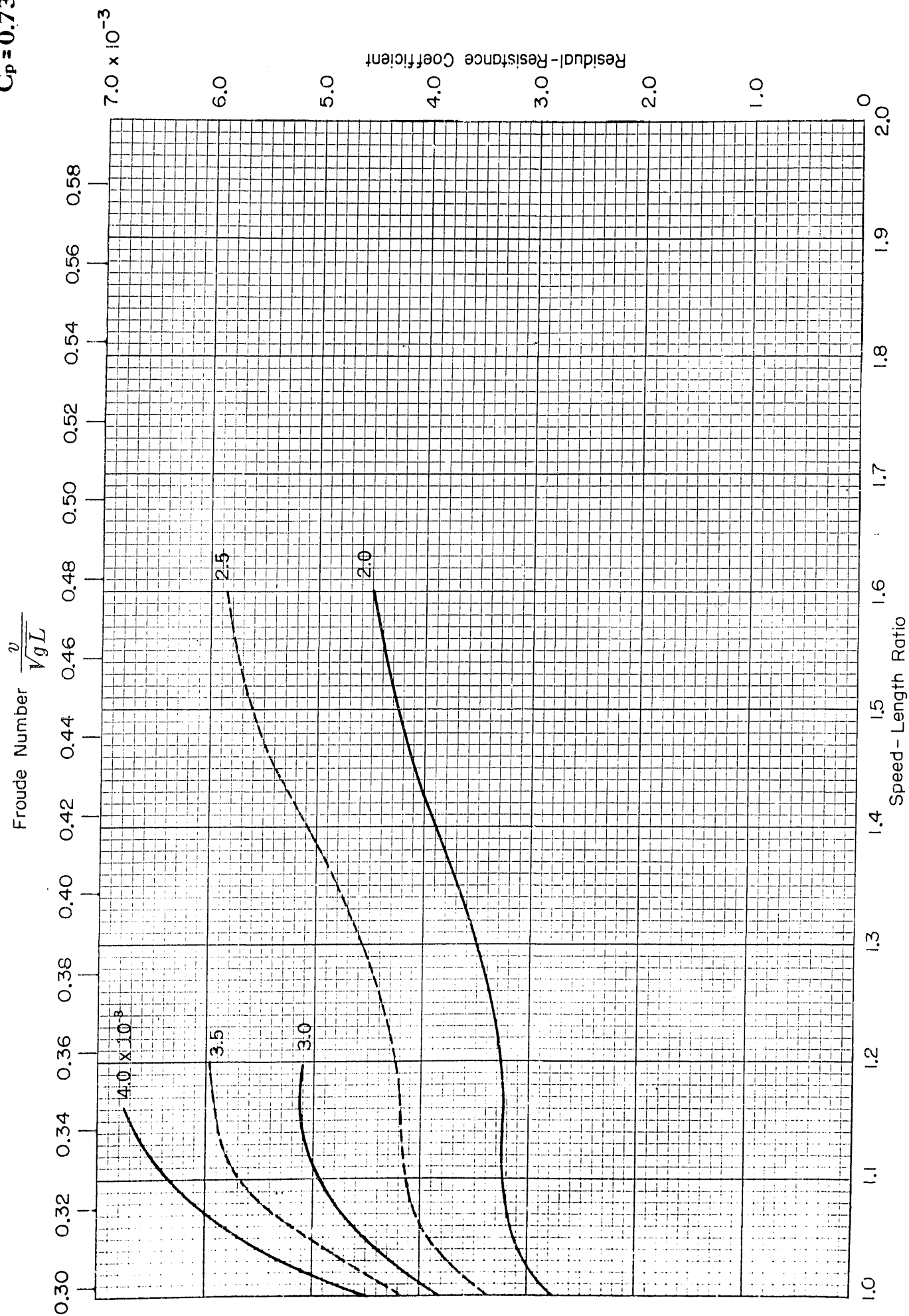
0.15 0.16 0.17 0.18 0.19 0.20 0.21 0.22 0.23 0.24 0.25 0.26 0.27 0.28 0.29



3.0×10^{-3}
 2.0
 1.0

0.5 0.6 0.7 0.8 0.9 1.0

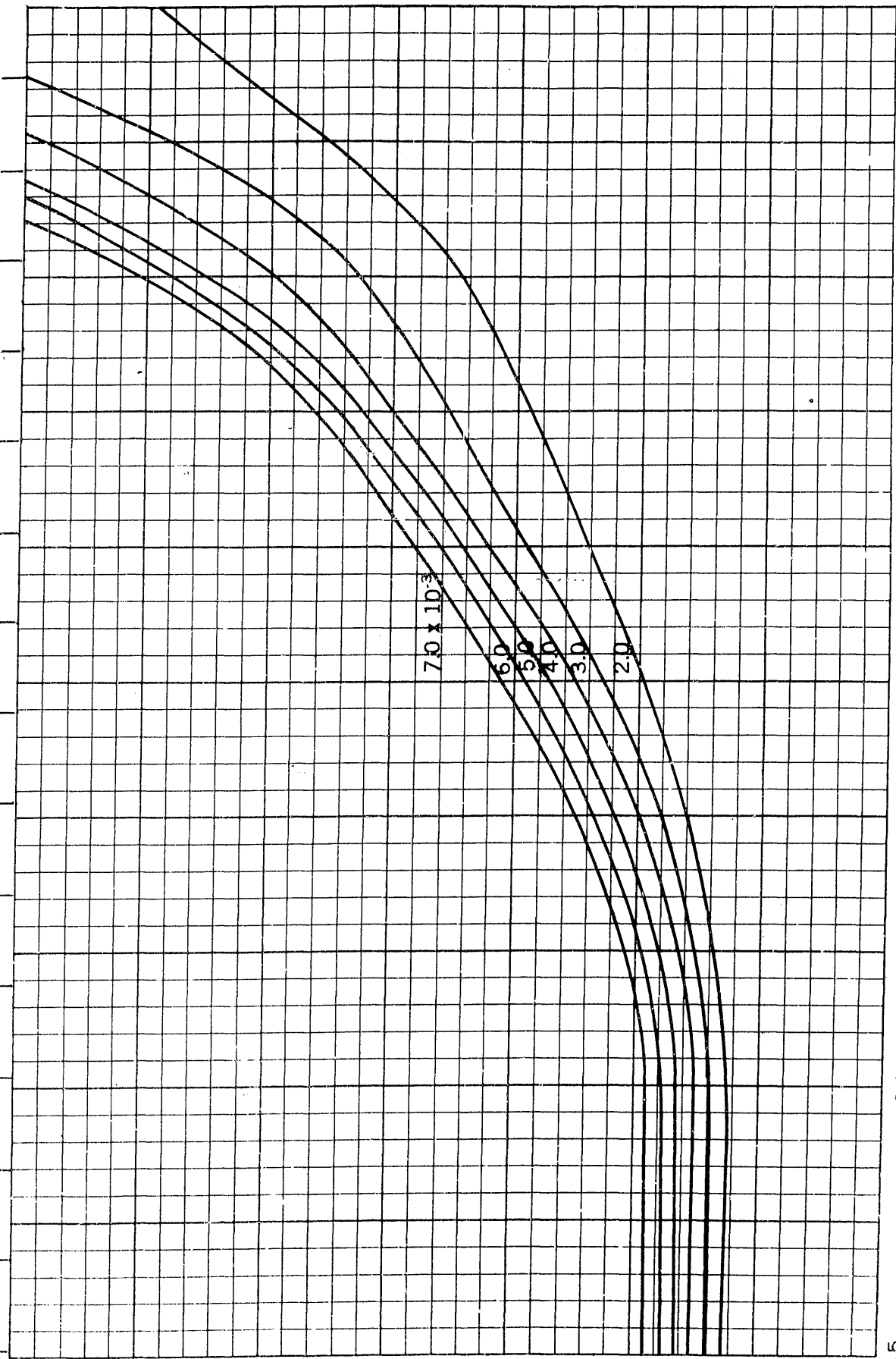
$B/H=3.75$
 $C_p=0.73$



$B/H=3.75$
 $C_p=0.74$

Froude Number $\frac{v}{\sqrt{gL}}$

0.15 0.16 0.17 0.18 0.19 0.20 0.21 0.22 0.23 0.24 0.25 0.26 0.27 0.28 0.29

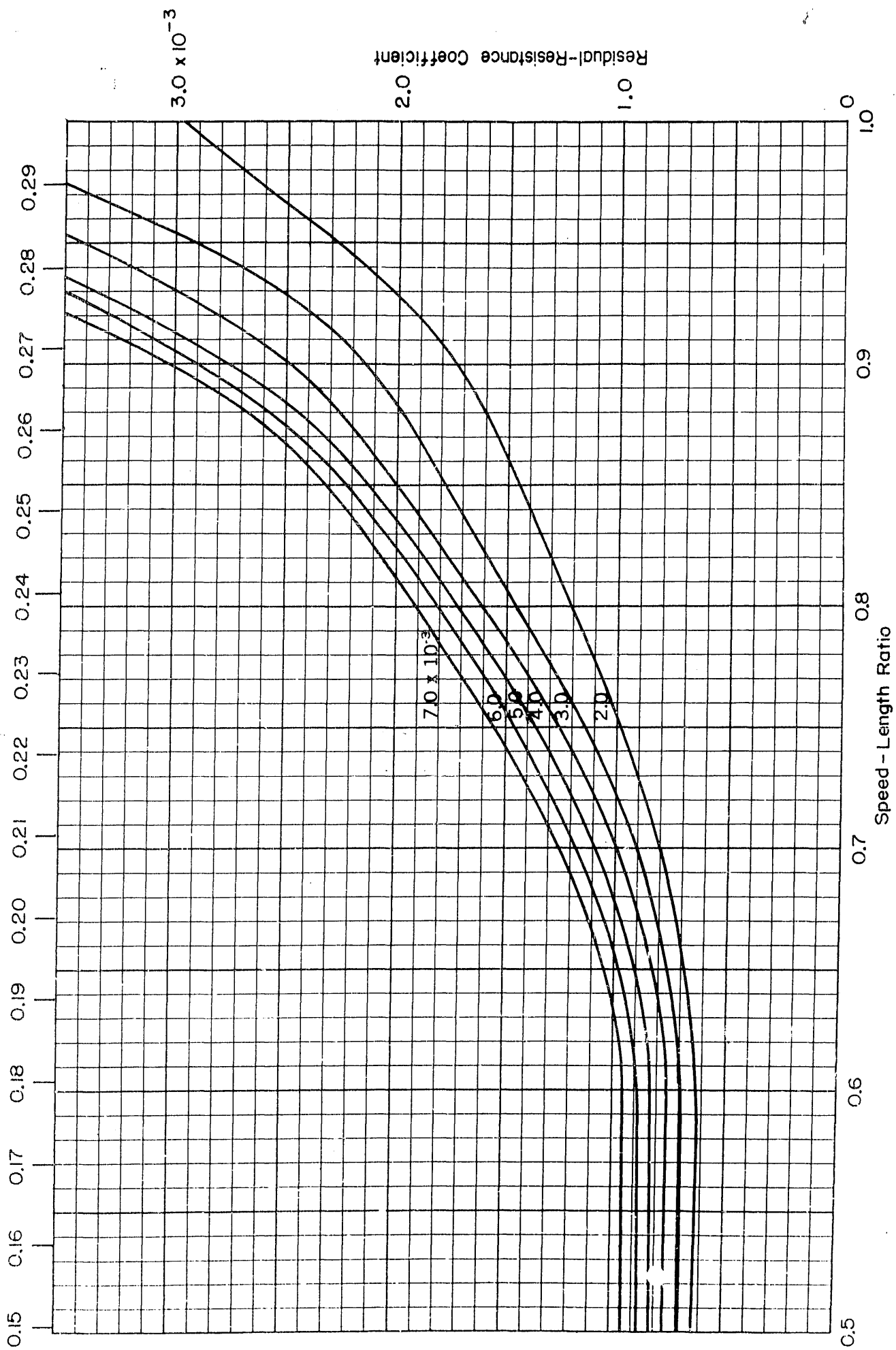


Residual-Resistance Coefficient
3.0 $\times 10^{-3}$
2.0
1.0
0

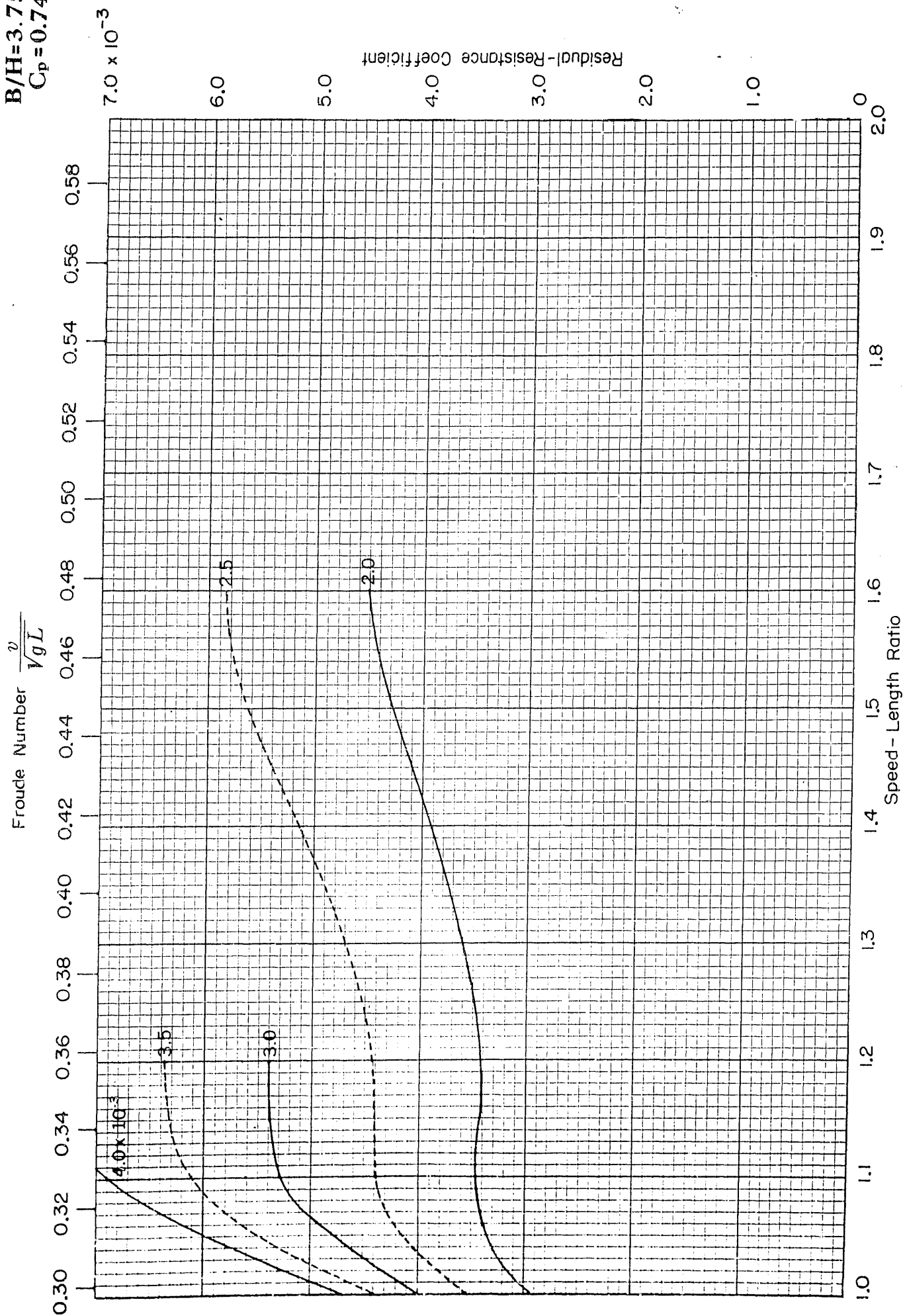
0.5 0.6 0.7 0.8 0.9 1.0
Speed - Length Ratio

$B/H=3.75$
 $C_p=0.74$

Froude Number $\frac{v}{\sqrt{gL}}$

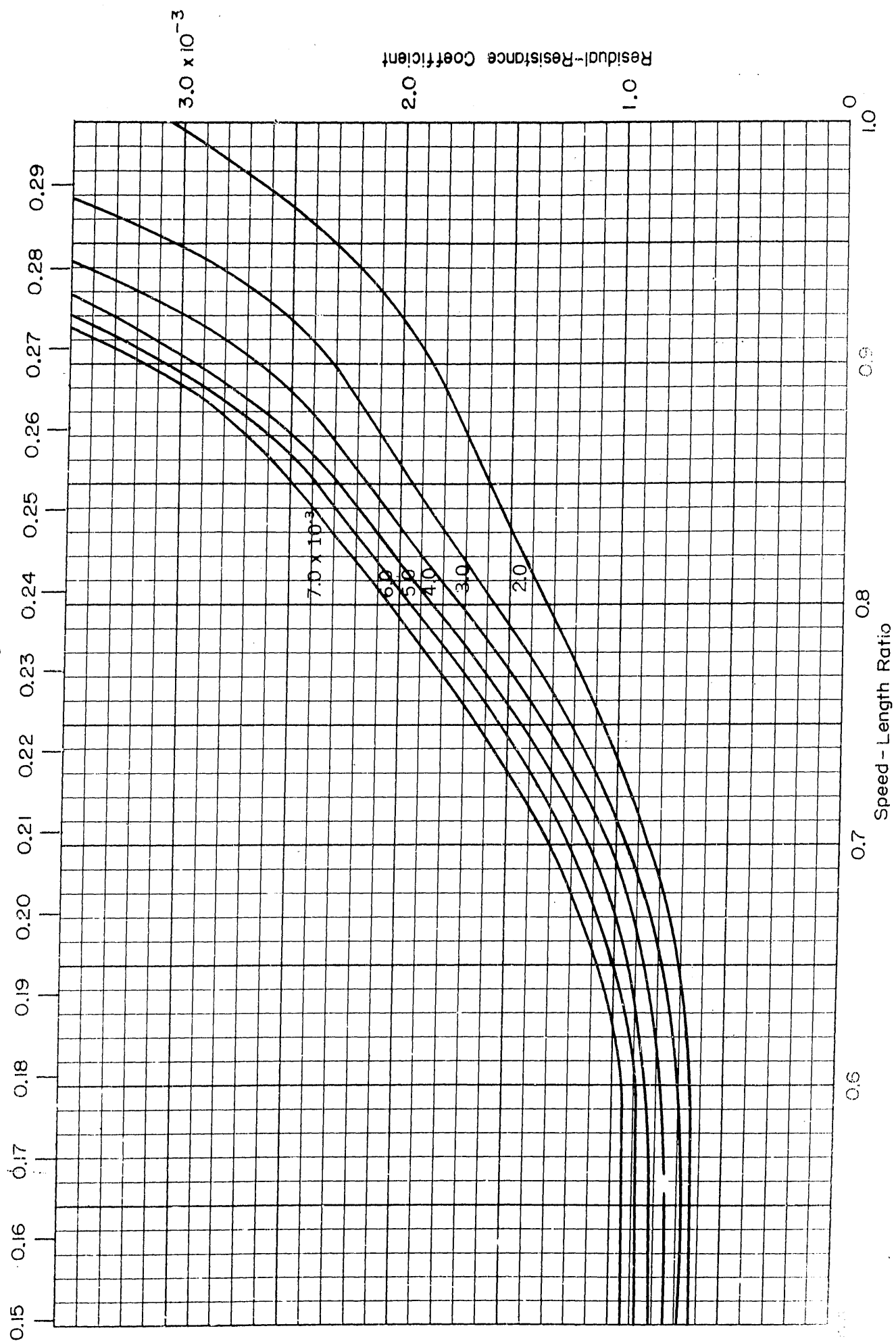


$B/H=3.75$
 $C_p=0.74$



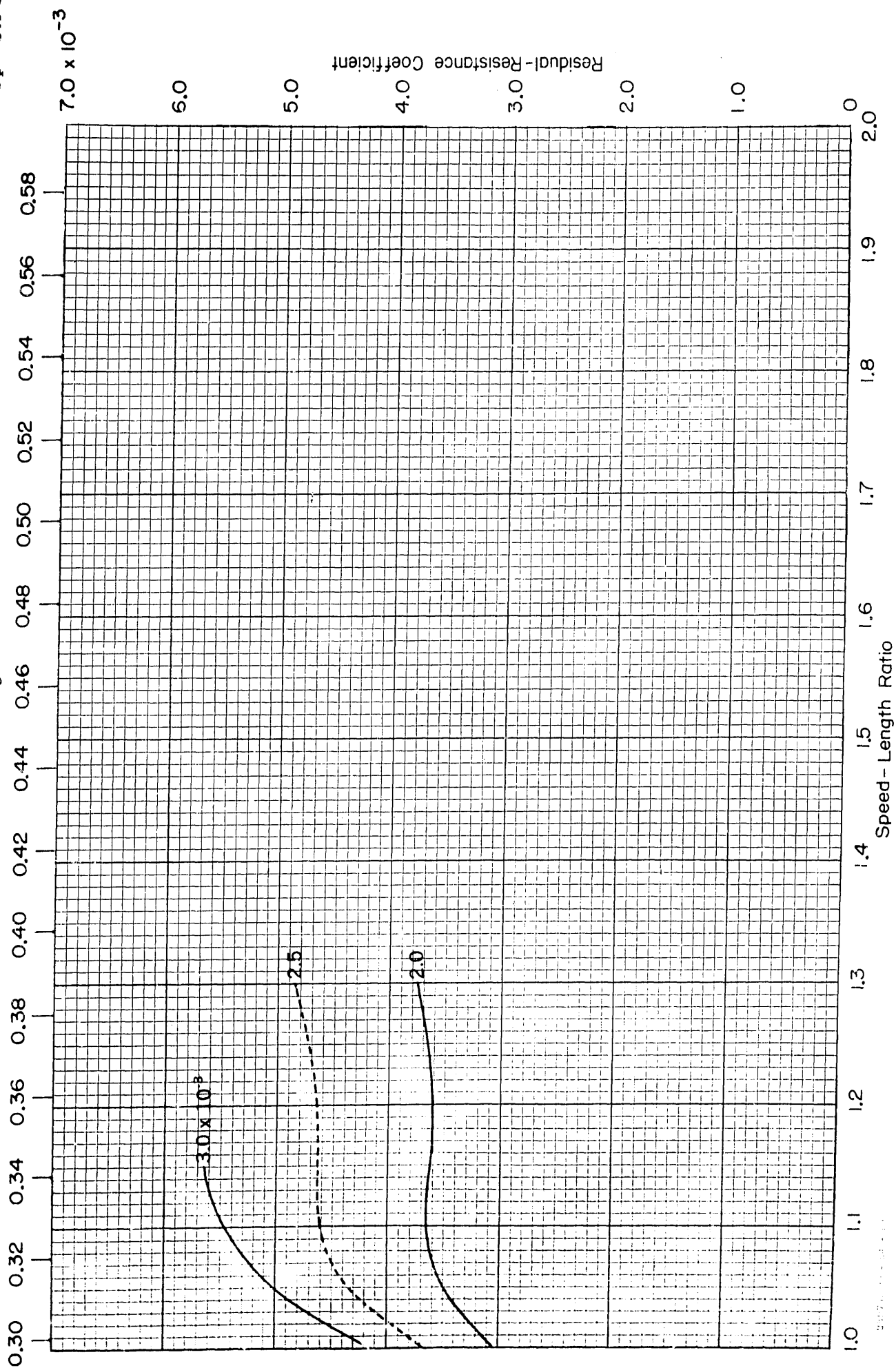
$B/H=3.75$
 $C_p=0.75$

Froude Number $\frac{v}{\sqrt{gL}}$



$B/H=3.75$
 $C_p=0.75$

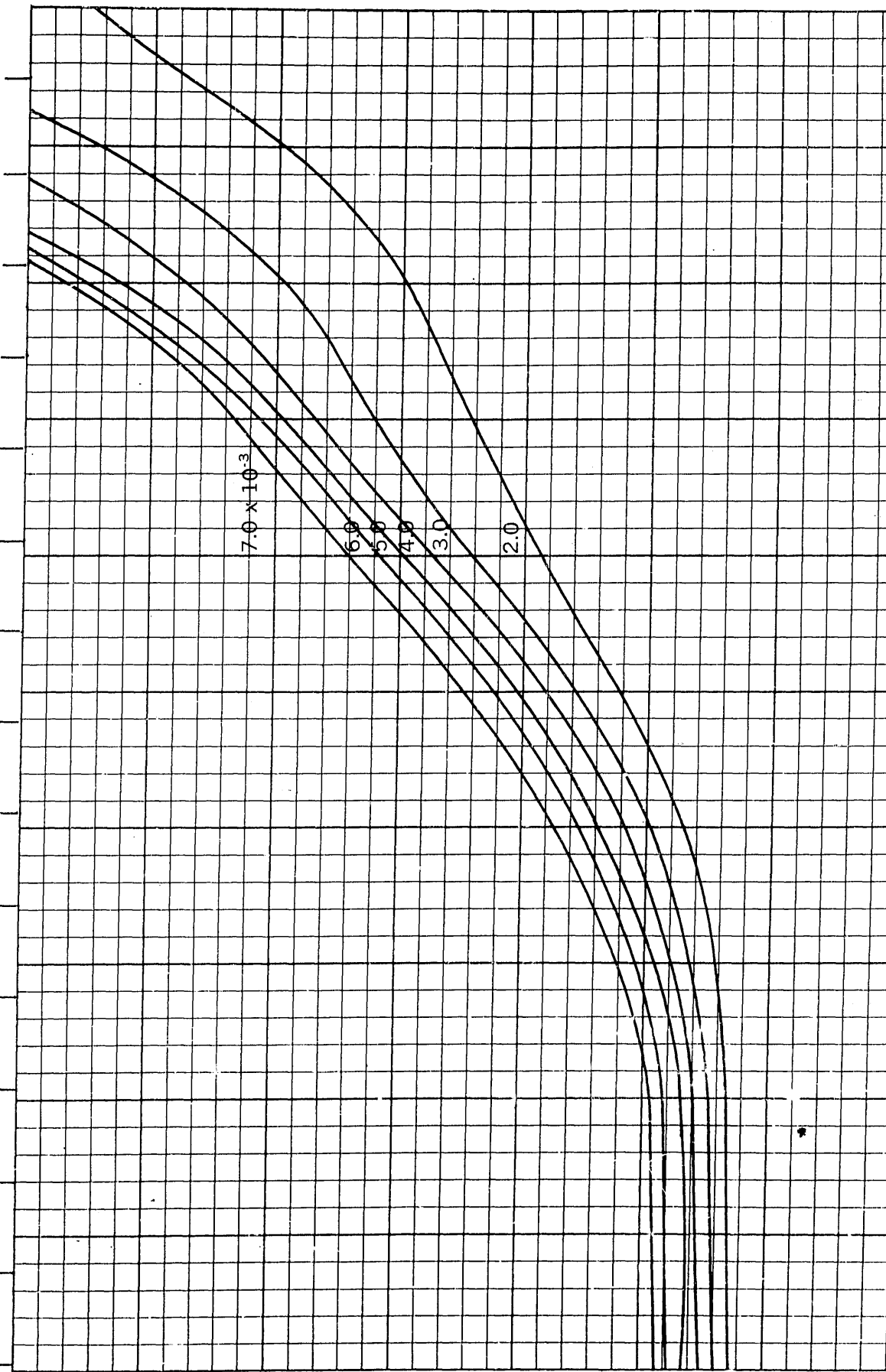
Froude Number $\frac{v}{\sqrt{gL}}$



$B/H=3.75$
 $C_p=0.76$

Froude Number $\frac{v}{\sqrt{gL}}$

0.15 0.16 0.17 0.18 0.19 0.20 0.21 0.22 0.23 0.24 0.25 0.26 0.27 0.28 0.29



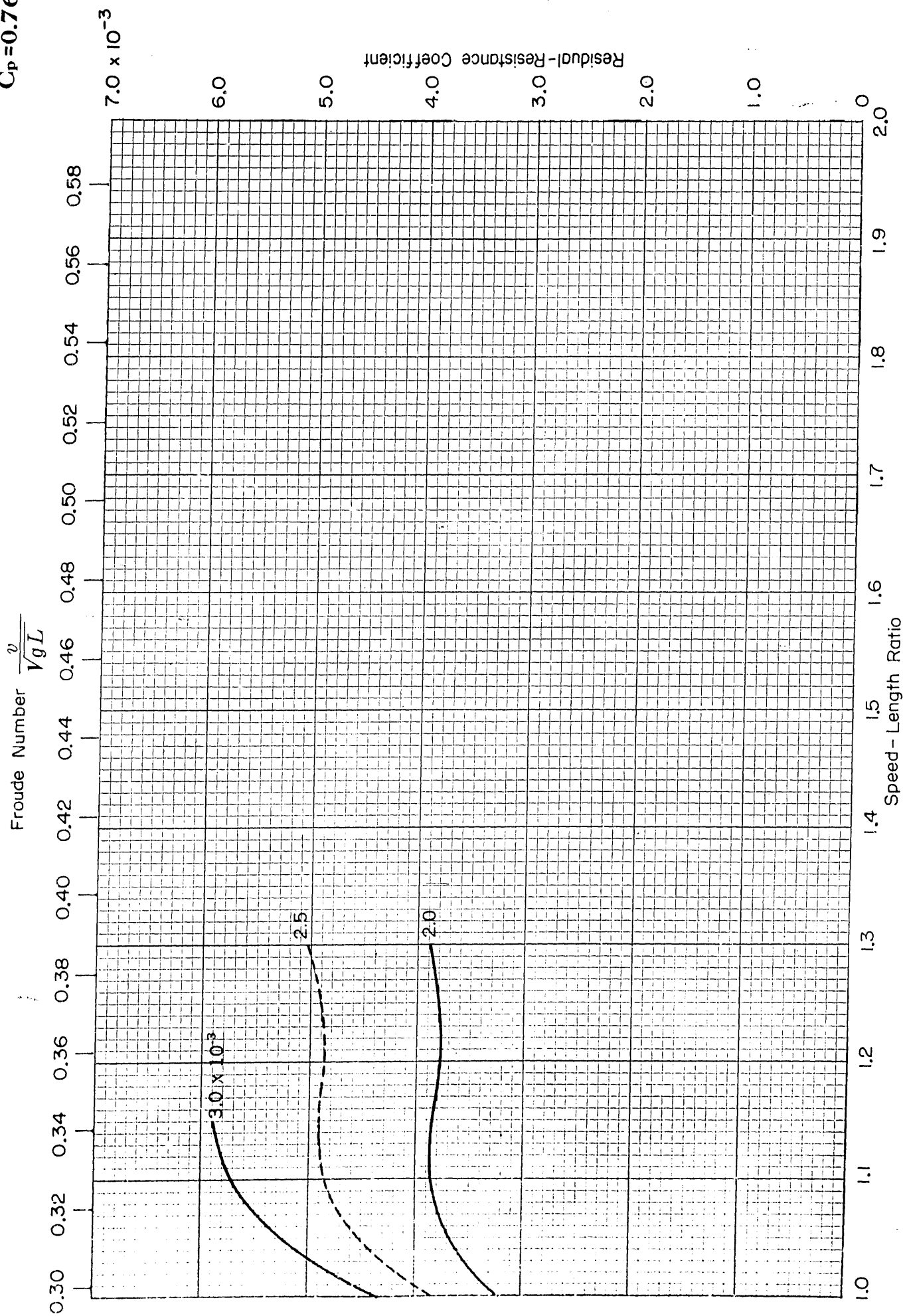
Residual-Resistance Coefficient

3.0 $\times 10^{-3}$

0 1.0 0.9 0.8 0.7 0.6 0.5

Speed - Length Ratio

$B/H=3.75$
 $C_p=0.76$



$B/H=3.75$
 $C_p=0.77$

Froude Number $\frac{v}{\sqrt{gL}}$

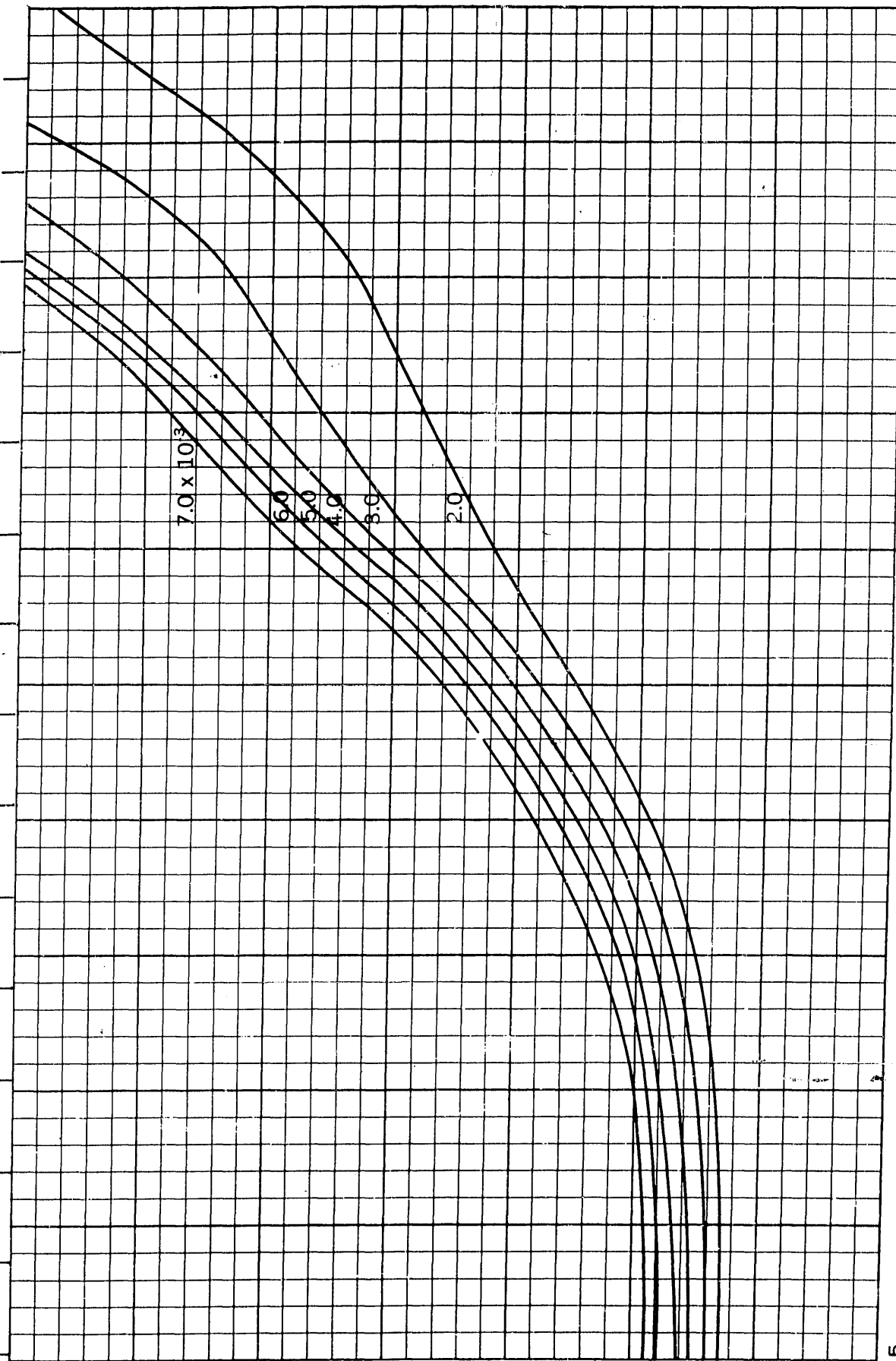
0.15 0.16 0.17 0.18 0.19 0.20 0.21 0.22 0.23 0.24 0.25 0.26 0.27 0.28 0.29

0.5 0.6 0.7 0.8 0.9 1.0

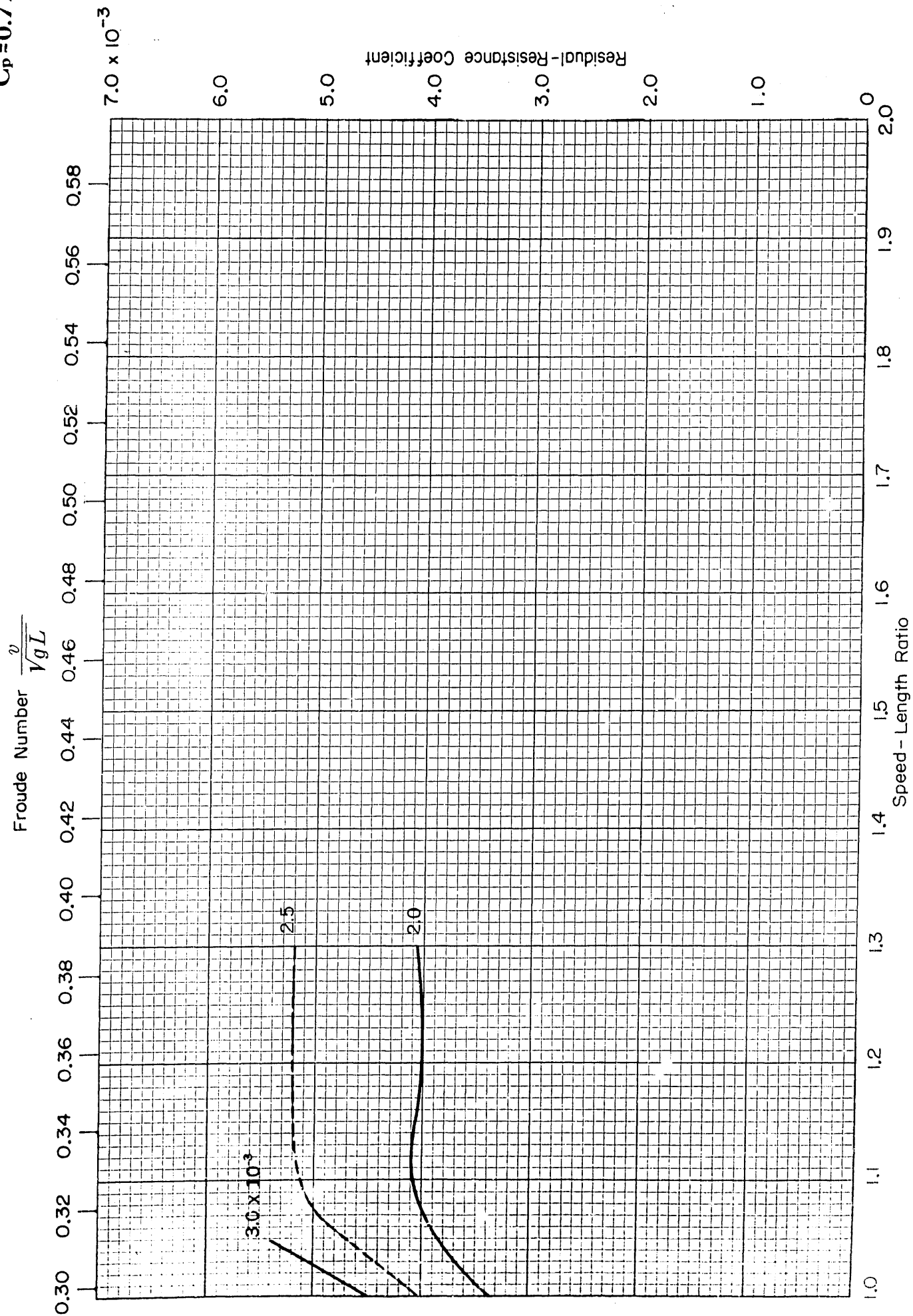
Speed - Length Ratio

Residual-Resistance Coefficient

3.0×10^{-3}



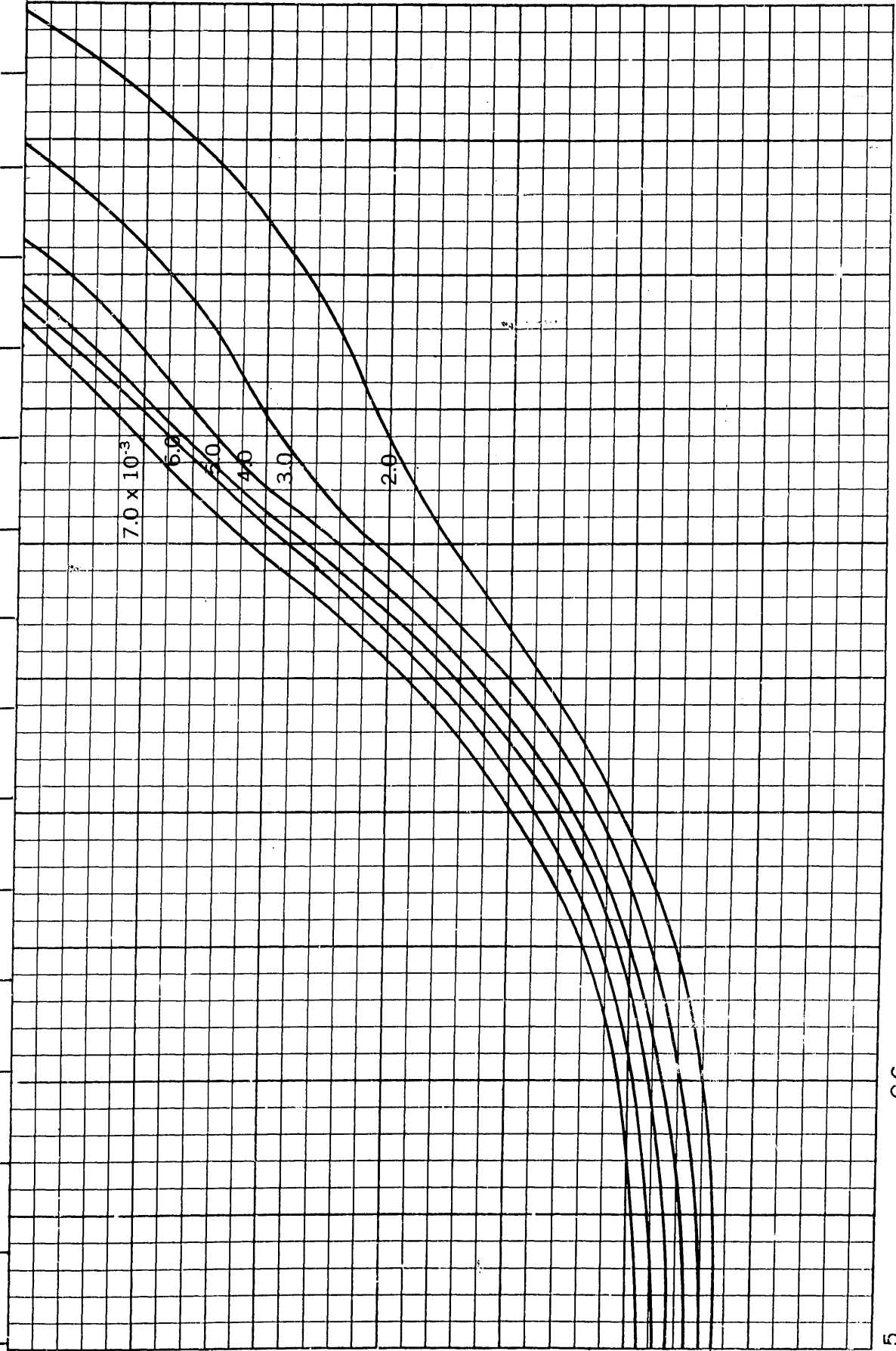
$B/H=3.75$
 $C_p=0.77$



$B/H=3.75$
 $C_p=0.78$

Froude Number $\frac{v}{\sqrt{gL}}$

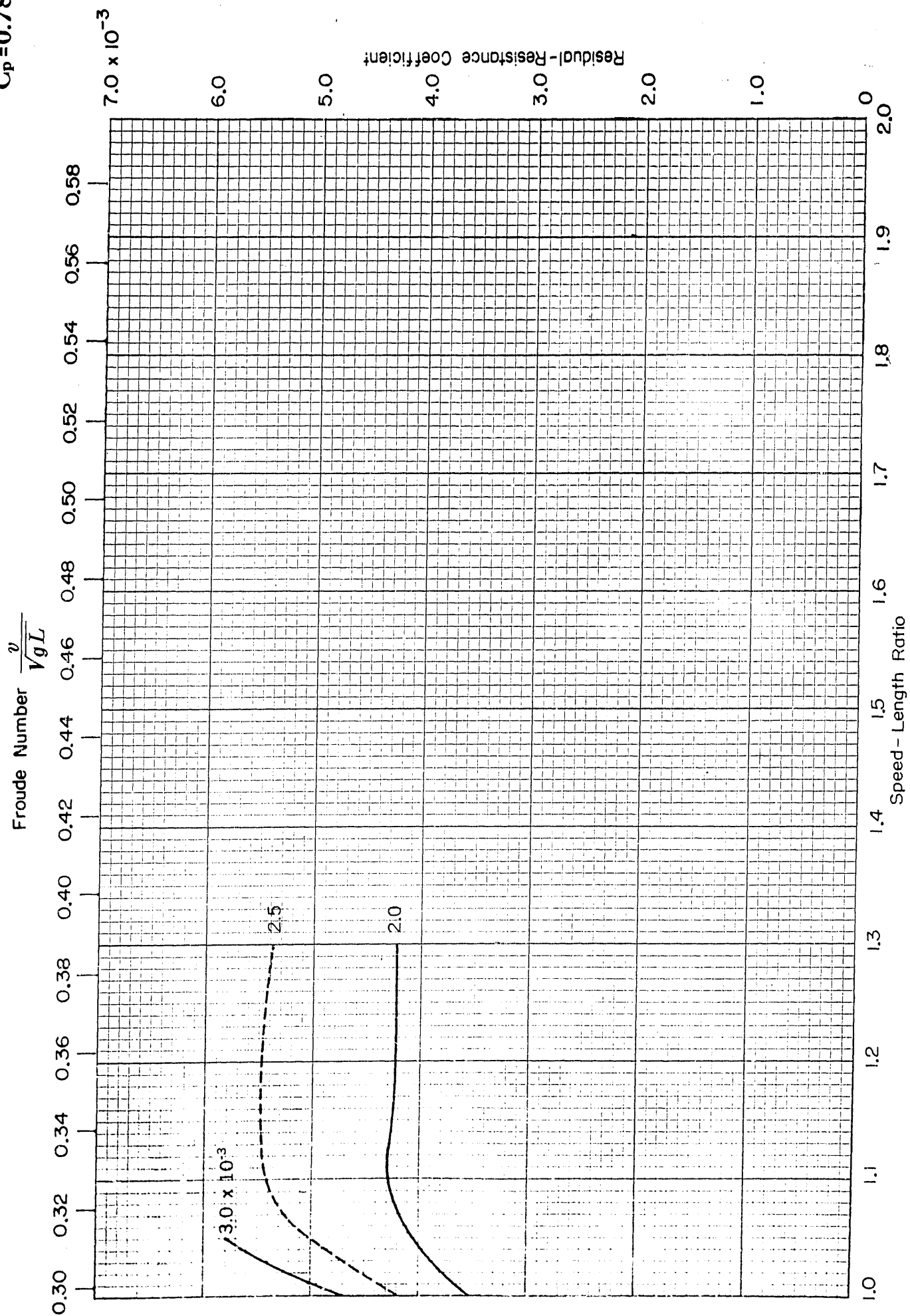
0.15 0.16 0.17 0.18 0.19 0.20 0.21 0.22 0.23 0.24 0.25 0.26 0.27 0.28 0.29



Residual-Resistance Coefficient

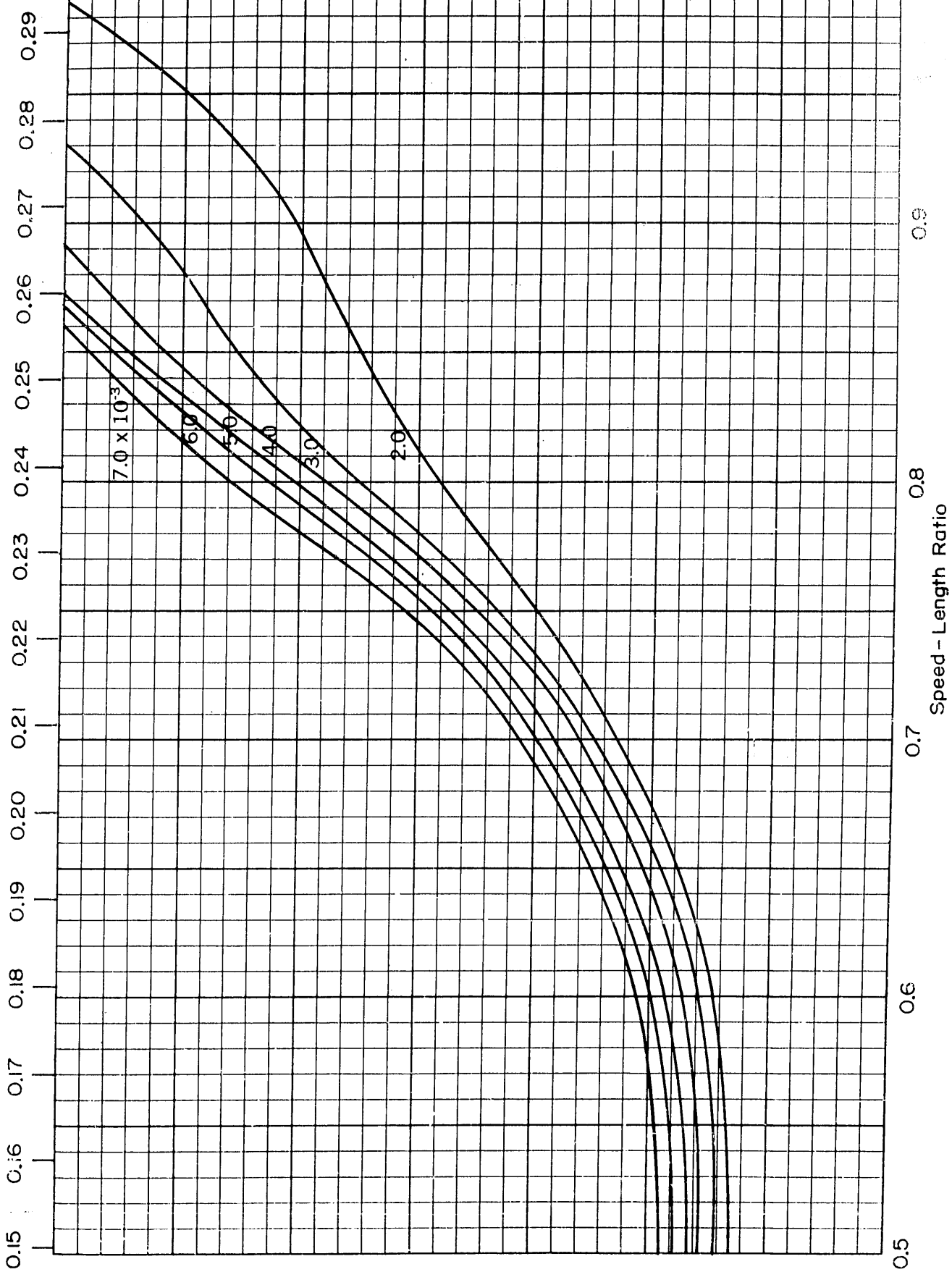
0 1.0
Speed - Length Ratio

$B/H=3.75$
 $C_p=0.78$



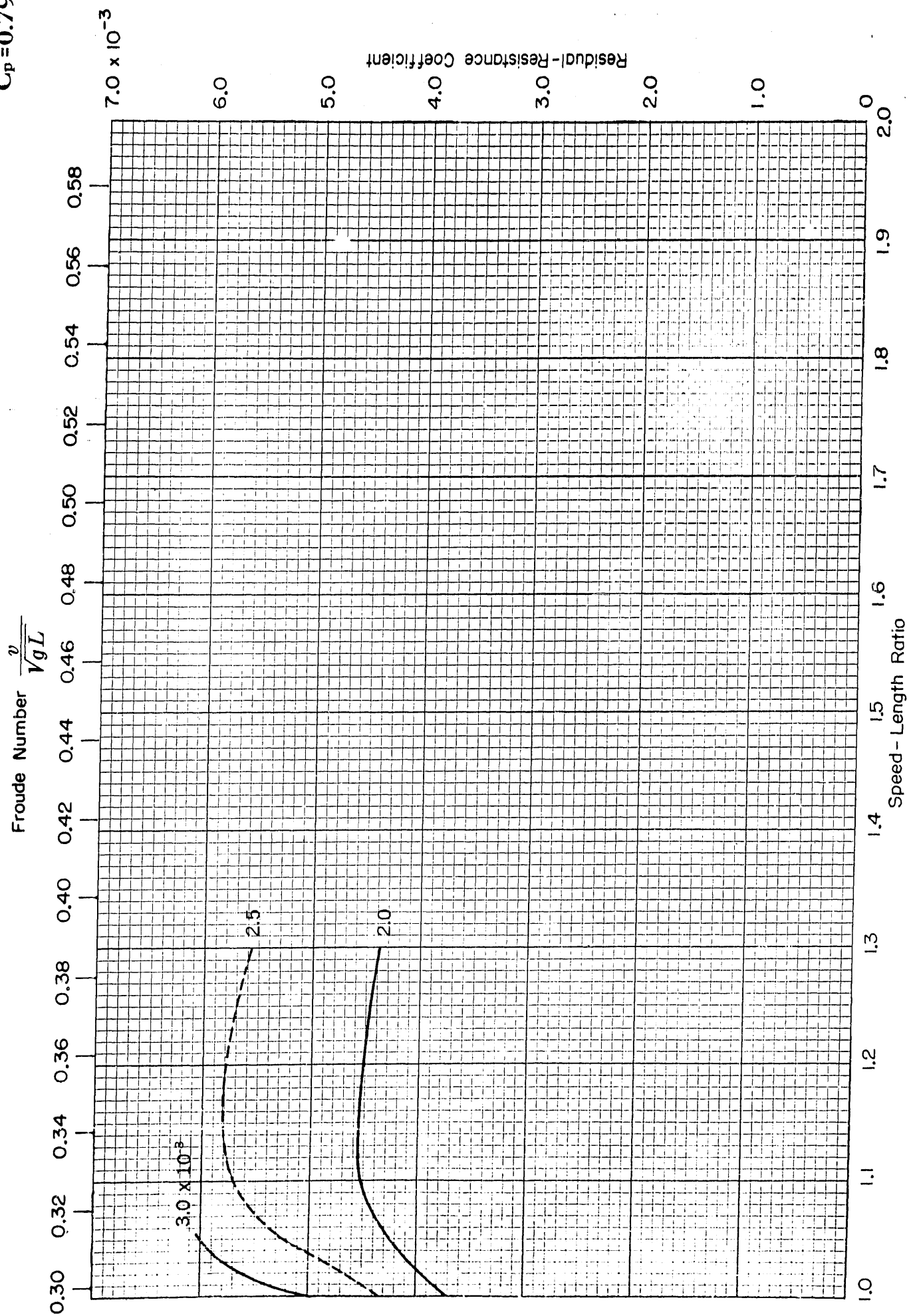
$B/H=3.75$
 $C_p=0.79$

Froude Number $\frac{v}{\sqrt{gL}}$



Residual-Resistance Coefficient

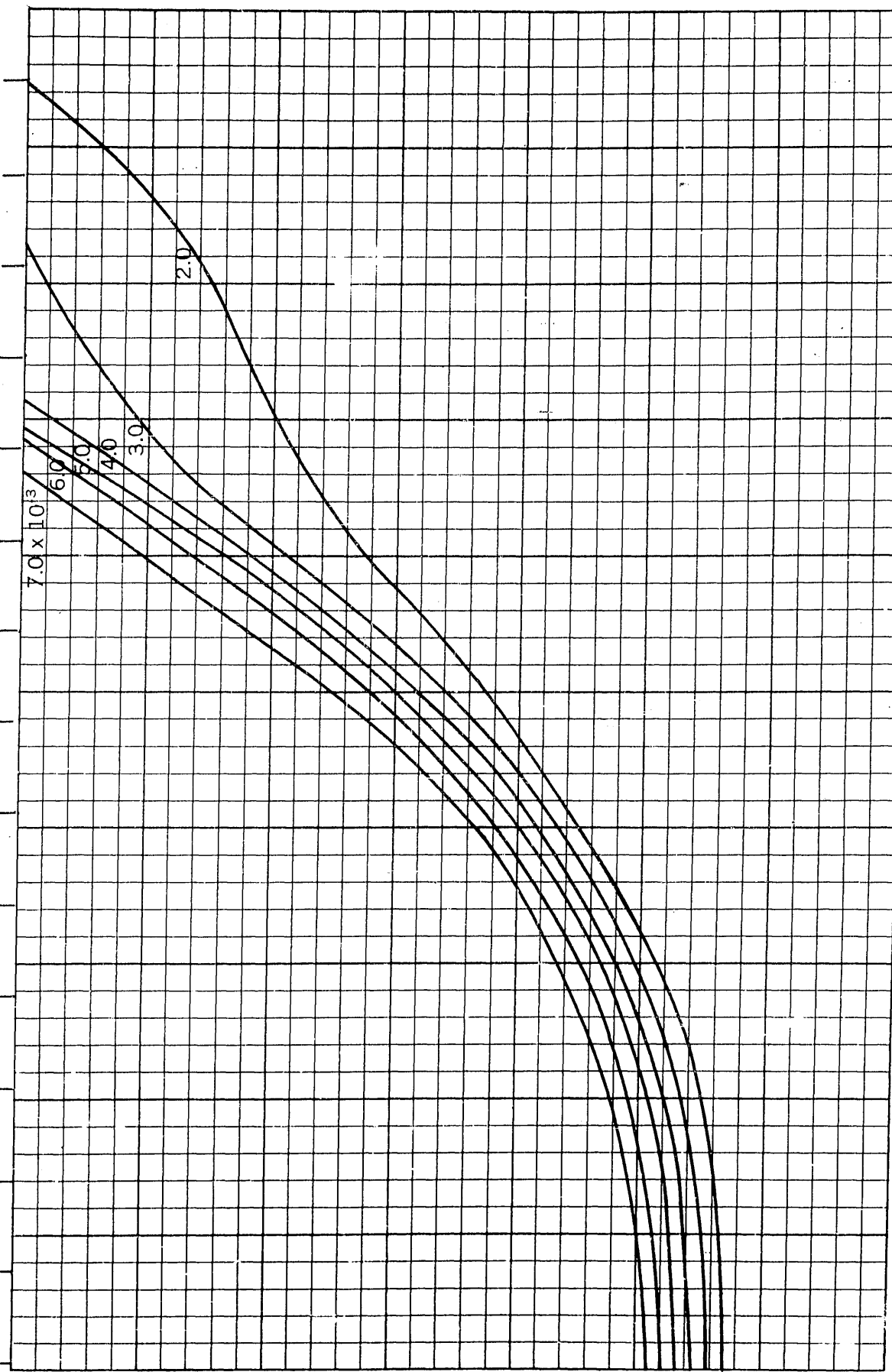
$B/H=3.75$
 $C_p=0.79$



$B/H=3.75$
 $C_p=0.80$

Froude Number $\frac{v}{\sqrt{gL}}$

0.15 0.16 0.17 0.18 0.19 0.20 0.21 0.22 0.23 0.24 0.25 0.26 0.27 0.28 0.29



0.5

0.6

0.7

0.8

0.9

1.0

1.0
2.0
 3.0×10^{-3}

3.0×10^{-3}

$B/H=3.75$
 $C_p=0.80$

Froude Number $\frac{v}{\sqrt{gL}}$

0.30 0.32 0.34 0.36 0.38 0.40 0.42 0.44 0.46 0.48 0.50 0.52 0.54 0.56 0.58

7.0×10^{-3}

6.0

5.0

4.0

3.0

2.0

1.0

0

Residual-Resistance Coefficient

2.0

1.9

1.8

1.7

1.6

1.5

1.4

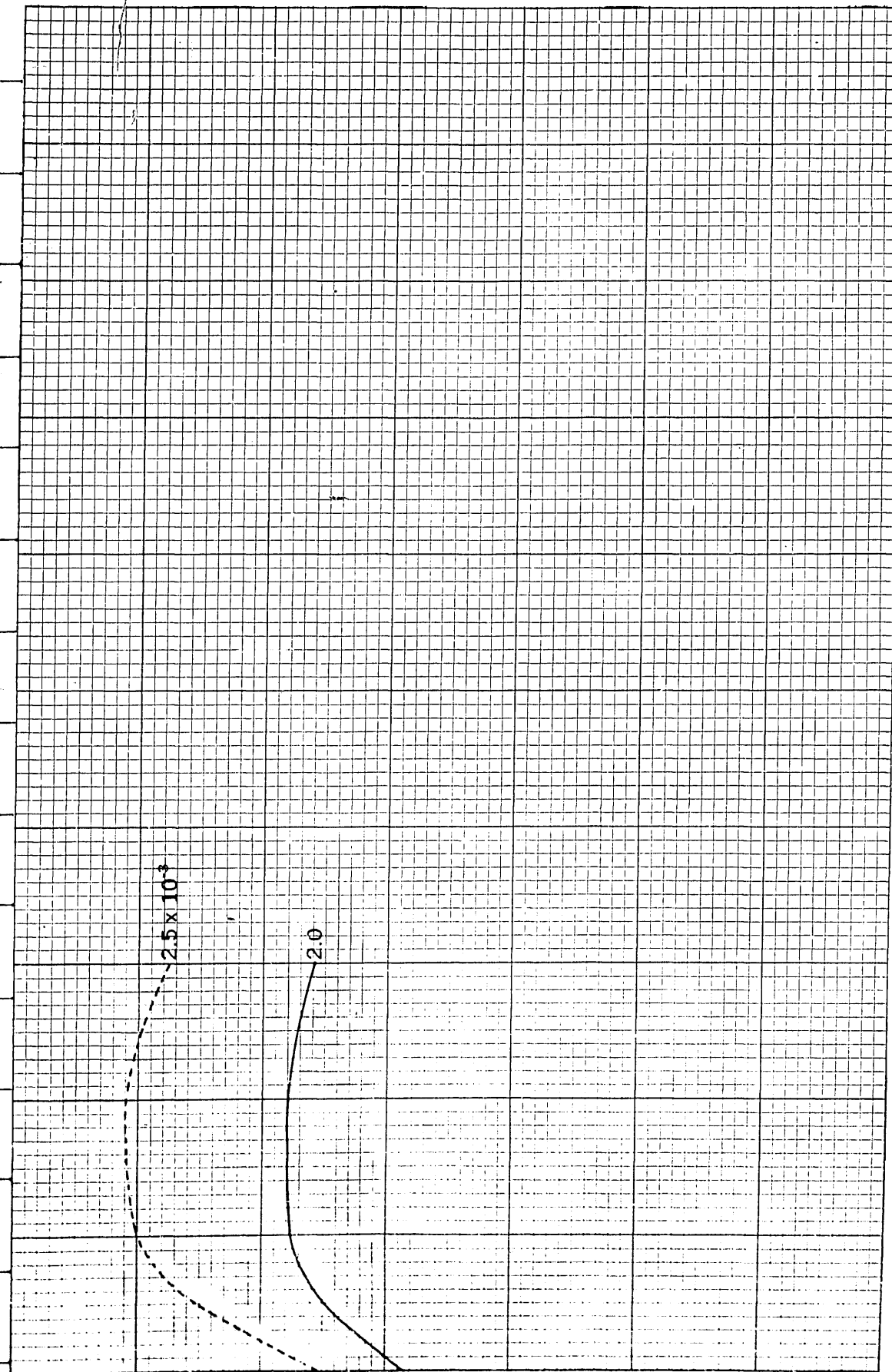
1.3

1.2

1.1

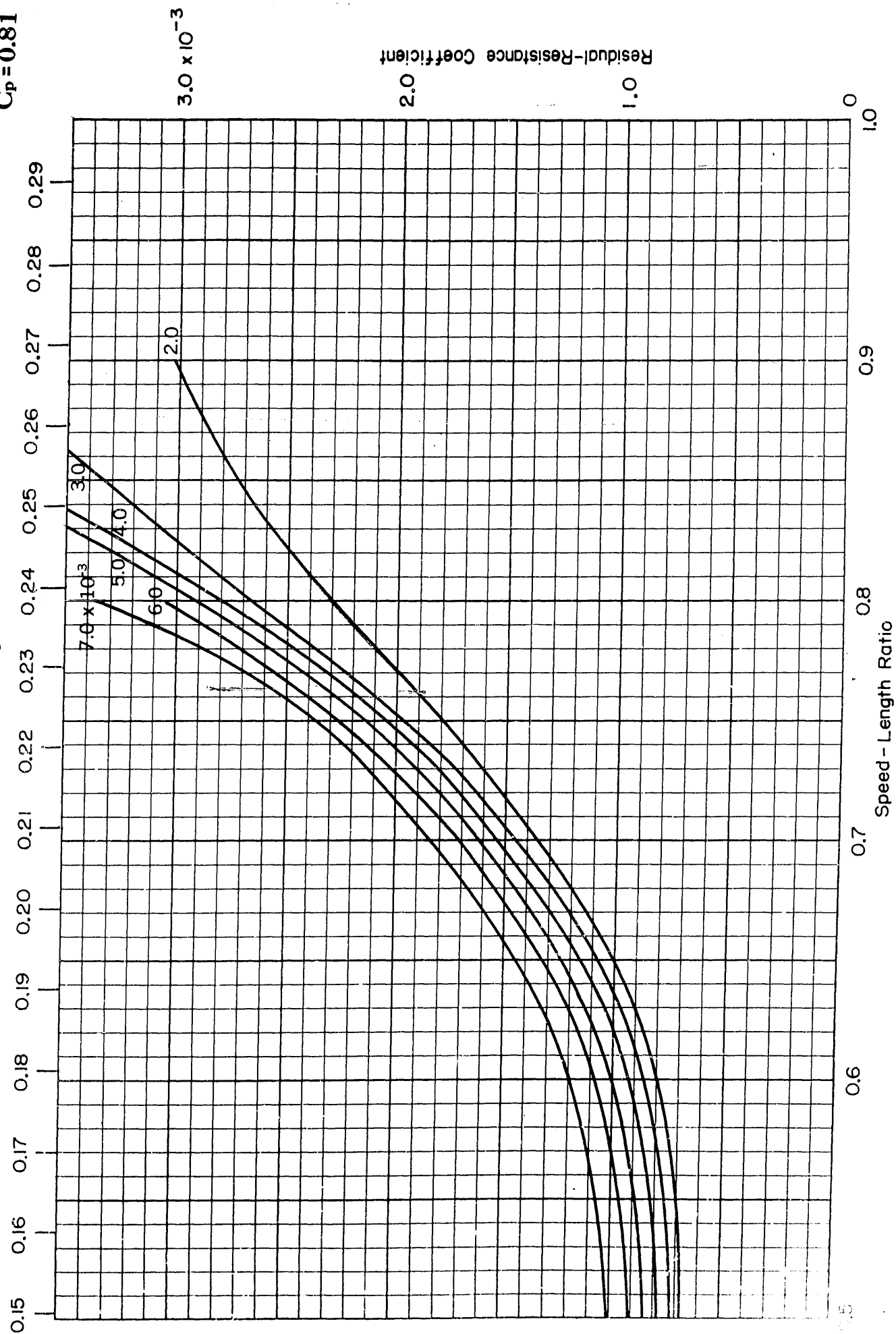
1.0

Speed-Length Ratio



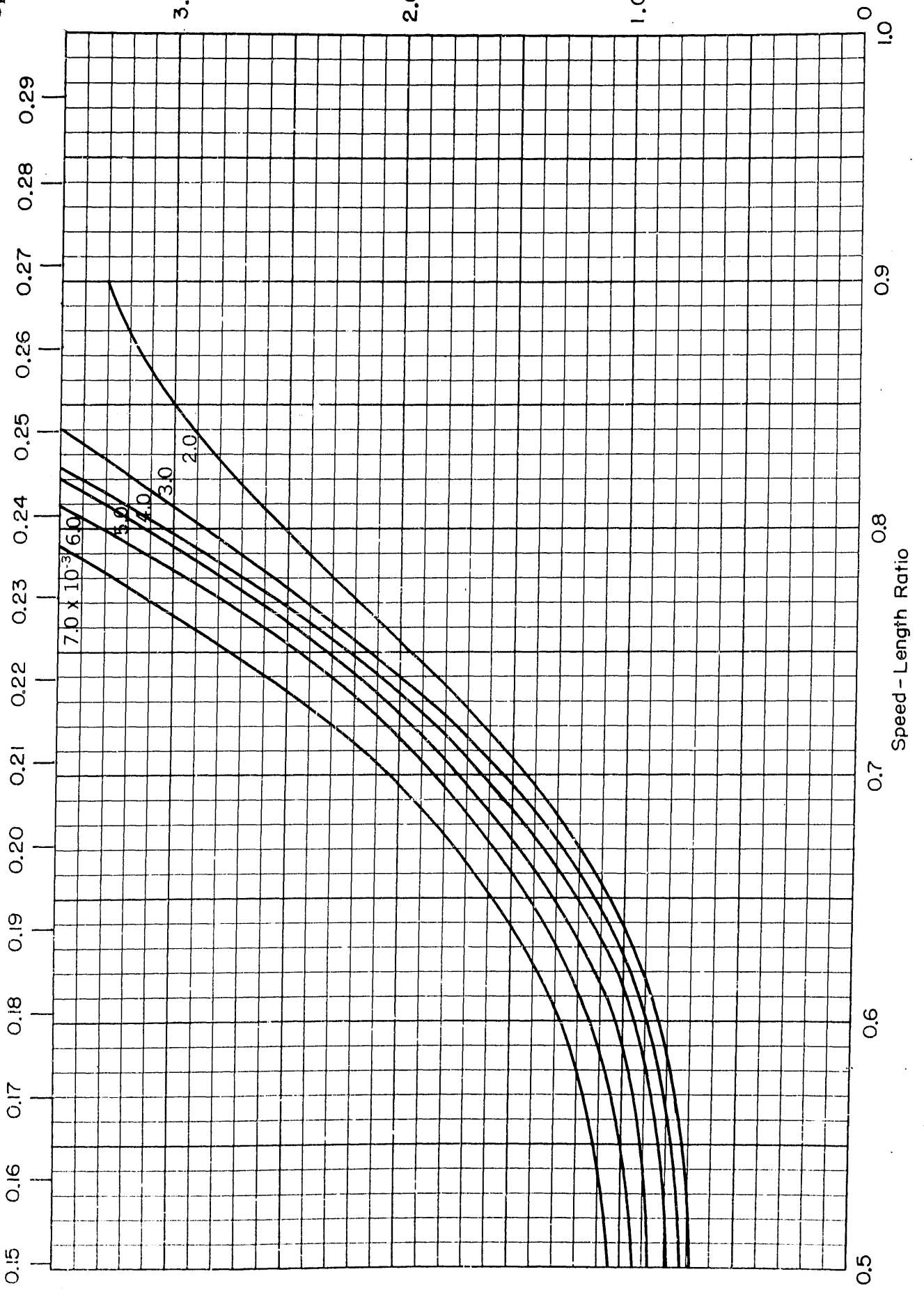
$B/H=3.75$
 $C_p=0.81$

Froude Number $\frac{v}{\sqrt{gL}}$



$B/H=3.75$
 $C_p=0.82$

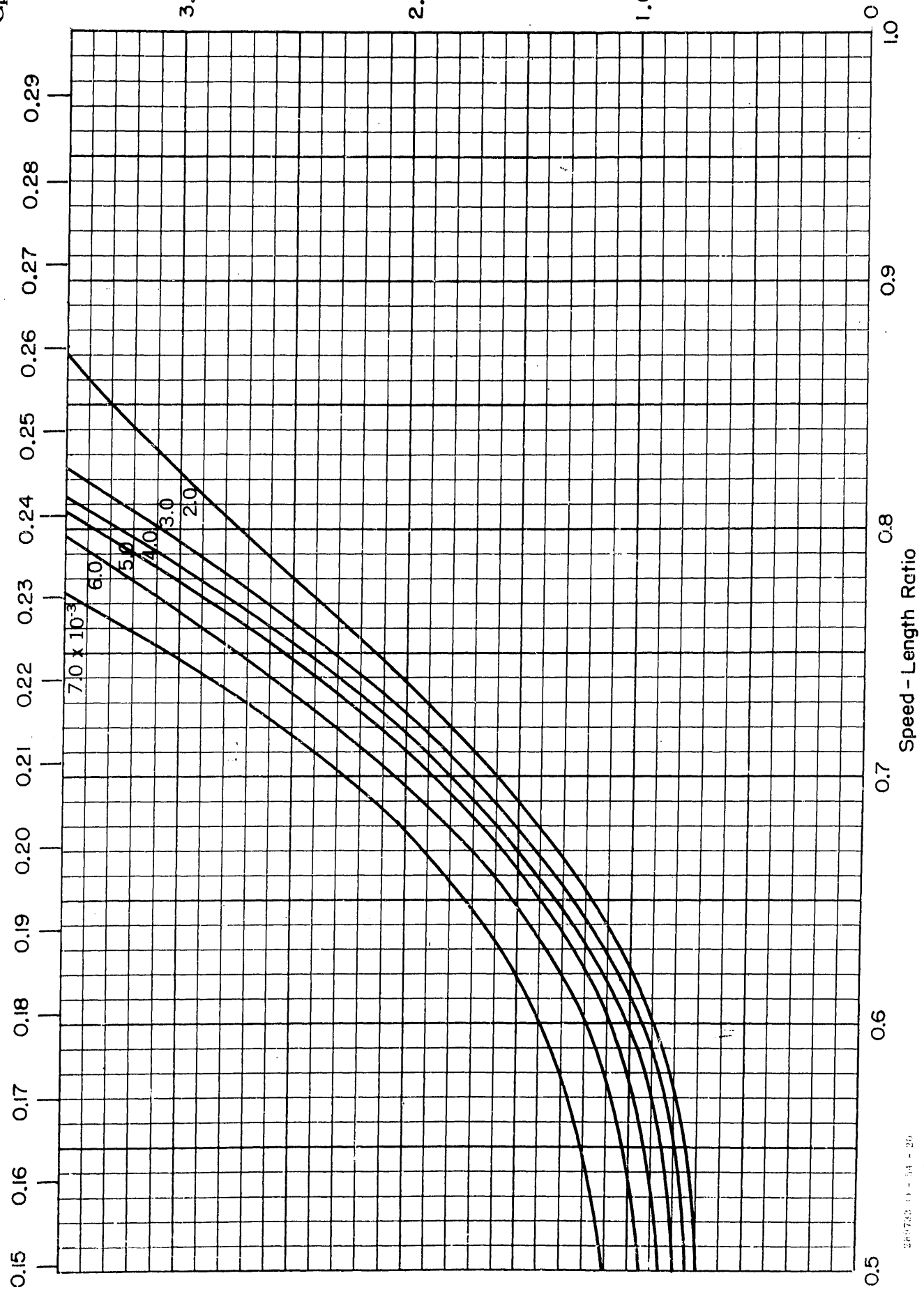
Froude Number $\frac{v}{\sqrt{gL}}$



Residual-Resistance Coefficient

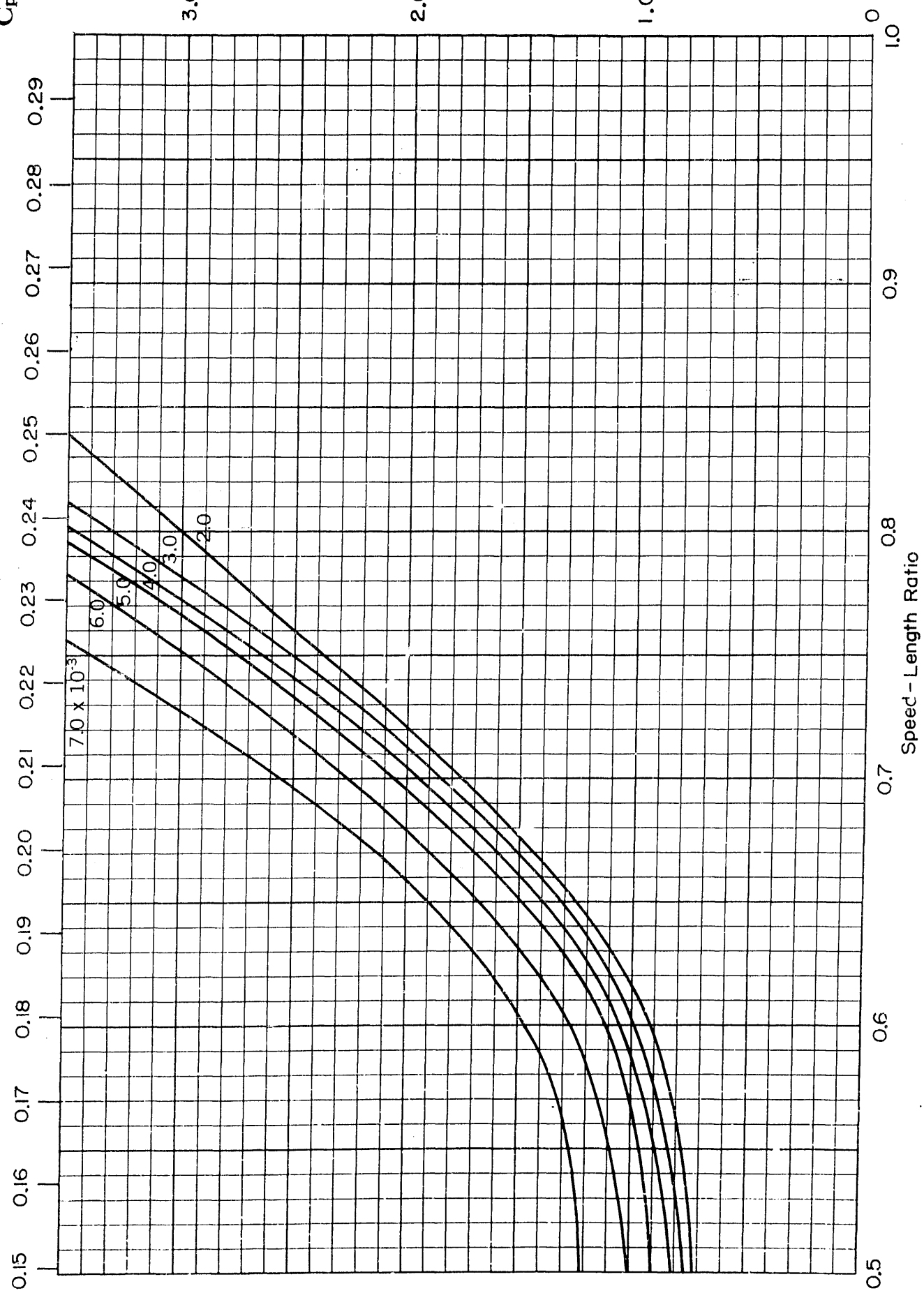
$B/H=3.75$
 $C_p=0.83$

Froude Number $\frac{v}{\sqrt{gL}}$



Froude Number $\frac{v}{\sqrt{gL}}$

$B/H=3.75$
 $C_p=0.84$

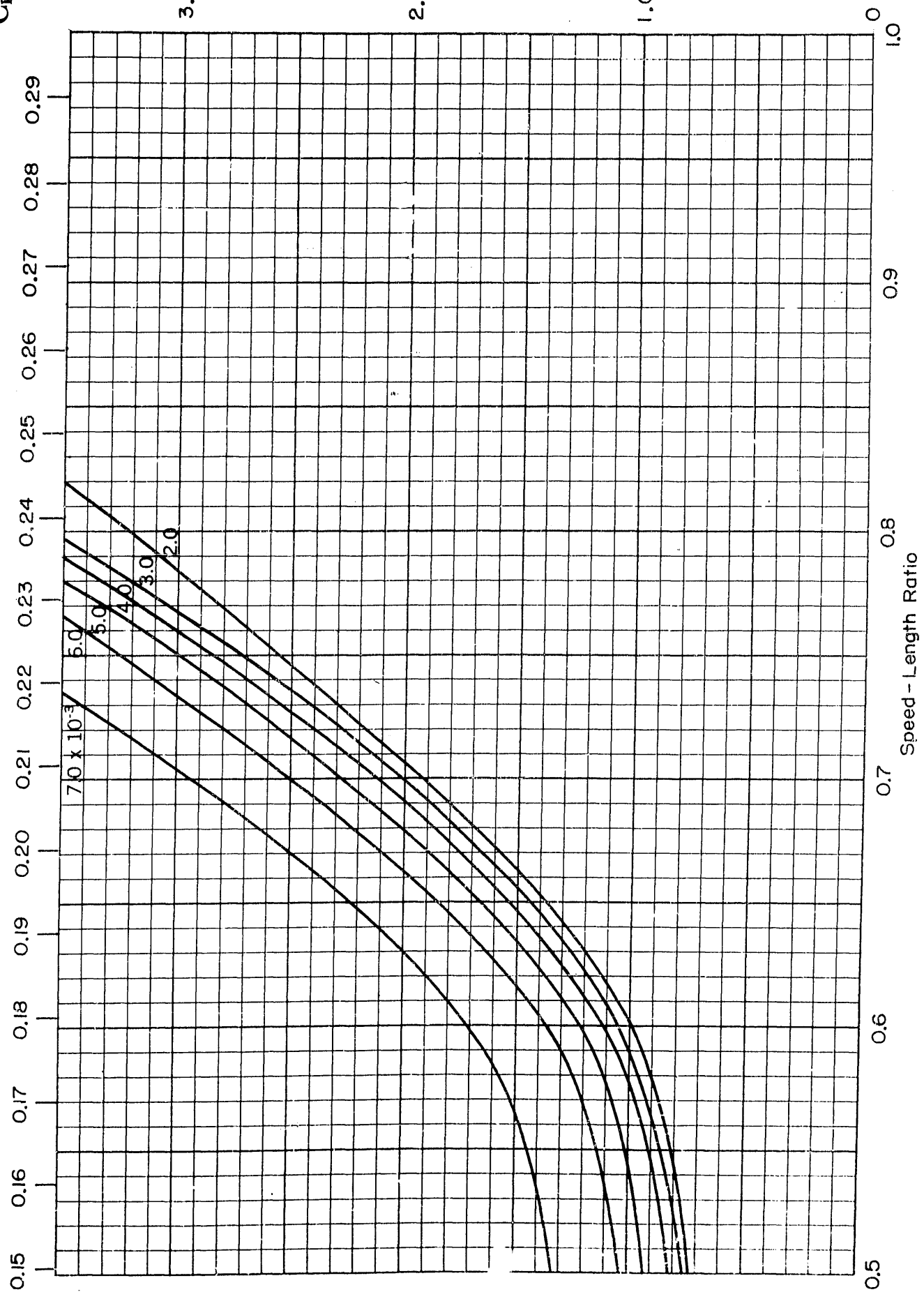


Residual-Resistance Coefficient

3.0×10^{-3}

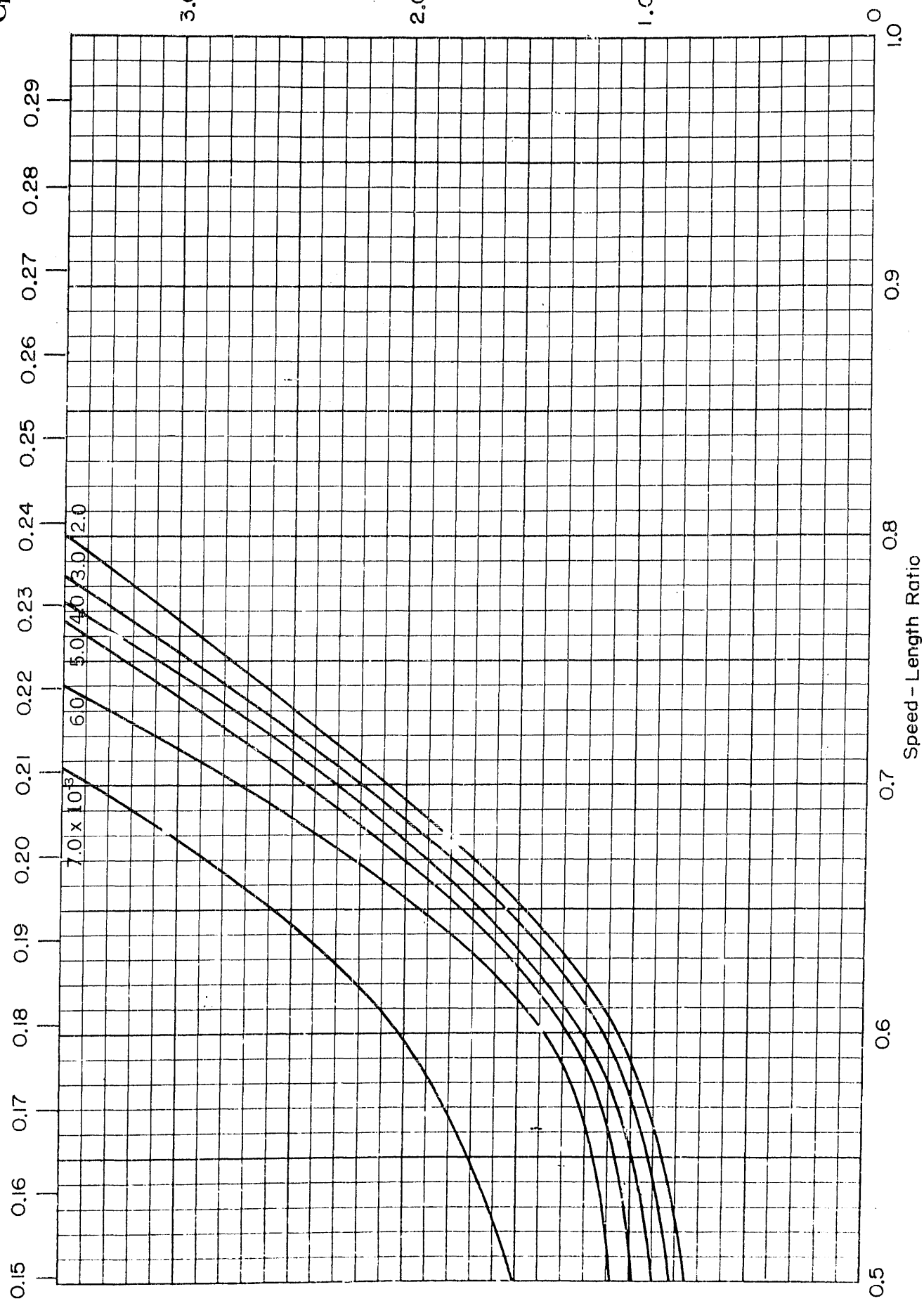
$B/H=3.75$
 $C_p=0.85$

Froude Number $\frac{v}{\sqrt{gL}}$



$B/H=3.75$
 $C_p=0.86$

Froude Number $\frac{v}{\sqrt{gL}}$



Residual-Resistance Coefficient

APPENDIX 6

TABLES OF THE SCHOENHERR FRICTIONAL-RESISTANCE COEFFICIENTS VERSUS
REYNOLDS NUMBERS

Supplementary Table of Residual-Resistance Coefficients which are Not Constant Below a Speed-Length Ratio of 0.50

Values of $C_r \times 10^3$																			
		$C_Y = 2.0 \times 10^{-3}$			$C_Y = 3.0 \times 10^{-3}$			$C_Y = 4.0 \times 10^{-3}$			$C_Y = 5.0 \times 10^{-3}$			$C_Y = 6.0 \times 10^{-3}$			$C_Y = 7.0 \times 10^{-3}$		
$\frac{V_k}{V_L}$	C_P	0.30	0.40	0.50	0.30	0.40	0.50	0.30	0.40	0.50	0.30	0.40	0.50	0.30	0.40	0.50	0.30	0.40	0.50
0.81														0.900	0.900	0.910	0.975	0.980	1.010
0.82														0.905	0.905	0.940	0.990	0.995	1.050
0.83										0.850	0.850	0.860	0.860	0.910	0.910	0.955	1.015	1.025	1.105
0.84										0.860	0.860	0.860	0.905	0.915	0.915	1.005	1.040	1.050	1.215
0.85										0.870	0.870	0.930	0.930	0.920	0.920	1.035	1.050	1.075	1.335
0.86										0.890	0.890	0.890	0.980	0.950	0.950	1.080	1.070	1.095	1.510

Schoenherr Frictional Resistance Coefficients for
Reynolds Numbers from 1.00 to 9.99 x 10⁵

The values for the frictional resistance coefficients must be multiplied by 10⁻³.

Reynolds Number 10 ⁵ x	0.00	0.01	0.02	0.03	0.04	0.05	0.06	0.07	0.08	0.09	0.10
1.0	7.179	7.163	7.147	7.130	7.114	7.098	7.083	7.068	7.052	7.037	7.022
1.1	7.022	7.007	6.993	6.979	6.964	6.950	6.936	6.922	6.909	6.895	6.881
1.2	6.881	6.869	6.856	6.844	6.831	6.819	6.807	6.795	6.782	6.770	6.758
1.3	6.758	6.746	6.735	6.723	6.712	6.700	6.689	6.678	6.667	6.656	6.645
1.4	6.645	6.635	6.624	6.614	6.603	6.593	6.583	6.573	6.563	6.553	6.543
1.5	6.543	6.534	6.525	6.517	6.508	6.499	6.489	6.479	6.469	6.459	6.449
1.6	6.449	6.440	6.431	6.422	6.413	6.404	6.395	6.387	6.378	6.370	6.361
1.7	6.361	6.353	6.345	6.336	6.328	6.320	6.312	6.304	6.297	6.289	6.281
1.8	6.281	6.273	6.266	6.258	6.251	6.243	6.236	6.229	6.221	6.214	6.207
1.9	6.207	6.200	6.193	6.186	6.179	6.172	6.165	6.158	6.152	6.145	6.138
2.0	6.138	6.131	6.125	6.118	6.112	6.105	6.099	6.092	6.086	6.079	6.073
2.1	6.073	6.067	6.060	6.054	6.047	6.041	6.035	6.029	6.024	6.018	6.012
2.2	6.012	6.006	6.000	5.994	5.988	5.982	5.976	5.971	5.965	5.960	5.954
2.3	5.954	5.948	5.943	5.937	5.931	5.926	5.921	5.915	5.910	5.904	5.899
2.4	5.899	5.894	5.889	5.883	5.878	5.873	5.868	5.863	5.857	5.852	5.847
2.5	5.847	5.842	5.837	5.832	5.827	5.822	5.817	5.812	5.807	5.802	5.797
2.6	5.797	5.792	5.788	5.783	5.779	5.774	5.769	5.765	5.760	5.756	5.751
2.7	5.751	5.746	5.742	5.737	5.733	5.728	5.724	5.719	5.715	5.710	5.706
2.8	5.706	5.702	5.698	5.693	5.689	5.685	5.681	5.677	5.672	5.668	5.664
2.9	5.664	5.660	5.656	5.652	5.648	5.644	5.640	5.636	5.632	5.628	5.624
3.0	5.624	5.620	5.616	5.612	5.608	5.605	5.601	5.597	5.593	5.589	5.585
3.1	5.585	5.581	5.577	5.574	5.570	5.566	5.562	5.558	5.555	5.551	5.547
3.2	5.547	5.543	5.540	5.536	5.533	5.529	5.525	5.522	5.518	5.515	5.511
3.3	5.511	5.508	5.504	5.501	5.497	5.494	5.491	5.487	5.484	5.480	5.477
3.4	5.477	5.474	5.470	5.467	5.464	5.461	5.457	5.454	5.451	5.447	5.444
3.5	5.444	5.441	5.437	5.434	5.431	5.428	5.424	5.421	5.418	5.414	5.411
3.6	5.411	5.408	5.405	5.402	5.399	5.396	5.392	5.389	5.386	5.383	5.380
3.7	5.380	5.377	5.374	5.371	5.368	5.365	5.362	5.359	5.356	5.353	5.350
3.8	5.350	5.347	5.344	5.341	5.338	5.336	5.333	5.330	5.327	5.324	5.321
3.9	5.321	5.318	5.316	5.313	5.310	5.308	5.305	5.302	5.299	5.297	5.294
4.0	5.294	5.291	5.289	5.286	5.283	5.281	5.278	5.275	5.272	5.270	5.267
4.1	5.267	5.264	5.262	5.259	5.257	5.254	5.251	5.249	5.246	5.244	5.241
4.2	5.241	5.239	5.236	5.233	5.231	5.229	5.226	5.224	5.221	5.219	5.216
4.3	5.216	5.214	5.211	5.209	5.206	5.204	5.201	5.199	5.196	5.194	5.191
4.4	5.191	5.189	5.186	5.184	5.181	5.179	5.177	5.174	5.172	5.169	5.167
4.5	5.167	5.165	5.162	5.160	5.158	5.156	5.153	5.151	5.149	5.146	5.144
4.6	5.144	5.142	5.140	5.137	5.135	5.133	5.131	5.129	5.126	5.124	5.122
4.7	5.122	5.120	5.118	5.115	5.113	5.111	5.109	5.107	5.104	5.102	5.100
4.8	5.100	5.098	5.096	5.094	5.092	5.089	5.087	5.085	5.083	5.081	5.079
4.9	5.079	5.077	5.075	5.073	5.071	5.068	5.066	5.064	5.062	5.060	5.058

Reynolds Number $10^5 \times$	0.00	0.01	0.02	0.03	0.04	0.05	0.06	0.07	0.08	0.09	0.10
5.0	5.058	5.056	5.054	5.052	5.050	5.047	5.045	5.043	5.041	5.039	5.037
5.1	5.037	5.035	5.033	5.031	5.029	5.027	5.025	5.023	5.021	5.019	5.017
5.2	5.017	5.015	5.013	5.011	5.009	5.007	5.006	5.004	5.002	5.000	4.998
5.3	4.998	4.996	4.994	4.992	4.990	4.988	4.987	4.985	4.983	4.981	4.979
5.4	4.979	4.977	4.975	4.974	4.972	4.970	4.968	4.966	4.965	4.963	4.961
5.5	4.961	4.959	4.957	4.956	4.954	4.952	4.950	4.948	4.947	4.945	4.943
5.6	4.943	4.941	4.939	4.938	4.936	4.934	4.932	4.930	4.929	4.927	4.925
5.7	4.925	4.923	4.922	4.920	4.918	4.916	4.915	4.913	4.911	4.910	4.908
5.8	4.908	4.906	4.905	4.903	4.901	4.899	4.898	4.896	4.894	4.893	4.891
5.9	4.891	4.889	4.888	4.886	4.884	4.882	4.881	4.879	4.877	4.876	4.874
6.0	4.874	4.872	4.871	4.869	4.868	4.866	4.864	4.863	4.861	4.860	4.858
6.1	4.858	4.856	4.855	4.853	4.852	4.850	4.849	4.847	4.846	4.844	4.843
6.2	4.843	4.841	4.840	4.838	4.837	4.835	4.834	4.832	4.831	4.829	4.828
6.3	4.828	4.826	4.825	4.823	4.822	4.820	4.819	4.817	4.816	4.814	4.813
6.4	4.813	4.811	4.810	4.808	4.807	4.805	4.804	4.802	4.801	4.799	4.798
6.5	4.798	4.796	4.795	4.793	4.792	4.790	4.789	4.787	4.786	4.784	4.783
6.6	4.783	4.781	4.780	4.778	4.777	4.775	4.774	4.772	4.771	4.769	4.768
6.7	4.768	4.767	4.765	4.764	4.762	4.761	4.760	4.758	4.757	4.755	4.754
6.8	4.754	4.753	4.751	4.750	4.748	4.747	4.746	4.744	4.743	4.741	4.740
6.9	4.740	4.739	4.737	4.736	4.735	4.733	4.732	4.731	4.730	4.728	4.727
7.0	4.727	4.726	4.724	4.723	4.722	4.720	4.719	4.718	4.717	4.715	4.714
7.1	4.714	4.713	4.711	4.710	4.709	4.707	4.706	4.705	4.704	4.702	4.701
7.2	4.701	4.700	4.698	4.697	4.696	4.694	4.693	4.691	4.689	4.688	4.687
7.3	4.688	4.687	4.686	4.684	4.683	4.682	4.681	4.680	4.678	4.677	4.676
7.4	4.676	4.675	4.674	4.672	4.671	4.670	4.669	4.668	4.666	4.665	4.664
7.5	4.664	4.663	4.662	4.660	4.659	4.658	4.657	4.656	4.654	4.653	4.652
7.6	4.652	4.651	4.650	4.648	4.647	4.646	4.645	4.644	4.642	4.641	4.640
7.7	4.640	4.639	4.638	4.636	4.635	4.634	4.633	4.632	4.630	4.629	4.628
7.8	4.628	4.627	4.626	4.624	4.623	4.622	4.621	4.620	4.618	4.617	4.616
7.9	4.616	4.615	4.614	4.613	4.612	4.610	4.609	4.608	4.607	4.606	4.605
8.0	4.605	4.604	4.603	4.602	4.601	4.599	4.598	4.597	4.596	4.595	4.594
8.1	4.594	4.593	4.592	4.591	4.590	4.588	4.587	4.586	4.585	4.584	4.583
8.2	4.583	4.582	4.581	4.580	4.579	4.577	4.576	4.575	4.574	4.573	4.572
8.3	4.572	4.571	4.570	4.569	4.568	4.566	4.565	4.564	4.563	4.562	4.561
8.4	4.561	4.560	4.559	4.558	4.557	4.555	4.554	4.553	4.552	4.551	4.550
8.5	4.550	4.549	4.548	4.547	4.546	4.545	4.544	4.543	4.542	4.541	4.540
8.6	4.540	4.539	4.538	4.537	4.536	4.535	4.534	4.533	4.532	4.531	4.530
8.7	4.530	4.529	4.528	4.527	4.526	4.525	4.524	4.523	4.522	4.521	4.520
8.8	4.520	4.519	4.518	4.517	4.516	4.515	4.514	4.513	4.512	4.511	4.510
8.9	4.510	4.509	4.508	4.507	4.506	4.505	4.504	4.503	4.502	4.501	4.500
9.0	4.500	4.499	4.498	4.497	4.496	4.495	4.494	4.493	4.492	4.491	4.490
9.1	4.490	4.489	4.488	4.487	4.486	4.485	4.484	4.483	4.482	4.481	4.480
9.2	4.481	4.480	4.479	4.478	4.477	4.476	4.475	4.474	4.473	4.472	4.471
9.3	4.472	4.471	4.470	4.469	4.468	4.467	4.466	4.465	4.464	4.463	4.462
9.4	4.463	4.462	4.461	4.460	4.459	4.458	4.457	4.456	4.455	4.454	4.453
9.5	4.454	4.453	4.452	4.451	4.450	4.449	4.448	4.447	4.446	4.445	4.444
9.6	4.445	4.444	4.443	4.442	4.441	4.440	4.439	4.438	4.437	4.436	4.435
9.7	4.436	4.435	4.434	4.433	4.432	4.431	4.430	4.429	4.428	4.427	4.426
9.8	4.427	4.426	4.425	4.424	4.423	4.422	4.421	4.420	4.419	4.418	4.417
9.9	4.418	4.417	4.416	4.415	4.414	4.413	4.412	4.411	4.410	4.409	4.408

Schoenherr Frictional Resistance Coefficients for
Reynolds Numbers from 1.00 to 9.99×10^6

The values for the frictional resistance coefficients must be multiplied by 10^{-3} .

Reynolds Number $10^6 \times$	0.00	0.01	0.02	0.03	0.04	0.05	0.06	0.07	0.08	0.09	0.10
1.0	4.410	4.402	4.394	4.386	4.378	4.371	4.363	4.355	4.347	4.339	4.331
1.1	4.331	4.324	4.316	4.309	4.302	4.295	4.287	4.280	4.273	4.265	4.258
1.2	4.258	4.252	4.245	4.239	4.232	4.226	4.219	4.213	4.206	4.200	4.193
1.3	4.193	4.187	4.181	4.176	4.170	4.164	4.158	4.152	4.147	4.141	4.135
1.4	4.135	4.130	4.125	4.119	4.114	4.109	4.104	4.099	4.093	4.088	4.083
1.5	4.083	4.078	4.073	4.069	4.064	4.059	4.054	4.049	4.045	4.040	4.035
1.6	4.035	4.031	4.026	4.022	4.017	4.013	4.008	4.004	3.999	3.995	3.990
1.7	3.990	3.986	3.982	3.977	3.973	3.969	3.965	3.961	3.957	3.952	3.948
1.8	3.948	3.944	3.940	3.936	3.932	3.929	3.925	3.921	3.917	3.913	3.909
1.9	3.909	3.906	3.903	3.900	3.897	3.894	3.890	3.887	3.884	3.881	3.878
2.0	3.878	3.874	3.870	3.866	3.862	3.858	3.854	3.850	3.846	3.842	3.838
2.1	3.838	3.835	3.831	3.828	3.824	3.821	3.818	3.814	3.811	3.807	3.804
2.2	3.804	3.801	3.798	3.795	3.792	3.789	3.785	3.782	3.779	3.776	3.773
2.3	3.773	3.770	3.767	3.765	3.762	3.759	3.756	3.753	3.751	3.748	3.745
2.4	3.745	3.742	3.740	3.737	3.735	3.732	3.729	3.727	3.724	3.722	3.719
2.5	3.719	3.716	3.714	3.711	3.709	3.706	3.703	3.701	3.698	3.696	3.693
2.6	3.693	3.691	3.688	3.686	3.683	3.681	3.678	3.676	3.673	3.671	3.668
2.7	3.668	3.666	3.663	3.661	3.658	3.656	3.654	3.651	3.649	3.646	3.644
2.8	3.644	3.642	3.640	3.637	3.635	3.633	3.631	3.629	3.626	3.624	3.622
2.9	3.622	3.620	3.618	3.615	3.613	3.611	3.609	3.607	3.604	3.602	3.600
3.0	3.600	3.598	3.596	3.594	3.592	3.590	3.588	3.586	3.584	3.582	3.580
3.1	3.580	3.578	3.576	3.574	3.572	3.570	3.568	3.566	3.564	3.562	3.560
3.2	3.560	3.558	3.556	3.555	3.553	3.551	3.549	3.547	3.546	3.544	3.542
3.3	3.542	3.540	3.538	3.536	3.534	3.533	3.531	3.529	3.527	3.525	3.523
3.4	3.523	3.521	3.519	3.517	3.515	3.514	3.512	3.510	3.508	3.506	3.504
3.5	3.504	3.502	3.501	3.499	3.497	3.496	3.494	3.492	3.490	3.489	3.487
3.6	3.487	3.485	3.484	3.482	3.481	3.479	3.477	3.476	3.474	3.473	3.471
3.7	3.471	3.469	3.468	3.466	3.465	3.463	3.461	3.460	3.458	3.457	3.455
3.8	3.455	3.453	3.452	3.450	3.449	3.447	3.445	3.444	3.442	3.441	3.439
3.9	3.439	3.437	3.436	3.434	3.433	3.431	3.429	3.428	3.426	3.425	3.423
4.0	3.423	3.422	3.420	3.419	3.417	3.416	3.414	3.413	3.411	3.410	3.408
4.1	3.408	3.407	3.405	3.404	3.402	3.401	3.400	3.398	3.397	3.395	3.394
4.2	3.394	3.393	3.391	3.390	3.388	3.387	3.386	3.384	3.383	3.381	3.380
4.3	3.380	3.379	3.377	3.376	3.374	3.373	3.372	3.369	3.368	3.366	3.365
4.4	3.366	3.365	3.363	3.362	3.361	3.360	3.358	3.357	3.356	3.354	3.353
4.5	3.353	3.352	3.351	3.349	3.348	3.347	3.346	3.345	3.344	3.343	3.341
4.6	3.341	3.340	3.339	3.337	3.336	3.335	3.334	3.333	3.331	3.330	3.329
4.7	3.329	3.328	3.327	3.325	3.324	3.323	3.322	3.321	3.319	3.318	3.317
4.8	3.317	3.316	3.315	3.313	3.312	3.311	3.310	3.309	3.307	3.306	3.305
4.9	3.305	3.304	3.303	3.302	3.301	3.300	3.299	3.297	3.296	3.295	3.294

Reynolds Number $10^6 \times$	0.00	0.01	0.02	0.03	0.04	0.05	0.06	0.07	0.08	0.09	0.10
5.0	3.294	3.293	3.292	3.291	3.290	3.289	3.288	3.286	3.285	3.284	3.283
5.1	3.283	3.282	3.281	3.280	3.279	3.278	3.277	3.275	3.274	3.273	3.272
5.2	3.272	3.271	3.270	3.269	3.268	3.267	3.266	3.264	3.263	3.262	3.261
5.3	3.261	3.260	3.259	3.258	3.257	3.256	3.255	3.254	3.253	3.252	3.251
5.4	3.251	3.250	3.249	3.248	3.247	3.246	3.245	3.244	3.243	3.242	3.241
5.5	3.241	3.240	3.239	3.238	3.237	3.236	3.235	3.234	3.233	3.232	3.231
5.6	3.231	3.230	3.229	3.228	3.227	3.226	3.225	3.224	3.223	3.222	3.221
5.7	3.221	3.220	3.219	3.218	3.217	3.216	3.215	3.214	3.213	3.212	3.211
5.8	3.212	3.211	3.210	3.209	3.208	3.207	3.206	3.205	3.204	3.203	3.202
5.9	3.202	3.201	3.200	3.199	3.198	3.197	3.196	3.195	3.194	3.193	3.192
6.0	3.193	3.192	3.191	3.190	3.189	3.188	3.187	3.186	3.185	3.184	3.183
6.1	3.184	3.183	3.182	3.181	3.180	3.179	3.178	3.177	3.176	3.175	3.174
6.2	3.176	3.175	3.174	3.173	3.172	3.171	3.170	3.169	3.168	3.167	3.166
6.3	3.167	3.166	3.165	3.164	3.163	3.162	3.161	3.160	3.159	3.158	3.157
6.4	3.159	3.158	3.157	3.156	3.155	3.154	3.153	3.152	3.151	3.150	3.149
6.5	3.151	3.150	3.149	3.148	3.147	3.146	3.145	3.144	3.143	3.142	3.141
6.6	3.143	3.142	3.141	3.140	3.139	3.138	3.137	3.136	3.135	3.134	3.133
6.7	3.135	3.134	3.133	3.132	3.131	3.130	3.129	3.128	3.127	3.126	3.125
6.8	3.127	3.126	3.125	3.124	3.123	3.122	3.121	3.120	3.119	3.118	3.117
6.9	3.120	3.119	3.118	3.117	3.116	3.115	3.114	3.113	3.112	3.111	3.110
7.0	3.112	3.111	3.110	3.109	3.108	3.107	3.106	3.105	3.104	3.103	3.102
7.1	3.104	3.103	3.102	3.101	3.100	3.099	3.098	3.097	3.096	3.095	3.094
7.2	3.097	3.096	3.095	3.094	3.093	3.092	3.091	3.090	3.089	3.088	3.087
7.3	3.090	3.089	3.088	3.087	3.086	3.085	3.084	3.083	3.082	3.081	3.080
7.4	3.083	3.082	3.081	3.080	3.079	3.078	3.077	3.076	3.075	3.074	3.073
7.5	3.077	3.076	3.075	3.074	3.073	3.072	3.071	3.070	3.069	3.068	3.067
7.6	3.069	3.068	3.067	3.066	3.065	3.064	3.063	3.062	3.061	3.060	3.059
7.7	3.062	3.061	3.060	3.059	3.058	3.057	3.056	3.055	3.054	3.053	3.052
7.8	3.056	3.055	3.054	3.053	3.052	3.051	3.050	3.049	3.048	3.047	3.046
7.9	3.049	3.048	3.047	3.046	3.045	3.044	3.043	3.042	3.041	3.040	3.039
8.0	3.043	3.042	3.041	3.040	3.039	3.038	3.037	3.036	3.035	3.034	3.033
8.1	3.037	3.036	3.035	3.034	3.033	3.032	3.031	3.030	3.029	3.028	3.027
8.2	3.031	3.030	3.029	3.028	3.027	3.026	3.025	3.024	3.023	3.022	3.021
8.3	3.025	3.024	3.023	3.022	3.021	3.020	3.019	3.018	3.017	3.016	3.015
8.4	3.019	3.018	3.017	3.016	3.015	3.014	3.013	3.012	3.011	3.010	3.009
8.5	3.013	3.012	3.011	3.010	3.009	3.008	3.007	3.006	3.005	3.004	3.003
8.6	3.007	3.006	3.005	3.004	3.003	3.002	3.001	3.000	2.999	2.998	2.997
8.7	3.002	3.001	3.000	2.999	2.998	2.997	2.996	2.995	2.994	2.993	2.992
8.8	2.996	2.995	2.994	2.993	2.992	2.991	2.990	2.989	2.988	2.987	2.986
8.9	2.991	2.990	2.989	2.988	2.987	2.986	2.985	2.984	2.983	2.982	2.981
9.0	2.986	2.985	2.984	2.983	2.982	2.981	2.980	2.979	2.978	2.977	2.976
9.1	2.980	2.979	2.978	2.977	2.976	2.975	2.974	2.973	2.972	2.971	2.970
9.2	2.975	2.974	2.973	2.972	2.971	2.970	2.969	2.968	2.967	2.966	2.965
9.3	2.969	2.968	2.967	2.966	2.965	2.964	2.963	2.962	2.961	2.960	2.959
9.4	2.964	2.963	2.962	2.961	2.960	2.959	2.958	2.957	2.956	2.955	2.954
9.5	2.959	2.958	2.957	2.956	2.955	2.954	2.953	2.952	2.951	2.950	2.949
9.6	2.954	2.953	2.952	2.951	2.950	2.949	2.948	2.947	2.946	2.945	2.944
9.7	2.949	2.948	2.947	2.946	2.945	2.944	2.943	2.942	2.941	2.940	2.939
9.8	2.944	2.943	2.942	2.941	2.940	2.939	2.938	2.937	2.936	2.935	2.934
9.9	2.939	2.938	2.937	2.936	2.935	2.934	2.933	2.932	2.931	2.930	2.929

Schoenherr Frictional Resistance Coefficients for
Reynolds Numbers from 1.00 to 9.99×10^7

The values for the frictional resistance coefficients must be multiplied by 10^{-3} .

Reynolds Number $10^7 \times$	0.00	0.01	0.02	0.03	0.04	0.05	0.06	0.07	0.08	0.09	0.10
1.0	2.934	2.929	2.925	2.920	2.916	2.911	2.907	2.902	2.898	2.893	2.889
1.1	2.889	2.885	2.880	2.877	2.873	2.869	2.865	2.861	2.857	2.853	2.849
1.2	2.849	2.845	2.842	2.838	2.835	2.831	2.827	2.824	2.820	2.817	2.813
1.3	2.813	2.810	2.806	2.803	2.799	2.796	2.793	2.790	2.786	2.783	2.780
1.4	2.780	2.777	2.774	2.770	2.767	2.764	2.761	2.758	2.755	2.752	2.749
1.5	2.749	2.746	2.743	2.741	2.738	2.735	2.732	2.729	2.727	2.724	2.721
1.6	2.721	2.718	2.716	2.713	2.711	2.708	2.706	2.703	2.701	2.698	2.696
1.7	2.696	2.694	2.691	2.689	2.686	2.684	2.682	2.679	2.677	2.674	2.672
1.8	2.672	2.670	2.667	2.665	2.662	2.660	2.658	2.656	2.653	2.651	2.649
1.9	2.649	2.647	2.645	2.643	2.641	2.639	2.637	2.635	2.632	2.630	2.628
2.0	2.628	2.626	2.624	2.622	2.620	2.618	2.616	2.614	2.613	2.611	2.609
2.1	2.609	2.607	2.605	2.603	2.601	2.599	2.597	2.595	2.594	2.592	2.590
2.2	2.590	2.588	2.586	2.585	2.583	2.581	2.579	2.577	2.576	2.574	2.572
2.3	2.572	2.570	2.568	2.567	2.565	2.563	2.561	2.560	2.558	2.557	2.555
2.4	2.555	2.553	2.552	2.550	2.549	2.547	2.545	2.544	2.542	2.541	2.539
2.5	2.539	2.537	2.536	2.534	2.533	2.531	2.530	2.528	2.527	2.525	2.524
2.6	2.524	2.522	2.521	2.519	2.518	2.516	2.515	2.513	2.512	2.510	2.509
2.7	2.509	2.508	2.506	2.505	2.503	2.502	2.501	2.500	2.498	2.497	2.496
2.8	2.496	2.495	2.493	2.492	2.490	2.489	2.488	2.487	2.485	2.484	2.483
2.9	2.483	2.482	2.480	2.479	2.477	2.476	2.475	2.474	2.472	2.471	2.470
3.0	2.470	2.469	2.468	2.466	2.465	2.464	2.463	2.461	2.460	2.458	2.457
3.1	2.457	2.456	2.455	2.454	2.453	2.452	2.451	2.450	2.448	2.447	2.446
3.2	2.446	2.445	2.444	2.442	2.441	2.440	2.439	2.438	2.437	2.436	2.435
3.3	2.435	2.434	2.433	2.431	2.430	2.429	2.428	2.427	2.426	2.425	2.424
3.4	2.424	2.423	2.422	2.420	2.419	2.418	2.417	2.416	2.415	2.414	2.413
3.5	2.413	2.412	2.411	2.410	2.409	2.408	2.407	2.406	2.405	2.404	2.403
3.6	2.403	2.402	2.401	2.400	2.399	2.398	2.397	2.396	2.395	2.394	2.393
3.7	2.393	2.392	2.391	2.390	2.389	2.388	2.387	2.386	2.385	2.384	2.383
3.8	2.383	2.382	2.381	2.381	2.380	2.379	2.378	2.377	2.376	2.375	2.374
3.9	2.374	2.373	2.372	2.372	2.371	2.370	2.369	2.368	2.367	2.366	2.365
4.0	2.365	2.364	2.363	2.363	2.362	2.361	2.360	2.359	2.358	2.357	2.356
4.1	2.356	2.355	2.354	2.354	2.353	2.352	2.351	2.350	2.350	2.349	2.348
4.2	2.348	2.347	2.346	2.346	2.345	2.344	2.343	2.342	2.341	2.341	2.340
4.3	2.340	2.339	2.338	2.338	2.337	2.336	2.335	2.334	2.334	2.333	2.332
4.4	2.332	2.331	2.330	2.330	2.329	2.328	2.327	2.326	2.326	2.325	2.324
4.5	2.324	2.323	2.323	2.323	2.321	2.320	2.320	2.319	2.318	2.318	2.317
4.6	2.317	2.316	2.316	2.315	2.314	2.313	2.313	2.312	2.311	2.311	2.310
4.7	2.310	2.309	2.309	2.308	2.307	2.306	2.306	2.305	2.304	2.304	2.303
4.8	2.303	2.302	2.302	2.301	2.300	2.299	2.299	2.298	2.297	2.297	2.296
4.9	2.296	2.295	2.295	2.294	2.293	2.292	2.292	2.291	2.290	2.290	2.289

Reynolds Number $10^7 \times$	0.00	0.01	0.02	0.03	0.04	0.05	0.06	0.07	0.08	0.09	0.10
5.0	2.289	2.288	2.288	2.287	2.286	2.285	2.285	2.284	2.283	2.283	2.282
5.1	2.282	2.281	2.281	2.280	2.279	2.278	2.278	2.277	2.276	2.276	2.275
5.2	2.275	2.274	2.274	2.273	2.273	2.272	2.271	2.271	2.270	2.270	2.269
5.3	2.269	2.268	2.268	2.267	2.267	2.266	2.265	2.265	2.264	2.264	2.263
5.4	2.263	2.262	2.262	2.261	2.261	2.260	2.259	2.259	2.258	2.258	2.257
5.5	2.257	2.256	2.256	2.255	2.255	2.254	2.253	2.253	2.252	2.252	2.251
5.6	2.251	2.250	2.250	2.249	2.249	2.248	2.247	2.247	2.246	2.246	2.245
5.7	2.245	2.244	2.244	2.243	2.243	2.242	2.241	2.241	2.240	2.240	2.240
5.8	2.240	2.239	2.239	2.238	2.238	2.237	2.236	2.236	2.235	2.235	2.235
5.9	2.235	2.234	2.234	2.233	2.233	2.232	2.231	2.231	2.230	2.230	2.229
6.0	2.229	2.228	2.228	2.227	2.227	2.226	2.225	2.225	2.224	2.224	2.223
6.1	2.223	2.222	2.222	2.221	2.221	2.220	2.219	2.219	2.218	2.218	2.218
6.2	2.218	2.217	2.217	2.216	2.216	2.215	2.214	2.214	2.213	2.213	2.213
6.3	2.213	2.212	2.212	2.211	2.211	2.210	2.209	2.209	2.208	2.208	2.208
6.4	2.208	2.207	2.207	2.206	2.206	2.205	2.204	2.204	2.203	2.203	2.203
6.5	2.203	2.202	2.202	2.201	2.201	2.200	2.199	2.199	2.198	2.198	2.198
6.6	2.198	2.198	2.197	2.197	2.196	2.196	2.195	2.195	2.194	2.194	2.194
6.7	2.194	2.193	2.193	2.192	2.192	2.191	2.190	2.190	2.189	2.189	2.189
6.8	2.189	2.188	2.188	2.187	2.187	2.186	2.185	2.185	2.184	2.184	2.184
6.9	2.184	2.183	2.183	2.182	2.182	2.181	2.180	2.180	2.179	2.179	2.179
7.0	2.179	2.179	2.178	2.178	2.177	2.177	2.176	2.176	2.175	2.175	2.175
7.1	2.175	2.175	2.174	2.174	2.173	2.173	2.172	2.172	2.171	2.171	2.171
7.2	2.171	2.171	2.170	2.170	2.169	2.169	2.168	2.168	2.167	2.167	2.167
7.3	2.167	2.167	2.166	2.166	2.165	2.165	2.164	2.164	2.163	2.163	2.163
7.4	2.163	2.163	2.162	2.162	2.161	2.161	2.160	2.160	2.159	2.159	2.159
7.5	2.159	2.158	2.158	2.157	2.157	2.156	2.155	2.155	2.154	2.154	2.154
7.6	2.154	2.154	2.153	2.153	2.152	2.152	2.151	2.151	2.150	2.150	2.150
7.7	2.150	2.150	2.149	2.149	2.148	2.148	2.147	2.147	2.146	2.146	2.146
7.8	2.146	2.146	2.145	2.145	2.144	2.144	2.143	2.143	2.142	2.142	2.142
7.9	2.142	2.142	2.141	2.141	2.140	2.140	2.139	2.139	2.138	2.138	2.138
8.0	2.138	2.138	2.137	2.137	2.137	2.136	2.136	2.136	2.135	2.135	2.135
8.1	2.135	2.135	2.134	2.134	2.133	2.133	2.132	2.132	2.131	2.131	2.131
8.2	2.131	2.131	2.130	2.130	2.129	2.129	2.128	2.128	2.127	2.127	2.127
8.3	2.127	2.127	2.126	2.126	2.125	2.125	2.124	2.124	2.123	2.123	2.123
8.4	2.124	2.124	2.123	2.123	2.122	2.122	2.121	2.121	2.120	2.120	2.120
8.5	2.120	2.120	2.119	2.119	2.118	2.118	2.117	2.117	2.116	2.116	2.116
8.6	2.116	2.116	2.115	2.115	2.114	2.114	2.113	2.113	2.112	2.112	2.112
8.7	2.113	2.113	2.112	2.112	2.111	2.111	2.110	2.110	2.109	2.109	2.109
8.8	2.110	2.110	2.109	2.109	2.108	2.108	2.107	2.107	2.106	2.106	2.106
8.9	2.106	2.106	2.105	2.105	2.104	2.104	2.103	2.103	2.102	2.102	2.102
9.0	2.103	2.103	2.102	2.102	2.102	2.101	2.101	2.101	2.100	2.100	2.100
9.1	2.100	2.100	2.099	2.099	2.099	2.098	2.098	2.098	2.097	2.097	2.097
9.2	2.097	2.097	2.096	2.096	2.096	2.095	2.095	2.095	2.094	2.094	2.094
9.3	2.094	2.094	2.093	2.093	2.093	2.092	2.092	2.092	2.091	2.091	2.091
9.4	2.090	2.090	2.089	2.089	2.089	2.088	2.088	2.088	2.087	2.087	2.087
9.5	2.087	2.087	2.086	2.086	2.086	2.085	2.085	2.085	2.084	2.084	2.084
9.6	2.084	2.084	2.083	2.083	2.083	2.082	2.082	2.082	2.081	2.081	2.081
9.7	2.081	2.081	2.080	2.080	2.080	2.079	2.079	2.079	2.078	2.078	2.078
9.8	2.078	2.078	2.077	2.077	2.077	2.076	2.076	2.076	2.075	2.075	2.075
9.9	2.075	2.075	2.074	2.074	2.074	2.073	2.073	2.073	2.072	2.072	2.072

Schoenherr Frictional Resistance Coefficients for
Reynolds Numbers from 1.00 to 9.99×10^8

The values for the frictional resistance coefficients must be multiplied by 10^{-8} .

Reynolds Number $10^8 \times$	0.00	0.01	0.02	0.03	0.04	0.05	0.06	0.07	0.08	0.09	0.10
1.0	2.072	2.069	2.066	2.064	2.061	2.058	2.055	2.053	2.050	2.048	2.045
1.1	2.045	2.042	2.040	2.037	2.035	2.032	2.030	2.027	2.025	2.022	2.020
1.2	2.020	2.018	2.015	2.013	2.010	2.008	2.006	2.004	2.002	2.000	1.998
1.3	1.998	1.996	1.994	1.991	1.989	1.987	1.985	1.983	1.982	1.980	1.978
1.4	1.978	1.976	1.974	1.972	1.970	1.968	1.966	1.964	1.963	1.961	1.959
1.5	1.959	1.957	1.955	1.954	1.952	1.950	1.948	1.947	1.945	1.944	1.942
1.6	1.942	1.940	1.939	1.937	1.936	1.934	1.932	1.931	1.929	1.928	1.926
1.7	1.926	1.924	1.923	1.921	1.920	1.918	1.917	1.915	1.914	1.912	1.911
1.8	1.911	1.910	1.908	1.907	1.905	1.904	1.903	1.901	1.900	1.898	1.897
1.9	1.897	1.896	1.894	1.893	1.891	1.890	1.889	1.888	1.886	1.885	1.884
2.0	1.884	1.883	1.882	1.880	1.879	1.878	1.877	1.876	1.874	1.873	1.872
2.1	1.872	1.871	1.870	1.868	1.867	1.866	1.865	1.864	1.862	1.861	1.860
2.2	1.860	1.859	1.858	1.857	1.856	1.854	1.853	1.852	1.851	1.850	1.849
2.3	1.849	1.848	1.847	1.846	1.845	1.843	1.842	1.841	1.840	1.839	1.838
2.4	1.838	1.837	1.836	1.835	1.834	1.833	1.832	1.831	1.830	1.829	1.828
2.5	1.828	1.827	1.826	1.825	1.824	1.823	1.822	1.821	1.820	1.819	1.818
2.6	1.819	1.818	1.817	1.816	1.815	1.814	1.813	1.812	1.811	1.810	1.809
2.7	1.810	1.809	1.808	1.807	1.806	1.805	1.804	1.803	1.802	1.801	1.800
2.8	1.801	1.800	1.799	1.798	1.797	1.796	1.795	1.794	1.793	1.792	1.791
2.9	1.792	1.791	1.790	1.790	1.789	1.788	1.787	1.786	1.785	1.784	1.783
3.0	1.784	1.783	1.782	1.782	1.781	1.780	1.779	1.778	1.778	1.777	1.776
3.1	1.776	1.775	1.775	1.774	1.773	1.772	1.771	1.770	1.770	1.770	1.769
3.2	1.769	1.768	1.768	1.767	1.766	1.765	1.765	1.764	1.763	1.762	1.762
3.3	1.762	1.761	1.761	1.760	1.759	1.758	1.758	1.757	1.756	1.756	1.755
3.4	1.755	1.754	1.754	1.753	1.752	1.751	1.751	1.750	1.749	1.749	1.748
3.5	1.748	1.747	1.747	1.746	1.746	1.745	1.744	1.744	1.743	1.743	1.742
3.6	1.742	1.741	1.741	1.740	1.740	1.739	1.738	1.738	1.737	1.737	1.736
3.7	1.736	1.735	1.735	1.734	1.734	1.733	1.733	1.732	1.731	1.731	1.730
3.8	1.730	1.729	1.729	1.728	1.728	1.727	1.726	1.726	1.725	1.725	1.724
3.9	1.724	1.723	1.723	1.722	1.722	1.721	1.720	1.720	1.719	1.719	1.718
4.0	1.718	1.717	1.717	1.716	1.716	1.715	1.715	1.714	1.714	1.713	1.713
4.1	1.713	1.712	1.712	1.711	1.711	1.710	1.710	1.709	1.709	1.708	1.708
4.2	1.708	1.707	1.707	1.706	1.706	1.705	1.705	1.704	1.704	1.703	1.703
4.3	1.703	1.702	1.702	1.701	1.701	1.700	1.700	1.699	1.699	1.698	1.698
4.4	1.698	1.697	1.697	1.696	1.696	1.695	1.695	1.694	1.694	1.693	1.693
4.5	1.693	1.692	1.692	1.691	1.691	1.690	1.690	1.689	1.689	1.688	1.688
4.6	1.688	1.687	1.687	1.686	1.686	1.685	1.685	1.684	1.684	1.683	1.683
4.7	1.683	1.683	1.682	1.682	1.681	1.681	1.680	1.680	1.680	1.679	1.679
4.8	1.679	1.679	1.678	1.678	1.677	1.677	1.676	1.676	1.676	1.675	1.675
4.9	1.675	1.674	1.674	1.673	1.673	1.672	1.672	1.671	1.671	1.670	1.670

Reynolds Number $10^5 \times$	0.00	0.01	0.02	0.03	0.04	0.05	0.06	0.07	0.08	0.09	0.10
5.0	1.670	1.670	1.669	1.669	1.668	1.668	1.668	1.667	1.667	1.666	1.666
5.1	1.666	1.666	1.665	1.665	1.664	1.664	1.664	1.663	1.663	1.662	1.662
5.2	1.662	1.662	1.661	1.661	1.660	1.660	1.660	1.659	1.659	1.658	1.658
5.3	1.658	1.658	1.657	1.657	1.656	1.656	1.656	1.655	1.655	1.654	1.654
5.4	1.654	1.654	1.653	1.653	1.652	1.652	1.652	1.651	1.651	1.650	1.650
5.5	1.650	1.650	1.649	1.649	1.648	1.648	1.648	1.647	1.647	1.646	1.646
5.6	1.646	1.646	1.645	1.645	1.644	1.644	1.644	1.643	1.643	1.642	1.642
5.7	1.642	1.642	1.641	1.641	1.640	1.640	1.640	1.639	1.639	1.638	1.638
5.8	1.638	1.638	1.637	1.637	1.637	1.636	1.636	1.635	1.635	1.635	1.635
5.9	1.635	1.635	1.634	1.634	1.634	1.633	1.633	1.633	1.633	1.632	1.632
6.0	1.632	1.632	1.631	1.631	1.630	1.630	1.630	1.629	1.629	1.628	1.628
6.1	1.628	1.628	1.627	1.627	1.627	1.626	1.626	1.626	1.626	1.625	1.625
6.2	1.625	1.625	1.624	1.624	1.624	1.623	1.623	1.623	1.623	1.622	1.622
6.3	1.622	1.622	1.621	1.621	1.621	1.620	1.620	1.620	1.620	1.619	1.619
6.4	1.619	1.619	1.618	1.618	1.618	1.617	1.617	1.617	1.617	1.616	1.616
6.5	1.616	1.616	1.615	1.615	1.615	1.614	1.614	1.614	1.614	1.613	1.613
6.6	1.613	1.613	1.612	1.612	1.612	1.611	1.611	1.611	1.611	1.610	1.610
6.7	1.610	1.610	1.609	1.609	1.609	1.608	1.608	1.608	1.608	1.607	1.607
6.8	1.607	1.607	1.606	1.606	1.606	1.605	1.605	1.605	1.605	1.604	1.604
6.9	1.604	1.604	1.603	1.603	1.603	1.602	1.602	1.602	1.602	1.601	1.601
7.0	1.601	1.601	1.600	1.600	1.600	1.599	1.599	1.599	1.599	1.598	1.598
7.1	1.598	1.598	1.597	1.597	1.597	1.596	1.596	1.596	1.596	1.595	1.595
7.2	1.595	1.595	1.594	1.594	1.594	1.593	1.593	1.593	1.593	1.592	1.592
7.3	1.592	1.592	1.591	1.591	1.591	1.590	1.590	1.590	1.590	1.589	1.589
7.4	1.589	1.589	1.588	1.588	1.588	1.587	1.587	1.587	1.587	1.586	1.586
7.5	1.586	1.586	1.586	1.585	1.585	1.585	1.585	1.585	1.584	1.584	1.584
7.6	1.584	1.584	1.584	1.583	1.583	1.583	1.583	1.583	1.582	1.582	1.582
7.7	1.582	1.582	1.581	1.581	1.581	1.580	1.580	1.580	1.580	1.579	1.579
7.8	1.579	1.579	1.578	1.578	1.578	1.577	1.577	1.577	1.577	1.576	1.576
7.9	1.576	1.576	1.576	1.575	1.575	1.575	1.575	1.575	1.574	1.574	1.574
8.0	1.574	1.574	1.574	1.573	1.573	1.573	1.573	1.573	1.572	1.572	1.572
8.1	1.572	1.572	1.571	1.571	1.571	1.570	1.570	1.570	1.570	1.569	1.569
8.2	1.569	1.569	1.569	1.568	1.568	1.568	1.568	1.568	1.567	1.567	1.567
8.3	1.567	1.567	1.566	1.566	1.566	1.565	1.565	1.565	1.564	1.564	1.564
8.4	1.564	1.564	1.564	1.563	1.563	1.563	1.563	1.563	1.562	1.562	1.562
8.5	1.562	1.562	1.562	1.561	1.561	1.561	1.561	1.561	1.560	1.560	1.560
8.6	1.560	1.560	1.560	1.559	1.559	1.559	1.559	1.559	1.558	1.558	1.558
8.7	1.558	1.558	1.558	1.557	1.557	1.557	1.557	1.557	1.556	1.556	1.556
8.8	1.556	1.556	1.555	1.555	1.555	1.554	1.554	1.554	1.553	1.553	1.553
8.9	1.553	1.553	1.553	1.552	1.552	1.552	1.552	1.552	1.551	1.551	1.551
9.0	1.551	1.551	1.551	1.550	1.550	1.550	1.550	1.550	1.549	1.549	1.549
9.1	1.549	1.549	1.549	1.548	1.548	1.548	1.548	1.547	1.547	1.547	1.547
9.2	1.547	1.547	1.547	1.546	1.546	1.546	1.546	1.546	1.545	1.545	1.545
9.3	1.545	1.545	1.545	1.544	1.544	1.544	1.544	1.544	1.543	1.543	1.543
9.4	1.543	1.543	1.543	1.542	1.542	1.542	1.542	1.542	1.541	1.541	1.541
9.5	1.541	1.541	1.541	1.540	1.540	1.540	1.540	1.540	1.539	1.539	1.539
9.6	1.539	1.539	1.539	1.538	1.538	1.538	1.538	1.538	1.537	1.537	1.537
9.7	1.537	1.537	1.537	1.536	1.536	1.536	1.536	1.536	1.535	1.535	1.535
9.8	1.535	1.535	1.535	1.534	1.534	1.534	1.534	1.534	1.533	1.533	1.533
9.9	1.533	1.533	1.533	1.532	1.532	1.532	1.532	1.532	1.531	1.531	1.531

Schoenherr Frictional Resistance Coefficients for
Reynolds Numbers from 1.00 to 9.99×10^9

The values for the frictional resistance coefficients must be multiplied by 10^{-3} .

Reynolds Number $10^9 \times$	0.00	0.01	0.02	0.03	0.04	0.05	0.06	0.07	0.08	0.09	0.10
1.0	1.531	1.529	1.527	1.526	1.524	1.522	1.520	1.518	1.517	1.515	1.513
1.1	1.513	1.511	1.510	1.508	1.507	1.505	1.503	1.502	1.500	1.499	1.497
1.2	1.497	1.496	1.494	1.493	1.491	1.490	1.488	1.487	1.485	1.484	1.482
1.3	1.482	1.481	1.480	1.478	1.477	1.476	1.475	1.473	1.471	1.470	1.469
1.4	1.469	1.468	1.467	1.465	1.464	1.463	1.462	1.461	1.459	1.458	1.457
1.5	1.457	1.456	1.455	1.453	1.452	1.451	1.450	1.448	1.447	1.447	1.446
1.6	1.446	1.445	1.444	1.443	1.442	1.441	1.440	1.439	1.437	1.437	1.436
1.7	1.436	1.435	1.434	1.433	1.432	1.431	1.430	1.429	1.428	1.427	1.426
1.8	1.426	1.425	1.424	1.423	1.422	1.421	1.420	1.419	1.418	1.417	1.416
1.9	1.416	1.415	1.414	1.414	1.413	1.412	1.411	1.410	1.410	1.409	1.408
2.0	1.408	1.407	1.406	1.406	1.405	1.404	1.403	1.402	1.402	1.401	1.400
2.1	1.400	1.399	1.398	1.398	1.397	1.396	1.395	1.394	1.394	1.393	1.392
2.2	1.392	1.391	1.391	1.390	1.389	1.388	1.388	1.387	1.386	1.386	1.385
2.3	1.385	1.384	1.384	1.383	1.382	1.381	1.381	1.380	1.379	1.379	1.378
2.4	1.378	1.377	1.377	1.376	1.375	1.374	1.374	1.373	1.372	1.372	1.371
2.5	1.371	1.370	1.370	1.369	1.369	1.368	1.367	1.367	1.366	1.366	1.365
2.6	1.365	1.364	1.364	1.363	1.363	1.362	1.361	1.361	1.360	1.360	1.359
2.7	1.359	1.358	1.358	1.357	1.357	1.356	1.355	1.355	1.354	1.354	1.353
2.8	1.353	1.352	1.352	1.351	1.351	1.350	1.350	1.349	1.349	1.348	1.348
2.9	1.348	1.347	1.347	1.346	1.346	1.345	1.345	1.344	1.344	1.343	1.343
3.0	1.343	1.342	1.342	1.341	1.341	1.340	1.340	1.339	1.339	1.338	1.338
3.1	1.338	1.337	1.337	1.336	1.336	1.335	1.335	1.334	1.334	1.333	1.333
3.2	1.333	1.332	1.332	1.331	1.331	1.330	1.330	1.329	1.329	1.328	1.328
3.3	1.328	1.327	1.327	1.326	1.326	1.325	1.325	1.324	1.324	1.323	1.323
3.4	1.323	1.323	1.322	1.322	1.321	1.321	1.321	1.320	1.320	1.319	1.319
3.5	1.319	1.319	1.318	1.318	1.317	1.317	1.317	1.316	1.316	1.315	1.315
3.6	1.315	1.314	1.314	1.313	1.313	1.312	1.312	1.311	1.311	1.310	1.310
3.7	1.310	1.310	1.309	1.309	1.308	1.308	1.308	1.307	1.307	1.306	1.306
3.8	1.306	1.306	1.305	1.305	1.304	1.304	1.304	1.303	1.303	1.302	1.302
3.9	1.302	1.302	1.301	1.301	1.301	1.300	1.300	1.300	1.300	1.299	1.299
4.0	1.299	1.299	1.298	1.298	1.297	1.297	1.297	1.296	1.296	1.295	1.295
4.1	1.295	1.295	1.294	1.294	1.293	1.293	1.293	1.292	1.292	1.291	1.291
4.2	1.291	1.291	1.290	1.290	1.290	1.289	1.289	1.289	1.288	1.288	1.288
4.3	1.288	1.288	1.287	1.287	1.286	1.286	1.286	1.285	1.285	1.284	1.284
4.4	1.284	1.284	1.283	1.283	1.283	1.282	1.282	1.282	1.282	1.281	1.281
4.5	1.281	1.281	1.280	1.280	1.280	1.279	1.279	1.279	1.279	1.278	1.278
4.6	1.278	1.278	1.277	1.277	1.277	1.276	1.276	1.276	1.276	1.275	1.275
4.7	1.275	1.275	1.274	1.274	1.274	1.273	1.273	1.273	1.273	1.272	1.272
4.8	1.272	1.272	1.271	1.271	1.271	1.270	1.270	1.270	1.270	1.269	1.269
4.9	1.269	1.269	1.268	1.268	1.268	1.267	1.267	1.267	1.267	1.266	1.266

Reynolds Number $10^5 \times$	0.00	0.01	0.02	0.03	0.04	0.05	0.06	0.07	0.08	0.09	0.10
5.0	1.266	1.266	1.265	1.265	1.265	1.264	1.264	1.264	1.264	1.263	1.263
5.1	1.263	1.263	1.262	1.262	1.262	1.261	1.261	1.261	1.261	1.260	1.260
5.2	1.260	1.260	1.259	1.259	1.259	1.259	1.259	1.259	1.258	1.258	1.258
5.3	1.258	1.258	1.257	1.257	1.257	1.256	1.256	1.256	1.256	1.255	1.255
5.4	1.255	1.255	1.254	1.254	1.254	1.253	1.253	1.253	1.253	1.252	1.252
5.5	1.252	1.252	1.252	1.251	1.251	1.251	1.251	1.251	1.250	1.250	1.250
5.6	1.250	1.250	1.249	1.249	1.249	1.248	1.248	1.248	1.247	1.247	1.247
5.7	1.247	1.247	1.246	1.246	1.246	1.245	1.245	1.245	1.244	1.244	1.244
5.8	1.244	1.244	1.244	1.243	1.243	1.243	1.243	1.243	1.242	1.242	1.242
5.9	1.242	1.242	1.242	1.241	1.241	1.241	1.241	1.241	1.240	1.240	1.240
6.0	1.240	1.240	1.239	1.239	1.239	1.239	1.239	1.239	1.238	1.238	1.238
6.1	1.238	1.238	1.238	1.237	1.237	1.237	1.237	1.237	1.236	1.236	1.236
6.2	1.236	1.236	1.236	1.235	1.235	1.235	1.235	1.235	1.234	1.234	1.234
6.3	1.234	1.234	1.233	1.233	1.233	1.232	1.232	1.232	1.232	1.231	1.231
6.4	1.231	1.231	1.231	1.230	1.230	1.230	1.230	1.230	1.229	1.229	1.229
6.5	1.229	1.229	1.229	1.228	1.228	1.228	1.228	1.228	1.227	1.227	1.227
6.6	1.227	1.227	1.227	1.226	1.226	1.226	1.226	1.226	1.225	1.225	1.225
6.7	1.225	1.225	1.225	1.224	1.224	1.224	1.224	1.224	1.223	1.223	1.223
6.8	1.223	1.223	1.223	1.222	1.222	1.222	1.222	1.222	1.221	1.221	1.221
6.9	1.221	1.221	1.221	1.220	1.220	1.220	1.220	1.220	1.219	1.219	1.219
7.0	1.219	1.219	1.219	1.218	1.218	1.218	1.218	1.218	1.217	1.217	1.217
7.1	1.217	1.217	1.217	1.216	1.216	1.216	1.216	1.216	1.215	1.215	1.215
7.2	1.215	1.215	1.215	1.214	1.214	1.214	1.214	1.214	1.213	1.213	1.213
7.3	1.213	1.213	1.213	1.213	1.213	1.212	1.212	1.212	1.212	1.212	1.212
7.4	1.212	1.212	1.212	1.211	1.211	1.211	1.211	1.211	1.210	1.210	1.210
7.5	1.210	1.210	1.210	1.209	1.209	1.209	1.209	1.209	1.208	1.208	1.208
7.6	1.208	1.208	1.208	1.207	1.207	1.207	1.207	1.207	1.206	1.206	1.206
7.7	1.206	1.206	1.206	1.205	1.205	1.205	1.205	1.205	1.204	1.204	1.204
7.8	1.204	1.204	1.204	1.204	1.204	1.203	1.203	1.203	1.203	1.203	1.203
7.9	1.203	1.203	1.203	1.202	1.202	1.202	1.202	1.202	1.201	1.201	1.201
8.0	1.201	1.201	1.201	1.201	1.201	1.200	1.200	1.200	1.200	1.200	1.200
8.1	1.200	1.200	1.200	1.199	1.199	1.199	1.199	1.199	1.198	1.198	1.198
8.2	1.198	1.198	1.198	1.197	1.197	1.197	1.197	1.197	1.196	1.196	1.196
8.3	1.196	1.196	1.196	1.196	1.196	1.195	1.195	1.195	1.195	1.195	1.195
8.4	1.195	1.195	1.195	1.194	1.194	1.194	1.194	1.194	1.193	1.193	1.193
8.5	1.193	1.193	1.193	1.193	1.193	1.192	1.192	1.192	1.192	1.192	1.192
8.6	1.192	1.192	1.192	1.191	1.191	1.191	1.191	1.191	1.190	1.190	1.190
8.7	1.190	1.190	1.190	1.190	1.190	1.189	1.189	1.189	1.189	1.189	1.189
8.8	1.189	1.189	1.189	1.188	1.188	1.188	1.188	1.188	1.187	1.187	1.187
8.9	1.187	1.187	1.187	1.187	1.187	1.186	1.186	1.186	1.186	1.186	1.186
9.0	1.186	1.186	1.186	1.185	1.185	1.185	1.185	1.185	1.184	1.184	1.184
9.1	1.184	1.184	1.184	1.184	1.184	1.183	1.183	1.183	1.183	1.183	1.183
9.2	1.183	1.183	1.183	1.182	1.182	1.182	1.182	1.182	1.181	1.181	1.181
9.3	1.181	1.181	1.181	1.181	1.181	1.180	1.180	1.180	1.180	1.180	1.180
9.4	1.180	1.180	1.180	1.180	1.180	1.179	1.179	1.179	1.179	1.179	1.179
9.5	1.179	1.179	1.179	1.179	1.179	1.178	1.178	1.178	1.178	1.178	1.178
9.6	1.178	1.178	1.178	1.177	1.177	1.177	1.177	1.177	1.176	1.176	1.176
9.7	1.176	1.176	1.176	1.176	1.176	1.175	1.175	1.175	1.175	1.175	1.175
9.8	1.175	1.175	1.175	1.174	1.174	1.174	1.174	1.174	1.173	1.173	1.173
9.9	1.173	1.173	1.173	1.173	1.173	1.172	1.172	1.172	1.172	1.172	1.172

APPENDIX 7

TABLES OF DENSITY AND KINEMATIC VISCOSITY OF WATER

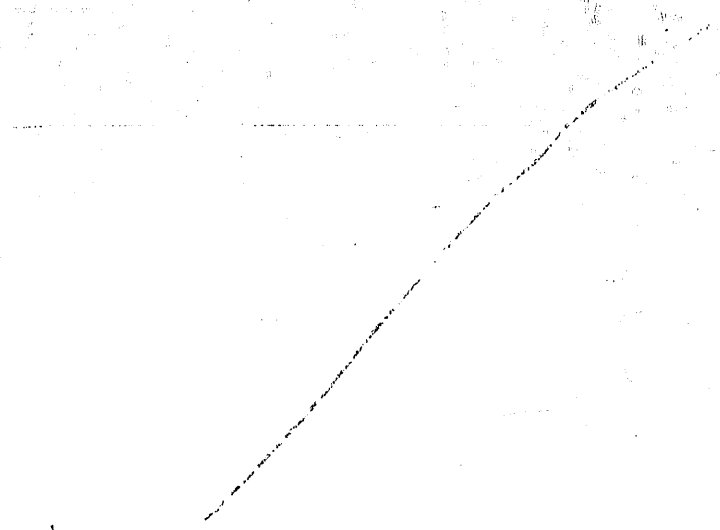


Table of Density of Water

These values were adopted by the American Towing Tank Conference in 1942.
The fifth significant figures are doubtful.

Density of Fresh Water ρ $\text{lb} \times \text{sec}^2/\text{ft}^4$	Temperature degree F	Density of Sea Water ρ_s $\text{lb} \times \text{sec}^2/\text{ft}^4$	Density of Fresh Water ρ $\text{lb} \times \text{sec}^2/\text{ft}^4$	Temperature degree F	Density of Sea Water ρ_s $\text{lb} \times \text{sec}^2/\text{ft}^4$
1.9399	32	1.9947	1.9381	61	1.9901
1.9399	33	1.9946	1.9379	62	1.9898
1.9400	34	1.9946	1.9377	63	1.9895
1.9400	35	1.9945	1.9375	64	1.9893
1.9401	36	1.9944	1.9373	65	1.9890
1.9401	37	1.9943	1.9371	66	1.9888
1.9401	38	1.9942	1.9369	67	1.9885
1.9401	39	1.9941	1.9367	68	1.9882
1.9401	40	1.9940	1.9365	69	1.9879
1.9401	41	1.9939	1.9362	70	1.9876
1.9401	42	1.9937	1.9360	71	1.9873
1.9401	43	1.9936	1.9358	72	1.9870
1.9400	44	1.9934	1.9355	73	1.9867
1.9400	45	1.9933	1.9352	74	1.9864
1.9399	46	1.9931	1.9350	75	1.9861
1.9398	47	1.9930	1.9347	76	1.9858
1.9398	48	1.9928	1.9344	77	1.9854
1.9397	49	1.9926	1.9342	78	1.9851
1.9396	50	1.9924	1.9339	79	1.9848
1.9395	51	1.9923	1.9336	80	1.9844
1.9394	52	1.9921	1.9333	81	1.9841
1.9393	53	1.9919	1.9330	82	1.9837
1.9392	54	1.9917	1.9327	83	1.9834
1.9390	55	1.9914	1.9324	84	1.9830
1.9389	56	1.9912	1.9321	85	1.9827
1.9387	57	1.9910	1.9317	86	1.9823
1.9386	58	1.9908			
1.9384	59	1.9905			
1.9383	60	1.9903			

Table of Kinematic Viscosity of Water

These values were adopted by the American Towing Tank Conference in 1942.
The fifth significant figures are doubtful.

Kinematic Viscosity of Fresh Water $\nu \times 10^5$ ft ² /sec	Temperature degree F	Kinematic Viscosity of Sea Water $\nu_s \times 10^5$ ft ² /sec	Kinematic Viscosity of Fresh Water $\nu \times 10^5$ ft ² /sec	Temperature degree F	Kinematic Viscosity of Sea Water $\nu_s \times 10^5$ ft ² /sec
1.9291	32		1.1937	61	1.2470
1.8922	33		1.1769	62	1.2303
1.8565	34		1.1605	63	1.2139
1.8219	35		1.1444	64	1.1979
1.7883	36		1.1287	65	1.1822
1.7558	37		1.1133	66	1.1669
1.7242	38		1.0983	67	1.1519
1.6935	39		1.0836	68	1.1372
1.6638	40		1.0692	69	1.1229
	41	1.6846	1.0552	70	1.1088
1.6349	42	1.6568	1.0414	71	1.0951
1.6068	43	1.6298	1.0279	72	1.0816
1.5795	44	1.6035	1.0147	73	1.0684
1.5530	45	1.5780	1.0018	74	1.0554
1.5272	46	1.5531	0.98918	75	1.0427
1.5021	47	1.5289	0.97680	76	1.0303
1.4776	48	1.5053	0.96466	77	1.0181
1.4538	49	1.4823	0.95276	78	1.0062
1.4306	50	1.4599	0.94111	79	0.99447
1.4080	51	1.4381	0.92969	80	0.98299
1.3860	52	1.4168	0.91850	81	0.97172
1.3646	53	1.3961	0.90752	82	0.96067
1.3437	54	1.3758	0.89676	83	0.94982
1.3233	55	1.3561	0.88621	84	0.93917
1.3034	56	1.3368	0.87586	85	0.92875
1.2840	57	1.3180	0.86570	86	0.91847
1.2651	58	1.2996			
1.2466	59	1.2817			
1.2285	60	1.2641			